MODELING AND CONTROL USING DELTA DOMAIN TECHNIQUE AND ITS APPLICATION IN BIOMEDICAL DIGITAL FILTERS

A thesis submitted in partial fulfillment of the requirements for the degree of

DOCTOR OF PHILOSOPHY

by

NARAYAN CHANDRA SARCAR

Registration No. 010 of 2006

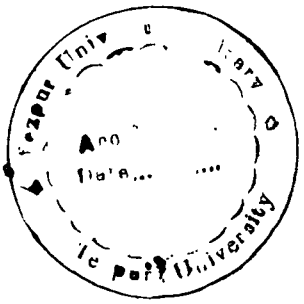

DEPARTMENT OF ELECTRONICS AND COMMUNICATION ENGINEERING
SCHOOL OF ENGINEERING
TEZPUR UNIVERSITY, NAPAAM
TEZPUR - 784028 INDIA
January 2009

Dedicated

to

My Parents,

Smt. Asha Lata & Shri Kshitish Ch. Sarcar,

Wife and Children

ABSTRACT

A paradigm shift from continuous-time to discrete-time signals and systems studies originated during sixties employing shift operator in the time domain analysis & design, while z-transformation in its complex domain counterparts. Despite the fact that real world physical signals and processes remain continuous in time, but due to certain limitations of continuous-time analysis, synthesis and design tools there have been rapid proliferation of digital techniques due to low hardware and software cost and hassle free implementation. The advent of very high speed digital computers and rapid development of VLSI technology have led fast sampling to avoid loss of information.

Unfortunately, the traditional shift-operator model becomes uninformative at fast sampling rates. An alternative parameterization based on signal differencing has been advocated by Middleton and Goodwin to overcome these difficulties. The delta operator parameterization has a close connection with continuous-time and in fact converges to the continuous-time description as the sampling period tends to zero. It therefore provides a unified framework for system studies, where continuous-time results can be achieved from the discrete-time description of the system.

In the present work classical control design methods in the complex delta domain using the concept of model matching in the Truxal framework is attempted. These controller design techniques consist of designing a controller to compensate a given plant in the complex delta domain, so that the controlled system follows the reference model. The reference model structure, which satisfies the classical time, frequency and complex domain specifications in the complex delta domain, is developed. Discrete-time modeling of the control systems in complex delta domain and development of low order controller based on performance specifications are the main objective of the work undertaken. Two methods are developed to design controllers in the frequency domain,-Optimal Generalised Delta Time Moments (OGDTMs) and Optimal frequency fitting (OFF). These methods are applied to design rational, discrete-time controller for single-input, single-output (SISO), multi-input, multi-output (MIMO) systems and systems with time delay.

Reference Model: Apart from the time and frequency domain specifications such as percentage overshoot, peak time, rise time, delay time, settling time, gain margin, phase

margin, resonant frequency and resonant peak, complex domain specifications are frequently associated with damping ratio (ξ) and frequency of natural oscillation (ω_n).

For a discrete time higher order system, relations between the specifications in the time, frequency and complex delta domain are complicated. In many cases, however, the dynamic characteristics of higher order control systems are well represented by those of a second order system or model for which the relationships between specifications are simpler. Hence the second order reference model transfer function of a closed loop model based on performance specification in discrete delta domain is chosen for this work.

For a pole-zero form of transfer function in z-domain, expression has been derived in terms of a set of complex z- domain specifications. Time domain specifications in delta domain has also been derived however no study has been made so far to relate frequency domain specifications in the complex delta domain. An attempt is however made to address these issues in this work.

Optimal GDTM: In the present work, the concept of model matching method in the complex delta domain discussed above has been developed replacing successive derivative operations of the function with forward difference operations and evaluating them at finite values close to zero. These values of the delta function are defined as generalised delta time moments (GDTM). Therefore the efficacy of the controller design scheme based on GDTM greatly relies on the selection of real frequency points and normally trial and error method is resorted to seek compromise. In the present work, genetic algorithms (GA) are used as an optimisation tool to find the optimal frequency point and hence Optimal GDTM (OGDTM).

Optimal Frequency Fitting: In this work another algorithm of controller design is developed based on selection of optimal complex frequency points using GA. In this method two transfer functions are matched at a number of frequency points in the low frequency range and the controller parameters are computed after evaluating a set of linear algebraic equations at these complex frequency points adopting the method of least square. Therefore the efficacy of the controller design scheme in this method greatly relies on the selection of complex frequency points in the complex delta domain and normally trial and error method is resorted to seek compromise. Genetic algorithm is used as an optimisation tool to find the optimal complex frequency point in this Optimal Frequency Fitting (OFF) method. The computational algorithm of both the design methods are numerically stable at high sampling frequency and yields a continuous-time

like controller, which depicts the advantage of delta operator modelling in control system design.

Genetic Algorithms: Genetic algorithms (GA) have been widely used in many applications to produce a global optimal solution. GA accommodates all facets of soft computing, namely, uncertainty, imperfection, non-linearity and robustness. It is domain independent adaptive and inherently parallel and can handle multiple objectives with no explicit mixing required to define a composite objective function.

In the controller design problems, in order to compute the optimal frequency points, both real and complex, a fitness function is developed which is the difference between the step response of the reference model and the designed controlled system in which GA was entrusted to find the optimal frequency points in the given search space and therefore to find OGDTM and OFF. A fitness function is computed using roulette-wheel /tournament selection method.

In the proposed methods GA is used as a global search tool to optimally locate the real and complex frequency points based on a scalar cost function developed between the error of the reference model and closed loop controlled systems. Hence these algebraic methods are a once-through design method without resort to any trial-and-error procedure. Therefore with minimum amount of effort, this method gives practically realizable PI, PID and other higher order controllers conforming to desired industrial specifications.

Biomedical digital filters: Digital filter is another important field in signal processing and biomedical is an essential area of its application. By using the delta operator based technique, digital filter has been designed for high performance inverter application. Exhaustive study has already been made in modeling and analysis of biomedical digital filters in complex z-domain. In the present work, application of delta operator parameterization has been extended to design of biomedical digital filter to remove high frequency, low frequency and 60 Hz power line interference from the ECG.

Hence, the delta domain methods developed and presented highlights the benefits of using delta operator in system theory and signal processing. To illustrate each method, several simulation results are provided with some practical plant models taken from the literature. The results clearly illustrate the usefulness of the methods developed in the thesis for practical problems and demonstrate that the proposed methods offer a viable and often attractive alternative to some prevalent methods.

DECLARATION

I hereby declare that the thesis entitled **"MODELING AND CONTROL USING DELTA DOMAIN TECHNIQUE AND ITS APPLICATION IN BIOMEDICAL DIGITAL FILTERS"** is an outcome of my research carried out at the Department of Electronics and Communication Engineering, School of Engineering, Tezpur University, Napam, Tezpur, India. The work is original and has not been submitted in part of full, for any other degree or diploma of any other University or Institute.

Date: 21/01/2009

(Narayan Chandra Sarcar)

Tezpur University

Napaam, Tezpur-784028
Assam (India)

This is to certify that the thesis entitled *"Modeling and Control Using Delta Domain Technique and its Application in Biomedical Digital Filters"* submitted to the School of Engineering, Tezpur University in part fulfillment for the award of the degree of Doctor of Philosophy in Electronics and Communication Engineering is a record of research work carried out by Mr Narayan Chandra Sarcar under our supervision and guidance.

All help received by him from various sources have been duly acknowledged. No part of this thesis has been submitted elsewhere for award of any other degree.

(Prof P Sarkar)
Co-Supervisor
Date:

(Prof M Bhuyan)
Supervisor
Date: 21-01-09

TEZPUR UNIVERSITY

This is to certify that the thesis entitled **"Modeling and Control Using Delta Domain Technique and its Application in Biomedical Digital Filters"** submitted by Mr. Narayan Chandra Sarcar to the Tezpur University in the Department of Electronics and Communication Engineering under the School of Engineering in partial fulfillment for the award of the degree of Doctor of Philosophy in Electronics and Communication Engineering has been examined by us and found to be satisfactory.

The committee recommends for the award of the degree of Doctor of Philosophy.

Supervisor External

Examiner

Date:

ACKNOWLEDGEMENTS

The success of my research work would have been uncertain without the help and guidance of dedicated band of people. Thus as token of appreciation of their effort in making of the research work a success, I find it most pleasant to express my true and sincere acknowledgement for their contribution and record my obligation

In the beginning, I would like to express my sincere gratitude to Dr. Manebendra Bhuyan, Professor & Head, Department of Electronics and Communication Engineering, Tezpur University under whose supervision I could complete my research work. I am really grateful in all my humility for imparting his valuable time inspite of his exigent schedule and appointments. I am profoundly stimulated by his enthusiasm and sincere advice and appreciate from insight his care and dedication in constructively censuring my performance including my thesis. I express my pleasure from the bottom of my heart being privileged to work under academician of his repute and persistent intellectual guidance.

I would also like to be sincerely thankful to my research co-supervisor, Dr. Prashant Sarkar, Prof & Head, Department of Electrical Engineering, National Institute of Technical Teacher's Training and Research, Kolkata, co-supervisor, for his expert guidance, sincere advice, constructive support and encouragement during entire period of research. I am intensely indebted to share his precious moments and also for sparing valuable time from his busy schedule while the thesis was being written. It is my pleasure to work under such a profound and intellectual dignitary.

I owe my heartfelt gratitude and indebtedness to Prof. M.K.Chowdhury, Vice Chancellor, Tezpur University, for providing all necessary facilities for completion of my research work.

I am very thankful to all members of Department of Electronics and Communication Engineering and central library, Tezpur University and Department of Electrical Engineering, NITTTR, Kolkata for providing with lab facilities and best study material related to the research and also for their constant support and encouragement.

I also would like to thanks to Dr. A.K.Wahi, Director and Mr. Gopal Chaturvedi, Secretary of Institute of Technology & Management, for extending their full support and encouragement for my research work

Last but not the least, I would like to thank my wife Ratna, daughters Arpita and Ankita for their constant moral support and encouragement for keeping patience and being so understanding during my entire research work

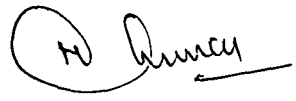

Date: 21/01/2009

(Narayan Chandra Sarcar)
Dept. of Electronics & Comm. Engineering
School of Engineering
Tezpur University

Table of Contents:

List of Figures:

List of Tables:

List of Principal Symbols:

s	Complex variable in s-plane
q	Shift operator
z	Complex variable in z-plane
δ	Time domain delta operator
γ	Complex variable in γ-plane
GA	Genetic Algorithms
SISO	Single-input, Single-output System
MIMO	Multi-input, Multi-output System
TF	Transfer Function
SS	State-space
TFM	Transfer Function Matrix
DTM	Delta Time Moment
OGDTM	Optimal Generalized Delta Time Moment
TM	Time Moment
OFF	Optimal Frequency Fitting
ECG	Electrocardiogram
PCT	Pseudo continuous time
DDC	Direct digital control
CEF	Continued Fraction Expansion
TDC	True Digital Control
LQG	Linear Quadratic Gaussian
LTR	Loop Transfer Recovery
VLSI	Very Large Scale Integration
CCF	Complex Curve Fitting
DDM	Dominant Data Matching
D/A	Digital to Analog Converter
A/D	Analog to Digital Converter
ZOH	Zero Order Hold
CPA	Classical Pade Approximation
EMM	Exact Model Matching
AMM	Approximate Model Matching

PI	Propotional plus integral
PID	Proportional plus integral plus derivative
LMS	Least Mean Square
TD	Time Delay
$x(t)$	Continuous & discrete-time generalized signal
$x_c(t)$	Continuous-time signal
$x(k\Delta)$	Discrete-time signal
$X(s)$	Laplace transform of signal $x_c(t)$
$X(z)$	z-transform of signal $x(k\Delta)$
$X(\gamma)$	δ-transform of $x(k\Delta)$
$u(t)$	Control signal both continuous & discrete-time
$u_c(t)$	Continuous-time control signal
$u(k\Delta)$	Discrete-time control signal
$U(s)$	Laplace transform of control signal
$U(z)$	z-transform of control signal
$U(\gamma)$	δ-transform of control signal
$y(t)$	Output signal both continuous & discrete-time
$y_c(t)$	Continuous-time output signal
$y(k\Delta)$	Discrete-time output signal
Δ	Sampling time
$Y(s)$	Laplace transform of output signal
$Y(z)$	z-transform of output signal
$Y(\gamma)$	δ-transform of output signal
$P_\delta(\gamma)$	Plant transfer function in δ-domain
$P_c(s)$	Plant transfer function in s-domain
d/dt	Time domain differential operator $_{dt}$
z_i	Zeros in s-plane
p_i	Poles in s-plane
$z_{q;i}$	Poles in the z-plane
$p_{q;i}$	Poles in the z-plane
$z_{\delta,i}$	Zeros in the γ-plane
$p_{\delta,i}$	Poles in the γ-plane
$F(\gamma)$	Delta transform of function $f(t)$
γ^{-1}	Inverse delta transform operator

$S_{11}^{\prime 2}$	Generalized integral operator for continuous and discrete-time functions
$E(\gamma,-t)$	Generalized exponential function for continuous & discrete-time functions
ω	Frequency in rad./sec.
ω_s	Sampling frequency in rad./sec.
ω_n	Undamped natural frequency in rad./sec.
ω_d	Damped natural frequency in rad./sec.
ψ_l	Normalized frequency points in γ-plane
$(\boldsymbol{A_c;B_c;C_c})$	Continuous-time state-space coefficients matrices
$(\boldsymbol{A_q;B_q;C_q})$	Discrete-shift state-space coefficients matrices
$(A_\delta;B_\delta;C_\delta)$	Dlta state-space coefficients matrices
$G_c(s)$	Transfer function/Matrix in s-domain
$G_q(z)$	Transfer function/matrix in z-domain
$G_\delta(\gamma)$	Transfer function/Matrix in δ-domain
$D_c(s)$	Denominator of s-plane polynomial / matrix Polynomial
$N_c(s)$	Numerator of s-plane polynomial/matrix polynomial
$D_q(z)$	Denominator of z-plane polynomial/matrix polynomial
$N_q(z)$	Numerator of z-plane polynomial/matrix polynomial
$D_\delta(\gamma)$	Denominator of γ-plane polynomial/matrix polynomial
$N_\delta(\gamma)$	Numerator of γ-plane polynomial/matrix polynomial
$\alpha i,\ \beta i$	Controller coefficients
$a_l\ ;\ b_l$	Plant Coefficients

Chapter 1

1 Introduction:

1.1 Motivation:

A paradigm shift from continuous-time to discrete-time signals and system studies originated during sixties employing the techniques of the shift operator in the time domain analysis and design, while z-transformation in its complex domain counterparts. Despite the fact that most real world physical signals and processes remain continuous in time, but due to certain limitations of continuous-time analysis, synthesis and design tools, there have been rapid proliferation of digital techniques with wide acceptability mainly due to low hardware and software cost and easy implementation. Discrete-time signal processing and discrete-time control popularly known as digital control or sample-data control have emerged out as a separate field of study and offer many conveniences such as:

- Stability of control
- Flexibility
- Lower cost
- Greater reliability and equipment life
- Human factors favouring Digital Interface
- Ease in implementation
- Extremely high accuracy and negligible drift with time
- Standard hardware modules across a wide range of applications
- Ability to self-check
- Greater range of control algorithms
- Digital algorithms are mostly algebraic that avoid calculus

Inspite of the fact that discrete-time signals and systems offer many advantages but, its major drawback is that the resultant signal or system as obtained after sampling of continuous-time counterpart is largely dependent on the selection of sampling frequency. While the choice of Nyquist frequency as the sampling frequency is the minimum requirement to retain the bandwidth in the corresponding discrete-time there is no fixed criteria what shall be the maximum sampling frequency. It largely depends on the intuition of the designer looking into the stability

of the overall systems, implementation issues and availability of the hardwares etc. However, in order to implement a continuous-time system in the corresponding discrete-time it can be institutively assumed that one should take the sampling frequency as large as possible, thereby making sampling time very near to zero. Unfortunately, the traditional shift-operator or z-transformation representation of the discrete-time systems becomes uninformative at fast sampling rates and resultant numerical algorithms become numerically ill-conditioned.

An alternative to the shift operator in time domain called delta operator and gamma transform in place of z-transform has been advocated by Middleton and Goodwin [1],[2] to overcome the above difficulties. Discrete-time signals and systems representation using the above technique not only ensure greater range of stability and numerical conditioning but also allows continuous-time results to be obtained as a special case from the resultant discrete-time system when the sampling period is zero. In recent years, the delta operator has been widely used to many areas in control and signal processing as an alternative to shift operator. The delta operator establishes a special rapprochement between analog and discrete dynamic models and allows for investigating the asymptotic behaviour of discrete time models as the sampling period converges to zero. Moreover, it has certain numerical advantages compared to the shift operator parameterization. It, therefore, provides a unified framework for system studies, where continuous-time results can be achieved from the discrete-time description of the system.

The term delta operator used in this thesis is to model a time domain signal or system in discrete-time and denoted by 'δ' while, the term δ-domain is the corresponding complex transformed domain denoted by the complex variable 'γ'. Therefore, the notation 'δ' is to be used as a time domain operator while the notation 'γ' is to be used as a complex domain operator for the analysis, design and simulation studies presented in this thesis.

1.2 Objective of the thesis:

The aim of the first part of the thesis is to develop a unified framework for representation of dynamic discrete-time systems in the complex delta domain such

that the resultant systems converge to its analog counterparts at fast sampling limit. In the sequel, we utilize the properties of the delta operator to develop the reference model parameters which satisfy the given classical time, frequency and complex domain specifications with a view to employ these reference models for controller design in a model matching framework.

The aim of the second part of the thesis is to develop methods for controller design in the complex delta domain using a variant of time moment in which Genetic algorithms (GA) have been used to optimally select either the real or complex frequency points. The controller design methods developed in the complex delta domain mainly use the transfer function description and are applicable to single-input single-output (SISO), multi-input multi-output systems (MIMO) and system with time delays. All methods included in the thesis are, however, directly applicable even if the original description of the system is given in state-space.

Finally, the third part of the thesis deals with filter design in the complex delta domain for biomedical applications.

1.3 Contribution of the thesis:

The properties of the delta operator are utilized to design reference model system in the complex delta domain denoted by the complex variable γ. The coefficients of this reference model are computed from the given time, frequency and transformed domain specifications so that the overall controlled system match the reference model approximately in a model matching framework. A newly defined set of parameters called the Optimal Generalized Delta Time Moments (OGDTM) is introduced. This OGDTM is a new variant developed from the concept of traditional time moment so far used for continuous-time signals and systems. The discrete-time time moment in the delta domain is called Delta time moment (DTM). A more general version of DTM is Generalised delta time moment (GDTM). The proposed OGDTM is developed by invoking GAs, an artificial intelligence tool to find a set of real frequency points after minimising a scalar cost function. This newly introduced set of parameters i.e. (OGDTM) has been successfully used for controller design in the complex delta domain.

A new method called the optimal frequency fitting (OFF) technique has also been introduced. The proposed OFF selects a set of complex frequency points after

minimising a scalar cost function by using GA. The OFF technique has been successfully applied for controller design of SISO, MIMO and system with time delays. The design method as proposed either using OGDTM or OFF is a comprehensive linear algebraic framework based on approximate model matching and are applicable to systems that are stable / unstable, minimum phase / non-minimum-phase. The proposed design methods as developed in the complex delta domain provide a unified framework for the design of a digital controller which converges to its corresponding analog controller when the sampling time approaches zero. Both of these properties have been well exploited in analysis, design and simulation studies. The concept of delta domain technique has also been used for biomedical signal processing in which design of digital filters has been attempted to remove artifacts of Electrocardiogram (ECG) signals.

In the context of the above, we now include a brief review of the related literature.

1.4 Historical Overview:

In this section, we present a brief historical overview of the evolution of delta operator, time moment, Genetic algorithms and biomedical digital signal processing with a view to its eventual applications in control system design and biomedical digital filter design problems. The discourse is mainly focused on issues that are relevant to this research and is by no means an exhaustive exposition of all the available contributions to these theories. We start with an introduction to the development of delta operator modelling and control followed by a brief discussion on time moment, Genetic algorithms and their present state of the art and application in control system focusing on model matching based controller design methodologies and biomedical filter design applications.

1.4.1 Delta operator :

There have been a large volume of works accumulated since sixties on discrete-time system studies using the shift-operator in time domain and z-transformation in the complex domain [3], [4], [5], [6]. The development of delta operator formulation by Middleton and Goodwin [1] in 1986 makes it possible to understand both continuous-time and discrete-time control and identification theory

within a unified framework, while substantially improving the numerical robustness with respect to the traditional shift-operator representation of discrete-time systems.

The delta operator theory of modelling of discrete-time is based on discrete differential or 'finite difference' operator. The calculus of finite differences has been in use in numerical analysis for several centuries and a good account of it is described in Middleton and Goodwin [7]. Although Gupta [8] in sixties has introduced ξ-transform which is nothing but the complex domain version of the delta operator called γ- domain. Similarly, Neuman C.P. [9] has defined the delta operator as the discrete approximation of the differential operator, the application of which converts all the relationships of sample-data systems to their continuous-time counterparts at the fast sampling limit. However, the actual benefits of it's use in control system analysis and design was fully explored by Middleton and Goodwin [10]. Subsequently, Mukhopadhyay *et. al.* have shown that delta operator formulation is a sub-class of a more general operator called γ-operator [11]. Since its inception, delta operator has been extensively used in controlled system design and implementation. To highlight the important applications of delta operator in systems and control, following areas may be mentioned such as literature on classical and modern control [12-14], predictive control [15], adaptive control [16-17], robust, H_∞ and optimal control [18-28], Linear Quadratic Gaussian (LQG) Control of Networked control [29], signal processing [30 - 42] and identification [43-48] etc.

1.4.2 Time moment:

Time moment, a traditional tool, has been extensively used in the reduced order modelling literatures [49-52]. Time moments are evaluated from a time dependent function about a point by the method of integration. A set of time functions of the high-order system are matched with those of the reduced model and the number of time-moments matched depends on the desired order of the reduced model. In the frequency domain, many variants of the time moments based methods [52] have been reported for control system design and implementation mostly with industrial settings. The classical techniques of control system design for continuous-time systems using frequency response plots of Bode and Nichols, root locus diagrams of Evans or the Nyquist plots are well documented in the literature. The methods are graphical and of a trial-and-error nature and are normally limited to SISO systems. These neo-classical design techniques have been further refined by

Rosenbrock [53], MacFarlane [54], Mayne [55], Hung and Anderson [56] and others [57].

The development of state variable techniques during sixties has witnessed a radical change from the frequency domain to time domain because of its several advantages over the classical transfer function approach. However, state-space design technique requires information about all the states while measuring the output in order to design an elegant controller. This can be achieved either through multitude of sensors or an asymptotic observer. For higher order systems, this mandates an implementation, which is highly complicated. Such sophisticated controllers may be reasonable in aerospace applications but in an industrial setting long-term reliability and economics prevent such sophistication. Optimal control approach requires the solution of higher order nonlinear differential equations and, moreover, it is often difficult to translate industrial specifications into the weighting matrices of the performance index and vice versa.

One of the important aspects of controller design and implementation is the order of the resultant controller and the subsequent hardware complexity. Practicing engineers prefer implementable controllers of low complexity. The problem of designing control systems via model matching approach may be stated as follows: Given a process whose performance is unsatisfactory and a closed-loop reference model having the desired performance, derive a controller such that the performance of the augmented process matches that of the model. Work on controller design for model matching dates back several decades, e.g., the Guillemin-Truxal design procedure yields a controller TF which matches a reference model in a unity-feedback configuration [58]. In sampled-data theory most of the techniques for control system analysis and synthesis were originally developed for continuous-time systems and were subsequently converted to or adopted for discrete-time systems. Problems of sample-rate selection, quantization effects, frequency warping, computational time-delay etc. that are particular to digital control systems have been addressed in Tzafestas [59]. The other problems in the implementation of digital controllers due to finite speed memory limitations, acquisition and processing time-delay are summed up in Hanselmann [60].

Design of digital controllers employing the technique of frequency response matching has been of interest of several investigators. Rattan et al. [61] has exhibited

a design technique in which frequency response of the closed-loop system was matched with that of a reference model. The method required the evaluation of complex integrals and the final design and stability of the system were sensitive to the chosen frequency band [62]. Shieh et al. [63] has presented a method in which the discrete open-loop frequency response was matched at a number of important frequency points known as the dominant data set. The controller transfer function coefficients were obtained as a solution of a set of non-linear equations based on the dominant data set. In the method of Shi and Gibbard [63] a discrete transfer function was selected as the reference model from which an equivalent open-loop transfer function was obtained. The controller parameters were obtained such that the frequency response of the discrete open-loop system matches that of the discrete open-loop reference model. A constrained minimization technique involving a simplex algorithm was employed to restrict the poles and zeros of the controllers to desirable regions in the unit circle disc.

Janiszowski [64] proposed controller algorithms for minimizing a quadratic performance index by appropriate weighting of controller outputs and errors. Zafiriou and Morari [65] provided a review of several digital control algorithms. A rule based algorithm has been suggested for the design of controllers which is applicable for large sampling times and the resultant system is free from inter sample ripples. A design method has been proposed by Houpis [66] where a sampled-data system is approximated by a pseudo-continuous-time (PCT) control system. This approach is a valuable technique when the sampling time is small. Whitbeck and Hofmann [67] have detailed the analogies between system formulations in the s and w' domains. It is established that direct digital control (DDC) law synthesis in the w' domain is a viable and practical alternative to design by emulation of a continuous system. A comprehensive and computationally simple DDC design technique has been given by Knowles [68]. A digital controller design method based on series expansion of the pulse transfer function has been proposed by Inooka et al. [69]. Inooka has extended his series expansion method for the design of double loop systems [70]. This method leads to a controller of higher order. Another technique based on the minimization of output error has been proposed by Porat and Friedlander [71]. This leads to a non-linear problem and the calculation of the parameters involves non-linear computational techniques. This drawback has been removed by Obinata et al. [72] by

minimizing an equation error of the closed-loop system. Forsythe [73, 74] has proposed a simple design method based on Taylor series expansion technique. Design techniques for exact and approximate model matching have been proposed in Kucera et al. [75] and Pal [76] among many others for continuous-time systems.

In the recent literature on delta operator modelling and control, Young et al. [12], have promoted the concepts of true digital control (TDC), which rejects the idea that a digital control system should be initially designed in continuous-time terms. Rather it was suggested that the designer should consider the design from a digital-sample data standpoint, even when rapidly sampled, near continuous time operation is required. The design of simple but powerful digital controllers for rapidly sampled system that can function in a near continuous-time fashion is one particular aspect of the general TDC approach which can be achieved using delta operator modelling of discrete-time systems. The explicit methods for proportional plus integral control of the delta operator systems are the outcome of such a strategy. Based on delta representation, Collins et al. [77] have derived a set of discrete-time H_∞ design equations. Erwin et al. [18], [19] have addressed the H2 and mixed H2/ H∞ controller synthesis problems, while Katab et.al. [78], have worked on robust stability. Suchomski [23] designed robust PI & PID controller using delta operator. In the area of generalized predictive control, the works of Lauritsen et al. [15] are worth mentioning. Works on adaptive control of delta operator systems are also reported by Masaru et al. [17]. Tadjine et al. [20] and Linbo et al. [29] have reformulated LQG/LTR control design by using delta operator. The problems of robust stability for linear time varying uncertain systems were investigated by Alexander et. al. [79] and Kai-yu Wu [26]. Hui-Guang Li et al. [24] has derived Robot based optimal control law. In this direction the work of Bengt Lennartson [25] on low order sampled data H_∞ control using delta operator and LMIs is worth mentioning. Wang Qing et al. [27] have described the delta operator based system with external disturbances. They have discussed the robust stabilization problem and H_∞ control problem based on the conception of quadratic stability and quadratic stabilization by applying linear matrix inequality method to design robust stabilizers, and robust H_∞ controllers. Qiu Jiqing et al. [28] investigated the problem of state feedback control for a class of time-delay systems with linear factional uncertainties using delta operator. Linbo Xie et al. [29] have addressed the stochastic control problem of networked control systems. They

designed networked control system for state feedback and output feedback control laws in delta operator by using a dynamic programming approach.

Modern control system design techniques like Linear Quadratic Gaussian (LQG) synthesis and H_∞ robust optimal control law normally result in higher order controllers that are difficult to use for simulation, analysis and controller synthesis and the complexity of such controllers makes practical implementation very difficult as well as uneconomical specially for industrial process control. On the other hand, need also exists for a design method to provide simple low order implementable controllers that can adequately control plants or processes regardless of their complexity or order.

Design techniques for exact and approximate model matching have been proposed in Kucera et al. [75] and Pal [76] among many others for continuous-time and discrete time systems. A unified controller design method in the complex delta domain is proposed by Sarkar et al [13-14] which is a sub-class of Pade' approximation technique, where the concept of time moments is developed in the delta domain namely - D elta Time Moments taking successive derivative of the function and evaluating their values about zero.

In the present work, classical control design methods in the complex delta domain using the concept of model matching in the Truxal framework is attempted. These controller design techniques involve designing a controller to compensate a given plant in the complex delta domain, so that the controlled system follows the reference model. The reference model structure, which satisfies the classical time, frequency and complex domain specifications in the complex delta domain, is developed. Discrete-time modelling of the control systems in complex delta domain and development of low order controller based on performance specifications are the main objective of the work undertaken. Two methods are developed to design controllers in the frequency domain i.e. Optimal Generalised Delta Time Moments (OGDTMs) and Optimal frequency fitting (OFF). These methods are applied to design rational, discrete-time controller for single-input, single-output (SISO), multi-input, multi-output (MIMO) systems and system with time delay.

1.4.3 Genetic algorithms:

Now a days genetic algorithms (GA) [80],[81] have been in wide use in many applications in systems and control studies to produce a global optimal

solution. GA accommodates all facets of soft computing, namely, uncertainty, imperfection, non-linearity and robustness. It can handle all search spaces, including non-smooth, multimodal and discontinuous spaces. GA works with a coding of the parameters set with finite length string of an optimisation problem. The traditional practice is to use binary bit strings, but it can also take real or integer string. It searches from a population of strings (chromosomes) made up of sub strings (encoded elements of parameter set). It uses the objective or fitness function to achieve the desired solution. It typically employs three operations, namely selection, recombination and mutation. Each of this operation is applied to the population once per generation, and several generations are required to achieve satisfactory results.

There have been a good number of applications of GA reported in control system design and implementation in recent time. Versak et al. [82] have used GA for auto tuning of inverted pendulum systems and experimentally verified the result against given robustness margin and reliability. In the work of Porter et.al [83],[84], an unconstrained digital PID controller was taken up to design a model following flight control system for F-16 aircraft. Jones et al. [85] have proposed GA as a means of auto tuning PID controller. The technique involves firstly using online data and the genetic algorithms to identify a model of the process. Then the identified model, the genetic algorithm and simulation methods are used to offline tune the PID controller so as to minimize a time domain based cost function. Genetic algorithms for H_2/H_∞ optimum PID control have been proposed by Chen et al. [86] for robust performance design for systems under parameter perturbation and uncertain disturbance. Jones et al. [87] have employed on-line frequency domain identification scheme for auto tuning of PID controller to provide prescribed gain and phase margin. While Kundu et al. [88] have used GA for optimal feedback controller design. The application of genetic algorithms for gain scheduling controls has been reported by Gray et al. [89] in which GA is used to optimised the activation point of the individual controllers. An exhaustive search to establish the optimum number controller coupled with optimization of the corresponding activation point by GA shows the relationship between controller performance and complexity. Application of GA for controller design in power system has been reported by Reformat et al. [90] in which a new method of designing control system which relies on a combination of advanced system simulator and genetic computations. The combination of electromagnetic

transients program and genetic algorithms resulted in a tool for optimal control design in the area of power system. Output feed back controller design is a difficult area when the system models are in transfer matrix form. Badran et al. [91] has proposed an optimal output feed back method using GA. C_{AO} et al. [92] have used GA for optimisation of control parameter using a stochastic approach. In the latest works on controllers based on GA, Nasri et al. [93] has also addressed on application of PID control for brushless DC motor. Design of fractional order controller is a relatively challenging area in system theory with emerging application areas in nano technology and micro electromechanical systems. GA applications have also been reported in fractional PID controller design by Arman Kiani et al. [94]. Optimization of decentralized PI/PID controller based on genetic algorithm has been reported Li et al. [95]. Mohsan Sayed has used GA in designing Optimal PID Controller with genetic algorithms in view of controller location in the plant [96].

1.4.4 Biomedical signal processing:

In the literature on signal processing, Markku et al. [31],[33] has demonstrated that delta operator has superior roundoff noise performance leads to significantly lower implementation complexity and up to 50% savings in hardware. Tenali Harju et al. [32] has shown that the digital filters that use the delta operator are less sensitive to filter coefficient quantization than filters using the shift operator when the poles and zeroes lie near the point $z = \pm 1$ and through other fixed-point neighbours of the floating point coefficients besides the one obtained by direct rounding is very likely to yield better sets of coefficients in terms of magnitude response characteristics. Juha Kauraniemi et al. [37-38] have worked on efficient direct form structures and shown that excellent roundoff noise performance is achieved at the cost of only a minor additional implementation complexity when compared with the corresponding delay realization. They have also performed detailed analysis of the computationally efficient transposed direct form-II delta structure focusing on the roundoff noise minimization in fixed-point implementations. Bauer et al. [97] addressed the zero input behaviour of digital filters in delta operator representation. Qiang Li [98] has studied the properties of information matrices of the delta operator-based algorithms for adaptive signal processing. Hong Shim [99] has studied the design of Kalman filter with the singularly perturbation technique using the delta operator approach. Ngai Wong et al. [100] addressed the problem of optimization of the free parameter of

the delta operator, with scaling of the structure to prevent arithmetic overflow with modified direct form-II second-order section in which the Δs and filter coefficients at different branches are separately scaled to achieve improved roundoff noise gain minimization. The work of Mehmet Hendekli et al. [101] on a multi channel form of the two-dimensional delta domain lattice filter is worth mentioning. Newman and Holmes [102] have presented a practical overview describing the use of the delta operator for IIR digital filters, and shown how the operator can be used in power electronic inverter applications to achieve substantial performance benefit compared to equivalent shift-based implementations. The design methods of Hao Liu [103] employ LMI approach for guaranteed cost filtering of delta operator polytype uncertain linear systems with time delay.

Tompkin [104] and Rangayan [105] have extensively studied the biomedical signal processing and illustrated results of different type digital filters used for biomedical signal processing. Mc Sharry et al. [106] have presented a dynamical model based on three coupled ordinary differential equations which is capable of generating realistic synthetic electrocardiogram (ECG) signals specifying the mean and standard deviation of the heart rate and the morphology of the PQRST cycle to access biomedical signal processing techniques which are used to compute clinical statistics from the ECG. Ramli et al. [107] have investigated the use of signal analysis technique to extract the important features from the 12 lead ECG signal using the cross-correlation analysis technique. Ju-Won Lee et al. [108] have designed optimal adaptive filter with a dynamic structure which can adjust the filter coefficient and produce a suitable order in different environments for ECG signals. Sameni et al. [109] proposed a nonlinear Bayesian filtering framework for the filtering of single channel noisy ECG recordings. Garcés Correa et al. [110] have proposed a cascade of three adaptive filters based on a least mean squares (LMS) algorithm, the first one eliminates line interference, the second adaptive filter removes the ECG artifacts and the last one cancels EOG spikes. Each stage uses a finite impulse response (FIR) filter, which adjusts its coefficients to produce an output similar to the artifacts present in the signals obtained.

From the above literature survey it is established that modelling, control and biomedical signal processing of dynamical systems in the complex delta domain are an important area in the system theory where a lot of scope is there for investigation.

1.5 Modelling of discrete-time systems using delta operator

In this section we discuss some aspects of linear discrete-time modelling using delta operator and its transform domain complex variable γ. We look into how discrete-time models can be derived by sampling of continuous-time systems and how input-output descriptions relate to state-space models. We consider both the discrete-time domain and transformed domain representations using delta operator and complex domain gamma transform. In conventional shift-operator representations of discrete-time systems, it is not possible to develop dynamic systems models which can support very high sampling rates. Further, such representations do not converge to its continuous-time counterparts. Therefore, in discrete-time representations it is not possible to implement a continuous-time system by making sampling period near to zero or sampling frequency very high. To avoid such difficulties, delta operator can be used for modelling signals and systems. These delta operator representations show a close agreement to continuous-time representations, and as a matter of fact, they meet to the expected continuous-time equivalents as the sampling period tend to zero.

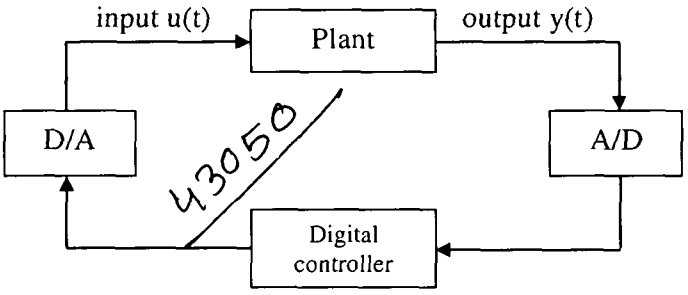

Figure 1.1: Digital control of a continuous time plant

1.6 Sampled-data systems

The use of digital computers in implementation of control systems has become very widespread. The discrete nature of digital computers makes it convenient to use discrete-time models of the controlled systems whereas the process itself evolves in continuous time. Let us consider a sampled data system with input $u(k\Delta)$, where Δ is the sampling period and k is an indexing discrete-time parameter, which is processed by a digital to analog (D/A) converter to give the continuous-time input $u(t)$. Usually, the D/A-converter is designed in such a way, that the value of $u(t)$ is held constant between samples, known as zero-order hold (ZOH). The continuous-time output $y(t)$

is then sampled with a period Δ using an analog to digital (A/D) converter to give the sampled output $y(k\Delta)$. A typical scheme is shown in Figure 1.1. In practice one must prefilter the continuous-time output to avoid aliasing problems. The prefilter should be of low-pass nature with a break frequency around the Nyquist-frequency π/Δ . In the following we will neglect the effect of this pre-filter.

The notation *'t'* used in this thesis as the independent time-variable in both continuous-time and in discrete-time. In discrete-time, the independent variable *'t'* can only assume values, that are multiples of the sampling period Δ, i.e. $t = k\Delta$. Wherever required specifically, the notation $t = k\Delta$ is also used for discrete-time. The distinction should be clear from the context. The class of system under consideration in this thesis is limited to linear finite-dimensional time-invariant systems. When working with digital control systems it is convenient to find an equivalent discrete-time description of the composite system consisting of D/A-converter, continuous-time system and A/D converter, i.e. to find a direct relation between the sampled signals $u(k\Delta)$ and $y(k\Delta)$ as illustrated in Figure 1.1. In this thesis, we consider the case of deterministic systems only.

1.6.1 Sampling of continuous-time systems

Let us consider a linear continuous time SISO model represented by state and output equations

$$\begin{aligned} \frac{dx(t)}{dt} &= \boldsymbol{A}_c\, x(t) + \boldsymbol{B}_c\, u(t) \\ y(t) &= \boldsymbol{C}_c x(t) + D_c u(t) \end{aligned} \tag{1.1}$$

Where $x \in \Re^n$ is the state, $u \in \Re^m$ is the control input, $y \in \Re^p$ is the output variable and $\boldsymbol{A}_c, \boldsymbol{B}_c, \boldsymbol{C}_c, D_c$ are normal notations of state space representation. An equivalent complex s-domain transfer matrix representation is of the form

$$G_c(s) = \boldsymbol{C}_c(s\boldsymbol{I} - \boldsymbol{A}_c)^{-1}\boldsymbol{B}_c + D_c \tag{1.2}$$

For the sake of clarity, it is suitable to introduce the realization set S_c noted as

$$S_c \overset{def}{=} \left\{ (\boldsymbol{A}_c, \boldsymbol{B}_c, \boldsymbol{C}_c, D_c) : \quad G_c(s) = \boldsymbol{C}_c(s\boldsymbol{I} - \boldsymbol{A}_c)^{-1}\boldsymbol{B}_c + D_c \right\} \tag{1.3}$$

Where, $G_c(s)$ is the transfer function matrix. Then,

$$Y(s) = \left\{C_c (sI - A_c)^{-1} B_c + D_c \right\} U(s)$$

$$Y(s) = \left\{C_c \frac{adj(sI - A_c)}{det(sI - A_c)} B_c + D_c \right\} U(s) \qquad (1\ 4)$$

where I is the identity matrix of appropriate dimension and adj (·) is the adjoint matrix. $Y(s)$ and $U(s)$ are the Laplace transforms of the input and output signal vectors and

$$D_c(s) = det(sI - A_c) \qquad (1.5)$$

$$N_c(s) = C_c\, adj(sI - A_c) B_c \qquad (1.6)$$

where in general $N_c(s)$ is numerator polynomial matrix and $D_c(s)$ is a n^{th} order denominator polynomial. For strictly proper rational systems, the degree of denominator polynomial and numerator polynomial are

$$deg\ D_c(s) = n$$
$$deg\ N_c(s) = m \leq n - 1$$

We now consider sampling with a zero-order hold, i.e. the input signal is held constant between the sampling instants. This is commonly done in digital control and is easily implemented by using a D/A converter, which latches the signal between the sampling instants. Given a state value x(kΔ) at some sampling time t = kΔ, where k is an integer, the states can be computed for t ≥ kΔ from the exact solution of eqn (1.1) given as [10],

$$x(t) = e^{A_c(t-k\Delta)} x(k\Delta) + \int_{k\Delta}^{t} e^{A_c(k\Delta-\tau)} B_c\, u(\tau)\, d\tau \qquad (1.7)$$

where $$e^{A_c t} = I + A_c t + \frac{1}{2!}(A_c t)^2 + \frac{1}{3!}(A_c t)^3 + ...$$

and $$\frac{d}{dt} e^{A_c t} = A_c e^{A_c t} = e^{A_c t} A_c$$

where we have assumed right continuity of the control signal. Hence, at the next sampling instant the state is given by

$$\begin{aligned} x((k+1)\Delta) &= e^{A_c\Delta} x(k\Delta) + \left[\int_{k\Delta}^{(k+1)\Delta} e^{A_c((k+1)\Delta-\tau)} B_c\, d\tau \right] u(k\Delta) \\ &= e^{A_c\Delta} x(k\Delta) + \int_{0}^{\Delta} e^{A_c(\Delta-\tau)} B_c\, u(k\Delta)\, d\tau \end{aligned} \qquad (1.8)$$

from this we have a discrete-time state-space description as

$$\begin{aligned} q\, x(t) &= A_q x(t) + B_q u(t) \\ y(t) &= C_q x(t) + D_q u(t) \end{aligned} \qquad (1.9)$$

where $$A_q = e^{A_c \Delta} = \sum_{k=0}^{\infty} \frac{(A_c \Delta)^k}{k!}$$

$$\begin{aligned} B_q &= \int_0^{\Delta} e^{A_c(\Delta-\tau)} B_c \, d\tau \\ &= A_c^{-1}[e^{A_c \Delta} - I] \text{ if } A_c \text{ is nonsingular} \\ C_q &= C_c \\ D_q &= D_c \end{aligned} \tag{1.10}$$

and t is a multiple of the sampling period Δ such that $k\Delta \le t < (k+1)\Delta$ [10]. The operator q is called the forward shift operator, that is, qx(kΔ) = x((k+1)Δ). It is interesting to observe that if the actual continuous-time signal *u(t)* is in fact constant between the sampling instants then the sampling involves no approximation. In this case, the difference equation (1.8) gives the exact value of the state and the output at the sampling instants.

We now investigate more closely the limiting properties of the discrete-time shift operator state-space model in eqn.(1.8). As the sampling period tends to zero, the limit values of the system matrices follow from eqn.(1.9)

$$\lim_{\Delta \to 0} A_q = I \tag{1.11}$$

$$\lim_{\Delta \to 0} B_q = 0 \tag{1.12}$$

The above results show that the shift-operator model is unstable at very high sampling frequencies. At very high sampling frequencies the sample periods are very small, and therefore there is no appreciable change in the successive samples of state, that is $x(t + \Delta) \approx x(t)$. The effect of the input from one sample to the next will also cease at fast sampling rate. In the complex z-domain, an equivalent z transfer matrix realization set are

$$S_q \overset{def}{=} \left\{ (A_q, B_q, C_q, D_q) : \quad G_q(z) = C_q(zI - A_q)^{-1} B_q + D_q \right\} \tag{1.13}$$

where $G_q(z)$ is the z- transfer function matrix. Then,

$$\begin{aligned} Y(z) &= \left\{ C_q (zI - A_q)^{-1} B_q + D_q \right\} U(z) \\ Y(z) &= \left\{ C_q \frac{adj(zI - A_q)}{det(zI - A_q)} B_q + D_q \right\} U(z) \end{aligned} \tag{1.14}$$

where $\boldsymbol{I}$ is the unity matrix of appropriate dimension, $adj(\cdot)$ is the adjoint matrix and Y(z) and U(z) are the z-transforms of input and output signal vectors. Also,

$$D_q(z) = det(z\boldsymbol{I} - \boldsymbol{A}_q) \tag{1.15}$$

$$N_q(z) = \boldsymbol{C}_q\, adj(z\boldsymbol{I} - \boldsymbol{A}_q)\boldsymbol{B}_q \tag{1.16}$$

where in general $N_q(z)$ is a polynomial matrix and $D_q(z)$ is an n^{th} order polynomial. For proper rational systems, the degree of denominator polynomial and numerator polynomial are

$$deg\ D_q(z) = n$$

$$deg\ N_q(z) = m \leq n - 1$$

In the limit of high sampling rate, the transfer matrix representation in the z-domain follow from eqns.(1.11) and (1.12) :

$$\lim_{\Delta \to 0} G_q(z) = 0 \tag{1.17}$$

It is easy to see that the transfer matrix representation in the z-domain is uninformative at very high sampling rate.

1.7 Delta operator parameterization

We discuss here an alternative formulation of discrete-time systems, the so called delta operator parameterization. One of the most important work on such parameterization is due to Middleton and Goodwin [10], where the following points of motivation for this alternative discrete-time operator are given:

- It highlights the similarities between discrete-time and continuous-time systems. This allows physical continuous-time insights in the discrete-time case.
- It allows a unified system theory in which discrete-time and continuous-time results can be derived simultaneously.
- Most continuous-time results can be obtained as a limiting case (when the sampling period tends to zero) of the discrete-time results.

- It is possible to use short sampling periods without incurring numerical difficulties such as a high sensitivity to round-off errors in coefficient representation.
- The coefficients of the discrete-time transfer function are similar to the continuous-time and it becomes easier to tune controller parameters for improved dynamic performance.
- The frequency and transient responses of the continuous-time system can be accurately estimated from the discretized system.
- It offers substantial numerical advantages at high sampling rates.

1.7.1 Definition

The delta operator is defined in the time-domain as

$$\delta = \frac{q-1}{\Delta} \tag{1.18}$$

where Δ is the sampling period and q is the forward shift operator. Operating δ on a differentialable signal $x(t)$ gives

$$\delta x(t) = \frac{x(t+\Delta) - x(t)}{\Delta} \tag{1.19}$$

In the limiting case we can see that

$$\lim_{\Delta \to 0} \delta x(t) = \frac{d}{dt} x(t) \tag{1.20}$$

which demonstrates the close relationship between the discrete-time delta operator and the continuous-time differential operator $\frac{d}{dt}$ at high sampling rates. It is to be noted that equation (1.18) is a simple linear transformation and thus system modeling using delta operator parameterization offers exactly the same flexibility as q-operator parameterization, i.e. the class of describable systems is not changed. Similar relation exists in the complex domain as well. The delta transform operator γ is defined as

$$\gamma = \frac{z-1}{\Delta} \tag{1.21}$$

where z is the complex domain transform operator for discrete-time system, like the Laplace transform operator for continuous-time system. Since eqn.(1.21) is a linear

transform relation which and scales the complex z-domain by $(\frac{1}{\Delta})$ and shifts the origin by $(-\frac{1}{\Delta})$ to the complex delta domain in γ-plane, therefore all the linear system properties and representations of the complex z-domain can be transformed to the delta domain with equal flexibility as offered by the z-domain.

1.7.2 State space representation

Using the delta operator, the discrete-time representation of the shift operator (q) model is given by

$$\begin{aligned} \delta x(t) &= \boldsymbol{A}_\delta x(t) + \boldsymbol{B}_\delta u(t) \\ y(t) &= \boldsymbol{C}_\delta x(t) + D_\delta u(t) \end{aligned} \tag{1.22}$$

where $$\delta x(t) = \begin{cases} \dfrac{x(t+\Delta) - x(t)}{\Delta} & : \ \Delta \neq 0 \\ \dfrac{dx(t)}{dt} & : \ \Delta = 0 \end{cases}$$

$$\boldsymbol{A}_\delta = \frac{\boldsymbol{A}_q - \boldsymbol{I}}{\Delta}$$

$$\boldsymbol{B}_\delta = \frac{\boldsymbol{B}_q}{\Delta}$$

The connection between the delta operator (δ) state-space representation to that of the shift operator (q) follows directly by inspection

$$\boldsymbol{A}_q = \boldsymbol{I} + \Delta \boldsymbol{A}_\delta \tag{1.23}$$

$$\boldsymbol{B}_q = \Delta \boldsymbol{B}_\delta \tag{1.24}$$

$$\boldsymbol{C}_q = \boldsymbol{C}_\delta \tag{1.25}$$

$$\boldsymbol{D}_q = \boldsymbol{D}_\delta \tag{1.26}$$

The above equations (1.24 -1.26) provide a direct connection between the state-space matrices of the q-operator and the delta operator. Although this is mathematically correct, it is not advisable to determine the delta operator realization in this way as the poor numerical properties of the q-operator representation, especially at fast sampling rates, is then carried over to the delta operator. A better procedure is to directly derive the delta operator matrices as suggested in [10].

$$\boldsymbol{A}_\delta = \Omega \boldsymbol{A}_c$$

$$\boldsymbol{B}_\delta = \Omega \boldsymbol{B}_c$$

$$\boldsymbol{C}_\delta = \boldsymbol{C}_c \qquad (1.27)$$

$$\boldsymbol{D}_\delta = \boldsymbol{D}_c$$

where $\boldsymbol{A}_c$ and $\boldsymbol{B}_c$ are continuous-time matrices and

$$\Omega = \frac{1}{\Delta}\int_0^{\Delta} e^{A_c \tau}\, d\tau$$

$$= I + \frac{\boldsymbol{A}_c \Delta}{2!} + \frac{\boldsymbol{A}_c^2 \Delta}{3!} + \ldots\ldots \qquad (1.28)$$

The δ-operator representations result in more reasonable limiting properties of the discrete-time. We have from eqns.(1.27) and (1.28)

$$\lim_{\Delta \to 0} \boldsymbol{A}_\delta = \boldsymbol{A}_c \qquad (1.29)$$

$$\lim_{\Delta \to 0} \boldsymbol{B}_\delta = \boldsymbol{B}_c \qquad (1.30)$$

The results above show that the continuous-time state-space matrices are recovered as a limit case at high sampling rate.

1.7.3 Transfer function representation

For continuous-time systems we have the complex domain Laplace transform variable s, which is closely related to the derivative operator d/dt and for discrete time systems, the complex domain transform variable z is associated with the forward shift operator q. Similarly the complex variable γ is associated with the forward difference operator δ by the relation called delta transformation. The delta transform of the discrete signal $f(t)$ in the complex δ-domain is defined by [10]

$$F_\delta(\gamma) = S_0^{\infty} f(t)\, E(\gamma, -t) \qquad (1.31)$$

where the generalized integration operator S is defined as:

$$S_{t_1}^{t_2} f(t)\, d\tau \cong \begin{cases} \int_{t_1}^{t_2} f(\tau)\, d\tau & : \Delta = 0 \\ \Delta \sum_{k=\frac{t_1}{\Delta}}^{k=\frac{t_2}{\Delta}-1} f(k\Delta) & : \Delta \neq 0 \end{cases}$$

and
$$E(\gamma,-t) \cong \begin{cases} e^{-\gamma t} & : \Delta = 0 \\ (1+\Delta\gamma)^{\frac{-t}{\Delta}} & : \Delta \neq 0 \end{cases} \tag{1.32}$$

In the continuous time i.e. when $\Delta = 0$, the delta transform defined above converges to the Laplace transform (with s replaced by γ). In discrete time, the delta transform defined above is related to z-transform as follows:

$$F_\delta(\gamma) = \Delta F_q(z)\Big|_{z=1+\gamma\Delta} = \Delta \sum_{k=0}^{\infty} f(k\Delta)(1+\Delta\gamma)^{-k} \tag{1.33}$$

where k is the indexing discrete-time parameter and $t = k\Delta$ are discrete time instants for $k \in [0,\infty]$.

Therefore, for zero initial conditions, operating on a function by delta operator is equivalent to multiplying the function's transform by γ. By operating on delta operator state space model in eqn. (1.22), we obtain the δ-transfer matrix representation as :

$$G_\delta(\gamma) = \boldsymbol{C}_\delta(\gamma \boldsymbol{I} - \boldsymbol{A}_\delta)^{-1}\boldsymbol{B}_\delta \tag{1.34}$$

where $G_\delta(\gamma)$ is the transfer function matrix in the delta domain. If $Y(\gamma)$ and $U(\gamma)$ are the delta transform of input and output signal vectors,

$$\begin{aligned} Y(\gamma) &= \left\{\boldsymbol{C}_\delta\,(\gamma \boldsymbol{I} - \boldsymbol{A}_\delta)^{-1}\,\boldsymbol{B}_\delta + D_\delta\right\}U(\gamma) \\ Y(\gamma) &= \left\{\boldsymbol{C}_\delta \frac{adj(\gamma \boldsymbol{I} - \boldsymbol{A}_\delta)}{det(\gamma \boldsymbol{I} - \boldsymbol{A}_\delta)}\boldsymbol{B}_\delta + D_\delta\right\}U(\gamma) \end{aligned} \tag{1.35}$$

where $\boldsymbol{I}$ is the unity matrix of appropriate dimension and $adj\,(\cdot)$ is the adjoint matrix from where we identify

$$D_\delta(\gamma) = det(\gamma \boldsymbol{I} - \boldsymbol{A}_\delta) \tag{1.36}$$

$$N_\delta(\gamma) = \boldsymbol{C}_\delta\, adj(\gamma \boldsymbol{I} - \boldsymbol{A}_\delta)\boldsymbol{B}_\delta \tag{1.37}$$

where in general $N_\delta(\gamma)$ is a polynomial matrix and $D_\delta(\gamma)$ is an n^{th} order polynomial. For proper rational systems, the degree of denominator polynomial and numerator polynomial matrix are

$$deg\ D_\delta(\gamma) = n$$

$$deg\ N_\delta(\gamma) = m \leq n - 1$$

When the sampling period decreases and approaches near to zero, the resulting complex domain delta transfer matrix converges to the corresponding continuous-time transfer matrix model. This follow from eqns. (1.29) and (1.30)

$$\lim_{\Delta \to 0} G_{\delta}(\gamma) = G_{c}(s) \tag{1.38}$$

This emphasizes the relationship between continuous-time descriptions and delta operator descriptions. For small sampling intervals, the continuous-time parameters can be recovered from the discrete-time δ-description. Similar relationships between the transfer function polynomial coefficients parameters in continuous and discrete-time do not exist for description in the z-domain.

1.7.4 Poles and zeros of sampled systems

We consider here the pole and zero locations of a sampled transfer function. Considering the continuous-time system

$$G_{c}(s) = \frac{N_{c}(s)}{D_{c}(s)} = K \frac{\prod_{i=1}^{m}(s - z_{i})}{\prod_{i=1}^{n}(s - p_{i})} \tag{1.39}$$

where z_i and p_i denote the zeros and poles of the transfer function, respectively, and $n > m$. The input and output signals of the system are now sampled directly with a zero order hold to give both delta domain and z-domain descriptions.

1.7.5 Pole locations

In the z-domain the poles of the sampled transfer function are obtained by mapping of the continuous-time poles [10]

$$p_{q,i} = e^{p_i \Delta}, \qquad i = 1, \cdots, n$$

It can be seen that at fast sampling,

$$\lim_{\Delta \to 0} p_{q,i} = 1, \qquad i = 1, \cdots, n$$

That is, at fast sampling, the poles of the z-domain representation cluster around the point (1, 0) in the complex plane. It seems reasonable, that a much better numerical precision could be obtained by shifting the origin from (1, 0) to (0, 0) in the complex plane. This is exactly what is achieved by using the variable γ. In delta domain, the poles become [10]

$$p_{\delta,i} = \frac{e^{p_i \Delta} - 1}{\Delta}, \qquad i = 1, \cdots\cdots, n \tag{1.40}$$

and the continuous-time poles are recovered in the limit as $\Delta \rightarrow 0$

$$\lim_{\Delta \to 0} p_{\delta,i} = p_i, \qquad i = 1, \cdots\cdots, n$$

1.7.6 Zero locations

The zero locations of the sampled system, in general can not be determined by a simple mapping of the continuous-time zeros.[10] In addition, some extra zeros are introduced by the sampling process if the relative degree of the continuous time transfer function is greater than 1. This follows from the fact that the orders of $N_\delta(\gamma)$ and $N_q(z)$, in general, are $n-1$, while the order of $N_c(s)$ is m. It is possible to divide the zeros of the sampled system into two categories; zeros that originate from the continuous-time zeros and that introduced by the sampling process. The later category is referred to as sampling zeros. In the z-domain we may write, as $\Delta \rightarrow 0$

$$N_q(z) = K(z - 1)^m N_{q,\, n-m}(z)$$

where $N_{q,n-m}(z)$ is a polynomial of degree $n - m - 1$. The sampling zeros can be found as the zeros of $N_{q,\, n-m}(z)$. Note that these zeros depend only on the relative degree of the continuous-time transfer function. As shown in [111], the zeros of $N_{q,n-m}(z)$ are located at fixed locations in the left half plane. At least one zero of $N_{q,\, n-m}$ will be non-minimum phase (outside the unit circle) if the relative degree of the continuous-time system is greater than 2, i.e. $n - m > 2$. Hence, with sufficiently fast sampling, the sampled transfer function will be non-minimum phase if $n - m > 2$ even if the continuous-time system is minimum-phase. This is a highly undesirable discrepancy between the continuous-time and the sampled system descriptions. The remaining m zeros, which can be thought of as mapped continuous-time zeros, will tend to 1 as $e^{z_i \Delta}$. The result in the delta domain can be obtained by transforming the q-domain results. It can be shown that if

$$N_\delta(\gamma) = K \prod_{i=1}^{n-1} (\gamma - z_{\delta,i}) \tag{1.41}$$

then $$\lim_{\Delta \to 0} z_{\delta,i} = z_i, \qquad i = 1, \cdots\cdots, m$$

and $$\lim_{\Delta\to 0}\prod_{i=m+1}^{n-1}(\gamma - z_{\delta,i}) = N_{\delta,n-m}(\gamma) \qquad (1.42)$$

where $N_{\delta\, n\text{-}m}(\gamma) = N_{q,n\text{-}m}(1 + \Delta\gamma)$ is a polynomial of degree (n - m - 1). Again the limiting sampling zeros are found as the zeros of a fixed polynomial $N_{\delta,n\text{-}m}(\gamma)$ and at least one zero gives non-minimum-phase if n - m > 2. Moreover

$$\lim_{\Delta\to 0} z_{\delta,i} = -\infty, \qquad i = m = 1, \cdots\cdots, n-1$$

The mapped continuous-time zeros are recovered from the discrete-time description. The sampling zeros are associated with highest order terms of the numerator polynomial $N_\delta(\gamma)$. As mentioned, this opens a possibility of discarding these higher order terms in control system then the design will not fail because of the presence of non-minimum phase zeros introduced by the sampling process [10]. A more detailed analysis of this property of delta domain parameterization can be found in [112].

1.8 Mapping between s-domain and delta domain

Analysis and design of continuous-time control system relies upon the pole-zero configurations in the *s*-plane. Similarly, the locations of the poles and zeros of discrete delta transfer function determine the response of the discrete-time system at the sampling instants. In parallel with the mapping of the *s*-plane into the *z*-plane, we highlight the mapping of the *s*-plane into the γ-plane (delta domain) by using the delta transformation.

We divide the *s*-plane ($s = \delta + j\omega$) into an infinite number of parallel periodic strips. The primary strip extends from $\omega = \frac{-\omega_s}{2}$ to $\omega = \frac{+\omega_s}{2}$, where $\omega_s = \frac{2\pi}{\Delta}$ is the radian sampling frequency. The complementary strips extend from $\omega = \frac{-\omega_s}{2}$ to $\omega = \frac{-3\omega_s}{2}$, $\omega = \frac{-3\omega_s}{2}$ to $\omega = \frac{-5\omega_s}{2}$ for negative frequencies and from $\omega = \frac{\omega_s}{2}$ to $\omega = \frac{3\omega_s}{2}$, $\omega = \frac{3\omega_s}{2}$ to $\omega = \frac{5\omega_s}{2}$ for positive frequencies etc.

The primary strip in the left half of the analog s-plane is mapped into the sampling disc in the γ-plane by the appropriate transformation. The poles in the *s*-

plane are mapped into the γ-plane by eqn.(1.40) above. Since, for n = -2, -1, 1, 2, all the complementary strips in the left half of the s-plane are also mapped into the same sampling circle in the γ-plane. All points in the left half of the s-plane are mapped into the interior of the sampling circle in the γ-plane. All points along the imaginary axis of the s-plane are mapped onto the sampling circle in the γ-plane. All points in the right-half of the s-plane are mapped into the exterior of the sampling circle in the γ-plane. In the fast sampling limit, the sampling circle opens to envelop the entire left of the s-plane.[113]

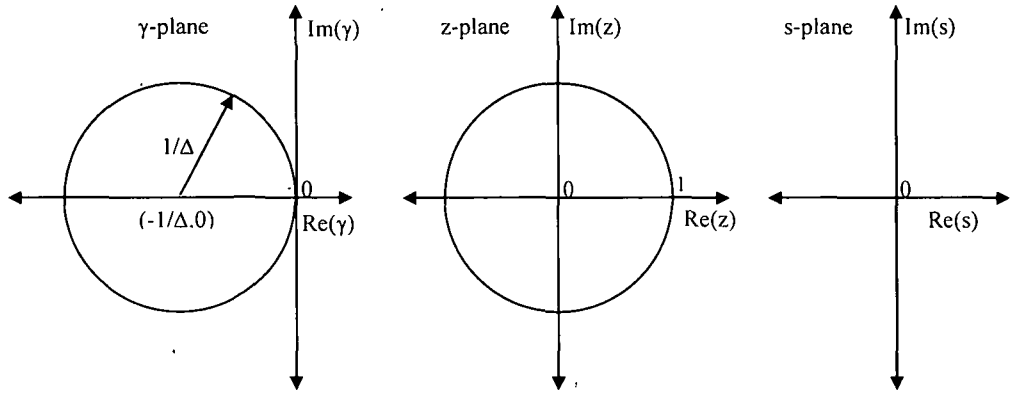

Figure 1.2: Hurwitz stability region for the poles in the complex z and γ-plane

From eqn. (1.21) we can relate complex s, z and γ as

$$\gamma = \frac{z-1}{\Delta} \tag{1.43}$$

$$\gamma = \frac{e^{(\sigma+j n\omega_s)\Delta}-1}{\Delta} \tag{1.44}$$

$$\gamma = \frac{e^{\sigma\Delta}e^{(j n 2\pi)}-1}{\Delta} \tag{1.45}$$

$$\gamma = \frac{e^{(\sigma\Delta)}-1}{\Delta} \tag{1.46}$$

Considering eqn.(1.46), it may be noted that mapping between the s and γ-planes is irrespective of the type of hold circuit used for the discrete-time system. This is so because the poles of a system describe the natural response of a system when the input forcing signal is zero . Obviously, the input hold circuit cannot affect the natural response of the system and therefore has no effect on the poles of the system. Such a simple situation does not hold for the zeros of a system which describe non-zero input

forcing signals which cause zero output from the system. Obviously these zeros are intimately related to the type of input hold circuit used for the discrete-time system, and hence, there will exist no simple mapping from continuous-time zeros to discrete-time as is the case continuous-time poles. Following are the mapping details:

- For $s = 0 \Rightarrow \gamma = 0$ and s $\rightarrow\infty$ along the real axis, $\gamma \rightarrow \frac{-1}{\Delta}$ along the real axis. This mapping is shown in Figure 1.3. Therefore, poles in the γ-plane near the real axis between the origin and the point $\gamma \rightarrow \frac{-1}{\Delta}$ coincide with a well damped system response, with the response becoming quicker as the poles move to the left, analogous to the continuous-time case. Furthermore, this mapping highlights the fact that there is a finite limit as to how fast a sampled data system can respond; that is, it is obvious that it can respond no quicker than the sampling interval Δ.

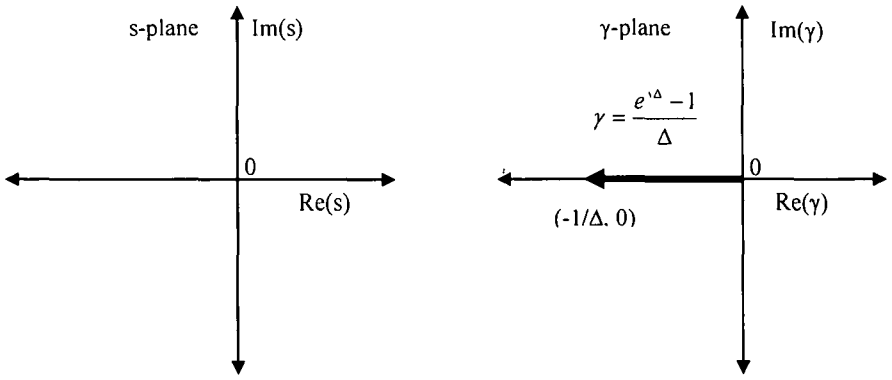

Figure 1.3: Mapping of negative real axis of the s-plane to the γ-plane

- Assuming a continuous time pole s = σ + jω, and substituting this in eqn.(1.46), we have;

$$1 + \Delta\gamma = e^{(-\sigma + j\omega)\Delta} = e^{-\sigma\Delta}(\cos\omega\Delta + j\sin\omega\Delta)$$

Now suppose that γ is a complex number given by $\gamma = x + jy$

in this case
$$\cos\omega\Delta = e^{\sigma\Delta}(1 + \Delta x)$$
$$\sin\omega\Delta = e^{\sigma\Delta}(\Delta y)$$

and
$$\left(x + \frac{1}{\Delta}\right) + y^2 = \frac{1}{(\Delta e^{\sigma\Delta})^2}$$

Therefore, the straight line locus $s = -\sigma + j\omega$ (where $\sigma = \xi\omega_n$ and $\omega = \omega_n\sqrt{1-\xi^2}$) with σ constant in the s-domain maps to a circle with centre at $\frac{-1}{\Delta}$ and radius $\frac{1}{\Delta e^{\sigma\Delta}}$ in the γ-plane. This is shown in Figure 1.4. This is also called the constant damping factor, or the constant settling time loci in the s-plane and the corresponding contour in the γ-plane. This highlights the interesting result that poles near the real axis in the γ-plane can represent a very poorly damped system response if the poles are to the left of $-1/\Delta$.

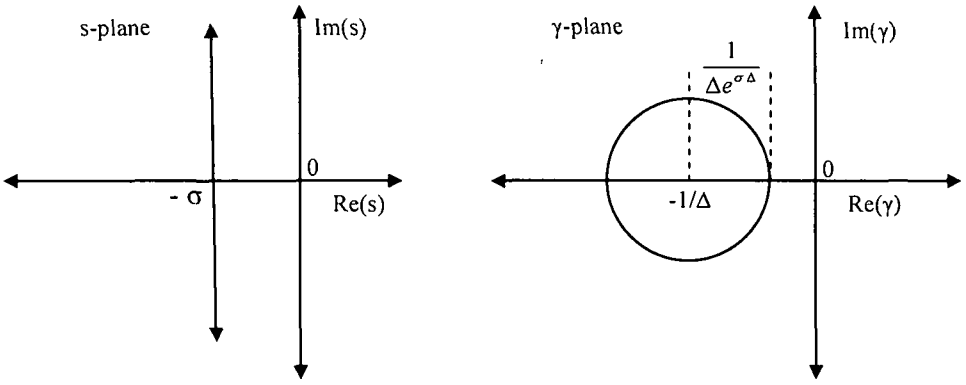

Figure 1.4: Mapping the loci of poles with constant real part in the s-plane to the γ-plane

- Furthermore, it is interesting to note how the loci of poles with a fixed damping ratio in the s-plane maps to the γ-plane. The locus of poles with a constant damping ratio (ξ) is given by the equation:

$$s = -\omega \cot\phi + j\omega \qquad (1.47)$$

where, $\xi = \cos\phi$. Poles defined by this equation are mapped to the poles in the γ-plane defined by

$$\gamma = \frac{e^{-\Delta\omega\cos\phi}e^{j\omega\Delta} - 1}{\Delta} \qquad (1.48)$$

This is an exponentially decaying spiral as shown in Figure 1.5.

- The contours of constant damped natural frequency in the analog s-plane map into radial lines emanating at an angle $\omega\Delta$ from $-1/\Delta$ in the γ-plane as shown in Figure 1.6. Finally, by substituting $\sigma = 0$ into eqn.(1.46) the s-plane stability boundary is seen to map to the circle shown in Figure 1.2.

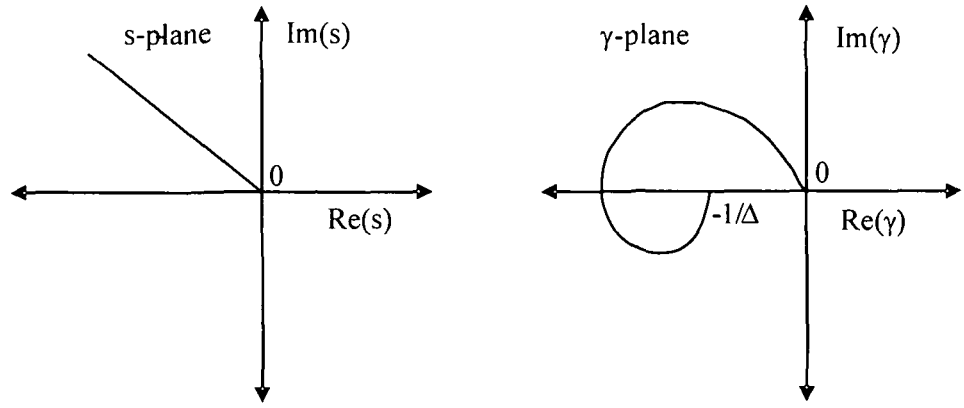

Figure 1.5: Mapping the loci of poles with constant damping ratio in the s-plane and the loci they map into the γ-plane

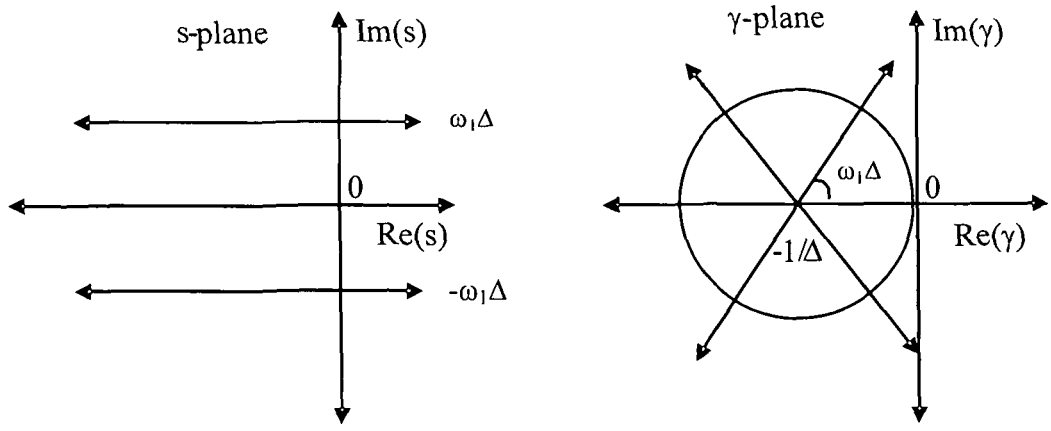

Figure 1.6: Mapping the loci of poles with constant damped natural frequency in the s-plane and the loci they map into the γ-plane

1.9 Stability region in the γ-plane

The stability region of the delta operator is obtained by a mapping of the stability region of the q-operator. From Figure 1.2 it is clear that the stability region of the δ-operator is enclosed by a circle with radius $1/\Delta$ and centre $(-1/\Delta, 0)$. It may be noted that the stability regions in the δ-domain i.e., in complex γ- plane vary with the sampling period, as $\Delta \rightarrow 0$ the stability region converges to the open left-half of γ-plane, which coincides with the stability region for the continuous-time system in the *s*-plane. Mutual relationship in between complex s, z and γ domain is shown in figure 1.7.

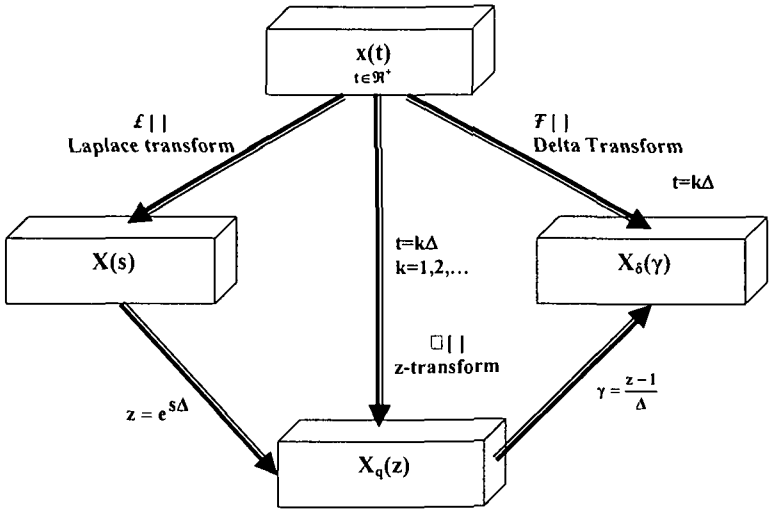

Figure 1.7: Mutual relationships between time and complex s, z and delta domain

1.10 Tables of Delta Transform

In terms of the complex variable γ, we define Discrete delta Transform pair as

$$T[f(k\Delta)] \cong F_\delta(\gamma) = \Delta\sum_{k=0}^{\infty}(1+\Delta\gamma)^{-k} f(k\Delta) \tag{1.49}$$

$$T^{-1}[F_\delta(\gamma)] = f(k\Delta) = \frac{1}{2\pi j}\oint(1+\Delta\gamma)^{k-1} F_\delta(\gamma)\,d\gamma \tag{1.50}$$

and discrete delta transform is related to the z-transform as

$$F_\delta(\gamma) = \Delta F_q(z)\Big|_{z=1+\Delta\gamma} \tag{1.51}$$

where $F_q(z) = Z[f(k\Delta)]$.

conversely

$$F_q(z) = \frac{1}{\Delta}F_\delta(\gamma)\Big|_{\gamma=\frac{z-1}{\Delta}} \tag{1.52}$$

Equations (1.51) and (1.52) allow us to derive a table of delta transforms from the corresponding z-transforms as shown in Appendix-1.1 and its properties in Appendix 1.2. As we have seen earlier and from Appendix 1.1 that δ-transform converge to the associated Laplace transform as Δ→0 that is,

$$\lim_{\Delta\to 0} F_\delta(\gamma) = F(s)\Big|_{s=\gamma} \tag{1.53}$$

1.11 Optimization using Genetic Algorithms.

Genetic Algorithms are general search techniques based on the mechanisms of natural selection and natural genetics. This class of methods is based on the notion of survival of the fittest. In GA search points are represented by genetic strings. The search process starts at a number of points-called populations of points. The acceptability of a search point is judged by the value of its fitness function, Genetic operators called reproduction, crossover and mutation are applied on these genetic strings to generate new search points in order to find the optimum solution. Despite the apparent simplicity of the procedure, GA exhibit substantial computational power in the search of arbitrary spaces. Numerous applications have illustrated the robust search ability of GA.

In the present work, the author has applied the Genetic algorithms to find the optimum frequency points for controller design for different methods.

1.11.1 Biological Background

Chromosome:

All living organisms consist of cells. In each cell there is the same set of chromosomes which consists of genes and DNA and serves as a model for the whole organism. Each gene encodes a particular protein and each gene encodes a trait, for example colour of eyes. Possible settings for a trait (e.g. blue, brown) are called alleles. Each gene has its own position in the chromosome called locus. All the chromosomes in a complete set of genetic material is called genome. Particular set of genes in genome is called genotype.

Reproduction:

During reproduction, first occurs recombination (or crossover) when genes from parents form in some way the whole new chromosome. The new created offspring can then be mutated by which elements of DNA are a bit changed. These changes are mainly caused by errors in copying genes from parents. The fitness of an organism is measured by success of the organism in its life.

Search Space:

When we solve some problem, we usually look for some solution, which will be the best among others. The space of all feasible solutions is called search space,

each point represent one feasible solution. Each feasible solution can be "marked" by its value or fitness for the problem.

One does not know where to look for the solution and where to start. There are many methods, how to find some suitable solution, for example hill climbing, tabu search, simulated annealing and genetic algorithms.

1.11.2 Historical Background of the Genetic Algorithms:

Idea of evolutionary computing was introduced in the 1960s by I. Rechenberg in his work *"Evolution strategies"*. His idea was then developed by other researchers. Genetic Algorithms were invented by John Holland [80] and developed by him and his students and colleagues. This lead to Holland's book *"Adaption in Natural and Artificial Systems"* published in 1975. In 1992 John Koza has used genetic algorithm to evolve programs to perform certain tasks. He called his method *"genetic programming"* (GP). Simulating evolution for useful purposes has been proposed and evaluated in different ways. Genetic algorithms, as practiced today, come in different flavours: genetic algorithms; evolutionary strategies; and evolutionary programming.

An offshoot of genetic algorithms is the concept of genetic programming. GA derive their strengths by simulating the natural search and selection process associated with natural genetics. GA accommodate all the facets of soft computing, namely uncertainty, imprecision, non-linearity, and robustness. GA can be used as advanced operators which include techniques for discovering multiple solutions, combinations of Neural, Fuzzy, and chaos theory, and multiple objective optimizations.

GA is characterized by the mechanism of natural selection and natural Genetics. Genetic algorithms is a multiple point probabilistic search technique, consists of three basic operations, namely reproduction, crossover and mutation. The search is started from a randomly selected population of points. Each of the points is represented by a genetic string called chromosome. The strength of a GA string is measured by its 'fitness value'. Based on the fitness values of the population strings, two parent strings are then generated from the parent strings by using the mechanism of crossover where one half of the first parent string is combined with the other half of the second parent. Mutation is then applied on the child strings by complementing the child strings at selected bit positions, thus introducing variety in the child population.

The algorithm consists of the following steps and corresponding flowchart of simple GA approach is shown in Figure 1.8:

Generate a population of solution stings;

set generation count = 1;

repeat, { while the number of generation ≠ maximum generation

set p = 1;

repeat, {while p ≠ number of population /2

repeat, { select two parent strings;

Generate two child strings using crossover and mutation;

p = p+1 }

generation count = generation count + 1; }

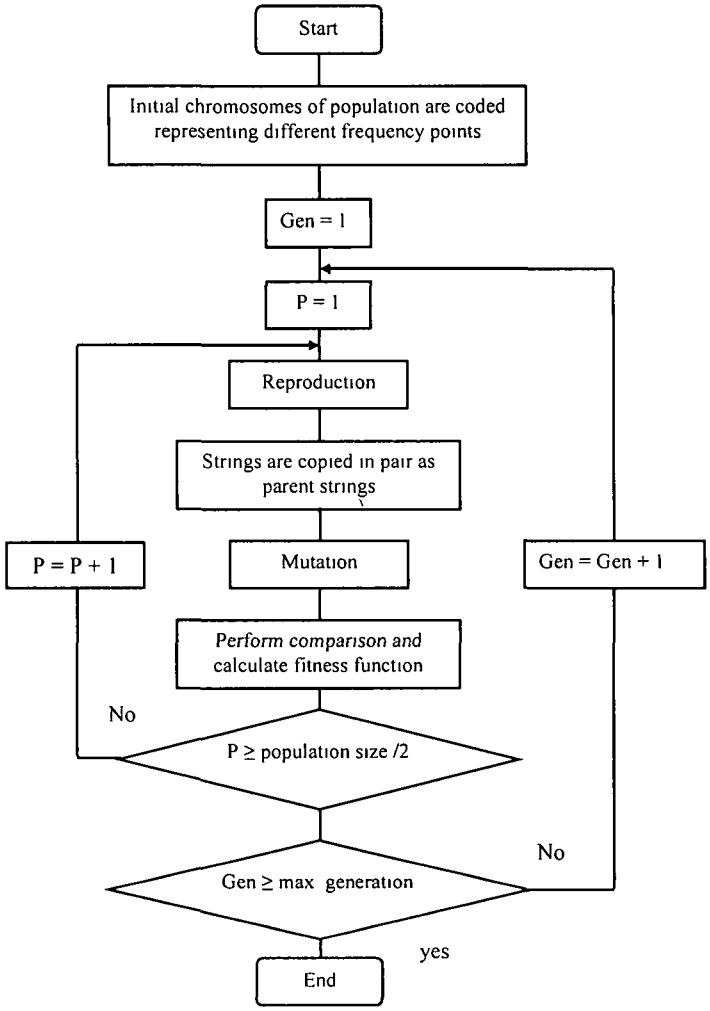

Figure 1 8: Flowchart of simple Genetic algorithm approach to find optimal frequency point

1.11.3 Principles of Genetic Algorithms:

Unlike many methods, GA use probabilistic transition rules to guide their search. The method is not a simple random search or is not a decision making tool depending on the simple probability act just like a toss of a coin. GA use random choice as a tool to guide a search toward region of the search space with likely improvement.

To demonstrate the working principle of GA, the following maximization problem is considered [81], where x is a vector with L lower and U upper bound.

$$Maximaze \quad f(x), x_i^{(L)} \le x_i \le x_i^U, \quad i = 1, 2, ...N$$

Although a maximization problem is considered here, a minimization problem can also be handled using GA. The working of GA is completed by performing the following tasks:

Coding:

To implement GA in the solution of the above maximization problem, variable x_i's are first coded in some string structures. Variable x_i's are coded by binary representation having 0's and 1's. The length of the coded string is usually determined according to the desired solution accuracy. For example, if four bits are used to code each variable in a two variable function optimization problem, the strings (0000, 0000) and (1111, 1111) would represent the points $(x_1^{(L)}, x_2^{(L)})$ and $(x_1^{(U)}, x_2^{(U)})$, respectively, because the substring (0000) and (1111) have the minimum and maximum decoded values. Any other eight bit string can be found to represent a point in the search space according to a fixed mapping rule. Usually, the following linear mapping rule is used [81]

$$x_i = x_i^{(L)} + \frac{x_i^{(U)} - x_i^{(L)}}{2^{L_i} - 1} \, decoded\, value\, (S_i)$$

In the above equation, the variable x_i is coded in a substring S_i of length l_i. The decoded value of a binary substring S_i is calculated as

$$\sum_{i=0}^{l-1} 2^i S_i$$

Where $S \in (0, 1)$ and has a decoded value equal (S_{l-1} S_{l-2}.....S_2 S_1 S_0). For example, a four bit string (0111) has decoded value equal to ((1) 2^0 + (1) 2^1 +(1) 2^2 +(0) 2^3) or 7. It is worthwhile to mention here that with four bits to code each variable, there are only 2^4 or 16 distinct substrings possible, because each bit position can take a value either 0 or 1. The accuracy that can be obtained with a four bit coding is only approximately $1/16^{th}$ of the search space. But as the string length is increased by one, the obtainable accuracy increases exponentially to $1/32^{th}$ of the search space.

Initialization:

Referring to the maximization problem a set of binary strings representing the variable x_i are generated at random to make the initial population. The string in GA corresponds to 'chromosome' and bits in a string refer 'genes' in natural genetics.

Fitness Function:

Every member string in a population is judged by the functional value of the fitness function. As GA follow the rule of survival of the fittest principle of nature to make a search process therefore, the algorithms are naturally suitable for solving maximization problems by some suitable transformation. In general, a fitness function *F(x)* is first derived from the objective function and used in successive genetic operations.

Genetic Operators:

With an initial population of individuals of various fitness values, the operators of GA begin to generate a new and improved population from the old one. A simple genetic algorithm consists of three operations: reproduction, crossover and mutation. Through these operations a new population of points is evaluated. The population is iteratively operated by the above three operators and evaluated until the goal or termination criterion is met. One cycle of these operations and subsequent evaluation procedure is known as a generation in GA.

Reproduction:

Reproduction is usually the first operator applied on a population. Reproduction selects strings according to the fitness values in a population and forms a mating pool. Selecting strings according to their fitness values means that string with a higher value have a higher probability of contributing one or more off-springs

to the next generation. The i^{th} string in the population is selected with a probability proportional to fitness functional value F_i. Since the population size is usually kept fixed in a simple GA, the sum of the probability of each string being selected for the mating pool must be one. Therefore, the probability for selecting the i^{th} string is

$$P_i = \frac{F_i}{\sum_{j=1}^{n} F_j}$$

where n is the population size. There are many methods how to select the best chromosomes, i.e. Roulette-wheel selection, Boltzman selection, Tournament selection, Rank selection and Steady state selection etc.

Let us imagine the selection scheme is roulette-wheel with its circumference marked for each string proportionate to the string's fitness. The roulette-wheel is spun n times, each time selecting an instance of the string chosen by the roulette-wheel pointer. Since the circumference of the wheel is marked according to a string's fitness, the roulette-wheel mechanism is expected to make $\frac{F_i}{\bar{F}}$ copies of the i^{th} string in the mating pool. The average fitness of the population is calculated as,

$$\bar{F} = \sum_{i=1}^{n} \frac{F_i}{n} \qquad = \frac{1}{n} \sum_{i=1}^{n} F_i$$

Table 1.1 shows individual fitness values of five frequency points and Figure 1.9 shows a roulette-wheel for said five individual frequency points having different fitness values. Since the fifth individual has a higher fitness value than any other, it is expected that the roulette-wheel selection will choose the fifth individual more than any other individual. This roulette-wheel selection scheme can be simulated easily.

Table 1.1: Five individual fitness values

Frequency Point	Fitness
1	5.0
2	10.0
3	20.0
4	25.0
5	40.0

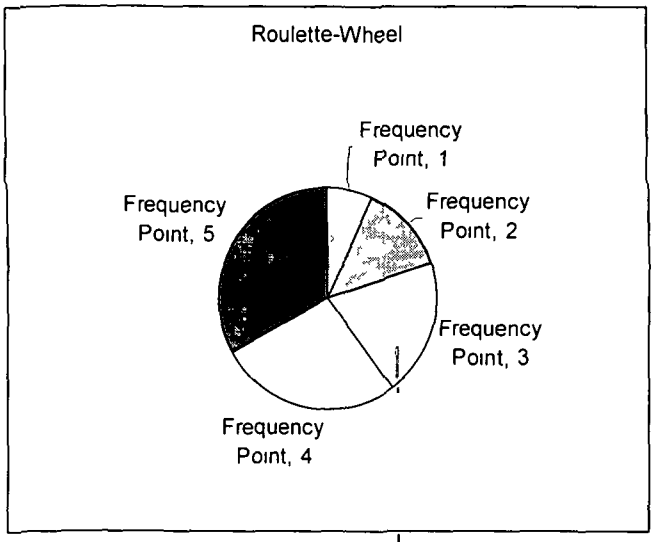

Figure 1.9: Roulette-Wheel marked for five frequency points according to their fitness value

Using the fitness value F_i of all strings, the probability of selecting a string P_i can be calculated. Therefore, the cumulative probability (P_i) of each string being copied can be calculated by adding the individual probabilities from the top of the list.

Crossover:

Crossover probability says how often will be crossover performed. If there is no crossover, offspring is exact copy of parents. If there is a crossover, offspring is made from parts of parents' chromosome. If crossover probability is 100%, then all offspring is made by crossover. Crossover is made in hope that new chromosomes will have good parts of old chromosomes and maybe the new chromosomes will be better

In reproduction, good strings in a population are probabilistically assigned a larger number of copies and a mating pool is formed. But no new string is formed in the reproduction phase. In the crossover operation, new strings are created by exchanging information among strings of the mating pool. Many crossover operators exist in the GA literature. In most crossover operator, two strings are picked from the mating pool randomly and some portions of the strings are exchanged between the strings. A single point crossover operator is performed by randomly choosing a crossing site along the string and by exchanging all bits on the right side of the crossing site as shown.

0 0 0 | 1 0 0 0 0 0 | 1 0 1

| ⇒ |

1 1 1 | 1 0 1 1 1 1 | 1 0 0

The two strings participating in the crossover operation are known as parent strings and the resulting strings are known as children strings. It can be expected that good substrings from parent strings can be combined to form a better child string, if an appropriate site is chosen. Since the knowledge of an appropriate site is usually not known beforehand, a random site is often chosen. With a random site, the children strings produced may or may not have a combination of good substrings from parent strings, depending on the position of crossover point.

Mutation:

Mutation probability defines how often will be parts of chromosome mutated. If there is no mutation, offspring is taken after crossover without any change. If mutation is performed, part of chromosome is changed. If mutation probability is 100%, whole chromosome is changed Mutation is made to prevent falling GA into local extreme, but it should not occur very often, because then GA will in fact change to random search.

A crossover operator is mainly responsible for the search of new strings, even though a mutation operator is also used for this purpose. The mutation operator changes 1 to 0 and vice versa in a bit position with a small mutation probability, p_m. Changing bit with probability p_m can be simulated by choosing a number between 0 to 1 randomly. If the random number is smaller than p_m, the randomly selected bit is altered; otherwise the bit is kept unchanged. The need for mutation is to create a point in the neighbourhood of the current point, thereby achieving a local search around the current solution. The mutation is also used to maintain diversity in the population. For example, consider the following population having four eight-bit strings:

0 1 1 0 1 1 0 0

0 0 1 0 0 0 1 1

0 1 0 1 1 1 1 1

0 1 1 1 0 0 0 0

It can be seen that all four strings have a 0 in the left-most position. If the true optimum solution requires 1 in that position, then neither reproduction nor crossover operator described above will be able to create 1 in that position. The inclusion of mutation introduces some probability of turning 0 to 1.

These three operators are simple and straightforward. A large vol ume of research works have so far been conducted to improve the efficiency of GA. Some variations have been introduced in GA operators. In most cases, the variants are developed to suit particular problems.

Other Parameters of GA:

There are also some other parameters of GA such as population size. Population size defines how many chromosomes are present in population of one generation. If there are too few chromosomes, GA have a few possibilities to perform crossover and only a small part of search space is explored. On the other hand, if there are too many chromosomes, GA slows down. Research shows that after some limit, which depends mainly on encoding and the problem, it is not useful to increase population size, because it does not make solving the problem faster.

While finding optimal frequency points, we got the best results considering the following GA parameters i.e. the crossover probability 77% - 85%, Mutation probability 0.77% - 0.85%, population size 30 - 35, number of generation for evolution 30 - 50 and selection method either Roulette wheel or tournament selection method.

1.11.4 Advantages of GA:

As seen from the above description of the working principles of GA, they are radically different from most of the traditional optimization methods. General advantages are described in the following paragraphs.

GA work with as string coding of variables instead of the variables. The advantage of working with a coding of variables is that the coding discretizes the search space, even though the function may be continuous. On the other hand, since GA require only function values at various discrete points a discrete or discontinuous function can be handled with no extra cost. This allows GA to be applied to a wide

variety of problems. Another advantage is that the GA operators exploit the similarities in string-structures to make an effective search.

The most striking difference of GA is that it works with a population of points instead of a single point. Because there is more than one string being processed simultaneously, it is very likely that the expected GA solution may be a global solution. Even though some traditional algorithms are population-based, like Box's evolutionary optimization and complex search methods, those methods do not use previously obtained information efficiently. In GA, previously found good information is emphasized using reproduction operator and propagated adaptively through crossover an mutation operators. Another advantage with a population based search algorithm is that multiple optimal solutions can be captured in the population easily, thereby reducing the effort to use the same algorithm many times.

In discussing GA operators or their working principles in the previous section, nothing bas been mentioned about the gradient or any other auxiliary problem information. In fact, GA do not require any auxiliary information except the objective function values. Although the direct search methods used in traditional optimization methods do not explicitly require the gradient information, some of those methods use search directions that are similar in concept to the gradient of the function. Moreover, some direct search methods work under the assumption that the function to be optimized is unimodal and continuous. In GA, no such assumption is necessary.

Another difference in the operation of GA is the use of probabilities in their operators. None of the genetic operators work deterministically. The basic problem with most of the traditional methods is that they use fixed transition rules to move from one point to another. For instance, in the steepest descent method, the search direction is always calculated as the negative of the gradient at any point, because in that direction the reduction in the function value is maximum. In trying to solve a multimodal problem with many local optimum points, search procedures may easily get trapped in one of the local optimum points. But in GA, an initial random population is used, to start with, the search can proceed in any direction and no major decisions are made in the beginning. Later on, when the population begins to converge in some bit positions, the search direction narrows and a near optimal solution is achieved. This nature of narrowing the search space as the search progresses is adaptive and is a unique characteristic of Genetic Algorithms.

1.12 Organization of the thesis

Including this introductory chapter, the thesis has been divided into seven chapters. A brief description of the contents of each chapter is given below. In Chapter-1, a short historical perspective of the state of the art of control theory is followed by a brief survey of the existing literature on discrete-time systems including brief details of Genetic Algorithms which is used for optimization. Reference model selection based on performance specification in delta domain has been presented in Chapter-2. Two frequency domain methods for controller design of SISO system are presented in Chapter-3. The controller design techniques of Chapter-3 are extended to MIMO systems in Chapter-4 and to time delay systems in Chapter-5. In Chapter-6 biomedical digital filters design methods have been presented in delta domain to remove artifacts from Electrocardiogram (ECG) signals. The main contributions of the thesis and scope of further work are included in Chapter-7. An algebraic framework for application of delta operator time moments for system parameter identification is also presented in Appendix-A which will constitute the scope of further work.

Chapter 2

Reference Model:

2.1 Introduction:

Model matching type of controller design greatly depends on the development of a reference model incorporating all of the time, frequency and complex domain design specifications. The desired open or closed loop system performance should be clearly defined for the model. In this chapter we discuss the discrete-time systems in delta operator representation in details.

2.2 Classical Control View Points:

Specification for the transient performance of closed loop control systems are generally formulated in time, frequency or complex s or z domains. The time-domain specifications are percentage overshoot (M_p), rise time (t_r) and settling time (t_s) for step response. In the frequency domain, specifications such as gain margin *(GM)* and phase margin *(PM)* are used with the open loop response, while resonant frequency (ω_r) and the peak value at resonance (M_r) are employed for the closed loop response. Specifications frequently associated with the complex domain are damping ratio (ξ) and frequency of undamped oscillation (ω_n).[3]

Analog control systems design is based on the pole-zero configuration of Laplace transform form of transfer function in the s-plane. Similarly, the poles and zeros of the delta transfer functions determine the response of discrete-time systems at the sampling instants. Since the δ-operator scales and shifts the origin by $1/\Delta$ of the z-plane unit circle, hence the same methodology translates into the delta operator framework. These translations of control systems characteristics are now discussed. The stability region of the γ-plane is the interior $|(1+\Delta\gamma)|< 1$ of the sampling circle. The location of the underdamped poles (for $0 < \xi < 1$) of 2nd order characteristic equation in s-plane are given as: [3]

$$s^2 + 2\xi\omega_n s + \omega_n^2 = 0 \qquad (2.1)$$

In equation (2.1), ω_n is the undamped natural frequency i.e. the radial distance from the poles to the origin of the s-plane and ξ is the dimensionless damping ratio i.e. the cosine of the angle between the radial lines to the poles and the negative real axis. In

turn, the location of the poles in (2.1) lead naturally to rules-of-thumb for the design of analog control system. The relationship among various classical control parameters are:

1. Rise time $(t_r) \cong \frac{1.8}{\omega_n}$
2. Settling time $(t_s) \cong \frac{4.5}{\sigma}$, where $\sigma = \xi \omega_n$ is the damping factor (the real part of the poles).
3. Peak time $(t_p) = \frac{\pi}{\omega}$ where $\omega_d = \omega_n\sqrt{1-\xi^2}$ is the damped natural frequency (the imaginary part of the poles).
4. Peak overshoot $(M_p) = \exp\left(\frac{-\pi\xi}{\sqrt{1-\xi^2}}\right)$

Each of these transient response specifications in s-domain is a function of a single parameter. The mapping of the salient s-plane contour such as the contours of constant settling time, peak overshoot and peak time etc into the γ-plane according to the transformation $\gamma = \frac{(e^{s\Delta}-1)}{\Delta}$ is already illustrated in Chapter 1.

To visualize the mapping of the foregoing control system characteristics, we may apply $\gamma = \frac{(z-1)}{\Delta}$ to scale and shift the z- plane [6].

The mapping of s-plane contour into γ-plane contour can be summarised as:

- In the analog s-plane, the contour of constant settling time (the contour of constant damping factor) for stable systems are vertical lines passing through $s = -\sigma$ along the negative real axis. These contours of constant attenuation map into the scaled and shifted circles $\gamma = \frac{(1-e^{-\sigma\Delta})}{\Delta}$ in the γ-plane (Figure 1.4)
- The contours of constant peak overshoot (the contour of constant damping ratio ξ) map into scaled and shifted spiral in the γ-plane (Figure 1.5).
- The contours of constant peak time (the contour of constant damping natural frequency ω_n) in the analog s–plane map into radial lines emanating (at the angle $\omega_n\Delta$ from $-1/\Delta$) in the γ-plane (Figure 1.6). And in the fast sampling limit, these γ-plane contours revert to their respective analog s-plane contours.

2.3 Parameterization of Control system specifications in Delta domain:

For higher order discrete system, relations between the specifications in the time, frequency and complex delta domain may be very complicated. In many cases, however, the dynamic characteristics of high order control systems are well represented by those of a second order system or model for which the relationships between specifications are simpler. The second order transfer function of the closed loop model in discrete delta domain is chosen as:

$$M_\delta(\gamma) = \frac{A\gamma + B}{\gamma^2 + C\gamma + D} \tag{2.2}$$

For a pole-zero form of transfer function in z-domain, Kuo [3] has derived expression, in terms of a set of complex z-domain specification for the time domain specifications. Jury, [114] has developed relationship between the system frequency response and it's time response; however Shi and Gibbard [63] has related both time and frequency domain specifications with the complex z-domain specifications. In δ-domain specifications however no study has been made so far to relate time and frequency domain specifications with the complex delta domain specifications. In the following sections, an attempt has been made to address these issues.

2.4 Second order reference model in delta domain:

Let us consider a second order reference model in delta domain. The location of the complex conjugate poles (p_δ, p^*_δ) and the real zero - $Z_{\delta 1}$ of the delta transfer function $M_\delta(\gamma)$ given in equation (2.2) are shown in the Figure–2.1.

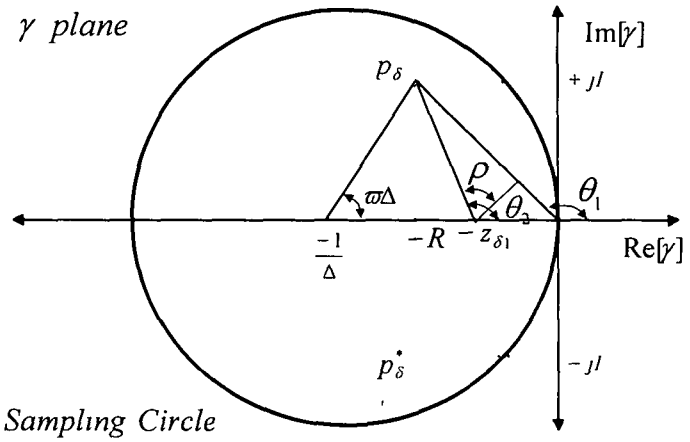

Fig-2 1 Poles and Zeros location of the reference model

The zero is arbitrarily assigned along the real axis by the angle ρ as shown in the Figure-2.1. It has been assumed that the specifications for the closed loop system performance are expressed in the complex γ-plane in terms of the damping ratio ξ, the undamped natural frequency ω_n and the angle ρ. The purpose is to express numerator and denominator coefficients *A, B, C* and *D* of closed loop transfer function of equation (2.2) in terms of these parameters. For our analysis, a second order discrete system with unity feedback is considered. Let us assume the open loop transfer function is $F_\delta(\gamma)$ hence the closed loop transfer function can be expressed in terms of open loop transfer function as:

$$M_\delta(\gamma) = \frac{F_\delta(\gamma)}{1 + F_\delta(\gamma)} \tag{2.3}$$

or,
$$M_\delta(\gamma) = \frac{A(\gamma + z_{\delta 1})}{(\gamma - p_\delta)(\gamma - p_\delta^*)} \tag{2.4}$$

or
$$M_\delta(\gamma) = \frac{A(\gamma + z_{\delta 1})}{\left[\gamma - \left(-\frac{1 - e^{-\sigma\Delta + j\omega_d\Delta}}{\Delta}\right)\right]\left[\gamma - \left(-\frac{1 - e^{-\sigma\Delta - j\omega_d\Delta}}{\Delta}\right)\right]} \tag{2.5}$$

where ω_d (rad/sec) is the damped natural frequency of the reference model and is related to ω_n (natural frequency in rad/sec) by

$$\omega_d = \omega_n\sqrt{1 - \xi^2} \quad \& \quad \sigma = \xi\omega_n \tag{2.6}$$

Δ is the sampling period, and is related to the sampling frequency ω_s (rad/sec) by

$$\Delta = \frac{2\pi}{\omega_s} \tag{2.7}$$

If we denote the real and imaginary part of p_δ as -*R* and *I* respectively, the poles may be expressed as

$$p_\delta = -R + jI \quad and \quad p^*_\delta = -R - jI \tag{2.8}$$

where

$$R = \frac{I - e^{-\sigma\Delta}\cos\omega_d\Delta}{\Delta} \tag{2.9}$$

and $$I = \frac{e^{-\sigma\Delta}\sin\omega\Delta}{\Delta} \tag{2.10}$$

from geometry of Figure-2.1, we can write

$$\rho = \theta_2 - \theta_1 + \frac{\pi}{2} \tag{2.11}$$

Where $$\theta_1 = \tan^{-1}\left(\frac{I}{-R}\right) \tag{2.12}$$

$$\theta_2 = \tan^{-1}\left(\frac{I}{Z_{\delta 1} - R}\right) \tag{2.13}$$

from eqn (2.11), $$\tan(\rho - 90^\circ) = \tan(\theta_2 - \theta_1) \tag{2.14}$$

Expanding the right hand side and expanding for $tan(\theta_2 - \theta_1)$ from eqn (2.12) and (2.13) we obtain the real zero as

$$Z_{\delta 1} = \frac{\tan\left(\rho - \frac{\pi}{2}\right)\left(R^2 + I^2\right)}{\left\{R\tan\left(\rho - \frac{\pi}{2}\right) - I\right\}} \tag{2.15}$$

It is to be noted that Z_{δ_1} is permitted to lie in the range (-∞, 0) on the real axis and ρ will vary from a lower limit ρ_l *to* $+\pi/2$. The lower limit of ρ is

$$\rho = \lim_{Z\delta 1 \to 0}(\rho) = \lim_{Z\delta 1 \to \infty}\left(\theta_2 - \theta_1 + \frac{\pi}{2}\right) \tag{2.16}$$

Substituting the eqns. (2.12) and (2.13) gives:

$$\rho_l = \frac{\pi}{2} - \tan^{-1}\left(\frac{I}{-R}\right) \tag{2.17}$$

From eqn (2.2) and (2.5) we get:

$$C = 2\frac{1 - e^{-\sigma\Delta}\cos\omega\Delta}{\Delta} \tag{2.18}$$

$$D = \left(\frac{1 - e^{-\sigma\Delta}\cos\omega\Delta}{\Delta}\right)^2 + \left(\frac{e^{-\sigma\Delta}\sin\omega\Delta}{\Delta}\right)^2 \tag{2.19}$$

The gain in eqn (2.4) affects only the steady state response of the closed loop system. It is assumed that under steady state conditions the difference between the output and input signals is zero. Hence from eqn (2.2) and (2.4) we can write

$$\frac{Y(\gamma)}{U(\gamma)} = \frac{A\gamma + B}{\gamma^2 + C\gamma + D}\bigg|_{at\,\gamma = 0} = \frac{B}{D} = 1 \tag{2.20}$$

i.e. $$B = D \tag{2.21}$$

and $$\frac{AZ_{\delta 1}}{p_\delta p^*_\delta} = 1 \tag{2.22}$$

$$AZ_{\delta 1} = B \quad or \quad A = \frac{B}{Z_{\delta 1}} \tag{2.23}$$

Finally the open loop Transfer function is obtained as:

$$F_\delta(\gamma) = \frac{A\gamma + B}{\gamma\{\gamma + (C - A)\}} \tag{2.24}$$

The A, B, C *and* D coefficients, together with the zero Z_{δ_1}, can all be expressed in terms of the complex delta domain specification (ξ, ω_n and ρ) using eqns (2.6) to (2.23).

2.5 Conversion of complex domain specifications:

2.5.1 Conversion to time domain.

The analysis of conversion of complex domain specifications is based on the discrete time response $y(k\Delta)$ of the closed loop system in eqn (2.4) to a unit step input signal. When a closed loop system is subjected to a unit step input, the output sequence is obtained by applying the Cauchy's inversion integral theorem as

$$y(k\Delta) = \frac{1}{2\pi j}\oint_\Gamma \frac{A(\gamma + z_{\delta 1})(1 + \Delta\gamma)^k\, d(\gamma\Delta)}{\gamma(\gamma - p_\delta)(\gamma - p^*_\delta)} \tag{2.25}$$

where Γ is the closed contour encloses all the singularities of the integrand. Applying the residue theorem of the complex variables to eqn (2.25), y(kΔ) is written as:

$$y(k\Delta) = 1 + 2\left|\frac{A\,(p_\delta + z_{\delta 1})}{p_\delta(p_\delta - p^*_\delta)}\right|\left|(1 + \Delta p_\delta)\right|^k \cos(k\phi + \theta) \tag{2.26}$$

where $$\phi = \angle(1 + \Delta p_\delta) \tag{2.27}$$

$$\theta = \angle(p_\delta + z_{\delta 1}) - (p_\delta - p^*_\delta) - \frac{\pi}{2}$$

or $$\theta = \theta_2 - \theta_1 - \frac{\pi}{2} \tag{2.28}$$

From eqns (2.11) and (2.28), we see that θ is related to ρ through

$$\theta = \rho - \pi \tag{2.29}$$

Also, we can readily show that the following relationship holds between ρ and the closed loop poles & zero locations:

$$|\sec\rho| = 2\left|\frac{A\,(p_\delta + z_{\delta 1})}{p_\delta (p_\delta - p_\delta^*)}\right| \tag{2.30}$$

where A is given in the eqn. (2.22), Substituting eqns (2.29) and (2.30) into output sequence is written as:

$$y(k\Delta) = 1 + |\sec\rho|\,|(1+\Delta p_\delta)|^k \cos(k\phi + \rho - \pi) \tag{2.31}$$

Equations (2.26) and (2.31) give the response to $y_c(t)$ only at the sampling instants, therefore $y(k\Delta)$ can be approximated as $y_c(t)$ that passes all the points of $y(k\Delta)$.

let $t = k\Delta$, then:

$$|(1+\Delta p_\delta)|^k = |(1+\Delta p_\delta)|^{\frac{t}{\Delta}} = e^{-\xi\omega_n t} \tag{2.32}$$

and

$$\phi_1 = \omega\Delta = \omega_n\sqrt{1-\xi^2}\,\Delta \tag{2.33}$$

therefore, a continuous time function that passes through the points of $y(k\Delta)$ is

$$y_c(t) = 1 + |\sec\rho|\,e^{-\xi\omega_n t}\cos\left(\omega_n\sqrt{1-\xi^2}\,t + \rho - \pi\right) \tag{2.34}$$

where ρ is in radians. The time for this response to reach its first peak value is:

$$t_p = \frac{1}{\omega_n\sqrt{1-\xi^2}}\left[\tan^{-1}\left(\frac{-\xi}{\sqrt{1-\xi^2}}\right) - \rho + \pi\right] \tag{2.35}$$

Let us assume that the maximum value of $y_c(t)$ occurs at its first peak. The associated maximum overshoot in the response is thus

$$M_p = y_c(t)\big|_{t=t_p} - 1$$

$$M_p = |\sec\rho|\sqrt{1-\xi^2}\,\exp\left[\frac{-\xi}{\sqrt{1-\xi^2}}\left(\tan^{-1}\frac{-\xi}{\sqrt{1-\xi^2}} - \rho + \pi\right)\right] \tag{2.36}$$

The settling time t_s, is defined as the time for the envelope, which bounds the oscillatory response to the unit step input, to reach 5% of the final value.

Setting $y_c(t)\,/_{t\,=\,ts}$ = 1+0.05 and cos(·) =1 in the equation (2.34) we find

$$t_s = -\ln(0.05\,|\cos\rho|)\frac{\sqrt{1-\xi^2}}{\omega\xi} \tag{2.37}$$

The three parameters M_p, t_p and t_s are functions of the complex domain parameters ξ, ω_n and ρ only. Therefore they are not only a convenient set of parameters for specifying the time domain performance of the closed loop system, but are also linked by relatively simple expressions to the complex δ-domain.

2.5.2 Conversion to frequency domain:

2.5.2.1 Open loop specifications

Based on eqn (2.24), the open loop frequency response is

$$F_\delta\left(\frac{e^{j\omega\Delta}-1}{\Delta}\right)=F_\delta(\gamma)\Big|_{\gamma=\frac{e^{j\omega\Delta}-1}{\Delta}}$$

or

$$F_\delta(\gamma)=\frac{A\left(\frac{e^{j\omega\Delta}-1}{\Delta}\right)+B}{\left(\frac{e^{j\omega\Delta}-1}{\Delta}\right)^2+(C-A)\left(\frac{e^{j\omega\Delta}-1}{\Delta}\right)} \tag{2.38}$$

There are two specifications commonly used with open loop frequency responses, namely the phase margin *(PM)* and the gain margin *(GM)*. The phase margin (in degrees) is defined as:

$$PM=\psi_f(\omega)\Big|_{\omega=\omega_c}-(-180^\circ) \tag{2.39}$$

where $\psi_f(\omega)$ is the phase angle of $F_\delta\left(\frac{e^{j\omega\Delta}-1}{\Delta}\right)$ and ω_c is the gain crossover frequency at which the magnitude of $F_\delta\left(\frac{e^{j\omega\Delta}-1}{\Delta}\right)$ equals unity, or 0 dB

It can be shown that these quantities (*PM* and *Gain crossover frequency*) are related to system coefficients A, B, C *and* D as:

$$\omega_c=\left(\frac{2}{\Delta}\sin^{-1}\left(\frac{-b_1\pm\sqrt{b_1^2-4a_1c_1)}}{2a_1}\right)^{\frac{1}{2}}\right) \tag{2.40}$$

where the parameters a_1, b_1 and c_1 are given by:

$$a_1=\frac{16}{\Delta^3}(C-A)-\frac{16}{\Delta^4} \tag{2.41}$$

$$b_1=\frac{4AB}{\Delta}-\frac{4}{\Delta^2}(C^2-2AC) \tag{2.42}$$

and

$$c_1=B^2 \tag{2.43}$$

$$\text{and } PM = \tan^{-1}\left[\frac{b_2 A\left(a_2^2 - b_2^2 + (C-A)a_2\right) - (Aa_2 + B)(2a_2 b_2 + b_2(C-A))}{b_2 A(2a_2 b_2 + b_2(C-A) + (Aa_2 + B)(a_2^2 - b_2^2 + (C-A)a_2}\right] + 180^\circ \tag{2.44}$$

where a_2 and b_2 are given as follows:

$$a_2 = \frac{-2}{\Delta}\sin^2\left(\frac{\omega_c \Delta}{2}\right) \tag{2.45}$$

$$b_2 = \frac{1}{\Delta}\sin(\omega_c \Delta) \tag{2.46}$$

The Gain Margin (*GM*) is defined in decibels as:

$$GM = -20\log_{10}\left|\tau_f(\omega)\right|_{\omega=\omega_c}\Big| \tag{2.47}$$

Where $\tau_f(\omega)$ is the magnitude of $F_\delta\left(\frac{e^{j\omega\Delta}-1}{\Delta}\right)$ and ω_f is the phase crossover frequency at which ψ_f is -180°. The phase crossover frequency and the Gain Margin are related to the system coefficients as:

$$\omega_f = \frac{2}{\Delta}\sin^{-1}\left(\frac{B\Delta^2(A-C)}{4(A-B\Delta)}\right)^{1/2} \quad \textit{is Phase crossover frequency} \tag{2.48}$$

and

$$GM = -20\log_{10}\left|\left[\frac{\left(\frac{-2A}{\Delta}\sin^2\left(\frac{\omega_f\Delta}{2}\right)+B\right)+j\left(\frac{A}{\Delta}\sin(\omega_f\Delta)\right)}{\left[\frac{4}{\Delta^2}\sin^4\left(\frac{\omega_f\Delta}{2}\right)-\frac{1}{\Delta^2}\sin^2(\omega_f\Delta)-\frac{2(C-A)}{\Delta}\sin^2\left(\frac{\omega_f\Delta}{2}\right)\right]+j\left[\frac{-4}{\Delta^2}\sin^2\left(\frac{\omega_f\Delta}{2}\right)\sin(\omega_f\Delta)-\frac{(C-A)}{\Delta}\sin(\omega_f\Delta)\right]}\right]\right| \tag{2.49}$$

2.5.2.2 Closed loop Specifications:

The closed loop transfer function in δ-domain is obtained from eqn.(2.3) as:

$$M_\delta(\gamma) = \frac{A\gamma + B}{\gamma^2 + C\gamma + D} \qquad \text{where } \gamma = \frac{e^{j\omega\Delta}-1}{\Delta} \tag{2.50}$$

The specifications, most frequently used to define the properties of a closed loop system are Bandwidth (ω_b), Resonant Frequency (ω_r) and Peak Resonance (M_r).

The Bandwidth (ω_b) is defined as the frequency at which the magnitude $|M_\delta(\gamma)|$ drops to 70.7% of its zero frequency value, or 3 dB. Bandwidth (ω_b) measures the transient response properties and given by:

$$\omega_b = \frac{1}{\Delta}\cos^{-1}\left(\frac{-J \pm \sqrt{(J^2 - 4KG)}}{2G}\right) \tag{2.51}$$

Where

$$J=2\left\{(CD-2AB)\Delta^3+(2A^2-2C^2-2D)\Delta^2+4C\Delta-4\right\} \quad (2.52)$$

$$K=4-C\Delta+(4A^2-C^2-3D)\Delta^2+2(CD-2AB)\Delta^3-2D^2\Delta^4 \quad (2.53)$$

$$G=4\left(D\Delta^2+1-C\Delta\right) \quad (2.54)$$

The resonant frequency (ω_r) is defined as the frequency at which the peak resonance M_r occurs. The resonant frequency (ω_r) for the closed loop transfer function of the eqn (2.50) is given by

$$\omega_r=\frac{1}{\Delta}\cos^{-1}\left(\frac{-T\pm\sqrt{(T^2-4SU)}}{2S}\right) \quad (2.55)$$

The peak resonance M_r is defined as maximum value of $|M_\delta(\gamma)|$ at $\omega=\omega_r$. In general, peak resonance gives the indication of the relative stability of a stable feedback control system. The M_r is found to be :

$$M_r=\frac{N+O\cos(\omega_r\Delta)}{\left(2R\cos^2(\omega_r\Delta)\right)+\left(Q\cos(\omega_r\Delta)\right)+(P-R)} \quad (2.56)$$

where

$$N=\left(\frac{A}{\Delta}\right)^2+\left(B\Delta^2-A\Delta\right)^2 \quad (2.57)$$

$$O=2A\Delta\left(B\Delta^2-A\Delta\right) \quad (2.58)$$

$$P=1+\left(C\Delta-2\right)^2+\left(D\Delta^2+1-C\Delta\right)^2 \quad (2.59)$$

$$Q=2\left(C\Delta-2\right)\left(1+(1+D\Delta^2-C\Delta)\right) \quad (2.60)$$

$$R=2(1+D\Delta^2-C\Delta) \quad (2.61)$$

$$S=2RO \quad (2.62)$$

$$T=4RN \quad (2.63)$$

$$U=QN+RO-PO \quad (2.64)$$

2.6 Derivation of A, B, C and D coefficients and conversion of specification by tabular form.

Equations (2.35) to (2.56) provide for discrete systems a set of mathematical relations for conversion from the complex delta- domain parameters ξ, ω_n, and α, to the time response specifications M_p, t_p and t_s and to the frequency response specifications *PM*, *GM*, ω_c, ω_f, ω_r, ω_b and M_r. These conversions are rather complicated even in the simple second order case. Moreover they do not provide direct conversion in the reverse

sense i.e from either the frequency domain or the time domain to the complex delta domain or between the frequency and time domain. In order to provide flexibility of conversion between domains and in particular, to relate specifications to the *A, B, C* and *D coefficients or to the pole / zero locations of the discrete transfer function, a tabular* form of presentation is convenient as shown in Table 2.1 to Table 2.3

2.7 Simulation results:

A plant taken from Shi and Gibbard [63] to analyse the discrete second order transfer function in the δ- domain given the closed loop specifications:

$$\omega_n = 0.84 \quad rad./\sec. \quad \xi = 0.7 and\ t_p \approx 5 \sec$$

Let us consider the sampling period as 0.5 sec. The above are a convenient set of specifications drawn from both complex domain (ω_n, ξ) and the time domain (t_p). From eqn (2.6), ω_d = 0.6 rad./sec. With $\omega_d\Delta$ and ξ known, the positions of the closed loop poles can be found eqn (2.8) to (2.10) as p_δ, p^*_δ = - 0.5759 ± 0.4404 i. However they do not characterize the system performance completely as zero has strong influence on the system transient response. It can be seen from figure 2.2 and 2.3 and also from Table-2.1 that as ρ varies from ± 10° to ± 80°, then tp/Δ and M_p changes significantly. The corresponding coefficients of the closed loop model may be selected from the quantitative values of the time domain specifications as per Table-2.2 & Table-2.3. Such as with tp/Δ ≈ 10, ρ is found to be -40°.The required transfer function with ξ=0.7, ρ = -40°, ω_n = 0.84 and Δ=0.5 sec is

$$M_\delta(\gamma) = \frac{0.2064\gamma + 0.5257}{\gamma^2 + 1.1519\gamma + 0.5257} \qquad (2.65)$$

The responses to Step and Impulse inputs, pole zero plots, Bode, Nyquist and Nichols plots are shown in figure (2.2 – 2.7) for the transfer function of the reference model given in eqn (2.65).

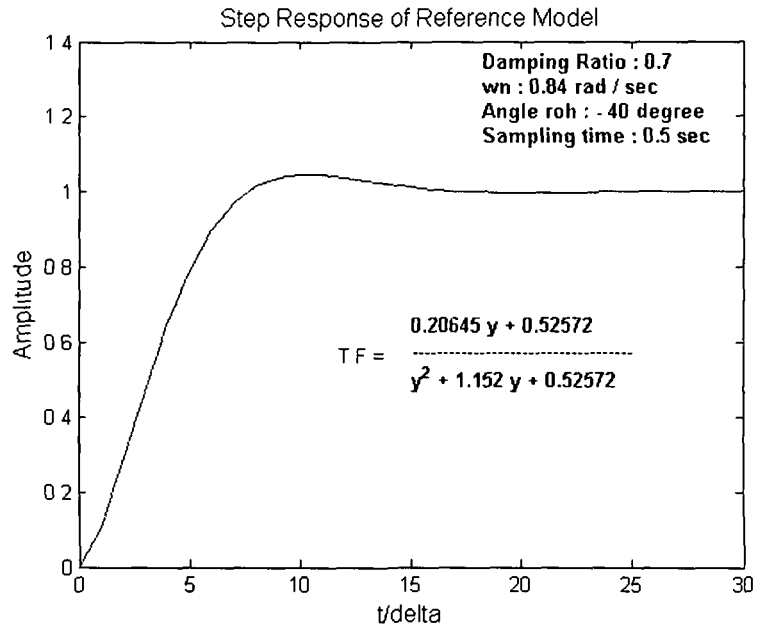

Figure 2.2: Step response of the reference model with ρ = -40°

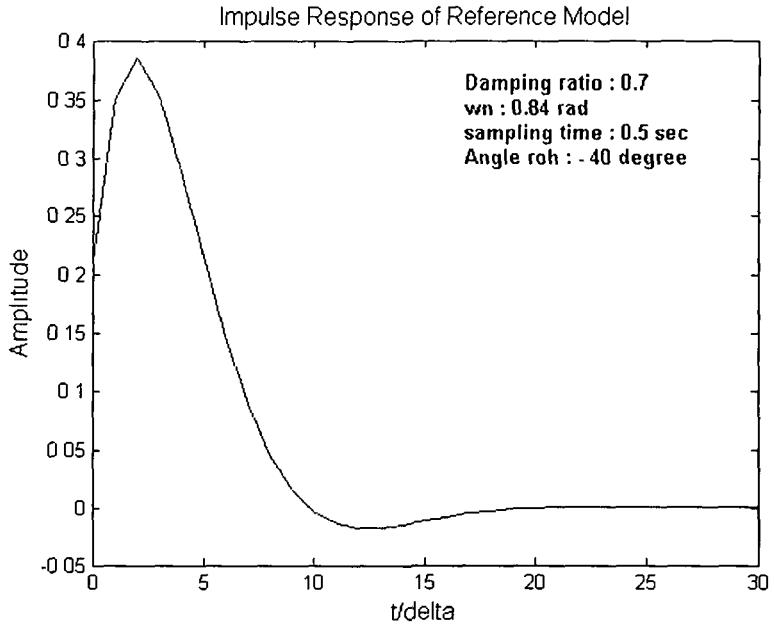

Figure 2.3: Impulse response of the reference model with ρ = -40°

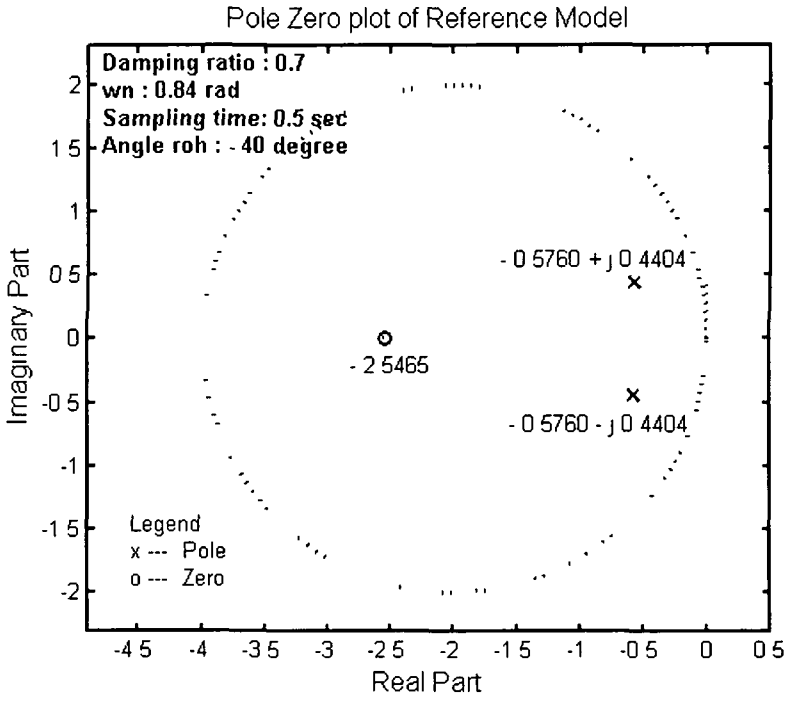

Figure 2.4 . Pole Zero plot of the Reference Model with ρ = - 40° in delta domain

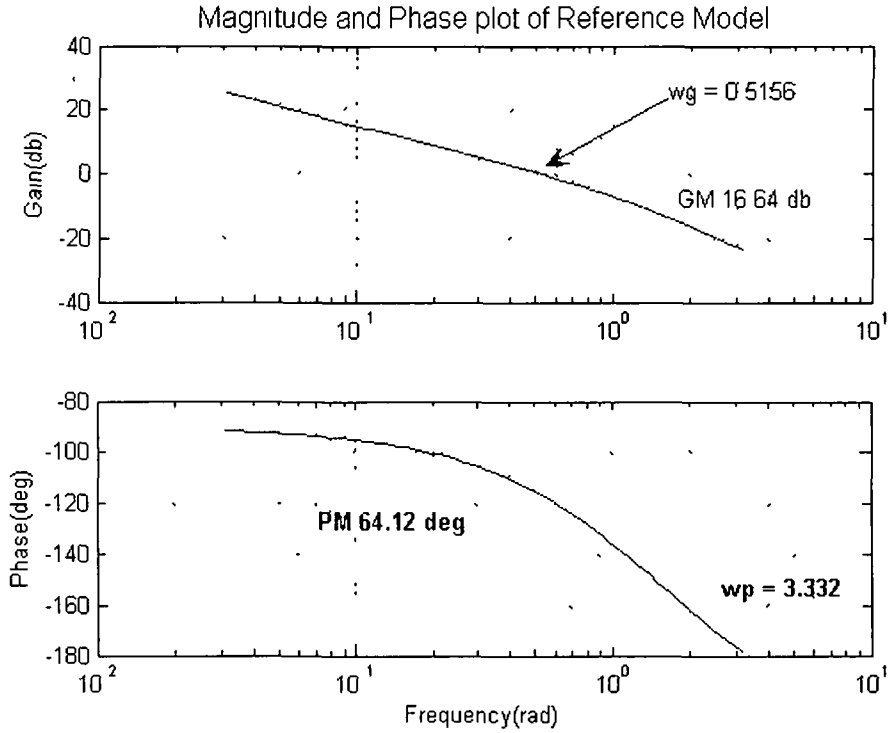

Figure 2 5 Magnitude and Phase plot of the reference model with ρ = - 40°

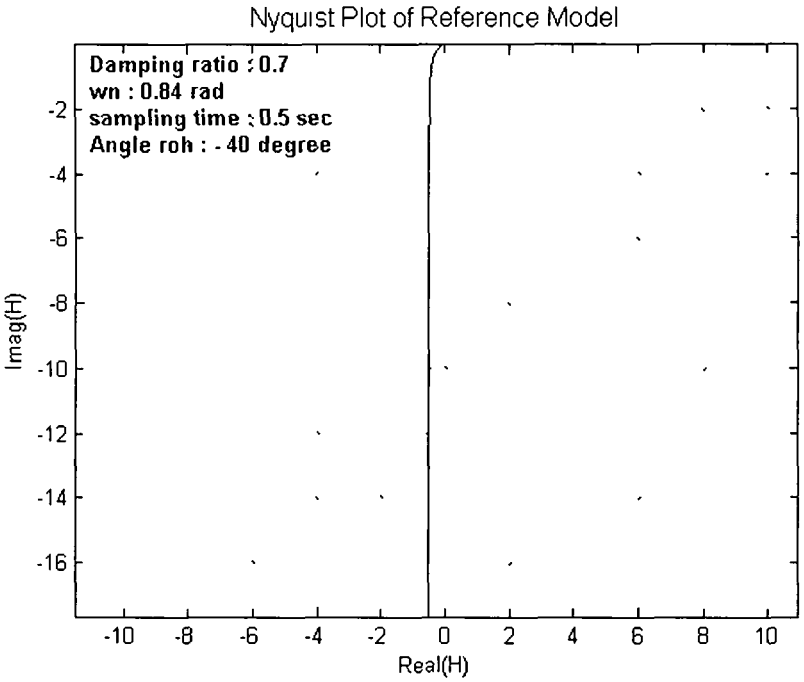

Figure 2 6 Nyquist plot of the reference model with ρ = - 40°

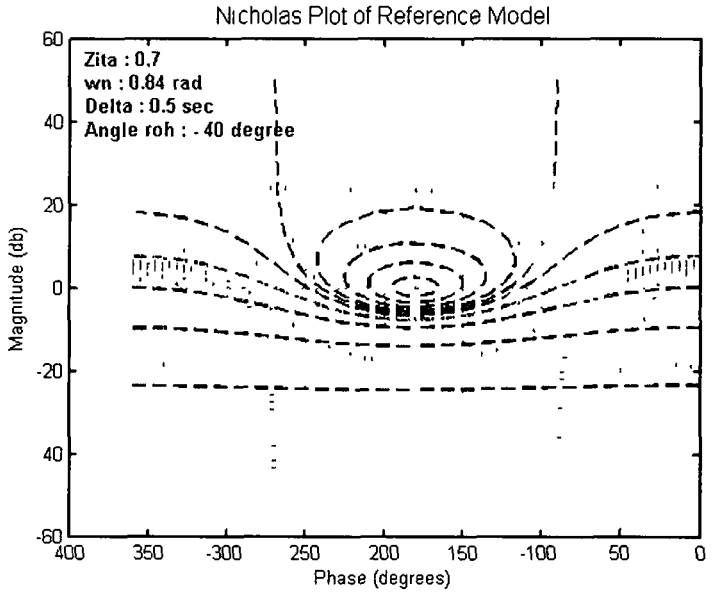

Figure 2 7 : Nichols plot of the reference model with ρ = - 40°

Table –2.1

Close loop System in γ plane				Close loop step response		
ρ	ωΔ	Poles	Zeros	t_p/Δ	%Mp	t_s/Δ
1	0.2999	-0.5759+0.4404 i	-0.9007	7.8307	7.1451	10.1900
10	0.2999	-0.5759+0.4404 i	-0.8042	7.3070	8.4616	10.2416
20	0.2999	-0.5759+0.4404 i	-0.7140	6.7251	10.5225	10.4011
30	0.2999	-0.5759+0.4404 i	-0.6332	6.1432	13.5479	10.6788
40	0.2999	-0.5759+0.4404 I	-0.5560	5.5613	18.1738	11.0960
50	0.2999	-0.5759+0.4404 i	-0.4775	4.9794	25.6998	11.6927
60	0.2999	-0.5759+0.4404 i	-0.3926	4.3975	39.2036	12.5472
70	0.2999	-0.5759+0.4404 i	-0.2943	3.8156	68.0051	13.8388
80	0.2999	-0.5759+0.4404 i	-0.1710	3.2337	158.9355	16.1444
-1	0.2999	-0.5759+0.4404 i	-0.9251	7.9471	6.9047	10.1901
-10	0.2999	-0.5759+0.4404 i	-1.0549	8.4707	6.0098	10.2416
-20	0.2999	-0.5759+0.4404 I	-1.2646	9.0526	5.3079	10.4011
-30	0.2999	-0.5759+0.4404 i	-1.6341	9.6345	4.8538	10.6788
-40	0.2999	-0.5759+0.4404 i	-2.5464	10.2164	4.6245	11.0961
-50	0.2999	-0.5759+0.4404 i	-10.2796	10.7983	4.6446	11.6927
-60	0.2999	-0.5759+0.4404 i	+2.8142	11.3802	5.0321	12.5472
-70	0.2999	-0.5759+0.4404 i	+0.8292	11.9621	6.1997	13.8388
-80	0.2999	-0.5759+0.4404 i	+0.2735	12.5441	10.2911	16.1444

Table –2.2

ρ	Close loop Frequency response			Open loop Frequency response		
	$\omega_b\Delta$	$\omega_r\Delta$	M_r(dB)	PM	GM (dB)	$\omega_c\Delta$
1	0.5438	0.2136	0.2986	61.575	4.9664	0.4371
10	0.5872	0.2404	-0.4880	60.74	2.1117	0.4744
20	0.6461	0.2684	-0.7829	59.463	-1.1294	0.5167
30	0.7217	0.2953	-1.1978	57.679	-4.928	0.5611
40	0.8242	0.3214	-1.7861	55.186	-10.388	0.6095
50	0.9753	0.3468	-2.6433	51.661	-24.289	0.6649
60	1.2304	0.3714	-3.9592	46.536	-15.208	0.7326
70	1.8099	0.3945	-6.1803	38.695	-7.6129	0.8222
80	3.1416-1.7255i	0.4138	-10.774	25.626	-3.303	0.9564

Table –2.2 (continued)

ρ	Close loop Frequency response			Open loop Frequency response		
	$\omega_b\Delta$	$\omega_r\Delta$	M_r(dB)	PM	GM (dB)	$\omega_c\Delta$
-1	0.5352	0.2074	-0.2646	61.728	5.6249	0.4289
-10	0.5004	0.1782	-0.1424	62.309	8.8679	0.3918
-20	0.4673	0.1423	-0.0575	62.777	13.656	0.3507
-30	0.4413	0.1018	-0.0150	63.043	22.987	0.3101
-40	0.4242	0.0592	-0.0017	62.967	24.486	0.2704
-50	0.4246	0.0607	-0.0019	62.248	14.319	0.2318
-60	0.1650	0.4572+ 1.0249i	14.941+5.5507i	43.701	6.6343	0.2538
-70	0.2085	0.4041+ 0.5475i	6.6354+1.8064i	-22.492	-4.7682	0.3861
-80	3.1416-0.9139i	0.3633	-1.4782	55.843	-9.061	0.7180

Table – 2.3

ρ	System Parameters			
	A	B	C	D
1	0.5837	0.52572	1.152	0.5257
10	0.6536	0.52572	1.152	0.5257
20	0.7362	0.52572	1.152	0.5257
30	0.8303	0.52572	1.152	0.5257
40	0.9455	0.52572	1.152	0.5257
50	1.1008	0.52572	1.152	0.5257
60	1.3388	0.52572	1.152	0.5257
70	1.786	0.52572	1.152	0.5257
80	3.0736	0.52572	1.152	0.5257
-1	0.5683	0.52572	1.152	0.5257
-10	0.4983	0.52572	1.152	0.5257
-20	0.4157	0.52572	1.152	0.5257
-30	0.3217	0.52572	1.152	0.5257
-40	0.2064	0.52572	1.152	0.5257
-50	0.0511	0.52572	1.152	0.5257
-60	0.1868	-0.52572	1.152	0.5257
-70	0.634	-0.52572	1.152	0.5257
-80	1.9217	-0.52572	1.152	0.5257

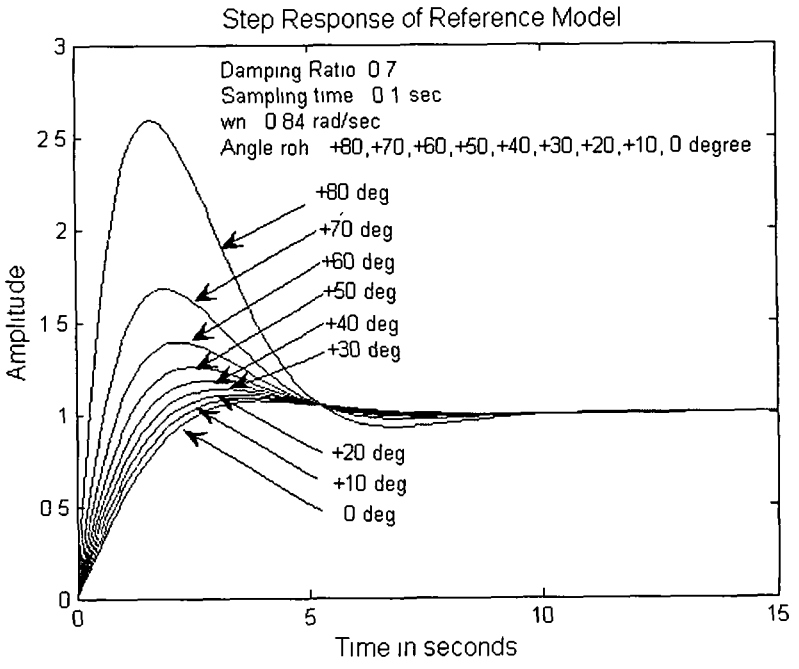

Figure 2.8 Step responses of the reference model with different +ρ

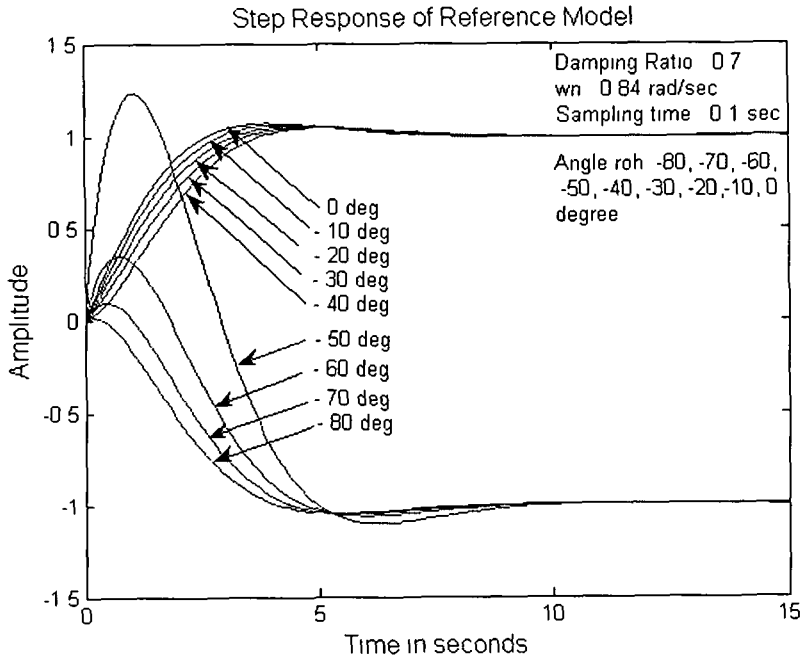

Figure 2.9 Step responses of the reference model with different - ρ

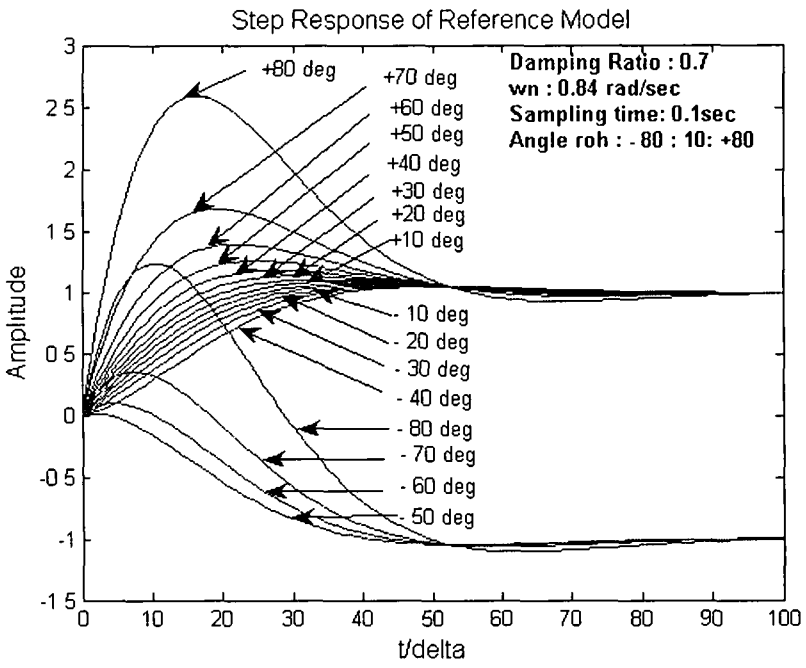

Figure 2.10 Step responses of the reference model with Different ranges of - ρ to + ρ

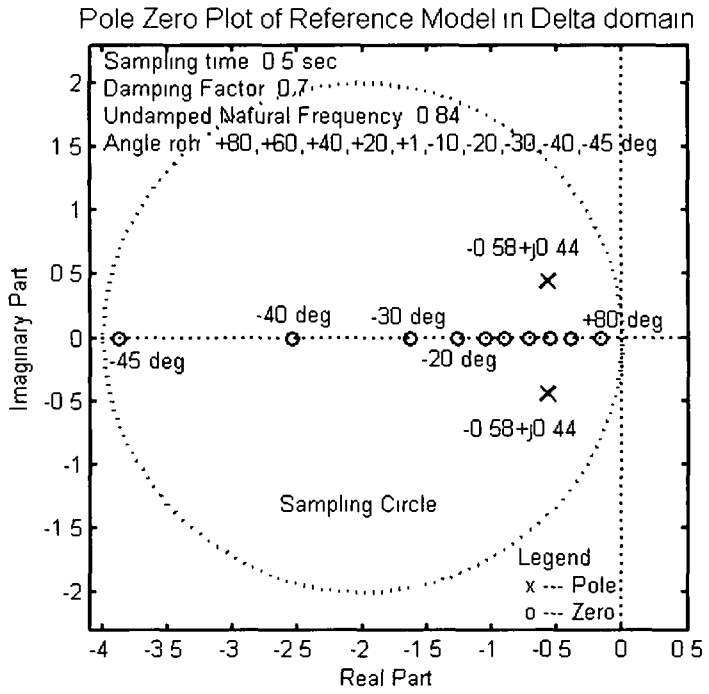

Figure 2.11 Pole Zero Plot of the reference model with ρ = + 80° to - 45° in delta domain

Typical design specifications for closed loop control systems with different ranges of $\omega\Delta$ from 0 1 to 1.5 for ρ = + 60° and - 45° is given in Table 2.4 and corresponding pole zero plot and step responses is shown in figure (2.12 – 2.14)

Table – 2.4

Sampling Time: 0.5 sec , Damping Ratio : 0.7

ρ	ωΔ	ω_n	Poles	zero	tp /Δ	ts /Δ	Mp%	A	B	C
+ 60	0 1	0 2801	-0 1958 ± 0 1810i	-0 3123	21 9166	30 7188	8 4617	0 2277	0 0711	0 3916
+ 60	0 2	0 5601	-0 3888 ± 0 3266i	-0 5776	10 9583	15 3594	8 4617	0 4464	0 2578	0 7776
+ 60	0 3	0 8402	-0 5761 ± 0 4405i	-0 8044	7 3055	10 2396	8 4617	0 6538	0 5259	1 1522
+ 60	0 6	1 6803	-1 0833 ± 0 6272i	-1 3124	3 6528	5 1198	8 4617	1 1939	1 5668	2 1665
+ 60	0 7	1 9604	-1 2298 ± 0 6487i	-1 4382	3 1309	4 3884	8 4617	1 3442	1 9332	2 4596
+ 60	0 9	2 5205	-1 4855 ± 0 6484i	-1 6421	2 4352	3 4132	8 4617	1 5998	2 6270	2 9709
+ 60	1 1	3 0806	-1 6914 ± 0 6064i	-1 7953	1 9924	2 7926	8 4617	1 7983	3 2284	3 3827
+ 60	1 3	3 6407	-1 8504 ± 0 5389i	-1 9093	1 6859	2 3630	8 4617	1 9454	3 7144	3 7008
+ 60	1 5	4 2008	-1 9675 ± 0 4586i	-1 9925	1 4611	2 0479	8 4617	2 0483	4 0813	3 9350
- 45	0 1	0 2801	-0 1958 ± 0 1810i	-4 8135	31 5159	34 0983	4 5992	0 0148	0 0711	0 3916
- 45	0 2	0 5601	-0 3888 ± 0 3266i	-4 1450	15 7580	17 0492	4 5992	0 0622	0 2578	0 7776
- 45	0 3	0 8402	-0 5761 ± 0 4405i	-3 8772	10 5053	11 3661	4 5992	0 1356	0 5259	1 1522
- 45	0 6	1 6803	-1 0833 ± 0 6272i	-3 4353	5 2527	5 6831	4 5992	0 4561	1 5668	2 1665
- 45	0 7	1 9604	-1 2298 ± 0 6487i	-3 3273	4 5023	4 8712	4 5992	0 5810	1 9332	2 4596
- 45	0 9	2 5205	-1 4855 ± 0 6484i	-3 1384	3 5018	3 7887	4 5992	0 8370	2 6270	2 9709
- 45	1 1	3 0806	-1 6914 ± 0 6064i	-2 9755	2 8651	3 0998	4 5992	1 0850	3 2284	3 3827
- 45	1 3	3 6407	-1 8504 ± 0 5389i	-2 8322	2 4243	2 6229	4 5992	1 3115	3 7144	3 7008
- 45	1 5	4 2008	-1 9675 ± 0 4586i	-2 7048	2 1011	2 2732	4 5992	1 5089	4 0813	3 9350

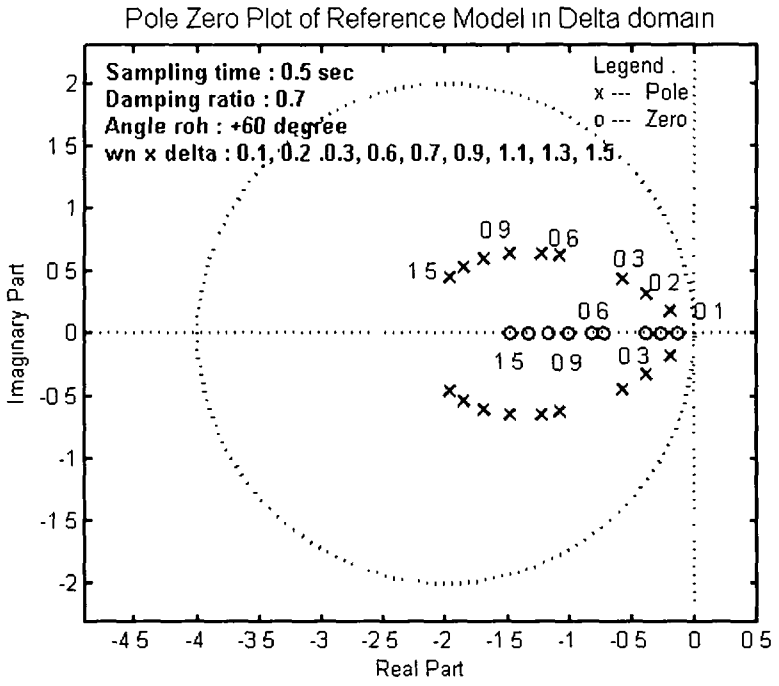

Figure 2.12 Pole Zero Plot of the reference model with ρ = + 60° and different range of ωΔ in delta domain

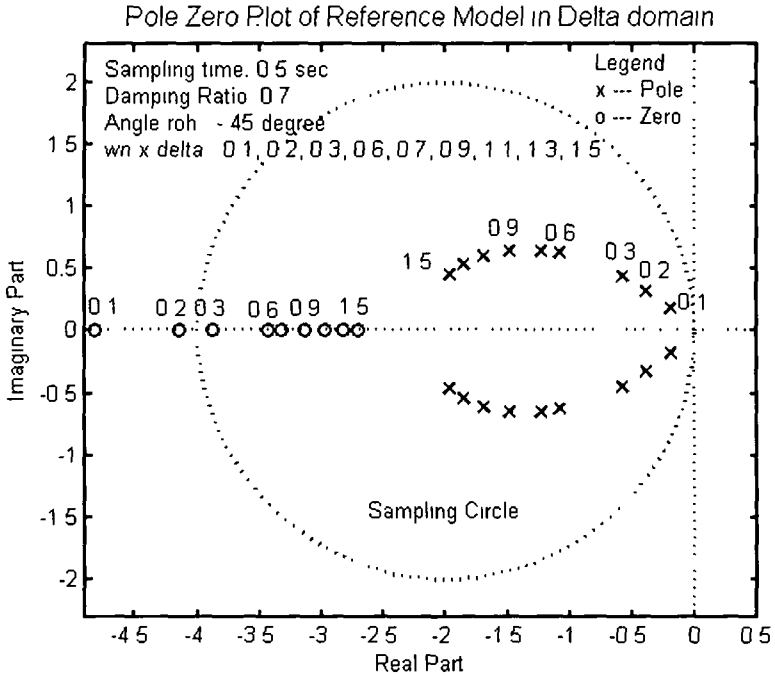

Figure 2.13 Pole Zero Plot of the reference model with ρ = -45° and different range of ωΔ in delta domain

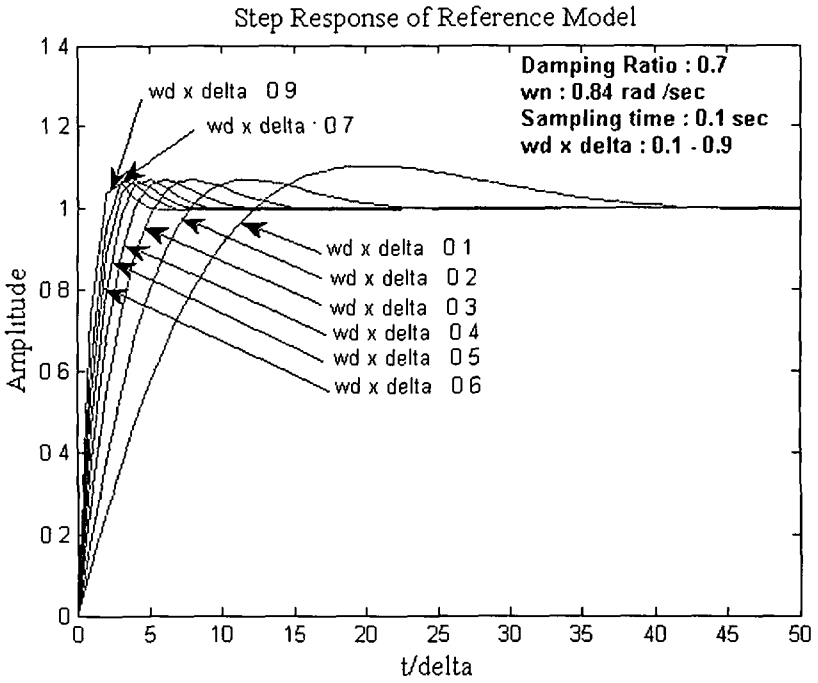

Figure 2.14 Step response of the reference model with different range of $\omega\Delta$ in delta domain

Design specifications for closed loop control systems with different damping ratio ξ = 0.3- 0.9 for ρ =- 20° is shown in Table -2.5 and corresponding pole zero plot is shown in figure (2.15)

Table -2.5

Sampling Time: 0.5 sec, Angle ρ = -20 degree

ρ (deg)	ξ	$\omega\Delta$	Poles	zero	tp /Δ	ts /Δ	Mp%	A	B	C
-20	0.3	0.4007	-0 3764 ± 0 6877i	-4 8737	7.9519	24.269	37.27	0 1261	0.6146	0 7528
-20	0 4	0 3849	-0 4330 ± 0 6349i	-2 9243	7 9991	18 202	25.44	0.2019	0.5905	0.8660
-20	0 5	0.3637	-0 4849 ± 0 5768i	-2.0648	8.1573	14.561	16.61	0.2750	0 5678	0.9698
-20	0.6	0.3360	-0 5324 ± 0 5125i	-1.5791	8.4737	12 134	10 06	0.3459	0.5462	1.0649
-20	0.7	0 2999	-0 5760 ± 0.4404i	-1.2647	9.0527	10.401	5.31	0.4157	0.5257	1 1520
-20	0.8	0.2520	-0 6159 ± 0 3564i	-1.0414	10.1721	9.101	2.09	0.4862	0 5063	1.2318
-20	0.9	0 1831	-0 6524 ± 0 2495i	-0.8688	12 9505	8 089	0 34	0.5616	0.4879	1.3049

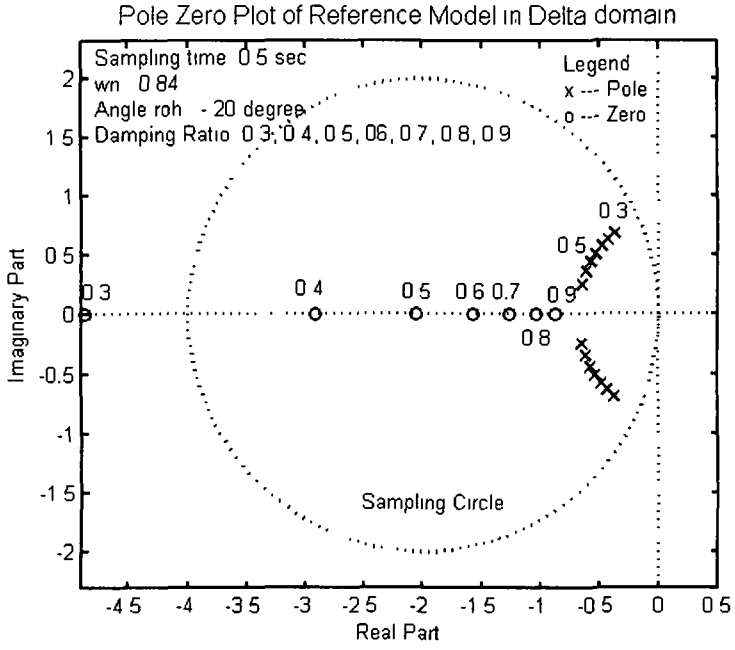

Figure 2.15 Pole Zero Plot of the reference model with $\rho = -20°$ and damping ratio ξ in the range of 0.3 to 0.9

2.8 Conclusion:

The table 2.1 to 2.5 shows the extensive numerical data which relates the time and frequency domain specifications to the complex delta domain parameters. For convenience, normalized variables are shown in the tables such as t_p/Δ etc, which is the approximate number of samples needed for the system output to reach its first peak value. Furthermore, all frequency variables are presented as $\omega\Delta$ so that the primary frequency range 0 to $\omega_s/2$ is normalized to 0 - π.

The step responses vary with the change of zero locations chosen arbitrarily by changing the angle ρ. From step responses and pole zero plots shown in figure 2.8 – 2.15 it is clear that as the parameters like angle ρ, $\omega\Delta$, ξ are varying, for some values of these parameters, the reference model poles shifted towards the sampling circle and the zero crosses the boundary of sampling circle and hence the model becomes unstable.

Chapter 3

Controller Design for SISO Systems

3.1 Introduction:

The configuration shown in Figure 3.1 is the basic standard controller with negative feed back. Let us consider $P_\delta(\gamma)$ is the delta domain equivalent of the continuous-time plant with a zero-order hold (ZOH) and $C_\delta(\gamma)$ the transfer function (TF) of a rational cascade-controller, the parameters of which are to be determined.

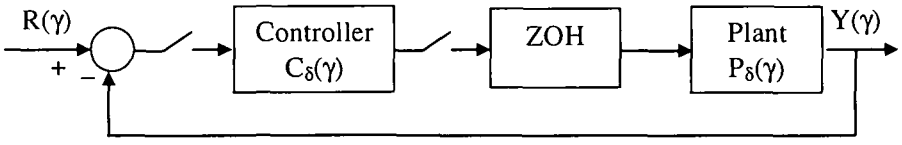

Figure 3.1 The standard unity negative feedback sampled data configuration

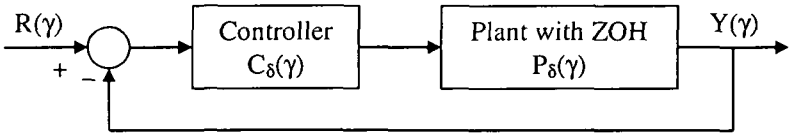

Figure 3.2 The δ-domain representation of the system in figure 3.1

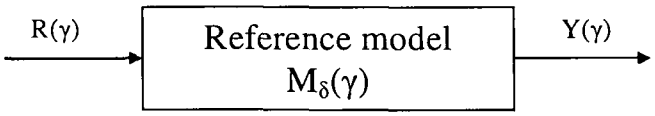

Figure 3.3 The Reference Model of Closed loop system in δ-domain

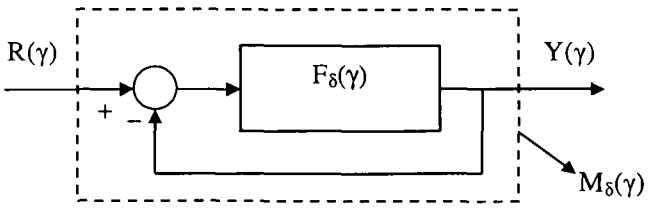

Figure 3.4 Equivalent open loop model of figure 3.3

The delta domain representation of the system is shown in Figure 3.2. The design method is based on the frequency domain approximate model matching

concept described in the later part of this chapter. The design requirements i.e. the desired time and frequency domain specifications are translated into a rational transfer function model. The controller parameters are then determined such that the closed-loop system with the above controller (Figure 3.2) approximates to the specification of the model in some sense.

Specifications for the desired performance of the closed-loop systems are formulated in the time domain (percentage overshoot, rise-time), frequency domain (gain margin, phase margin, resonant frequency etc.) or complex domain (damping ratio, frequency of damped oscillation) as discussed in chapter 2. The closed loop reference model that satisfies a given set of desired performance specifications is shown in Figure 3.3 In the design method we use an open loop-equivalent specification model $F_\delta(\gamma)$ as in Figure 3.4 of the closed-loop reference model (Figure 3.3), such that $F_\delta(\gamma)$ with unity-negative feedback equals $M_\delta(\gamma)$. Therefore the system in Figure 3.4 is equivalent to the given closed-loop specification model in Figure 3.3 we have

$$M_\delta(\gamma) = \frac{F_\delta(\gamma)}{1+F_\delta(\gamma)} \tag{3.1}$$

Solving for $F_\delta(\gamma)$, we have

$$F_\delta(\gamma) = \frac{M_\delta(\gamma)}{1-M_\delta(\gamma)} \tag{3.2}$$

Hence for the desired specification model $M_\delta(\gamma)$, the open-loop equivalent specification model $F_\delta(\gamma)$ may be obtained from equation (3.2). We choose a realizable discrete-time controller transfer function $C_\delta(\gamma)$ of order $q << n$.

We have proposed two methods for controller design of SISO systems in delta domain. The method is an extension of the continuous-time Classical Pade Approximation (CPA) technique in the delta domain defined as Optimal Generalized Delta Time Moment (OGDTM) technique and the second is the complex Optimal Frequency Fitting (OFF) technique. The OGDTM technique is computationally simpler and the OFF technique accommodates both the real and imaginary parts of the frequency response of the process plant and reference model while computing the coefficients of the controller. To get the optimal frequency points, genetic algorithm is used as a tool for optimization. The orders of the controller discussed are assumed known *a-priori* and the output of the controlled process matches that of the reference model.

3.2 Time Moment:

In this section we discuss the concepts of time moment for continuous-time systems, the discrete-time moments for discrete-time systems with shift operator parameterization and in the sequel, define the delta time moments (DTM) for discrete-time systems with delta operator parameterization.

Time moments are important parameters and we briefly discuss the concepts of time moment for continuous and discrete-time systems.

3.2.1 Continuous-time systems:

The i^{th} moment of a continuous real function $f(t)$ of independent variable t about the point $t = a$ is defined by [52]

$$T_i = \int_{-\infty}^{+\infty} (t-a)^i f(t)dt \tag{3.3}$$

If the function is defined for t ∈ [0 ; ∞] then the moments become :

$$T_i = \int_{0}^{+\infty} (t-a)^i f(t)dt \tag{3.4}$$

and if $a = 0$, then the moments are called the time moments about the origin :

$$T_i = \int_{0}^{+\infty} t^i f(t)dt \tag{3.5}$$

A time-invariant, asymptotically-stable dynamic system with n state variables, m input and p output variables as described in state space form (1.1) and its transfer matrix description as in (1.2) in the complex s-domain is considered here.

Let us consider an non-reducible SISO system i.e. with $p = 1$, $m = 1$ and assuming that the numerator and denominator polynomials of the transfer function are co-prime. Expanding the transfer function in eqn.(1.2) into a Maclaurian series about s = 0, yields:

$$G_c(s) = -\sum_{i=0}^{\infty} C_c A_c^{-(i+1)} B_c s^i \tag{3.6}$$

Assuming A_c to be nonsingular, the quantities

$$T_i = (-1)^i i!\, C_c A_c^{-(i+1)} B_c , \qquad i \in [0,\infty] \tag{3.7}$$

where, T_i's are called the time moments of the system. By definition, the impulse-response $g(t) = C_c \exp(A_c t) B_c$ is the inverse Laplace transform of the transfer function, or equivalently,

$$G_c(s) = \int_0^\infty e^{-st} g(t)dt \tag{3.8}$$

Using power series expansion of e^{-st} of (3.8) we get:

$$G_c(s) = \sum_{i=0}^{\infty} (-i) T_i \frac{s^i}{i!} \tag{3.9}$$

From equations (3.6) and (3.7) we get:

$$\begin{aligned} T_i &= (-1)^i \frac{d^i G_c(s)}{ds^i}\Big|_{s=0} \\ &= (-1)^i i! C_c A_c^{-(i+1)} B_c \end{aligned} \tag{3.10}$$

3.2.2 Time moment in discrete-shift operator systems:

Let us consider the independent discrete-time variable t_k, such that a discrete-time function $f(t_k)$ be defined over t_k, where k ∈ {positive integers}. The i[th] moment about $t_k = a$ is then: [52]

$$T_{zi} = \sum_{k=0}^{\infty} (t_k - a)^i f(t_k) \tag{3.11}$$

Similarly, the i[th] moment about the origin is given by:

$$T_{zi} = \sum_{k=0}^{\infty} (t_k)^i f(t_k) \tag{3.12}$$

For a discrete-time system, let us consider the impulse response $g(t)$ of the continuous time system $G_c(s)$ which is sampled with a constant sampling period Δ. Then the i[th] time moment of the discrete-time function $g(k\Delta)$ is given by

$$T_{zi} = \sum_{k=0}^{\infty} (k\Delta)^i g(k\Delta) \tag{3.13}$$

By definition, the z-transform denoted by $G_q(z)$ is given by

$$G_q(z) = \sum_{k=0}^{\infty} g(k\Delta) z^{-k} \tag{3.14}$$

The (impulse) sampled version of $G_c(s)$, that is denoted by $G_c^*(s)$ is obtained by substituting $z = e^{s\Delta}$ in the above relation :

$$G_c^*(s) = \sum_{k=0}^{\infty} g(k\Delta) e^{-ks\Delta} \tag{3.15}$$

The expansion of the exponential term gives :

$$G_c^*(s) = \sum_{k=0}^{\infty} g(k\Delta)\left\{1 - ks\Delta + \frac{(ks\Delta)^2}{2!} - \frac{(ks\Delta)^3}{3!} + \cdots\cdots\right\} \tag{3.16}$$

Using the definition of T_{z_l} as stated in eqn. (3.13), the above relation becomes :

$$G_c^*(s) = \sum_{k=0}^{\infty}\left\{T_{z0} - T_{z1}s + \frac{T_{z2}s^2}{2!} - \frac{T_{z3}s^3}{3!} + \cdots\cdots\right\} \tag{3.17}$$

The discrete time moments may then be expressed as

$$T_{z_l} = (-1)^l \frac{d^l G_c^*(s)}{ds^l}\Big|_{s=0} \tag{3.18}$$

The similarity and difference between the expressions for T_{z_l} and T_l may be noted. Now, changing the variable s to z (where, $z = e^{s\Delta}$, or, $s = \ln z/\Delta$) so that

$$ds = \frac{dz}{\Delta z} \tag{3.19}$$

the expression for T_{z_l} becomes

$$T_{z_l} = (-1)^l (\Delta z \frac{d}{dz})^l G_q(z)\Big|_{z=1} \tag{3.20}$$

$$T_{z_l} = (-1)^l \Delta^l [\frac{d^l}{dz^l} G_q(z)]\Big|_{z=1} \tag{3.21}$$

Defining the power series expansion of $G_q(z)$ about z = 1 as,

$$G_q(z) = \sum_{i=0}^{\infty} d_i (z-1)^i \tag{3.22}$$

one may derive the time moments T_{z_l} from the above coefficients d_i as :

$$T_{z_l} = \frac{i!\Delta^i}{(-1)^i} d_i \tag{3.23}$$

For the sake of computational ease, the coefficients d_i may be obtained by substituting z = (p +1) in $G_q(z)$ and by using the continued division process These coefficients d_i are called the modified proportional time moments of $G_q(z)$.

3.2.3 Time moment in discrete-delta operator systems:

With the concepts of time moments of continuous as well as discrete-time system with shift operator parameterization, now we introduce the time moments for discrete-delta operator parameterizations. The major contributions of the thesis in the areas of modeling and controller design for SISO and MIMO systems rely on these

newly introduced concepts of Delta Time Moments (DTM) in the delta domain; and their generalizations that follow in the sequel and called the Optimal Generalized Delta Time moments (OGDTM).

Using delta transformation definition, if $g(k\Delta)$ is the impulse response of a linear discrete-time system then its transfer function in the complex delta domain can be written as:[10]

$$G_\delta(\gamma) = \Delta \sum_{k=0}^{\infty} g(k\Delta)\,(1+\Delta\gamma)^{-k} \tag{3.24}$$

From the definition of γ given in eqn.(1.46), with the limit $z \to 1$, $\gamma = 0$ as:

$$\gamma = \lim_{z\to 1} \frac{z-1}{\Delta} = 0 \tag{3.25}$$

Expanding $G_\delta(\gamma)$ into its power series expansion about $\gamma = 0$ as:

$$G_\delta(\gamma) = c_0 + c_1\gamma + c_2\gamma^2 + \cdots\cdots \qquad = \sum_{i=0}^{\infty} c_i\,\gamma^i \tag{3.26}$$

Now successive differentiation of eqn.(3.24) is performed and evaluating them at $\gamma = 0$, we can get

$$G_\delta(\gamma)\Big|_{\gamma=0} = \Delta \sum_{k=0}^{\infty} g(k\Delta) = T_{\gamma 0}$$

$$G_\delta^{(1)}(\gamma)\Big|_{\gamma=0} = -\Delta \sum_{k=0}^{\infty} (k\Delta)\, g(k\Delta) = -T_{\gamma 1}$$

$$G_\delta^{(2)}(\gamma)\Big|_{\gamma=0} = \Delta \sum_{k=0}^{\infty} k(k+1)\Delta^2\, g(k\Delta) = T_{\gamma 2}$$

$$G_\delta^{(3)}(\gamma)\Big|_{\gamma=0} = -\Delta \sum_{k=0}^{\infty} k(k+1)(k+2)\Delta^3\, g(k\Delta) = -T_{\gamma 3}$$

$$\vdots \qquad\qquad \vdots \qquad\qquad \vdots \qquad\qquad \vdots$$

$$G_\delta^{(i)}(\gamma)\Big|_{\gamma=0} = (-1)^i \Delta \sum_{k=0}^{\infty} k(k+1)(k+2)\ \ldots\ (k+i-1)\Delta^i\, g(k\Delta) = (-1)^i T_{\gamma i} \tag{3.27}$$

where $T_{\gamma i}$ is defined as the i^{th} Time Moment in the delta domain i.e. the i^{th} Delta Time Moment (DTM). It easily follows that:

$$T_{\gamma i} = (-1)^i \Delta \sum_{k=0}^{\infty} \frac{(k+i-1)!}{(k-1)!} \Delta^{(i)}\, g(k\Delta) \tag{3.28}$$

On successive differentiation of eqn.(3.26) and evaluating them at $\gamma = 0$, we get

$$
\begin{aligned}
G_\delta(\gamma)\ \big|_{\gamma=0} &= c_0 \\
G_\delta^{(1)}(\gamma)\ \big|_{\gamma=0} &= c_1 \\
G_\delta^{(2)}(\gamma)\ \big|_{\gamma=0} &= 2!\,c_2 \\
G_\delta^{(3)}(\gamma)\ \big|_{\gamma=0} &= 3!\,c_2 \\
\vdots \qquad\quad \vdots &\qquad \vdots \\
G_\delta^{(i)}(\gamma)\ \big|_{\gamma=0} &= i!\,c_i
\end{aligned}
$$

while from eqn. (3.27) and eqn. (3.28), it follows that

$$c_i = \frac{1}{i!}\frac{d^i G_\delta(\gamma)}{d\gamma}\bigg|_{\gamma=0} = \frac{(-1)^i}{i!}T_{\gamma i} \tag{2.29}$$

Here c_i may conveniently be called the proportional delta time moment, and is normally used in all calculations in place of the actual DTM $T_{\gamma i}$. Now let us consider the time domain linear state-space delta operator model of eqn. (1.22) and the corresponding frequency domain transfer function in eqn.(1.34), assuming p = 1 and m = 1 for a SISO system. Expansion of eqn.(1.34) about $\gamma = 0$ and assuming that the system matrix A_δ is non-singular, we obtain:

$$G_\delta(\gamma) = (-1)^i \sum_{i=0}^{\infty} C_c A_\delta^{-(i+1)} B_\delta \gamma^i \tag{3.30}$$

The delta time moment series is $T_{\gamma i}$ then given by

$$T_{\gamma i} = (-1)^i\, i! C_c A_\delta^{-(i+1)} B_\delta \tag{3.31}$$

Where $i \in [0 ; \infty]$

3.3 Generalised Delta Time Moments:

Let us consider a real function $f(x)$ with derivatives $f^{(i)}(x)$, $i \in [1, \infty]$ in some region around the point x_0. The values of $f(x)$ be given for the real numbers $x_0, x_1, x_2, \ldots \ldots x_n$ of the variable x; where $x_i = x_0 + h_i$, $i \in [1; n]$ and $h > 0$. By using the notation of the calculus of divided differences we have

$$f[x_0] \cong f(x_0)$$

$$f[x_0, x_1] \cong \frac{(f[x_0] - f[x_1]}{(x_0 - x_1)}$$

$$f[x_0, x_1, x_2] \cong \frac{(f[x_0, x_1] - f[x_1, x_2]}{(x_0 - x_2)}$$

$$f[x_0, x_1, x_2] \cong \frac{(f[x_0\, x_1] - f[x_2\, x_1]}{(x_0 - x_2)}$$

$$\vdots \qquad\qquad \vdots \qquad\qquad \vdots$$

$$f[x_0, x_1, \ldots\ldots\ldots, x_k] \cong \frac{(f[x_0\, x_1 \ldots . x_{k-1}] - f[x_1\, x_2 \ldots\ldots x_k]}{(x_0 - x_k)} \qquad (3.32)$$

Let us suppose in the interval *(a, b)* bounded by the greatest and least of $x_0, x_1, \ldots . x_n$, the function $f(x)$ of the real variable x, and its first $(n - 1)$ derivatives are finite and continuous and that $f^{(n)}(x)$ exists. It may then be shown that [115]

$$f[x_0, x_1, x_2 \ldots . x_n] = h^{-n} \sum_{i=0}^{n} \frac{(-1)^{n-i}}{i!\,(n-i)!} f(x_i) = \frac{1}{n!} f^{(n)}(\eta) \qquad (3.33)$$

where η lies in the interval $x_0 \leq \eta < x_0 + nh$. Now let $\psi(x)$ be a second real function with finite and continuous derivatives $\psi^{(i)}(x)$ around the point $x = x_0$, such that

$$\Psi(x_i) = f(x_i), \qquad i = 1, 2, 3, \ldots\ldots\ldots, n \qquad (3.34)$$

Then from equation (3.33),

$$\psi^{(n)}(\zeta) = f^{(n)}(\eta)$$

where ζ lies in the interval $x_0 \leq \zeta \leq x_0 + nh$. Now if the parameter h takes a very small non-negative value; we have

$$f^{(i)}(x_0) \cong \Psi^{(i)}(x_0), \quad i \in [0, n] \qquad (3.35)$$

Thus, for a suitably small value of the parameter h, for a given $f(x)$ another real valued function $\psi(x)$ may always be constructed using (3.34) so that the approximate relations in (3.35) are satisfied.

Now by approximating the differential operators $G_\delta^{(i)}(\gamma)\big|_{\gamma=0}$ by the divided difference equivalents, a new set of parameters called generalized delta time moments (GDTM) are obtained.

Let $G_\delta(\gamma)$ be the n^{th} order transfer function of a SISO linear discrete time invariant system described by

$$G_\delta(\gamma) = \frac{N_\delta(\gamma)}{D_\delta(\gamma)} = k\frac{1 + b_1\gamma + b_2\gamma^2 + b_3\gamma^3 + \cdots\cdots + b_m\gamma^m}{1 + a_1\gamma + a_2\gamma^2 + a_3\gamma^3 + \cdots\cdots + a_n\gamma^n} \qquad (3.36)$$

where $m < n$. It is assumed that $G_\delta(\gamma)$ is irreducible i.e $N_\delta(\gamma)$ and $D_\delta(\gamma)$ have no zeros in common. The delta time moments $T_{\gamma i}$, $i \in [0, \infty]$ of $N_\delta(\gamma))$ are defined as

$$T_{\gamma i} = (-1)^i \frac{d^i G_\delta(\gamma)}{d\gamma^i}\Big|_{\gamma=0} \tag{3.37}$$

and $T_{\gamma i}$ are proportional to c_i, where

$$G_\delta(\gamma) = \sum_{i=0}^{\infty} c_i \gamma^i \tag{3.38}$$

If we replace (γ) with a small suitable positive real number (frequency) (μ_i) such that $\mu_{ii} = i.\mu_i$ and define *(m+n)* distinct values of a function $f_1, f_2, \ldots\ldots f_{m+n}$ such that

$$f_i = G_\delta(\mu_{ii}), \qquad i \in [1,\ m+n] \tag{3.39}$$

Then f_i are defined as the Generalized delta time moments (GDTMs).

3.4 Optimal Generalised Delta Time Moment:

The concept of optimal generalised delta time moment (OGDTM) is presented here. It may be seen from section 3.3 that the GDTMs are computed from a set of real frequency points with trial and error methods only with no emphasis on how such parameters can be computed and what shall be the overall performance of the resultant system. The success of such methods largely depends on the intuition of the designer and after choosing a particular set of GDTM the performance of the overall system is determined as an end result. In order to get rid of such situation GA is applied to minimize a *apriori* performance index to compute these parameters called Optimal Generalised Delta Time Moments (OGDTM). In the controller design problem presented in the next section these parameters set is computed by minimizing the cost function developed between the step response of the reference model and the overall controlled system. The algorithms for computing OGDTM using GA is presented in figure 3.5:

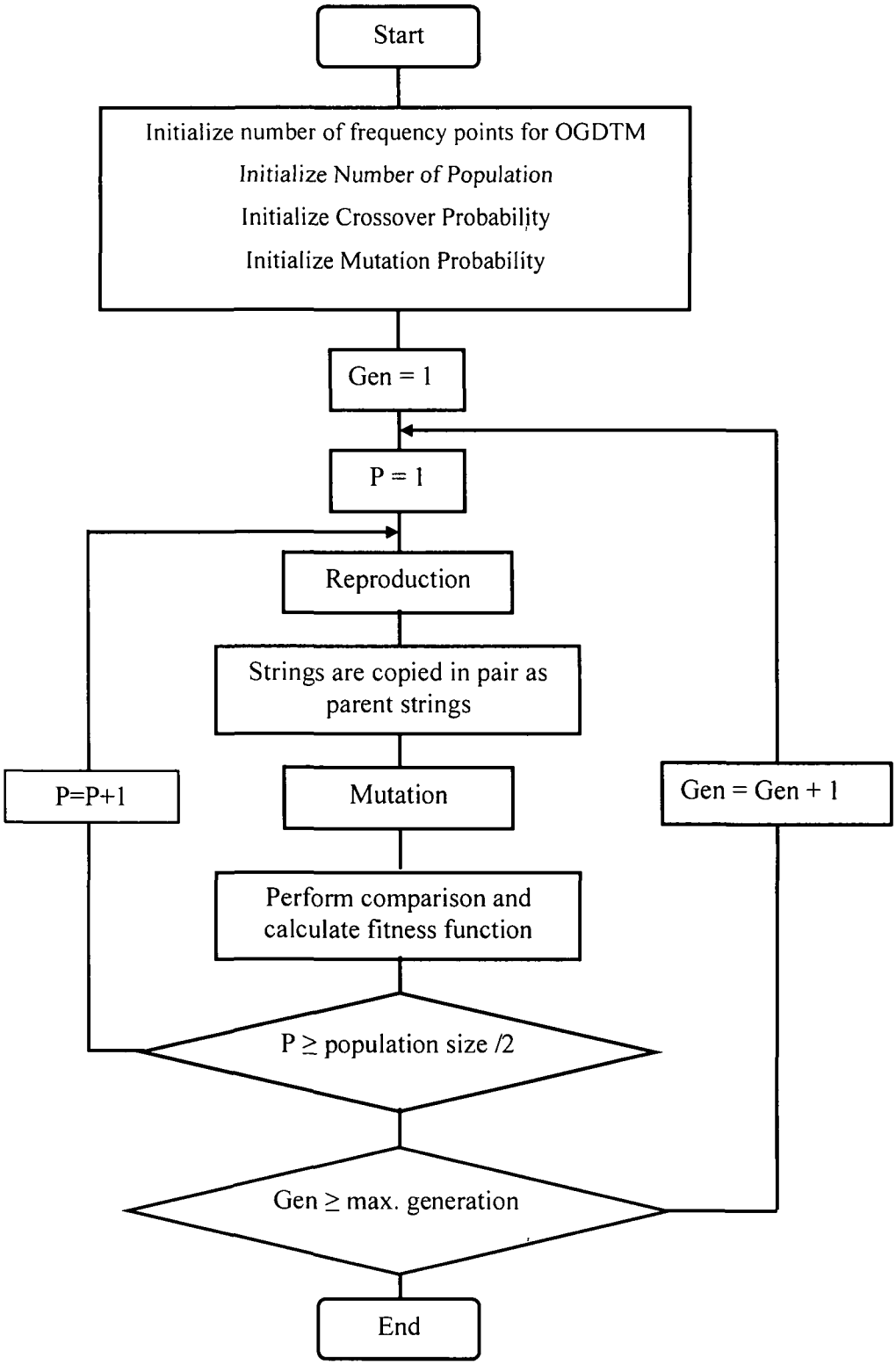

Figure 3.5: Flow chart of steps to compute OGDTM

3.5 Controller design by OGDTM matching method:

In the present work we propose a unified controller design method in the complex delta domain by using OGDTM. The proposed method of controller design based on OGDTM is developed using a computational framework which is a variant of classical Pade approximation technique. The design method is computationally simple and requires only the solution of a set of linear algebraic equations. The computational algorithms invoke GA to determine optimal real frequency points after minimizing a cost function and are numerically stable and yield a continuous-time like controller at very fast sampling rate. The proposed method is based on model matching framework which requires brief discussion on exact model matching (EMM) and approximate model matching (AMM).

3.5.1 Exact Model Matching (EMM):

Let us consider the delta-operator representation of discrete-time unity feedback system, shown in Figure 3.2. In the system, $P_\delta(\gamma)$ and $C_\delta(\gamma)$ are the plant and controller transfer function respectively and are given by:

$$P_{\delta(m,n)}(\gamma) = \frac{\sum_{i=0}^{m} b_i \gamma^i}{\sum_{i=0}^{n} a_i \gamma^i}; \; m \le n \tag{3.40}$$

and

$$C_{\delta(p\,q)}(\gamma) = \frac{\sum_{i=0}^{p} \beta_i \gamma^i}{\sum_{i=0}^{q} \alpha_i \gamma^i}; \; p \le q \tag{3.41}$$

The subscripts (m, n) and (p, q) in equations (3.40) and (3.41) represent the order of the numerator and denominator of the plant and controller respectively. The closed-loop transfer function $G_\delta(\gamma)$ is then given by

$$G_{\delta(m+p,n+q)}(\gamma) = \frac{\left(\sum_{i=0}^{m} b_i \gamma^i \sum_{i=0}^{p} \beta_i \gamma^i\right)}{\left[\sum_{i=0}^{n} a_i \gamma^i \sum_{i=0}^{q} \alpha_i \gamma^i + \sum_{i=0}^{m} b_i \gamma^i \sum_{i=0}^{p} \beta_i \gamma^i\right]} \tag{3.42}$$

The denominator of equation (3.42) represents the characteristic polynomial of the closed-loop system and is of order *(n + q)*. The unknowns of equation (3.41) are

the $\beta_i s$ and $\alpha_i s$ corresponding to the compensator $C_\delta(\gamma)$. In the exact model matching problem, it is desired to find the unknown parameters $\beta_i s$ and $\alpha_i s$ of $C_\delta(\gamma)$ such that the closed-loop transfer function, $G_\delta(\gamma)$ exactly matches a general specification transfer function, $M_\delta(\gamma)$, given by

$$M_{\delta(k,l)}(\gamma) = \frac{\sum_{i=0}^{k} d_i \gamma^i}{\sum_{i=0}^{l} c_i \gamma^i}; \; k \le l \tag{3.43}$$

Therefore, for exact model matching, we have

$$G_\delta(\gamma) = M_\delta(\gamma) \tag{3.44}$$

or,
$$\frac{P_\delta(\gamma)C_\delta(\gamma)}{1 + P_\delta(\gamma)C_\delta(\gamma)} = M_\delta(\gamma) \tag{3.45}$$

Solving for $C_\delta(\gamma)$, we have

$$C_\delta(\gamma) = \frac{M_\delta(\gamma)}{P_\delta(\gamma)[1 - M_\delta(\gamma)]} \tag{3.46}$$

and substituting for $P_\delta(\gamma)$ and $M_\delta(\gamma)$ from equations (3.40) and (3.43), we finally get

$$C_\delta(\gamma) = C_{\delta(k+n,\, m+l)}(\gamma) = \frac{\sum_{i=0}^{k} d_i \gamma^i \sum_{i=0}^{n} a_i \gamma^i}{\left[\sum_{i=0}^{m} b_i \gamma^i \sum_{i=0}^{l} c_i \gamma^i - \sum_{i=0}^{m} b_i \gamma^i \sum_{i=0}^{k} d_i \gamma^i\right]} \tag{3.47}$$

The equation (3.47) is called "Synthesis equation" or Truxal's method which is extended here for delta-operator systems for designing $C_\delta(\gamma)$. Though computation of the design based on exact model matching method is simple but it may often lead to higher order controller, sometimes the order of which is higher than the plant, the implementation of which in hardware may in many cases is not cost effective. The controller may also be unstable and unrealizable. Further, the structure and order of the controller cannot be fixed a priori as has been done in equation (3.41).

3.5.2 Approximate Model Matching (AMM):

In approximate model matching (AMM) concept for controller design of delta-operator systems, the equation (3.44) is only approximately satisfied, i.e.

$$G_\delta(\gamma) \approx M_\delta(\gamma) \tag{3.48}$$

Therefore the problems encountered in exact model matching method can be effectively resolved. It is further possible to design compensator of chosen order and with a structure that approximately satisfies the various specifications embodied in the desired transfer function, $M_\delta(\gamma)$. The method provides added flexibility of making a trade-off between the order complexity of the controller and the extent to which the desired specifications are met. Therefore for $C_\delta(\gamma)$ to be physically realizable, following condition should satisfy with the degrees

$$(m+l) \geq (k+n) \qquad or \qquad (l-k) \geq (n-m) \tag{3.49}$$

i.e $M_\delta(\gamma)$ must be selected so that the excess of finite poles over finite zeros for the closed-loop function is at least equal to the pole-zero excess of the plant transfer function, $P_\delta(\gamma)$. Hence to make both the exact model matching and approximate model matching methods to be feasible, the above degree constraint on the choice of $M_\delta(\gamma)$ must be imposed. In the time moment matching technique, few proportional time moments of the respective models are made identical, i.e.

$$\frac{d^{\iota}G_\delta(\gamma)}{d\gamma^{\iota}}\Big|_{\gamma=0} = \frac{d^{\iota}M_\delta(\gamma)}{d\gamma^{\iota}}\Big|_{\gamma=0} \qquad \text{for } \iota = 0,1,2,\cdots,(k+l+1) \tag{3.50}$$

equivalently,

$$g_{\delta\iota} = m_{\delta\iota} \tag{3.51}$$

where $g_{\delta\iota}$ and $m_{\delta\iota}$ are the coefficients of the power series expansion about $\gamma = 0$ i.e.

$$G_\delta(\gamma) = \sum_0^\infty g_{\delta\iota}\gamma^{\iota} \tag{3.52}$$

and

$$M_\delta(\gamma) = \sum_0^\infty m_{\delta\iota}\gamma^{\iota} \tag{3.53}$$

3.5.3 Optimal Generalised Delta Moment Matching (OGDTM)

In the case of optimal generalised delta moment matching (OGDTM), the divided difference equivalents are

$$G_\delta(\mu_\iota) = M_\delta(\mu_\iota), \qquad \iota \in [0,\ k+l+1] \tag{3.54}$$

where μ_ι is a very small positive number such that $0 < \mu_\iota << 1$ computed using GA. The *(k+l+2)* distinct values, $G_\delta(\mu_\iota)$ and $M_\delta(\mu_\iota)$ of the function $G_\delta(\gamma)$ and $M_\delta(\gamma)$ evaluated at different values of μ_ι are defined as OGDTMs of the functions $G_\delta(\gamma)$

and $M_\delta(\gamma)$ respectively. The two functions $G_\delta(\gamma)$ and $M_\delta(\gamma)$, then have identical initial *(k+l+2)* OGDTMs.

3.5.4. Steps for Controller Design by OGDTM Matching:

The following are the steps for controller design problem using the concepts of OGDTM matching. Here we consider for a SISO system.

- **Step 1:** We choose a closed-loop reference model TF, $M_\delta(\gamma)$ that satisfies the desired specifications.
- **Step 2:** The controller TF is now chosen as

$$C_\delta(\gamma) = \frac{\beta_0 + \beta_1\gamma + \cdots + \beta_p\gamma^p}{\alpha_0 + \alpha_1\gamma + \cdots + \alpha_q\gamma^q} \tag{3.55}$$

- **Step 3:** The performance index (fitness function) $PI = \sum_{i=0}^{n}(y_{ref_i}^2 - y_{cl_i}^2)$ is set, where y_{ref} and y_{cl} are the step responses of the reference model and the closed loop over all controlled system.
- **Step 4:** Setting the parameters of GA (number of parameters, number of population, crossover probability, Mutation probability etc.) and GA is run to compute μ_{ii}
- **Step 5:** Now we compute $G_\delta(\gamma)\big|_{\gamma=\mu_{ii}} \triangleq M_\delta(\gamma)\big|_{\gamma=\mu_{ii}}$ for $i \in [1,(p+q+2)]$ (3.56)
- **Step 6:** The equivalent open loop model $F_\delta(\gamma)$ as

$$F_\delta(\gamma) = \frac{M_\delta(\gamma)}{1 - M_\delta(\gamma)} = \frac{\sum_{j=0}^{k} d_j\gamma^j}{\sum_{j=0}^{l} c_j\gamma^j - \sum_{j=0}^{k} d_j\gamma^j} \tag{3.57}$$

- **Step 7:** We find the open-loop equivalent expression as

$$P_\delta(\gamma)C_\delta(\gamma) \triangleq F_\delta(\gamma) \tag{3.58}$$

$$\frac{\sum_{j=0}^{m} b_j\gamma^j \sum_{j=0}^{p}\beta_j\gamma^j}{\sum_{j=0}^{n} a_j\gamma^j q\sum_{j=0}^{}\alpha_j\gamma^j} \triangleq \frac{\sum_{j=0}^{k} d_j\gamma^j}{\sum_{j=0}^{l} c_j\gamma^j - \sum_{j=0}^{k} d_j\gamma^j} \tag{3.59}$$

From which we can write

$$\sum_{j=0}^{p}\beta_j\gamma^j\left[\sum_{j=0}^{m}b_j\gamma^j\left(\sum_{j=0}^{l}c_j\gamma^j-\sum_{j=0}^{k}d_j\gamma^j\right)\right]\triangleq\sum_{j=0}^{q}\alpha_j\gamma^j\left[\sum_{j=0}^{n}a_j\gamma^j\sum_{j=0}^{k}d_j\gamma^j\right] \quad (3.60)$$

Now by putting $\gamma=\mu_u$ where $\mu_u \triangleq i.\mu_t$, where μ_t is the point of expansion about the origin in equation (3.60) and from equation (3.57) with $\alpha_0=1$ we have

$$\begin{aligned}&\sum_{j=0}^{p}\beta_j(\mu_u)^j\left[\sum_{j=0}^{m}b_j(\mu_u)^j\left(\sum_{j=0}^{l}c_j(\mu_u)^j-\sum_{j=0}^{k}d_j(\mu_u)^j\right)\right]\\&-\sum_{j=1}^{q}\alpha_j(\mu_u)^j\left[\sum_{j=0}^{n}\alpha_j(\mu_u)^j\sum_{j=0}^{k}d_j(\mu_u)^j\right]=\left[\sum_{j=0}^{n}a_j(\mu_u)^j\sum_{j=0}^{k}d_j(\mu_u)^j\right]\end{aligned} \quad (3.61)$$

for $i\in[1,(p+q+1)]$

In the above equation, a_i, b_i, c_i, and d_i are known parameters i.e the coefficients in the plant and reference model transfer function and the terms in the parentheses [·] will be known constants, hence the unknown controller parameters β_i and α_i can be computed with a set of *(p+q+1)* linear simultaneous algebraic equations. The controller $C_\delta(\gamma)$ is of PI, PID or any other form with an integral term, and $\alpha_0=0$. Letting $\alpha_1=1$, equation (3.61) gets modified as

$$\begin{aligned}&\sum_{j=0}^{p}\beta_j(\mu_u)^j\left[\sum_{j=0}^{m}b_j(\mu_u)^j\left(\sum_{j=0}^{l}c_j(\mu_u)^j-\sum_{j=0}^{k}d_j(\mu_u)^j\right)\right]\\&-\sum_{j=2}^{q}\alpha_j(\mu_u)^j\left[\sum_{j=0}^{n}a_j(\mu_u)^j\sum_{j=0}^{k}d_j(\mu_u)^j\right]=(\mu_u)\left[\sum_{j=0}^{n}a_j(\mu_u)^j\sum_{j=0}^{k}d_j(\mu_u)^j\right]\end{aligned} \quad (3.62)$$

for $i\in[1,(p+q)]$

In the case of a PI controller, β_1 gives the proportional gain and β_0 gives the gain associated with the integral term, where β_0,β_1, and β_2 are respectively the proportional, integral and derivative gains in the case of a PID controller. The controller parameters can be determined by solving the (p+q+1) linear equations.

- **Step 8:** If the closed-loop system approximately satisfies the desired specifications, then STOP otherwise GO TO STEP 4 after changing GA parameters if not satisfactory.

3.5.6. Simulation results:

For illustrating the methodology of the OGDTM scheme, described above, we consider the following plants with unsatisfactory step responses

3.5.6.1 Simple open loop plant:

The OGDTM technique has been tested on the following simple plant model [76] with transfer function given as:

$$G_c = \frac{3}{s^2 + 4s + 3} \tag{3.63}$$

To exhibit the properties of the delta operator representation in the complex delta domain, the above continuous-time plant transfer function is discretised incorporating a sampler and zero order hold (ZOH) with sampling periods Δ = 0.1, 0.01, 0.001 seconds respectively. It may be seen that the discrete models converges to the corresponding continuous-time model as the sampling frequency is increased, in other words when the sampling time is reduced. In this particular example at Δ = 0.001 sec. the discrete model at eqn. (3.66) whose coefficients are very near to that of the continuous-time plant model at eqn. (3.63) validate the uniqueness of delta operator to represent dynamic model in a unified framework.

- **Sampling time (Δ) = 0.1 seconds**

Plant transfer function in delta domain is $P_\delta(\gamma) = \dfrac{0.13153\gamma + 2.4664}{\gamma^2 + 3.5434\gamma + 2.4664}$ (3.64)

- **Sampling time (Δ) = 0.01 seconds**

Plant transfer function in delta domain is $P_\delta(\gamma) = \dfrac{0.014802\gamma + 2.9407}{\gamma^2 + 3.9505\gamma + 2.9407}$ (3.65)

- **Sampling time (Δ) = 0.001 seconds**

Plant transfer function in delta domain is $P_\delta(\gamma) = \dfrac{0.001498\gamma + 2.994}{\gamma^2 + 3.995\gamma + 2.994}$ (3.66)

It is to be noted that in a continuous-time transfer function model with no finite zeros when discretised, the order of the numerator polynomial becomes the same as the order of the denominator polynomial thereby a strictly proper transfer function after discretisation becomes biproper. These additional zeros are called sampling zeros which has been discussed in chapter-1. Therefore, in discrete-time controller design adequate attention has to be paid to these zeros in the design

technique. As presented in the chapter-2, a set of 2nd order reference models has been developed in the complex delta domain for a given set of time, frequency and complex domain specifications and for zero placing, a geometric criteria is developed in which real zeros can be placed arbitrarily by varying the angle (ρ).

Following GA parameters are used to compute the OGDTMs to design a PID controller $C_\delta(\gamma) = k_p + k_d\,\gamma + \frac{k_i}{\gamma}$, where k_p, k_d and k_i are proportional, derivative and integral constants.

- Method of selection : Tournament selection method
- Number of tournaments: 2
- Number of generation for evolution: 30
- Population size : 31
- Crossover probability: 0.77
- Number of crossover : 2
- Mutaion probability: 0.0077

In Table 3.1, the parameters of the reference model with ω_n = 0.85 rad/sec. and damping ratio ξ =0.7 and PID controller transfer functions are shown for different sampling time Δ=0.1 sec., 0.01sec. and 0.001 sec. corresponding to the plant models obtained at these sampling frequencies. The reference models zeros are placed by varying the angle ρ and the controller parameters are computed from OGDTMs. In Table 3.2 a comparison of the pole zero locations of the reference model and the closed loop system for the same Δ, ρ and μ_i are presented. From the table it may be seen that the pole zero are appropriately matched. Table 3.3 shows the time domain specifications of the reference model and the closed loop system while Table 3.4 shows the frequency domain part of the same. It may be seen from both the tables (3.3 & 3.4) that time and frequency domain specifications of the reference model and the closed loop system with PID controller closely match. Comparison of the step responses, pole zero plot and the frequency domain Nyquist plot of the reference model and the closed loop system with the above PID setting are presented in figure 3.6 – 3.17 which match the response characteristics closely. This depicts the efficacy of the proposed OGDTM for classical control design in the complex delta domain.

Table – 3.1

Δ	ρ	OGDTM (μ_t)	Reference Model $M_\delta(\gamma)$	Controller $C_\delta(\gamma)$
0.1	+50°	0.8768	$\frac{1.2617\gamma+0.6653}{\gamma^2+1.176\gamma+0.6653}$	$1.173+0.46936\gamma+\frac{4.041}{\gamma}$
0.1	+20°	0.7168	$\frac{0.7937\gamma+0.6653}{\gamma^2+1.176\gamma+0.6653}$	$1.1094+0.24336\gamma+\frac{1.5006}{\gamma}$
0.1	-20°	0.3314	$\frac{0.38226\gamma+0.6653}{\gamma^2+1.176\gamma+0.6653}$	$0.61987+0.12309\gamma+\frac{0.83282}{\gamma}$
0.1	-40°	0.4572	$\frac{0.11368\gamma+0.6653}{\gamma^2+1.176\gamma+0.6653}$	$0.3723+0.018427\gamma+\frac{0.62846}{\gamma}$
0.01	-40°	0.3471	$\frac{0.08877\gamma+0.7015}{\gamma^2+1.176\gamma+0.7015}$	$0.3417+0.02127\gamma+\frac{0.6459}{\gamma}$
0.001	-40°	0.3471	$\frac{0.0849\gamma+0.7052}{\gamma^2+1.176\gamma+0.7052}$	$0.3383+0.02166\gamma+\frac{0.6478}{\gamma}$

:

Table –3.2

Δ	ρ	Closed Loop System : $G_\delta(\gamma)$	Zeros	Poles
0.1	+50°	$\frac{0.061735\gamma^3+1.3124\gamma^2+3.4327\gamma+9.9668}{1.0617\gamma^3+4.8558\gamma^2+5.8992\gamma+9.9668}$	-18.7519 -1 2531 ± 2 6532i	-3.7598 -0.4069 ± 1.5268i
0.1	+20°	$\frac{0.032009\gamma^3+0.74615\gamma^2+2.9336\gamma+3.7013}{1.032\gamma^3+4.2896\gamma^2+5.4001\gamma+3.7013}$	-18.7519 -2.2793± 0.9854i	-2.7162 -0.7201 ± 0 8954i
0.1	-20°	$\frac{0.01619\gamma^3+0.38513\gamma^2+1.6384\gamma+2.0541}{1.0162\gamma^3+3.9286\gamma^2+4.1049\gamma+2.0541}$	-18.7519 -2.5179 ± 0.6527i	-2.6179 -0.5701 ± 0.5443i
0.1	-40°	$\frac{0.002424\gamma^3+0.09441\gamma^2+1.0009\gamma+1.5501}{1.0024\gamma^3+3.6379\gamma^2+3.4674\gamma+1.5501}$	-18.7519 -18.3451 , -1.8591	-2.4889 -0.3807 ± 0.3854i
0.01	-40°	$\frac{\mathbf{0.0003148\gamma^3+0.0676\gamma^2+1.0143\gamma+1.899}}{\mathbf{1.0003\gamma^3+4.0181\gamma^2+3.955\gamma+1.8995}}$	-198.6 -138.7 , -2.19	-0.0287 -0.1387±0.0058i
0.001	-40°	$\frac{\mathbf{0.000324\gamma^3+0.06536\gamma^2+1.0138\gamma+1.9336}}{\mathbf{\gamma^3+4.0604\gamma^2+4.0078\gamma+1.9396}}$	-1858.1 -3.4 , -2.2	-0.0029 -0.0006 ±0.0006i

Table -3.3

Δ	ρ	μ_t	t_p/Δ			t_s/Δ			Mp%			Status
			plant	Ref. Model	C-L system	plant	Ref. Model	C-L system	plant	Ref. Model	C-L system	
0.1	+50°	0.8768	22	26	21	15	58	123	1.88	25.69	40.06	Stable
0.1	+20°	0.7168	22	35	29	15	61	46	1.88	10.52	10.39	Stable
0.1	-20°	0.3314	22	46	45	15	66	63	1.88	5.31	5.3159	Stable
0.1	-40°	0.4572	22	52	53	15	70	72	1.88	4.62	4.74	Stable
0.01	-40°	0.3471	221	51	518	158	700	714	1.88	4.62	4.68	Stable
0.001	-40°	0.3471	2221	51092	5173	1588	7126	7256	1.88	4.83	4.88	Stable

Table-3.4

Δ	ρ	Gain Margin			Phase Margin		
		plant	Ref. Model	C-L System	plant	Ref. Model	C-L System
0.1	+50°	28.64	∞	∞	∞	60.22	27.08
0.1	+40°	28.64	∞	∞	∞	67.07	62.27
0.1	-20°	28.64	∞	∞	∞	68.14	67.49
0.1	-40°	28.63	796.4	∞	∞	65.68	65.65
0.01	-40°	268.4	∞	∞	∞	66.14	66.19
0.001	-40°	2668	∞	∞	∞	66.19	66.25

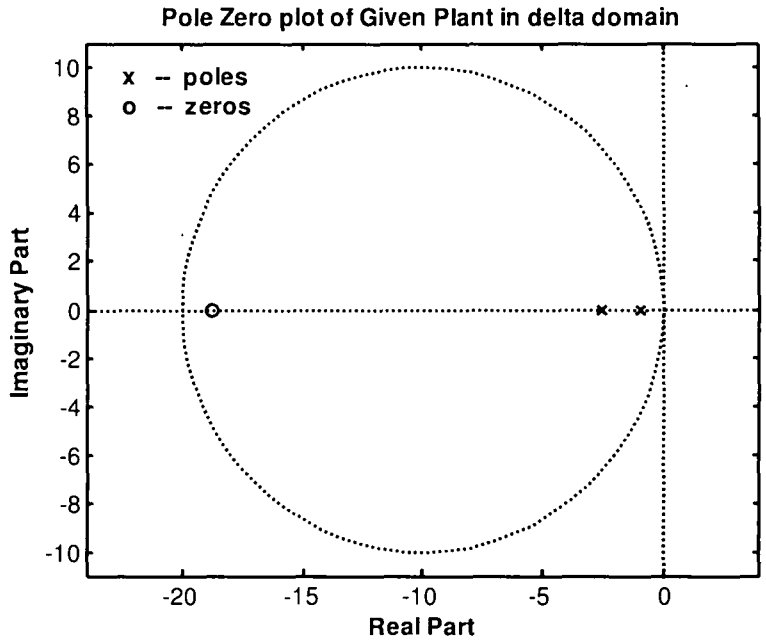

Figure 3.6: Pole zero plot of given plant in delta domain with sampling time Δ=0.1 sec

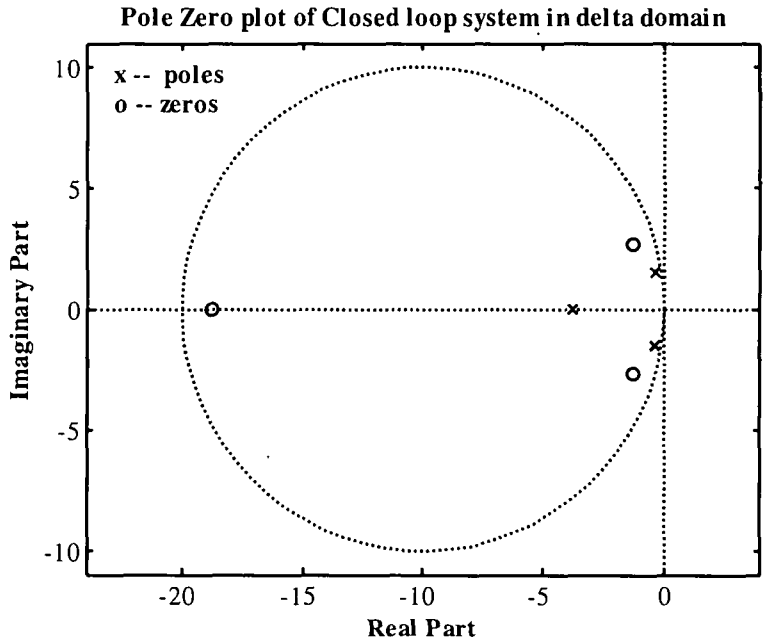

Figure 3.7 : Pole zero plot of closed loop system in delta domain with Δ=0.1, ω_n=0.84 rad/sec, ξ=0.7, ρ=+50° & optimal frequency point μ_t=0.8768

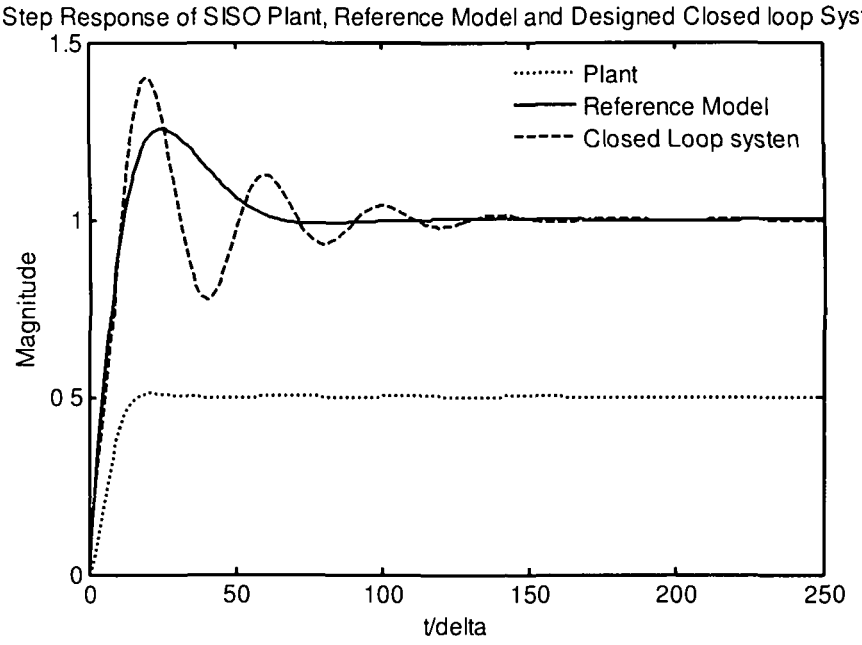

Figure 3.8: Step responses of reference model, open loop and closed loop plant with PID controller with Δ=0.1 sec, ω_n=0.84 rad/sec, ξ=0.7, ρ=+50° & optimal frequency point μ_t=0.8768

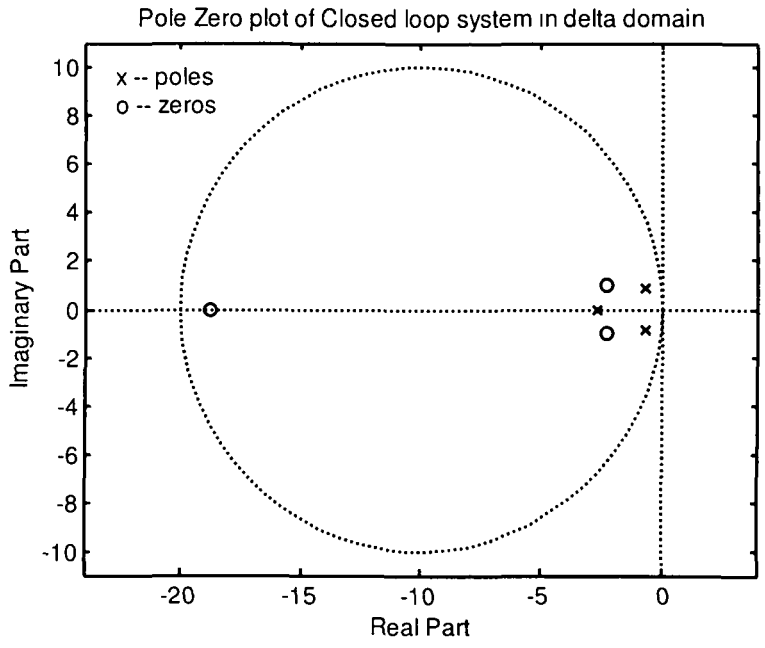

Figure 3.9 : Pole zero plot of closed loop system in delta domain with Δ=0.1, ω_n=0.84 rad/sec, ξ=0.7, ρ=+20° & optimal frequency point μ_t=0.7168

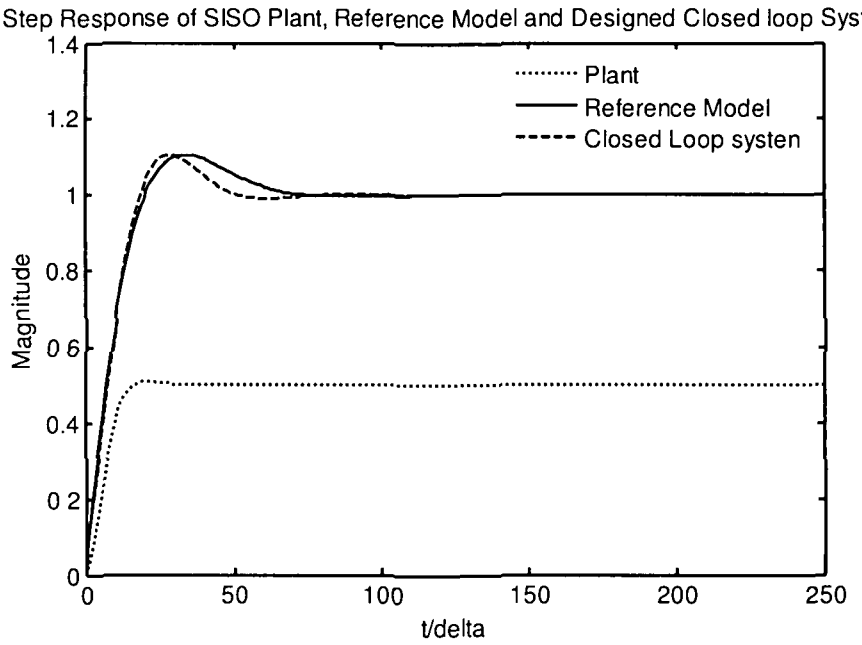

Figure 3.10 : Step responses of reference model, open loop and closed loop plant with PID controller with Δ=0.1 sec, ω_n=0.84 rad/sec, ξ=0.7, ρ=+20° & optimal frequency point μ_t=0.7168

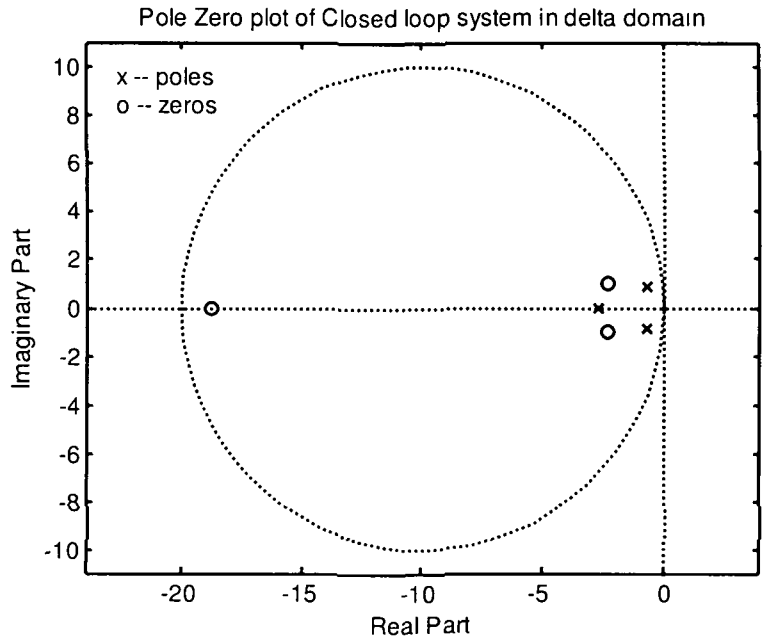

Figure 3.11 : Pole zero plot of closed loop system in delta domain with Δ=0.1, ω_n=0.84 rad/sec, ξ=0.7, ρ= -20° & optimal frequency point μ_t=0.3314

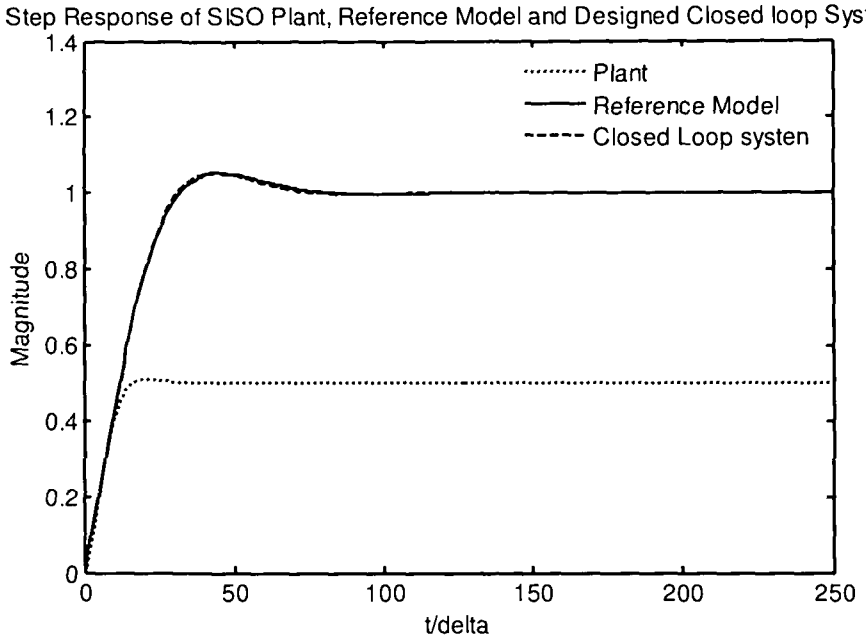

Figure 3.12 : Step responses of reference model, open loop and closed loop plant with PID controller with Δ=0.1 sec, ω_n=0.84 rad/sec, ξ=0.7, ρ=-20° & optimal frequency point μ_t=0.3314

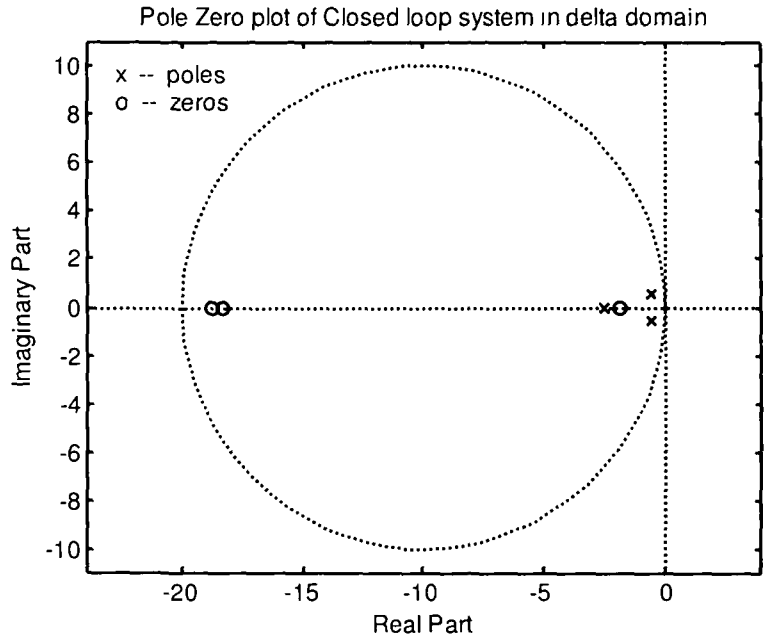

Figure 3.13 : Pole zero plot of closed loop system in delta domain with Δ=0.1, ω_n=0.84 rad/sec, ξ=0.7, ρ= -40° & optimal frequency point μ_t=0.4572

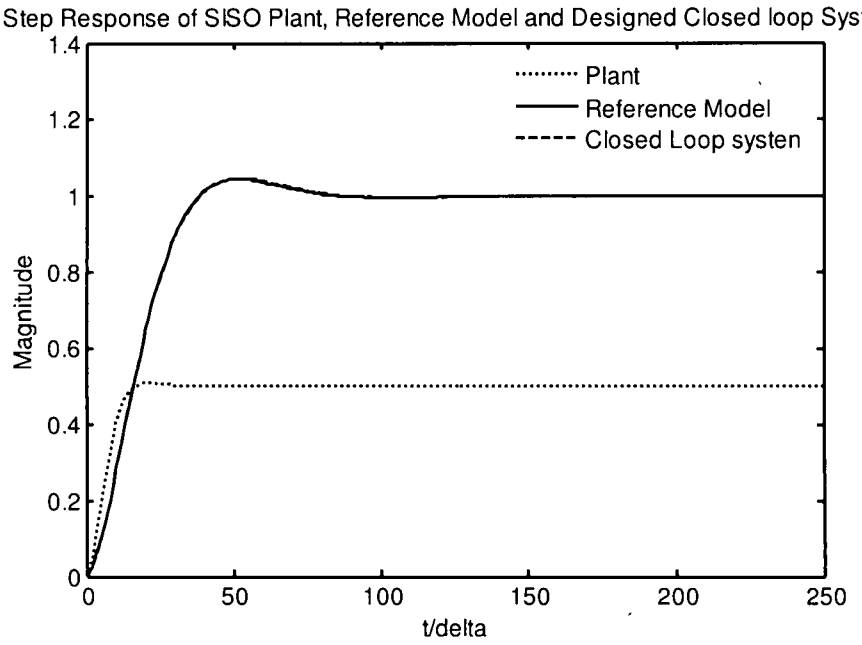

Figure 3.14 : Step responses of reference model, open loop and closed loop plant with PID controller with Δ=0.1 sec, ω_n=0.84 rad/sec, ξ=0.7, ρ=-40° & optimal frequency point μ_t=0.4572

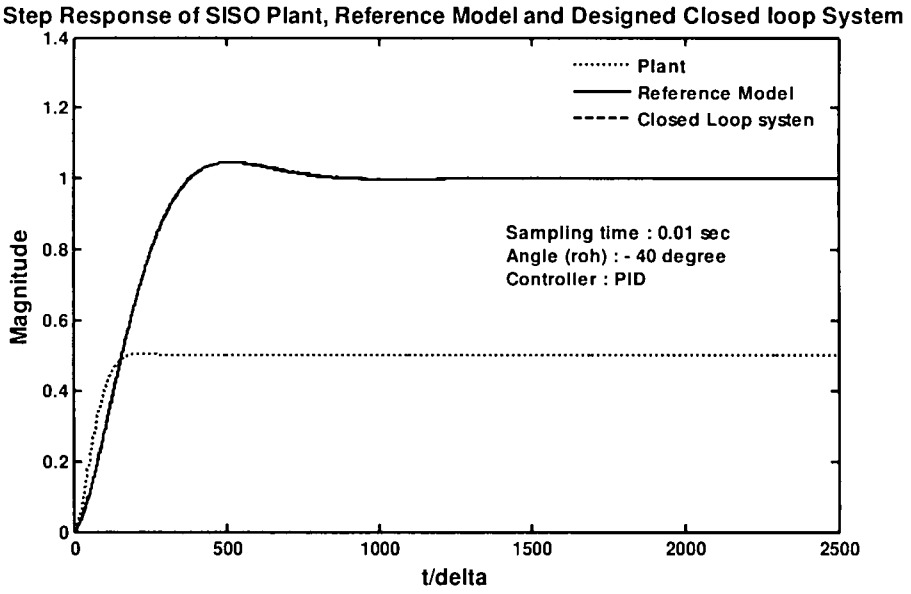

Figure 3.15 : Step responses of reference model, open loop and closed loop plant with PID controller with Δ=0.01 sec, ω_n=0.84 rad/sec, ξ=0.7, ρ=- 40° & optimal frequency point μ_t=0.3471

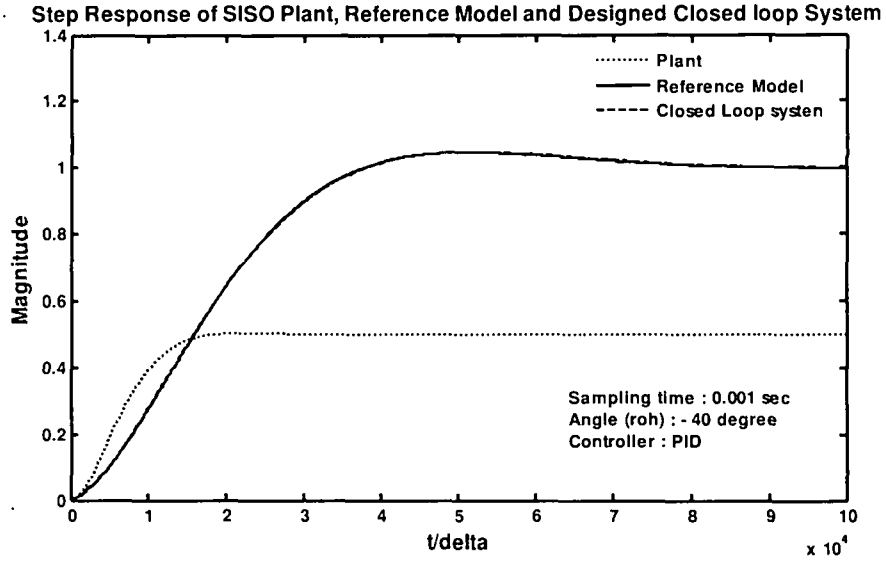

Figure 3.16 : Step responses of reference model, open loop and closed loop plant with PID controller with Δ=0.001 sec, ω_n=0.84, ξ=0.7, ρ=- 40° & optimal frequency point μ_t=0.3471

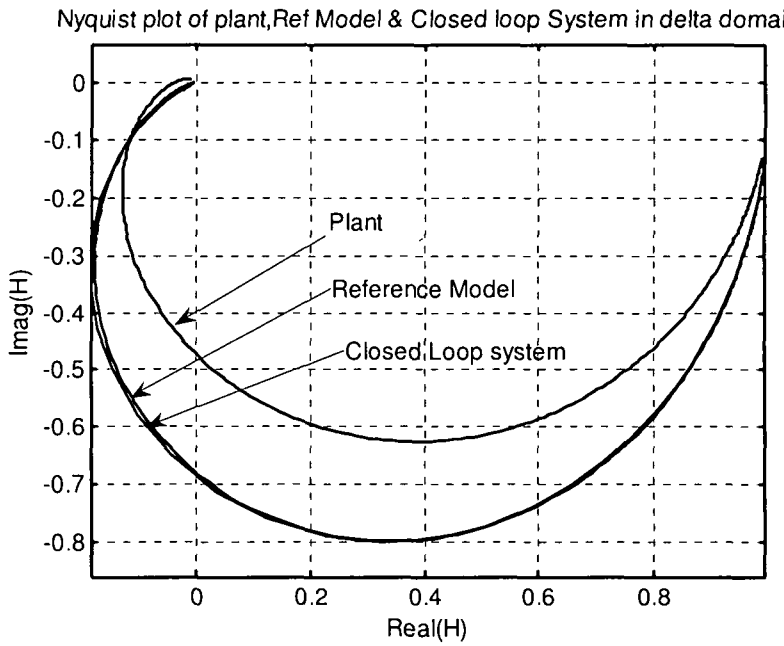

Figure 3.17 : Nyquist plots of reference model, open loop and closed loop plant with PID controller with Δ=0.1 sec, ω_n=0.84 rad/sec, ξ=0.7, ρ=-40° & optimal frequency point μ_t=0.4572

3.5.6.2 Higher order plant:

For testing the robustness of the OGDTM technique, mow we consider a sixth order transfer function of a typical open loop helicopter engine given by [116]

$$P_c(s) = \frac{248.04\,s^4 + 1483.339\,s^3 + 91930.803\,s^2 + 468732.64\,s + 634950.95}{s^6 + 26.2401\,s^5 + 1363.07\,s^4 + 26802.8\,s^3 + 326900\,s^2 + 859173\,s + 528055} \quad (3.67)$$

The open loop step response of the helicopter engine transfer function given in eqan. (3.67) is found to be oscillatory in nature. To compensate the engine, a controller is required to be designed. In this example also the OGDTM mothedology will be used to design a digital PID controller in the delta domain.

The helicopter engine transfer function is therefore discretised incorporating a sampler and ZOH with sampling periods Δ = 0.01 & 0.1 seconds respectively and corresponding to these sampling periods, the coefficients of second order reference model in delta domain is computed for ω_n = 0.84 rad/sec and ξ = 0.7 by varying the position of zero locations at different angle (ρ).

For computation of the OGDTMs, the following GA parameters are considered

- Method of selection : Roulette wheel
- Number of generation for evolution: 35
- Population size : 31
- Crossover probability: 0.8
- Number of crossover : 2
- Mutaion probability: 0.008

The plant transfer function and subsequent reference model sampled with different sampling time are given as under:

• Sampling time (Δ) = 0.01 seconds and angle (ρ) = - 40 degree

$$P_\delta(\gamma) = \frac{1.152\,\gamma^5 + 233.837\,\gamma^4 + 2559.328\,\gamma^3 + 88308.615\,\gamma^2 + 421544.924\,\gamma + 552166.985}{\gamma^6 + 36.2\,\gamma^5 + 1574.684\,\gamma^4 + 29215.76\,\gamma^3 + 303273.399\,\gamma^2 + 761032.006\,\gamma + 459207.971} \quad (3.68)$$

$$M_\delta(\gamma) = \frac{0.087658\,\gamma + 0.70146}{\gamma^2 + 1.1761\,\gamma + 0.70146} \quad (3.69)$$

Applying GA, the Optimal GDTM Point (μ_t) is found to be 0.6303 and at this optimal frequency point the parameters of required PID controller is computed as:

$$C_\delta(\gamma) = 0.0037587 - 0.00067514\,\gamma + \frac{0.54818}{\gamma} \qquad (3.70)$$

• Sampling time (Δ) = 0.01 seconds and angle (ρ) = +20 degree

Since sampling time is same hence $p_\delta(\gamma)$ will also be same as in (3.68) however the parameters of reference model will vary since the location of zero has been changed due to change in angle (ρ)

$$M_\delta(\gamma) = \frac{0.80512\,\gamma + 0.70146}{\gamma^2 + 1.1761\,\gamma + 0.70146} \qquad (3.71)$$

Using GA, the Optimum GDTM Point (μ_t) is found to be 0.8820 and parameters of the desired PID controller is computed as

$$C_\delta(\gamma) = 0.2899 + 0.0010384\,\gamma + \frac{1.315}{\gamma} \qquad (3.72)$$

The unit step responses of the reference model and closed-loop system in delta domain are shown in Figure 3.18 &3.19 respectively.

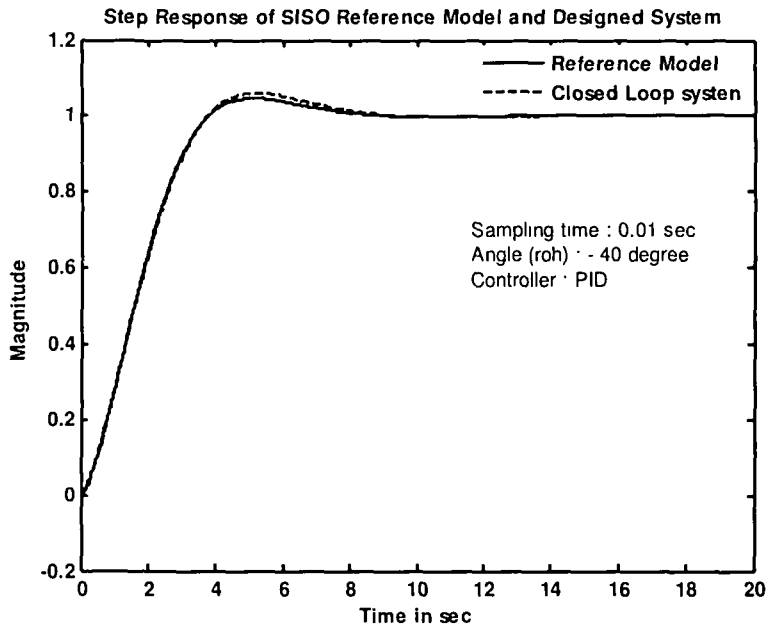

Figure 3.18: Step responses of reference model, open loop and closed loop plant with PID controller with Δ=0.01 sec, ω_n=0.84 rad/sec, ξ=0.7, ρ=- 40° & optimal frequency point μ_t=0.6303

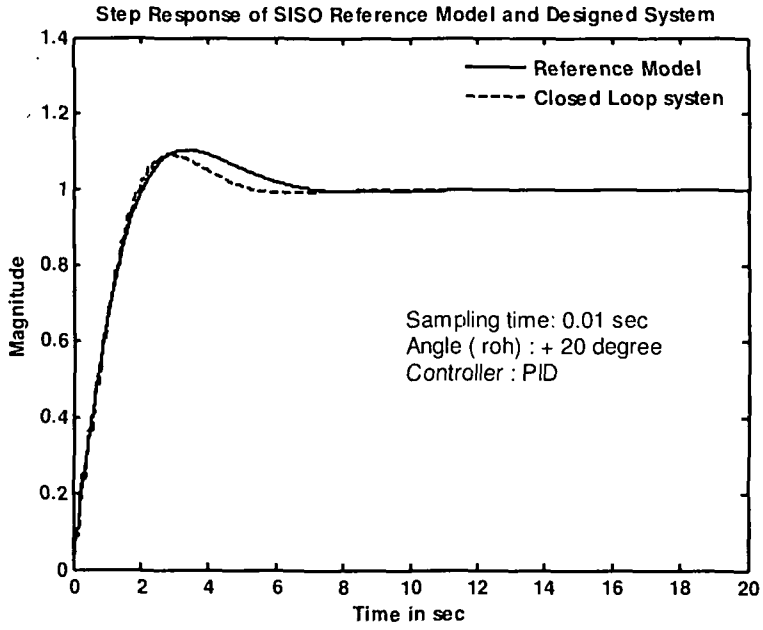

Figure 3.19: Step responses of reference model, open loop and closed loop plant with PID controller with Δ=0.01 sec, ω_n=0.84 rad/sec, ξ=0.7, ρ=+20° & optimal frequency point μ_t=0.8820

- **Sampling time (Δ) = 0.1 seconds and angle (ρ) = - 40 degree**

$$P_\delta(\gamma) = \frac{3.035\,\gamma^5 + 147.94\,\gamma^4 + 2715.6\,\gamma^3 + 22616.18\,\gamma^2 + 68142.71\,\gamma + 67413.16}{\gamma^6 + 59.03\,\gamma^5 + 1295.98\,\gamma^4 + 13131.16\,\gamma^3 + 61840.89\,\gamma^2 + 109345.43\,\gamma + 56063.95} \tag{3.73}$$

Corresponding reference model is

$$M_\delta(\gamma) = \frac{0.11368\,\gamma + 0.6653}{\gamma^2 + 1.1761\,\gamma + 0.6653} \tag{3.74}$$

Setting the above parameters of GA, the Optimum GDTM Point (μ_t) is found to be 0.5910 and we obtain the parameters of desired PID controller as

$$C_\delta(\gamma) = 0.037179 - 0.003178\,\gamma + \frac{0.53276}{\gamma} \tag{3.75}$$

The unit step responses of the reference model and closed-loop system in delta domain are shown in Figure 3.20.

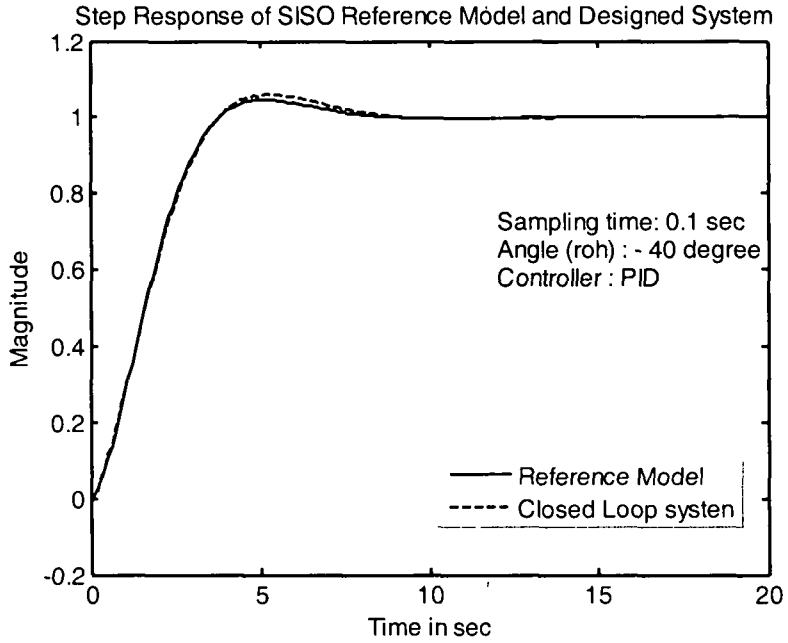

Figure 3.20 : Step responses of reference model, open loop and closed loop plant with PID controller with Δ=0.1 sec, ω_n=0.84 rad/sec, ξ=0.7, ρ=- 40° & optimal frequency point μ_t=0.5910

- **Sampling time (Δ) = 0.1 seconds and angle (ρ) = +20 degree**

Since sampling time is the same, hence $p_\delta(\gamma)$ will also be the same as in (3.73) however the parameters of reference model will change due to change in location of zero. The referemce model transfer function is given as:

$$M_\delta(\gamma) = \frac{0.79375\,\gamma + 0.6653}{\gamma^2 + 1.1761\,\gamma + 0.6653} \qquad (3.76)$$

Using GA for given set of parameters, the Optimum GDTM Point (μ_t) is found to be 0.7640 and corresponding PID controller transfer function is given as

$$C_\delta(\gamma) = 0.3272 + 0.0049804\,\gamma + \frac{1.2548}{\gamma} \qquad (3.77)$$

The unit step responses of the reference model and closed-loop system in delta domain are shown in Figure 3.21.

The various time and frequency domain performance specifications for the controller parameters at different sampling time and different angle (ρ) are given in Table 3.5.

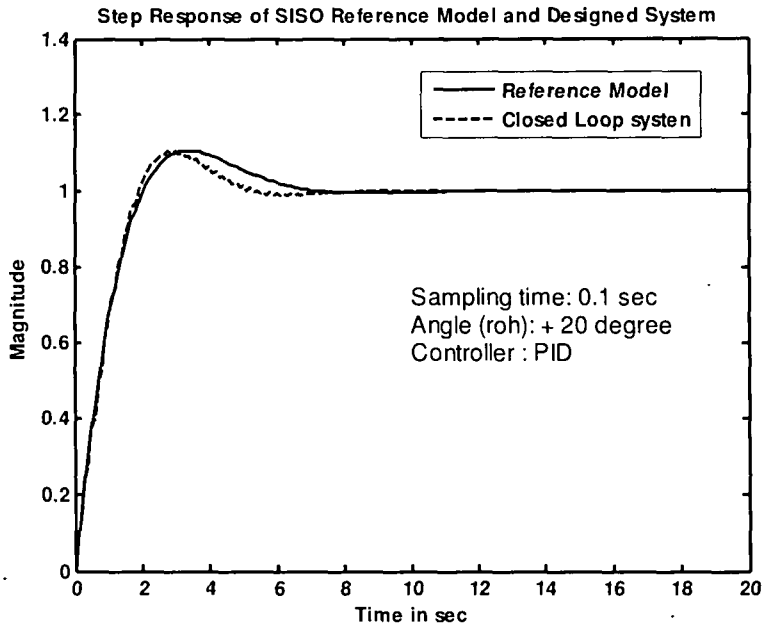

Figure 3.21 : Step responses of reference model, open loop and closed loop plant with PID controller with Δ=0.1 sec, ω_n=0.84 rad/sec, ξ=0.7, ρ= +20° & optimal frequency point μ_t=0.7640

Table 3.5:

Δ (Sec.)	Angle (ρ)	OGDTM (μ_{ti})	%MP	t_p/Δ	t_r/Δ	t_s/Δ	GM	PM
0.01	- 40°	0.6306	0.0	456	737	940	249.9	66.49
0.01	+ 20°	0.8820	0.0	421	712	898	30.47	83.14
0.1	- 40°	0.5910	42.16	19	21	44	03.94	38.82
0.1	+ 20°	0.7640	30.92	37	84	95	03.77	22.53

3.5.6.3 Closed loop oscillatory plant :

To illustrate the methodology of the OGDTM scheme described above, another simple continuous time plant J.Pal [76] is taken as

$$G_c = \frac{200}{2s^2 + 10s + 100} \tag{3.78}$$

The Closed loop step response of the transfer function is oscillatory and therefore to compensate the plant it is desired to design a digital PID controller in the delta domain. The plant TFs is therefore discretised incorporating a sampler and zero

order hold (ZOH) with sampling periods $\Delta = 0.1$sec. and corresponding plant transfer function in delta domain is given in eqan. (3.79). The parameters of the reference model for $\omega_n = 0.84$ rad/sec and $\xi = 0.7$ & 0.5 is computed for different zero locations i.e at different angle (ρ) in delta domain.

. The following GA parameters are considered to compute OGDTM (μ_{ti}) values

- Method of selection : Roulette wheel
- Number of generation for evolution: 30
- Population size : 31
- Crossover probability: 0.77
- Number of crossover : 2
- Mutaion probability: 0.0077

Applying GA with above parameters and by varying the zero locations of reference model i.e. by changing the angel ρ, different OGDTMs are computed. The resulting discrete-time plant and 2nd order reference model, PID controller and Closed loop control system TFs, pole zero locations of closed loop system, time and frequency domain specifications are shown in Table 3.6 – 3.9 as under:

Plant transfer function in delta domain: $$P_\delta(\gamma) = \frac{4.0926\gamma + 75.4824}{\gamma^2 + 7.7088\gamma + 37.7412} \qquad (3.79)$$

Table – 3.6

$\omega_n = 0.84$ and $\xi = 0.7$				
Δ	ρ	OGDTM (μ_t)	$M_\delta(\gamma)$	$C_\delta(\gamma)$
0.1	+30°	0.9857	$\frac{0.91437\gamma + 0.6653}{\gamma^2 + 1.176\gamma + 0.6653}$	$0.06163 + 0.02804\gamma + \frac{0.7645}{\gamma}$
0.1	+10°	0.9528	$\frac{0.6877\gamma + 0.6653}{\gamma^2 + 1.176\gamma + 0.6653}$	$0.01957 - 0.01639\gamma + \frac{0.5338}{\gamma}$
0.1	-20°	0.9135	$\frac{0.3823\gamma + 0.6653}{\gamma^2 + 1.176\gamma + 0.6653}$	$0.03068 - 0.01273\gamma + \frac{0.3596}{\gamma}$
0.1	-40°	0.7404	$\frac{0.1137\gamma + 0.6653}{\gamma^2 + 1.176\gamma + 0.6653}$	$0.07185 - 0.01620\gamma + \frac{0.2773}{\gamma}$
$\omega_n = 0.84$ and $\xi = 0.5$				
0.1	-40°	0.4651	$\frac{0.06084\gamma + 0.2414}{\gamma^2 + 0.7002\gamma + 0.2414}$	$-0.08324 + 0.02657\gamma + \frac{0.1641}{\gamma}$

Table –3.7

$\omega_n = 0.84$ and $\xi = 0.7$				
Δ	ρ	**Closed Loop System : $G_\delta(\gamma)$**	**Zero Location**	**Pole Locations**
0.1	+30°	$\frac{0.1148\gamma^3 + 1.8644\gamma^2 - 1.5232\gamma + 57.7031}{1.1148\gamma^3 + 9.5732\gamma^2 + 36.218\gamma + 57.7031}$	-18.4436 1.0989 ±5.1043i	-3.5406 -2.5235 ± 2.8725i
0.1	+30°	$\frac{0.0671\gamma^3 + 1.1576\gamma^2 + 0.7071\gamma + 40.294}{1.0671\gamma^3 + 8.8665\gamma^2 + 38.4483\gamma + 40.294}$	-18.4436 0.5969 ± 5.6743i	-1.4465 -3.4312 ± 3.7856i
0.1	-20°	$\frac{0.05208\gamma^3 + 0.8349\gamma^2 - 0.8447\gamma + 27.1427}{1.0521\gamma^3 + 8.5438\gamma^2 + 36.8965\gamma + 27.1428}$	-18.4436 1.2058 ± 5.1772i	-0.9037 -3.6086 ± 3.9403i
0.1	-40°	$\frac{0.06631\gamma^3 + 0.9289\gamma^2 - 4.2883\gamma + 20.9301}{1.0663\gamma^3 + 8.6377\gamma^2 + 33.4529\gamma + 20.9301}$	-18.4436 2.2173 ± 3.4926i	-0.7612 -3.6697 ± 3.5099i
$\omega_n = 0.84$ and $\xi = 0.5$				
0.1	-40°	$\frac{0.10873\gamma^3 + 1.6647\gamma^2 - 5.6166\gamma + 12.3835}{1.1087\gamma^3 + 9.3735\gamma^2 + 32.1295\gamma + 12.3835}$	-18.4436 1.5666 ± 1.9290i	-0.4386 -4.0078 ± 3.0659i

Table-3.8

$\omega_n = 0.84$ and $\xi = 0.7$												
Δ	ρ	μ_t	t_p/Δ			t_s/Δ			Mp%			**Status**
			plant	**Ref. Model**	**C-L system**	**plant**	**Ref. Model**	**C-L system**	**plant**	**Ref. Model**	**C-L system**	
0.1	+30°	0.9857	4	32	15	156	60	18	88.86	13.54	7.24	Stable
0.1	+10°	0.9528	4	38	23	156	62	28	88.86	8.45	0	Stable
0.1	-20°	0.9135	4	46	25	156	66	45	88.86	5.31	0	Stable
0.1	-40°	0.7404	4	52	25	156	70	55	88.86	4.62	0	Stable
$\omega_n = 0.84$ and $\xi = 0.5$												
0.1	-40°	0.4651	4	87	25	156	118	95	88.86	4.62	0	Stable

Table-3.9

Δ	ρ	Gain Margin			Phase Margin		
		plant	**Ref. Model**	**C-L System**	**plant**	**Ref. Model**	**C-L System**
0.1	+30°	1.14	∞	2.65	4.53	65.58	64.66
0.1	+40°	1.14	∞	4.59	4.53	68.02	75.34
0.1	-20°	1.14	∞	5.47	4.53	68.14	78.16
0.1	-40°	1.14	796.41	4.23	4.53	65.68	75.26
$\omega_n = 0.84$ and $\xi = 0.5$							
0.1	-40°	1.14	∞	4.66	4.53	65.89	76.60

The unit step responses of the uncompensated plant, reference model and closed-loop system in delta domain for different values of 'ρ' are shown in Figure 3.22 to 3.26.

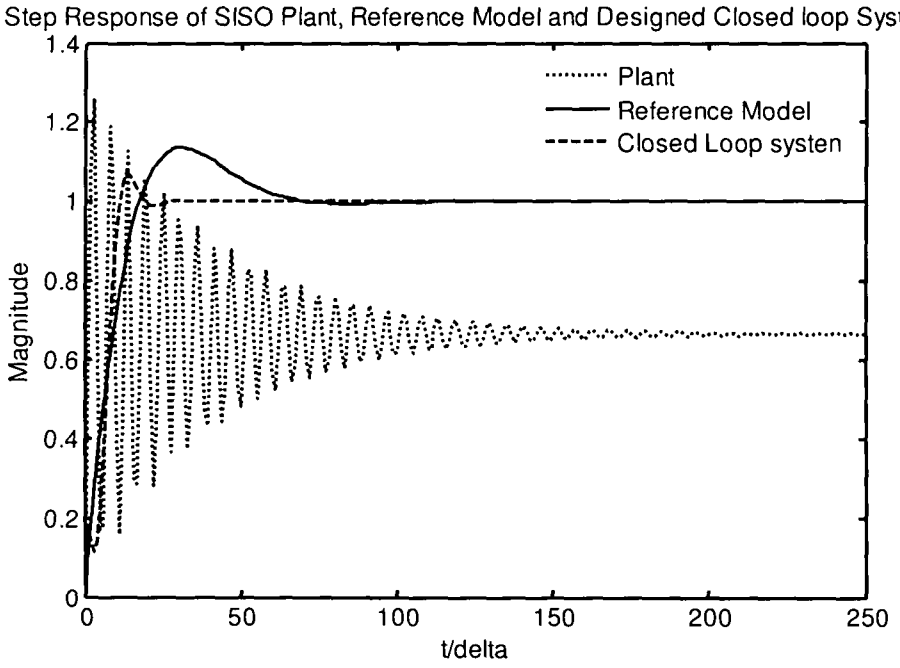

Figure 3.22 : Step responses of reference model, open loop and closed loop plant with PID controller with Δ=0.1, ρ=+30° & optimal frequency point μ_t=0.9857

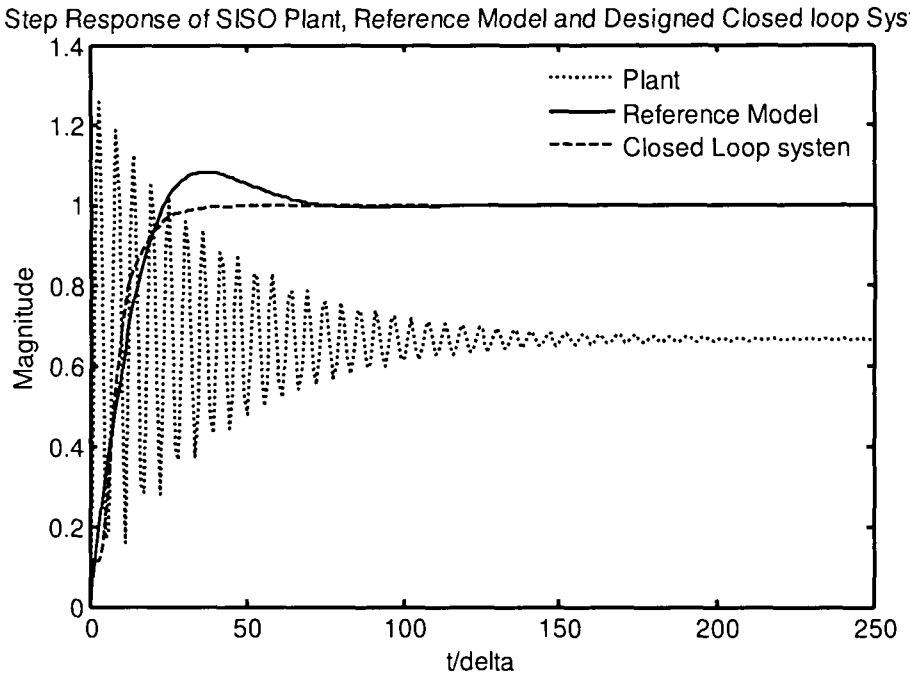

Figure 3.23 : Step responses of reference model, open loop and closed loop plant with PID controller with Δ=0.1, ρ=+10° & optimal frequency point μ_f=0.9528

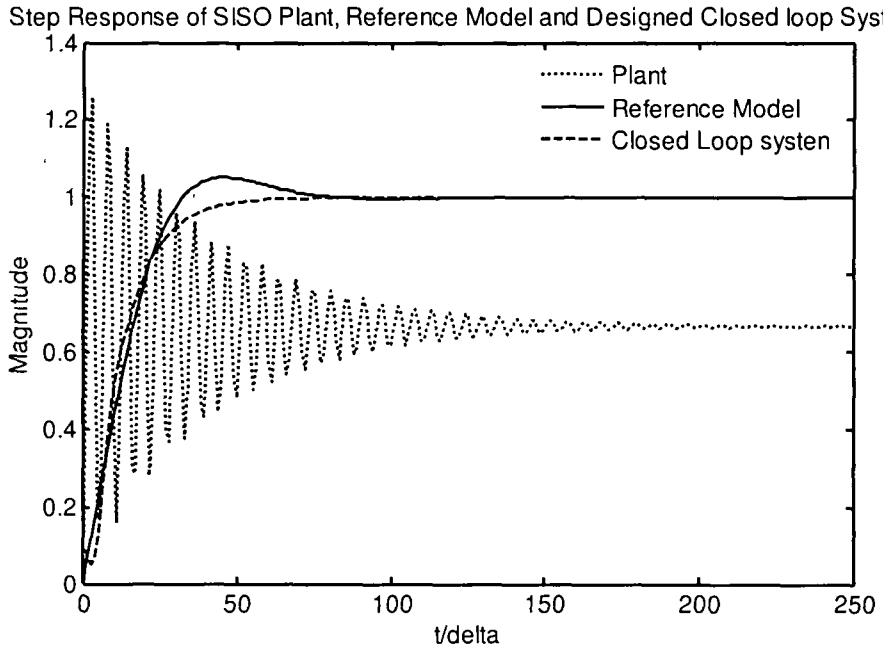

Figure 3.24 : Step responses of reference model, open loop and closed loop plant with PID controller with Δ=0.1, ρ=-20° & optimal frequency point μ_f=0.9135

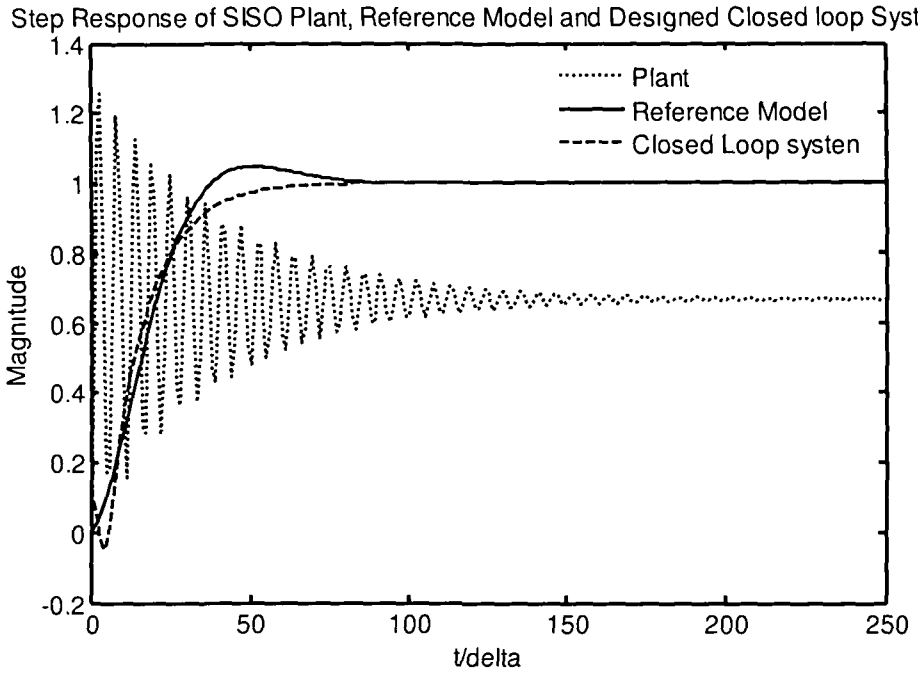

Figure 3.25 : Step responses of reference model, open loop and closed loop plant with PID controller with Δ=0.1, ρ=-40° & optimal frequency point μ_t=0.7404

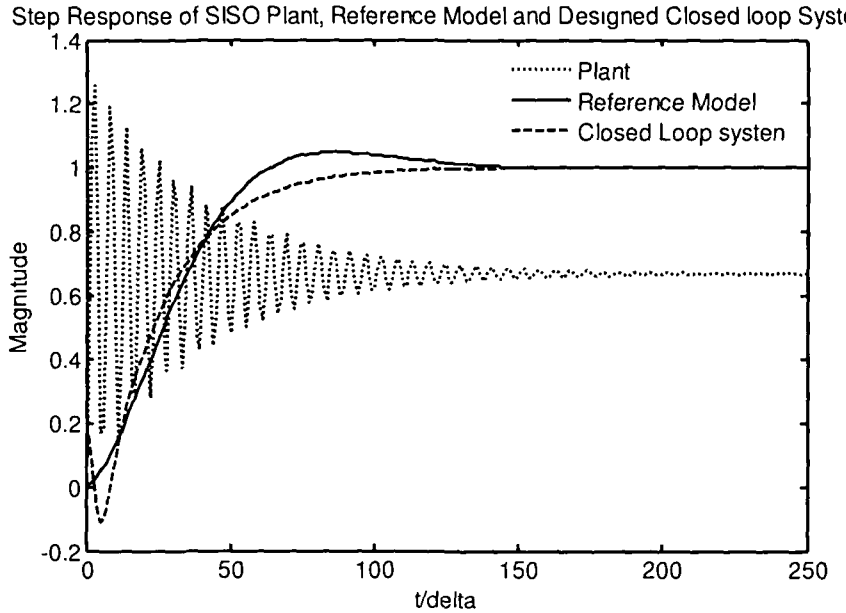

Figure 3.26 : Step responses of reference model, open loop and closed loop plant with PID controller with Δ=0.1, ρ=-40°, ξ=0.5 & optimal frequency point μ_r=0.4651

The Nyquist plot of uncompensated plant, reference model and closed-loop system and pole zero plot in delta domain are shown in Figure 3.27

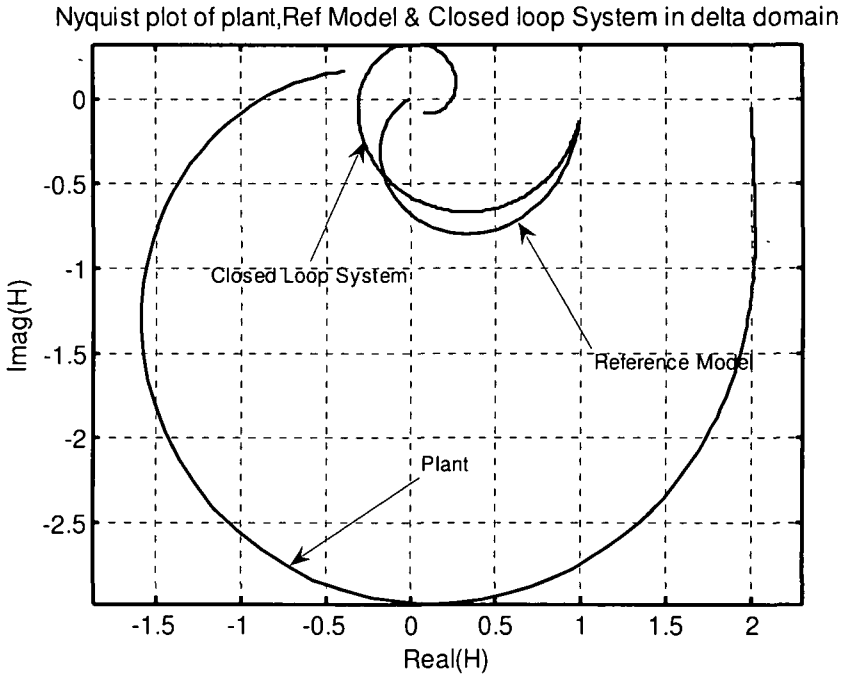

Figure 3.27 : Nyquist plot of plant, Reference model and plant with PID controller for Δ=0.1, ρ=-40°, ξ=0.7 & optimal frequency point μ_t=0.7404

3.6 Optimal Frequency Fitting method

In Optimal frequency fitting method, two transfer functions are matched at a number of frequency points in the low frequency range and the resultant linear algebraic equations are solved to arrive at a optimal frequency point. This method is based on approximate frequency fitting and the efficacy of the controller design greatly relies on the selection of complex frequency points in the complex delta domain and normally trial and error method is resorted to seek compromise. In the present work, genetic algorithm is used as an optimisation tool to find the optimal complex frequency points and hence Optimal Frequency Fitting. The computational algorithm of the design method is numerically stable at high sampling frequency and yields a continuous-time like controller, which depicts the advantage of delta operator modelling in control system design.

3.6.1 Frequency response in delta domain

The frequency response of the delta transfer function of equation 3.24 is defined as

$$G_\delta(\gamma)\Big|_{\gamma=\frac{e^{j\omega\Delta}-1}{\Delta}} = |G_\delta|e^{j\phi} \tag{3.80}$$

$$\gamma = \frac{e^{j\omega\Delta}-1}{\Delta} = |\gamma|e^{j\theta} \tag{3.81}$$

Where

ω is the frequency in rad /sec of the input sinusoidal signal

$|\gamma|$ and θ are the magnitude and phase of the transformed variable γ

$|G_\delta|$ and □ are magnitude and phase of the transfer function $G_\delta(\gamma)$

If the value of ωΔ is very small, $\frac{(e^{j\omega\Delta}-1)}{\Delta} \cong j\omega$ which shows that for large sampling frequency we get back the frequency response of the original continuous time system. This property of the delta operator unifies both discrete and continuous time systems.

3.6.2 Controller design :

The computation of controller parameters $C_\delta(\gamma)$ using optimal frequency fitting is not straight forward. First of all the frequency response of the open loop reference model $F_\delta(\gamma)$ is computed at optimum frequency points depending upon the number of controller parameters that are to be evaluated. Since the plant $P_\delta(\gamma)$ is known, its frequency response is also known and may be computed at the same frequency points as those of the open loop reference model. The frequency response of the controller may therefore be computed from those of the plant $P_\delta(\gamma)$ and the open loop reference model $F_\delta(\gamma)$ at those optimum frequency points. The frequency points of interest are computed using genetic algorithm so that the augmented system with controller matches the steady state frequency response of the chosen reference model closely. The computational procedure is now depicted in the following steps:

Step 1: We choose a closed-loop reference model TF, $M_\delta(\gamma)$ that satisfies the desired specifications and also select a controller transfer function as

$$C_\delta(\gamma) = \frac{\beta_0 + \beta_1\gamma + \cdots + \beta_p\gamma^p}{\alpha_0 + \alpha_1\gamma + \cdots + \alpha_q\gamma^q} \tag{3.82}$$

The unknown parameters β_i & α_i of the controller are to be determined and in general $p \le q$.

- **Step 2:** Let the performance index $PI = \sum_{i=0}^{n}(y_{ref_i}^2 - y_{cl_i}^2)$, where y_{ref} and y_{cl} are the step responses of the reference model and the closed loop over all controlled system.
- **Step 3:** Setting the parameters of GA (number of parameters , number of population, crossover probability, Mutation probability etc.) and run the GA and compute μ_{ii}
- **Step 4 :** Referring to the Figure 3.2, the closed-loop TF, may be written as

$$G_\delta(\gamma) = \frac{P_\delta(\gamma)C_\delta(\gamma)}{1 + P_\delta(\gamma)C_\delta(\gamma)}$$

The closed-loop system is to satisfy the reference model specifications, so $G_\delta(\gamma)$ should be equivalent to $M_\delta(\gamma)$ in some sense. In the proposed method we find $C_\delta(\gamma)$ such that $G_\delta(\gamma)$ and $M_\delta(\gamma)$ have identical *(p+q+2)* Optimum frequency points. i.e.,

$$G_\delta(\gamma)\big|_{\gamma=\mu_{ii}} \triangleq M_\delta(\gamma)\big|_{\gamma=\mu_{ii}} \text{ for } i \in [1,(p+q+2)] \tag{3.83}$$

- **Step 5:** From $M_\delta(\gamma)$ we find the equivalent open loop model $F_\delta(\gamma)$ using equation (3.84). Then $F_\delta(\gamma)$ along with a unity negative feedback would equal $M_\delta(\gamma)$. Thus

$$F_\delta(\gamma) = \frac{M_\delta(\gamma)}{1 - M_\delta(\gamma)} = \frac{\sum_{j=0}^{k} d_j\gamma^j}{\sum_{j=0}^{l} c_j\gamma^j - \sum_{j=0}^{k} d_j\gamma^j} \tag{3.84}$$

- **Step 6:** Now the open-loop equivalent expression given in (3.85) is to be computed as

$$P_\delta(\gamma)C_\delta(\gamma) \triangleq F_\delta(\gamma) \quad or \quad C_\delta(\gamma) \triangleq \frac{F_\delta(\gamma)}{P_\delta(\gamma)} \tag{3.85}$$

$$C_\delta(\gamma) \triangleq X_\delta(\gamma) \tag{3.86}$$

Where $X_\delta(\gamma)$ is known, as both $F_\delta(\gamma)$ and $P_\delta(\gamma)$ are completely specified. In the above relation, $X_\delta(\gamma)$ cannot, in general, be used as the required controller. This is because $X_\delta(\gamma)$ may not be realizable and even if it is realizable, its order may be too high to be practically implemented.

- **Step 7:** Approximating the known $X_\delta(\gamma)$ and computing

$$C_\delta(\gamma)\Big|_{\gamma=\frac{e^{j\omega\Delta}-1}{\Delta}} \triangleq X_\delta(\gamma)\Big|_{\gamma=\frac{e^{j\omega\Delta}-1}{\Delta}} \tag{3.87}$$

and substituting equation (3.82) in (3.87) with $\alpha_q = 1$, we get,

$$\sum_{i=0}^{p}\beta_i|\gamma|^i e^{j\theta i} - |X_\delta| e^{j\phi}\sum_{i=1}^{q-1}\alpha_i|\gamma|^i e^{j\theta i} \cong |\gamma|^q |X_\delta| e^{j(\phi+\theta q)} \tag{3.88}$$

Where

$$\gamma = |\gamma| e^{j\theta} \qquad and \qquad X_\delta(\gamma) = |X_\delta| e^{j\phi}$$

Let us define the normalised frequency variable $\psi = \omega\Delta$, where ω is the angular frequency in rad/sec, therefore θ and ϕ are functions of ψ. Finally separately equating the real and the imaginary parts of equation (3.88) we get

$$\sum_{i=0}^{p}\beta_i R_i(\psi) - \sum_{i=1}^{q-1}\alpha_i S_i(\psi) \cong T(\psi) \tag{3.89}$$

$$\sum_{i=0}^{p}\beta_i U_i(\psi) - \sum_{i=1}^{q-1}\alpha_i V_i(\psi) \cong W(\psi) \tag{3.90}$$

where,

$$R_i(\psi) = |\gamma|^i \cos\theta i$$

$$S_i(\psi) = |X_\delta||\gamma|^i \cos(\theta i + \phi)$$

$$U_i(\psi) = |\gamma|^i \sin\theta i$$

$$V_i(\psi) = |X_\delta||\gamma|^i \cos(\theta i + \phi)$$

$$T(\psi) = |X_\delta||\gamma|^r \cos(\theta q + \phi)$$

$$W(\psi) = |X_\delta||\gamma|^r \sin(\theta q + \phi)$$

The left hand side expressions of eqns. (3.89) and (3.90) are real function of ψ with unknown coefficients β_i and α_i and $T(\psi)$ and $W(\psi)$ are two real known functions

of ψ. Hence designating the l.h.s functions of equations (3.89) and (3.90) as $\Phi_R(\psi)$ and $\Phi_I(\psi)$ respectively, relations may be written for convenience as:

$$\Phi_R(\psi) \cong T(\psi) \tag{3.91}$$

$$\Phi_I(\psi) \cong W(\psi) \tag{3.92}$$

In order to force two real functions $\Phi_R(\psi)$ and $\Phi_I(\psi)$ to be equivalent to their approximates $-T(\psi)$ and $W(\psi)$ respectively, one may equate approximate number of initial few terms of the corresponding Taylor series expansions about $\psi = 0$. Thus, to accomplish appropriate matching of the l.h.s. functions in eqns. (3.82) and (3.83) with the corresponding functions on the r.h.s, the initial N derivatives (where N is at least equal to (p+q+1)) of the corresponding functions are equated at $\psi = 0$ to get:

$$\frac{d^k}{d\psi^k}[\Phi_R(\psi)]\Big|_{\psi=0} = \frac{d^k}{d\psi^k}[T(\psi)]\Big|_{\psi=0} \tag{3.93}$$

$$\frac{d^k}{d\psi^k}[\Phi_I(\psi)]\Big|_{\psi=0} = \frac{d^k}{d\psi^k}[W(\psi)]\Big|_{\psi=0} \quad ; \quad k \in [0, N-1] \tag{3.94}$$

Using the results of Pal, [76] the derivative operations $\Phi_R(\psi)$ approximately matches $T(\psi)$ if

$$\Phi_R(\psi)\Big|_{\psi=\psi_k} = T(\psi)\Big|_{\psi=\psi_k}; \qquad k \in [0, N-1] \tag{3.95}$$

where ψ_k are small positive values around $\psi = 0$. Similarly,

$$\Phi_I(\psi)\Big|_{\psi=\psi_k} = W(\psi)\Big|_{\psi=\psi_k}; \qquad k \in [0, N-1] \tag{3.96}$$

The relations in eqns. (3.95) and (3.96) may be written in a matrix form as

$$Ax = b \tag{3.97}$$

Here A is a $2(N) \times (p+q+1)$ matrix given by

$$A = \begin{bmatrix} R_{1,1} & R_{1,2} & \cdots & R_{1,p+1} & S_{1,1} & \cdots & S_{1,q} \\ U_{1,1} & U_{1,2} & \cdots & U_{1,p+1} & V_{1,1} & \cdots & V_{1,q} \\ \vdots & \vdots & \vdots & \vdots & \vdots & \vdots & \vdots \\ R_{i,1} & R_{i,2} & \cdots & R_{i,p+1} & S_{i,1} & \cdots & S_{i,q} \\ U_{i,1} & U_{i,2} & \cdots & U_{i,p+1} & V_{i,1} & \cdots & V_{i,q} \\ \vdots & \vdots & \vdots & \vdots & \vdots & \vdots & \vdots \\ R_{N,1} & R_{N,2} & \cdots & R_{N,p+1} & S_{N,1} & \cdots & S_{N,q} \\ U_{N,1} & U_{N,2} & \cdots & U_{N,p+1} & V_{N,1} & \cdots & V_{N,q} \end{bmatrix}$$

$$X = \left[\beta_0, \beta_1, \beta_2 \cdots \beta_p, \quad \alpha_0, \alpha_1, \alpha_2, \cdots \alpha_{q-1}\right]^T \tag{3.98}$$

$$b = \left[T_1 \cdots T_2 \cdots T_i \cdots T_N, \quad W_1 \cdots W_2 \cdots W_k \cdots W_N\right]^T \tag{3.99}$$

where

$$R_{i,j} = \left|\gamma^j\right| \cos\theta j$$
$$S_{i,k} = \left|X_\delta\right| \left|\gamma\right|^k \cos(\theta k + \phi)$$
$$U_{i,j} = \left|\gamma^j\right| \sin\theta j$$
$$V_{i,k} = \left|X_\delta\right| \left|\gamma\right|^k \sin(\theta k + \phi)$$
$$T_i = \left|X_\delta\right| \left|\gamma\right|^r \cos(\phi + \theta q)$$
$$W_i = \left|X_\delta\right| \left|\gamma\right|^r \sin(\phi + \theta q); \quad \text{and} \quad i \in [1, N]; j \in [1, p]; k \in [1, q-1]$$

It is clear from eqn.(3.99) that N values of ψ give 2N linear algebraic equations in the unknown parameters of the controller. For (p+q+1) number of unknowns, N is at leas equal to (p+q+1)/2. In the case when 2N > (p+q+1), the parameters of the controller may be determined by the least squares solution of (3.99) as:

$$x = (A^T A)^{-1} A^T b \tag{3.100}$$

The optimal frequency point searched by using genetic algorithm with the parameter set in step-3, lie around the point $\omega = 0$ or $\psi = 0$ ($\psi = \omega\Delta$). For various systems, the sampling period Δ may be different and so will be the sampling frequency ω_s. But $\omega_s \Delta / 2$ is always a constant and equals π. Therefore, for matching purpose the initial frequency points are chosen as $\psi_k = k\eta$; $k \in [1, N]$ where η is small positive number and $\eta << 1$ so that $\psi = [0, \pi]$. for $k \in [1, N]$.

- **Step 8:** If the closed-loop system approximately satisfies the desired specifications, then STOP otherwise GO TO STEP 3 and by changing GA parameters simulation is to be done again.

In the case of a PI controller, β_1 gives the proportional gain and β_0 gives the gain associated with the integral term, where β_0, β_1, and β_2 are respectively the proportional, integral and derivative gains in the case of a PID controller.

3.6.4 Simulation results:

To illustrate the methodology of optimal frequency fitting technique we consider a 3rd order continuous time plant transfer function [117] given as:

$$P_c(s) = \frac{(s+2)}{(s+1)(s+3)(s+4)} \tag{3.101}$$

The open loop step response of the transfer function given in (3.101) is not satisfactory therefore to satisfy the required time and frequency domain specifications it is desired to design a digital PID controller in the delta domain. The plant TFs is therefore discretised incorporating a sampler and zero order hold with sampling periods Δ = 0.01 & 0.1 sec. respectively and corresponding 2nd order reference model in delta domain are also developed for different angles (ρ) considering ω_n =0.5 rad/sec, 0.84 rad/sec and ξ = 0.707.

The obtain the Optimum frequency points, the following GA parameters have been considered

- Method of selection : Tournament selection method
- Number of tournaments: 2
- Number of generation for evolution: 30
- Population size : 31
- Crossover probability: 0.77
- Number of crossover : 2
- Mutaion probability: 0.0077

Applying genetic algorithm with above parameters the desired PID controller are obtained for different zero locations. Details of optimal frequency points obtained for different angles (ρ) and sampling frequency (Δ) are given in Table 3.10.

The continuous time plant given in equation (3.101) is discretized with sampler and ZOH and given in equation (3.102). It is obserbed that the continuous time transfer function (3.101) has only on zero however after sampling in delta domain one more zero is inducted which is known as sampling zero. Care must be taken while considering sampling zero which may lead the system towards non minimum phase system. The desired reference models for the given specification parameters stated above are computed at different sampling periods. The plant and corresponding controller transfer functions are given as under:

For sampling time (Δ) = 0.01 sec the plant transfer function in delta domain is

$$P_\delta(\gamma) = \frac{0.0049\gamma^2 + 0.9803\gamma + 1.9218}{\gamma^3 + 7.8715\gamma^2 + 18.4308\gamma + 11.5307} \tag{3.102}$$

• For **Angle (ρ) = + 20 degree, ω_n = 0.5 rad/sec and ξ = 0.707.** the ref. model TF is

$$M_\delta(\gamma) = \frac{0.48175\,\gamma + 0.24912}{\gamma^2 + 0.707\,\gamma + 0.24912} \tag{3.103}$$

and desired PID controller

$$C_\delta(\gamma) = 2.1268 - 0.34231\,\gamma + \frac{4.9434}{\gamma} \tag{3.104}$$

The unit step responses of the reference model and closed-loop system in delta domain are shown in Figure- 3.28.

• For **Angle (ρ) = - 40 degree, ω_n = 0.5 rad/sec and ξ = 0.707** the ref. model TF is

$$M_\delta(\gamma) = \frac{0.05784\,\gamma + 0.24912}{\gamma^2 + 0.707\,\gamma + 0.24912} \tag{3.105}$$

and desired PID controller

$$C_\delta(\gamma) = 0.31734 - 0.2069\,\gamma + \frac{2.1525}{\gamma} \tag{3.106}$$

The unit step responses of the reference model and closed-loop system in delta domain are shown in Figure - 3.29 .

• For **Angle (ρ) = - 40 degree, ω_n = 0.84 rad/sec and ξ = 0.707** the ref. model TF is

$$M_\delta(\gamma) = \frac{0.09835\gamma + 0.70142}{\gamma^2 + 1.1877\,\gamma + 0.70142} \tag{3.117}$$

and desired PID controller

$$C_\delta(\gamma) = -1.25 - 3.4661e^{-5}\,\gamma + \frac{3.8632627}{\gamma} \tag{3.118}$$

The unit step responses of the reference model and closed-loop system in delta domain are shown in Fig.- 3.30.

• **Angle (ρ) = +40 degree, ω_n = 0.84 rad/sec and ξ = 0.707** the ref. model TF is

$$M_\delta(\gamma) = \frac{1.0894\,\gamma + 0.70142}{\gamma^2 + 1.1877\gamma + 0.70142} \tag{3.119}$$

and desired PID controller

$$C_\delta(\gamma) = 10.9039 - 1.9312\,\gamma + \frac{11.713}{\gamma} \tag{3.120}$$

The unit step responses of the reference model and closed-loop system in delta domain are shown in Figure 3.31. The unit step responses of other values of 'ρ' and ω_n have also shown in figure 3.32– 3.35.

The various time and frequency domain performance measures with these controllers are given in Table 3.10. From the above it is seen that the synthesised controllers with Optimum frequency fitting yield very good low and high frequency matching. It may further be seen that the controller gain in this design is smaller than the critical value and hence enough stability margin is assured.

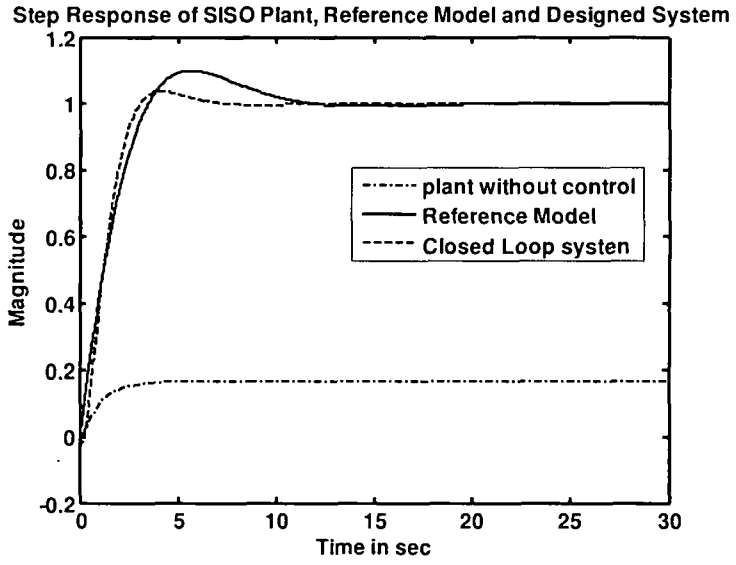

Figure 3.28: Step responses with $\Delta = 0.01$ sec, $\rho = +20°$ and ω_n=0.5 rad/sec

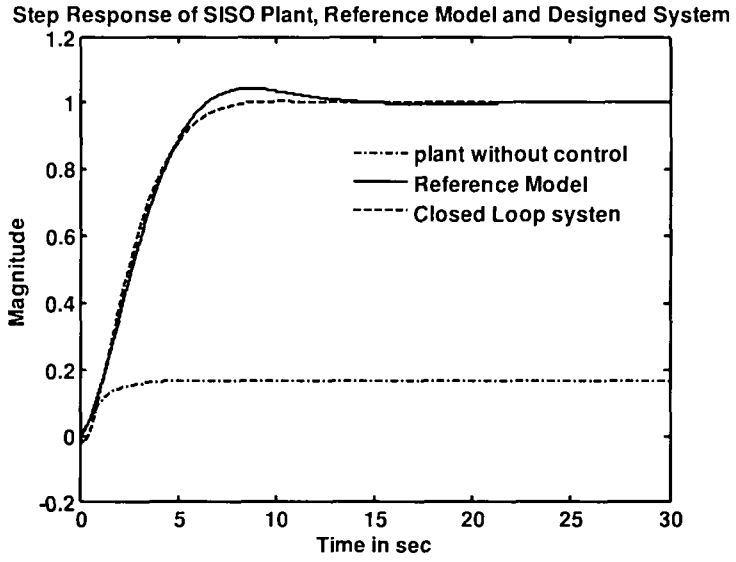

Figure 3.29: Step responses of plant, reference model and closed loop plant with $\Delta = 0.01$ sec, $\rho = -40°$ and ω_n=0.5 rad/sec

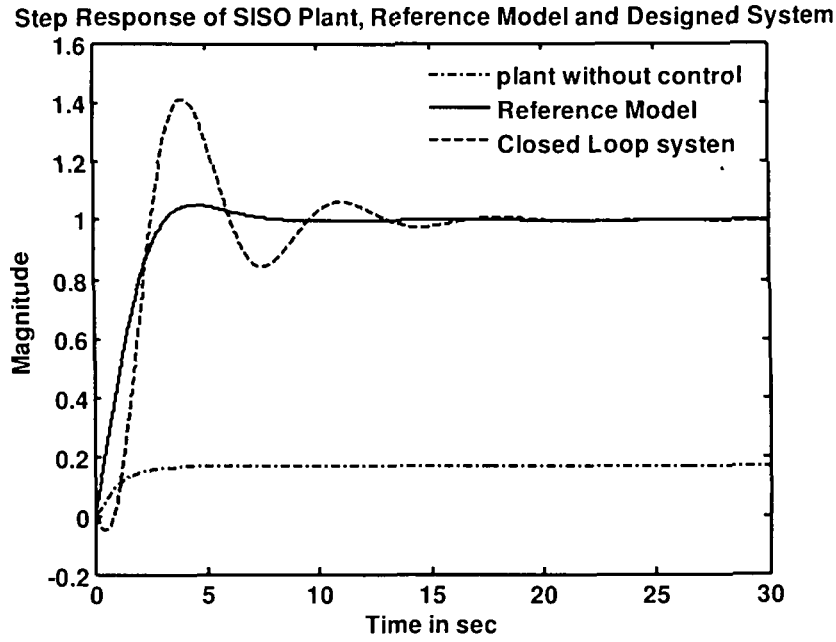

Figure 3.30: Step responses of plant, reference model and closed loop plant with $\Delta = 0.01$ sec, $\rho = -40°$ & $\omega_n = 0.84$ rad/sec

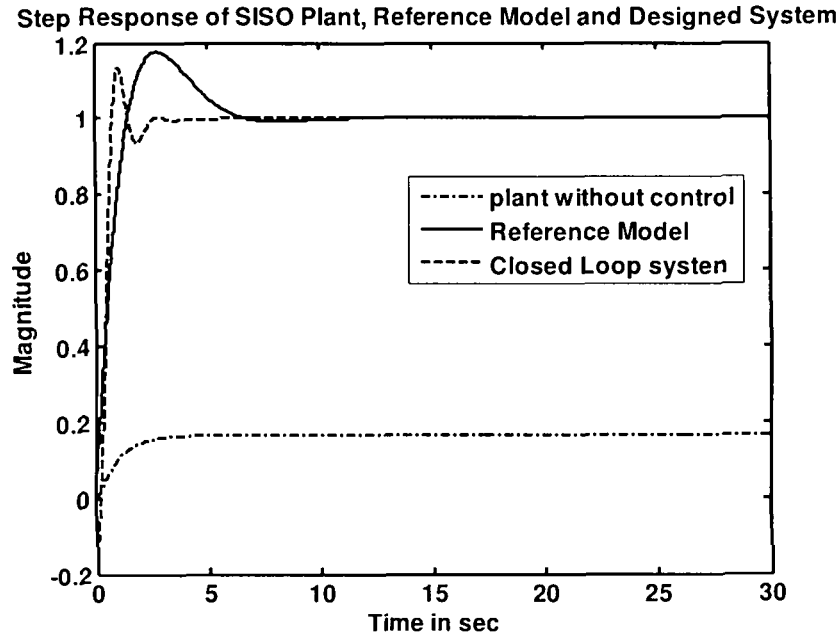

Figure 3.31: Step responses of plant, reference model and closed loop plant with $\Delta = 0.01$ sec, $\rho = +40°$ & $\omega_n = 0.84$ rad/sec

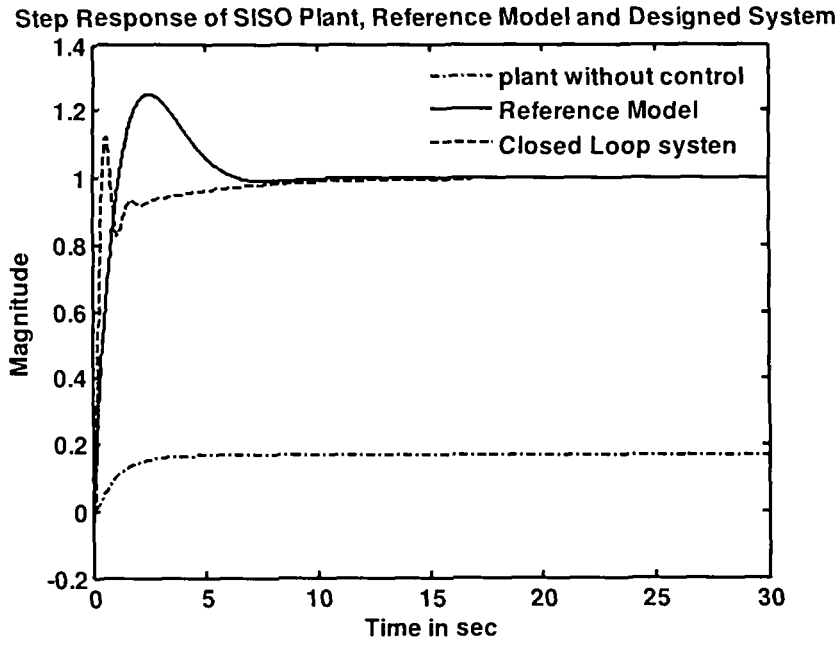

Figure 3.32: Step responses of plant, reference model and closed loop plant with $\Delta = 0.01$ sec, $\rho = +50°$ & $\omega_n = 0.84$ rad/sec

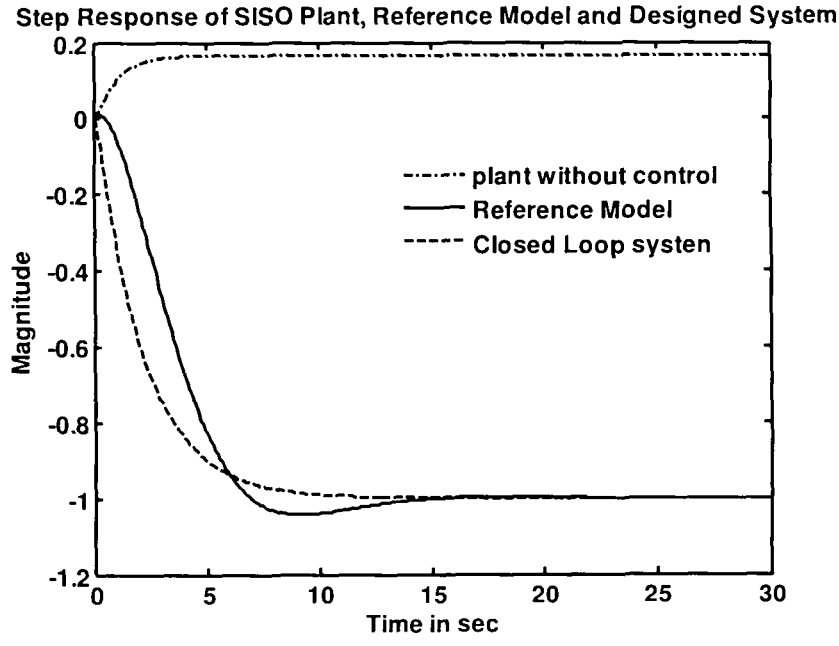

Figure 3.33 : Step responses of plant, reference model and closed loop plant with $\Delta = 0.01$ sec, $\rho = -50°$ & $\omega_n = 0.5$ rad/sec

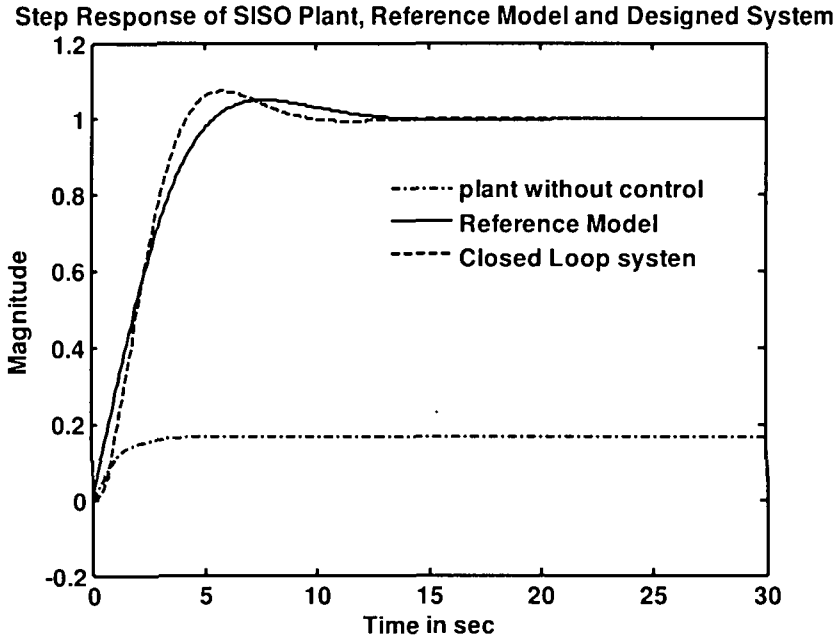

Figure 3.34: Step responses of plant, reference model and closed loop plant with Δ = 0.1 sec, $\rho = -20°$ & ω_n=0.5 rad/sec

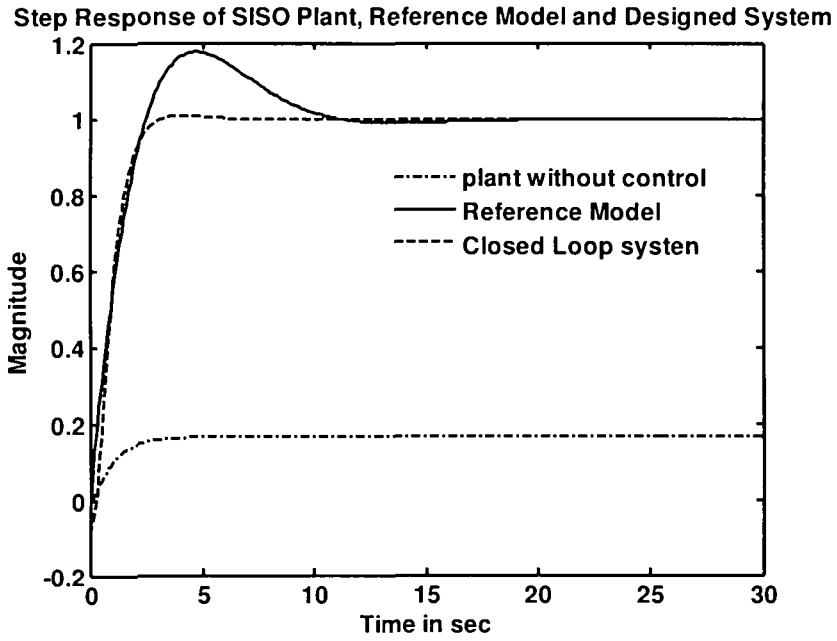

Figure 3.35: Step responses of plant, reference model and closed loop plant with Δ = 0.1 sec, $\rho = +40°$ & ω_n=0.5 rad/sec

Table 3.10: Comparison of performance System with PID controllers

Δ Sec.	ω_n rad/sec	Angle (ρ) in degree	Opt. freq points	Real and Imaginary values	%MP	t_p/Δ	t_s/Δ	GM	PM
0.01	0.5	- 40	0.1033	-0.0005+0.3098i	-	1567	2752	111	∞
0.01	0.5	-30	0.0482	-0.0008+0.4042i	-	1356	2391	40.4	∞
0.01	0.5	+ 20	0.0875	-0.0003+0.2626i	-	1398	2464	75.8	∞
0.01	0.5	+30	0.1111	-0.0006+0.3334i	-	1376	2424	54.3	∞
0.01	0.5	+40	0.1347	-0.0008+0.4042i	-	1356	2391	40.4	∞
0.01	0.84	-40	0.0001	-0.0000+0.0003i	-	1421	2600	29.1	∞
0.01	0.84	+40	0.1347	-0.0008+0.4042i	-	849	1463	18.8	87.1
0.1	0.84	-40	0.0246	-0.0003+0.0738i	54.72	66	284	1.45	18.47
0.1	0.84	+40	0.1269	-0.0072+0.3805i	74.68	25	287	1.34	1.54
0.1	0.5	-40	0.0875	-0.0034+0.2626i	16.31	-	114	4.04	51 71
0.1	0.5	+20	0.0792	-0.0029+0.2391i	38.77	48	143	2.79	32.74
0.1	0.5	+40	0.1190	-0.0064+0.3569i	36.38	41	92	2.77	35.12

3.7 Conclusions:

Two new algebraic methods for design of linear time invariant discrete-time systems in delta-operator parameterisation are reported in this chapter. These frequency domain methods are based on the principle of approximate frequency fitting which is a sub class of approximate model matching and uses a viable alternative of the classical Pade' approximation. The desired performance is converted into a transfer function model, which is matched with the augmented system to have identical optimal frequency point. This method is effectively applied to different SISO processes. This is a once-through design method without any trial-and-error procedure. With a minimum amount of effort, this method gives practically realizable controllers conforming to desired industrial specifications. The methods optimal generalized delta time moment matching and optimum frequency fitting are used to obtain PI, PID or higher order controller structures. This ensures that the steady state values of the output of the closed-loop system and the reference model are close to each other. On completion of one design–simulation run, the designer understanding of the possible improvement of system dynamics works and the available trade-offs between the desired specifications and controller complexity become more apparent. The computational work consists of solving only linear equations to determine the controller parameters and obtaining system responses to a unit step input.

Chapter 4

Controller Design for MIMO Systems

4.1 Introduction:

In recent years, considerable research efforts have been concentrated on development of time domain methods for controller design based on state-space description. Although the state-space methods are computationally elegant, they require measurement of all the states leading to increased cost for control system design. In addition, if all the states are not available for measurement, an observer is also required to be designed to estimate the states. This complicates the structure of the control system and reduces the reliability of the overall system. In an alternative approach in this chapter, delta operator formulated simple lower-order dynamic controller design methods are developed that use only the available outputs for feedback purpose.

From a practical point of view, methods using only output feedback are normally preferred. A drawback of pole-placement techniques is that no zero-placement is done explicitly, while the transient response of a system depends very much on the positions of the poles as well as the zeros.

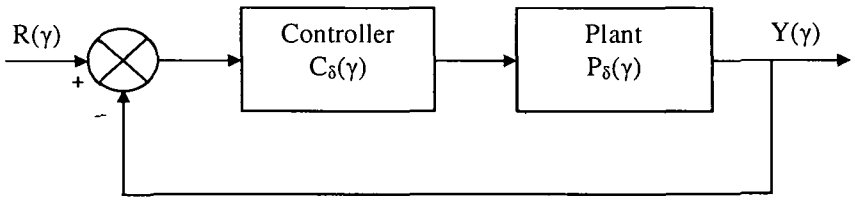

Figure: 4.1 Standard unity negative feedback system

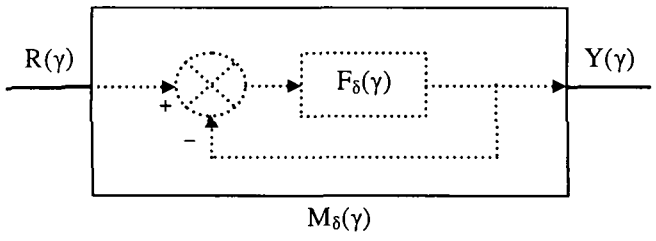

Figure: 4.2 Reference Model for desired closed-loop control system

In model-matching type of controller design technique, a controller is designed such that the closed loop system behaviour follows that of a reference model. The reference model is chosen to exhibit the desired transient and steady state responses. Methods based on exact model matching often yield good matching at the cost of controller complexity. The resultant controllers may be of higher order and may sometimes be unrealizable.

In this chapter two methods are proposed for designing cascade rational controllers for linear discrete-time multivariable industrial systems in delta domain using output feedback. The methods are based on the principle of approximate model-matching as opposed to exact model-matching design procedures. In this chapter SISO design methods of chapter-3 are extended to multivariable systems. The design methods are applicable to unstable/or non-minimum phase systems.

The objective of the MIMO controller design methods based on the concept of Aproximate Model Matching (AMM), is to find the controller transfer function $C_\delta(\gamma)$ as shown in Figure 4.1, such that the closed loop system has satisfactory stability properties and the transient response to a specified demand vector r(t) follows closely that of the reference model transfer function matrix $M_\delta(\gamma)$ of Figure 4.2. The precise design objectives and the degree of interaction permissible will, however, vary from application to application. The important general properties considered in the present work are

- Stability
- Closed-loop transient performance
- Steady-state response and steady-state errors
- Interaction minimization between various input-output loops

To achieve the above objectives in controller design, the methodology developed in chapter-3 and extensively used for SISO controller design is extended here to MIMO systems. In the design methods developed in this chapter we adopt similar procedures.

4.2 Problem definition:

Considering the standard MIMO unity negative feedback configuration of the multivariable system given in Figure 4.1, let the multi-input multi-output transfer function model of the plant to be controlled be $P_\delta(\gamma)_{pvm}$ and the cascade controller be $C_\delta(\gamma)_{pvm}$. The closed-loop transfer function $G_\delta(\gamma)$ is then given by

$$G_\delta(\gamma) = [I + P_\delta(\gamma) C_\delta(\gamma)]^{-1} P_\delta(\gamma) C_\delta(\gamma) \qquad (4.1)$$

Let the desired plant specifications be satisfied by a closed-loop reference model transfer function matrix $M_\delta(\gamma)$. Usually a low interaction level is desired in multivariable control systems such that the response of $y_i(t)$ to the demand $r_i(t) = \gamma^{-1} R_i(\gamma)$ should satisfy the standard classical requirements of suitable rise time, overshoot, settling time etc., and $y_j(t)$, $j \neq i$ should remain small. The off-diagonal terms in $M_\delta(\gamma)$ are therefore assumed to have negligible contribution to the time and frequency responses and are ideally chosen as zero. Hence we assume

$$M_\delta(\gamma) = diag\{ M_{\delta,ii}(\gamma) \}; \qquad i \in [1, p] \qquad (4.2)$$

such that $M_{\delta,ij}(\gamma) = 0$ for $i \neq j$. The diagonal entries in $M_\delta(\gamma)$ are chosen to satisfy specifications like damping factor ξ, peak overshoot M_p, time for peak overshoot t_p, gain margin, phase margin etc. The AMM problem is mathematically equivalent to

$$G_\delta(\gamma) = M_\delta(\gamma) \qquad (4.3)$$

The problem is now to find the controller transfer function $C_\delta(\gamma)_{pxm}$, such that the outputs of the system in Figure 4.1 i.e. the cascaded controller with plant under unity feedback match those of the reference closed-loop model. Let the plant and the desired controller be square transfer function matrices with same number of inputs and outputs i.e. p = m, such that

$$G_\delta(\gamma) = [G_{\delta,ij}(\gamma)]; \qquad i, j \in [1, p] \qquad (4.4)$$

A cascade controller transfer function matrix $C_\delta(\gamma)$ is assumed of the form [13]

$$C_\delta(\gamma) = [C_{\delta,ij}(\gamma)]; \qquad i, j \in [1, p] \qquad (4.5)$$

where

$$C_{\delta,ij}(\gamma) = \frac{\beta_{0,ij} + \beta_{1,ij}\gamma + \cdots + \beta_{r,ij}\gamma^r}{\alpha_{0,ij} + \alpha_{1,ij}\gamma + \cdots + \gamma^q} \qquad (4.6)$$

where r is the order of each scalar transfer function of $C_\delta(\gamma)$ and β's and α's are the $(2r+1)$ unknown parameters of each entry (SISO transfer function) in the transfer function matrix $C_\delta(\gamma)$.

In the design method we use an equivalent open-loop reference model specification transfer function model $F_\delta(\gamma)$ that is derived from the given desired closed-loop reference model $M_\delta(\gamma)$ so that

$$F_\delta(\gamma) = [\, I - M_\delta(\gamma) \,]^{-1} M_\delta(\gamma) \qquad (4.7)$$

therefore the approximate model matching problem is now reduced to

$$[P_\delta(\gamma)]_{(p\times p)}\,[C_\delta(\gamma)]_{(p\times p)} \equiv [\,F_\delta(\gamma)\,]_{(p\times p)} \tag{4.8}$$

We now extend the SISO methods of Optimal GDTM and Optimal frequency fitting method developed in Chapter-3 to obtain the unknown parameters of the transfer function model $C_\delta(\gamma)$, for multivariable systems.

4.3 Optimal GDTM matching method:

The Optimal GDTM technique has been discussed in chapter-3 for controller design of SISO systems. In this section we discuss controller design of MIMO systems using the Optimal GDTM technique. The design methodology is based on Delta Time Moment (DTM) technique however it is further generalized and optimized by using this proposed method. The DTM technique referred by P.Sarkar et.al.[13-14] does not permit easy computation of the DTM series of $F_\delta(\gamma)$, which is obtained recursively from $M_\delta(\gamma)$. On the contrary, the Optimal GDTM method is straight forward and avoids the problems encountered in computation of DTMs. The concept of OGDTM introduced in chapter-3 is directly used to compute the coefficients of the element transfer functions of the controller. As discuss in Section 4.2, the aproximate model matching technique using OGDTM is mathematically equivalent to

$$P_\delta(\gamma)C_\delta(\gamma)\Big|_{\gamma=\mu_{ti}} = F_\delta(\gamma)\Big|_{\gamma=\mu_{ti}} \tag{4.9}$$

where $\mu_{ti} = \mu.i, \quad i \in [\,0, \infty\,]$ and μ_t is a small positive number such that $\mu_t << 1$. The above relation can be written as

$$C_\delta(\gamma)\Big|_{\gamma=\mu_{ti}} = [P_\delta(\gamma)^{-1}\,F_\delta(\gamma)]\Big|_{\gamma=\mu_{ti}} \tag{4.10}$$

Now defining the following structures for MIMO representation, we can write

$$F = F_\delta(\gamma)\Big|_{\gamma=\mu_{ti}} = \begin{bmatrix} f'_{11} & f'_{12} & f'_{13} & f'_{14} & \cdots\cdots & f'_{1m} \\ f'_{21} & f'_{22} & f'_{23} & f'_{24} & \cdots\cdots & f'_{2m} \\ \vdots & \vdots & \vdots & \vdots & & \vdots \\ \vdots & \vdots & \vdots & \vdots & & \vdots \\ f'_{p1} & f'_{p2} & f'_{p3} & f'_{p4} & \cdots\cdots & f'_{pm} \end{bmatrix} \tag{4.11}$$

$$P = P_\delta(\gamma)\Big|_{\gamma=\mu_{ti}} = \begin{bmatrix} p'_{11} & p'_{12} & p'_{13} & p'_{14} & \cdots\cdots & p'_{1m} \\ p'_{21} & p'_{22} & p'_{23} & p'_{24} & \cdots\cdots & p'_{2m} \\ \vdots & \vdots & \vdots & \vdots & & \vdots \\ \vdots & \vdots & \vdots & \vdots & & \vdots \\ p'_{p1} & p'_{p2} & p'_{p3} & p'_{p4} & \cdots\cdots & p'_{pm} \end{bmatrix} \tag{4.12}$$

$$Q_\delta(\gamma) = [P_\delta(\gamma)]^{-1} F_\delta(\gamma)\Big|_{\gamma=\mu_{ti}} \tag{4.13}$$

and

$$Q = Q_\delta(\gamma) = \begin{bmatrix} q_{11}^i & q_{12}^i & q_{13}^i & q_{14}^i & \cdots\cdots & q_{1m}^i \\ q_{21}^i & q_{22}^i & q_{23}^i & q_{24}^i & \cdots\cdots & q_{2m}^i \\ \vdots & \vdots & \vdots & \vdots & & \vdots \\ \vdots & \vdots & \vdots & \vdots & & \vdots \\ q_{p1}^i & q_{p2}^i & q_{p3}^i & q_{p4}^i & \cdots\cdots & q_{pm}^i \end{bmatrix} \tag{4.14}$$

$$C_\delta(\gamma) = \begin{bmatrix} \frac{n_{11}}{d_{11}} & \frac{n_{12}}{d_{12}} & \frac{n_{13}}{d_{13}} & \frac{n_{14}}{d_{14}} & \cdots\cdots & \frac{n_{1m}}{d_{1m}} \\ \frac{n_{21}}{d_{21}} & \frac{n_{22}}{d_{22}} & \frac{n_{23}}{d_{23}} & \frac{n_{24}}{d_{24}} & \cdots\cdots & \frac{n_{2m}}{d_{2m}} \\ \vdots & \vdots & \vdots & \vdots & & \vdots \\ \vdots & \vdots & \vdots & \vdots & & \vdots \\ \frac{n_{p1}}{d_{p11}} & \frac{n_{p2}}{d_{p2}} & \frac{n_{p3}}{d_{p13}} & \frac{n_{p4}}{d_{p4}} & \cdots\cdots & \frac{n_{pm}}{d_{pm}} \end{bmatrix} \tag{4.15}$$

and the (j, k)th elements of $C_\delta(\gamma)$ is

$$\frac{\beta_{0,jk} + \beta_{1,jk}\gamma + \cdots + \beta_{r,jk}\gamma^r}{\alpha_{0,jk} + \alpha_{1,jk}\gamma + \cdots + \gamma^r} = \frac{n_{jk}(\gamma)}{d_{jk}(\gamma)} \tag{4.16}$$

We assume a square plant transfer function $P_\delta(\gamma)$ and Controller transfer function $C_\delta(\gamma)$ such that p = m. Further we consider that the denominator polynomials of the elements of the controller transfer function are monic (α_r = 1). In order to satisfy the relation in equation (4.10), from equations (4.14) and (4.15) we can write,

$$\frac{n_{jk}(\gamma)}{d_{jk}(\gamma)}\Big|_{\gamma=\mu_{ti}} = q_{jk}^i \tag{4.17}$$

Equation (4.17) has (2r+1) unknowns for each (j, k). Therefore, substituting $\gamma = \mu_{ti}$, $i \in [1, 2r + 1]$ for $\mu_t << 1$, a real positive number (frequency), we obtain (2r+1) linear algebraic equations, which can be written in closed form as under

$$\{[\beta_{0,jk} + \beta_{1,jk}\gamma + \cdots + \beta_{r-1,jk}\gamma^{r-1} + \beta_{r,jk}\gamma^r] = q_{jk}^i[\alpha_{0,jk} + \alpha_{1,jk}\gamma + \cdots + \alpha_{r-1,jk}\gamma^{r-1} + \gamma^r]\}\Big|_{\gamma=\mu_{ti}} \tag{4.18}$$

Defining,

$$w_{jk}^i = [1, \gamma, \gamma^2, \cdots, \gamma^r \quad -q_{jk}^i \; -q_{jk}^i\gamma \; - \cdots - q_{jk}^i\gamma^{r-1}]\Big|_{\gamma=\mu_{ti}} \tag{4.19}$$

$$v_{jk}^{l} = q_{jk}^{l}\,\gamma^{r}\Big|_{\gamma=\mu_{tl}} \tag{4.20}$$

$$Z_{jk} = [\,\beta_{0,jk}, \beta_{1,jk}, \ldots\ldots \beta_{r-1,jk}, \beta_{r,jk} \;\vdots\; \alpha_{0,jk}, \alpha_{1,jk}, \ldots\ldots \alpha_{r-1,jk}\,]^{T}\Big|_{\gamma=\mu_{tl}} \tag{4.21}$$

we can now write from equations (4.19),(4.20) and (4.21)

$$w_{i,jk}^{l} Z_{jk} = v_{i,jk}^{l} \tag{4.22}$$

then for i = 1, 2, 3, ..., 2r + 1 we can write,

$$Z_{jk} = [W_{jk}]^{-1} V_{jk} \tag{4.23}$$

where

$$W_{jk} = \begin{bmatrix} w_{jk}^{1} \\ w_{jk}^{2} \\ \vdots \\ w_{jk}^{2r+1} \end{bmatrix}_{(2r+1 \times 2r+1)} \tag{4.24}$$

and

$$V_{jk} = \begin{bmatrix} v_{jk}^{1} \\ v_{jk}^{2} \\ \vdots \\ v_{jk}^{2r} \end{bmatrix}_{(2r+1 \times 1)} \tag{4.25}$$

thus equation (4.24 & 4.25) gives the parameters of (j, k)th transfer function of the controller transfer function. Complete transfer function can be obtained for j ∈ [1, p] and k ∈ [1, m]. The advantage of this method is evident from equation (4.13), where the polynomial matrix inversion is avoided by substituting $\gamma = \mu_{tl}$. where μ_t is a small positive number less than one, which ensures better low frequency matching. Therefore, the steady-state responses of the closed-loop system are better matched with those of the reference model.

4.4 Simulation results:

The OGDTM method developed was tested on the systems as described below:

4.4.1 Simple multivariable plant:

We consider here an example to demonstrate the application of OGDTM method for controller design [53]. The Optimal frequency points considered are μ_{ti} = μ_t.i, i ∈ [1, 2].

$$P_c(s)=\begin{bmatrix} \dfrac{1-s}{(1+s)^2} & \dfrac{2-s}{(1+s)^2} \\ \dfrac{1-3s}{3(1+s)^2} & \dfrac{1-s}{(1+s)^2} \end{bmatrix}$$

Now the continuous plant transfer function is sampled with ZOH with sampling period Δ = 0.1 second and corresponding plant TF in delta domain with common denominator is given as:

$$P_\delta(\gamma)=\begin{bmatrix} \dfrac{-0.8580\gamma+0.9056}{\gamma^2+1.9033\gamma+0.9056} & \dfrac{-0.8113\gamma+1.8112}{\gamma^2+1.9033\gamma+0.9056} \\ \dfrac{-0.8892\gamma+0.3019}{\gamma^2+1.9033\gamma+0.9056} & \dfrac{-0.8580\gamma+0.9056}{\gamma^2+1.9033\gamma+0.9056} \end{bmatrix}$$

The 2nd order reference model with ω_n= 0.84 rad/sec, damping factor ξ=0.7 and angle (ρ) = - 40° is

$$M_\delta(\gamma)=\begin{bmatrix} \dfrac{0.11368\gamma+0.6653}{\gamma^2+1.176\gamma+0.6653} & 0 \\ 0 & \dfrac{0.11368\gamma+0.6653}{\gamma^2+1.176\gamma+0.6653} \end{bmatrix}$$

Following GA parameters are used to compute the OGDTMs for a PI controller $C_\delta(\gamma)=k_p+\dfrac{k_i}{\gamma}$, where k_p and k_i are proportional and integral constants.

- Method of selection : Tournament selection method
- Number of tournaments: 2
- Number of generation for evolution: 35
- Population size : 32
- Crossover probability: 0.85
- Number of crossover : 2
- Mutaion probability: 0.0085

Using above GA parameters the optimal frequency point μ_t is computed for different locations of zeros of reference model by changing the values of angle 'ρ'. The proposed design method yields the following PI controller for OGDTM point (μ_{ti} 0.1269 .

$$C_\delta(\gamma) = \begin{bmatrix} -1.5444 + \dfrac{1.8945}{\gamma} & 1.0646 - \dfrac{3.7770}{\gamma} \\ 1.8642 - \dfrac{0.6396}{\gamma} & -1.5444 + \dfrac{1.8945}{\gamma} \end{bmatrix}$$

The unit step responses of the uncontrolled plant, reference model and the augmented plant with controller are given in figures 4.3 to 4.6 and corresponding control efforts are shown in figure 4.7. It may be seen from the figures that the unit step responses of the closed-loop system are close to those of the reference model. It may also be seen that the off diagonal elements of the designed multivariable PI controller are not zeros, this is because of the plant transfer function including interaction terms has been taken into consideration in the design process.

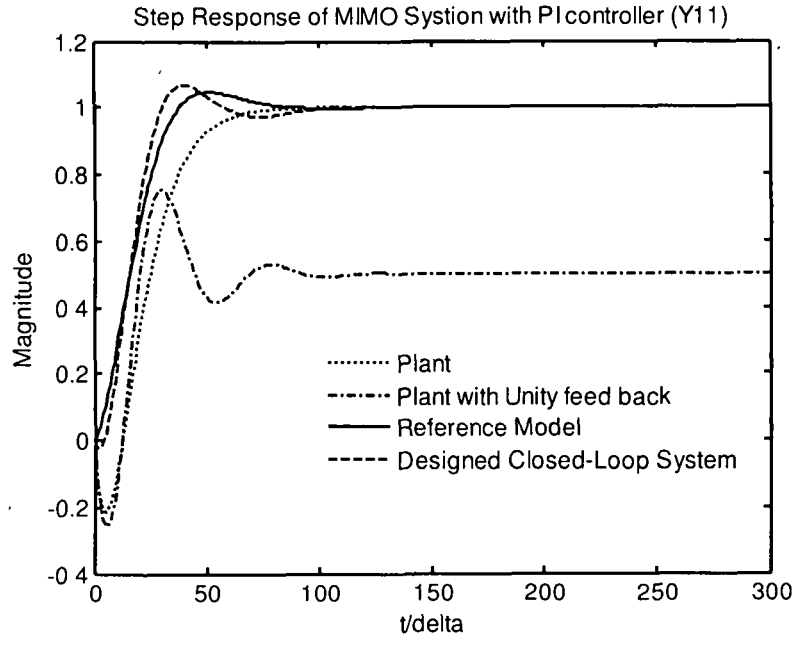

Figure 4.3: Step responses of uncontrolled plant, reference model and closed loop system with PI controller using OGTM, output y11, Δ = 0.1 sec and ρ = - 40°

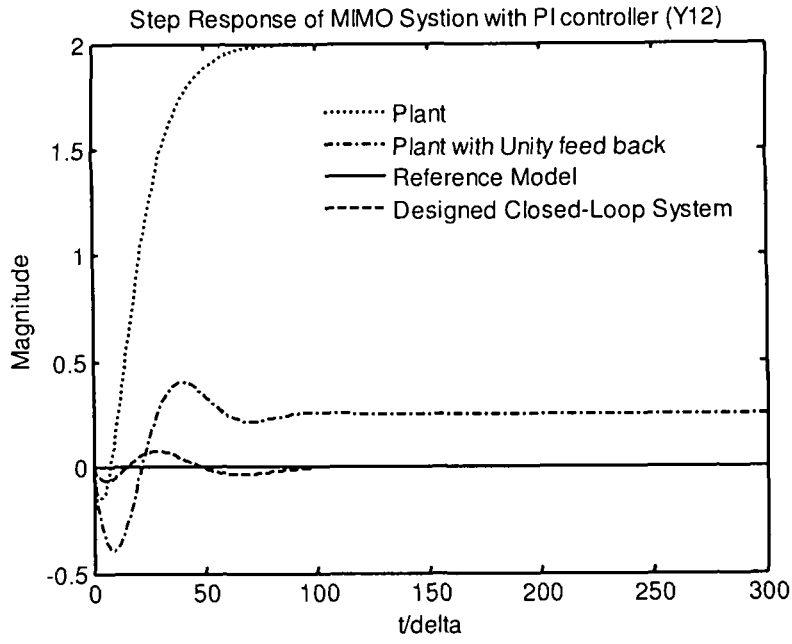

Figure 4.4: Step responses of uncontrolled plant, reference model and closed loop system with PI controller using OGTM, output y12, $\Delta = 0.1$ sec and $\rho = -40°$

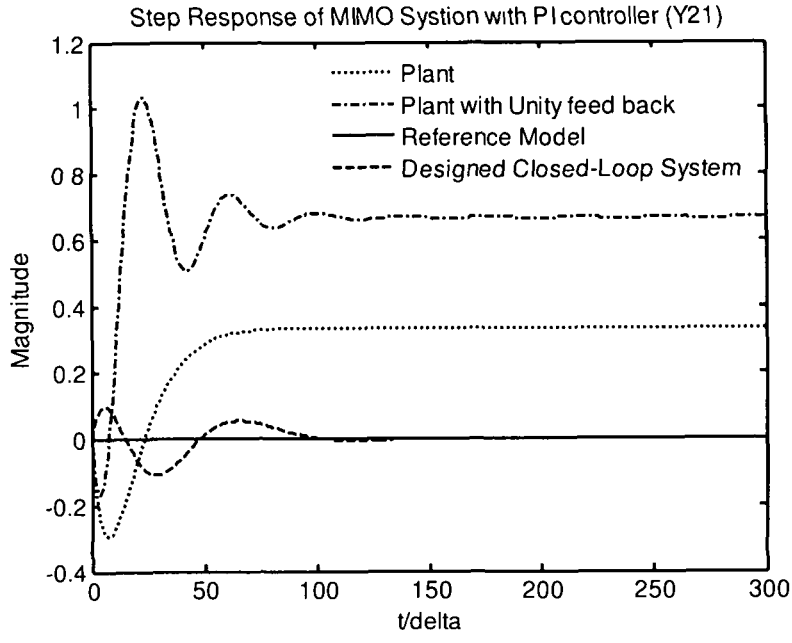

Figure 4.5: Step responses of uncontrolled plant, reference model and closed loop system with PI controller using OGTM, output y21, $\Delta = 0.1$ sec and $\rho = -40°$

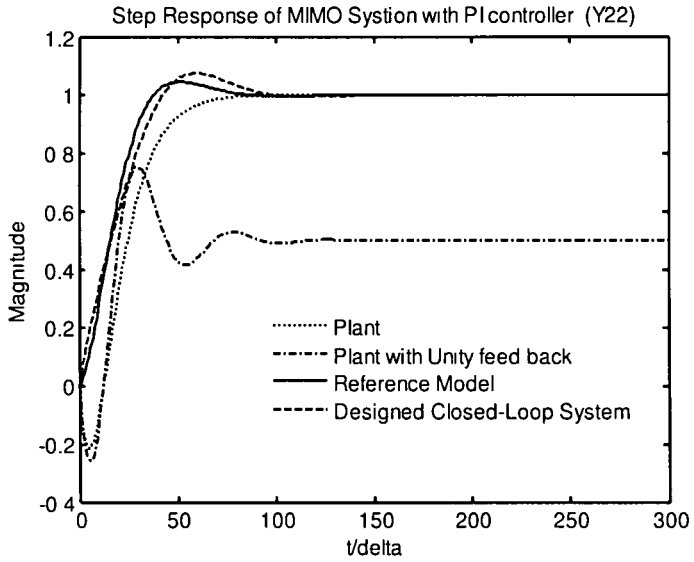

Figure 4.6: Step responses of uncontrolled plant, reference model and closed loop system with PI controller using OGTM, output y22, $\Delta = 0.1$ sec and $\rho = -40°$

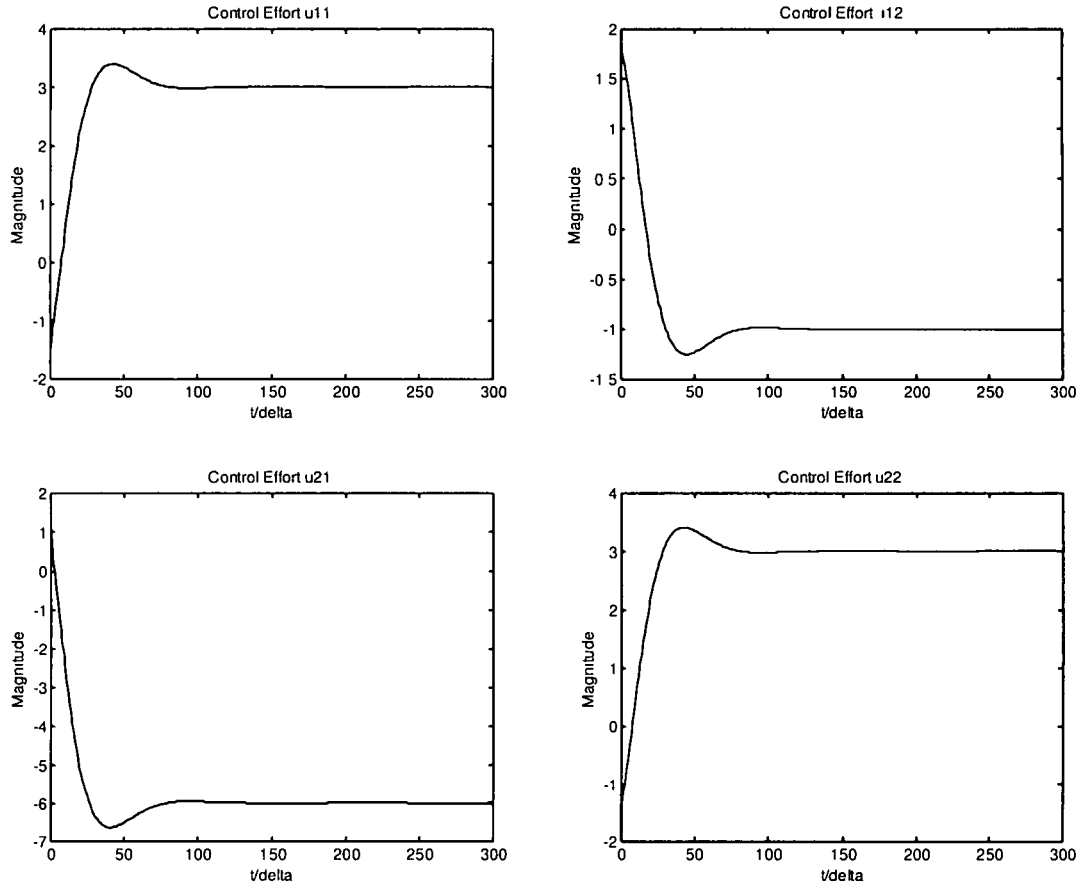

Figure 4.7: Control Efforts U11, U12, U21, U22 with PI controller using OGTM, $\Delta = 0.1$ sec and $\rho = -40°$

The 2nd order reference model with ω_n= 0.84 rad/sec, damping factor ξ=0.7 and angle (ρ) = +40° is

$$M_\delta(\gamma) = \begin{bmatrix} \dfrac{1.0623\gamma + 0.6653}{\gamma^2 + 1.176\gamma + 0.6653} & 0 \\ 0 & \dfrac{1.0623\gamma + 0.6653}{\gamma^2 + 1.176\gamma + 0.6653} \end{bmatrix}$$

Using GA with the parameter stated above, the OGDTM Point (μ_{ti}) is found to be 0.4258 and we obtain the desired PI controller as

$$C_\delta(\gamma) = \begin{bmatrix} -8.3160 + \dfrac{8.7921}{\gamma} & 7.7296 - \dfrac{17.5386}{\gamma} \\ 8.7069 - \dfrac{2.9611}{\gamma} & -8.3160 - \dfrac{8.7921}{\gamma} \end{bmatrix}$$

The unit step responses of the reference model and the augmented plant with controller are given in figures 4.8 to 4.10 and control efforts are shown in figure 4.11 In this case also the unit step responses Y11 and Y22 of the designed closed-loop system are close to those of the reference model with initial oscillation. It may also be seen that the off diagonal elements of the designed multivariable PI controller are not zeros, this is because of the plant transfer function including interaction terms has been taken into consideration in the design process.

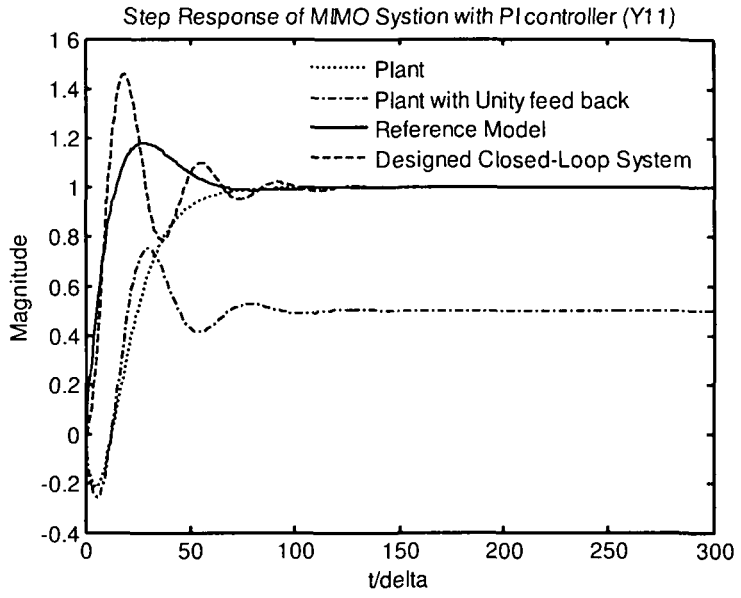

Figure 4.8: Step responses of uncontrolled plant, reference model and closed loop system with PI controller using OGTM, output y11, Δ = 0.1 sec and ρ = +40°

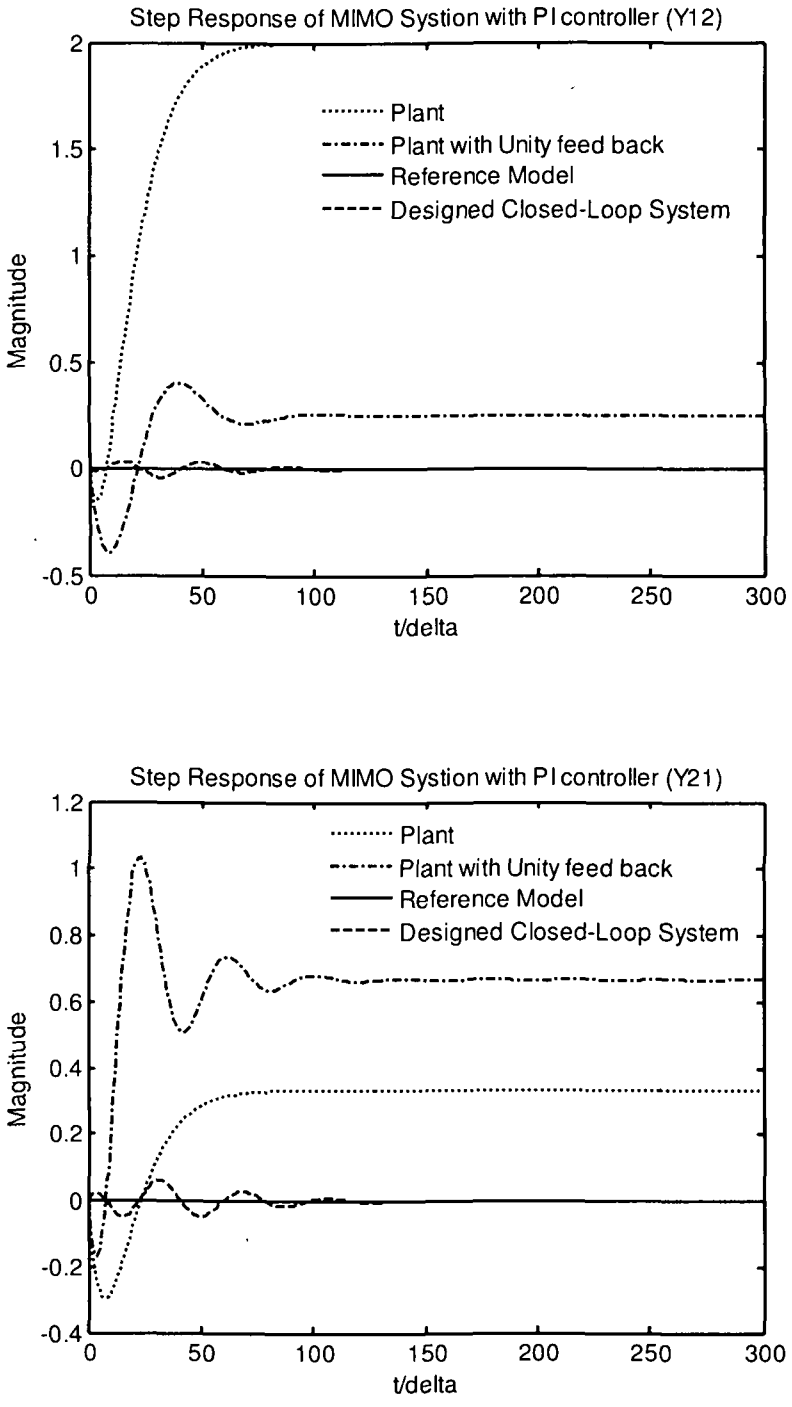

Figure 4.9: Step responses of uncontrolled plant, reference model and closed loop system with PI controller using OGTM, output y12, y21, $\Delta = 0.1$ sec and $\rho = +40°$

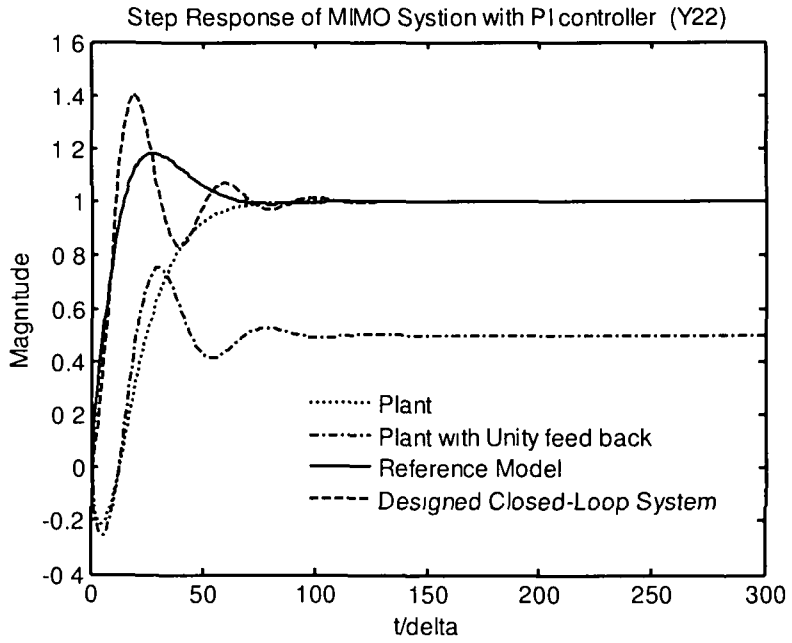

Figure 4.10: Step responses of uncontrolled plant, reference model and closed loop system with PI controller using OGTM, output y22, $\Delta = 0.1$ sec and $\rho = +40°$

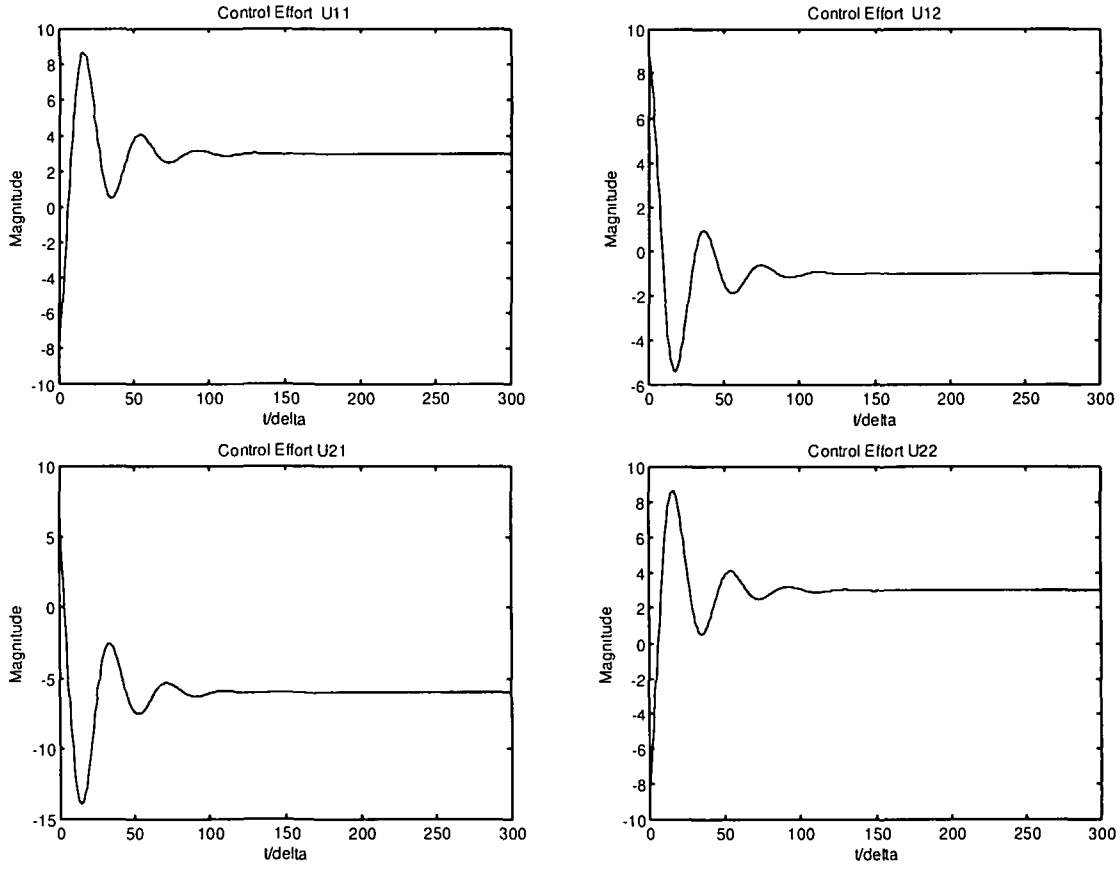

Figure 4.11: Control Efforts U11, U12, U21, U22 with PI controller using OGTM, $\Delta = 0.1$ sec and $\rho = +40°$

4.4.2 Pressurized flow box:

To test the robustness of the OGDTM technique developed, we consider the following open loop transfer function matrix of a pressurised flow box [56] to demonstrate controller design.

$$P_c(s)=\begin{bmatrix} \dfrac{0.0336}{s+0.395} & \dfrac{1.03s}{s^2+0.395s+1.26e-04} \\ \dfrac{9.66e-04s+0.117e-04}{s^2+0.395s+1.26e-04} & \dfrac{-0.01141}{s^2+0.39s+1.26e-04} \end{bmatrix}$$

Now sampling the above plant with sampler with sampling period $\Delta = 0.1$ second and ZOH, we get the corresponding plant TF in delta domain with common denominator as:

$$P_\delta(\gamma)=\begin{bmatrix} \dfrac{0.0329\gamma^2+0.0128\gamma+4\,07E-06}{\gamma^3+0.7746\gamma^2+0.1501\gamma+4.7849E-05} & \dfrac{0.0009\gamma^2+0.0004\gamma+4.4431e-06}{\gamma^3+0.7746\gamma^2+0.1501\gamma+4.7849E-05} \\ \dfrac{\gamma(1.0099\gamma+0.3911)}{\gamma^3+0.7746\gamma^2+0.1501\gamma+4.7849E-05} & \dfrac{-0.0006\gamma^2-0.0114\gamma-0.0043}{\gamma^3+0.7746\gamma^2+0.1501\gamma+4.7849E-05} \end{bmatrix}$$

The 2nd order reference model with ω_n= 0.84 rad/sec, damping factor ξ=0.7 and angle ρ = - 40° is

$$M_\delta(\gamma)=\begin{bmatrix} \dfrac{0.1137\gamma+0.6653}{\gamma^2+1.176\gamma+0.6653} & 0 \\ 0 & \dfrac{0.1137\gamma+0.6653}{\gamma^2+1.176\gamma+0.6653} \end{bmatrix}$$

Following GA parameters are used to compute the OGDTMs for a PI controller

- Method of selection : Roulette wheel
- Number of generation for evolution: 30
- Population size : 31
- Crossover probability: 0.77
- Number of crossover : 2
- Mutaion probability: 0.0077

the OGDTM point μ_t is computed for angle ρ =-40° with above GA parameters and found to be 0.561 and corresponding PI controller is obtained as:

$$C_\delta(\gamma) = \begin{bmatrix} -4.3779 + \dfrac{7.1192}{\gamma} & 571.7276 + \dfrac{2.6673}{\gamma} \\ 0.5317 + \dfrac{0.0098}{\gamma} & -18.6362 - \dfrac{0.0935}{\gamma} \end{bmatrix}$$

The unit step responses of the reference model and the augmented plant with controller are given in figures 4.12 to 4.15 and corresponding control efforts are shown in figure 4.16. It may be seen from the figures that the unit step responses of the closed-loop system are close to those of the reference model. It may also be seen that the off diagonal elements of the designed multivariable PI controller are not zeros, this is because of the plant transfer function including interaction terms has been taken into consideration in the design process.

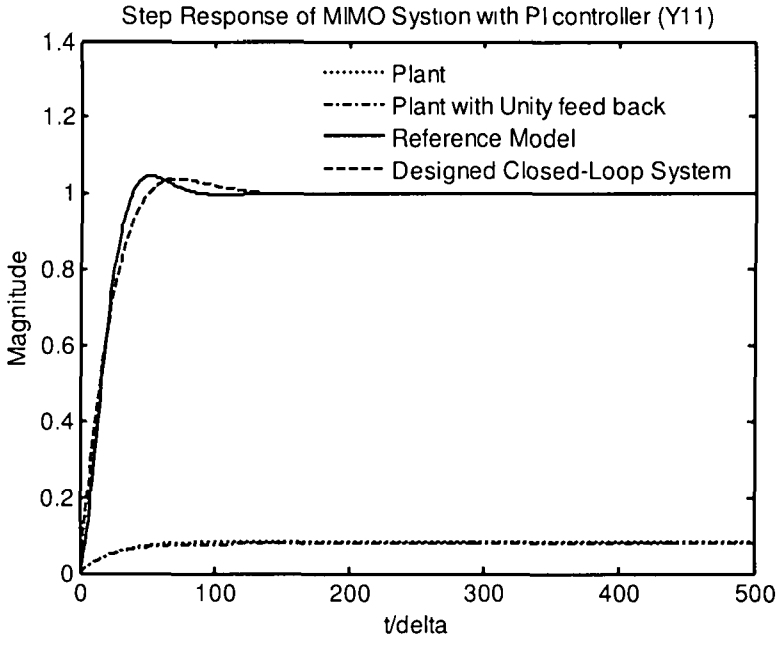

Figure 4.12: Step responses of uncontrolled plant, reference model and closed loop system with PI controller using OGTM, output y11, Δ = 0.1 sec and ρ = -40°

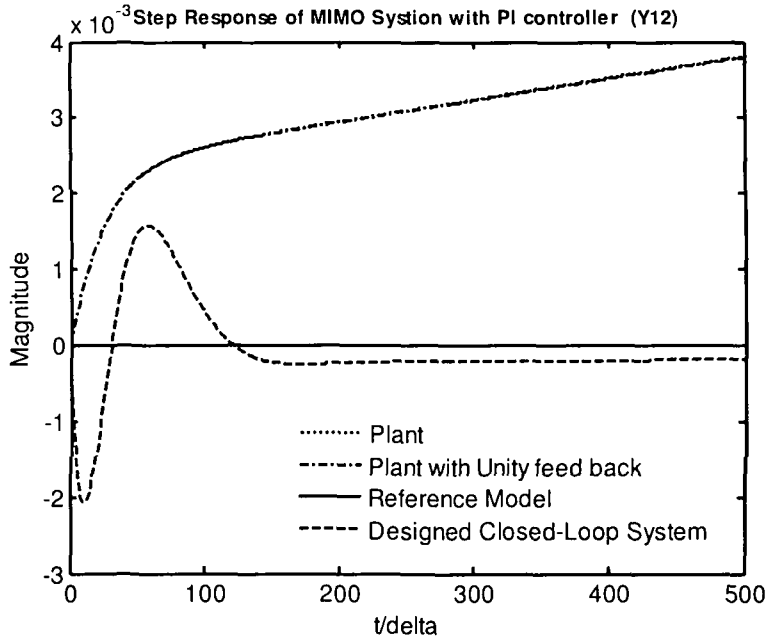

Figure 4.13: Step responses of uncontrolled plant, reference model and closed loop system with PI controller using OGTM, output y12, $\Delta = 0.1$ sec and $\rho = -40°$

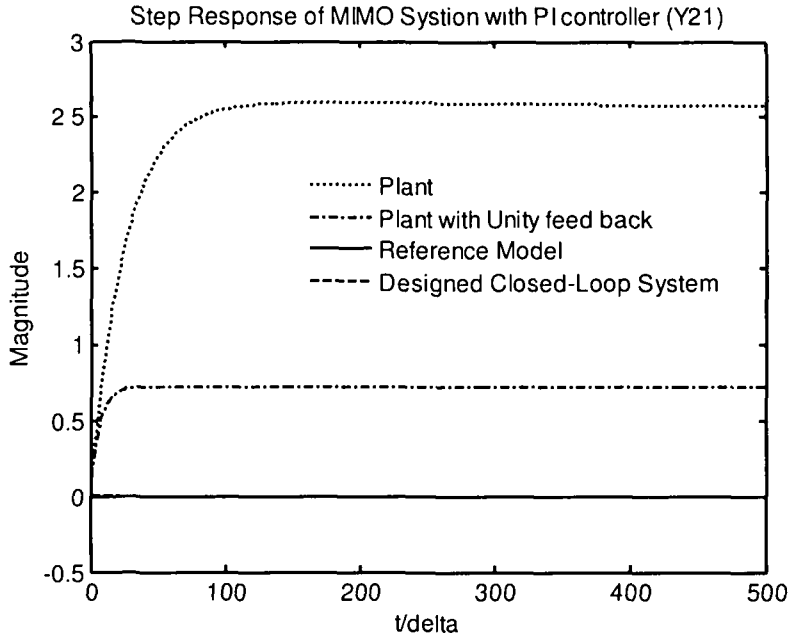

Figure 4.14: Step responses of uncontrolled plant, reference model and closed loop system with PI controller using OGTM, output y21, $\Delta = 0.1$ sec and $\rho = -40°$

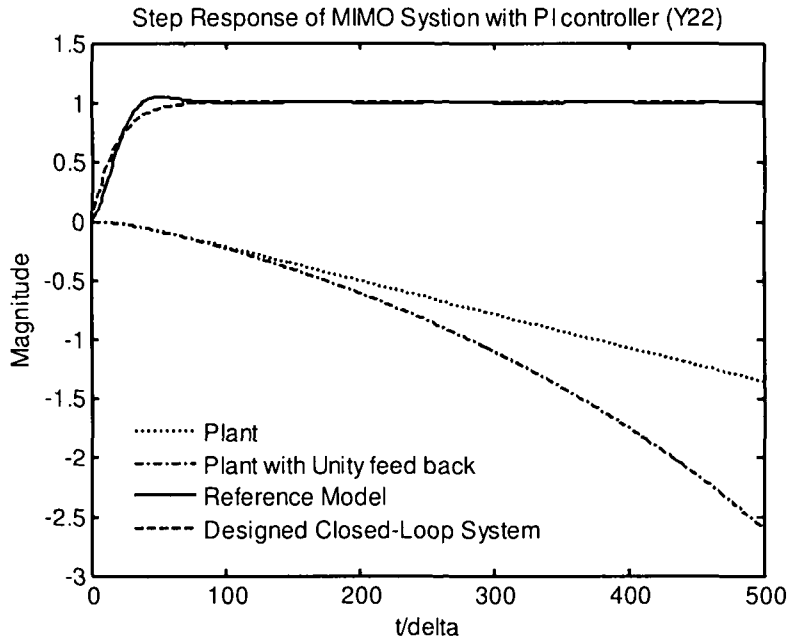

Figure 4.15: Step responses of uncontrolled plant, reference model and closed loop system with PI controller using OGTM, output y22, $\Delta = 0.1$ sec and $\rho = -40°$

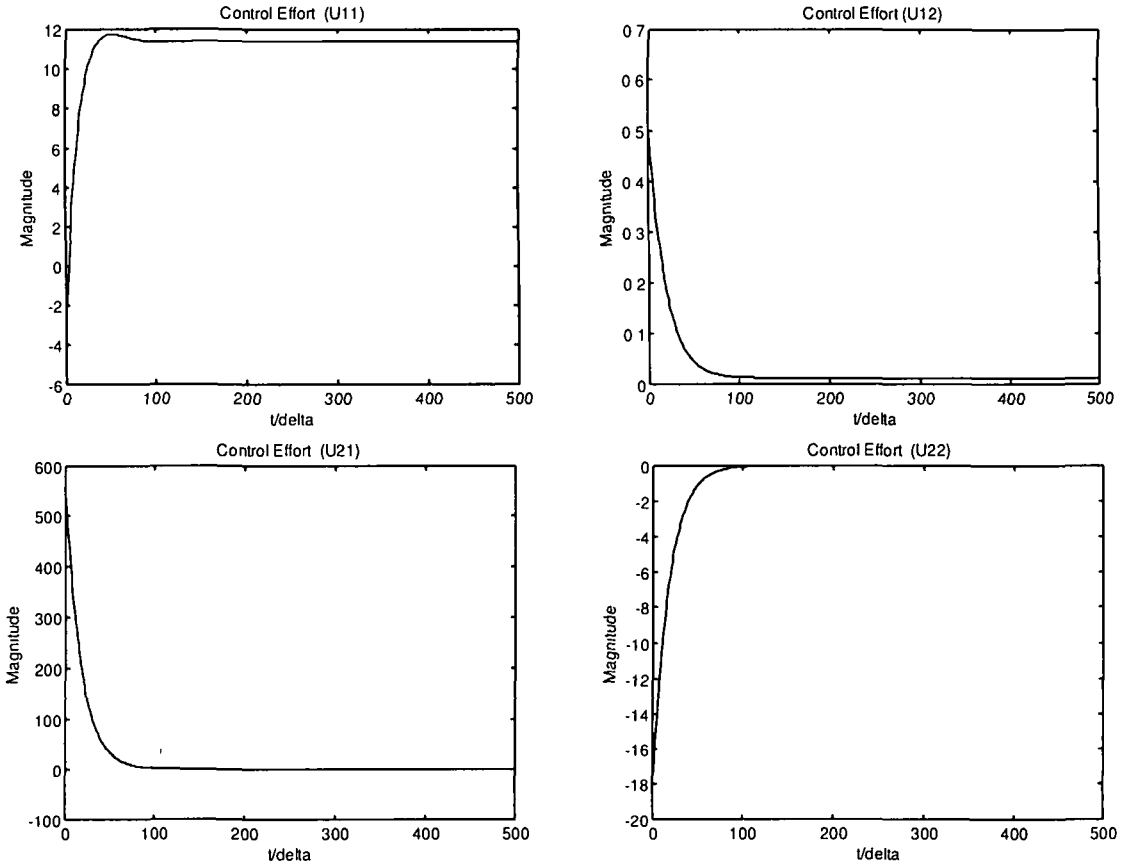

Figure 4.16: Control Efforts U11, U12, U21, U22 with PI controller using OGTM, $\Delta = 0.1$ sec and $\rho = -40°$

4.4.3 Gas fired furnace:

Now we consider another MIMO plant of a gas fired furnace [118] to test the OGDTM methodology. The four input and four output furnace is described by the following transfer function matrix.

$$P_c(s) = \begin{bmatrix} \frac{1}{4s+1} & \frac{0.7}{5s+1} & \frac{0.3}{5s+1} & \frac{0.2}{5s+1} \\ \frac{0.6}{5s+1} & \frac{1}{4s+1} & \frac{0.4}{5s+1} & \frac{0.35}{5s+1} \\ \frac{0.35}{5s+1} & \frac{0.4}{5s+1} & \frac{1}{4s+1} & \frac{0.6}{5s+1} \\ \frac{0\,2}{5s+1} & \frac{0.3}{5s+1} & \frac{0.7}{5s+1} & \frac{0.1}{4s+1} \end{bmatrix}$$

the furnace transfer function is now discritized with sampler ZOH with sampling period Δ = 0.1 second and corresponding plant TF in delta domain with common denominator is obtained as:

$$P_\delta(\gamma) = \begin{bmatrix} \frac{0\,2469\gamma+0\,0489}{\gamma^2+0\,4449\gamma+0\,0489} & \frac{0\,1386\gamma+0\,0342}{\gamma^2+0\,4449\gamma+0\,0489} & \frac{0\,0594\gamma+0\,0147}{\gamma^2+0\,4449\gamma+0\,0489} & \frac{0\,0396\gamma+0\,0098}{\gamma^2+0\,4449\gamma+0\,0489} \\ \frac{0\,1188\gamma+0\,0293}{\gamma^2+0\,4449\gamma+0\,0489} & \frac{0\,2469\gamma+0\,0489}{\gamma^2+0\,4449\gamma+0\,0489} & \frac{0\,0792\gamma+0\,0196}{\gamma^2+0\,4449\gamma+0\,0489} & \frac{0\,0693\gamma+0\,0171}{\gamma^2+0\,4449\gamma+0\,0489} \\ \frac{0\,0693\gamma+0\,0171}{\gamma^2+0\,4449\gamma+0\,0489} & \frac{0\,0792\gamma+0\,0196}{\gamma^2+0\,4449\gamma+0\,0489} & \frac{0\,2469\gamma+0\,0489}{\gamma^2+0\,4449\gamma+0\,0489} & \frac{0\,1188\gamma+0\,0293}{\gamma^2+0\,4449\gamma+0\,0489} \\ \frac{0\,0396\gamma+0\,0098}{\gamma^2+0\,4449\gamma+0\,0489} & \frac{0\,0594\gamma+0\,0147}{\gamma^2+0\,4449\gamma+0\,0489} & \frac{0\,1386\gamma+0\,0342}{\gamma^2+0\,4449\gamma+0\,0489} & \frac{0\,2469\gamma+0\,0489}{\gamma^2+0\,4449\gamma+0\,0489} \end{bmatrix}$$

The reference model with ω_n= 0.84 rad/sec, ξ=0.7 and angle (ρ) = - 40° is obtained as:

$$M_\delta(\gamma) = diag\left[\frac{0.3234\,\gamma+0.2179}{\gamma^2+0.8881\gamma+0.2179}\right]$$

To obtain the OGDTM Point (μ_{ti}), following GA parameters are considered

- Method of selection : Tournament selection method
- Number of tournaments: 2
- Number of generation for evolution: 30
- Population size : 31
- Crossover probability: 0.80
- Number of crossover : 2
- Mutaion probability: 0.0080

and after simulation we got the OGDTM point 0.1505 and corresponding PI controller coefficients as:

$$C_s(\gamma)=\begin{bmatrix} 1.8409+\frac{0.6595}{\gamma} & -0.9447-\frac{0.4443}{\gamma} & -0.1539-\frac{0.0584}{\gamma} & 0.0332+\frac{0.0562}{\gamma} \\ -0.7690-\frac{0.3594}{\gamma} & 1\ 9288+\frac{0.7057}{\gamma} & -0\ 2744-\frac{0.0906}{\gamma} & -0.2747-\frac{0.1182}{\gamma} \\ -0.2747-\frac{0.1182}{\gamma} & -0.2744-\frac{0.0906}{\gamma} & 1.9288+\frac{0.7057}{\gamma} & -0.7690-\frac{0.3594}{\gamma} \\ 0.0332+\frac{0.0562}{\gamma} & -0.1539-\frac{0.0584}{\gamma} & -0\ 9447-\frac{0.4443}{\gamma} & 1.8409+\frac{0.6595}{\gamma} \end{bmatrix}$$

The unit step responses of the reference model and the augmented plant with controller are given in figures 4.17 to 4.18. As in earlier cases, it may be seen from the figures 4.17 & 4.18 that the unit step responses of the closed-loop system are close to those of the reference model which proves the robustness of the OGDTM methodology. The off diagonal elements of the designed multivariable PI controller are not zeros initially, this is because of the plant transfer function including interaction terms has been taken into consideration in the design process however its effect becomes zero as time is increased.

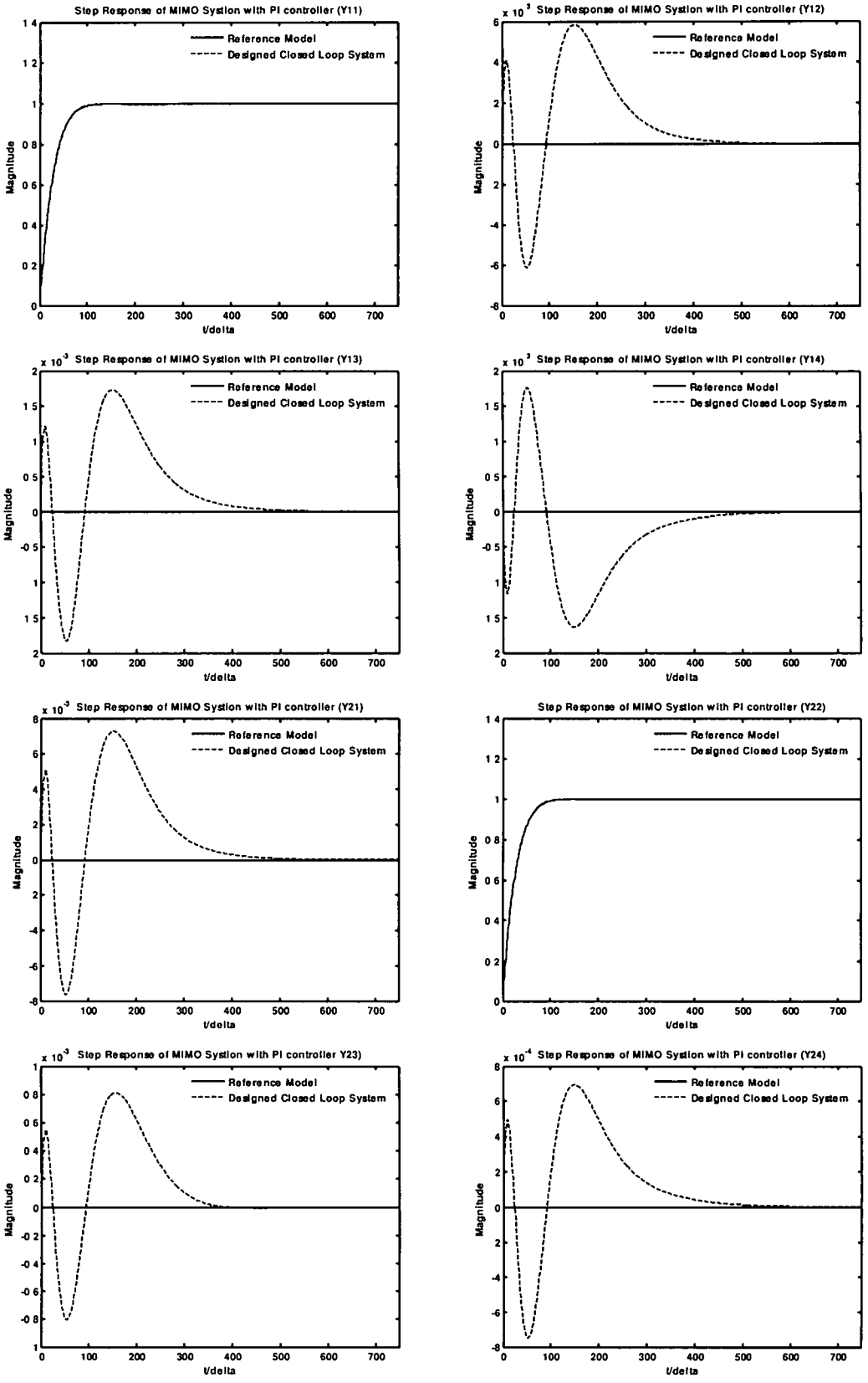

Figure 4 17 Step responses of uncontrolled plant, reference model and closed loop system with PI controller using OGDTM, output y11,y12,y13,y14,y21,y22,y23,y24, Δ = 0 1 sec and ρ = -40°

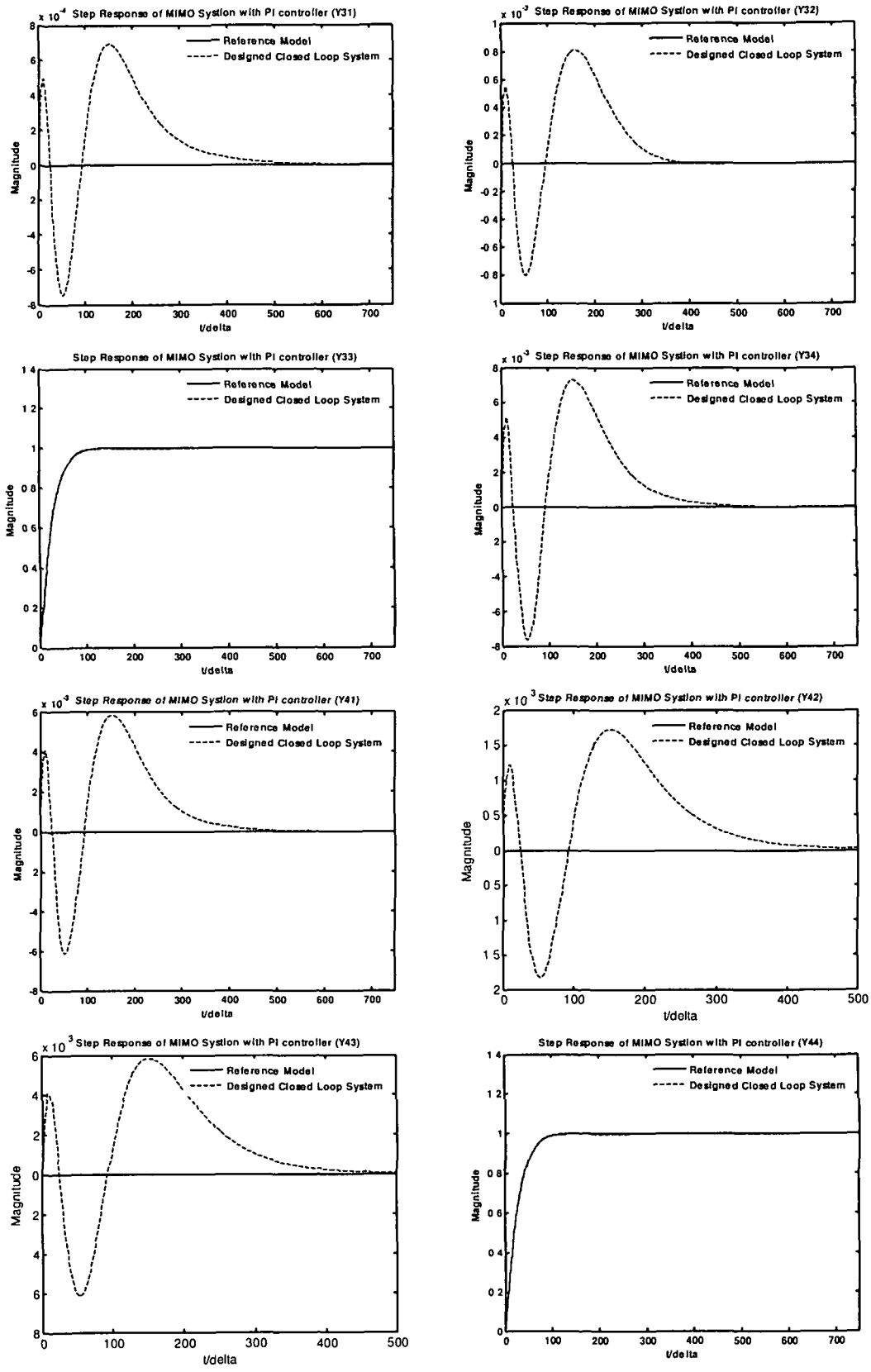

Figure 4 18 Step responses of uncontrolled plant, reference model and closed loop system with PI controller using OGDTM, output y31,y32,y33,y34,y41,y42,y43,y44, $\Delta = 0.1$ sec and $\rho = -40°$

4.5 Optimal Frequency Fitting method:

The optimal frequency fitting design method of SISO systems described in Chapter 3 has already been successfully tested. Here, in this section the same methodology is applies for controller design of MIMO processes. Let us assume the transfer function matrices of the plant and cascaded controller be $P_\delta(\gamma)$ and $C_\delta(\gamma)$ respectively. Therefore the closed-loop transfer function matrix $G_\delta(\gamma)$ can is given in terms of $P_\delta(\gamma)$ and $C_\delta(\gamma)$ as:

$$G_\delta(\gamma) = [I + P_\delta(\gamma)\, C_\delta(\gamma)]^{-1}\, P_\delta(\gamma)\, C_\delta(\gamma) \qquad (4.26)$$

The performance specifications of the closed-loop control system are translated into a reference transfer matrix $M_\delta(\gamma)$, which is of the form

$$M_\delta(\gamma) = diag\{\, M_{\delta,ii}(\gamma)\,\}; \qquad i \in [\,1,\, p\,] \qquad (4.27)$$

Here p is the number of inputs or outputs and the off-diagonal entries $M_\delta(\gamma)$, are chosen as 0 (zero) i.e. we try to enforce zero coupling. The equivalent open loop reference model transfer function matrix is $F_\delta(\gamma)$, such that $F_\delta(\gamma)$, with unity negative feedback becomes equal to $M_\delta(\gamma)$. Thus,

$$M_\delta(\gamma) = [1 + F_\delta(\gamma)]^{-1} F_\delta(\gamma) \qquad (4.28)$$

hence
$$F_\delta(\gamma) = M_\delta(\gamma)\,[1 - M_\delta(\gamma)]^{-1} \qquad (4.29)$$

For the closed-loop system $G_\delta(\gamma)$ to match the time and frequency responses of the closed-loop reference model $M_\delta(\gamma)$, they are to be equivalent in some sense. Alternatively, it may be said that the open-loop system $P_\delta(\gamma)\ C_\delta(\gamma)$ should be equivalent to open-loop reference model $F_\delta(\gamma)$ i.e.,

$$P_\delta(\gamma)\, C_\delta(\gamma) \cong F_\delta(\gamma) \qquad (4.30)$$

or
$$C_\delta(\gamma) \cong P_\delta(\gamma)^{-1} F_\delta(\gamma)$$

or
$$C_\delta(\gamma) \cong X_\delta(\gamma)$$

then
$$[C_{\delta,ij}(\gamma)] = [X_{\delta,ij}(\gamma)], \qquad i, j \in [1,\ p]$$

where $X_\delta(\gamma)$, is an entirely known transfer function matrix, as both $P_\delta(\gamma)$, and $F_\delta(\gamma)$, are completely specified. For SISO controller design problem discussed in section 3.6 of chapter-3, it was seen that the problem of designing the controller $C_\delta(\gamma)$, where

$C_\delta(\gamma)$, with pre-specified order and structure (Equation 3.91) was made to approximate the known $X_\delta(\gamma)$. Here for MIMO controller design we assume the structure of each element of the transfer function model $C_\delta(\gamma)$, as a scalar controller transfer function of order *r* given by:

$$C_\delta(\gamma) = \frac{\beta_{0,ij} + \beta_{1,ij}\gamma + \cdots + \beta_{r,ij}\gamma^r}{\alpha_{0,ij} + \alpha_{1,ij}\gamma + \cdots + \gamma^r} \tag{4.31}$$

where β's and α's are the *(2r+1)* unknown parameters of each scalar transfer function of $C_\delta(\gamma)$. Then, using the AFF technique which is mathematically equivalent to

$$C_{\delta,ij}(\gamma)\Big|_{\gamma=\frac{e^{j\omega\Delta}-1}{\Delta}} \triangleq X_{\delta,ij}(\gamma)\Big|_{\gamma=\frac{e^{j\omega\Delta}-1}{\Delta}} \tag{4.32}$$

From eqn.(4.32); we have,

$$\sum_{l=0}^{r}\beta_{l,ij}|\gamma|^l e^{j\theta l} - |X_{\delta,ij}|e^{j\phi}\sum_{l=0}^{r-1}\alpha_{l,ij}|\gamma|^l e^{j\theta l} \cong |X_{\delta,ij}||\gamma|^r e^{j(\phi+\theta r)} \tag{4.33}$$

where

$$\gamma = |\gamma|e^{j\theta} \quad \text{and} \quad X_{\delta,ij}(\gamma) = |X_{\delta,ij}|e^{j\phi}$$

Let us define $\psi = \omega\Delta$; therefore, θ and ϕ are functions of ψ. Finally equating the real and imaginary parts of eqn.(4.33) separately, we get

$$\sum_{l=0}^{r}\beta_{l,ij}R_{l,ij}(\psi) - \sum_{l=0}^{r-1}\alpha_{l,ij}S_{l,ij}(\psi) \cong T_{ij}(\psi) \tag{4.34}$$

$$\sum_{l=0}^{r}\beta_{l,ij}U_{l,ij}(\psi) - \sum_{l=0}^{r-1}\alpha_{l,ij}V_{l,ij}(\psi) \cong W_{ij}(\psi) \tag{4.35}$$

Where

$$R_{l,ij}(\psi) = |\gamma|^l \cos\theta l$$

$$S_{l,ij}(\psi) = |X_{\delta,ij}||\gamma|^l \cos(\theta l + \phi)$$

$$U_{l,ij}(\psi) = |\gamma|^l \sin\theta l$$

$$V_{l,ij}(\psi) = |X_\delta||\gamma|^l \cos(\theta l + \phi)$$

$$T_{ij}(\psi) = |X_{\delta,ij}||\gamma|^r \cos(\theta q + \phi)$$

$$W_{ij}(\psi) = |X_{\delta,ij}||\gamma|^r \sin(\theta q + \phi)$$

The left hand side (l.h.s) expressions of (4.34) and (4.35) are real functions of ψ with unknown coefficients $\beta_{l,ij}$ and $\alpha_{l,ij}$, $T_{ij}(\psi)$ and $W_{ij}(\psi)$ are also two real (known)

functions of ψ. Hence designating the l.h.s. functions as $\Phi_{R,ij}(\psi)$ and $\Phi_{I,ij}(\psi)$ respectively, relations (4.34) and (4.35) may be written for convenience as :

$$\Phi_{R,ij}(\psi) \cong T_{ij}(\psi) \tag{4.36}$$

$$\Phi_{I,ij}(\psi) \cong W_{ij}(\psi) \tag{4.37}$$

In order to force two real functions $\Phi_{R,ij}(\psi)$ and $\Phi_{I,ij}(\psi)$ to be equivalent with their approximates $T_{ij}(\psi)$ and $W_{ij}(\psi)$ respectively, one may equate approximate number of initial few terms of the corresponding Taylor series expansions about $\psi = 0$. Thus, to accomplish appropriate matching of the l.h.s. functions in eqns. (4.36) and (4.37) with the corresponding functions on the r.h.s, the initial N derivatives (where N is at least equal to *r*) of the corresponding functions are equated at $\psi = 0$ to give

$$\frac{d^k}{d\psi^k}[\Phi_{R,ij}(\psi)]\Big|_{\psi=0} = \frac{d^k}{d\psi^k}[T_{ij}(\psi)]\Big|_{\psi=0} \tag{4.38}$$

$$\frac{d^k}{d\psi^k}[\Phi_{I,ij}(\psi)]\Big|_{\psi=0} = \frac{d^k}{d\psi^k}[W_{ij}(\psi)]\Big|_{\psi=0} \quad ; \quad k \in [0, N-1]$$

Using the results of Pal [76] and Milne-Thompson [115], the derivative operations $\Phi_{R,ij}(\psi)$ approximately matches $T_{ij}(\psi)$ if

$$\Phi_{R,ij}(\psi)\Big|_{\psi=\psi_k} = T_{ij}(\psi)\Big|_{\psi=\psi_k}; \qquad k \in [0, N-1] \tag{4.39}$$

where ψ_k are small positive values around $\psi = 0$. Similarly,

$$\Phi_{I,ij}(\psi)\Big|_{\psi=\psi_k} = W_{ij}(\psi)\Big|_{\psi=\psi_k}; \qquad k \in [0, N-1] \tag{4.40}$$

The relations in eqns. (4.39) and (4.40) may be written in a matrix form as

$$A_{ij}\, x_{ij} = b_{ij} \tag{4.45}$$

Here A_{ij} is a 2(N) × (2r + 1) matrix given by

$$A_{ij} = \begin{bmatrix} R_{ij,1,1} & \cdots & R_{ij,1,q+1} & -S_{ij,1,1} & \cdots & -S_{ij,1,q} \\ U_{ij,1,1} & \cdots & U_{ij,1,q+1} & -V_{ij,1,1} & \cdots & -V_{ij,1,q} \\ \vdots & \ddots & \vdots & \vdots & \cdots & \vdots \\ R_{ij,k,1} & \cdots & R_{ij,k,q+1} & -S_{ij,k,1} & \cdots & -S_{ij,k,q} \\ U_{ij,k,1} & \cdots & U_{ij,k,q+1} & -V_{ij,k,1} & \cdots & -V_{ij,k,q} \\ \vdots & \ddots & \vdots & \vdots & \cdots & \vdots \\ R_{ij,N,1} & \cdots & R_{ij,N,q+1} & -S_{ij,N,1} & \cdots & -S_{ij,N,q} \\ U_{ij\,1,1} & \cdots & U_{ij,N,q+1} & -V_{ij\,N,1} & \cdots & -V_{ij,N,q} \end{bmatrix}$$

$$x_{ij} = [\beta_{ij,0}, \beta_{ij,1}, \beta_{ij,2} \cdots \beta_{ij,q}, \quad \alpha_{ij,0}, \alpha_1, \alpha_2, \cdots \alpha_{ij,q-1}]^T \qquad (4.46)$$

$$b_{ij} = [T_{ij,1} \cdots T_{ij,2} \cdots T_{ij,k} \cdots T_{ij,N}, \quad W_{ij,1} \cdots W_{ij,2} \cdots W_{ij,k} \cdots W_N]^T \qquad (4.47)$$

where

$$R_{ij,k,l} = |\gamma|^l \cos\theta l$$
$$S_{ij,k,m} = |X_\delta||\gamma|^m \cos(\theta m + \phi)$$
$$U_{ij,k,l} = |\gamma|^l \sin\theta l$$
$$V_{ij,k,m} = |X_\delta||\gamma|^m \sin(\theta m + \phi)$$
$$T_{ij,k} = |X_\delta||\gamma|^r \cos(\phi + \theta r)$$
$$W_{ij,k} = |X_\delta||\gamma|^r \sin(\phi + \theta r);$$

and $i \in [1, p]; j \in [1, p]$; are inputs and outputs; k ∈ [1, N] are the number f expansion points; l ∈ [0, r] and m ∈ [0, 2r+1]. It is clear from eqn.(4.45) that N values of ψ give 2N linear algebraic equations in the unknown parameters of the controller. For (2r + 1) number of unknowns.. In the case when 2N > (2r + 1), the parameters of the controller may be determined by the least squares solution of (4.45) as:

$$x_{ij} = (A_{ij}^T A_{ij})^{-1} A_{ij}^T b_{ij} \qquad (4.48)$$

The optimal frequency points searched by using genetic algorithms are confined to lie in a small zone around the point $\omega = 0$ or $\psi = 0$ ($\psi = \omega\Delta$). In effect, the matching is done for the effective range of the frequency response in discrete domain i.e., $\omega = [0, \omega_s / 2]$ or $\psi = [0, \pi]$. For various systems, the sampling period Δ may be different and so will be the sampling frequency ω_s. But $\omega_s \Delta / 2$ is always a constant and equals π. Therefore, for matching purpose the frequency points are chosen as $\psi_k = k\eta$; $k \in [1, N]$ where η is small positive number and $\eta << 1$ so that $\psi_k = [0, \pi]$. for $k \in [1, N]$.

4.6 Simulation results:

The optimal frequency fitting method as tested on plants as described in the following sections.

4.6.1 Simple multivariable plant:

We consider here the multivariable plant given in section 4.4.1 to demonstrate the application of optimal frequency fitting method of controller design. The plant $P_c(s)$ and corresponding plant TF with common denominator in delta domain with sampling period $\Delta = 0.1$ second is same as given in section 4.4.1.

The 2nd order reference model with $\omega_n = 0.84$ rad/sec, $\xi = 0.7$ and angle $(\rho) = -45°$ is

$$M_\delta(\gamma) = \begin{bmatrix} \dfrac{0.0227\gamma + 0.6653}{\gamma^2 + 1.176\gamma + 0.6653} & 0 \\ 0 & \dfrac{0.0227\gamma + 0.6653}{\gamma^2 + 1.176\gamma + 0.6653} \end{bmatrix}$$

To methodology was tested with the following GA parameters

- Method of selection : Roulette wheel
- Number of generation for evolution: 30
- Population size : 31
- Crossover probability: 0.77
- Number of crossover : 2
- Mutaion probability: 0.0077

and using above GA parameters, the real and imaginary parts of optimal frequency point found to be -0.0220+j0.6623 at $\mu_{ti} = 0.3314$ and we obtain the following PI controller transfer function matrix.

$$C_\delta(\gamma) = \begin{bmatrix} -1.4868 + \dfrac{1.8507}{\gamma} & 1.1701 - \dfrac{3.6399}{\gamma} \\ 1.6980 - \dfrac{0.6579}{\gamma} & -1.4868 + \dfrac{1.8507}{\gamma} \end{bmatrix}$$

The unit step responses of the reference model and the augmented plant with controller are given in figures 4.19 to 4.22 and corresponding control efforts are shown in figure 4.23. It may be seen from the figures that the unit step responses of the closed-loop system are close to those of the reference model and the off diagonal elements of the designed multivariable PI controller are not zeros, this is because of the plant transfer function including interaction terms has been taken into consideration in the design process.

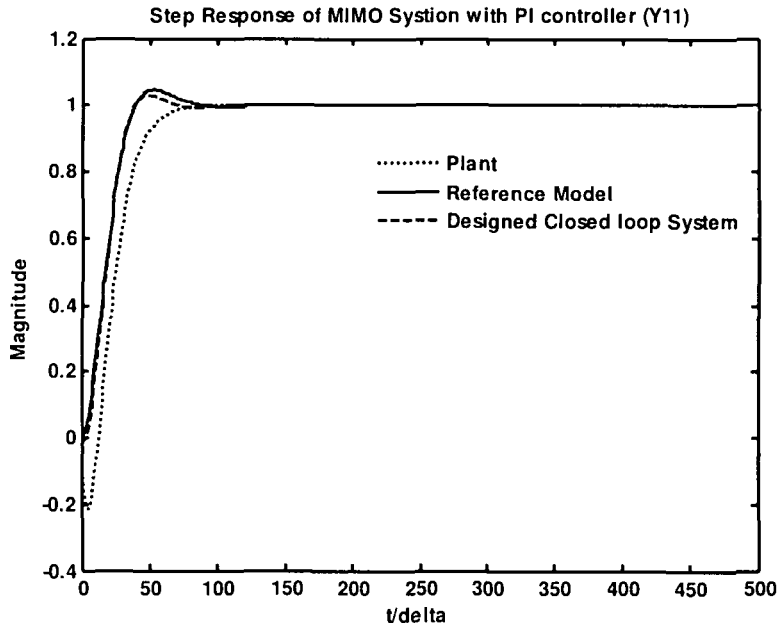

Figure 4.19: Step responses of plant, reference model and closed loop system with PI controller using OFF method, output y11, $\Delta = 0.1$ sec and $\rho = -45°$

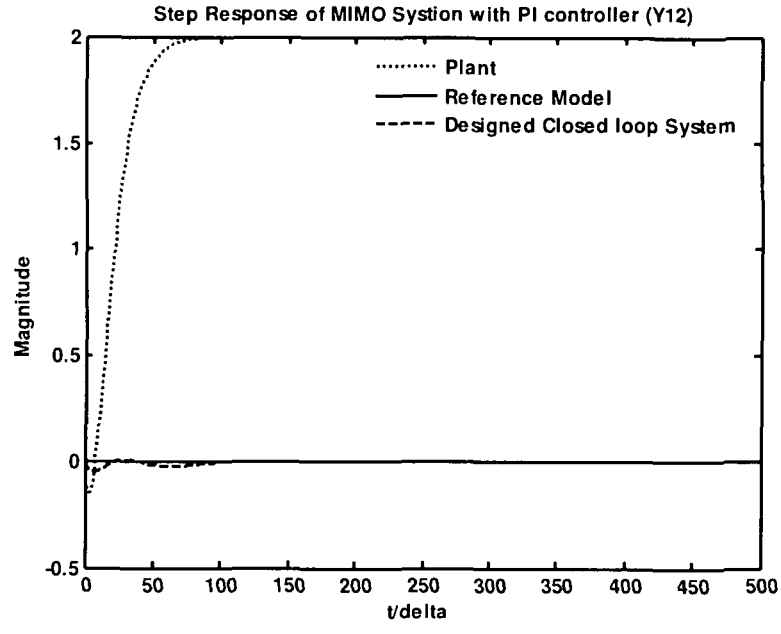

Figure 4.20: Step responses of plant, reference model and closed loop system with PI controller using OFF method, output y12, $\Delta = 0.1$ sec and $\rho = -45°$

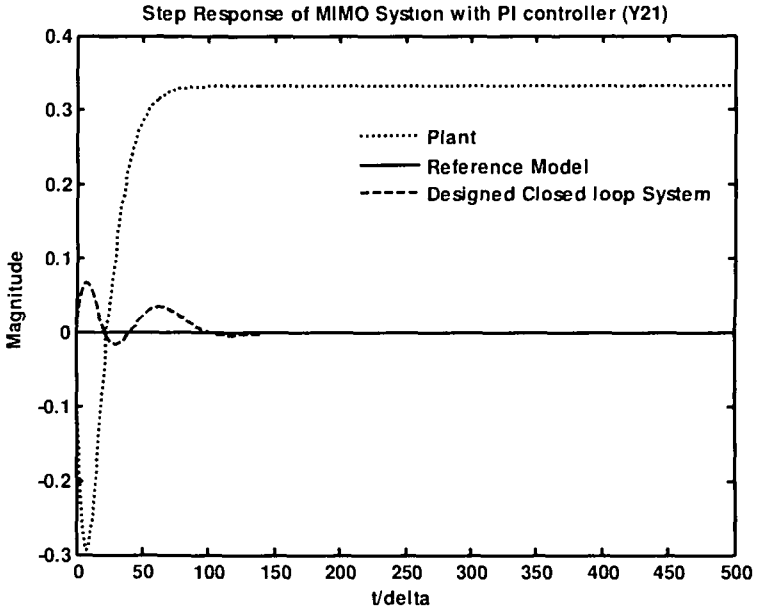

Figure 4.21: Step responses of plant, reference model and closed loop system with PI controller using OFF method, output y21, $\Delta = 0.1$ sec and $\rho = -45°$

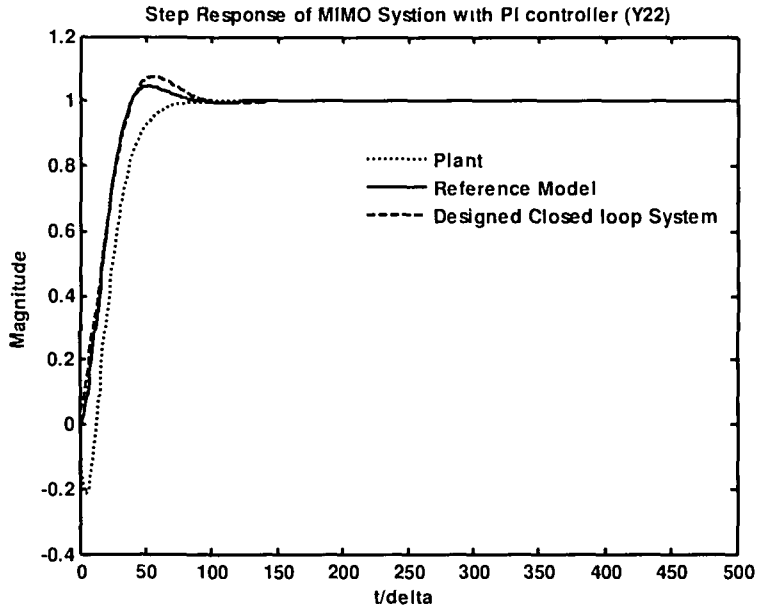

Figure 4.22: Step responses of plant, reference model and closed loop system with PI controller using OFF method, output y22, $\Delta = 0.1$ sec and $\rho = -45°$

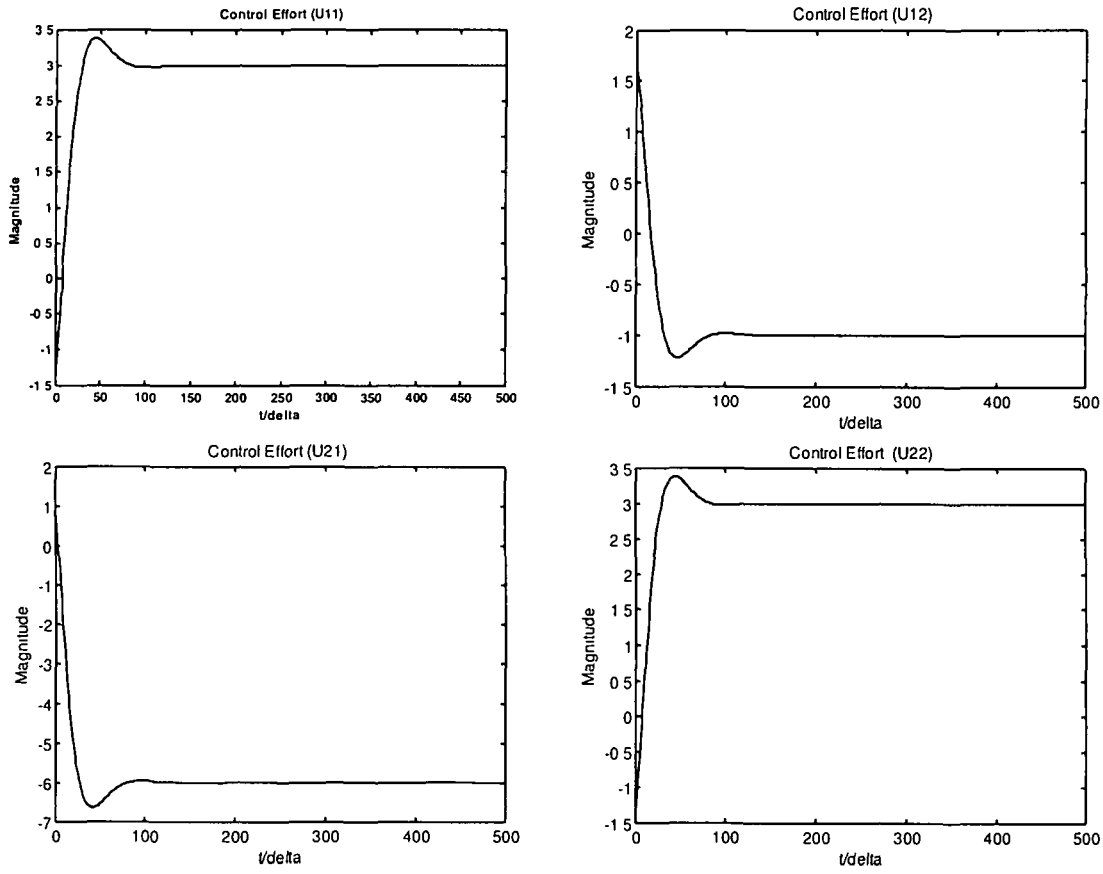

Figure 4.23: Control Efforts U11, U12, U21, U22 with PI controller using OFF method, $\Delta = 0.1$ sec and $\rho = -45°$

4.6.2 Gas turbine:

Next we consider a gas turbine [119] to test the controller design using optimal frequency fitting method. The uncontrolled plant is described by the transfer function matrix as :

$$P_c(s) = \begin{bmatrix} \dfrac{14.96s^2 + 1521.432s + 2543.2}{s^4 + 113.225s^3 + 1357.275s^2 + 3502.75s + 2525} & \dfrac{95150s^2 + 1132094.7s + 1805947}{s^4 + 113.225s^3 + 1357.275s^2 + 3502.75s + 2525} \\ \dfrac{85.2s^2 + 8642.668s + 12268.8}{s^4 + 113.225s^3 + 1357.275s^2 + 3502.75s + 2525} & \dfrac{12400s^2 + 1492588s + 2525880}{s^4 + 113.225s^3 + 1357.275s^2 + 3502.75s + 2525} \end{bmatrix}$$

The plant is sampled with sampler and zero order hold with sampling period $\Delta = 0.1$ second and corresponding plant TF in delta domain with common denominator is

$$P_\delta(\gamma)=\begin{bmatrix} \dfrac{10\gamma^2+111\gamma+140}{\gamma^4+19.29\gamma^3+113.87\gamma^2+223.01\gamma+136\ 14} & \dfrac{810\gamma^3+15400\gamma^2+80540\gamma+97370}{\gamma^4+19.29\gamma^3+113.87\gamma^2+223\ 01\gamma+136.14} \\ \dfrac{80\gamma^2+600\gamma+660}{\gamma^4+19\ 29\gamma^3+113.87\gamma^2+223.01\gamma+136\ 14} & \dfrac{1060\gamma^3+20320\gamma^2+107760\gamma+136190}{\gamma^4+19.29\gamma^3+113.87\gamma^2+223.01\gamma+136.14} \end{bmatrix}$$

The reference model with ω_n= 0.84 rad/sec, ξ=0.7 and angle ρ = - 40° is

$$M_\delta(\gamma)=\begin{bmatrix} \dfrac{0.1137\gamma+0.6653}{\gamma^2+1.176\gamma+0.6653} & 0 \\ 0 & \dfrac{0.1137\gamma+0.6653}{\gamma^2+1.176\gamma+0.6653} \end{bmatrix}$$

Following GA parameters are considered to design PI controller using OFF method

- Method of selection : Tournament selection method
- Number of tournaments: 2
- Number of generation for evolution: 35
- Population size : 31
- Crossover probability: 0.85
- Number of crossover : 2
- Mutaion probability: 0.0085

Using above GA parameters, the real and imaginary frequency point are found to be -0.0311+j0.7878 and μ_{ti} 0.3943 and we obtain the following PI controller controller transfer function matrix.

$$C_\delta(\gamma)=\begin{bmatrix} 0.0120-\dfrac{0.2339}{\gamma} & -0.0034+\dfrac{0.1685}{\gamma} \\ 0.0001+\dfrac{0.0012}{\gamma} & 0.0001-\dfrac{0.0002}{\gamma} \end{bmatrix}$$

The unit step responses of uncontrolled plant is given in figure 4.24 and corresponding step responses of the reference model and the augmented plant with controller are given in figures 4.25 to 4.28 along with the control effort in figure 4.29 . The unit step responses of the closed-loop system are close to those of the reference model.

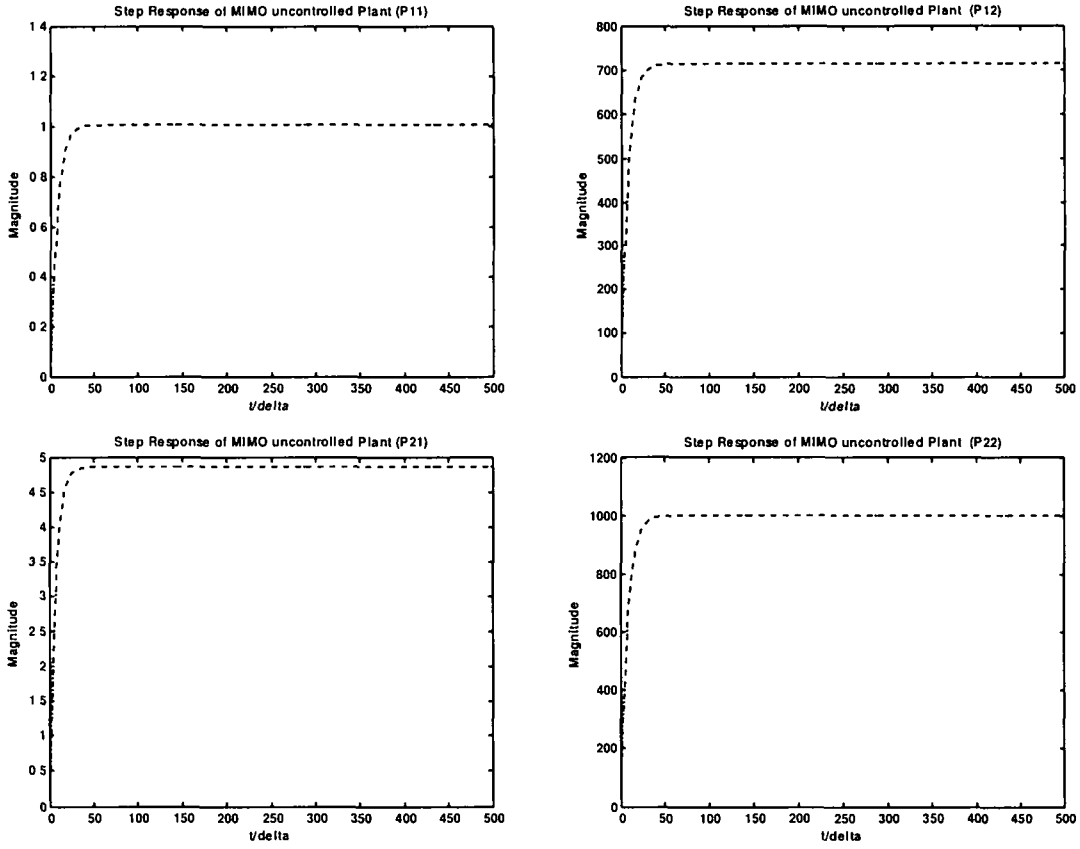

Figure 4.24: Step responses of p11, p12, p21, p22 , $\Delta = 0.1$ sec and $\rho = -40°$

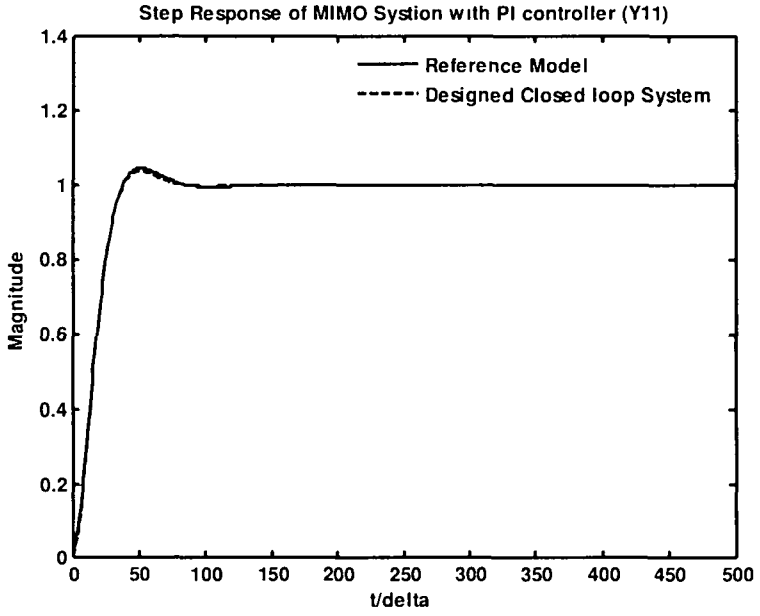

Figure 4.25: Step responses of reference model and closed loop system with PI controller using OFF method, output y11, $\Delta = 0.1$ sec and $\rho = -40°$

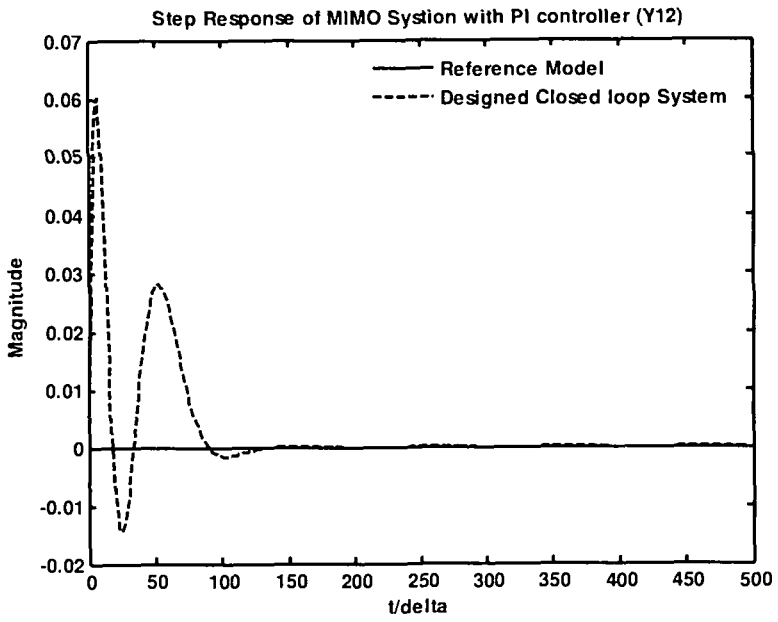

Figure 4.26: Step responses of reference model and closed loop system with PI controller using OFF method, output y12, $\Delta = 0.1$ sec and $\rho = -40°$

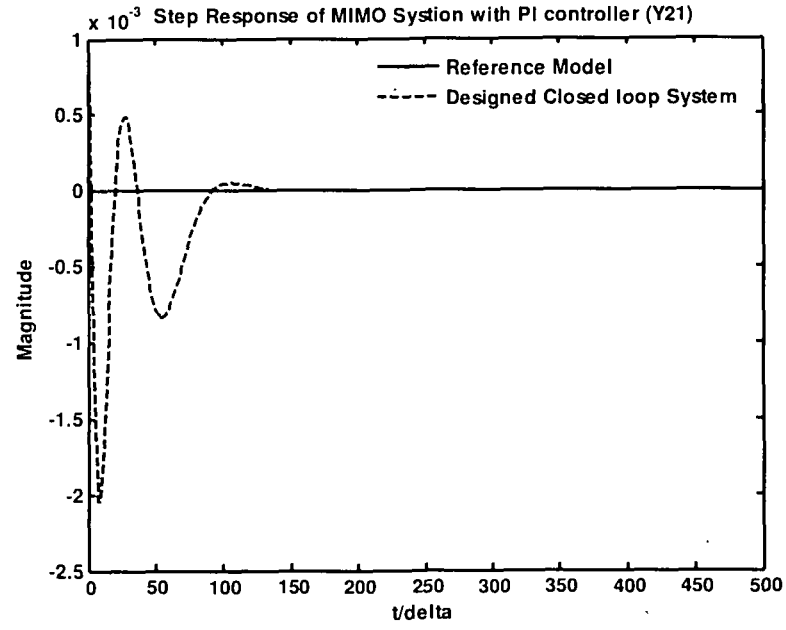

Figure 4.27: Step responses of reference model and closed loop system with PI controller using OFF method, output y21, $\Delta = 0.1$ sec and $\rho = -40°$

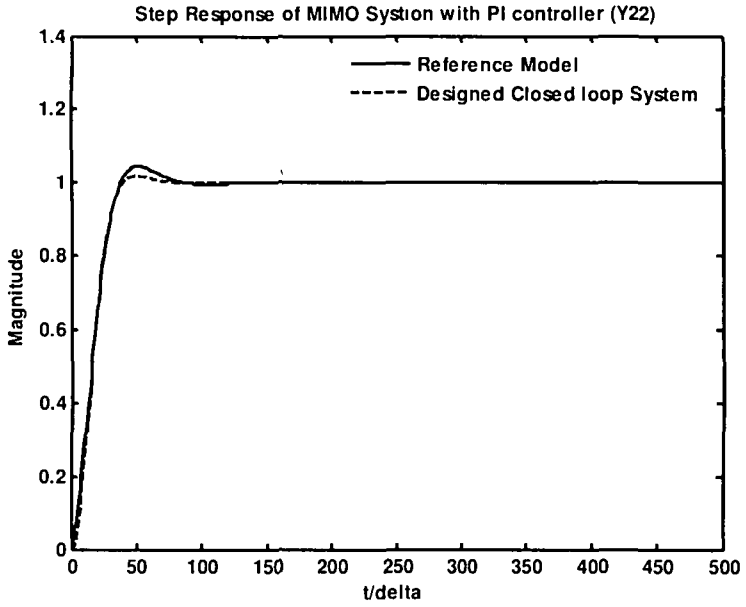

Figure 4.28: Step responses of reference model and closed loop system with PI controller using OFF method, output y22, $\Delta = 0.1$ sec and $\rho = -40°$

4.6.3 Multivariable gas fired furnace:

The four-input four-output gas fired furnace given in section 4.5.3 is revisited to test the robustness of optimal frequency fitting method. We chose here the sampling period $\Delta = 0.1$ second, therefore corresponding furnace TF matrix in delta domain with common denominator will be same as shown in section 4.5.3

The 2nd order reference model with $\omega_n = 0.84$ rad/sec, $\xi = 0.7$ and angle $(\rho) = -40°$ is

$$M_\delta(\gamma) = \begin{bmatrix} \frac{0.3234\gamma + 0.2179}{\gamma^2 + 0.8881\gamma + 0.2179} & 0 & 0 & 0 \\ 0 & \frac{0.3234\gamma + 0.2179}{\gamma^2 + 0.8881\gamma + 0.2179} & 0 & 0 \\ 0 & 0 & \frac{0.3234\gamma + 0.2179}{\gamma^2 + 0.8881\gamma + 0.2179} & 0 \\ 0 & 0 & 0 & \frac{0.3234\gamma + 0.2179}{\gamma^2 + 0.8881\gamma + 0.2179} \end{bmatrix}$$

Following GA parameters are considered to design PI controller using OFF method

- Method of selection : Tournament selection method
- Number of tournaments: 2
- Number of generation for evolution: 30
- Population size : 31
- Crossover probability: 0.77
- Number of crossover : 2
- Mutaion probability: 0.0077

Using genetic algorithm the real and imaginary parts of frequency point is found to be -0.0036+j 0.2694 and $\mu_{ti} = 0.1347$ and we obtain the following PI controller transfer function matrix.

$$C_\delta(\gamma) = \begin{bmatrix} 1.8444 + \frac{0.6461}{\gamma} & -0.9048 - \frac{0.4250}{\gamma} & -0.1526 - \frac{0.0562}{\gamma} & 0.0124 + \frac{0.0489}{\gamma} \\ -0.7373 - \frac{0.3438}{\gamma} & 1.9267 + \frac{0.6902}{\gamma} & -0.2814 - \frac{0.0915}{\gamma} & -0.2672 - \frac{0.1133}{\gamma} \\ -0.2672 - \frac{0.1133}{\gamma} & -0.2814 - \frac{0.0915}{\gamma} & 1.9267 + \frac{0.6902}{\gamma} & -0.7372 - \frac{0.3438}{\gamma} \\ 0.0124 + \frac{0.0489}{\gamma} & -0.1526 - \frac{0.0562}{\gamma} & -0.9048 - \frac{0.4250}{\gamma} & 1.84444 + \frac{0.6461}{\gamma} \end{bmatrix}$$

The unit step responses of the reference model and the augmented plant with controller are shown in figures 4.30 to 4.31 and control efforts are shown in figures

4.32. It may be seen from the figures that the unit step responses of the closed-loop system are close to those of the reference model.

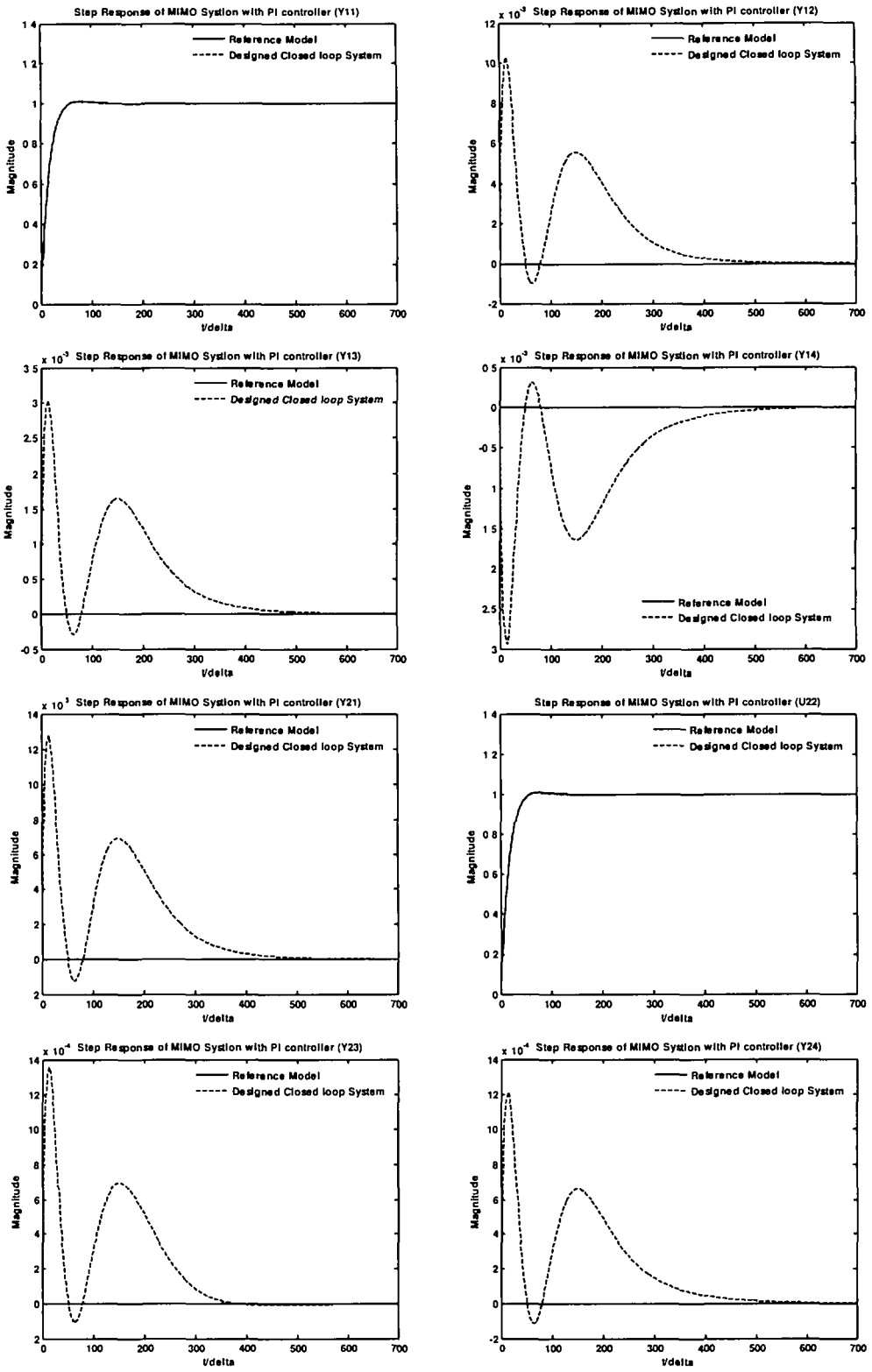

Figure 4.30: Step responses of reference model and closed loop system with PI controller using OFF method, output y11,y12,y13,y14,y21,y22,y23,y24, $\Delta = 0.1$ sec and $\rho = -40°$

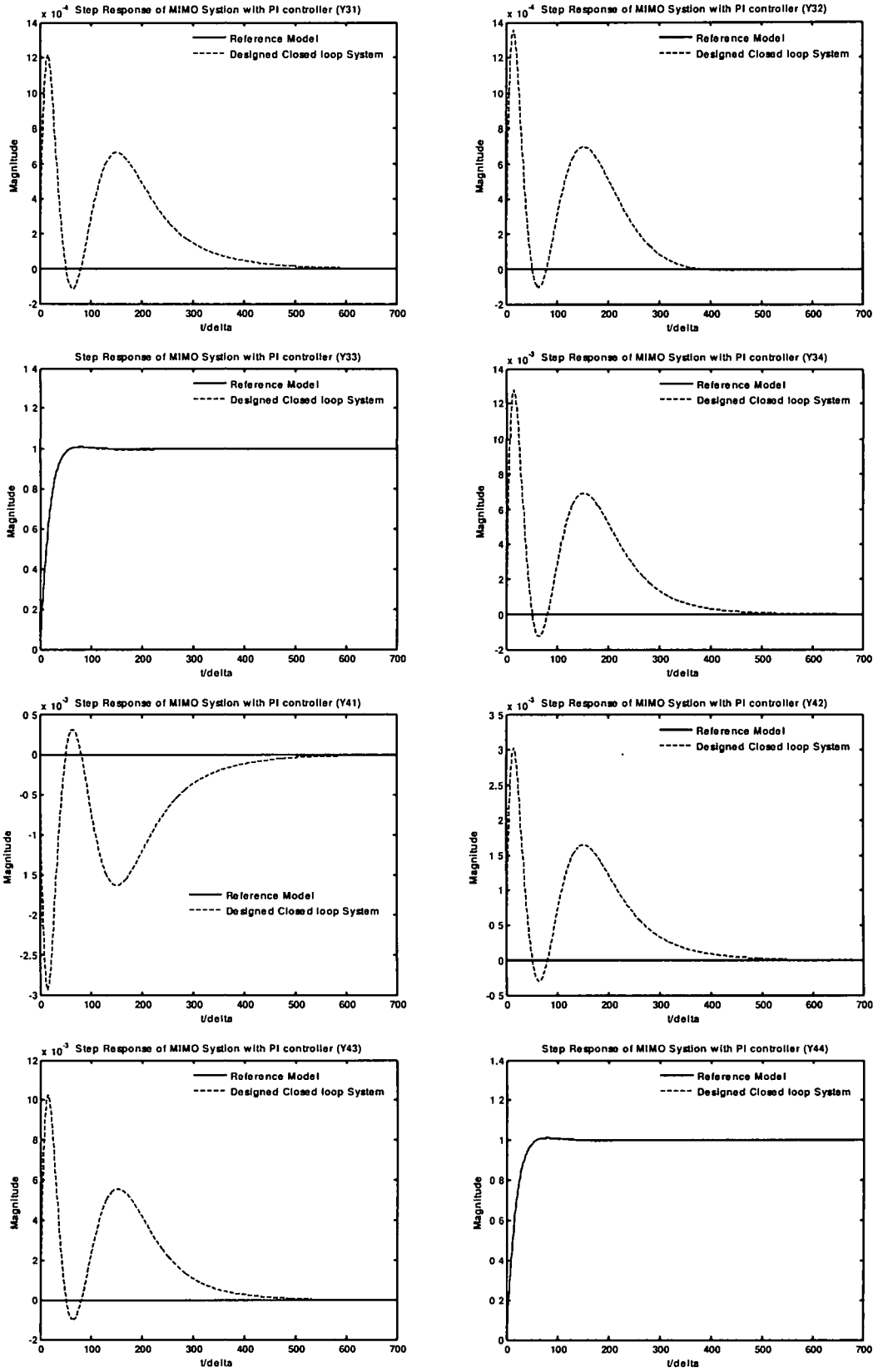

Figure 4.31: Step responses of reference model and closed loop system with PI controller using OFF method, output y31,y32,y33,y34,y41,y42,y43,y44, $\Delta = 0.1$ sec and $\rho = -40°$

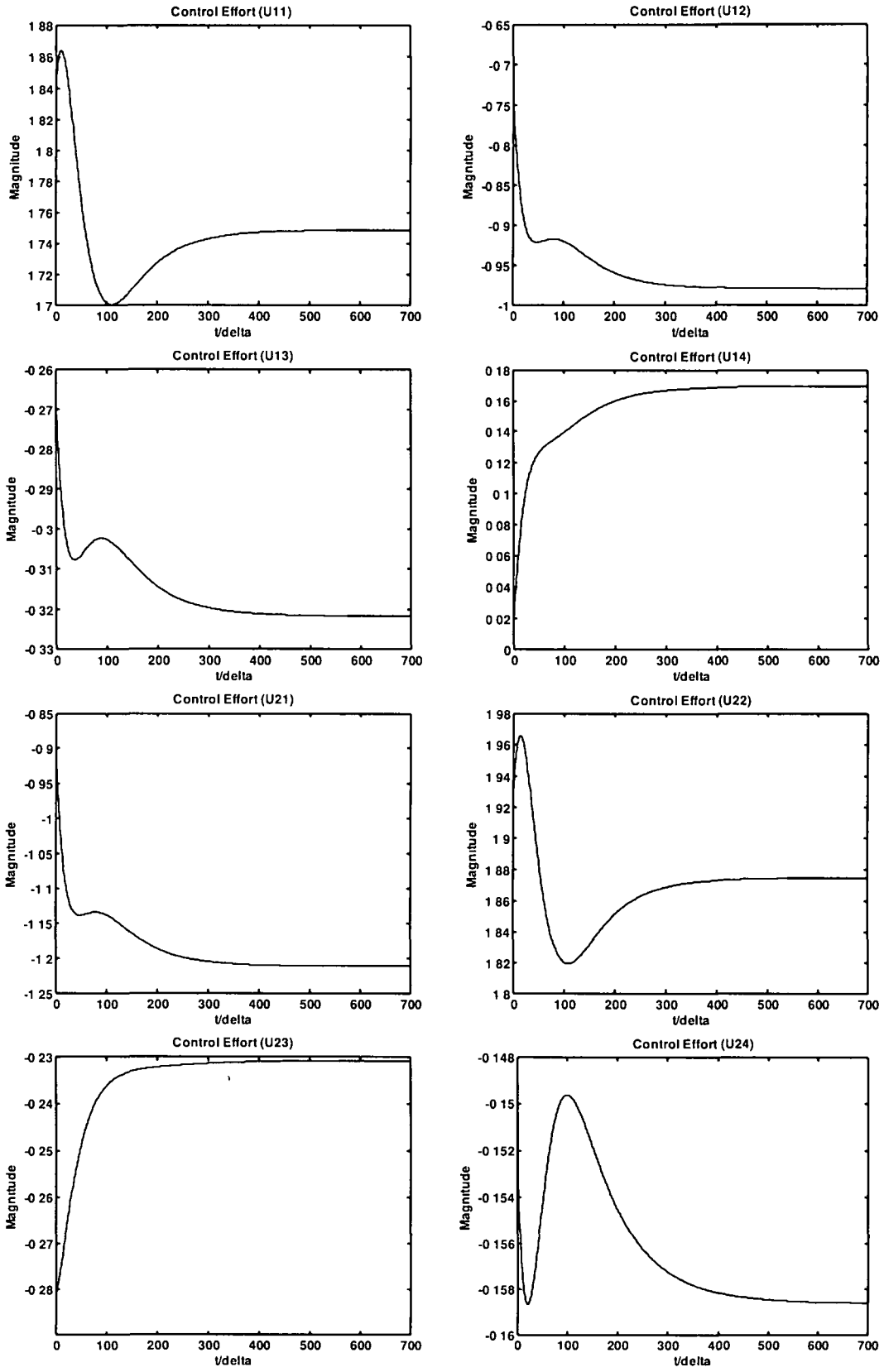

Figure 4 32 Control Efforts using OFF method, u11,u12,u13,u14,u21,u22,u23,u24 $\Delta = 0.1$ sec, $\rho = -40°$

4.7 Conclusion:

Two computationally simple design approaches to practical controller design for multivariable systems in δ-domain are presented in this chapter. The linear algebraic frameworks developed in the Chapter 3 for controller design of SISO systems have been extended for MIMO systems. Optimal GDTM and Optimal frequency fitting of the closed loop TFM with those of the reference TFM model have led to close matching of the step responses on each individual input output channel and simultaneous suppression of the interaction between various input-output loops. The methods have been applied to some practical plants. The effectiveness of the design methods in providing adequate control according to a predetermined design objective has been demonstrated. Salient features of the proposed methods are:

- To determine the controller parameters, only linear equations are required to be solved.
- Design does not require the controller to be confined to any particular structure.
- Plant may be described in transfer function or state space form hence polynomial matrix operations are not required.
- Complexity and structure of $C_\delta(\gamma)$ may be changed at designer's will to make a compromise between controller complexity and achievable performance.
- The increase in the computational effort is minimal with an increase in number of inputs and outputs.
- The methods can be extended to the design of digital controllers for multivariable systems with multiple time delays also which is discussed in the later chapters.
- The design procedures are goal-oriented. The end result is made to meet a predetermined objective i.e., to satisfy the given industrial specifications and is not a by-product of the design procedure.
- The algorithms are numerically robust and at high sampling limit converges to the corresponding continuous-time results leading to a unified treatment of both discrete-time and continuous-time systems.

The approach adopted in the proposed methods suppress interaction and also the desired main diagonal response requirements are simultaneously accomplished, i.e., in a single step rather than in two steps. The individual scalar controller TFs of

the controller TFM may be chosen to have a different order or structure. The solution of equations for a given individual controller TF is independent of the solution of equations of the other scalar TFs in the controller TFM. This offers flexibility to the designer to change the complexity or structure of any individual entry in the controller TFM. The designer, therefore, has freedom to make tradeoffs between the controller complexity and the performance requirement on each main diagonal. Higher-order plants do not require any special computational problem. Design for unstable MIMO system has been carried out by stabilizing the system in the first step using an inner loop. Unity rank output feedback, though known to be restrictive, has been used in order to illustrate the suitability of the method in designing controllers for unstable MIMO systems.

Chapter 5

Time Delay & Uncertain System Controllers

5.1 Controller Design for Systems with Time Delay

5.1.1 Introduction:

An important class of systems whose dynamic characteristics possess dead time or transportation lag is called system with time delay. Typical examples include heat flow, material transportation, hydraulic and pneumatic transmission, chemical reactors, distillation columns and several others in the process industries. Continuous-time systems with time delay do not have rational transfer function in s-domain. The presence of dead time in the continuous time process gives rise to a non-rational term $e^{-s\tau}$ in the plant transfer function and hence greatly complicates the design of a controller for the continuous-time process. The characteristic equation of such a system does not have a finite order. In fact, there are an infinite number of characteristic roots for a system with dead time. However, the presence of time delay in discrete-time systems does not lead to an irrational transfer function either in the shift operator or in the delta operator parameterization. The time delay in the case of discrete-time system may be considered as either an integer multiple or a non-integer multiple of the sampling time.

The problems posed by the time delay are degradation in performance on one hand, and complicated analytical aspect on the other. From the performance point of view, the closed-loop system will not perform as well as when $\tau = 0$. This is mainly because delay introduces a large phase lag and thus tends to destabilize the closed-loop system. To counteract this, the gain of the controller must be reduced below the value which could be used in the no-delay case, i.e. $\tau = 0$. As a consequence, the system will respond slow to set point changes or other kinds of command inputs and the achievable performance will thus be limited.

5.1.2 Time delay in s-domain:

The time domain model for a system with time delay 'τ' in the measurement of output may be formulated in state-space form as

$$\frac{dx(t)}{dt} = A_c x(t) + B_c u(t)$$
$$y(t+\tau) = C_c x(t) \tag{5.1}$$

Alternatively, in some systems the time delay may be associated with the input signal, and the appropriate model is then

$$\frac{dx'(t)}{dt} = A_c x'(t) + B_c u(t-\tau)$$
$$y(t) = C_c x'(t) \tag{5.2}$$

Note that the states have a different interpretation in the equivalent models given above. With zero initial conditions, including y(t) = 0 for t < 0, and taking the transform of equation (5.1)

$$sX(s) = A_c X(s) + B_c X(s) \tag{5.3}$$

and

$$e^{-s\tau}Y(s) = C_c X(s) \tag{5.4}$$

The same result is obtained for the input delay model of equation (5.2). It may be seen that the frequency response of a pure delay of τ seconds is given by

$$e^{-s\tau}\Big|_{s=j\omega} = e^{-j\omega\tau} \tag{5.5}$$

Thus the magnitude is unity and the phase increases linearly with frequency.

5.1.3 Time delay in δ-domain:

In discrete-time, the equivalent state-space representation can be written as

$$\delta x(t) = A_\delta x(t) + B_\delta u(t)$$
$$y(t+\tau) = C_\delta x(t) \tag{5.6}$$

Alternatively, in some systems the time delay may be associated with the input signal, and the appropriate model is then

$$\delta x'(t) = A_\delta x'(t) + B_\delta u(t-\tau)$$
$$y(t) = C_\delta x'(t) \tag{5.7}$$

In the delta domain, we get

$$\gamma X(\gamma) = A_\delta X(\gamma) + B_\delta X(\gamma) \tag{5.8}$$

and

$$E(\gamma, \tau) Y(\gamma) = C_\delta X(\gamma) \tag{5.9}$$

where

$$E(\gamma, \tau) \cong \begin{cases} e^{\gamma\tau} & : \Delta = 0 \\ (1+\Delta\gamma)^{\frac{\tau}{\Delta}} & : \Delta \neq 0 \end{cases}$$

The transfer function relating Y(γ) to U(γ) is thus

$$G_\delta(\gamma) = E(\gamma, -\tau) C_\delta [\gamma I - A_\delta]^{-1} B_\delta \qquad (5.10)$$

In discrete time, whenever we talk about delaying a sequence, y(t), by τ , it is taken as an integral number of samples; that is, $\tau = N\Delta$ where N is a positive integer. In this case, the transfer function of the delay term reduces to [10]

$$G_\delta^{\cdot}(\gamma) = \dot{E}(\gamma, -\tau) = (1+\gamma\Delta)^{-N} \qquad (5.11)$$

Thus, in discrete-time, a time delay gives rise to a rational transfer function. It should be noted that, unless the sampling rate is low compared with the delay, the order of the transfer function may be quite large.

5.1.4 Sampling in time delay systems:

In this section we now consider the mathematical modelling of a discrete-time system in delta operator parameterization with time delay which is a non-integer multiple of the sampling time. Let us consider the sampling of a continuous-time system with a zero-order hold and having a time delay either with the input or output signal [as in equations 5.1 or 5.2] and let $\tau = N\Delta + \eta$ (5.12)

where $N \in Z^+ \cup 0$ and $0 \leq \eta \leq \Delta$. Then proceeding as in Chapter 1, we have

$$x^{\cdot}(k\Delta + \Delta) = e^{A_c\Delta} x^{\cdot}(k\Delta) + \int_{k\Delta}^{(k+1)\Delta} e^{A_c((k+1)\Delta - t)} B_c u(t-\tau)\, dt \qquad (5.13)$$

$$\begin{aligned} &= e^{A_c\Delta} x^{\cdot}(k\Delta) + \left\{\frac{1}{\Delta}\int_\eta^\Delta e^{A_c(\Delta-\upsilon)} B_c\, d\upsilon\right\} u(t-\tau)\, dt \\ &+ \left\{\frac{1}{\Delta}\int_0^\eta e^{A_c(\Delta-\upsilon)} B_c\, d\upsilon\right\} u((k-N-1)\Delta \end{aligned} \qquad (5.14)$$

From equation (5.14), it follows that

$$\begin{aligned} \delta x^{\cdot}(k\Delta) = &\left(\frac{e^{A_c\Delta} - I}{\Delta}\right) x^{\cdot}(k\Delta) + \left\{\frac{1}{\Delta}\int_\eta^\Delta e^{A_c(\Delta-\upsilon)} B_c\, d\upsilon\right\} u((k-N)\Delta) \\ &+ \left\{\frac{1}{\Delta}\int_0^\eta e^{A_c(\Delta-\upsilon)} B_c\, d\upsilon\right\} u((k-N-1)\Delta) \end{aligned} \qquad (5.15)$$

This equation has the form

$$\delta x'(k\Delta) = A_\delta x'(k\Delta) + B_1 u((k-N-1)\Delta) + B_0 u((k-N)\Delta) \qquad (5.16)$$

and

$$y(k\Delta) = C_\delta x'(k\Delta) \qquad (5.17)$$

Taking transforms of equations (5.16) and (5.17) with zero initial conditions we have,

$$\gamma X(\gamma) = A_\delta X(\gamma) + B_1(1+\Delta\gamma)^{-(N+1)} U(\gamma) + B_0(1+\Delta\gamma)^{-N} U(\gamma) \qquad (5.18)$$

And

$$Y(\gamma) = C_\delta X(\gamma) \qquad (5.19)$$

So

$$Y(\gamma) = C_\delta[\gamma I - A_\delta]^{-1}(B_1 + B_0(1+\Delta\gamma))(1+\Delta\gamma)^{-(N+1)} U(\gamma) \qquad (5.20)$$

5.1.5 SISO Systems:

Let $P_\delta(\gamma)$ be the delta domain equivalent of the continuous-time plant $P_c(s)$ with a ZOH and $C_\delta(\gamma)$ be a digital cascade controller, the parameters of which are to be determined. Let the n-th order stable discrete-time SISO transfer function $P_\delta(\gamma)$ be given by

$$P_\delta(\gamma) = \frac{b_0 + b_1\gamma + b_2\gamma^2 \ldots\ldots + b_q\gamma^q}{a_0 + a_1\gamma + a_2\gamma^2 \ldots\ldots + a_p\gamma^p}(1+\Delta\gamma)^{-N} \qquad (5.21)$$

where n = p + N, and N is an integer such that N times Δ is the dead time τ present in the process (Δ is the sampling period). In case τ/Δ is a fraction, the same is dealt with in the above section.

For a meaningful choice of the reference model, it should contain the same amount of time delay as the plant, otherwise if the delay of the reference model is less than that of the plant then the controller will be non-causal and in the reverse case, there will be extra amount of dead time in the system. From a given set of specifications a delay-free proper rational transfer function $M_\delta(\gamma)$ is chosen. Then this $M_\delta(\gamma)$ combined with the delay term $(1+\Delta\gamma)^{-N}$, gives the required reference model, $M_\delta(\gamma)$ [10]. thus,

$$M_\delta(\gamma) = M(\gamma)(1+\Delta\gamma)^{-N} \qquad (5.22)$$

The equivalent open-loop model $F_\delta(\gamma)$ is defined as:

$$F_\delta(\gamma) = \frac{M_\delta(\gamma)}{1 - M_\delta(\gamma)} \qquad (5.23)$$

Thus $F_\delta(\gamma)$ alongwith unity negative feedback becomes equal to $M_\delta(\gamma)$. The two proposed SISO controller design methods of Sections 3.5 & 3.6 are used to design cascade controllers using the above $F_\delta(\gamma)$. Design results are given in the example sections.

Reference model transfer functions and its performance specifications for time delay system for different angles (ρ) with undamped natural frequency ω_n=10 rad/sec, damping ratio ξ=0.5, sampling time Δ=0.5 sec and delay time t_d=1 sec has been computed and shown in table 5.1 and table 5.2 and corresponding step responses for sampling time Δ=0.5 sec and Δ=0.1 sec are shown in figure 5.1 &5.2. Step response of reference model with ω_n=0.84 rad/sec, ξ=0.7, sampling time Δ=0.1 sec and delay time t_d=1 sec is given in figure 5.3.

Table-5.1

ω_n=10 rad/sec, ξ=0.5, Δ=0.5 sec and delay time t_d=1 sec

Angle ρ	Reference Model without time delay $M_\delta(\gamma)$	Reference Model with time delay $M_\delta(\gamma)_{td}$
-80°	$\frac{1.1974\gamma + 4.2719}{\gamma^2 + 4.1225\gamma + 4.2719}$	$\frac{4.7895\gamma^2 + 26.6667\gamma + 34.1753}{\gamma^5 + 10.1225\gamma^4 + 41.0068\gamma^3 + 83.1012\gamma^2 + 84.2427\gamma + 34.1753}$
-60°	$\frac{1.7974\gamma + 4.2719}{\gamma^2 + 4.1225\gamma + 4.2719}$	$\frac{7.1896\gamma^2 + 31.4669\gamma + 34.1753}{\gamma^5 + 10.1225\gamma^4 + 41.0068\gamma^3 + 83.1012\gamma^2 + 84.2427\gamma + 34.1753}$
-40°	$\frac{1.9334\gamma + 4.2719}{\gamma^2 + 4.1225\gamma + 4.2719}$	$\frac{7.7337\gamma^2 + 32.555\gamma + 34.1753}{\gamma^5 + 10.1225\gamma^4 + 41.0068\gamma^3 + 83.1012\gamma^2 + 84.2427\gamma + 34.1753}$
-20°	$\frac{2.0058\gamma + 4.2719}{\gamma^2 + 4.1225\gamma + 4.2719}$	$\frac{8.0232\gamma^2 + 33.134\gamma + 34.1753}{\gamma^5 + 10.1225\gamma^4 + 41.0068\gamma^3 + 83.1012\gamma^2 + 84.2427\gamma + 34.1753}$
+20°	$\frac{2.1167\gamma + 4.2719}{\gamma^2 + 4.1225\gamma + 4.2719}$	$\frac{8.4667\gamma^2 + 34.0211\gamma + 34.1753}{\gamma^5 + 10.1225\gamma^4 + 41.0068\gamma^3 + 83.1012\gamma^2 + 84.2427\gamma + 34.1753}$
+40°	$\frac{2.1891\gamma + 4.2719}{\gamma^2 + 4.1225\gamma + 4.2719}$	$\frac{8.7562\gamma^2 + 34.6\gamma + 34.1753}{\gamma^5 + 10.1225\gamma^4 + 41.0068\gamma^3 + 83.1012\gamma^2 + 84.2427\gamma + 34.1753}$
+60°	$\frac{2.3251\gamma + 4.2719}{\gamma^2 + 4.1225\gamma + 4.2719}$	$\frac{9.3003\gamma^2 + 35.6882\gamma + 34.1753}{\gamma^5 + 10.1225\gamma^4 + 41.0068\gamma^3 + 83.1012\gamma^2 + 84.2427\gamma + 34.1753}$
+80°	$\frac{2.9251\gamma + 4.2719}{\gamma^2 + 4.1225\gamma + 4.2719}$	$\frac{11.7004\gamma^2 + 40.4884\gamma + 34.1753}{\gamma^5 + 10.1225\gamma^4 + 41.0068\gamma^3 + 83.1012\gamma^2 + 84.2427\gamma + 34.1753}$

Table-5.2

ρ	Reference Model without delay					Reference Model with delay of-1 sec				
	M_p %	t_p/Δ	t_s/Δ	GM	PM	M_p %	t_p/Δ	t_s/Δ	GM	PM
-80°	3.1312	3	2	∞	63.3606	3.1581	5	4	2.0833	60.5405
-60°	1.2941	3	2	∞	61.8485	1.3023	5	4	2.0328	60.2145
-40°	0.8776	3	1	∞	60.4506	0.8817	5	3	2.0075	60.0350
-20°	0.6561	3	1	∞	59.4604	0.6579	5	3	1.9922	59.9201
+20°	5.8340	2	2	∞	57.6065	5.8324	4	4	1.9669	59.7156
+40°	9.4526	2	2	∞	56.1913	9.4486	4	4	1.9493	59.5624
+60°	16.2534	2	2	∞	53.1179	16.2444	4	4	1.9144	59.2295
+80°	46.2548	2	2	∞	38.4639	46.2173	4	4	1.7549	56.9343

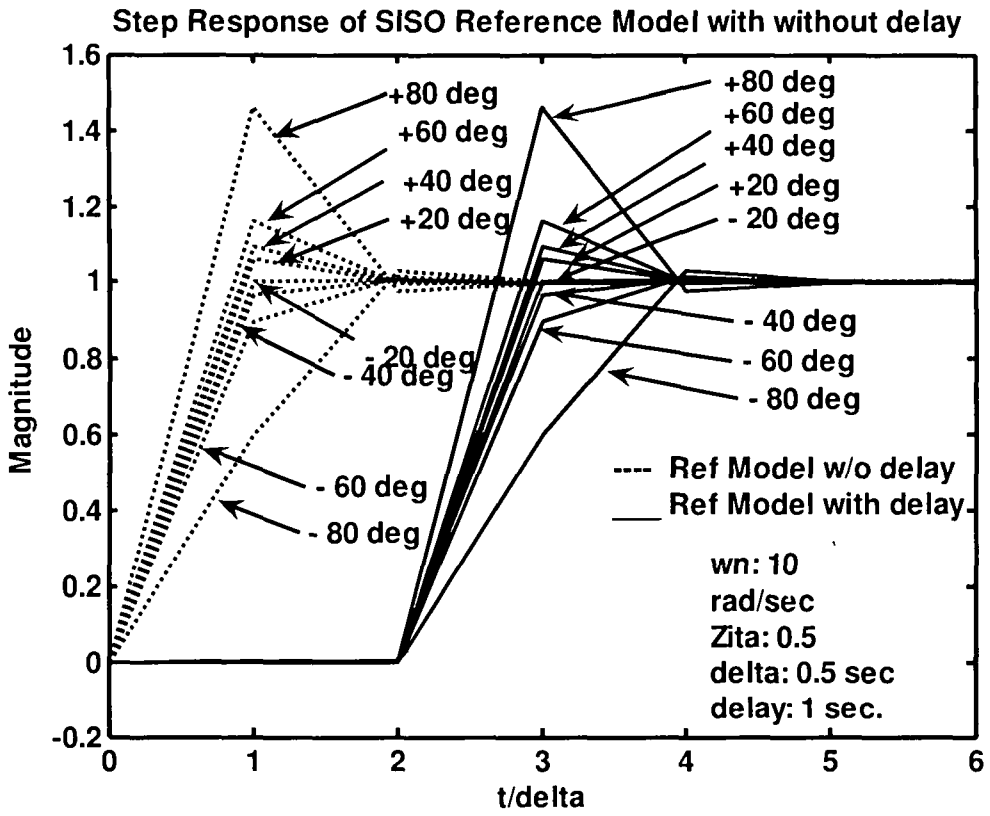

Figure 5.1: Step responses of Reference model with and without time delay with ω_n=10 rad/sec, ξ=0.5, Sampling time 0.5 sec and time delay 1 sec

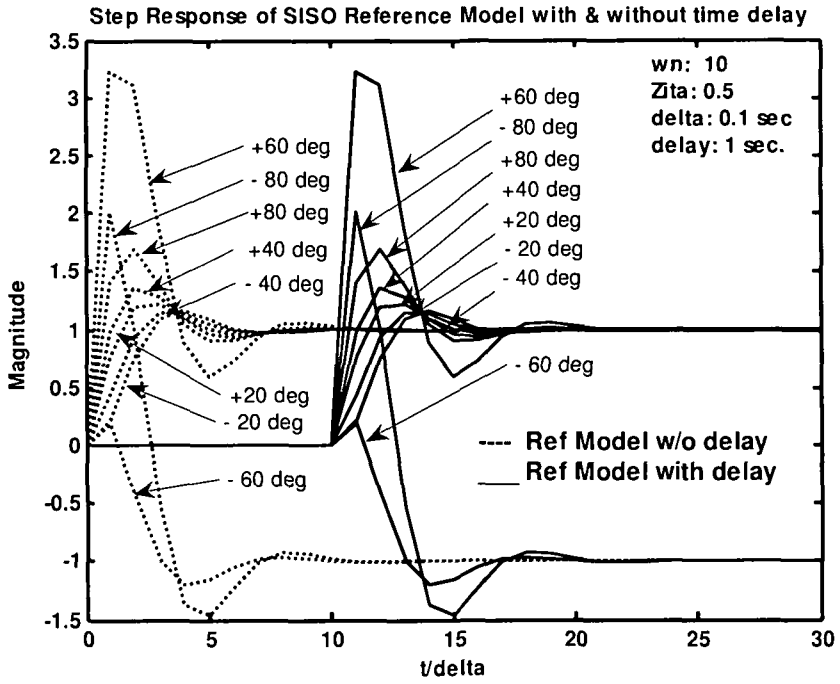

Figure 5.2: Step responses of Reference model with and without time delay with ω_n=10 rad/sec, ξ=0.5, Sampling time 0.1 sec and time delay 1 sec

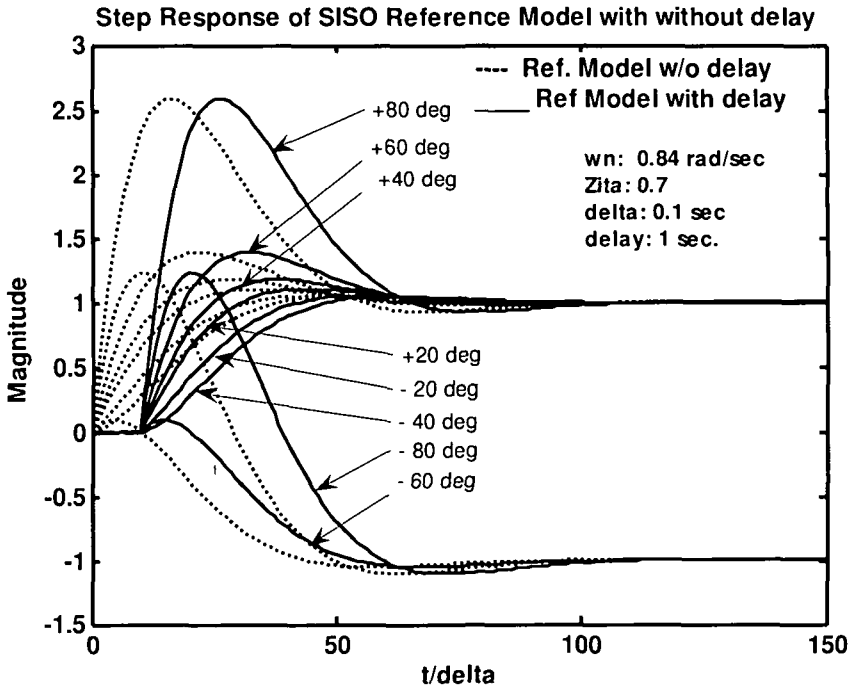

Figure 5.3: Step responses of Reference model with and without time delay with ω_n=0.84 rad/sec, ξ=0.7, Sampling time 0.1 sec and time delay 1 sec

5.1.6 Testing on SISO using OGDTM method:

OGDTM method is also tested on the following time delay systems

5.1.6.1 Simple time delay plant:

Here we consider a second order plant [76] given by

$$P_c(s) = \frac{Ke^{-s\tau}}{s^2 + 2\xi\omega_n s + \omega_n^2}$$

where ω_n = 10 rad/sec, ξ = 0.5, K = 200, τ = 1 sec. Let us choose a PID controller as

$$C_\delta(\gamma) = K_c\left[1 + \tau_1\gamma + \frac{1}{\tau_2}\gamma\right]$$

Discretizing the plant in delta domain incorporating a sampler and ZOH with sampling period Δ = 0.2, 0.5, 1 sec respectively and resulting discrete time models of the plant and reference model in delta domain for different value of angle ρ are given as under:

Δ = 0.2 sec, ρ = - 40°, ω_n = 10 rad /sec, ξ=0.5 and time delay 1 sec.

$$P_\delta(\gamma) = \frac{26544.55\gamma^2 + 328576.85\gamma + 979270.46}{\gamma^8 + 40.59\gamma^7 + 724.06\gamma^6 + 7411.59\gamma^5 + 47602.88\gamma^4 + 196379.02\gamma^3 + 507980.91\gamma^2 + 753041.25\gamma + 489635.23}$$

$$M_\delta(\gamma) = \frac{11787.23\gamma^2 + 156863.19\gamma + 489635.23}{\gamma^8 + 40.59\gamma^7 + 724.06\gamma^6 + 7411.59\gamma^5 + 47602.88\gamma^4 + 196379.02\gamma^3 + 507980.91\gamma^2 + 753041.25\gamma + 489635.23}$$

The following GA parameters are considered to compute OGDTM (μ_{ti}) values for the time delay systems

- Method of selection : Roulette wheel
- Number of generation for evolution: 30
- Population size : 31
- Crossover probability: 0.77
- Number of crossover : 2
- Mutaion probability: 0.0077

Using above GA parameters, the OGDTM point μ_t is found to be 0.4179 and we obtain the desired PID controller as

$$C_\delta(\gamma) = 0.29402 + 0.032446\gamma + \frac{0.40826}{\gamma}$$

Closed loop system transfer function cascaded with controller and plant with unity feed back is found as

$$G_\delta(\gamma) = \frac{861.26\gamma^4 + 18465.58\gamma^3 + 139218.69\gamma^2 + 422070.61\gamma + 399796.84}{\gamma^9 + 40.59\gamma^8 + 724.06\gamma^7 + 7411.59\gamma^6 + 47602.88\gamma^5 + 197240.28\gamma^4 + 526446.49\gamma^3 + 892259.94\gamma^2 + 911705.84\gamma + 399796.84}$$

The Unit step responses of the reference model and closed loop system are shown in figure 5.4.

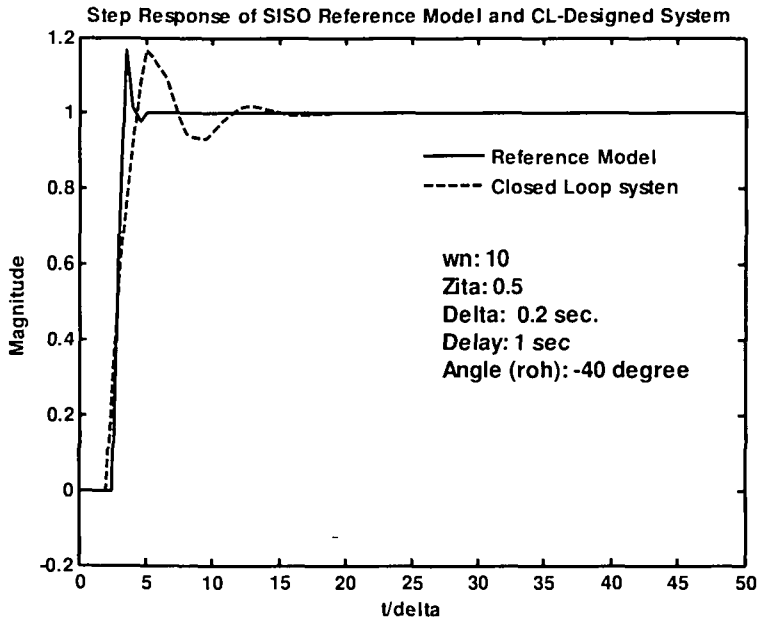

Figure 5.4: Step responses of Ref. model and closed loop plant with PID Controller for ρ= - 40°, ω_n=10 rad/sec, ξ=0.5, Δ= 0.2 sec and time delay 1 sec

Δ = 0.2 sec, ρ = + 40°, ω_n = 10 rad /sec, ξ=0.5 and time delay 1 sec.

Since sampling frequency is same so plant transfer function with 1 sec is same as above. However reference model for ρ =+40° is computed as

$$M_\delta(\gamma) = \frac{21308.56\gamma^2 + 204469.88\gamma + 489635.23}{\gamma^8 + 40.59\gamma^7 + 724.06\gamma^6 + 7411.59\gamma^5 + 47602.88\gamma^4 + 196379.02\gamma^3 + 507980.91\gamma^2 + 753041.25\gamma + 489635.23}$$

Using the same parameters of GA stated above, the OGDTM point μ_t is found to be 0.4258 and we obtain the desired PID controller as

$$C_\delta(\gamma) = 0.33587 + 0.053892\gamma + \frac{0.44419}{\gamma}$$

Closed loop system transfer function cascaded with controller and plant with unity feed back is found as

$$G_\delta(\gamma) = \frac{1430.55\gamma^4 + 26623.41\gamma^3 + 174926.12\gamma^2 + 474860.12\gamma + 434979.36}{\gamma^9 + 40.59\gamma^8 + 724.06\gamma^7 + 7411.59\gamma^6 + 47602.88\gamma^5 + 197809.57\gamma^4 + 534604.32\gamma^3 + 927967.37\gamma^2 + 964495.36\gamma + 434979.35}$$

The Unit step responses of the reference model and closed loop system are shown in figure 5.5.

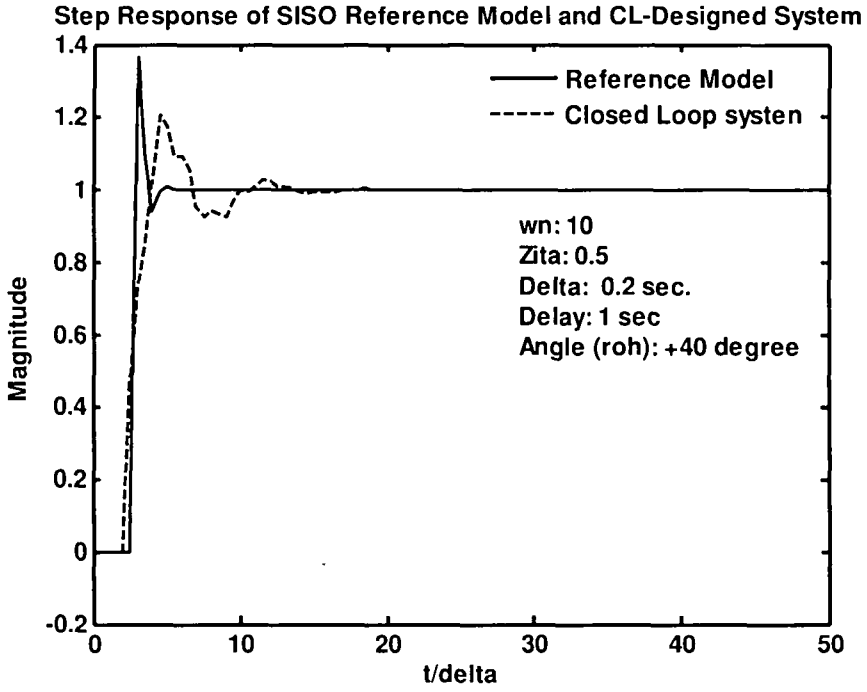

Figure 5.5: Step responses of Ref. model and closed loop plant with PID Controller for $\rho = +40°$, $\omega_n = 10$ rad/sec, $\xi = 0.5$, $\Delta = 0.2$ sec and time delay 1 sec

Δ = 0.5 sec, ρ = - 40°, ω_n=10 rad /sec, ξ=0.5 and delay 1 sec.

$$P_\delta(\gamma) = \frac{17.1934\gamma^2 + 68.5622\gamma + 68.3505}{\gamma^5 + 10.1225\gamma^4 + 41.0068\gamma^3 + 83.1012\gamma^2 + 84.2427\gamma + 34.1753}$$

$$M_\delta(\gamma) = \frac{7.7337\gamma^2 + 32.555\gamma + 34.1753}{\gamma^5 + 10.1225\gamma^4 + 41.0068\gamma^3 + 83.1012\gamma^2 + 84.2427\gamma + 34.1753}$$

Using genetic algorithms with the same parameters stated above, the OGDTM point μ_t is found to be 0.2134 and we obtain the desired PID controller as

$$C_\delta(\gamma) = 0.32127 + 0.034025\gamma + \frac{0.33001}{\gamma}$$

Closed loop system transfer function cascaded with controller and plant with unity feed back is found as

$$G_\delta(\gamma) = \frac{0.58501\gamma^4 + 7.8566\gamma^3 + 30.0269\gamma^2 + 44.5858\gamma + 22.5567}{\gamma^6 + 10.1225\gamma^5 + 41.5918\gamma^4 + 90.9578\gamma^3 + 114.2696\gamma^2 + 78.761\gamma + 22.5567}$$

The Unit step responses of the reference model and closed loop system are shown in figure 5.6.

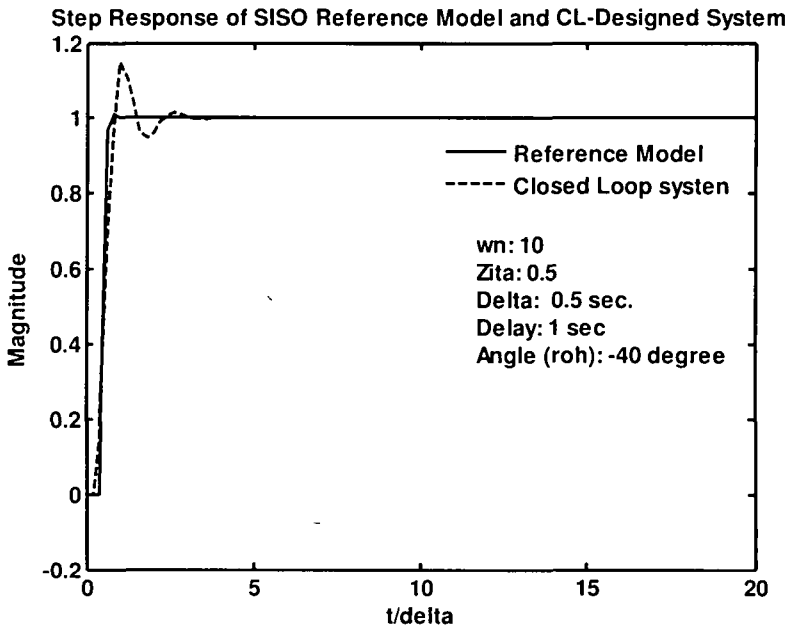

Figure 5.6: Step responses of Ref. model and closed loop plant with PID Controller for ρ= - 40°, ω_n=10 rad/sec, ξ=0.5, Δ= 0.5 sec and time delay 1 sec

Δ = 0.5 sec, ρ = + 40°, ω_n=10 rad /sec, ξ=0.5 and delay 1 sec.

Since sampling frequency is same so plant transfer function with 1 sec is same as above. However reference model for ρ =+ 40° is computed as

$$M_\delta(\gamma) = \frac{8.7562\gamma^2 + 34.6\gamma + 34.1753}{\gamma^5 + 10.1225\gamma^4 + 41.0068\gamma^3 + 83.1012\gamma^2 + 84.2427\gamma + 34.1753}$$

Using same parameters of genetic algorithms, the OGDTM point μ_t is found to be 0.1898 and we obtain the desired PID controller as

$$C_\delta(\gamma) = 0.34064 + 0.042161\gamma + \frac{0.34376}{\gamma}$$

Closed loop system transfer function cascaded with controller and plant with unity feed back is found as

$$G_\delta(\gamma) = \frac{0.72489\gamma^4 + 8.7474\gamma^3 + 32.1471\gamma^2 + 46.852\gamma + 23.4963}{\gamma^6 + 10.1225\gamma^5 + 41.5918\gamma^4 + 91.8486\gamma^3 + 116.3898\gamma^2 + 81.0272\gamma + 23.4963}$$

The Unit step responses of the reference model and closed loop system are shown in figure 5.7.

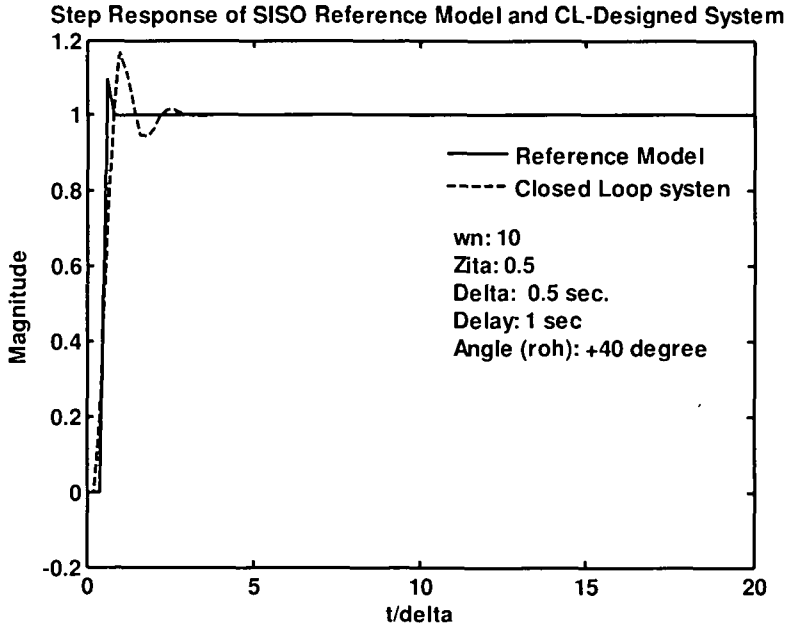

Figure 5.7: Step responses of Ref. model and closed loop plant with PID Controller for ρ= + 40°, ω_n=10 rad/sec, ξ=0.5, Δ= 0.5 sec and time delay 1 sec

Δ = 1 sec, ρ = - 40°, ω_n=10 rad /sec, ξ = 0.5 and time delay 1 sec.

$$P_\delta(\gamma) = \frac{2.0043\gamma^2 + 4.0239\gamma + 2.0195}{\gamma^4 + 4.0097\gamma^3 + 6.0292\gamma^2 + 4.0293\gamma + 1.0098}$$

$$M_\delta(\gamma) = \frac{1.0009\gamma^2 + 2.0107\gamma + 1.0098}{\gamma^4 + 4.0097\gamma^3 + 6.0292\gamma^2 + 4.0293\gamma + 1.0098}$$

Using genetic algorithms with same parameters stated above, the OGDTM point μ_t is found 0.0325 and we obtain the desired PID controller as

$$C_\delta(\gamma) = 0.37502 + 0.056641\gamma + \frac{0.25012}{\gamma}$$

$$G_\delta(\gamma) = \frac{0.11353\gamma^4 + 0.97959\gamma^3 + 2.1248\gamma^2 + 1.7638\gamma + 0.50512}{\gamma^5 + 4.1233\gamma^4 + 7.0088\gamma^3 + 6.154\gamma^2 + 2.7736\gamma + 0.50512}$$

The Unit step responses of the reference model and closed loop system are shown in figure 5.8.

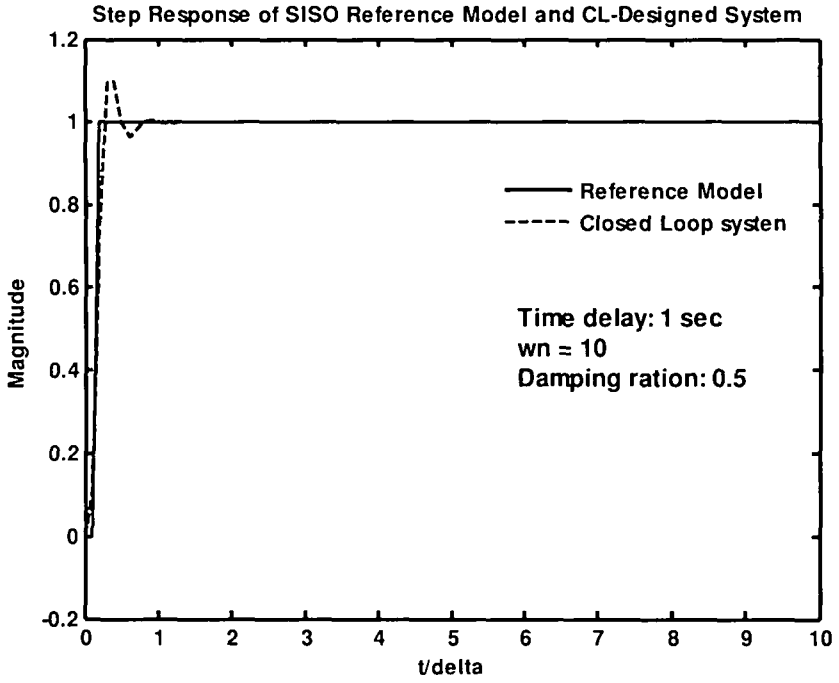

Figure 5.8: Step responses of Ref. model and closed loop plant with PID Controller for ρ= - 40°, ω_n=10 rad/sec, ξ=0.5, Δ= 1 sec and time delay 1 sec

Δ = 1 sec, ρ = + 50°, ω_n = 10 rad /sec, ξ = 0.5 and time delay 1 sec.

Since sampling frequency is same so plant transfer function with 1 sec is same as above. However reference model for ρ =+50° is computed as

$$M_\delta(\gamma) = \frac{1.0129\gamma^2 + 2.0227\gamma + 1.0098}{\gamma^4 + 4.0097\gamma^3 + 6.0292\gamma^2 + 4.0293\gamma + 1.0098}$$

Using genetic algorithms with same parameters, the OGDTM μ_t is found to be 0.0246 and we obtain the desired PID controller as

$$C_\delta(\gamma) = 0.37787 + 0.059015\gamma + \frac{0.25162}{\gamma}$$

Closed loop system transfer function cascaded with controller and plant with unity feed back is found as

$$G_\delta(\gamma) = \frac{0.11829\gamma^4 + 0.99486\gamma^3 + 2.144\gamma^2 + 1.7756\gamma + 0.50815}{\gamma^5 + 4.128\gamma^4 + 7.0241\gamma^3 + 6.1733\gamma^2 + 2.7854\gamma + 0.50815}$$

The Unit step responses of the reference model and closed loop system are shown in figure 5.9.

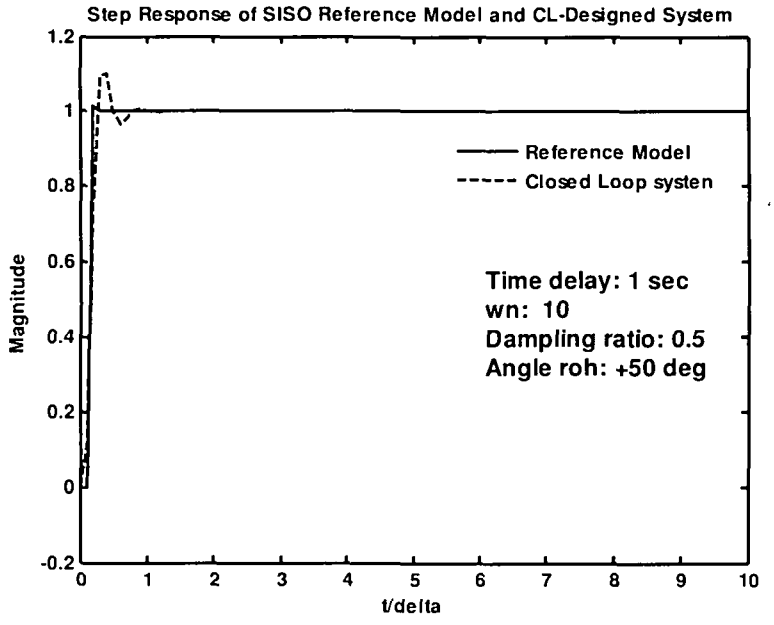

Figure 5.9: Step responses of Ref. model and closed loop plant with PID Controller for ρ= + 50°, ω_n=10 rad/sec, ξ=0.5, Δ= 1 sec and time delay 1 sec

Δ = 0.5 sec, ρ = -40°, ω_n = 0.84 rad /sec, ξ = 0.7 and time delay 1 sec.

$$P_\delta(\gamma) = \frac{17.1934\gamma^2 + 68.5622\gamma + 68.3505}{\gamma^5 + 10.1225\gamma^4 + 41.0068\gamma^3 + 83.1012\gamma^2 + 84.2427\gamma + 34.1753}$$

$$M_\delta(\gamma) = \frac{0.82581\gamma^2 + 3.7545\gamma + 4.2058}{\gamma^5 + 7.152\gamma^4 + 19.4377\gamma^3 + 24.9782\gamma^2 + 15.5246\gamma + 4.2058}$$

Using genetic algorithm with same parameters, the OGDTM μ_t is found 0.4072 and the desired PID controller is obtained as

$$C_\delta(\gamma) = 0.049553 - 0.001329\gamma + \frac{0.1795}{\gamma}$$

Closed loop system transfer function cascaded with controller and plant with unity feed back is given as

$$G_\delta(\gamma) = \frac{-0.022851\gamma^4 + 0.76087\gamma^3 + 6.3928\gamma^2 + 15.6936\gamma + 12.2686}{\gamma^6 + 10.1225\gamma^5 + 40.9839\gamma^4 + 83.862\gamma^3 + 90.6355\gamma^2 + 49.8689\gamma + 12.2686}$$

For same GA parameters, the OGDTM point μ_t for PI controller is found to be 0.9873 and controller transfer function is

$$C_\delta(\gamma) = 0.04852 + \frac{0.17964}{\gamma}$$

Closed loop system transfer function cascaded with PI controller and plant with unity feed back is given as

$$G_\delta(\gamma) = \frac{0.83423\gamma^3 + 6.4152\gamma^2 + 15.6326\gamma + 12.2782}{\gamma^6 + 10.1225\gamma^5 + 41.0068\gamma^4 + 83.9354\gamma^3 + 90.6579\gamma^2 + 49.8078\gamma + 12.2782}$$

The Unit step responses of the reference model and closed loop system cascaded with PID & PI controllers are shown in figure 5.10 & 5.11 respectively.

Δ = 0.5 sec, ρ = + 40°, ω_n = 0.84 rad /sec, ξ = 0.7 and time delay 1 sec.

Since sampling frequency is same so plant transfer function with 1 sec is same as above. However reference model for ρ =+ 40° is computes as

$$M_\delta(\gamma) = \frac{3.7821\gamma^2 + 9.6672\gamma + 4.2058}{\gamma^5 + 7.152\gamma^4 + 19.4377\gamma^3 + 24.9782\gamma^2 + 15.5246\gamma + 4.2058}$$

Using GA with same parameters, the OGDTM point μ_t is found to be 0.9786 and desired PID controller is obtained as

$$C_\delta(\gamma) = 0.20903 + 0.0024468\gamma + \frac{0.32032}{\gamma}$$

Closed loop system transfer function cascaded with controller and plant with unity feed back is given as

$$G_\delta(\gamma) = \frac{0.042068\gamma^4 + 3.7617\gamma^3 + 20.0061\gamma^2 + 36.2493\gamma + 21.8943}{\gamma^6 + 10.1225\gamma^5 + 41.0068\gamma^4 + 86.8628\gamma^3 + 104.2488\gamma^2 + 70.4245\gamma + 21.8943}$$

The Unit step responses of the reference model and closed loop system are shown in figure 5.12. Comparision of closed loop system with different controlles are given in table 5.4.

Table-5.3

Comparison of performance of various closed loop systems cascaded with the desired controller

Con trol ler	ρ	Δ sec	ω_n rad/ sec	ξ	Reference Model with delay of 1 sec					Closed loop system with controller				
					M_p %	t_p/Δ	t_s/Δ	GM	PM	M_p %	t_p/Δ	t_s/Δ	GM	PM
PID	- 40°	0 2	10	0 5	16 4	8	8	19 48	54 98	16 4	11	21	8 53	6 27
PID	+40°	0 2	10	0 5	36 3	7	9	15 23	32 61	20 4	10	19	8 22	7 30
PID	40°	0 5	10	0 5	0 87	5	3	20 07	60 03	14 9	6	10	30 24	37 80
PID	+40°	0 5	10	0 5	9 45	4	4	19 49	59 56	16 6	6	10	29 56	38 26
PID	- 40°	1	10	0 5	0 09	3	2	19 99	59 99	9 94	5	5	13 32	61 45
PID	+50°	1	10	0 5	1 29	3	2	19 87	59 88	9 94	5	5	13 27	61 43
PID	- 40°	0 5	0 84	0 7	4 60	13	9	29 17	60 85	5 05	14	14	34 74	38 51
PID	+40°	0 5	0 84	0 7	17 9	9	13	23 53	48 11	23 4	8	10	24 49	48 61
PI	- 40°	0 5	0 84	0 7	4 60	13	9	29 17	60 85	5 27	14	14	30 67	60 35

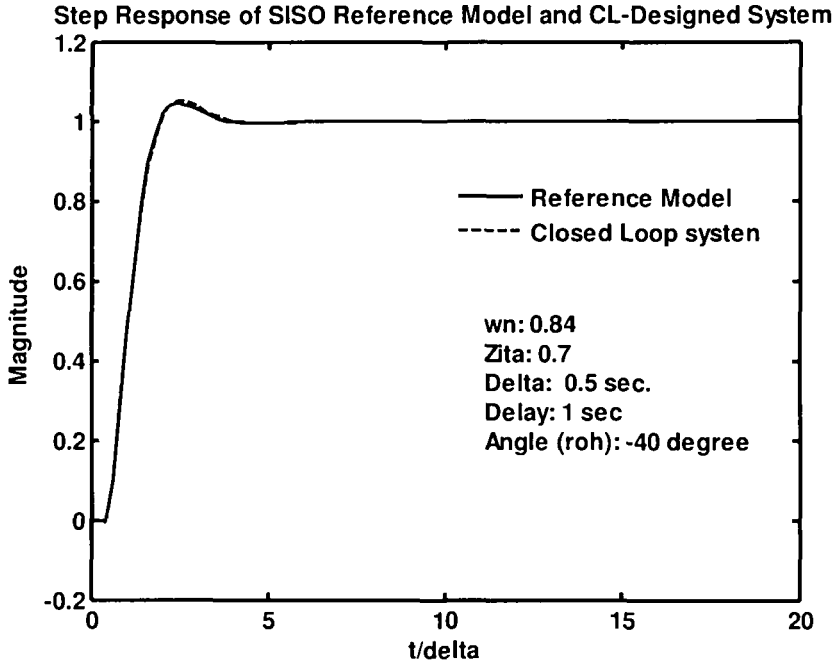

Figure 5.10: Step responses of Ref. model and closed loop plant with PID Controller for ρ= - 40°, ω_n=0.84 rad/sec, ξ=0.7, Δ= 0.5 sec using OGDTM

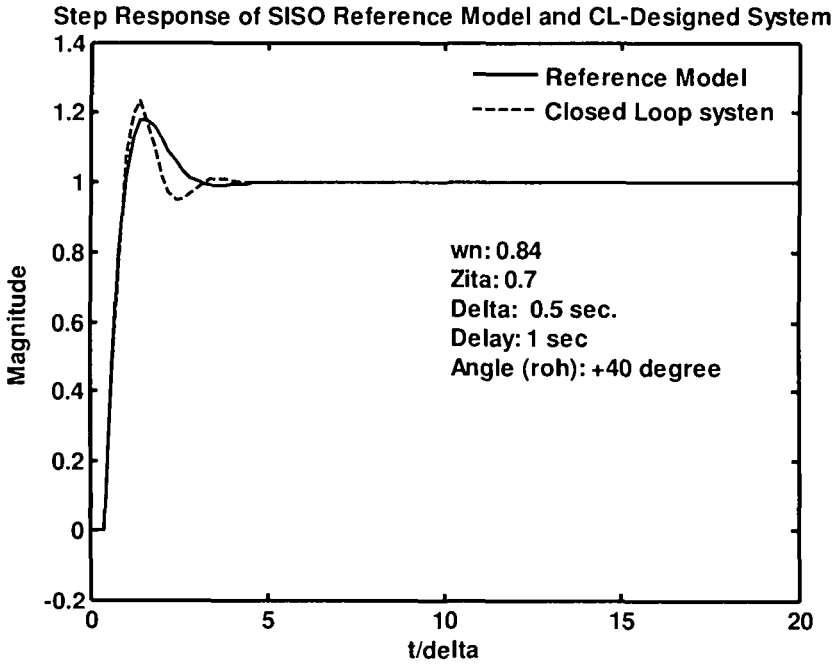

Figure 5.11: Step responses of Ref. model and closed loop plant with PID Controller for ρ= + 40°, ω_n=0.84 rad/sec, ξ=0.7, Δ= 0.5 sec using OGDTM

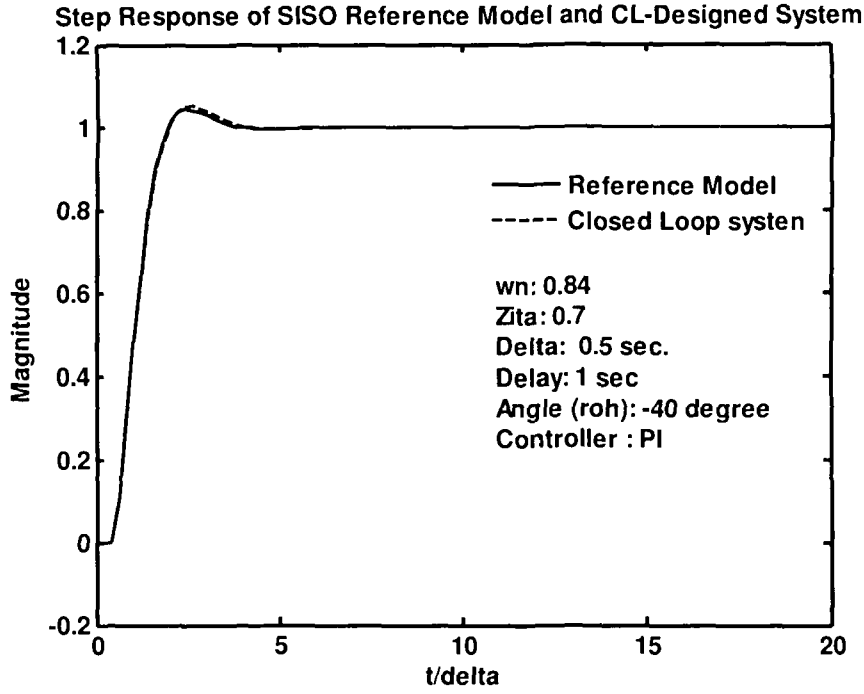

Figure 5.12: Step responses of Ref. model and closed loop plant with PI Controller for ρ= - 40°, ω_n=0.84 rad/sec, ξ=0.7, Δ= 0.5 sec using OGDTM

5.1.6.2 Stirred chemical reactor plant:

In the following example, we consider the time delay transfer function of continuous stirred chemical reactor plant [96].

$$P_c(s) = \frac{k_p e^{-\tau s}}{(1 + T_1 s)(1 + T_2 s)}$$

Where $k_p = 1.39$, $T_1 = 10.1$, $T_2 = 4.1$

Three values of τ are used to study how the performance of the controller is effected by the relative magnitude of the dead time τ when compared with the plant time constants T_1 and T_2

1. Reactor 1 has $\tau = \tau_1 = 0.8$ min., lower than both time constants.
2. Reactor 2 has $\tau = \tau_2 = 5.0$ min., comparable to the smaller time constant.
3. Reactor 3 has $\tau = \tau_3 = 10.0$ min., comparable to the larger time constant.

The continuous time transfer functions are given as :

Model of reactor 1

$$P_c(s) = \frac{1.39e^{-0.8s}}{(1 + 10.1s)(1 + 4.1s)}$$

Model of reactor 2

$$P_c(s) = \frac{1.39e^{-5s}}{(1 + 10.1s)(1 + 4.1s)}$$

Model of reactor 3

$$P_c(s) = \frac{1.39e^{-10s}}{(1 + 10.1s)(1 + 4.1s)}$$

The OGDTM method is applied here to all the reactors individually for design of the controller.

Reactor 1

For reference model in δ-domain, undamped natural frequency ω_n is chosen 0.2 rad/sec, damping ratio ξ is 0.8 and sampling period Δ is 0.1 sec. The plant is now discretized in the δ-domain after incorporating the sampler and ZOH with the $\Delta = 0.1$ sec. Very fast sampling is avoided to restrict the order of the resultant system. The resultant discrete rational transfer functions are given as under

$\Delta = 0.1$ sec, $\rho = -40°$, $\omega_n = 0.2$ rad /sec, $\xi = 0.8$

$$P_{\delta 1}(\gamma) = \frac{165928.45\gamma^2 + 4958995.16\gamma + 32997106.73}{\gamma^{11} + 90.34\gamma^{10} + 3630.58\gamma^9 + 85224.24\gamma^8 + 1288601.23\gamma^7 + 13029730.58\gamma^6 + 88307276.15\gamma^5 + 388814877.84\gamma^4 + 1024204501.39\gamma^3 + 1314072092.33\gamma^2 + 360838454.33\gamma + 23738925.71}$$

$$M_{\delta 1}(\gamma) = \frac{6034403.63\gamma^2 + 64280582.31\gamma + 39365460.22}{\gamma^{11} + 90.32\gamma^{10} + 3628.74\gamma^9 + 85151.48\gamma^8 + 1286926.85\gamma^7 + 13005083.81\gamma^6 + 88067371.61\gamma^5 + 387281145.72\gamma^4 + 1018100159.74\gamma^3 + 1301155218.38\gamma^2 + 354299639.42\gamma + 39365460.21}$$

PI Controller:

Following GA parameters are used to compute the OGDTMs to design a PI controller

- Method of selection : Tournament selection method

- Number of tournaments: 2
- Number of generation for evolution: 30
- Population size : 31
- Crossover probability: 0.77
- Number of crossover : 2
- Mutaion probability: 0.0077

Using GA, the OGDTM points μ_t is found to be 0.0089 and we obtain the following PI controller.

$$C_{\delta 1}(\gamma) = 1.2439 + \frac{0.09735}{\gamma}$$

and corresponding closed loop transfer function cascaded with PI controller is given as

$$G_{\delta 1}(\gamma) = \frac{206397.55\gamma^3 + 6184621.98\gamma^2 + 41527692.85\gamma + 3212281.19}{\gamma^{12} + 90.32\gamma^{11} + 3630.57\gamma^{10} + 85224.24\gamma^9 + 1288601.22\gamma^8 + 13029730.58\gamma^7 + 88307276.15\gamma^6 + 388814877.84\gamma^5 + 1024204501.39\gamma^4 + 1314278489.88\gamma^3 + 367023076.31\gamma^2 + 65266618.55\gamma + 3212281.19}$$

PID Controller:

Using same GA parameters, the OGDTM point μ_t for PID controller is found to be 0.0403. The transfer function of PID controller and closed loop system cascaded with the controller are given as:

$$C_{\delta 1}(\gamma) = 1.201 + 1.8028\gamma + \frac{0.097486}{\gamma}$$

$$G_{\delta 1}(\gamma) = \frac{299129.12\gamma^4 + 9139157.65\gamma^3 + 65457808.32\gamma^2 + 40113118.67\gamma + 3216748.09}{\gamma^{12} + 90.32\gamma^{11} + 3630.57\gamma^{10} + 85224.24\gamma^9 + 1288601.22\gamma^8 + 13029730.58\gamma^7 + 88307276.15\gamma^6 + 388814877.84\gamma^5 + 1024503630.51\gamma^4 + 132321129.97\gamma^3 + 426296262.65\gamma^2 + 638520044.37\gamma + 3216748.09}$$

The unit step responses of the reference model and the closed loop plant with the PI & PID controllers using OGDTM are shown in Figure 5.13 & 5.14 respectively.

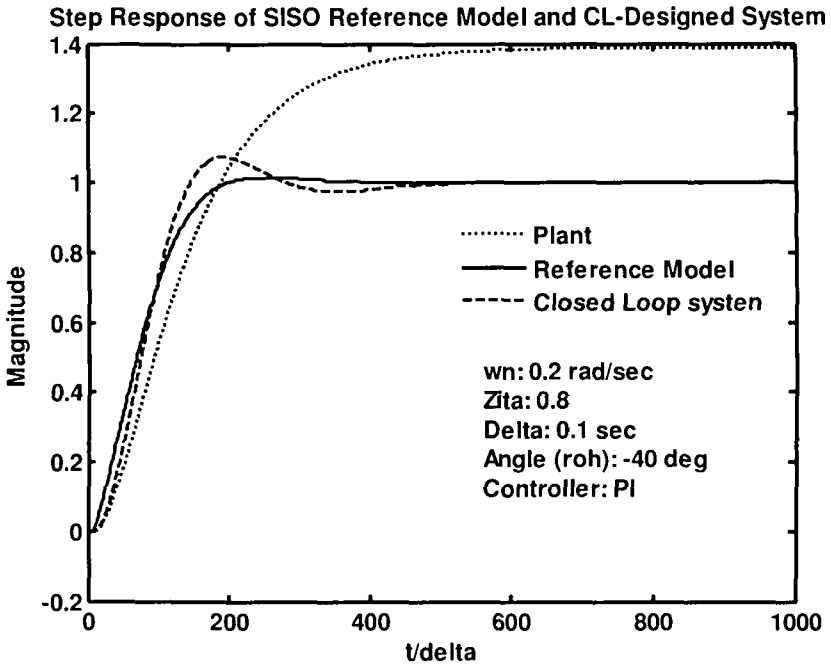

Figure 5.13: Step responses of Reference model and closed loop plant with PI Controller for ρ= - 40°, ω_n=0.2 rad/sec, ξ=0.8, Δ= 0.1 sec using OGDTM

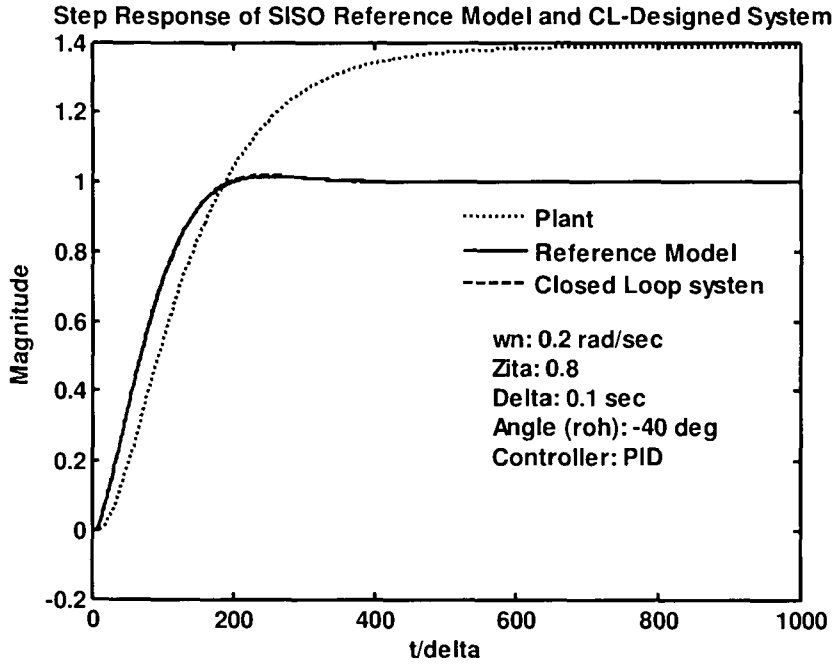

Figure 5.14: Step responses of Reference model and closed loop plant with PID Controller for ρ= - 40°, ω_n=0.2 rad/sec, ξ=0.8, Δ= 0.1 sec using OGDTM

Reactor 2:

For reactor 2, reference model in δ-domain is computed with undamped natural frequency ω_n = 0.2 rad/sec, damping ratio ξ =0.8 and sampling period Δ = 0.5 sec. The plant is discretized in the δ-domain after incorporating the sampler and ZOH with the sampling period Δ = 0.5 sec. Very fast sampling is avoided to restrict the order of the resultant system. The resultant discrete rational transfer functions are given as under

Δ = 0.5 sec, ρ = - 40°, ω_n=0.2 rad /sec, ξ=0.8

$$P_{\delta 1}(\gamma)=\frac{8.12\gamma^2+47.82\gamma+63.14}{\gamma^{13}+22.33\gamma^{12}+227.19\gamma^{11}+1392.26\gamma^{10}+5715.48\gamma^9+16535.69\gamma^8+34507.89\gamma^7+52213.47\gamma^6+56675.21\gamma^5+42876.28\gamma^4+21387.16\gamma^3+6347.11\gamma^2+917.93\gamma+45.42}$$

$$M_{\delta 1}(\gamma)=\frac{65.74\gamma^2+169.29\gamma+75.64}{\gamma^{13}+22.31\gamma^{12}+226.95\gamma^{11}+1389.93\gamma^{10}+5702.84\gamma^9+16491.62\gamma^8+34407.83\gamma^7+52075.67\gamma^6+56602.97\gamma^5+42990.98\gamma^4+21671.34\gamma^3+6626.95\gamma^2+1059.46\gamma+75.64}$$

PI Controller:

Using same GA parameters, the OGDTM point μ_t is found to be 0.0001 and we obtain the following PI controller.

$$C_{\delta 1}(\gamma)=0.88245+\frac{0.061126}{\gamma}$$

And corresponding closed loop transfer function cascaded with PI controller is given as

$$G_{\delta 1}(\gamma)=\frac{7.164\gamma^3+42.6844\gamma^2+58.6426\gamma+3.8597}{\gamma^{14}+22.33\gamma^{13}+227.19\gamma^{12}+1392.26\gamma^{11}+5715.49\gamma^{10}+16535.69\gamma^9+34507.89\gamma^8+52213.48\gamma^7+56675.21\gamma^6+42876.28\gamma^5+21387.15\gamma^4+6354.27\gamma^3+960.62\gamma^2+104.07\gamma+3.86}$$

PID Controller:

Using GA with same parameters, the OGDTM point μ_t for PID controller is found to be 0.0403. The transfer function of PID controller and closed loop system cascaded with the controller are given as:

$$C_{\delta 1}(\gamma)=0.87525+2.4019\gamma+\frac{0.061131}{\gamma}$$

$$G_{\delta 1}(\gamma)=\frac{19.49\gamma^4+121.94\gamma^3+194.01\gamma^2+58.19\gamma+3.86}{\gamma^{14}+22.33\gamma^{13}+227.19\gamma^{12}+1392\ 26\gamma^{11}+5715.49\gamma^{10}+16535.69\gamma^9+34507.89\gamma^8+52213.48\gamma^7+56675.21\gamma^6+42876.28\gamma^5+21406.66\gamma^4+6469.04\gamma^3+1111.93\gamma^2+103.61\gamma+3.86}$$

Δ = 0.5 sec, ρ = + 40°, ω_n=0.2 rad /sec, ξ=0.8

Plant transfer function in delta domain will be same as above because sampling period is considered 0.5 sec in this case also. However with the change of angle ρ i. e. +40°, the reference model in delta domain is computed as

$$M_{\delta 1}(\gamma) = \frac{255.98\gamma^2 + 549.78\gamma + 75.64}{\gamma^{13} + 22.31\gamma^{12} + 226.95\gamma^{11} + 1389.93\gamma^{10} + 5702.84\gamma^9 + 16491.62\gamma^8 + 34407.83\gamma^7 + 52075.67\gamma^6 + 56602.97\gamma^5 + 42990.98\gamma^4 + 21671.34\gamma^3 + 6626.95\gamma^2 + 1059.46\gamma + 75.64}$$

Using GA, the OGDTM point μ_i for PID controller is found to be 0.1190. The transfer function of PID controller and closed loop system cascaded with the controller are given as:

$$C_{\delta 1}(\gamma) = 1.3999 + 6.2811\gamma + \frac{0.111991}{\gamma}$$

$$G_{\delta 1}(\gamma) = \frac{50.99\gamma^4 + 311.64\gamma^3 + 464.43\gamma^2 + 93.75\gamma + 7.07}{\gamma^{14} + 22.33\gamma^{13} + 227.19\gamma^{12} + 1392.26\gamma^{11} + 5715.49\gamma^{10} + 16535.69\gamma^9 + 34507.89\gamma^8 + 52213.48\gamma^7 + 56675\ 21\gamma^6 + 42876.28\gamma^5 + 21438.15\gamma^4 + 6658.75\gamma^3 + 1382.37\gamma^2 + 139.18\gamma + 7.07}$$

The unit step responses of the reference model and the closed loop plant with the PI & PID controllers using OGDTM are shown in Figure 5.15, 5.16 & 5.17 respectively

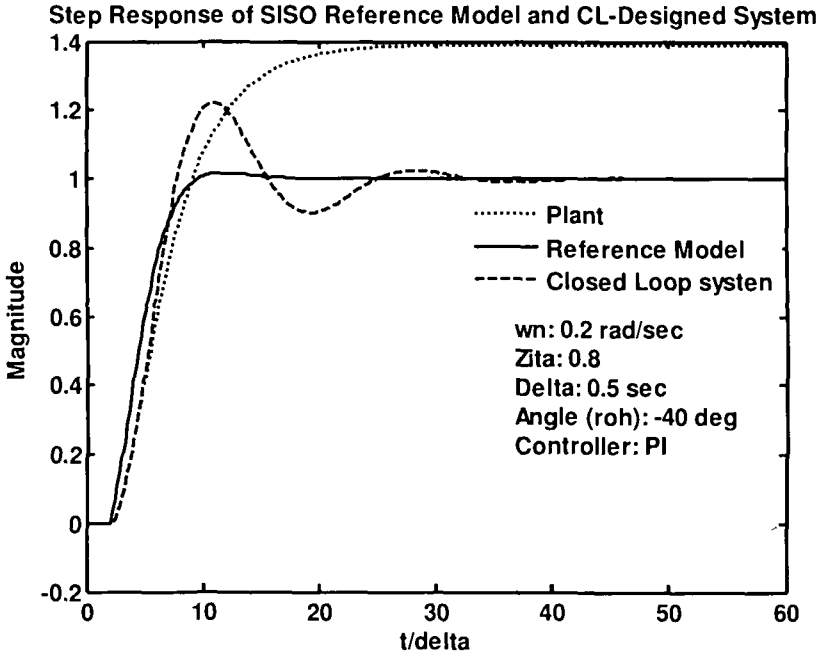

Figure 5.15: Step responses of Reference model and closed loop plant with PI Controller for ρ= - 40°, ω_n=0.2 rad/sec, ξ=0.8, Δ= 0.5 sec using OGDTM

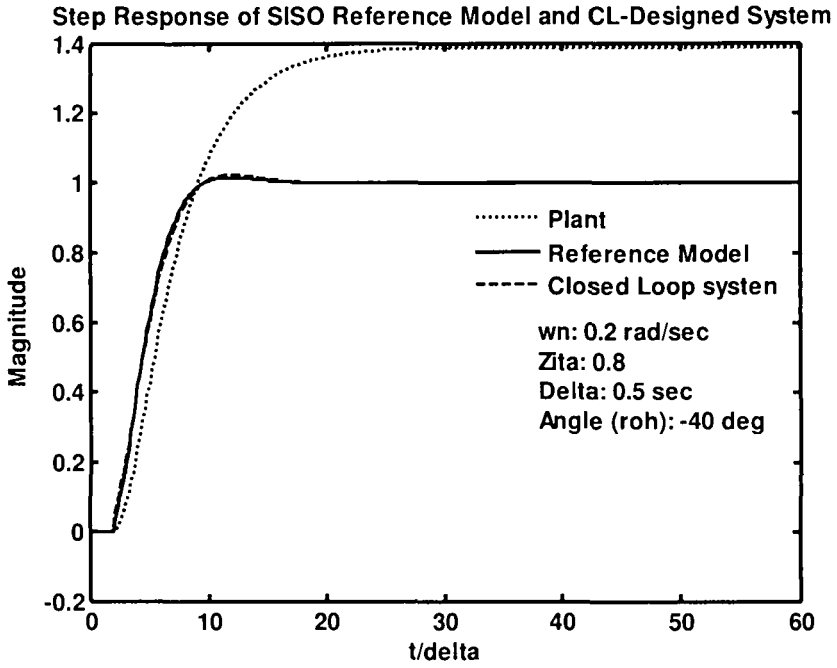

Figure 5.16: Step responses of Reference model and closed loop plant with PID Controller for ρ= - 40°, ω_n=0.2 rad/sec, ξ=0.8, Δ= 0.5 sec using OGDTM

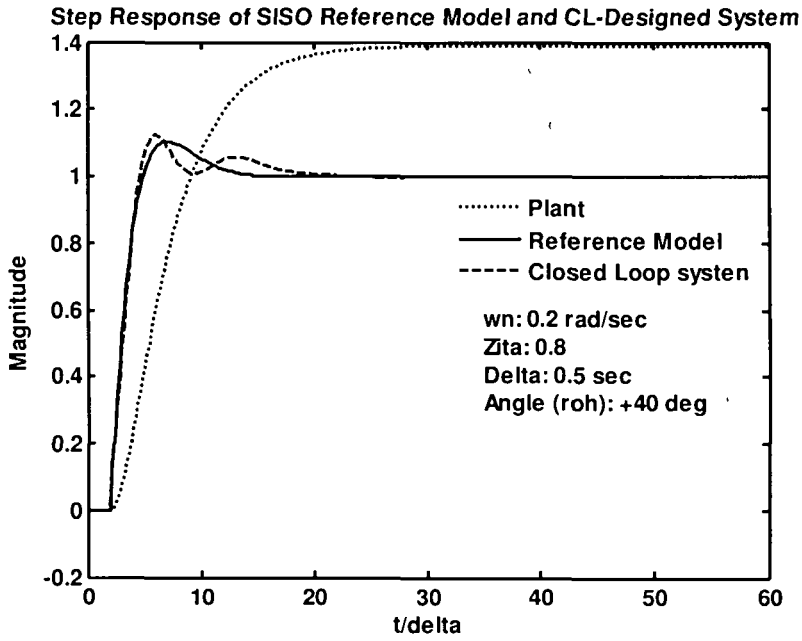

Figure 5.17: Step responses of Reference model and closed loop plant with PID Controller for ρ= + 40°, ω_n=0.2 rad/sec, ξ=0.8, Δ= 0.5 sec using OGDTM

Reactor 3:

For reactor 3, reference model in δ-domain with undamped natural frequency ω_n = 0.1 rad/sec& 0.05 rad/sec, damping ratio ξ =0.8 and sampling period Δ = 0.5 sec is computed. However with this sampling period the order of resusltant system in delta domain increased a lot and to restrict the order one shouls avoid fast sampling. The plant is discretized in the δ-domain after incorporating the sampler and ZOH with the sampling period Δ = 0.5 sec. The resultant discrete rational transfer functions are given as under

Δ = 0.5 sec, ρ = - 40°, ω_n=0.1 rad /sec, ξ=0.8

$$P_{\delta 1}(\gamma)=\frac{8313.13\gamma^2+48955.21\gamma+64657.91}{\gamma^{23}+42.33\gamma^{22}+853.72\gamma^{21}+10914.95\gamma^{20}+99249.57\gamma^{19}+682642.45\gamma^{18}+3687441.46\gamma^{17}+16031197.7\gamma^{16}+57025818.48\gamma^{15}+167816009.52\gamma^{14}+411429609.73\gamma^{13}+845523487.94\gamma^{12}+1447594733.75\gamma^{11}+2075756263.99\gamma^{10}+2475634652.47\gamma^{9}+2435682311.12\gamma^{8}+1955901494.17\gamma^{7}+1258945167.61\gamma^{6}+634136986.23\gamma^{5}+241236260.41\gamma^{4}+65670000.85\gamma^{3}+11722575.28\gamma^{2}+1172547.64\gamma+46516.48}$$

$$M_{\delta 1}(\gamma)=\frac{32423.16\gamma^2+74921.52\gamma+20150.39}{\gamma^{21}+42.15\gamma^{22}+846.67\gamma^{21}+10773.60\gamma^{20}+97455.27\gamma^{19}+666455.04\gamma^{18}+3577072.81\gamma^{17}+15440799.17\gamma^{16}+54486962.51\gamma^{15}+158895707.43\gamma^{14}+385545494.23\gamma^{13}+781081419\gamma^{12}+1321953782.41\gamma^{11}+1864841048.38\gamma^{10}+2181036672.34\gamma^{9}+2096239579.89\gamma^{8}+1633857087.92\gamma^{7}+1013020672.49\gamma^{6}+4858559244.04\gamma^{5}+172924192.01\gamma^{4}+4282828900.48\gamma^{3}+6646807.91\gamma^{2}+544127.71\gamma+20150.39}$$

PI Controller:

Using GA with same parameters, the OGDTM point μ_t is found to be 0.0001 and corresponding PI controller transfer function is obtained as:

$$C_{\delta 1}(\gamma)=0.4381+\frac{0.030894}{\gamma}$$

PID Controller:

The OGDTM point μ_t.for PID controller is found to be 0.0001 using same parameters of GA and the transfer function of PID controller is found as:

$$C_{\delta 1}(\gamma)=0.43475+1.1152\gamma+\frac{0.030896}{\gamma}$$

The unit step responses of the reference model and the closed loop plant with the PI & PID controllers using OGDTM are shown in Figure 5.18 & 5.19 respectively.

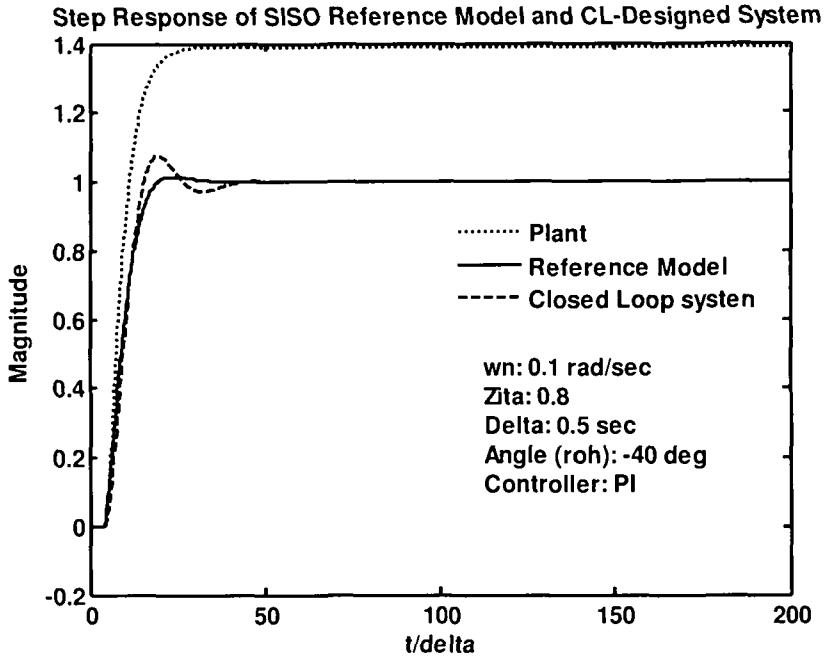

Figure 5.18: Step responses of Reference model and closed loop plant with PI Controller for ρ= - 40°, ω_n=0.1 rad/sec, ξ=0.8, Δ= 0.5 sec using OGDTM

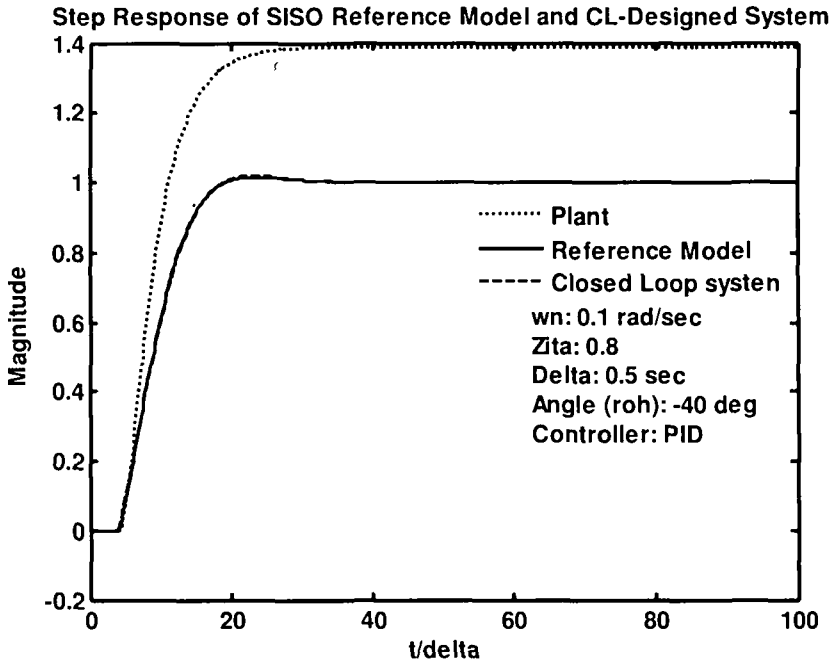

Figure 5.19: Step responses of Reference model and closed loop plant with PID Controller for ρ= - 40°, ω_n=0.1 rad/sec, ξ=0.8, Δ= 0.5 sec using OGDTM

Δ = 0.5 sec, ρ = + 40°, ω_n=0.1 rad /sec, ξ=0.8

Plant transfer function in delta domain will be same as above because sampling period is considered 0.5 sec in this case also. However with the change of angle i.e. ρ=+40°, the reference model in delta domain is computed as

$$M_{\delta 1}(\gamma)=\frac{133851.14\gamma^2+277777.468\gamma+20150.39}{\gamma^{23}+42.15\gamma^{22}+846.67\gamma^{21}+10773.60\gamma^{20}+97455.27\gamma^{19}+666455.04\gamma^{18}+3577072.81\gamma^{17}+15440799.17\gamma^{16}+54486962.51\gamma^{15}+158895707.43\gamma^{14}+385545494.23\gamma^{13}+781081419\gamma^{12}+1321953782.41\gamma^{11}+1864841048.38\gamma^{10}+2181036672.34\gamma^{9}+2096239579.89\gamma^{8}+1633857087.92\gamma^{7}+1013020672.49\gamma^{6}+4858559244.04\gamma^{5}+172924192.01\gamma^{4}+4282828900.48\gamma^{3}+6646807.91\gamma^{2}+544127.71\gamma+20150.39}$$

Controller:

Using GA with same parameters, the OGDTM point μ_1 for PI and PID controller is found to be 0.0002 and 0.008 respectively and corresponding controller transfer functions are found as:

PI controller $$C_{\delta 1}(\gamma)=0.76302+\frac{0.054419}{\gamma}$$

PID controller $$C_{\delta 1}(\gamma)=0.75669+3.9592\gamma+\frac{0.054381}{\gamma}$$

The unit step responses of the reference model and the closed loop plant with the PI & PID controllers using OGDTM are shown in Figure 5.20 & 5.21 respectively.

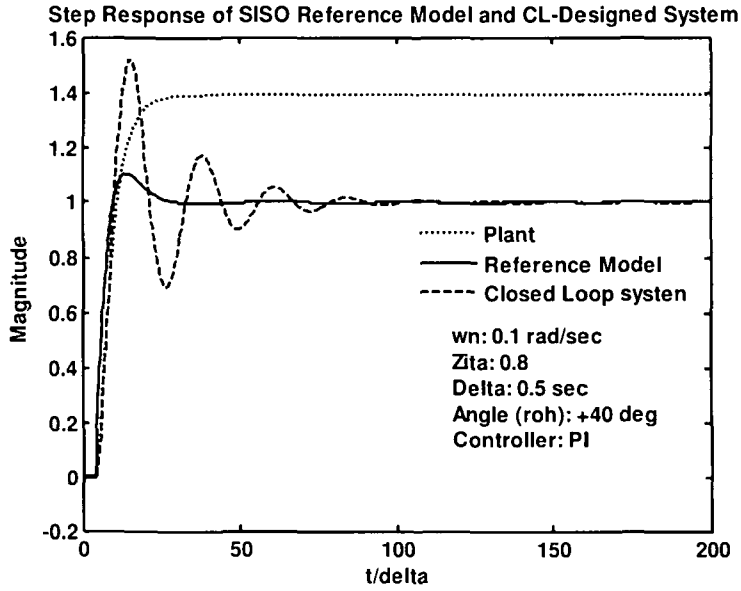

Figure 5.20: Step responses of Ref. model and closed loop plant with PI Controller for ρ= + 40°, ω_n=0.1 rad/sec, ξ=0.8, Δ= 0.5 sec using OGDTM

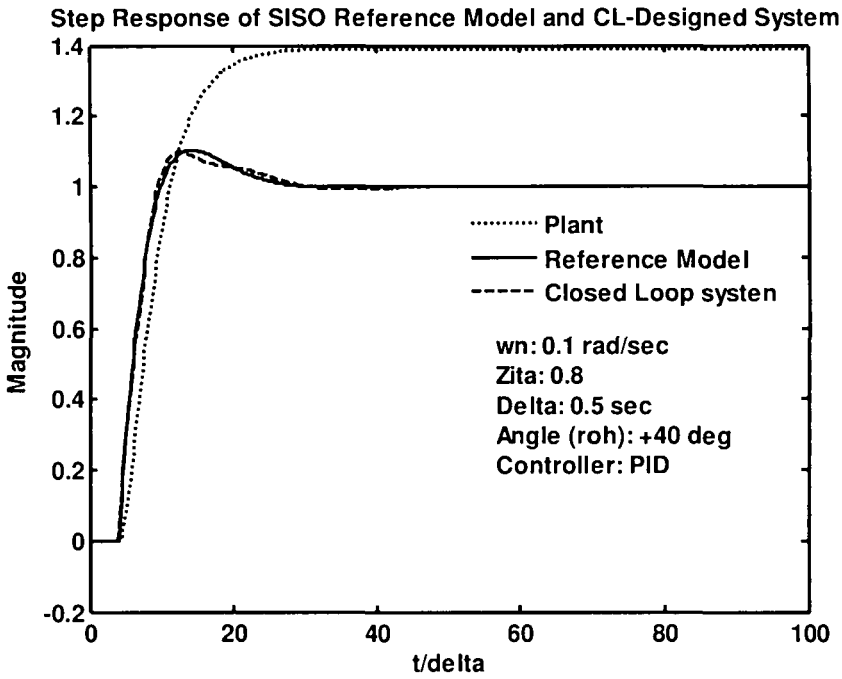

Figure 5.21: Step responses of Reference model and closed loop plant with PID Controller for $\rho = +40°$, $\omega_n = 0.1$ rad/sec, $\xi = 0.8$, $\Delta = 0.5$ sec using OGDTM

$\Delta = 1$ sec, $\rho = -40°$, $\omega_n = 0.1$ rad /sec, $\xi = 0.8$

$$P_{\delta 1}(\gamma) = \frac{0.014989\gamma^2 + 0.043349\gamma + 0.02836}{\gamma^{13} + 11.31\gamma^{12} + 58.43\gamma^{11} + 182.31\gamma^{10} + 382.39\gamma^9 + 567.89\gamma^8 + 612.27\gamma^7 + 482.97\gamma^6 + 276.95\gamma^5 + 112.99\gamma^4 + 31.46\gamma^3 + 5.54\gamma^2 + 0.5351\gamma + 0.020403}$$

$$M_{\delta 1}(\gamma) = \frac{0.032097\gamma^2 + 0.041331\gamma + 0.0092333}{\gamma^{13} + 11.15\gamma^{12} + 56.73\gamma^{11} + 173.74\gamma^{10} + 356.42\gamma^9 + 515.36\gamma^8 + 537\,62\gamma^7 + 406.84\gamma^6 + 221.11\gamma^5 + 83.97\gamma^4 + 21.16\gamma^3 + 3.23\gamma^2 + 0.2586\gamma + 0.00923}$$

Controller:

Using GA with same parameters, the OGDTM point μ_t for PI and PID controller is found to be 0.0002 and 0.008 respectively and corresponding controller transfer functions are found as:

$$\text{PI controller} \quad C_{\delta 1}(\gamma) = 0.56392 + \frac{0.02742}{\gamma}$$

$$\text{PID controller} \quad C_{\delta 1}(\gamma) = 0.44198 + 1.0813\gamma + \frac{0.03056}{\gamma}$$

And corresponding closed loop transfer function cascaded with PI and PID controller are found as:

PI:

$$G_{\delta 1}(\gamma)=\frac{0.00845\gamma^3+0.024856\gamma^2+0.017181\gamma+0.00077}{\gamma^{14}+11.31\gamma^{13}+58.43\gamma^{12}+182.31\gamma^{11}+382.38\gamma^{10}+567.89\gamma^9+612.27\gamma^8+482.97\gamma^7 \\ +276.95\gamma^6+112.99\gamma^5+31.45\gamma^4+5.54\gamma^3+0.5599\gamma^2+0.03758\gamma+0.00077}$$

PID

$$G_{\delta 1}(\gamma)=\frac{0.0162\gamma^4+0.0535\gamma^3+0.0503\gamma^2+0.0139\gamma+0.00087}{\gamma^{14}+11.31\gamma^{13}+58.43\gamma^{12}+182.31\gamma^{11}+382.38\gamma^{10}+567.89\gamma^9+612.27\gamma^8+482.97\gamma^7 \\ +276.95\gamma^6+112.99\gamma^5+31.47\gamma^4+5.59\gamma^3+0.5854\gamma^2+0.03426\gamma+0.00087}$$

The unit step responses of the reference model and the closed loop plant with the PI & PID controllers using OGDTM are shown in Figure 5.22 & 5.23 respectively. Comparision of closed loop system with different controlles are given in table 5.4.

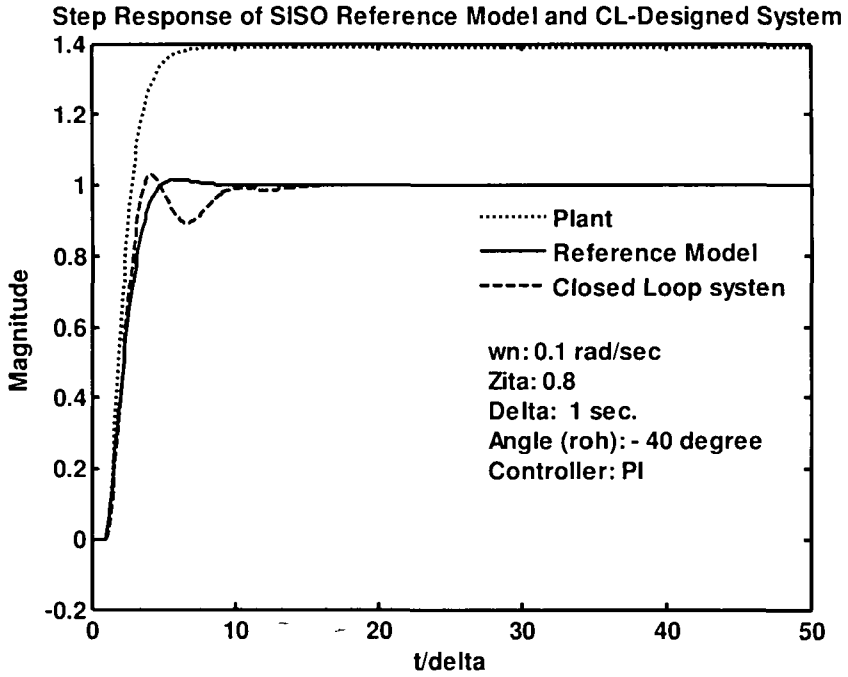

Figure 5.22: Step responses of Reference model and closed loop plant with PI Controller for ρ= - 40°, ω_n= 0.1 rad/sec, ξ=0.8, Δ= 1 sec using OGDTM

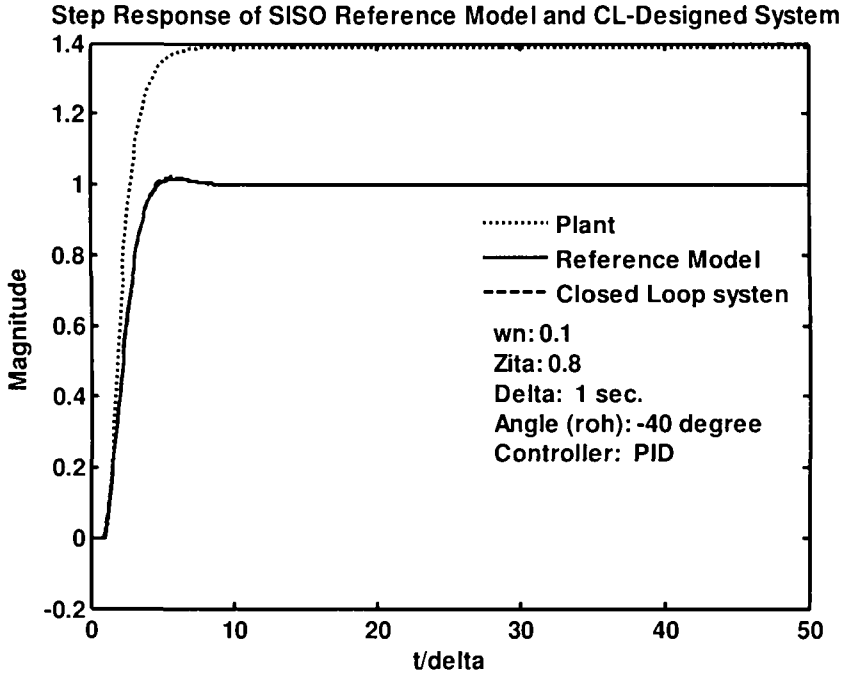

Figure 5.23: Step responses of Reference model and closed loop plant with PID Controller for ρ= - 40°, ω_n= 0.1 rad/sec, ξ=0.8, Δ= 1 sec using OGDTM

Table 5.4

Comparison of performance of various closed loop systems cascaded with the desired controller

Model	Controller	Δ sec.	ρ	ω_n (rad/sec)	ξ	M_p%	t_p/Δ	t_s/Δ (5%)	GM	PM
Reactor 1	PI	0.1	-40°	0.2	0.8	7.41	193	231	7.77	59.62
	PID	0.1	-40°	0.2	0.8	1.87	118	159	12.32	63.03
Reactor 2	PI	0.5	-40°	0.2	0.8	21.97	55	113	2.20	49.29
	PID	0.5	-40°	0.2	0.8	2.31	42	61	0.49	41.44
	PID	0.5	+40°	0.2	0.8	12.48	31	72	0.38	80.56
Reactor 3	PI	0.5	-40°	0.1	0.8	7.70	98	114	2.56	60.46
	PID	0.5	-40°	0.1	0.8	1.91	34	49	0.53	49.02
	PI	0.5	+40°	0.1	0.8	51.89	76	314	1.46	31.03
	PID	0.5	+40°	0.1	0.8	9.82	63	106	0.41	54.03
	PI	1	-40°	0.1	0.8	2.65	42	83	2.28	69.23
	PID	1	-40°	0.1	0.8	2.12	41	58	0.23	63.7

5.1.7 Testing on SISO System using OFF method:

The methodology of optimal frequency fitting method is tested on following SISO system.

5.1.7.1 Simulation results:

Here we consider as system for which the time delay is twice the dominant time constant of the process [116]. The continuous-time plant is given by

$$P_c(s) = \frac{1}{(1+s)(1+0.5s)} e^{-2s}$$

From the desired specifications the reference model in δ-domain is computed with undamped natural frequency ω_n= 0.3 rad/sec, damping ratio ξ 0.7 and sampling period Δ 0.5 sec. The plant is discretized in the δ-domain after incorporating the sampler and ZOH with the Δ = 0.5 sec. Very fast sampling is avoided to restrict the order of the resultant system. The resultant discrete rational transfer functions are given as under

Δ = 0.5 sec, ρ = +40°, ω_n=0.3 rad /sec, ξ=0.7

Plant Transfer Function in delta Domain

$$P_\delta(\gamma) = \frac{4.9542\gamma^2 + 25.8246\gamma + 31.8362}{\gamma^7 + 12.05\gamma^6 + 61.51\gamma^5 + 171.99\gamma^4 + 283.88\gamma^3 + 275.68\gamma^2 + 145.22\gamma + 31.84}$$

Reference Model Transfer Function in delta Domain

$$M_\delta(\gamma) = \frac{7.4225\gamma^2 + 16.8675\gamma + 4.0451}{\gamma^7 + 10.53\gamma^6 + 45.43\gamma^5 + 102.48\gamma^4 + 127.48\gamma^3 + 84.53\gamma^2 + 27.08\gamma + 4.05}$$

For computation of the optimal frequency point, the following GA parameters are considered

- Method of selection : Roulette wheel
- Number of generation for evolution: 35
- Population size : 31
- Crossover probability: 0.8
- Number of crossover : 2
- Mutaion probability: 0.008

Using OFF method the optimal frequency point is found to be 0.2999 with -0.1990 + 0.8697i as real and imaginary part and corresponding PID controller and system transfer function in delta domain are found to be

$$C_{\delta 1}(\gamma) = 0.28861 + 0.6421\gamma + \frac{0.090446}{\gamma}$$

$$G_{\delta 1}(\gamma) = \frac{3.1811\gamma^4 + 18.013\gamma^3 + 28.3438\gamma^2 + 11.524\gamma + 2.8794}{\gamma^8 + 12.05\gamma^7 + 61.50\gamma^6 + 171.99\gamma^5 + 287.07\gamma^4 + 293.69\gamma^3 + 173.57\gamma^2 + 43.36\gamma + 2.88}$$

The unit step responses of the reference model and the closed loop plant with the controller using Optimal Frequency fitting is shown in Figure 5.24.

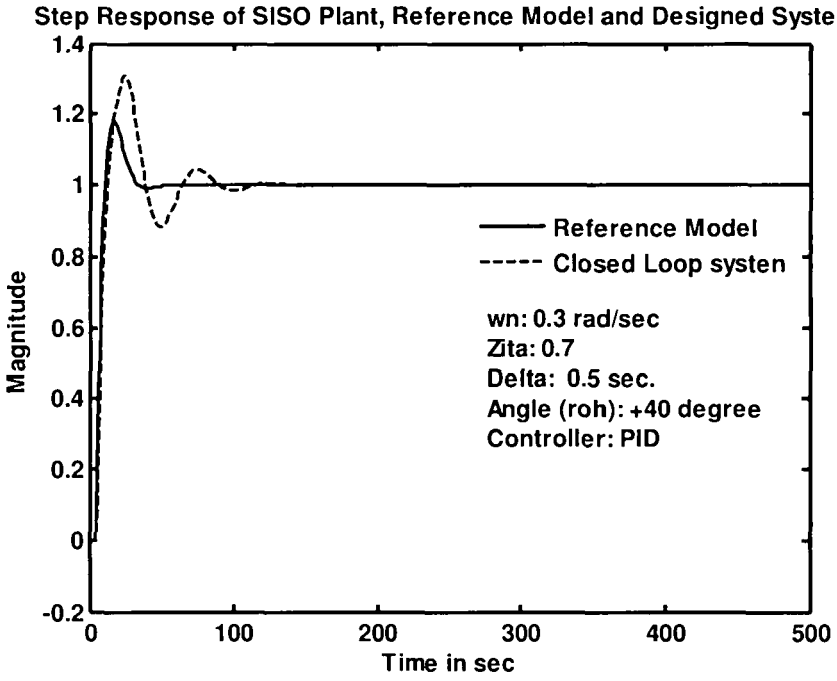

Figure 5.24: Step responses of Reference model and closed loop plant with PID Controller for ρ= + 40°, ω_n= 0.3 rad/sec, ξ=0.7, Δ= 0.5 sec using OFF method

Δ = 0.5 sec, ρ = +20°, ω_n=0.3 rad /sec, ξ=0.7

Plant Transfer Function in delta Domain is same because sampling period is same i.e 0.5 sec. hence the reference Model Transfer Function in delta domain for the above specifications is

$$M_\delta(\gamma) = \frac{5.6219\gamma^2 + 13.2664\gamma + 4.0451}{\gamma^7 + 10.53\gamma^6 + 45.43\gamma^5 + 102.48\gamma^4 + 127.48\gamma^3 + 84.53\gamma^2 + 27.08\gamma + 4.05}$$

Using same GA parameters, optimal frequency point is found to be 0.3156 with -0.2200 + 0.9120i as real and imaginary part. Corresponding PID controller and system transfer function in delta domain are found to be

$$C_{\delta 1}(\gamma) = 0.24832 + 0.55529\gamma + \frac{0.078402}{\gamma}$$

$$G_{\delta 1}(\gamma) = \frac{2.751\gamma^4 + 15.5713\gamma^3 + 24.4799\gamma^2 + 9.9305\gamma + 2.496}{\gamma^8 + 12.05\gamma^7 + 61.50\gamma^6 + 171.99\gamma^5 + 286.64\gamma^4 + 291.25\gamma^3 + 169.71\gamma^2 + 41.76\gamma + 2.49}$$

The unit step responses of the reference model and the closed loop plant with the controller using Optimal Frequency fitting is shown in Figure 5.25.

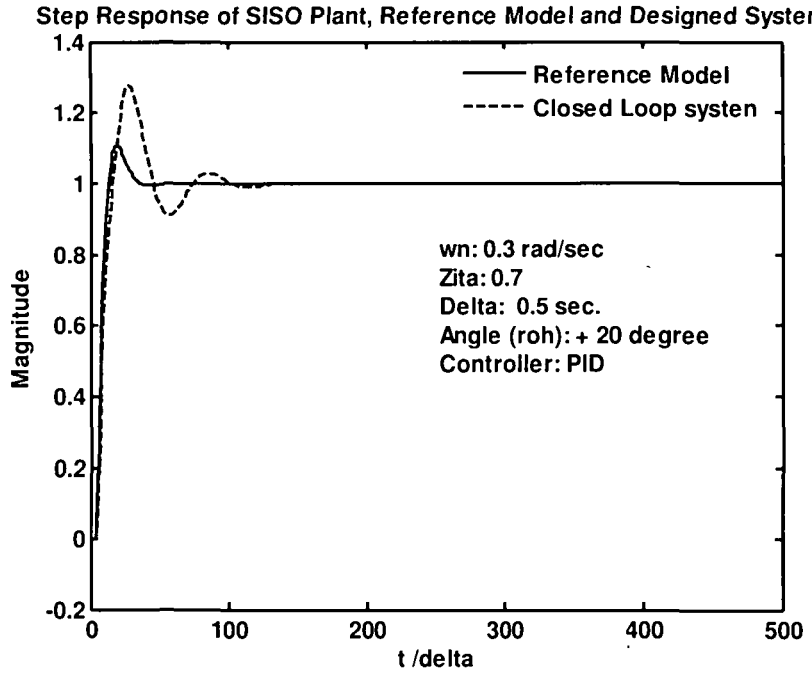

Figure 5.25: Step responses of Ref. model and closed loop plant with PID Controller for $\rho = +20°$, $\omega_n = 0.3$ rad/sec, $\xi = 0.7$, $\Delta = 0.5$ sec using OFF method

Δ = 0.5 sec, ρ = - 20°, ω_n=0.3 rad /sec, ξ=0.7

Plant Transfer Function in delta Domain is same because sampling period is same i.e 0.5 sec. hence the reference Model Transfer Function in delta Domain for above specifications are

$$M_{\delta}(\gamma) = \frac{5.6219\gamma^2 + 13.2664\gamma + 4.0451}{\gamma^7 + 10.53\gamma^6 + 45.43\gamma^5 + 102.48\gamma^4 + 127.48\gamma^3 + 84.53\gamma^2 + 27.08\gamma + 4.05}$$

Using GA, the optimal frequency point is found to be 0.3156 with -0.2200 + 0.9120i as real and imaginary part. The desired PID controller and systme transfer function in delta domain are found to be

$$C_{\delta 1}(\gamma) = 0.24832 + 0.55529\gamma + \frac{0.078402}{\gamma}$$

$$G_{\delta 1}(\gamma) = \frac{2.751\gamma^4 + 15.5713\gamma^3 + 24.4799\gamma^2 + 9.9305\gamma + 2.496}{\gamma^8 + 12.05\gamma^7 + 61.50\gamma^6 + 171.99\gamma^5 + 286.64\gamma^4 + 291.25\gamma^3 + 169.71\gamma^2 + 41.76\gamma + 2.49}$$

The unit step responses of the reference model and the closed loop plant with the controller using Optimal Frequency fitting is shown in Figure 5.26.

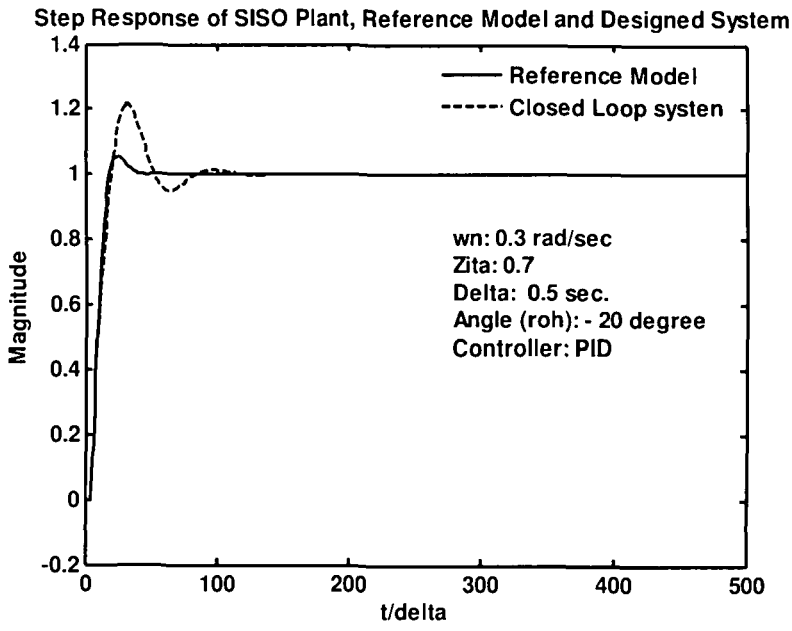

Figure 5.26: Step responses of Ref. model and closed loop plant with PID Controller for ρ= - 20°, ω_n= 0.3 rad/sec, ξ=0.7, Δ= 0.5 sec using OFF method

Δ = 0.5 sec, ρ = - 40°, ω_n=0.3 rad /sec, ξ=0.7

Plant Transfer Function in delta Domain is same because sampling period is same i.e 0.5 sec. hence the reference Model Transfer Function in delta Domain

$$M_{\delta}(\gamma) = \frac{1.0628\gamma^2 + 4.1481\gamma + 4.0451}{\gamma^7 + 10.53\gamma^6 + 45.43\gamma^5 + 102.48\gamma^4 + 127.48\gamma^3 + 84.53\gamma^2 + 27.08\gamma + 4.05}$$

Using GA, the optimal frequency point is found to be 0.7090 and -1.0282 + 1.7481i as real and imaginary part. The PID controller and system transfer function in delta domain are found to be

$$C_{\delta 1}(\gamma) = 0.23804 + 0.39707\gamma + \frac{0.042383}{\gamma}$$

$$G_{\delta 1}(\gamma) = \frac{1.9672\gamma^4 + 11.4343\gamma^3 + 18.9989\gamma^2 + 8.6728\gamma + 1.3493}{\gamma^8 + 12.05\gamma^7 + 61.50\gamma^6 + 171.99\gamma^5 + 285.86\gamma^4 + 287.12\gamma^3 + 164.23\gamma^2 + 40.51\gamma + 1.34}$$

The unit step responses of the reference model and the closed loop plant with the controller in Figure 5.27. Comparision of closed loop system with different controlles are shown in table 5.5

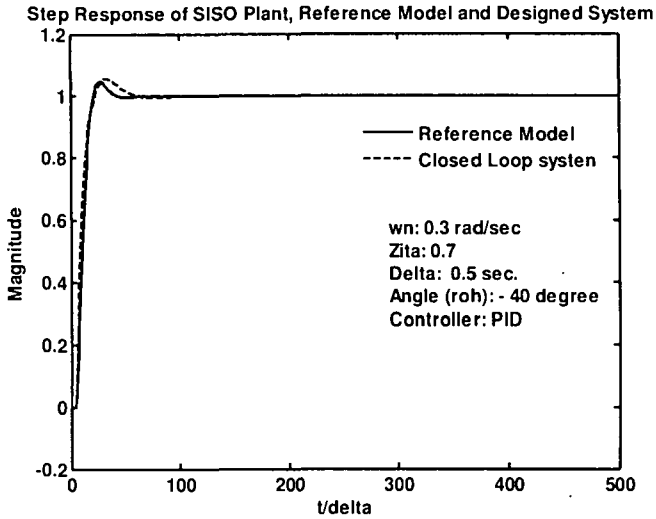

Figure 5.27: Step responses of Ref. model and closed loop plant with PID Controller for ρ= - 40°, ω_n= 0.3 rad/sec, ξ=0.7, Δ= 0.5 sec using OFF method

Table-5.5

Comparison of performance of various closed loop systems cascaded with the desired controller

Controller	ρ	Δ sec	ω_n rad/sec	ξ	Reference Model with delay of 1 sec					Closed loop system with controller				
					M_p %	t_p/Δ	t_s/Δ	GM	PM	M_p %	t_p/Δ	t_s/Δ	GM	PM
PID	+40°	0.5	0.3	0.7	18.14	17	27	2.63	48.13	30.65	25	59	2.53	34.83
PID	+20°	0.5	0.3	0.7	10.51	20	27	3.01	32.61	54.55	27	63	2.94	36.02
PID	- 20°	0.5	0.3	0.7	5.30	25	26	3.59	60.50	21.44	32	67	3.87	45.42
PID	-40°	0.5	0.3	0.7	4.61	28	19	3.25	61.15	5.47	34	37	3.26	61.56

5.1.8 Uncertainty in process model

Uncertainty is an inherent and inevitable characteristic of process models. The models that are used in the process industry are only approximations of the actual physical process. Usually the model uncertainty are due to process nonlinearity and process parameter variations, simplifying assumptions made during the modeling process, finite order or reduced order models obtained from identification/estimation procedures and errors introduced in experimental identification/ curve-fitting procedures, etc.[120]

Detailed analysis of a large scale process is often difficult and typically involves several approximations. Linearizing of the process model around different operating points results in different transfer function models. Even if the model is accurate, variations of real parameters affect the plant operation and the true model deviates considerably from the nominal model. For example, ambient temperature and pressure may vary about the nominal values. In the following, an uncertain plant is considered. It is shown that stability robustness can be maintained in the face of plant uncertainties if the reference model chosen for the nominal plant has sufficient robustness embedded in it.

5.1.8.1 Simulation results:

We consider the following uncertain process [120].

$$P_c(s) = \frac{K\, e^{-\tau s}}{1 + T s}$$

The nominal process model is given by

$$\tilde{P}_c(s) = \frac{12.5\, e^{-10 s}}{1 + 10 s}$$

the uncertainty ranges of various parameters are $K \in [11, 14]$; $\tau \in [9, 11]$; $T \in [7, 13]$

The following six extreme plants have been considered.

$$P_{c1}(s) = \frac{11\, e^{-9 s}}{1 + 7 s} \qquad P_{c2}(s) = \frac{14\, e^{-9 s}}{1 + 7 s}$$

$$P_{c3}(s) = \frac{14\, e^{-11 s}}{1 + 13 s} \qquad P_{c4}(s) = \frac{14\, e^{-10 s}}{1 + 7 s}$$

$$P_{c5}(s) = \frac{11e^{-11s}}{1+13s} \qquad P_{c6}(s) = \frac{11e^{-9s}}{1+13s}$$

The above plant are discretized incorporating system delays with sampler and ZOH. The sampling time Δ = 2 sec. is considered. The resulting nominal plant, perturbed plants obtained in the δ-domain are given as under:

$$\tilde{P}_{\delta}(\gamma) = \frac{0.0354\gamma + 0.0177}{\gamma^7 + 3.0906\gamma^6 + 4.0219\gamma^5 + 2.8399\gamma^4 + 1.1641\gamma^3 + 0.2725\gamma^2 + 0.0326\gamma + 0.0014}$$

$$P_{\delta 1}(\gamma) = \frac{0.0458\gamma + 0.0427}{\gamma^6 + 2.6243\gamma^5 + 2.8107\gamma^4 + 1.5607\gamma^3 + 0.4678\gamma^2 + 0.0701\gamma + 0.0039}$$

$$P_{\delta 2}(\gamma) = \frac{0.0582\gamma + 0.0544}{\gamma^6 + 2.6243\gamma^5 + 2.8107\gamma^4 + 1.5607\gamma^3 + 0.4678\gamma^2 + 0.0701\gamma + 0.0039}$$

$$P_{\delta 3}(\gamma) = \frac{0.0582\gamma + 0.0544}{\gamma^6 + 2.6243\gamma^5 + 2.8107\gamma^4 + 1.5607\gamma^3 + 0.4678\gamma^2 + 0.0701\gamma + 0.0039}$$

$$P_{\delta 4}(\gamma) = \frac{0.02912\gamma + 0.0272}{\gamma^7 + 3.1248\gamma^6 + 4.1228\gamma^5 + 2.9660\gamma^4 + 1.2482\gamma^3 + 0.3040\gamma^2 + 0.0389\gamma + 0.0019}$$

$$P_{\delta 5}(\gamma) = \frac{0.0127\gamma + 0.0272}{\gamma^7 + 3.0713\gamma^6 + 3.9639\gamma^5 + 2.7674\gamma^4 + 1.1157\gamma^3 + 0.2543\gamma^2 + 0.0290\gamma + 0.0011}$$

$$P_{\delta 6}(\gamma) = \frac{0.0225\gamma + 0.0245}{\gamma^6 + 2.5713\gamma^5 + 2.6782\gamma^4 + 1.4282\gamma^3 + 0.4016\gamma^2 + 0.0535\gamma + 0.0022}$$

The reference model in delta domain with ω_n=0.11 rad /sec, damping ratio ξ=0.8, time delay of 10 sec and sampling period Δ=2 sec for different values of angle angle (ρ) are computed for the nominal system and given as:

Angle ρ= -40°

$$M_{\delta}(\gamma) = \frac{0.00118\gamma^2 + 0.00091\gamma + 0.00016}{\gamma^8 + 3.16\gamma^7 + 4.26\gamma^6 + 3.16\gamma^5 + 1.39\gamma^4 + 0.372\gamma^3 + 0.057\gamma^2 + 0.0045\gamma + 00016}$$

Using GA with the following parameters, the OGDTM $\mu_{t\ is}$ found to be 0.0089 and corresponding PI controller and system transfer function for the nominal plant is obtained as:

- *Method of selection : Tournament selection method*
- Number of tournaments: 2
- Number of generation for evolution: 30
- Population size : 31
- Crossover probability: 0.77
- Number of crossover : 2
- Mutaion probability: 0.0077

PI controller $C_\delta(\gamma) = 0.040128 + \dfrac{0.0034992}{\gamma}$

$$G_\delta(\gamma) = \frac{0.00142\gamma^2 + 0.000834\gamma + 0.000062}{\gamma^8 + 3.09\gamma^7 + 4.02\gamma^6 + 2.84\gamma^5 + 1.16\gamma^4 + 0.27\gamma^3 + 0.034\gamma^2 + 0.0023\gamma + 000062}$$

Figures 5.28 show the reference and closed-loop unit step responses for the nominal plant with the PI controller. Unit step responses for various extreme plants with nominal controller are shown in figure 5.29.

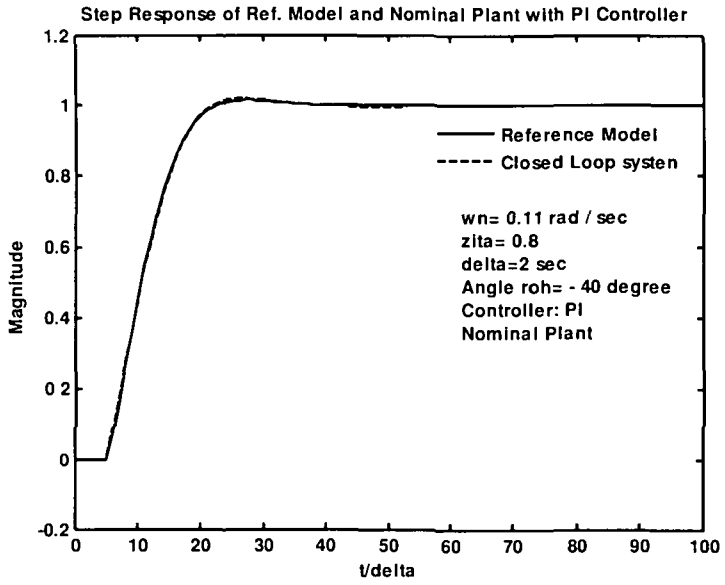

Figure 5.28: Step responses of Reference model and closed loop nominal plant with PI Controller for ρ= - 40°, ω_n= 0.11 rad/sec, ξ=0.8, Δ= 2 sec using OGDTM method

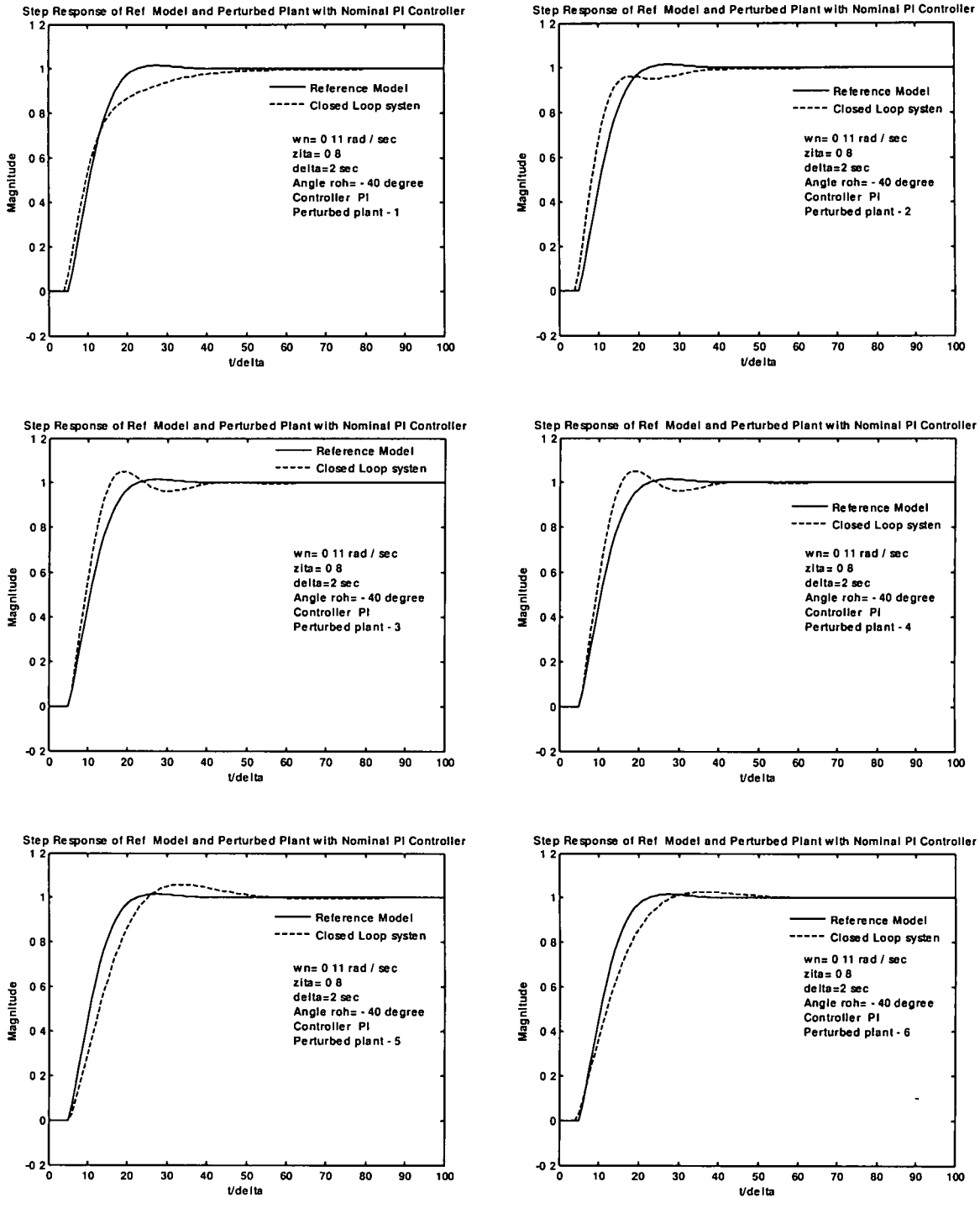

Figure 5.29: Step responses of various extreme plants $P_{\delta 1}(\gamma)$, $P_{\delta 2}(\gamma)$, $P_{\delta 3}(\gamma)$, $P_{\delta 4}(\gamma)$, $P_{\delta 5}(\gamma)$, $P_{\delta 6}(\gamma)P$ with nominal PI Controller using OGDTM

Angle ρ= -20°

Since sampling period is same i.e. 2 sec, hence the nominal and perturbed plants in delta domain will be same as for angle ρ= -40° , but the reference model transfer function is computed for the nominal system and given as:

$$M_\delta(\gamma) = \frac{0.0020\gamma^2 + 0.00132\gamma + 0.000158}{\gamma^8 + 3.16\gamma^7 + 4.26\gamma^6 + 3.16\gamma^5 + 1.39\gamma^4 + 0.371\gamma^3 + 0.057\gamma^2 + 0.0045\gamma + 00016}$$

Now using GA with same parameters, the OGDTM point is found to be 0.0167 and we obtain the following PI controller and system transfer function for the nominal plant as:

$$\text{PI controller} \quad C_\delta(\gamma) = 0.05096 + \frac{0.003920}{\gamma}$$

$$G_\delta(\gamma) = \frac{0.0018\gamma^2 + 0.00104\gamma + 0.000069}{\gamma^8 + 3.09\gamma^7 + 4.02\gamma^6 + 2.84\gamma^5 + 1.16\gamma^4 + 0.27\gamma^3 + 0.034\gamma^2 + 0.0025\gamma + 000069}$$

Angle ρ= +20°

Since sampling period is same i.e. 2 sec, hence the nominal and perturbed plants in delta domain will be same as above, the reference model transfer function is computed for the nominal system and given as:

$$M_\delta(\gamma) = \frac{0.00326\gamma^2 + 0.001195\gamma + 0.000158}{\gamma^8 + 3.16\gamma^7 + 4.26\gamma^6 + 3.16\gamma^5 + 1.39\gamma^4 + 0.371\gamma^3 + 0.057\gamma^2 + 0.0045\gamma + 00016}$$

Using GA with same parameters, the OGDTM point is found to be 0.0089 and we obtain the following PI controller and system transfer function for the nominal plant as:

$$\text{PI controller} \quad C_\delta(\gamma) = 0.06509 + \frac{0.004883}{\gamma}$$

$$G_\delta(\gamma) = \frac{0.0023\gamma^2 + 0.001133\gamma + 0.000086}{\gamma^8 + 3.09\gamma^7 + 4.02\gamma^6 + 2.84\gamma^5 + 1.16\gamma^4 + 0.27\gamma^3 + 0.034\gamma^2 + 0.0027\gamma + 000086}$$

Angle ρ= +40°

Since sampling period is same i.e. 2 sec, hence the nominal and perturbed plants in delta domain will be same as for angle ρ= -40° , but the reference model transfer function is computed for the nominal system and given as:

$$M_\delta(\gamma) = \frac{0.00408\gamma^2 + 0.00235\gamma + 0.000158}{\gamma^8 + 3.16\gamma^7 + 4.26\gamma^6 + 3.16\gamma^5 + 1.39\gamma^4 + 0.371\gamma^3 + 0.057\gamma^2 + 0.0045\gamma + 00016}$$

Using GA with same parameters, the OGDTM point is found to be 0.0089 and we obtain the following PI controller and system transfer function for the nominal plant as:

$$\text{PI controller} \quad C_\delta(\gamma) = 0.073258 + \frac{0.0057926}{\gamma}$$

$$G_\delta(\gamma) = \frac{0.00259\gamma^2 + 0.00150\gamma + 0.000103}{\gamma^8 + 3.09\gamma^7 + 4.02\gamma^6 + 2.84\gamma^5 + 1.16\gamma^4 + 0.27\gamma^3 + 0.035\gamma^2 + 0.0029\gamma + 000103}$$

Figures 5.30 to 5.33 show the reference model and closed-loop unit step responses for the nominal and various extreme plants with the nominal PI controller for angle ρ = - 40°, -20° , +20° and +40° respectively. Robustness is checked in terms of step responses and various time and frequency domain specifications are given in table 5.6

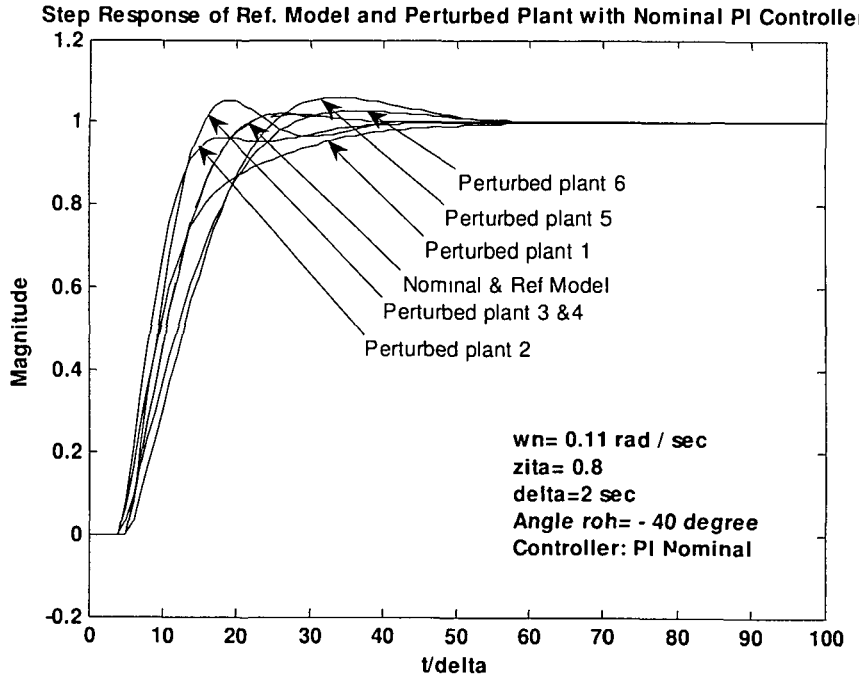

Figure 5.30: Step responses of Reference model and closed loop nominal & extreme plants with PI Controller for ρ= - 40°, ω_n= 0.11 rad/sec, ξ=0.8, Δ= 2 sec using OGDTM

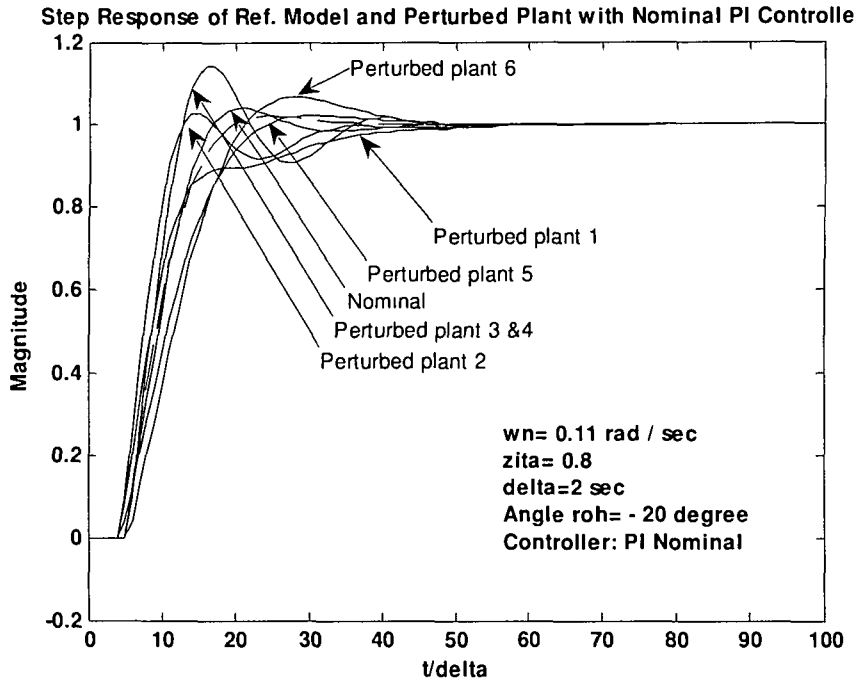

Figure 5.31: Step responses of Reference model and closed loop nominal & extreme plants with PI Controller for ρ= - 20°, ω_n= 0.11 rad/sec, ξ=0.8, Δ= 2 sec using OGDTM

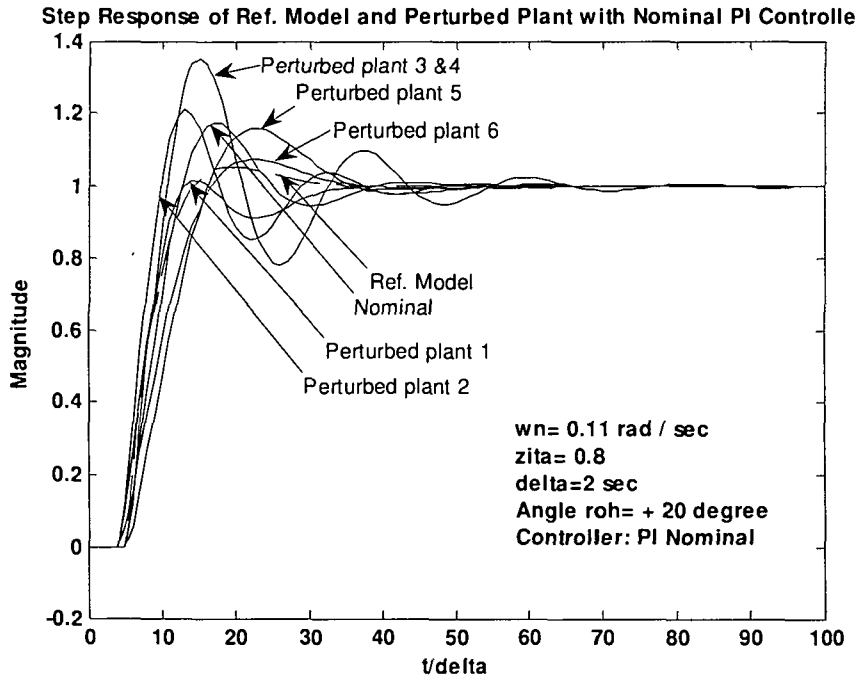

Figure 5.32: Step responses of Reference model and closed loop nominal & extreme plants with PI Controller for ρ= +20°, ω_n= 0.11 rad/sec, ξ=0.8, Δ= 2 sec using OGDTM

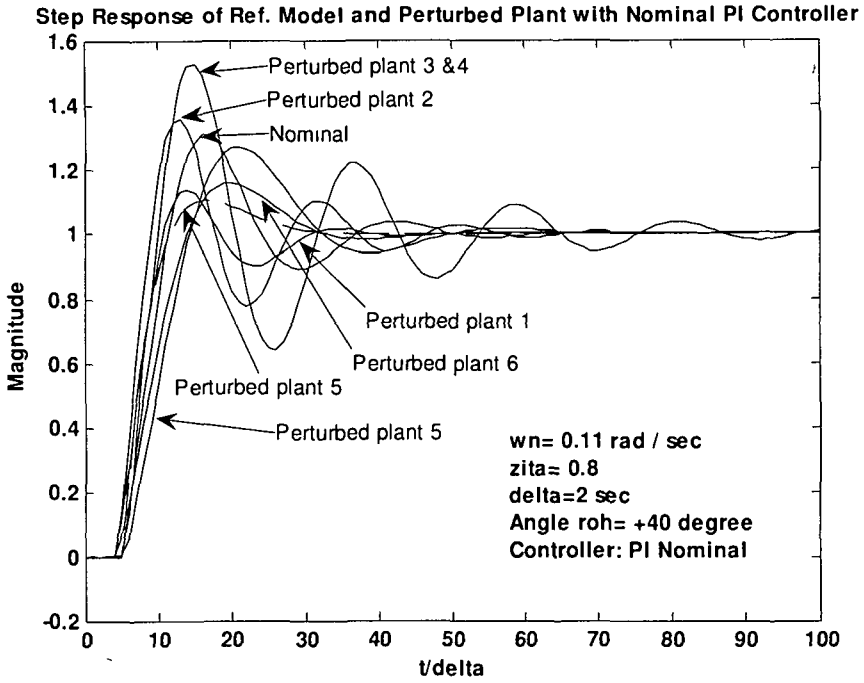

Figure 5.33: Step responses of Reference model and closed loop nominal & extreme plants with PI Controller for ρ= +40°, ω_n= 0.11 rad/sec, ξ=0.8, Δ= 2 sec using OGDTM

The nominal controller parameters are randomly varied to the extent of ±10%, ±20% and ±30% and corresponding time and frequency domain performance measures are computed and are given in table 5.7. Step responses of Reference model and closed loop nominal & extreme plants with varied parameter nominal PI Controller for ρ= -40°, ω_n= 0.11 rad/sec, ξ=0.8, Sampling time Δ= 2 sec using genetic algorithm for OGDTM method optimum frequency point is found to be 0.0089 for different parameter variation in the nominal controller are shown in figure 3.34 to 3.39. The Nominal controller transfer function is given as

$$C_{\delta nom}(\gamma) = 0.040128 + \frac{0.003499}{\gamma}$$

Table 5.6

Time and frequency response specifications due to Plant uncertainty for different angles with ω_n= 0.11 rad/sec, ξ=0.8, Sampling time Δ= 2 sec & PI controller

Plant	ρ	Reference Model					Closed loop system with nominal PI Controller				
		M_p%	t_p/Δ	t_s/Δ	GM	PM	M_p%	t_p/Δ	t_s/Δ	GM	PM
Nominal	- 40°	1.61	28	19	3.09	63.26	2.07	28	19	3.19	63.11
$P_{\delta 1}(\gamma)$	- 40°	1.61	28	19	3.09	63.26	0	--	32	3.51	74.15
$P_{\delta 2}(\gamma)$	- 40°	1.61	28	19	3.09	63.26	0	--	16	2.75	68.68
$P_{\delta 3}(\gamma)$	- 40°	1.61	28	19	3.09	63.26	5.25	20	20	2.37	62.68
$P_{\delta 4}(\gamma)$	- 40°	1.61	28	19	3.09	63.26	5.25	20	20	2.37	62.68
$P_{\delta 5}(\gamma)$	- 40°	1.61	28	19	3.09	63.26	5.95	34	39	3.71	59.96
$P_{\delta 6}(\gamma)$	- 40°	1.61	28	19	3.09	63.26	2,72	37	24	4.57	64.21
Nominal	- 20°	2.08	25	17	3.02	62.62	4.04	22	16	2.67	62.08
$P_{\delta 1}(\gamma)$	- 20°	2.08	25	17	3.02	62.62	0	--	31	2.87	74.37
$P_{\delta 2}(\gamma)$	- 20°	2.08	25	17	3.02	62.62	2.72	16	28	2.26	67.41
$P_{\delta 3}(\gamma)$	- 20°	2.08	25	17	3.02	62.62	14.01	17	32	1.96	60.22
$P_{\delta 4}(\gamma)$	- 20°	2.08	25	17	3.02	62.62	14.01	17	32	1.96	60.22
$P_{\delta 5}(\gamma)$	- 20°	2.08	25	17	3.02	62.62	6.67	29	34	3.17	59.04
$P_{\delta 6}(\gamma)$	- 20°	2.08	25	17	3.02	62.62	2.20	32	21	3.85	63.89
Nominal	+20°	5.31	20	21	2.61	58.64	17.47	18	32	2.11	54.25
$P_{\delta 1}(\gamma)$	+20°	5.31	20	21	2.61	58.64	1.51	16	28	2.26	68.59
$P_{\delta 2}(\gamma)$	+20°	5.31	20	21	2.61	58.64	20.86	14	27	1.78	57.21
$P_{\delta 3}(\gamma)$	+20°	5.31	20	21	2.61	58.64	35.27	16	50	1.55	47.50
$P_{\delta 4}(\gamma)$	+20°	5.31	20	21	2.61	58.64	35.27	16	50	1.55	47.50
$P_{\delta 5}(\gamma)$	+20°	5.31	20	21	2.61	58.64	15.82	24	32	2.51	52.38
$P_{\delta 6}(\gamma)$	+20°	5.31	20	21	2.61	58.64	7.39	23	28	3.05	58.43
Nominal	+40°	10.31	18	24	2.37	53.98	30.55	17	35	1.83	45.60
$P_{\delta 1}(\gamma)$	+40°	10.31	18	24	2.37	53.98	13.51	15	28	1.98	60.81
$P_{\delta 2}(\gamma)$	+40°	10.31	18	24	2.37	53.98	35.63	14	43	1.56	46.18
$P_{\delta 3}(\gamma)$	+40°	10.31	18	24	2.37	53.98	51.25	16	73	1.35	34.50
$P_{\delta 4}(\gamma)$	+40°	10.31	18	24	2.37	53.98	51.25	16	73	1.35	34.50
$P_{\delta 5}(\gamma)$	+40°	10.31	18	24	2.37	53.98	26.77	22	43	2.17	45.03
$P_{\delta 6}(\gamma)$	+40°	10.31	18	24	2.37	53.98	15.65	21	28	2.64	52.04

Table 5.7

Time and frequency domain specification due to variation in controller parameters with ρ= - -40°, ω_n= 0.11 rad/sec, ξ=0.8, Sampling time Δ= 2 sec & PI controller

Plant	PI Controller Transfer function	Closed loop system with nominal PI Controller				
		M_p%	t_p/Δ	t_s/Δ	GM	PM
	-30% Parameter Variation					
Nominal	$C_\delta(\gamma) = 0.02809 + \frac{0.002449}{\gamma}$	--	--	35	4.56	71.31
$P_{\delta 1}(\gamma)$		--	--	48	5.01	79.43
$P_{\delta 2}(\gamma)$		--	--	37	3.94	76.15
$P_{\delta 3}(\gamma)$		--	--	34	3.39	72.09
$P_{\delta 4}(\gamma)$		--	--	34	3.39	72.09
$P_{\delta 5}(\gamma)$		0.47	61	37	5.31	68.35
$P_{\delta 6}(\gamma)$		0.05	77	40	6.53	71.38
	-20% Parameter Variation					
Nominal	$C_\delta(\gamma) = 0.03210 + \frac{0.002799}{\gamma}$	--	--	28	3.99	68.59
$P_{\delta 1}(\gamma)$		--	--	42	4.38	77.75
$P_{\delta 2}(\gamma)$		--	--	32	3.44	73.81
$P_{\delta 3}(\gamma)$		--	--	26	2.97	69.11
$P_{\delta 4}(\gamma)$		--	--	26	2.97	69.11
$P_{\delta 5}(\gamma)$		1.74	47	31	4.64	65.48
$P_{\delta 6}(\gamma)$		0.5264	55	33	5.71	68.93
	-10% Parameter Variation					
Nominal	$C_\delta(\gamma) = 0.03612 + \frac{0.003149}{\gamma}$	0.09	37	23	3.55	65.87
$P_{\delta 1}(\gamma)$		--	--	36	3.90	75.99
$P_{\delta 2}(\gamma)$		--	--	28	3.06	71.32
$P_{\delta 3}(\gamma)$		--	--	17	2.64	65.98
$P_{\delta 4}(\gamma)$		--	--	17	2.64	65.98
$P_{\delta 5}(\gamma)$		3.60	39	26	4.12	62.68
$P_{\delta 6}(\gamma)$		1.44	44	28	5.08	66.54

Table 5.7 (continued)

Time and frequency domain specification due to variation in controller parameters with ρ= - -40°, ω_n= 0.11 rad/sec, ξ=0.8, Sampling time Δ= 2 sec & PI controller

Plant	PI Controller Transfer function	Closed loop system with nominal PI Controller				
		M_p%	t_p/Δ	t_s/Δ	GM	PM
	+10% Parameter Variation					
Nominal		5.29	24	25	2.91	60.35
$P_{\delta 1}(\gamma)$		--	--	29	3.19	72.23
$P_{\delta 2}(\gamma)$		1.04	17	13	2.50	65.87
$P_{\delta 3}(\gamma)$	$C_\delta(\gamma) = 0.04414 + \frac{0.003849}{\gamma}$	11.69	19	23	2.16	59.19
$P_{\delta 4}(\gamma)$		11.69	19	23	2.16	59.19
$P_{\delta 5}(\gamma)$		8.68	31	40	3.37	57.29
$P_{\delta 6}(\gamma)$		4.31	22	23	4.15	61.94
	+20% Parameter Variation					
Nominal		9.15	22	27	2.66	57.58
$P_{\delta 1}(\gamma)$		1.61	25	26	2.92	70.21
$P_{\delta 2}(\gamma)$	$C_\delta(\gamma) = 0.04815 + \frac{0.004199}{\gamma}$	6.43	16	26	2.29	62.89
$P_{\delta 3}(\gamma)$		18.36	18	33	1.98	55.50
$P_{\delta 4}(\gamma)$		18.36	18	33	1.98	55.50
$P_{\delta 5}(\gamma)$		11.75	29	39	3.09	54.68
$P_{\delta 6}(\gamma)$		6.17	30	34	3.81	59.74
	+30% Parameter Variation					
Nominal		13.40	21	27	2.46	54.80
$P_{\delta 1}(\gamma)$		--	--	15	2.70	68.09
$P_{\delta 2}(\gamma)$	$C_\delta(\gamma) = 0.05217 + \frac{0.004549}{\gamma}$	12.01	16	28	2.12	59.73
$P_{\delta 3}(\gamma)$		24.93	18	34	1.82	51.62
$P_{\delta 4}(\gamma)$		24.93	18	34	1.82	51.62
$P_{\delta 5}(\gamma)$		8.30	27	34	3.51	57.58
$P_{\delta 6}(\gamma)$						

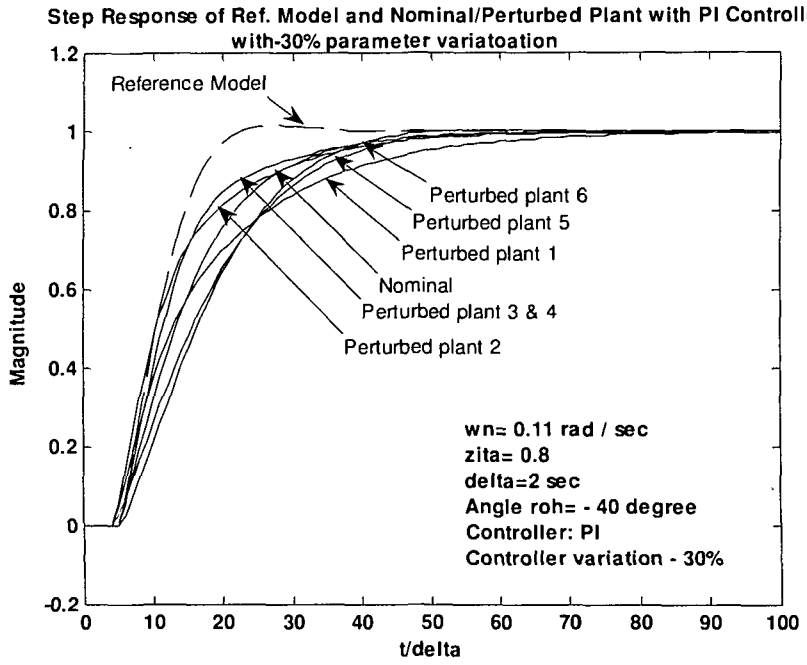

Figure 5.34: Step responses of Reference model and closed loop nominal & extreme plants with -30% varied parameter nominal PI Controller for ρ= -40°, ω_n= 0.11 rad/sec, ξ=0.8, Sampling time Δ= 2 sec using OGDTM

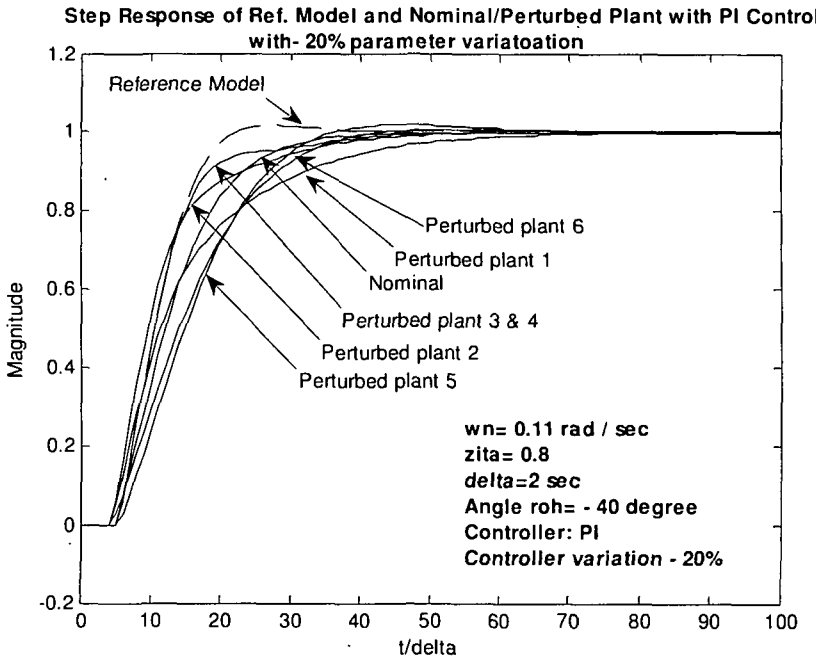

Figure 5.35: Step responses of Ref. model and closed loop nominal & extreme plants with -20% varied parameter nominal PI Controller for ρ= -40°, ω_n= 0.11 rad/sec, ξ=0.8, Δ= 2 sec using OGDTM

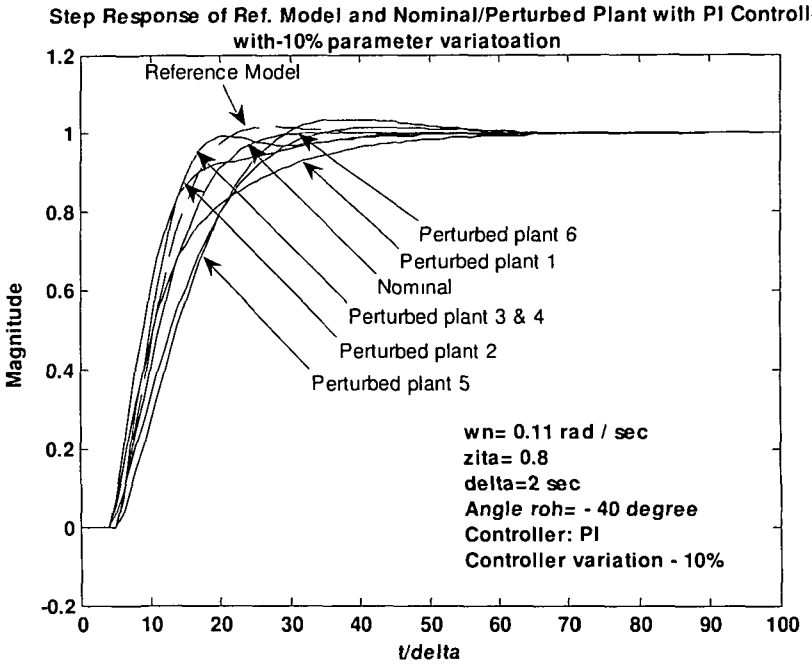

Figure 5.36: Step responses of Ref. model and closed loop nominal & extreme plants with -10% varied parameter nominal PI Controller for ρ= -40°, ω_n= 0.11 rad/sec, ξ=0.8, Δ= 2 sec using OGDTM

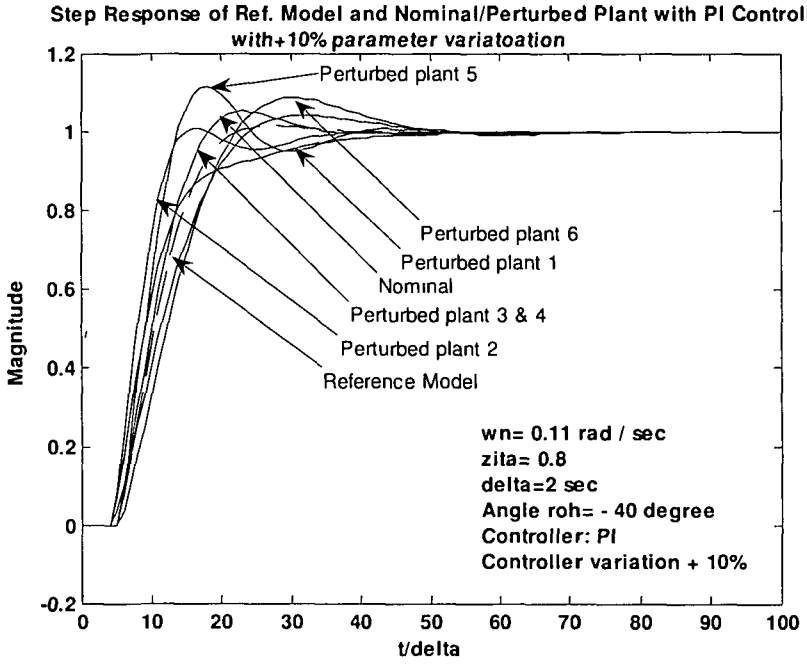

Figure 5.37: Step responses of Ref. model and closed loop nominal & extreme plants with +10% varied parameter nominal PI Controller for ρ= -40°, ω_n= 0.11 rad/sec, ξ=0.8, Δ= 2 sec using OGDTM

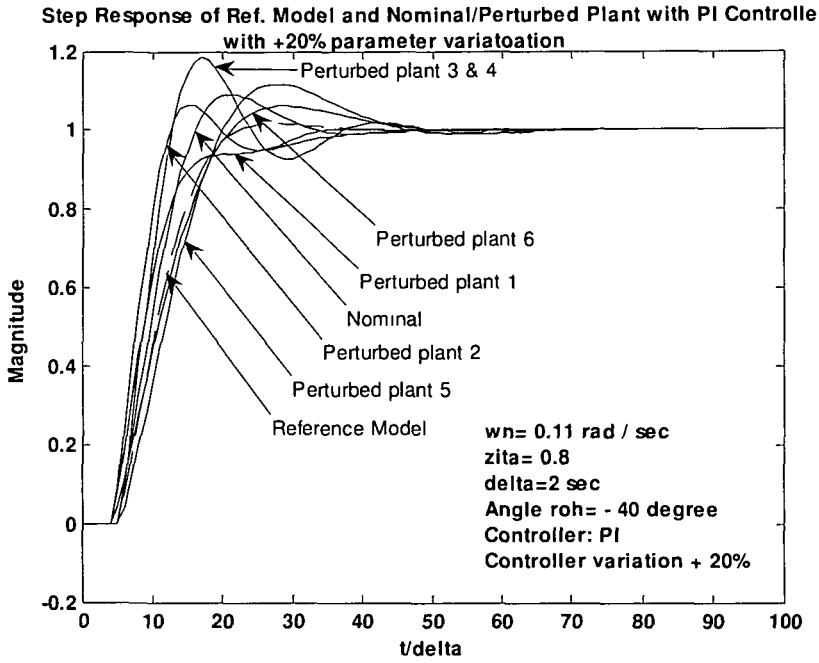

Figure 5.38: Step responses of Reference model and closed loop nominal & extreme plants with +20% varied parameter nominal PI Controller for ρ= -40°, ω_n= 0.11 rad/sec, ξ=0.8, Sampling time Δ= 2 sec using OGDTM

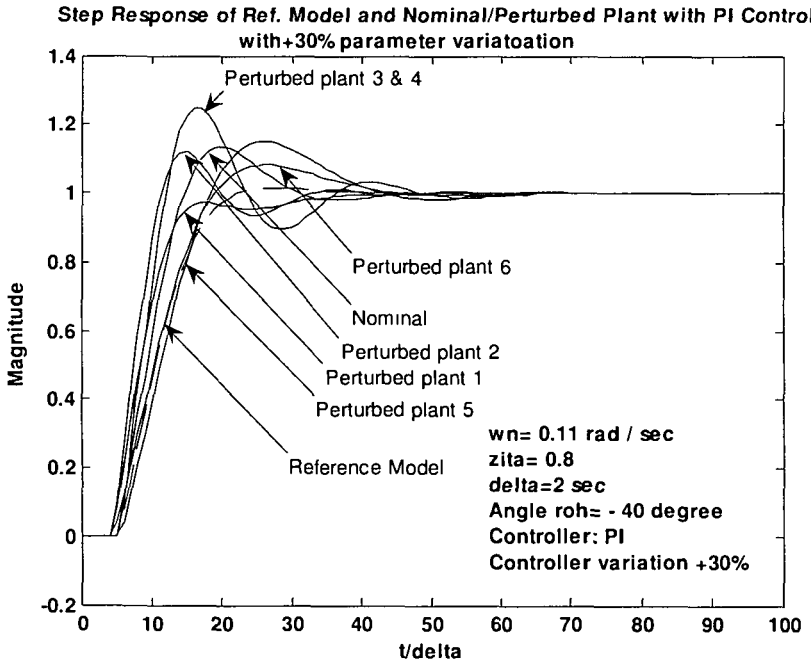

Figure 5.39: Step responses of Reference model and closed loop nominal & extreme plants with +30% varied parameter nominal PI Controller for ρ= -40°, ω_n= 0.11 rad/sec, ξ=0.8, Sampling time Δ= 2 sec using OGDTM

5.1.9 MIMO Systems:

We consider here the problem of controller design for a multivariable system with dead time. There is a great variety of processes whose dynamics are represented by multivariable transfer functions having multiple time delays. Some of the more important processes in this category are distillation columns, extraction and absorption processes, heat exchangers etc. These processes are multi-input multi-output systems with multiple time delays and strong interaction effects between various inputs and outputs. Let the transfer function model of the plant is

$$P_\delta(\gamma)=\begin{bmatrix} p_{\delta,11}(\gamma) & p_{\delta,12}(\gamma) & \cdots\cdots & p_{\delta,1m}(\gamma) \\ p_{\delta,21}(\gamma) & p_{\delta,22}(\gamma) & \cdots\cdots & p_{\delta,2m}(\gamma) \\ \vdots & \vdots & \vdots & \vdots \\ p_{\delta,p1}(\gamma) & p_{\delta,p2}(\gamma) & \cdots\cdots & p_{\delta,pm}(\gamma) \end{bmatrix} \qquad (5.24)$$

For square plant transfer function model, p = m. The individual scalar transfers function in the above may be expressed in a general form as

$$P_\delta(\gamma)=\frac{b_{0,ij}+b_{1,ij}\gamma+b_{2,ij}\gamma^2\cdots\cdots+b_{q,ij}\gamma^q}{a_0+a_{1,ij}\gamma+a_{2,ij}\gamma^2\cdots\cdots+a_{p,ij}\gamma^p}(1+\Delta\gamma)^{-N} \qquad (5.25)$$

The reference model TFM with multiple time delay is considered as

$$M_\delta(\gamma)=diag\left\{M_{ii}(\gamma)\,(1+\Delta\gamma)^{N_{ii}}\right\};\quad i\in[1,\ p];\ p=m \qquad (5.26)$$

The purpose is to design a multivariable controller $C_\delta(\gamma)$ that results in good set point tracking, low interaction and desired time response characteristics like settling time, rise time, allowable overshoot etc., for the main diagonal responses.

In this section we extend the MIMO controller design methods of Chapter-4 OGDTM and Optimal frequency fitting to design a controller TFM $C_\delta(\gamma)$ for MIMO systems with multiple delays. Design results are given in the example sections. The mathematical expressions for the controller design procedure follow closely those of Chapter-4, and are not included for brevity.

5.1.10 Simulation results with OGDTM method:

The OGDTM method is tested here on following MIMO system with time delay.

5.1.10.1 Distillation column with time delay:

We consider here the distillation column studied by Wood and Berry [121]. The plant transfer function is given by

$$P_\delta(\gamma)=\begin{bmatrix} \dfrac{12.8}{1+16.7s}e^{-s} & \dfrac{-18.9}{1+21s}e^{-3s} \\ \dfrac{6.6}{1+10.9s}e^{-7s} & \dfrac{-19.4}{1+14.4s}e^{-3s} \end{bmatrix}$$

The continuous plant models is discritized in δ-domain incorporating the sampler and ZOH at sampling period Δ=1 sec. Very fast sampling is avoided to restrict the order of the resultant system. The discrete transfer function in δ-domain is obtained as :

$$P_{\delta 11}(\gamma)=\frac{0.74397\gamma+0.74397}{\gamma^3+2.0581\gamma^2+1.1162\gamma+0.058123}$$

$$P_{\delta 12}(\gamma)=\frac{-0.87891\gamma-0.87891}{\gamma^5+4.0465\gamma^4+6.168\gamma^3+4.279\gamma^2+1.186\gamma+0.046503}$$

$$P_{\delta 21}(\gamma)=\frac{0.57856\gamma+0.57856}{\gamma^9+8.08\gamma^8+28.70\gamma^7+58.45\gamma^6+74.91\gamma^5+62.14\gamma^4+32.91\gamma^3+10.46\gamma^2+1.70\gamma+0.087}$$

$$P_{\delta 22}(\gamma)=\frac{-1.3015\gamma-1.3015}{\gamma^5+4.067\gamma^4+6.268\gamma^3+4.402\gamma^2+1.268\gamma+0.0671}$$

The reference model for undamped natural frequency ω_n=0.28 rad/sec and 0.3 rad /sec, damping factor ξ=0.8 and angle ρ = -40° are computed and given as:

Δ=1 sec, ρ= -40°,ω_n=0.28 rad/sec & ξ=0.8

Reference model

$$M_\delta(\gamma)=\begin{bmatrix} \dfrac{0.0.0684\gamma^2+0.1025\gamma+0.03412}{\gamma^4+2.308\gamma^3+1.6501\gamma^2+0.3762\gamma+0.03412} & 0 \\ 0 & \dfrac{0.0.0684\gamma^2+0.1025\gamma+0.03412}{\gamma^6+4.31\gamma^5+7.27\gamma^4+5.98\gamma^3+2.44\gamma^2+0.44\gamma+0.034} \end{bmatrix}$$

The following GA parameters are considered to compute OGDTM (μ_t) value

- Method of selection : Roulette wheel
- Number of generation for evolution: 35
- Population size : 32
- Crossover probability: 0.85

- Number of crossover : 2
- Mutaion probability: 0.0085

Using above GA parameters, the optimal frequency point μ_t is found to be 0.0718 and corresponding PI controller is obtained as:

$$C_\delta(\gamma)=\begin{bmatrix} 0.10091+\dfrac{0.02206}{\gamma} & -0.01652-\dfrac{0.01583}{\gamma} \\ 0.00078+\dfrac{0.00854}{\gamma} & -0.05453-\dfrac{0.011114}{\gamma} \end{bmatrix}$$

Δ=1 sec, ρ= -40°,ω_n=0.3 rad/sec & ξ=0.8

For the specifications given above, the reference model transfer functions are

$$M_\delta(\gamma)=\begin{bmatrix} \dfrac{0.10791\gamma^2+0.1788\gamma+0.0709}{\gamma^4+2.4522\gamma^3+1.9753\gamma^2+0.5941\gamma+0.0709} & 0 \\ 0 & \dfrac{0.10791\gamma^2+0.1788\gamma+0.0709}{\gamma^6+4.45\gamma^5+7.88\gamma^4+6.99\gamma^3+3.23\gamma^2+0.74\gamma+0.071} \end{bmatrix}$$

and using GA with same parameters, OGDTM point is found to be 0.0954 and the PI controller obtained are given as:

$$C_\delta(\gamma)=\begin{bmatrix} 0.1559+\dfrac{0.0312}{\gamma} & -0.02834-\dfrac{0.02101}{\gamma} \\ -0.00154+\dfrac{0.01277}{\gamma} & -0.08251-\dfrac{0.01429}{\gamma} \end{bmatrix}$$

The unit step responses of the reference model and closed-loop plant are shown in Figures 5.40 and 5.41 respectively, while the corresponding control efforts are shown in Figures 5.42 &5.43

5.1.11 Simulation results with Optimal frequency fitting method:

The optimal frequency fitting method is tested on following MIMO system with time delay

5.1.11.1 Distillation column (revisited):

We considered the plant in section 5.1.10.1 for controller design using the optimal frequency fitting method. Since the sampling period is kept same i.e. 1 sec to restrict the order of resultant transfer function, the plant transfer function in delta domain will be same as section 5.1.10.1. The reference model is computed for different values of

undamped natural frequencies and using genetic algorithm the optimal frequency points resultant PI controller obtained the Optimal frequency points considered are $\psi_i = \psi.i$, $i \in [1, 2]$.

Δ = 1 sec, ρ = - 40°, ω_n = 0.2 rad / sec & ξ = 0.8

Reference model transfer functions are

$$M_\delta(\gamma) = \begin{bmatrix} \dfrac{0.05736\gamma^2 + 0.1218\gamma + 0.0644}{\gamma^4 + 2.389\gamma^3 + 1.842\gamma^2 + 0.518\gamma + 0.064} & 0 \\ 0 & \dfrac{0.0573\gamma^2 + 0.1218\gamma + 0.0644}{\gamma^6 + 4.389\gamma^5 + 7.619\gamma^4 + 6.590\gamma^3 + 2.941\gamma^2 + 0.646\gamma + 0.064} \end{bmatrix}$$

GA parmeters are selected as

The following GA parameters are considered to compute OGDTM (μ_i) value

- Method of selection : Roulette wheel
- Number of generation for evolution: 30
- Population size : 31
- Crossover probability: 0.77
- Number of crossover : 2
- Mutaion probability: 0.0077

Using above parameters for GA, the optimal frequency point is found to be 0.0089 and -0.0002+0.0177i as the real and imaginary parts and corresponding PI controller is obtained as:

$$C_\delta(\gamma) = \begin{bmatrix} 0.22586 + \dfrac{0.025684}{\gamma} & -0.03059 - \dfrac{0.01861}{\gamma} \\ 0.071927 + \dfrac{0.008821}{\gamma} & -0.09688 - \dfrac{0.012727}{\gamma} \end{bmatrix}$$

Δ = 1 sec, ρ = - 40°, ω_n = 0.28 rad / sec & ξ = 0.7

Reference model transfer functions are

$$M_\delta(\gamma) = \begin{bmatrix} \dfrac{0.06839\gamma^2 + 0.1025\gamma + 0.03411}{\gamma^4 + 2.308\gamma^3 + 1.650\gamma^2 + 0.376\gamma + 0.034} & 0 \\ 0 & \dfrac{0.06839\gamma^2 + 0.1025\gamma + 0.03411}{\gamma^6 + 4.308\gamma^5 + 7.266\gamma^4 + 5.984\gamma^3 + 2.436\gamma^2 + 0.444\gamma + 0.034} \end{bmatrix}$$

Using the same GA parameters , the optimal frequency point is found to be 0.1269 and the real and imaginary parts are -0.0329+0.2510i. The PI controller transfer function is obtained as:

$$C_\delta(\gamma)=\begin{bmatrix} 0.08388+\dfrac{0.02775}{\gamma} & -0.01779-\dfrac{0.01855}{\gamma} \\ -0.01041+\dfrac{0.01274}{\gamma} & -0.04733-\dfrac{0.011318}{\gamma} \end{bmatrix}$$

The unit step responses of the reference model and closed-loop plant are shown in Figures 5.44 and 5.45 respectively, while the corresponding control efforts are shown in Figures 5.46 & 5.47.

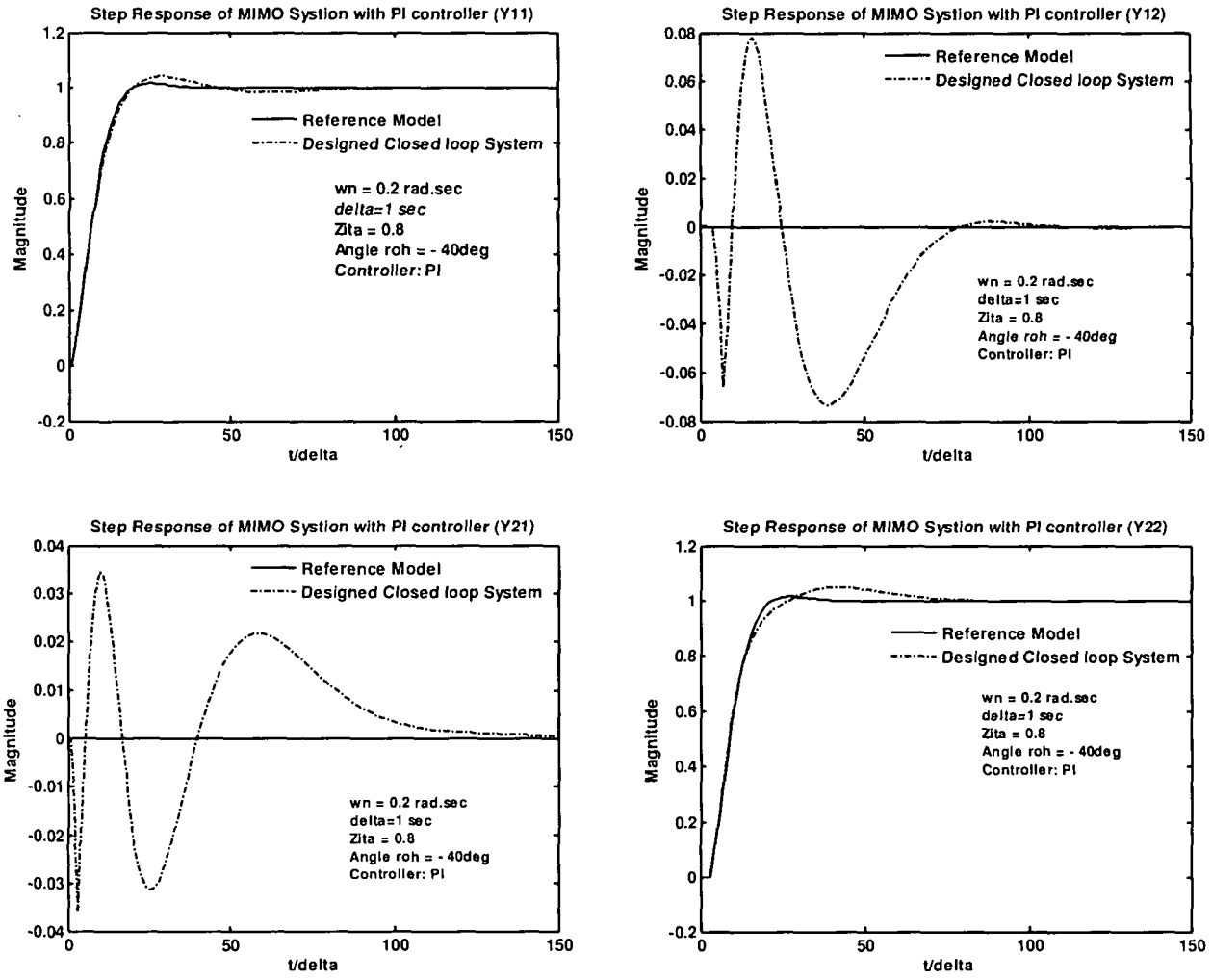

Figure 5.40: Step responses of the reference model and closed loop plant with PI controller using OGDTM, output y11,y12,y21,y22, Δ=1sec, ρ=-40°, ω_n=0.2 rad/sec & ξ=0.8

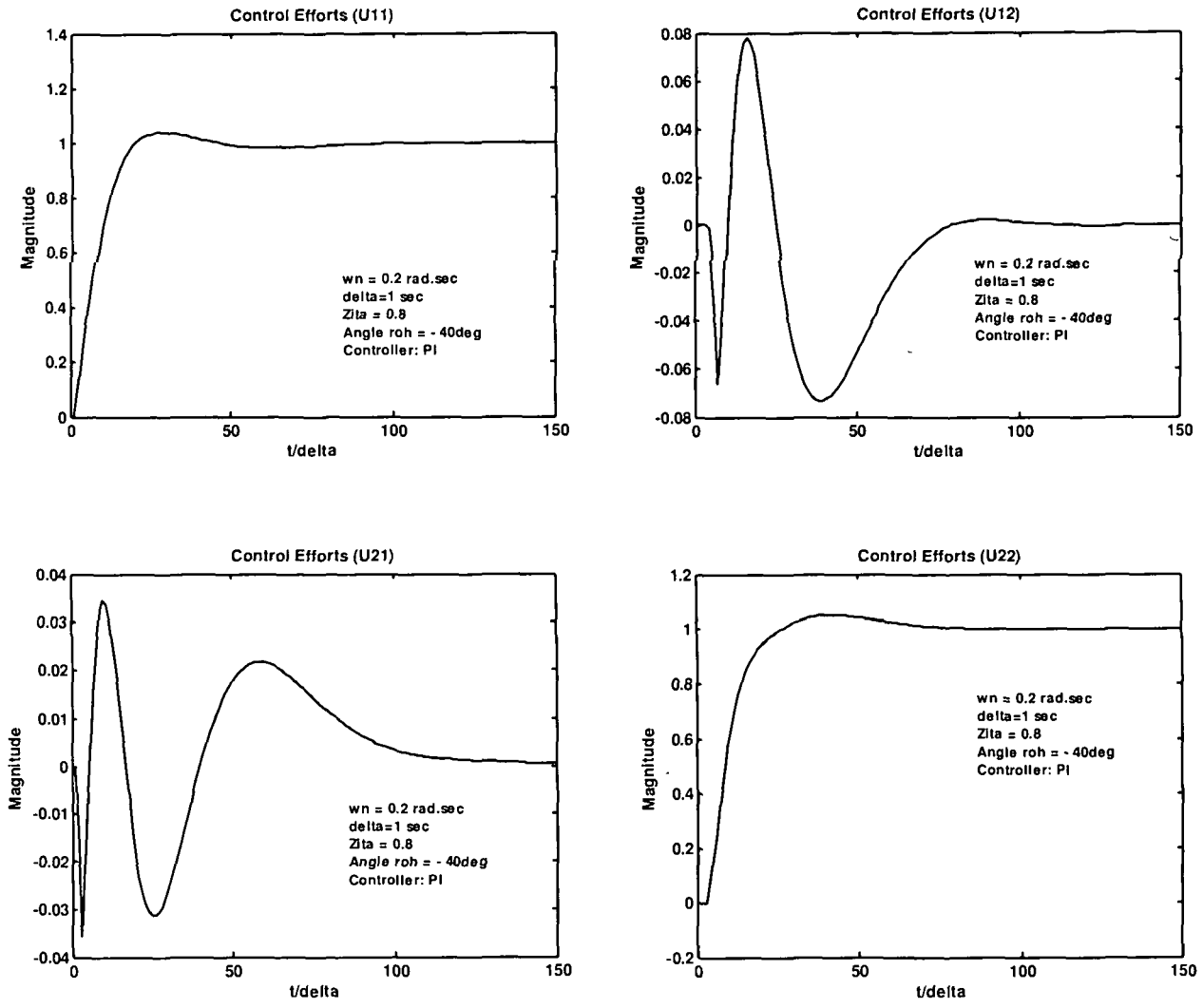

Figure 5.41: Step responses of Control effort using OGDTM, u11,u12,u21,u22, Δ = 1sec, ρ = - 40°, ω_n= 0.2 rad/sec & ξ = 0.8

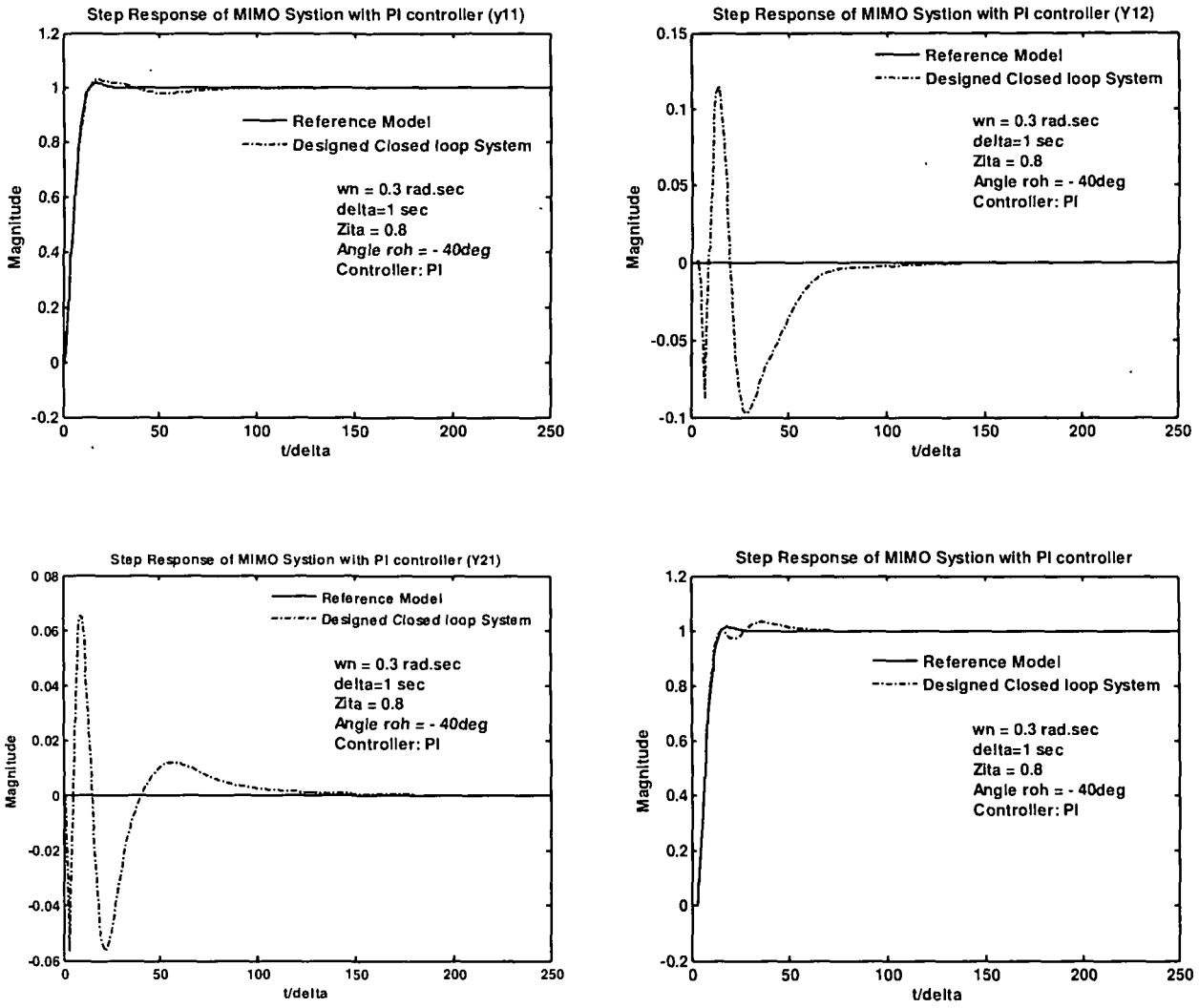

Figure 5.42: Step responses of the reference model and closed loop plant with PI controller using OGDTM, output y11,y12,y21,y22, Δ=1sec, ρ=-40°, ω_n=0.3 rad/sec & ξ=0.8

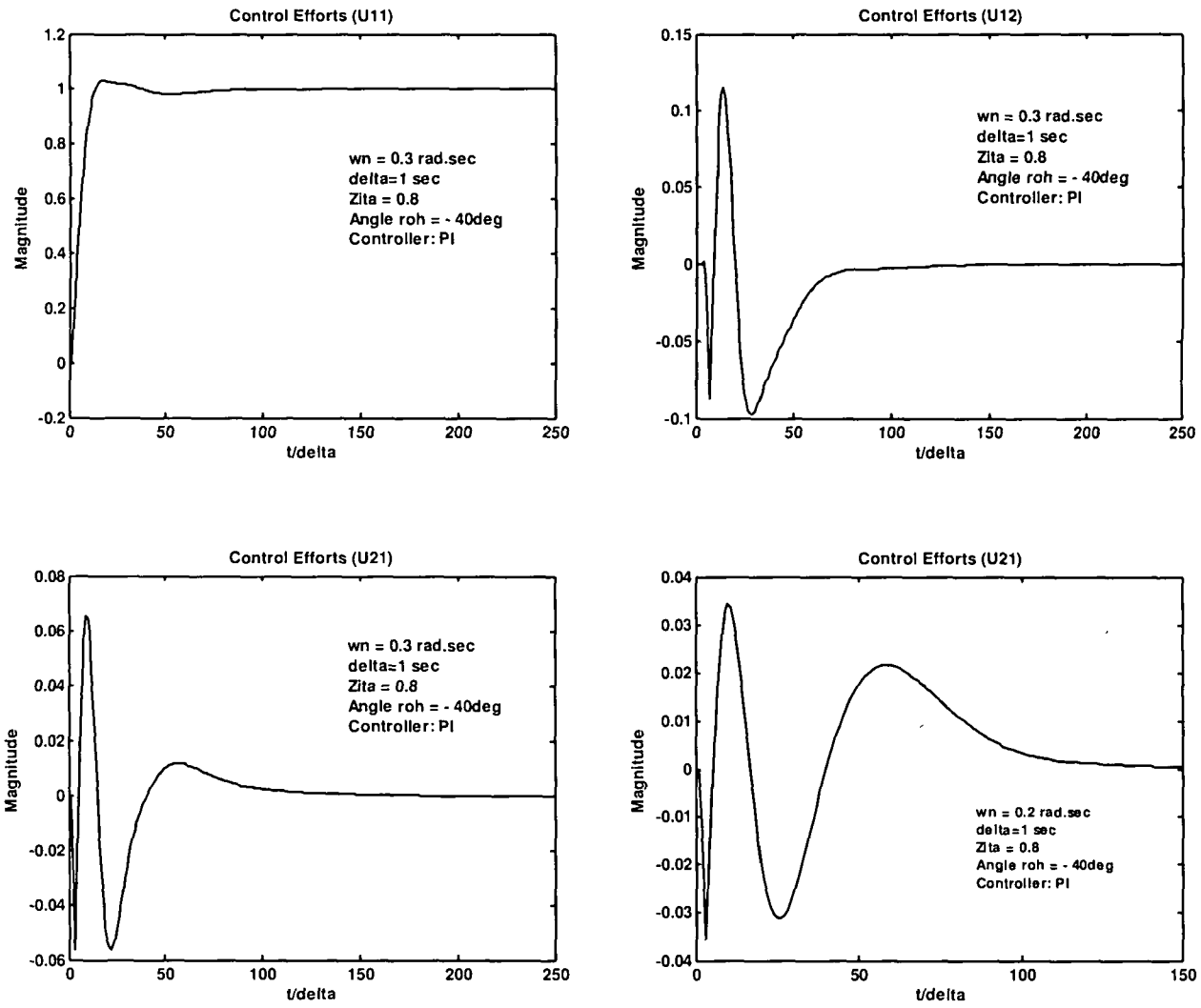

Figure 5.43: Step responses of Control effort using OGDTM, u11,u12,u21,u22, Δ = 1sec, ρ = - 40°, ω_n= 0.3 rad/sec & ξ = 0.8

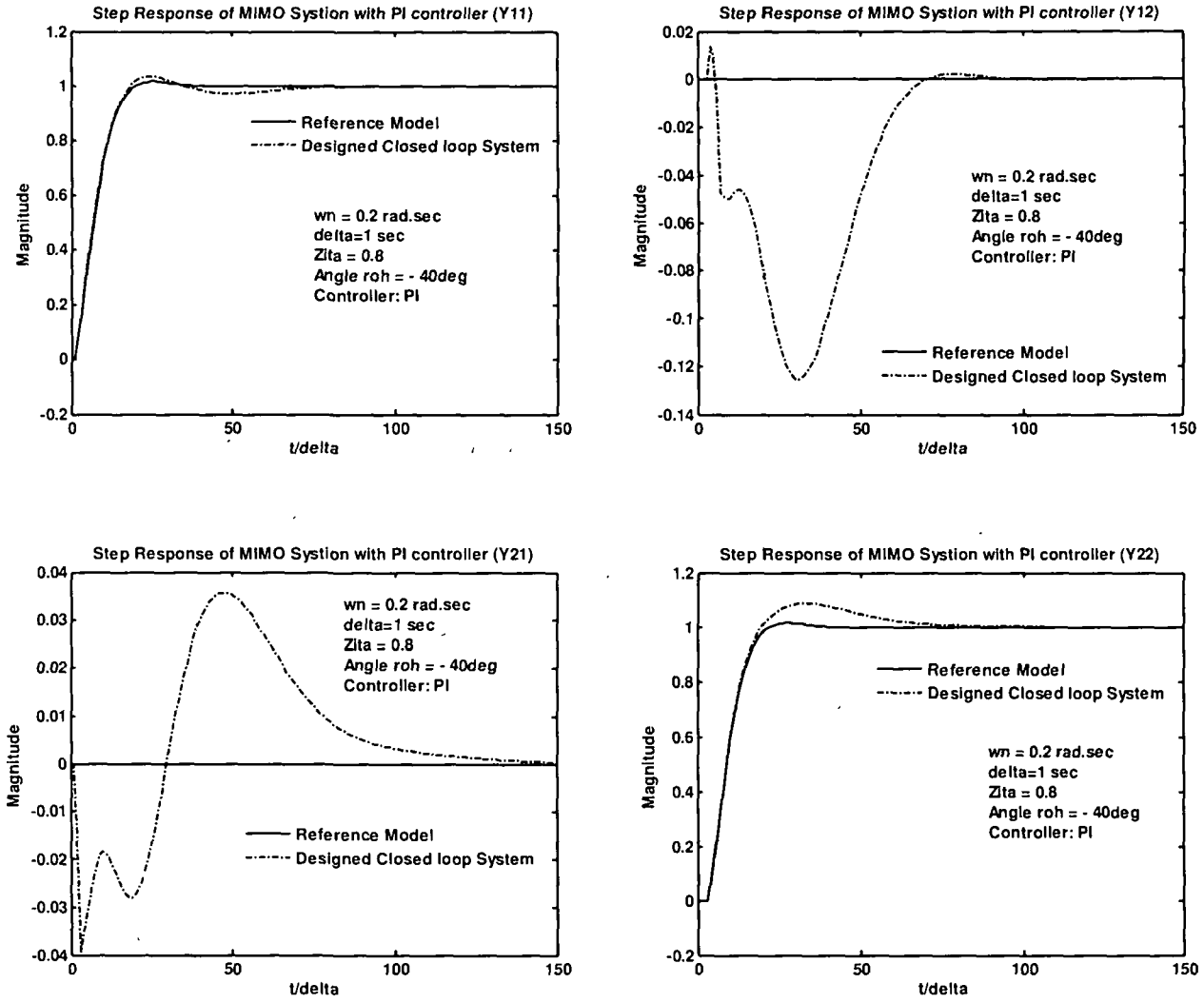

Figure 5.44: Step responses of the reference model and closed loop plant with PI controller using OFF method, output y11,y12,y21,y22, Δ=1sec, ρ=-40°, ω_n=0.2 rad/sec & ξ=0.8

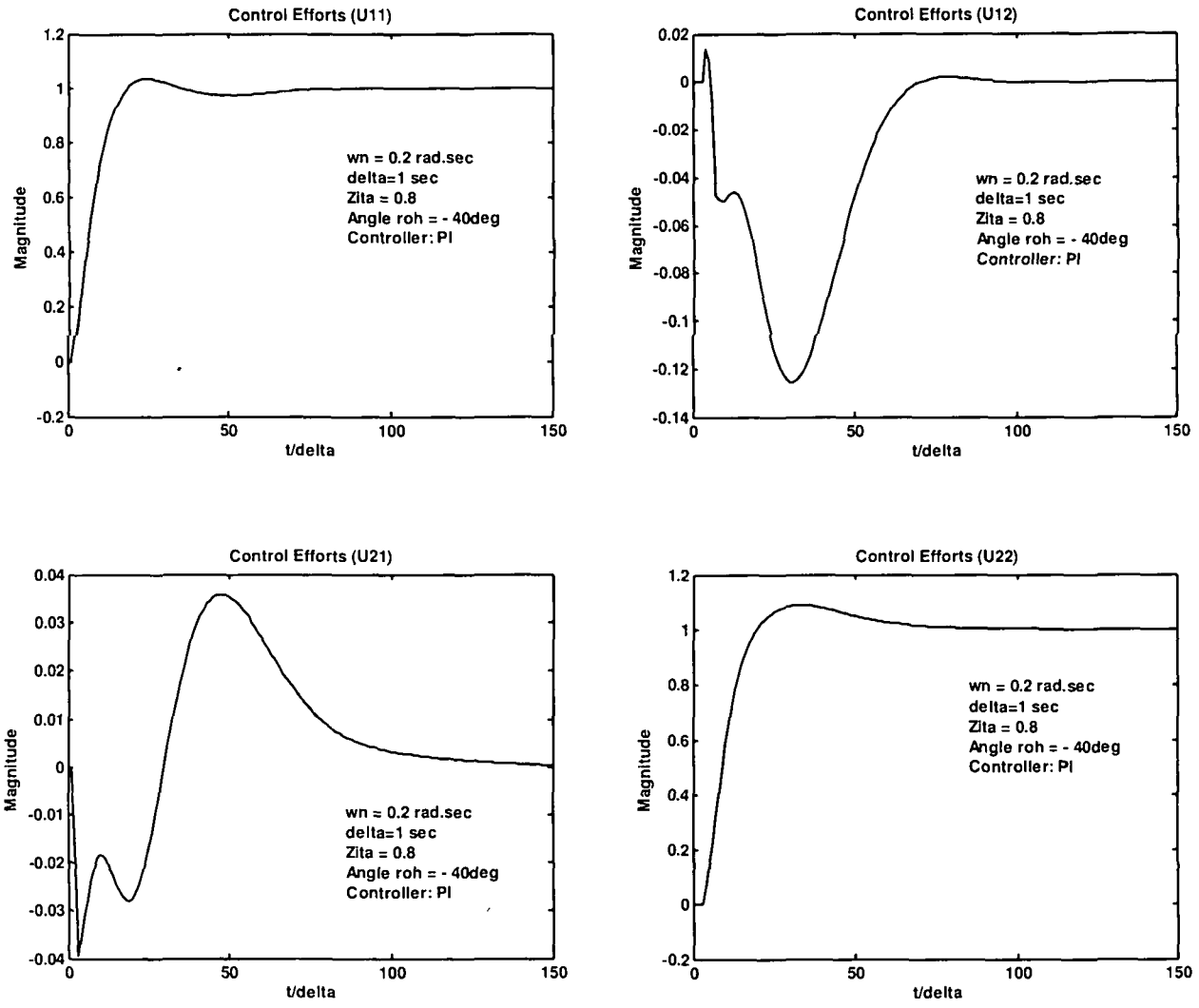

Figure 5.45: Step responses of Control effort using OFF method, u11,u12,u21,u22, Δ = 1sec, ρ = - 40°, ω_n= 0.2 rad/sec & ξ = 0.8

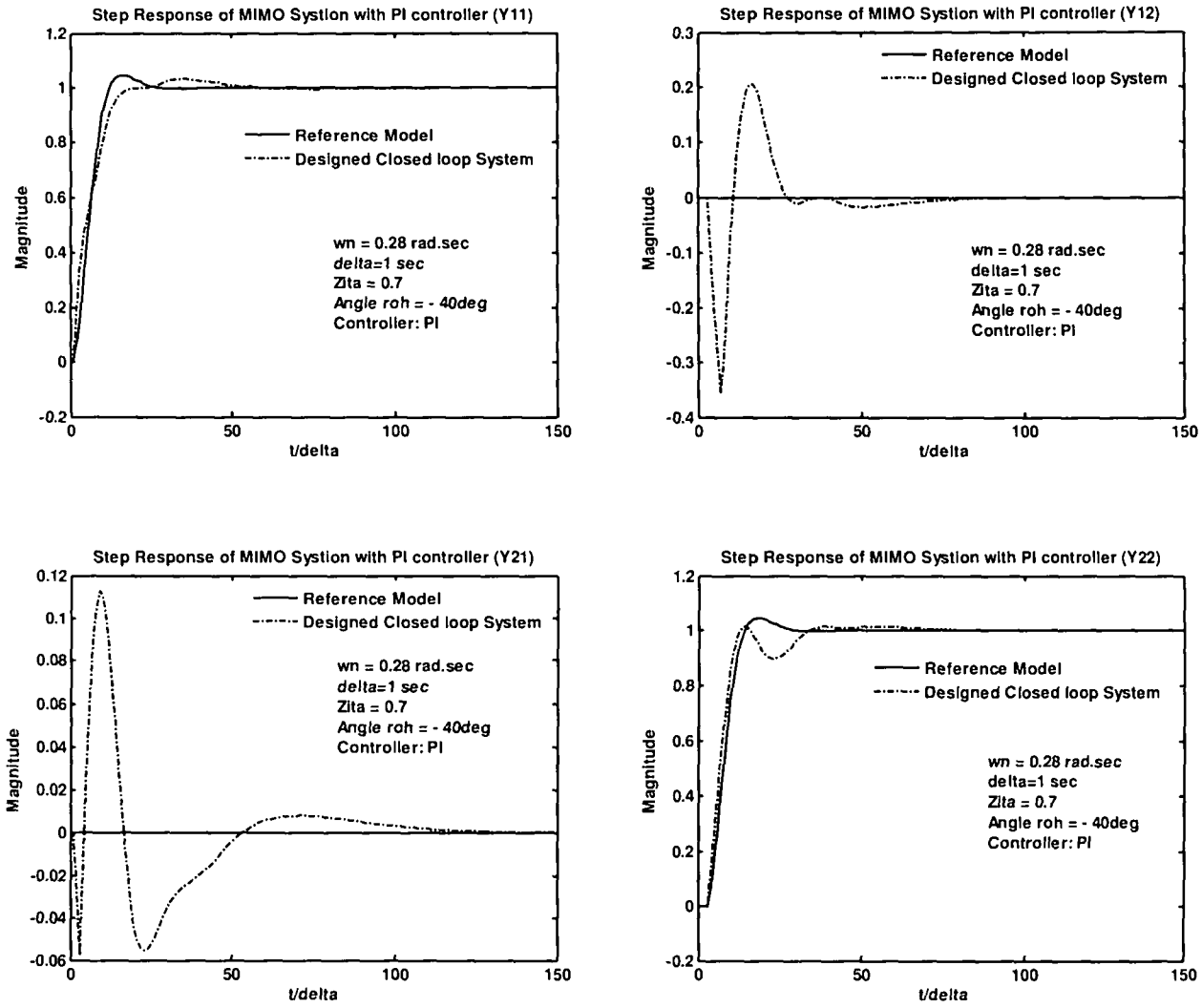

Figure 5.46: Step responses of the reference model and closed loop plant with PI controller using OFF method, output y11,y12,y21,y22, Δ=1sec, ρ=-40°, ω_n=0.28 rad/sec & ξ=0.7

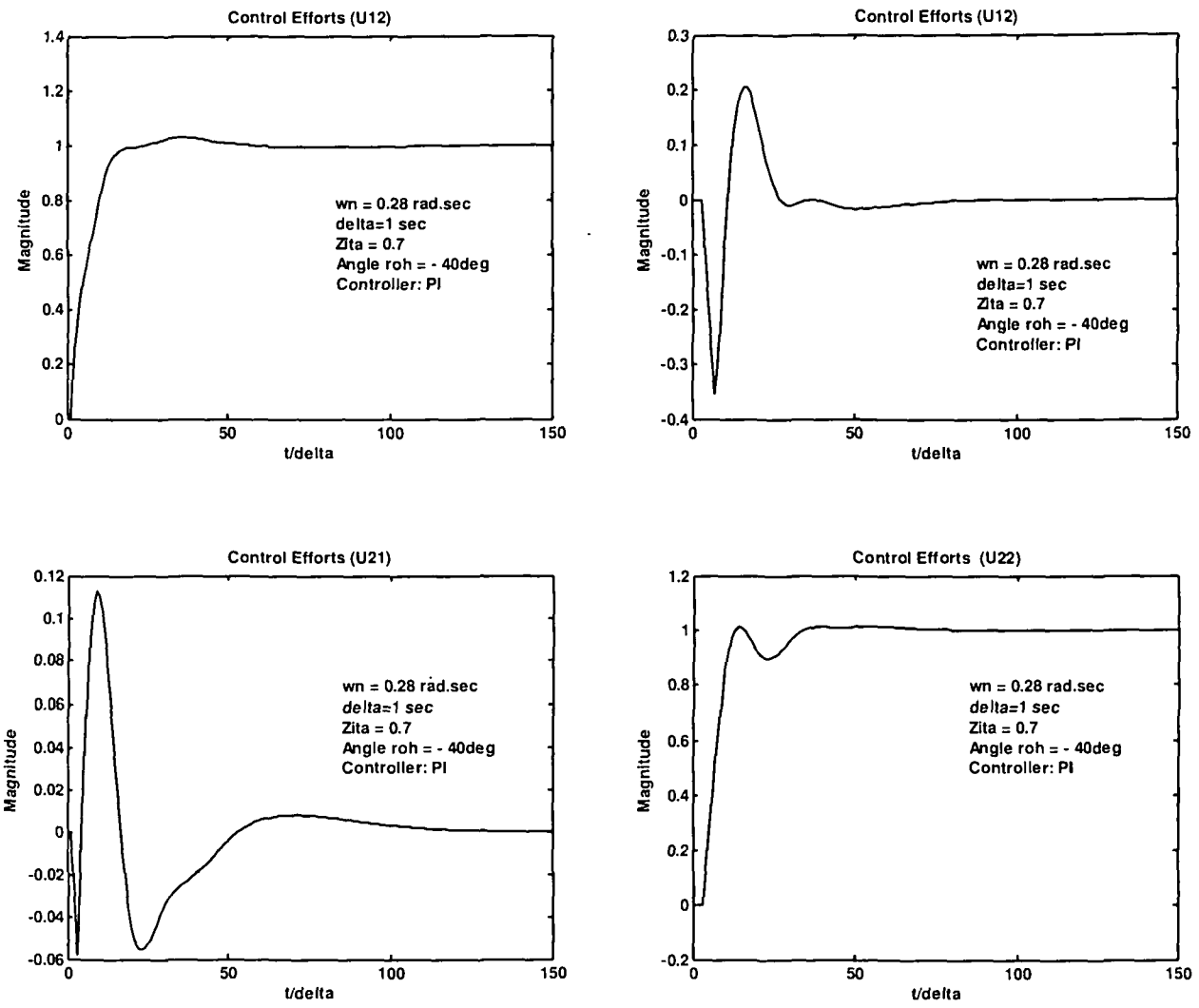

Figure 5.47: Step responses of Control effort using OFF method, u11,u12,u21,u22, Δ = 1sec, ρ = - 40°, ω_n= 0.28 rad/sec & ξ = 0.7

5.2 Conclusion:

Two new methods for designing controllers for systems with time delay have been proposed. The methods use the concept of approximate model matching approach to obtain the parameters of a cascade controller $C_\delta(\gamma)$ in the standard unity-feedback configuration. The design results in a closed-loop step response that closely matches the desired response.

We presented two methods namely the OGDTMs matching and the method of Optimal Frequency Fitting. In these methods we use the concept of matching the Optimal GDTMs and Optimal frequency fitting for obtaining the controller. The use of OGDTM and Optimal Frequency Fitting concepts have thus been effectively extended to processes involving time delay. The important features of the proposed method and the results are the following :

- Only output feedback is used.
- These provide low-order, practically implementable controllers.
- The methods are conceptually elegant and computationally simple, requiring the solutions of sets of linear algebraic equations. The merit of the methods in terms of computational ease becomes even more important when the plant is of high-order.
- The controlled system responses match very closely those of the desired model.
- Responses due to interactions are kept to acceptably low levels.
- The methods are easy to use and give good results.
- On completion of one design-simulation run, the designer's understanding of the possible betterment of system dynamics improves and the available trade off between the desired specifications and controller complexity become more apparent. It may be noted that the main computational work involved in each trial toward an acceptable compromise consists of solving only linear equations to determine the controller parameters and obtaining system responses to a unit step input.
- Implementation does not call for software/hardware modeling of the time-delay term (as in the smith's predictor method).

Chapter 6

Biomedical Digital Filters in Delta Domain:

6.1 Introduction:

Traditional digital signal processing algorithms, developed during the past five decades, employ the technique of the shift operator to represent the dynamics of sampled data systems. However, the shift operator does not overcome the gap between the high sampling rates of widely available digital signal processing chips, and relative slow dynamics of the continuous time processes. In such situations of processing and control data, often in real time at very high speeds, a more suitable mathematical operator is necessary. As discussed in chapter-1, Middleton and Goodwin [7],[10] developed a unified description of continuous time and discrete-time systems. It allows continuous-time results to be obtained as a particular special case of discrete-time ones, by setting the sampling period to zero.

The new approach is based on the introduction of the so-called delta (δ) operator as an alternative to the shift operator. In recent years, the delta operator methodology has been widely accepted as an effective tool for high-speed digital signal processing, and fast sampled data representation.

The delta operator establishes a special rapprochement between analog and discrete dynamic models and allows for investigating the asymptotic behaviour of discrete time models as the sampling period converges to zero. Numerous advantages, for using the delta operator have already been listed in chapter-1. As already discussed, in the shift form, as the sampling rate increases, the poles and zeros cluster around the point (1, j0) in the z-plane and the solution algorithms are better conditioned in delta than in shift form. From then on, the delta operator became more attractive, and interesting links between continuous-time and discrete-time signals and systems analysis had been established [122], [123]. On the other hand, some limitations of the delta domain setting have been also reported, e.g. it is a common opinion that the relevant delta operator based computations become more complicated [123] and sampling zeros are inducted during sampling which is to be taken care of.

The delta operator methodology promoted by Middleton and Goodwin [1] had been tested in a teaching environment at the University of Newcastle, Australia for years. Moreover, this encouraged professor Middleton to write the software and documentation for the Delta Toolbox [124] which can be downloaded from his personal site.

The use of the delta operator in the realizations of digital filters has recently gained interest due to its good finite-word-length performance under fast sampling. Juha Kauraniemi et.al [37] [38] have studied efficient direct form structures and analysed round off noise and found delta structure has the lower quantization noise level as its output. P.Tanelz Harp et.al, have worked on magnitude response optimization of delta operator filters" [32] and an algorithm to test for various symmetries in the magnitude response of two dimensional complex-coefficient delta operator formulated discrete-time systems have been developed by Hari c.Reddy [125]. Markku Eraluoto and Iiro Hartimo [31], [33] have worked on reducing implementation complexity of fast sampled digital IIR filters. The work of Newman et.al [102] on delta operator based IIR digital filter for high performance power electronic inverter applications is worth mentioning. A considerable amount of work has been done in delta operator based digital filters in different field and in continuation we have also tried to contribute our effort by designing digital filters in delta domain to filter out high frequency / low frequency noises as well as 50/60 Hz power line interference from ECG signal.

6.2 Preliminary:

6.2.1 Analog and Digital filter:

The processing of signals is called filtering. When applied to continuous time signals, this processing is called analog filtering and while the applied to discrete time signals, it is known as digital filtering. An analog filter uses analog electronic circuits made up from components such as resistors, capacitors and op-amps to produce the required filtering effect. Such filter circuits are widely used in the applications as noise reduction, video signal enhancement, graphic equalizers in hi-fi systems, and many other areas. There are well-established standard techniques for designing an analog filter circuit for a given requirement. At all stages, the signal being filtered is an electrical voltage or current.

Digital filters are fundamental to digital signal processing. A digital filter uses a digital processor to perform numerical calculations on sampled values of the signal. The processor may be a general-purpose computer such as a PC, or a specialized DSP (Digital Signal Processor) chip.

The analog input signal must first be sampled and digitized using an ADC (analog to digital converter). The resulting binary numbers, representing successive sampled values of the input signal, are transferred to the processor, which carries out numerical calculations on them. These calculations typically involve multiplying the input values by constants and adding the products together. If necessary, the results of these calculations, which now represent sampled values of the filtered signal, are output through a DAC (digital to analog converter) to convert the signal back to analog form. In a digital filter, the signal is represented by a sequence of numbers, rather than a voltage or current.

Digital filters are defined by their impulse response, *h[n],* or the filter output given unit sample impulse input signal. The frequency response of a digital filter can be found by taking the DFT or FFT of the filter impulse response. The frequency response of a filter consists of its magnitude and phase responses. The magnitude response indicates the ratio of a filtered sine wave's output amplitude to its input amplitude. The phase response describes the phase offset or time delay experienced by a sine wave passing through a filter. However the digital filters are often best described in terms of their frequency response i.e. how is a sinusoidal signal of a given frequency affected by the filter.

6.2.2 Advantages of digital filters:

The following list gives some of the main advantages of digital over analog filters.

- A digital filter is *programmable*, i.e. its operation is determined by a program stored in the processor's memory. This means the digital filter can easily be changed without affecting the circuitry (hardware). An analog filter can only be changed by redesigning the filter circuit.
- Digital filters are easily designed, tested and implemented on a general-purpose computer.

- The characteristics of analog filter circuits are subject to drift and are dependent on temperature. Digital filters do not suffer from these problems, and therefore they extremely stable with respect both to time and temperature.
- Digital filters can handle low frequency signals accurately. As the speed of DSP technology continues to increase, digital filters are being applied to high frequency signals in the RF (radio frequency) domain, which in the past was the exclusive preserve of analog technology.
- Digital filters are very much more versatile in their ability to process signals in a variety of ways; this includes the ability of some types of digital filter to adapt to changes in the characteristics of the signal.
- Fast DSP processors can handle complex combinations of filters in parallel or cascade, making the hardware requirements relatively simple and compact in comparison with the equivalent analog circuitry.

6.2.3 Operation of digital filters:

Suppose the signal which is to be digitally filtered is described by the function V = x (t), Where *t* is time. This signal is sampled at time intervals Δ. The sampled value at time $t = k\Delta$ is $x_k = x(k\Delta)$

Thus the digital values transferred from the ADC corresponding to t = 0, Δ, 2Δ, 3Δ, ... to the processor can be represented by the sequence $x_0, x_1, x_2, x_3, \ldots x_n$ and are stored in memory. In this case the sampled values x_{n+1}, x_{n+2} etc. are not available as they haven't happened yet. The digital output from the processor to the DAC consists of the sequence of values $y_0, y_1, y_2, y_3, \ldots, y_n$ In general, the value of y_n is calculated from the values $x_0, x_1, x_2, x_3, \ldots, x_n$. The way in which the *y*'s are calculated from the *x*'s determines the filtering action of the digital filter.

The following are few digital filters and their essential features:

i. Simple gain filter: $y_n = Kx_n$ (K = constant)

   K > 1 makes the filter an amplifier, while 0 < K < 1 makes it an attenuator. K < 0 corresponds to an inverting amplifier.

ii. Pure delay filter: $y_n = x_{n-1}$

The output value at time $t = n\Delta$ is simply the input at time $t = (n-1)\Delta$, i.e. the signal is delayed by time Δ.

iii. Two-term difference filter: $y_n = x_n - x_{n-1}$

The output value at $t = n\Delta$ is equal to the difference between the current input x_n and the previous input x_{n-1}. The output is the change in the input over the most recent sampling interval Δ. The effect of this filter is similar to that of an analog differentiator circuit.

iv. Two-term average filter: $y_n = (x_n + x_{n-1}) / 2$

The output is the average (arithmetic mean) of the current and previous input. This is a simple type of low pass filter as it tends to smooth out high-frequency variations in a signal.

v. Three-term average filter: $y_n = (x_n + x_{n-1} + x_{n-2}) / 3$

This is similar to the previous example, with the average being taken of the current and two previous inputs. As before, x_{-1} and x_{-2} are taken to be zero.

vi. Central difference filter: $y_n = (x_n - x_{n-2}) / 2$

This is similar in its effect to example (3). The output is equal to half the change in the input signal over the previous two sampling intervals:

6.2.4 Order of a digital filter:

The order of a digital filter can be defined as the number of previous inputs stored in the processor memory is used to calculate the current output.

i. zero order filter: $y_n = x_n$ or $y_n = Kx_n$

Here the current output y_n depends only on the current input x_n and not on any previous inputs.

ii. First order filter $y_n = x_{n-1}$ or $y_n = x_n - x_{n-1}$

In a first order filter, one previous sample (x_{n-1}) is required to calculate y_n. Therefore the order of a digital filter may be any positive integer.

All of the digital filter examples given in section 6.2.3 can be written in the following general forms:

Zero order: $y_n = a_0x_n$

First order: $y_n = a_0x_n + a_1x_{n-1}$

Second order: $y_n = a_0x_n + a_1x_{n-1} + a_2x_{n-2}$

Similar expressions can be developed for filters of any order.

6.2.5 Recursive and non-recursive filters:

For all the examples of digital filters discussed so far, the current output (y_n) is calculated solely from the current and previous input values (x_n, x_{n-1}, x_{n-2} ...). These are called as non-recursive filters.

A recursive filter is one which in addition to input values also uses previous output values. The expression for a recursive filter therefore contains not only terms involving the input values (x_n, x_{n-1}, x_{n-2}, ...) but also terms in y_{n-1}, y_{n-2}, ...

Recursive filters require more calculations to be performed, since there are previous output terms in the filter expression as well as input terms. To achieve a given frequency response characteristic using a recursive filter generally requires a much lower order filter, and therefore fewer terms to be evaluated by the processor, than the equivalent non-recursive filter.

6.2.6 FIR and IIR filters:

A non-recursive filter is known as an FIR (Finite Impulse Response) filter, and a recursive filter as an IIR (Infinite Impulse Response) filter. These terms refer to the differing "impulse responses" of the two types of filter. An FIR filter is one whose impulse response is of finite duration. An IIR filter is one whose impulse response (theoretically) continues for ever, because the previous output terms are feed back energy into the filter input and keep it going. But actual impulse responses of nearly all IIR filters reduce virtually to zero in a finite time.

6.2.7 The unit delay operator

The delay operators in z and delta domain are represented by the symbol z^{-1} & γ^{-1}. When applied to a sequence of digital values, this operator gives the previous value in the sequence. It therefore in effect introduces a delay of one sampling interval. The relations between z and δ domain unit delays are shown in Figure 6.1

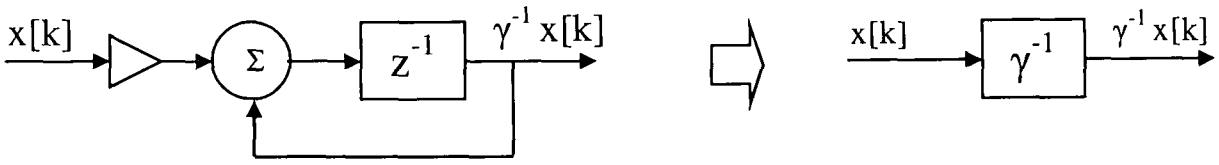

Figure 6.1: Construction of delay in delta domain

6.2.8 Steady State and Transient Response:

Since digital filters are linear systems, a sinusoidal input will produce a sinusoidal output of the same frequency assuming before a signal is applied to the input of a digital filter; the filter's internal state is equal to zero. However, when a sinusoidal signal is first applied to the input of a digital filter, the output initially exhibits a region of transition which is referred to transient response. For FIR filters, this transition region has duration in samples equal to the filter order. But for IIR filters, the length of the transition region is dependent on the filter order and the feedback coefficient values.

Assuming a continued application of the sinusoidal input, the filter will eventually settle into its steady-state region. If the input frequency changes or shows a discontinuity of any sort, another transient region will occur in the filter output. The frequency response of a digital filter is understood to represent its steady-state behaviour.

6.2.9 Signal conversion

The concept of converting a continuous time signal to discrete samples leads to the fact that to represent a continuous time signal can be done by its instantaneous amplitude values taken at periodic points in time. Simply to say, any continuous signal can be reconstructed perfectly with its sampled points without any loss of information as stated in the sampling theorem initially developed by Shannon [126].

The Sampling Theorem states that for band limited signals with maximum frequency f_{max}, the equally spaced sampling frequency fs must be greater than twice of the maximum frequency f_{max}, i.e., $fs > 2 \cdot f_{max}$. The frequency $2.f_{max}$ is called the Nyquist sampling rate and half of this value f_{max}, is sometimes called the Nyquist frequency. For any filter to recover the original signal it must satisfy the condition in sampling theorem, if fs is equal to or less than the twice of the maximum frequency adjacent samples get

overlapped and results to an effect called aliasing also explained as the higher frequencies are reflected in to the lower frequency range.

6.2.10 Shift operator based IIR digital filters

The shift operator q and its associated z-transform are synonymous as the way of implementing IIR digital filters. The application of the shift operator to a given input discrete-time sample x[k] is simply the future sample as in

$$x[k+1] = q\,x[k]$$

or equivalently $$x[k+1] = z\,x[k] \qquad (6.1)$$

If initial conditions are ignored, the shift operator q can simply be replaced by 'z' [117]. In a practical sense this is obviously not causal, but the inverse shift operator can be applied as a causal alternative

$$z^{-1}[k] = x[k-1] \qquad (6.2)$$

Any linear discrete-time system (2nd order in this case) can be described by a linear difference equation [122]

$$y[k] + a_1 y[k-1] + a_2[k-2] = b_0 x[k] + b_1 x[k-1] + b_2 x[k-2] \qquad (6.3)$$

It is to be noted that only a second order transfer function has been considered, as higher order transfer functions are preferably implemented as a cascade of first and second order functions, to minimize rounding and truncation effects [123]. Applying (6.2) results in the general form for the output of a second order infinite impulse response (IIR) filter, of

$$y[k] = b_0 x[k] + b_1 z^{-1} x[k] + b_2 z^{-2} x[k] - a_1 z^{-1} y[k] + a_2 z^{-2}[k] \qquad (6.4)$$

Finally, rearrangement of (6.4) provides the canonical form of the shift-based IIR filter, $H_q(z)$, which gives an output of Y(z) when applied to an input sequence X(z)

$$H_q(z) = \frac{b_0 + b_1 z^{-1} + b_2 z^{-2}}{1 + a_1 z^{-1} + a_2 z^{-2}} \qquad (6.5)$$

With the above structure if we have the knowledge of the filter coefficients, a_i & b_i , the shift-based 2nd order IIR filter can easily be realized and implemented. There are many methods for acquisition of these coefficients [122], the bilinear (*Tustin*)

transformation is the more popular choice, as it will always provide a stable digital filter as long as the analog filter is stable. This method involves the substitution of

$$s = \frac{2}{T}\frac{(z-1)}{(z+1)} \tag{6.6}$$

into the desired s-domain transfer function, and rearranging the result into the form of (6.5) to obtain the associated coefficient values. The transformation from the continuous Laplace s-domain into the discrete-time z-domain, maps the infinite frequency range [0, ∞] to the finite range [0, π] [127],[128]. This mapping is nonlinear and the frequency axis is compressed, with the effect becoming particularly significant for higher sampling frequencies. The importance of this compression for shift-based IIR filters is that as the sampling frequency increases, the poles of the filter converge toward 1 on the z-plane. This clustering makes very small changes in the pole locations (i.e., because of coefficient rounding) cause very large deviations from the intended transfer function.

To illustrate this effect let us consider a 3rd order butterworth filter [129] whose transfer function in s-domain is given as:

$$H_c(s) = \frac{1}{(s+1)(s^2+s+1)} \tag{6.7}$$

The transfer function (6.7) is discretized for various sampling time Δ = 1 sec to 0.01 sec using bilinear transformation and the pole zero plot in z-plane is shown in Figure 6.2. For stability, the poles must lie within the unit circle on the z-plane whereas the zeros can lie anywhere and therefore as the sampling time decreases or sampling frequency increases, the poles also move closer to the point [1, 0] as shown in Figure. 6.2.

6.2.11 Delta operator based IIR digital filters:

The delta operator was named and actively promoted in digital control by Middleton and Goodwin in 1986 [1],[7],[122]. However, the technique was known in the numerical analysis field some decades before as the "difference operator." A complete history of the origins of the delta operator is contained in [7]. For discrete systems the delta operator is a Euler approximation to a derivative [122]. The definition of delta operator has already been given in equation (1.19 – 1.21).

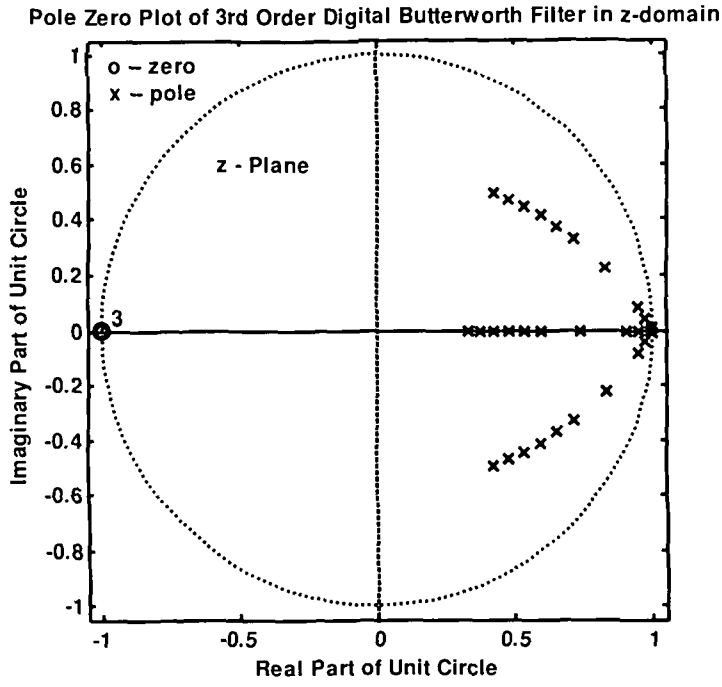

Figure 6.2: Pole clustering of 3rd order butterworth IIR digital filter in z-domain (Sampling Time Δ = 1 sec to 0.01 sec)

Just as the continuous time derivative operator d/dt has a s-domain equivalent "s " (ignoring initial conditions) using Laplace transforms, the *Delta transform* can be used to convert the discrete time operator to its equivalent; " γ". From [1] the Delta transform can be derived from the Laplace transform to illustrate the relationship between the two, and is summarized as follows.

If the Laplace transformation (single sided) formula

$$F(s) = L\{f(t)\} = \int_0^\infty e^{-st} f(t)\,dt \qquad (6.8)$$

is discretized by the substitution of kΔ, where Δ is sampling the time, for time and an infinite summation for the integral, we obtain

$$F'(s) = \sum_{k=0}^{\infty} \Delta e^{-sk\Delta} f(k\Delta) \qquad (6.9)$$

With substitution of $e^{s\Delta} = 1 + \gamma\Delta$ the result is the single sided *Delta transform*

$$F_\delta(\gamma) = D\{f[k]\} = \sum_{k=0}^{\infty} \Delta(1+\Delta\gamma)^{-k} f[k] \qquad (6.10)$$

Equation (6.10) can now be used to find the Delta transform of the derivative approximation [1].

$$D\{\delta f[k]\} = \gamma F_\delta(\gamma) - (1+\Delta\gamma) f[0] \qquad (6.11)$$

Comparison of (6.11) to the Laplace transform of the derivative operator in (6.12) shows that if Δ=0 then "γ" becomes interchangeable with "s "

$$L\left\{\frac{d}{dt} f(t)\right\} = sF(s) - f(0) \qquad (6.12)$$

Therefore, the delta operator has the particular property that as the sample time, Δ, approaches zero, it converges toward its continuous counterpart, the Laplace transform variable. In fact, it can be said that the continuous domain is actually a subset of the discrete-time delta representation. This property gives the delta operator its superior performance at high sample rates compared to the shift operator which does not converge. It is to be noted, e^{Δ} is a time shift of Δ, and is equivalent to z. Therefore, from the same substitution used to create (6.10), the shift and delta operators are found to be related by

$$z = 1 + \Delta\gamma \qquad (6.13)$$

It has been already discussed in details in chapter-1 with the mapping s, z and delta plane and it has been shown that the delta operator is associated with the γ-transform in exactly the same way that the shift operator q is associated with the z-transform, so it follows from (6.13) that

$$q = 1 + \delta\Delta \qquad (6.14)$$

This illustrates how the forward shift is made up of the present sample plus the difference (which is the derivative, multiplied by the time step Δ). We discretize the transfer function given in equation (6.7) for various sampling time Δ = 1 sec to 0.01 sec to find the transfer function in delta domain, and the pole-zero plot in delta domain is shown in figure 6.2. For stability, the poles must lie within the sampling circle on the γ-plane. In the case of delta parameterization it is clear from the figure 6.2 that on decreasing the sampling time or increasing sampling frequency, the poles remain with in the sampling circle however the zeros move towards left of the sampling circle as shown in Figure. 6.3.

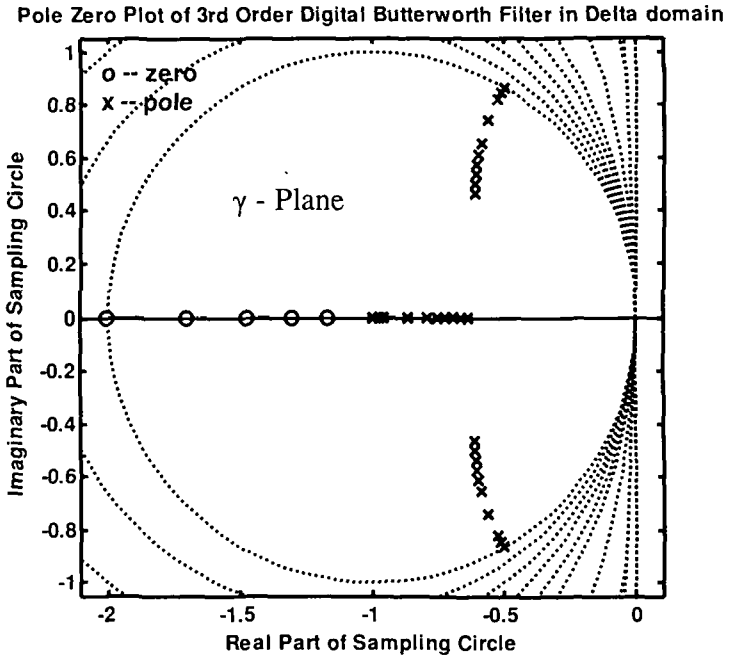

Figure 6.3: Pole-zero plot of 3rd order butterworth IIR digital filter in delta domain (Sampling Time Δ = 1 sec to 0.01 sec)

For comparison the location of poles and zeros for different sampling time are shown in table 6.1

For discrete implementation of analog prototypes using delta-operator based IIR digital filters there are two possibilities, first we define an analog prototype transfer function in s-domain. For convenience we consider a second order transfer function with coefficients as given in equation (6.15).

$$H_c(s) = \frac{\beta_0' s^2 + \beta_1' s + \beta_2'}{s^2 + \alpha_1' s + \alpha_2'} \qquad (6.15)$$

Then Equation (6.16) can be formed where the coefficients are equal to those in (6.15) for, Δ = 0, and diverge as Δ increases. The coefficients α_i and β_i defined in equation (6.16) could be found directly by applying the delta transform eqn. (6.10) to the sampled prototype system *h[n]* shown in equation (6.15).

$$H_\delta(\gamma) = \frac{\beta_0 \gamma^2 + \beta_1 \gamma + \beta_2}{\gamma^2 + \alpha_1 \gamma + \alpha_2} \qquad (6.16)$$

Table 6.1

Poles & zeros of 3rd order Butterworth digital filter in z and δ domain.

Sampling time Δ in	Poles & zeros in z-domain		Poles & zeros in delta domain	
	Poles	Zeros	Poles	Zeros
1 sec	0.4286 + 0.4949i 0.4286 - 0.4949i 0.3333	-1.0000 + 0.0000i -1.0000 - 0.0000i -1.0000	-0.6071 + 0.4620i -0.6071 - 0.4620i -0.6321	-3.1951 -1.1676 --
0.9 sec	0.4826 + 0.4717i 0.4826 - 0.4717i 0.3793	-1.0000 + 0.0000i -1.0000 - 0.0000i -1.0000	-0.6072 + 0.4980i -0.6072 - 0.4980i -0.6594	-3.6909 -1.3057
0.8 sec	0.5385 + 0.4441i 0.5385 - 0.4441i 0.4286	-1.0000 + 0.0000i -1.0000 - 0.0000i -1.0000	-0.6053 + 0.5352i -0.6053 - 0.5352i -0.6883	-4.3175 -1.4789
0.7 sec	0.5959 + 0.4117i 0.5959 - 0.4117i 0.4815	-1.0000 + 0.0000i -1.0000 - 0.0000i -1.0000	-0.6013 + 0.5736i -0.6013 - 0.5736i -0.7192	-5.1312 -1.7023
0.6 sec	0.6547 + 0.3738i 0.6547 - 0.3738i 0.5385	-1.0000 + 0.0000i -1.0000 - 0.0000i -1.0000	-0.5949 + 0.6131i -0.5949 - 0.6131i -0.7520	-6.2259 -2.0010
0.5 sec	0.7143 + 0.3299i 0.7143 - 0.3299i 0.6000	-1.0000 + 0.0000i -1.0000 - 0.0000i -1.0000	-0.5862 + 0.6536i -0.5862 - 0.6536i -0.7869	-7.7706 -2.4204
0.3 sec	0.8337 + 0.2216i 0.8337 - 0.2216i 0.7391	-1.0001 + 0.0001i -1.0001 - 0.0001i -0.9999	-0.5606 + 0.7370i -0.5606 - 0.7370i -0.8639	-14.0127 -4.1041
0.1 sec	0.9477 + 0.0823i 0.9477 - 0.0823i 0.9048	-1.0000 + 0.0000i -1.0000 - 0.0000i -0.9996	-0.9516 -0.5234 + 0.8228i -0.5234 -0.8228i	-45.4901 -12.5495
0.05 sec	0.9744 + 0.0422i 0.9744 - 0.0422i 0.9512	-1.0005 + 0.0008i -1.0005 - 0.0008i -0.9991	-0.9754 -0.5121 + 0.8444i -0.5121 - 0.8444i	-92.7929 -25.2270
0.01 sec	0.9950 + 0.0086i 0.9950 - 0.0086i 0.9900	-1.0016 + 0.0027i -1.0016 - 0.0027i -0.9969	-0.9950 -0.5025 + 0.8617i -0.5025 - 0.8617i	-471.3426 -126.6614
0.001 sec	0.9995 + 0.0009i 0.9995 - 0.0009i 0.9990	-1.0133 + 0.0236i -1.0133 - 0.0236i -0.9733	-0.9995 -0.5002 + 0.8656i -0.5002 - 0.8656i	-4.73020e+003 -1.26780e+003
0.0001 sec	1.0000 + 0.0001i 1.0000 - 0.0001i 0.9999	-1.3918 -0.8103 + 0.2613i -0.8103 - 0.2613i	-1.0000 -0.5000 + 0.8660i -0.5000 - 0.8660i	-4.73190e+004 -1.26790e+004

But this is a less straightforward approach than desired, The second possible method is to use the relationship between the shift and delta domains in (6.12) & (6.13) to utilize the coefficients developed using the bilinear transformation. However, it is an implementation method and not the design method that provides the delta its performance advantages over the shift at high sample rates [122]. Applying equation (6.5) and substituting in (6.17) we get simple derivation of the delta filter coefficients.

$$H_\delta(\gamma) = H_q(z)\Big|_{z=1+\gamma\Delta} \tag{6.17}$$

For the delta operator to be useful in digital filter applications, a causal form must also be available. This is the inverse delta operator i.e delay element in delta domain is equivalent to

$$\delta^{-1} = \frac{\Delta q^{-1}}{1 - q^{-1}}$$

or equivalent to

$$\gamma^{-1} = \frac{\Delta z^{-1}}{1 - z^{-1}} \tag{6.18}$$

The construction of equation (6.18) is shown in figure 6.1.

The 2nd, 3rd and 4th order digital filters with delay element in z domain are represented as

$$H_q(z) = \frac{b_0 + b_1 z^{-1} + b_2 z^{-2}}{1 + a_1 z^{-1} + a_2 z^{-2}} \tag{6.19}$$

$$H_q(z) = \frac{b_0 + b_1 z^{-1} + b_2 z^{-2} + b_3 z^{-3}}{1 + a_1 z^{-1} + a_2 z^{-2} + a_3 z^{-3}} \tag{6.20}$$

$$H_q(z) = \frac{b_0 + b_1 z^{-1} + b_2 z^{-2} + b_3 z^{-3} + b_4 z^{-4}}{1 + a_1 z^{-1} + a_2 z^{-2} + a_3 z^{-3} + a_4 z^{-4}} \tag{6.21}$$

By using equation (6.18), corresponding transfer functions of (6.19), (6.20) & (6.21) in delta domain are given as

$$H_\delta(\gamma) = \frac{\beta_0 + \beta_1 \gamma^{-1} + \beta_2 \gamma^{-2}}{1 + \alpha_1 \gamma^{-1} + \alpha_2 \gamma^{-2}} \tag{6.22}$$

$$H_\delta(\gamma) = \frac{\beta_0 + \beta_1 \gamma^{-1} + \beta_2 \gamma^{-2} + \beta_3 \gamma^{-3}}{1 + \alpha_1 \gamma^{-1} + \alpha_2 \gamma^{-2} + \alpha_3 \gamma^{-3}} \tag{6.23}$$

$$H_\delta(\gamma) = \frac{\beta_0 + \beta_1 \gamma^{-1} + \beta_2 \gamma^{-2} + \beta_3 \gamma^{-3} + \beta_4 \gamma^{-4}}{1 + \alpha_1 \gamma^{-1} + \alpha_2 \gamma^{-2} + \alpha_3 \gamma^{-3} + \beta_4 \gamma^{-4}} \tag{6.24}$$

The coefficients α_i & β_i of (6.22), (6.23) and (6.24) in terms of a_i and b_i are given in table 6.2, 6.3 & 6.4 respectively.

Table 6.2

Conversion table of 2nd order Delta & Shift coefficients	
$\beta_0 = b_0$	$\alpha_0 = 1$
$\beta_1 = \frac{2b_0 + b_1}{\Delta}$	$\alpha_1 = \frac{2 + a_1}{\Delta}$
$\beta_2 = \frac{b_0 + b_1 + b_2}{\Delta^2}$	$\alpha_2 = \frac{1 + a_1 + a_2}{\Delta^2}$

Table 6.3

Conversion table of 3rd order Delta & Shift coefficients	
$\beta_0 = b_0$	$\alpha_0 = 1$
$\beta_1 = \frac{3b_0 + b_1}{\Delta}$	$\alpha_1 = \frac{3 + a_1}{\Delta}$
$\beta_2 = \frac{3b_0 + 2b_1 + b_2}{\Delta^2}$	$\alpha_2 = \frac{3 + 2a_1 + a_2}{\Delta^2}$
$\beta_3 = \frac{b_0 + b_1 + b_2 + b_3}{\Delta^3}$	$\alpha_3 = \frac{1 + a_1 + a_2 + a_3}{\Delta^3}$

Table 6.4

Conversion table of 4th order Delta & Shift coefficients	
$\beta_0 = b_0$	$\alpha_0 = 1$
$\beta_1 = \frac{4b_0 + b_1}{\Delta}$	$\alpha_1 = \frac{4 + a_1}{\Delta}$
$\beta_2 = \frac{6b_0 + 3b_1 + b_2}{\Delta^2}$	$\alpha_2 = \frac{6 + 3a_1 + a_2}{\Delta^2}$
$\beta_3 = \frac{4b_0 + 3b_1 + 2b_2 + b_3}{\Delta^3}$	$\alpha_3 = \frac{4 + 3a_1 + 2a_2 + a_3}{\Delta^3}$
$\beta_4 = \frac{b_0 + b_1 + b_2 + b_3 + b_4}{\Delta^4}$	$\alpha_4 = \frac{1 + a_1 + a_2 + a_3 + a_4}{\Delta^4}$

From this the IIR canonical form of the delta domain transfer functions given in (6.22) to (6.24) is found which has the same form as its shift counterpart in (6.19) to (6.21). Therefore implementation of delta operator based IIR filters can be performed in the same manner as for the shift, except with γ^{-1} replacing the z^{-1}, and different coefficients.

The discrete stability regions for the s, z and δ domain has already been shown in figure 1.2 in chapter-1. The stability region of shift implementation is fixed, causing the clustering as shown in figure 6.2 however it can be seen that as Δ approaches zero, the stability region for the delta implementation will once again grow to approach that of the laplace domain or s-domain i.e. whole left half plane.

For shift-based filters, the spread of the coefficient values are fixed, and if this spread is too large then the coefficients reach a point where they cannot be implemented on a 16 bit fixed-point system. However for delta operator based digital filters, despite the variable being initially defined as the sample period, is free to be varied to optimize the numerical properties of the design [45]. Therefore, since the coefficients are a function as given in Table 6.2 to 6.4, the spread of the coefficients can be optimized to allow lower percentage rounding errors. In general, the choice of Δ determines the coefficient rounding and sensitivity, as well as the maximum variable size of the delta filter [42].

IIR digital filters can be implemented using either direct form I (DFI) or direct form II (DFII) structures, or their transposed versions DFIt and DFIIt as shown in Figure (6.4). The DFI form can be seen to be simply a diagrammatic version of (6.4), illustrating the order in which the additions and subtractions should take place. The DFIt, DFII, and DFIIt forms are rearrangements developed to achieve different numerical quantization responses.

While most shift-based digital filters can be implemented with any of these forms, this is not necessarily the case for fixed-point delta-based digital filters [44]. For the DFI form [Fig. 6.4(a)] the unstable pole at of the formula in (6.18) is not cancelled prior to the inverse delta operation, and it is therefore unstable. This causes the output of the operation to overflow. For the DFIt form Fig. 6.4(b) the unstable poles of (6.8) are cancelled prior to the inverse, but require double precision to function properly [38].

Mostly, these problems are avoided by use of the DFII and DFIIt forms Fig. 6.4(c) and (d). [42]

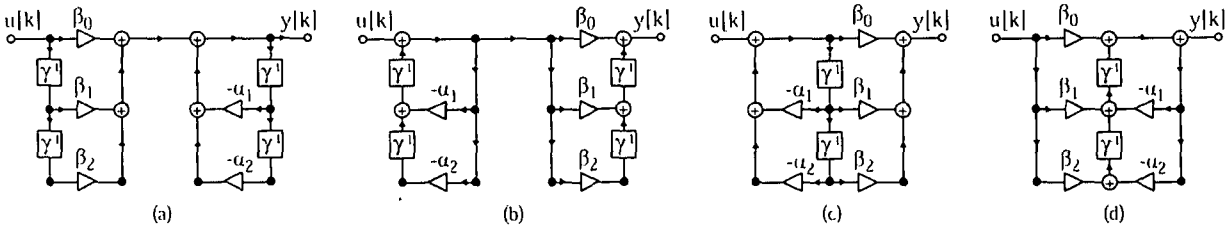

Figure 6.4: Direct form digital filter implementation structures:(a) DFI (b) DFIt (c) DFII (d) DFIIt

In this chapter, few biomedical time and frequency domain digital filters in delta domain is presented to remove low frequency, high frequency noises and 50/60 Hz power line interference in ECG signal.

6.3 Biomedical signals

6.3.1 The Nature of Biomedical signals :

The human body includes the nervous system, the cardiovascular system, and the muscular skeletal system etc. Each system is made up of several sub-systems that carry on many physiological processes. For example, the cardiac system performs the important task of rhythmic pumping of blood throughout the body to facilitate the delivery of nutrients, as well as pumping blood through the pulmonary system for oxygenation of the blood itself. [105]

Physiological processes are complex phenomena, including nervous or hormonal stimulation and control; inputs and outputs that could be the form of physical material, neurotransmitters, or information and action that could be mechanical, electrical, or biochemical. Most physiological processes are accompanied by or manifest themselves as signals that reflect their nature and activities. Such signals could be of many types, including biochemical in the form of hormones and neuro transmitters, electrical in the form of potential or current and physical in the form of pressure or temperature.

Disease or defects in a biological system cause alterations in its normal physiological processes, leading to pathological processes that affect the performance, health and general well being of the system. A pathological process is typically associated with signals that are different in some respects from the corresponding normal signals. If we possess a good understanding of a system of interest, it becomes possible to observe the corresponding signals and assess the state of the system. The task is not very difficult when the signal is simple and appears at the other surface of the body. For example, most infections cause a rise in the temperature of the body, which may be sensed very easily. Objectives or quantitative measurement of temperature requires an instrument, such as a simple thermometer. Electrical activity of the hearth is an important physiological signal.

6.3.2 The electrocardiogram (ECG):

The ECG is the electrical manifestation of the contractile activity of the heart, and can be recorded fairly easily with surface electrodes on the limbs or chest. The ECG is perhaps the most commonly known, recognized and used biomedical signal. The rhythm of the heart in terms of beats per minutes (bpm) may be easily estimated by counting the readily identifiable waves. More important is the fact the ECG waveshape is altered by cardiovascular disease and abnormalities such as myocardial ischemia and infarction, ventricular hypertrophy and condition problems.

6.3.2.1 Generation of ECG:

The heart is a four chambered pump with two atria for collection of blood and two ventricles for pumping out of blood. Figure 6.4 shows a schematic representation of the our chambers and the major vessels connecting to the heart. The resting or filling phase of a cardiac chamber is called diastole; the contracting or pumping phase is called systole. The right atrium (RA) collects impure blood from the superior and inferior vena cavae. During atrial contraction, blood is passed from the right atrium to the right ventricle (RV) through the tricuspid valve. During ventricular systole, the impure blood in the right ventricle is pumped out through the pulmonary valve to the lungs for purification (oxygenation).

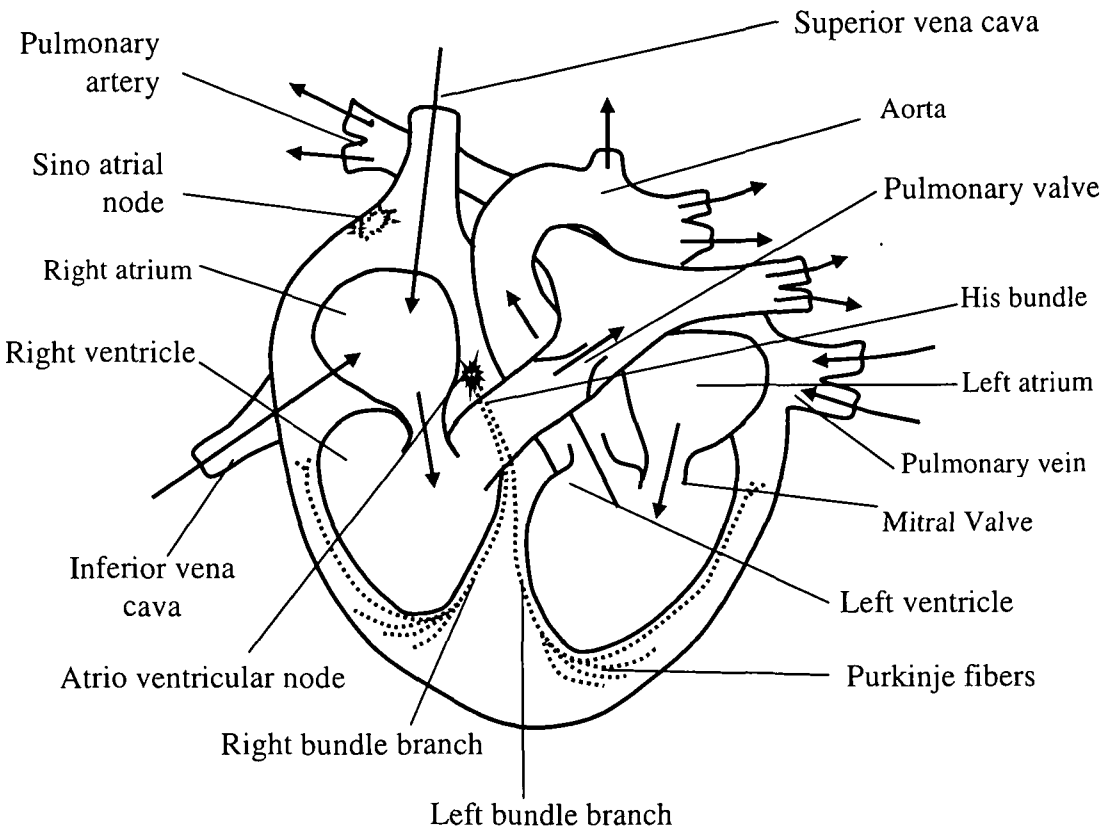

Figure 6.4: Schematic representation of the chambers, valves, vessels and conduction system of the heart

The left atrium (LA) receives purified blood from the lungs, which is passed on during atrial contraction to the left ventricle (LV) via the mitral valve. The left ventricle is the largest and most important cardiac chamber. The left ventricle contracts the strongest among the cardiac chambers. As it has to pump out the oxygenated blood through the aortic valve and the aorta against the pressure of the rest of the vascular system of the body. Due to the higher level of importance of contraction of the ventricles, the terms systole and diastole are applied to the ventricles by default.

The heart rate (HR) or cardiac rhythm is controlled by specialized pacemaker cells that form the sino-atrial (SA) node located at the junction of the superior vena cava and the right atrium [125]. The firing rate of the SA node is controlled by impulses from the autonomous and central nervous systems leading to the delivery of the neurotransmitters acetylcholine or epinephrine. The normal (resting) heart rate is about

70 bpm. The heart rate is lower during sleep, but abnormally low heart rates below 60 bpm during activity could indicate a disorder called *bradycardia.* The instantaneous heart rate could reach values as high as 200 bpm during vigorous exercise or athletic activity: a high resting heart rate could be due to illness, disease or cardiac abnormalities and is termed *tachycardia.*

The coordinated electrical events and a specialized conduction system intrinsic and unique to the heart play major roles in the rhythmic contractile activity of the heart. The SA mode is the basic, natural cardiac pacemaker that triggers its own train of action potentials. The action potential of the SA node propagates through the rest of the heart, causing a particular pattern of excitation and contraction The sequence of events and waves in a cardiac cycle is as follows [130]:

1. The SA node fires.
2. Electrical activity is propagated through the atrial musculature at comparatively low rates, causing slow moving depolarization (contraction) of the atria. This results in the P wave in the ECG as shown in Figure 6.5 (a) & (b) . Due to the slow contraction of the atria and their small size, the P wave is a slow, low amplitude wave, with an amplitude of about 0.1 – 0.2 mV and a duration of about 60–80 ms.
3. The excitation wave faces a propagation delay at the atrio ventricular (AV) node, which results in a normally iso-electric segment of about 60 - 80 ms after the P wave in the ECG. Known as the PQ segment. The pause assists in the completion of the transfer of blood from the atria to the ventricles.
4. The His bundle, the bundles branches, and the Purkinje system of specialized conduction fibres propagate the stimulus to the ventricles at a high rate.
5. The wave of stimulus spreads rapidly from the apex of the heart upwards, causing rapid depolarization (contraction) of the ventricles. This results in the QRS wave of the ECG. A sharp biphasic or triphasic wave of about 1 mV amplitude and 80 ms duration as shown in figure 6.5.
6. Ventricular muscle cells possess a relatively long action potential duration of 300–350 ms. The plateau portion of the action potential causes a normally iso-electric segment of about 100 – 120 ms after the QRS. Known as the ST Segment.

7. Re-polarization (relaxation) of the ventricles causes the slow T wave, with an amplitude of 0.1 – 0.3 mV and duration of 120 – 160 ms as shown in the figure 6.4

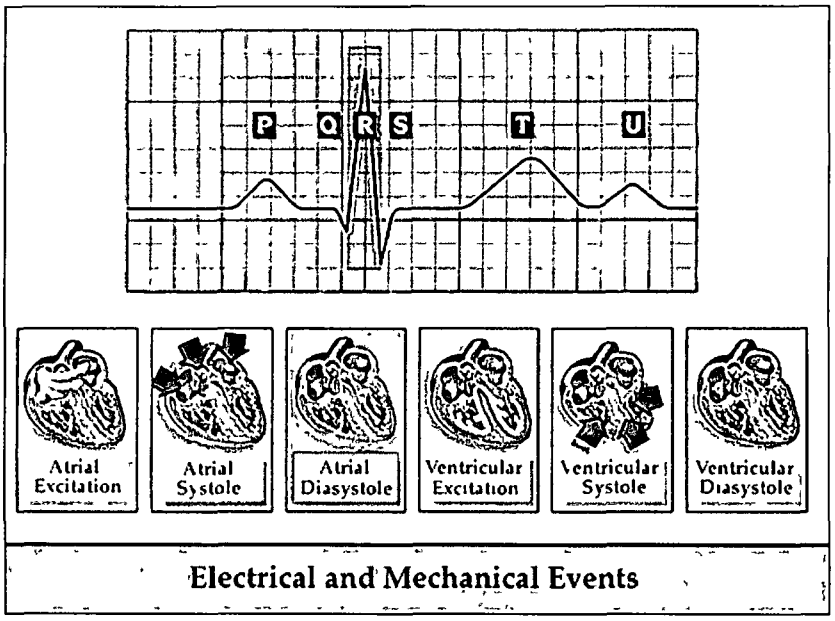

Figure 6.5(a): A typical QRS wave of ECG signal

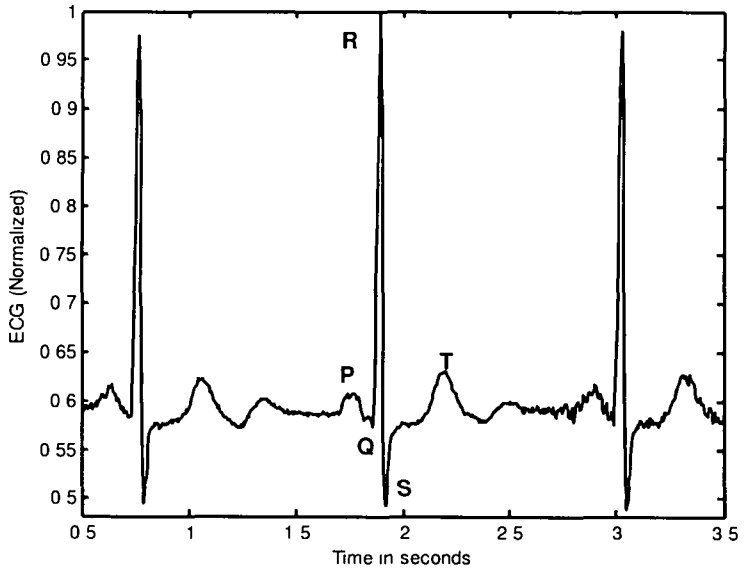

Figure 6.5(b): A typical QRS wave of ECG signal

Any disturbance in the regular rhythmic activity of the heart is termed arrhythmia. Cardiac arrhythmia may be caused by irregular firing patterns from the SA node, or by abnormal and additional pacing activity from other parts of the hearts. Many parts of the heart possess inherent rhythmicity and pacemaker properties: for examples, the SA node, the AV node, the Purkinje fibres, artial tissue and ventricular tissue. If the SA node is depressed or inactive, any one of the above tissue may take over the role of the pacemaker or introduce ectopic beats. Different types of abnormal rhythm (arrhythmia) result from variations in the site and frequency of impulse formation. Premature ventricular contractions (PVCs) caused by ectopic foci on the ventricles upset the regular rhythm and may lead to ventricular dissociation and fibrillation i.e a state of disorganized contraction of the ventricles independents of the artria, resulting in no effective pumping of blood and possibly death. The waveshapes of PVCs are usually very different conduction paths of the ectopic impulses and the associated abnormal contraction events. Figure 6.6 shows ventricular conduction.

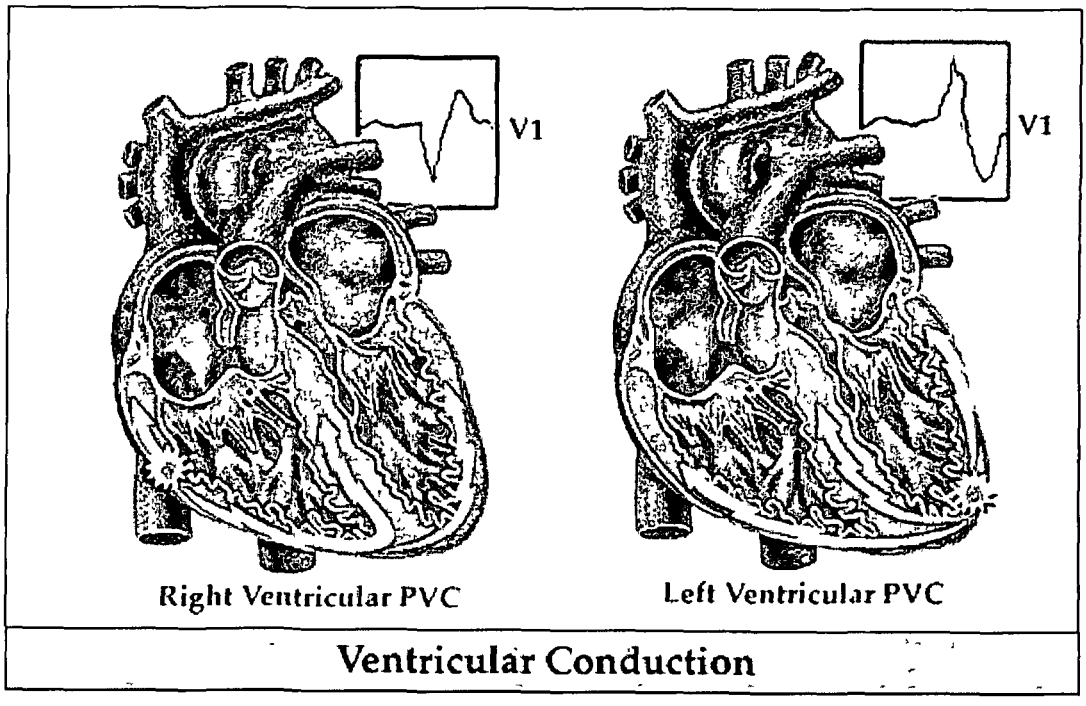

Figure 6.6: Ventricular conduction

6.3.2.2. ECG Signal acquisition:

In clinical practices, the standard 12 channel ECG is obtained using four limbs leads and chest leads in six position [104],[105],[130]. The right leg is used to place the reference electrode. The left arms, right arm, and left leg are used to get leads I, II and III. A combined reference known as Wilson's central terminal is formed by combining the left arm, right arm and left leg leads, and is used as the reference for chest leads. The augmented limb (aV) leads known as aVR (for right arm), aVL (for left arm), and aVF (for left foot) are obtained by using the exploring electrode on the limb indicated by the leads name, with the references being Wilson's central terminal without the exploring limbs lead. Fig. 6.7 shows the directions of the axes formed by the six limb leads. The hypothetical equilateral triangle formed by leads I, II and III is known as Einthoven's triangle. The center of the triangle represents Wilson's central terminal. Schematically, the heart is assumed to be placed at the center of the triangle. The six leads measure projections of the three dimensional (3D) cardiac electrical vector onto the axes illustrated in Fig 6.7 The six axes sample the 0^0 – 180^0 range in steps of approximately 30^0 . The projections facilitate viewing and analysis of the electrical activity of the heart and from different perspective in the frontal plane.

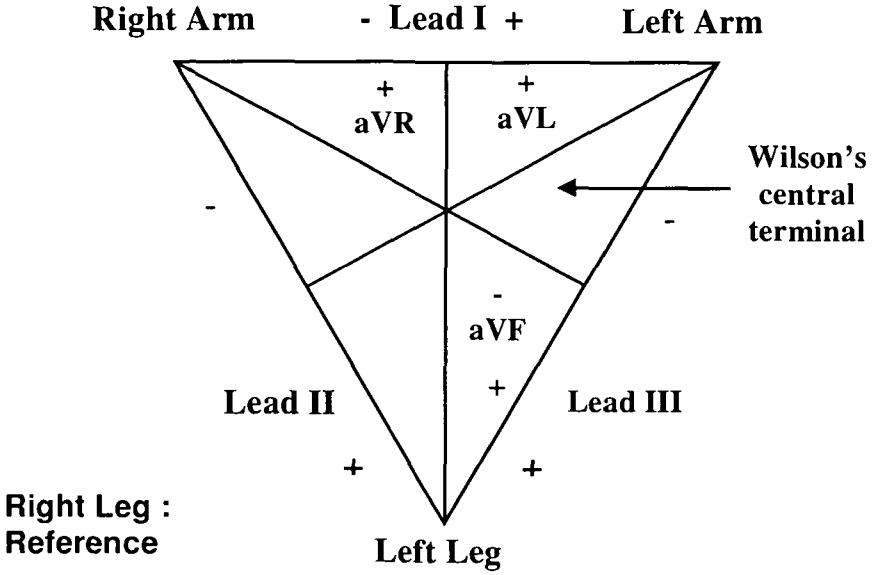

Figure 6.7: Einthoven's triangle and the axes of the six ECG leads formed by using four limb leads.

The six chest leads V1 to V6 are obtained from six standardized positions on the chest [125] with Wilson's central terminal as the reference. The positions for placement of the chest leads are indicated in figure 6.8. The V1 & V2 leads are placed at the fourth intercostals space just to the right and left of the sternum respectively. V4 is recorded at the fifth intercostals space at the midclavicular line. The V3 lead is placed half way between the V2 & V4 leads. The V5 and V6 leads are located at the same level as the V4 lead, but at the anterior axillary line and the midaxillary line respectively. The six chest leads permit viewing the cardiac electrical vector from different orientations I a cross sectional plane i.e. V5 and V6 most sensitive to left ventricular activity, V3 and V4 depicts septal activity best, V1 and V2 reflect well activity in the right half of the heart.

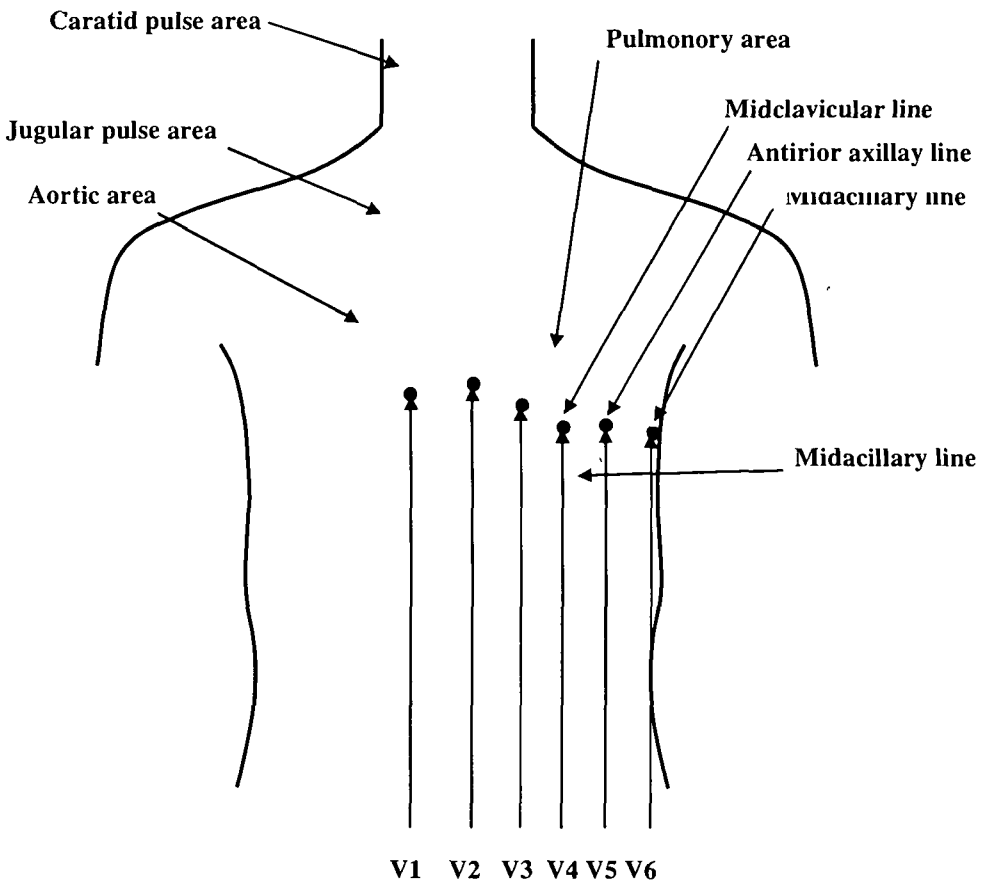

Figure 6.8: Positions for placement of the chest leads V1 – V6 for acquisition of ECG

Some of the important features of the standard clinical ECG are:

- A rectangular calibration pulse of 1 mV amplitude and 200 ms duration is applied to produce a pulse of 1 cm height on the paper plot.
- The paper speed used is 25 mm/s, resulting in a graphical scale of 0.04 s/mm or 40 ms/mm. The calibration pulse width will then be 5 mm.
- The ECG signal peak value is normally about 1 mV.
- The amplifier gain used is 1,000.
- Clinical ECG is usually filtered to a bandwidth of about 0.05 – 100 Hz, with a recommended sampling rate of 500 Hz for diagnostic ECG. Distortions in the shape of the calibration pulse may indicate improper filter settings or a poor signal acquisition system.
- ECG for heart rate monitoring could use a reduced bandwidth 0.05 – 500 Hz.

6.3.3 Filtering for removal of artifacts:

Most biomedical signals appear as weak signals in an environment that is teeming with many other signals of various origins. Any signal other than that of interest could be termed as an interference, artifact or simply noise. The source of noise could be physiological, the instrumentation used, or the environment of the experiment. The problems caused by artifacts in biomedical signals are vast in scope and variety; their potential for degrading the performance of the most sophisticated signal processing algorithms is high.

Our environment is full of stray EM waves, both natural and man-made. EM waves broadcast by radio and television (TV) stations and those radiated by florescent lighting devices, computer monitors, and other systems used in the laboratory or work environment are picked up the cables, devices and connectors. The 50 Hz or 60 Hz power supply waveform is notorious for the may ways in which it can get mixed with and corrupt the signal of interest. Such interference may be termed as being duet to the environment of the experiment. Simple EM shielding of cables and grounding of the chassis of equipment reduce EM and power supply interference in most cases.

The ECG is a relatively strong signal with a readily identifiable waveform. Most types of interference that affect ECG signal may be removed by band pass filters.

6.3.3.1 High frequency noise in the ECG:

Fig. 6.9 shows a segment of an ECG signal with high-frequency noise. The noise could be due to the instrumentation amplifiers, the recording system, pickup of ambient EM signals by the cables, and so on. The signal illustrated has also been corrupted by power-line interference at 60 Hz and its harmonics, which may also be considered as a part of high frequency noise relative to low frequency nature of the ECG signal.

6.3.3.2 Motion artifact in the ECG:

Low frequency artifacts and base line drift may be caused in chest lead ECG signals by coughing or breathing with large movement of the chest or when an arm or leg is moved in the case of limb lead ECG acquisition. The EEG is a common source of artifact in chest lead ECG. Poor contact and polarization of the electrodes may also cause low frequency artifacts. Base line drift may sometimes be caused by variations in temperature and bias in the instrumentation and amplifiers as well; Fig. 6.10 shows an ECG signal with low frequency artifact. Base line drift makes analysis of isoelectricity of the ST segment difficult. A large base line drift may cause the positive or negative peaks in the ECG to be clipped by the amplifiers or the ADC.

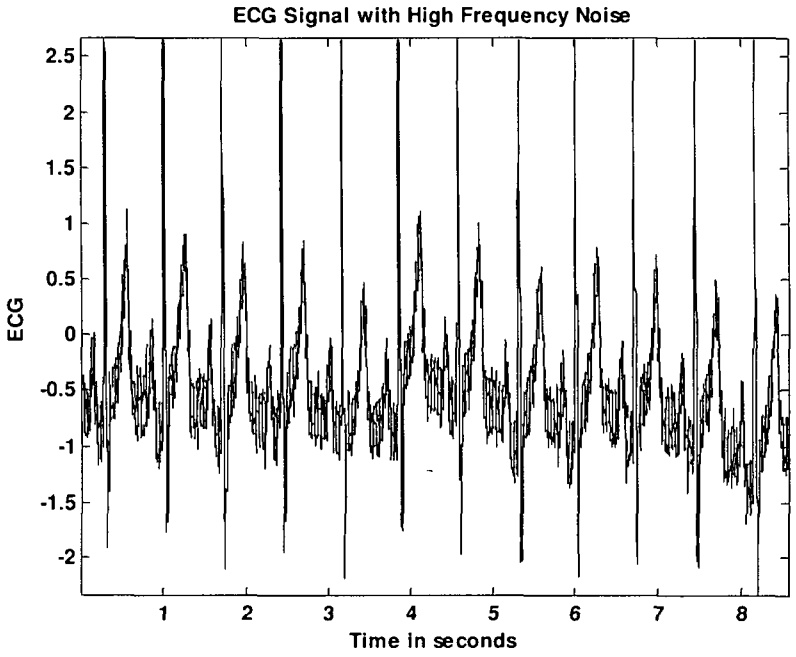

Figure 6.9: ECG signal with high frequency noise

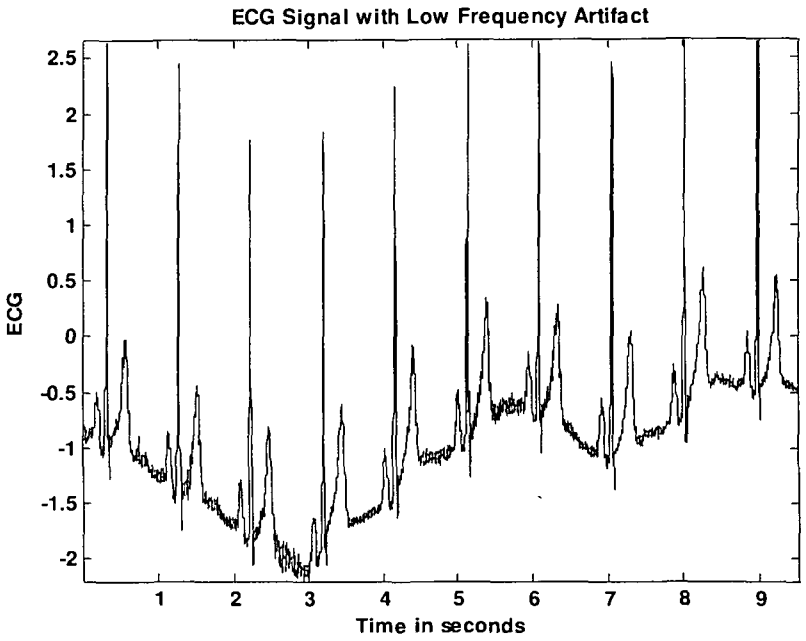

Figure 6.10: ECG signal with low frequency artifact

6.3.3.3 Power Line interference in ECG signals:

The most commonly encountered periodic artifact in biomedical signals is the power line interference at 50 Hz or 60 Hz. If the power-line waveform is not a pure sinusoid due to distortions or clipping, harmonics of the fundamental frequency could also appear. Harmonics will also appear if the interference is a periodic waveform that is not a sinusoid such as rectangular pulses. In the recent work of Yue-Der Lin [131] has developed method to detect and remove powerline interference from ECG.

Power-line interference is easily visible if present on well defined ECG signal waveforms. The power spectrum of the signal provides a clear indication of the presence of power line interference as an impulse or spike at 50 Hz or 60 Hz harmonics, if present, will appear as additional spikes at integral multiples of the fundamental frequency. Fig. 6.11 shows a segment of an ECG signal with 60 Hz interference. It is clear that the regular or periodic structure of the interference rides on top of the ECG waves. Figure 6.12 shows the FFT of the ECG signal with 60 Hz power line interference. If third and fifth harmonics are present, periodic interference is will also appear as a spike at 180 Hz and 300 Hz. The recommended sampling rate for ECG signals is 500 Hz; the higher rate

of 1,000 Hz was used in this case as the ECG was recorded as a reference signal with the PCG. The larger bandwidth also permits better illustration of artifacts and filtering.

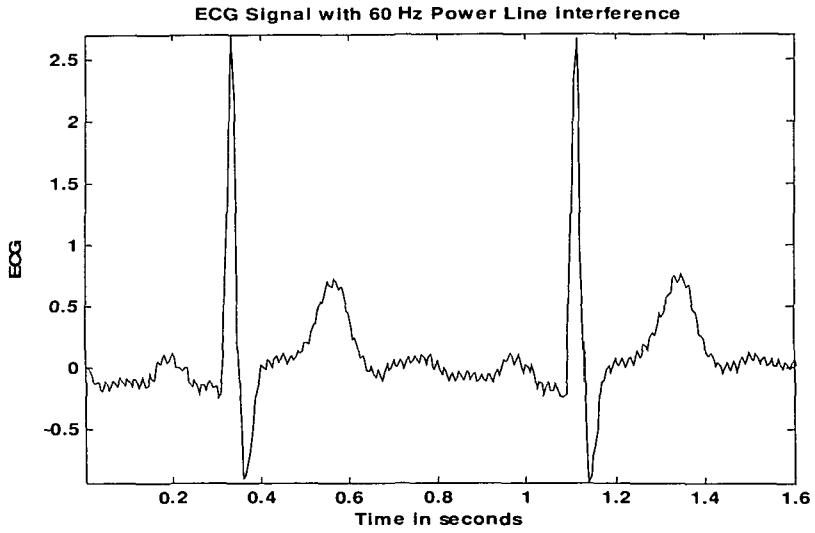

Figure 6.11: ECG signal with 60 Hz power line interference

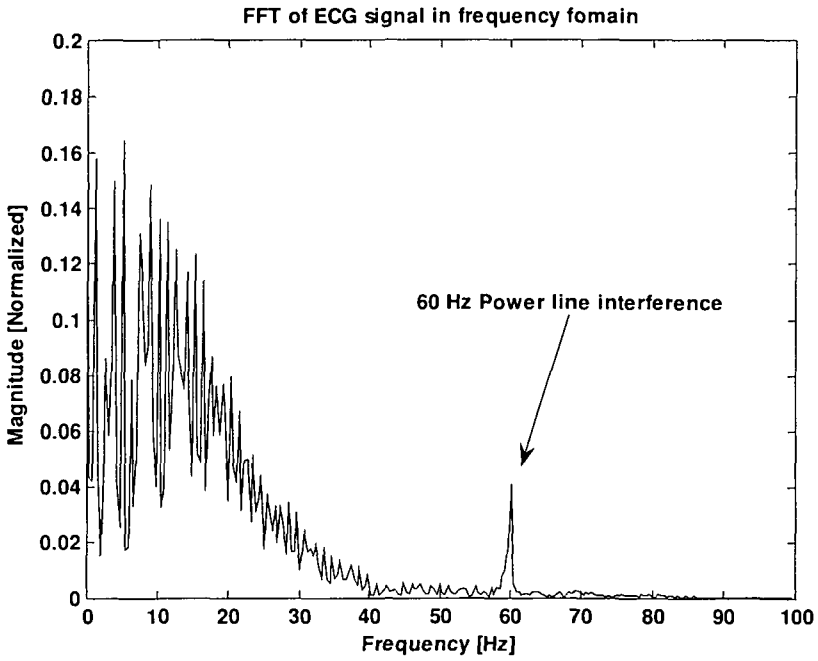

Figure 6.12: FFT of ECG signal

The bandwidth of interest of the ECG signal, which is usually in the range 0.05 – 100 Hz, includes the 60 Hz components; therefore lowpass filtering will not be

appropriate for removal of power-line interference. Lowpass filtering of the ECG to a bandwidth lower than 60 Hz could smooth and blur the QRS complex as well as affect the PQ and ST segments.

6.3.4 Time domain filters :

Certain types of noise may be filtered directly in the time domain using signal processing techniques or digital filters. An advantage of time-domain filtering is that spectral characterization of the signal and noise may not be required. Time-domain processing may also be faster in most cases than frequency filtering.

6.3.4.1 Moving average filters :

When an ensemble of several realizations of an event is not available we are then forced to consider temporal averaging for noise removal. As temporal statistics are computed using a few samples of the signal along the time points of time, such a filtering procedure is called a moving average (MA) filter.

The general form of an MA filter is:

$$y(n) = \sum_{k=0}^{N} b_k \, x(n-k) \qquad (6.25)$$

where x and y are the input and output of the filter, respectively. The b_k values are the filter coefficients or tap weights, k = 0,1,2, ...N. where N is the order of the filter. The effect of division by the number of samples used (N+1) is included in the values of the filter coefficients. A simple moving average filter for filtering noise is the von Hann of Hanning filter [104][105] given by

$$y(n) = \frac{1}{4}[x(n) + 2x(n-1) + x(n-2)] \qquad (6.26)$$

Applying the delta transform, and using equation (6.18) we get the transfer function $H_\delta(\gamma)$ of the filter in delta domain is

$$H_\delta(\gamma) = \frac{\frac{1}{4} + \frac{1}{\Delta}\gamma^{-1} + \frac{1}{\Delta^2}\gamma^{-2}}{1 + \frac{2}{\Delta}\gamma^{-1} + \frac{1}{\Delta^2}\gamma^{-2}} \qquad (6.27)$$

Where $X(\gamma)$ and $Y(\gamma)$ are the δ-transform of x(n) and y(n) respectively. The signal-flow diagram and pole zero plot of the Hanning filter in delta domain are shown in Figure 6.13 & 6.14 respectively.

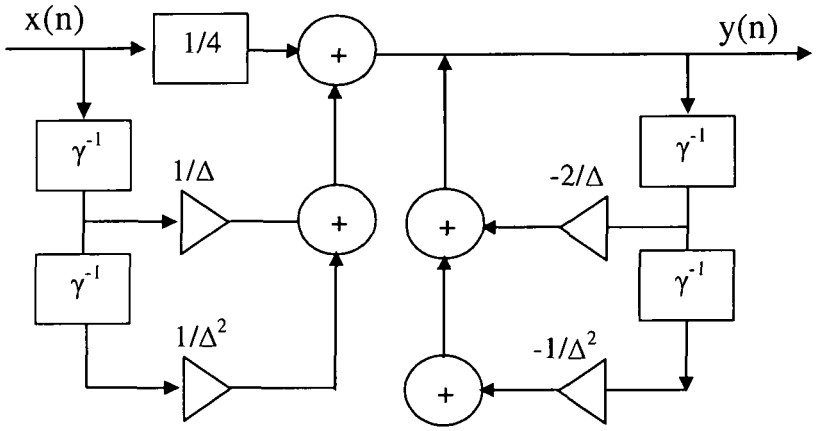

Figure 6.13: Signal flow diagram of Hanning filter in delta domain

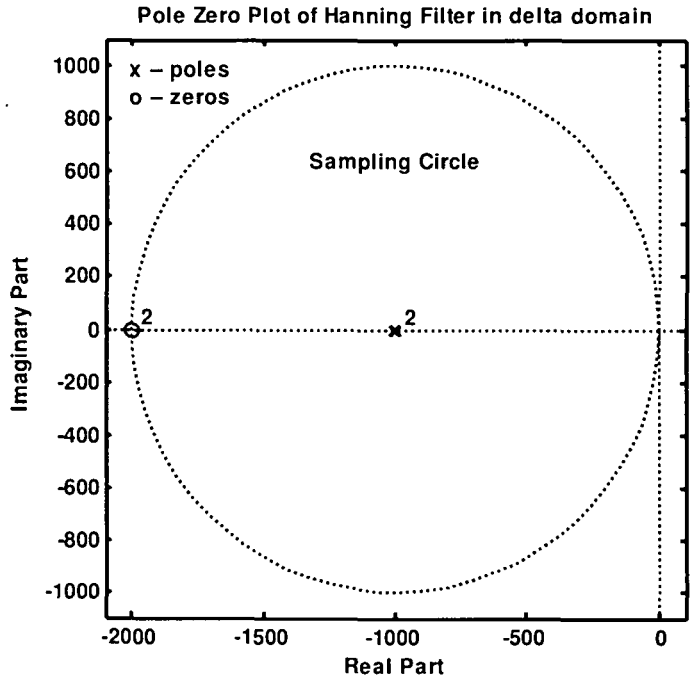

Figure 6.14: Pole zero plot of Hanning filter in delta domain

The frequency response of a filter is obtained by substituting $\gamma = \frac{e^{j\omega\Delta} - 1}{\Delta}$ or in the expression for $H_\delta(\gamma)$, where Δ is the sampling interval in seconds and ω is the radian frequency $\omega = 2\pi f$, where f is the frequency in Hz . We may set $\Delta = 1$ sec and deal with normalized frequency in the range $0 \le \omega < 2\pi$, or 0 0 $\le f < 1$, then $f = 1$ or $\omega = 2\pi$ represent the sampling frequency, with lower frequency values being represented as a normalized fraction of the sampling frequency.

The frequency response of the Hanning filter is given as :

From equation 6.18 we have $\gamma^{-1} = \frac{\Delta z^{-1}}{1 - z^{-1}}$ and we know $z^{-1} = e^{-j\omega\Delta}$

$$\gamma^{-1} = \frac{\Delta e^{-j\omega\Delta}}{1 - e^{-j\omega\Delta}} \qquad and \qquad \gamma^{-2} = \frac{\Delta^2 e^{-j2\omega\Delta}}{1 - 2e^{-j\omega\Delta} + e^{-j2\omega\Delta}} \tag{6.28}$$

Substituting in equation (6.27) we have

$$H_\delta(\omega) = \frac{\frac{1}{4} + \frac{e^{-j\omega\Delta}}{(1 - e^{-j\omega\Delta})} + \frac{e^{-j2\omega\Delta}}{(1 - 2e^{-j\omega\Delta} + e^{-j2\omega\Delta})}}{1 + \frac{2e^{-j\omega\Delta}}{\Delta(1 - e^{-j\omega\Delta})} + \frac{e^{-j2\omega\Delta}}{\Delta^2(1 - 2e^{-j\omega\Delta} + e^{-j2\omega\Delta})}} \tag{6.29}$$

let $e^{-j\omega} = \cos\omega - j\sin\omega$ and setting $\Delta = 1$ in equation (6.29)

$$H_\delta(\omega) = \frac{1}{4}[1 + 2e^{-j\omega} + e^{-j2\omega}] \tag{6.30}$$

$$H_\delta(\omega) = \frac{1}{4}[\{2 + 2\cos(\omega)\}e^{-j\omega}] \tag{6.31}$$

The magnitude and phase response are given as

$$|H_\delta(\omega)| = \left|\frac{1}{2}\{1 + \cos(\omega)\}\right| \tag{6.32}$$

and

$$\angle H_\delta(\gamma) = -\omega \tag{6.33}$$

the magnitude and phase responses of the Hanning filter are shown in figure 6.15. It is clear that the filter is a lowpass filter with linear phase

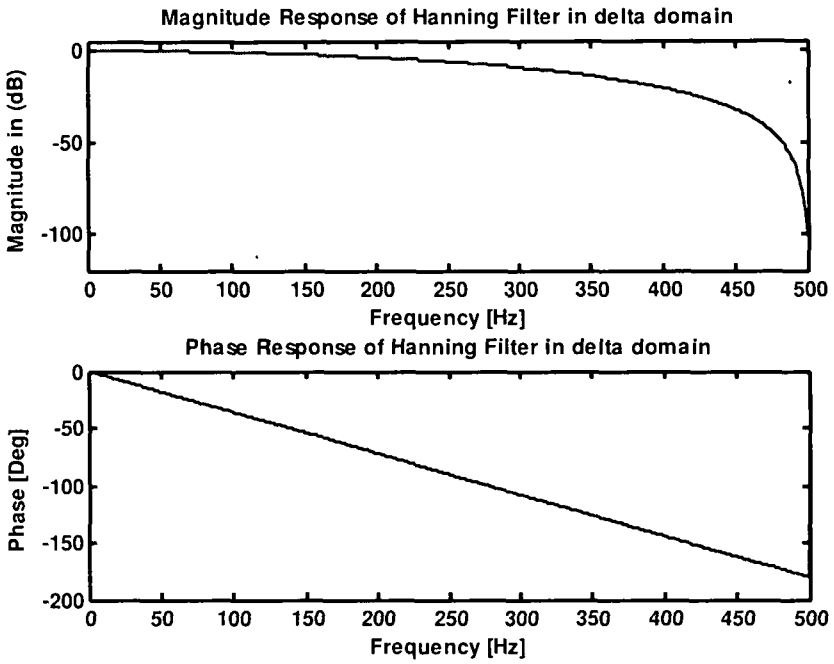

Figure 6.15: Magnitude and phase response of the Hanning filter in delta domain

Although we started with description of the Hanning filter in the time domain, subsequent analysis of the filter was performed in the frequency domain using the delta transform and the frequency response. System analysis is easier to perform in the delta domain in terms of the poles and zeros of the transfer function and in the frequency domain in terms of the magnitude and phase responses. The magnitude and phase responses assist in understanding the effect of the filter on the frequency components of the signal and noise.

It is seen from the magnitude response of the Hanning filter (Figure 6.15) that components beyond about 20% of the sampling frequency of 1,000 Hz are reduced in amplitude by more than 3 dB, that is, to less than half of their levels in the input. High frequency components beyond 40% of the sampling frequency are suppressed to less than 20 dB below their input levels. Figure 6.16 shows the filtering of ECG signal with high frequency noise using Hanning filter and figure 6.17 shows its FFT of filtered signal. It can be seen from the FFT that the high frequency noise is filtered using hanning filter in delta domain.

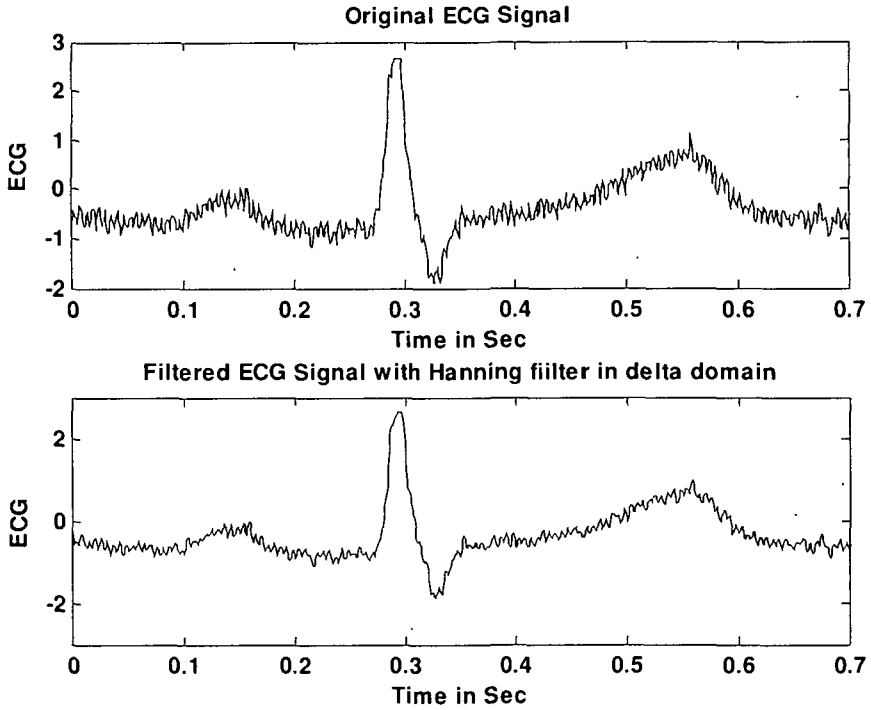

Figure 6.16: Filtering of ECG signal with high frequency noise using Hanning filter

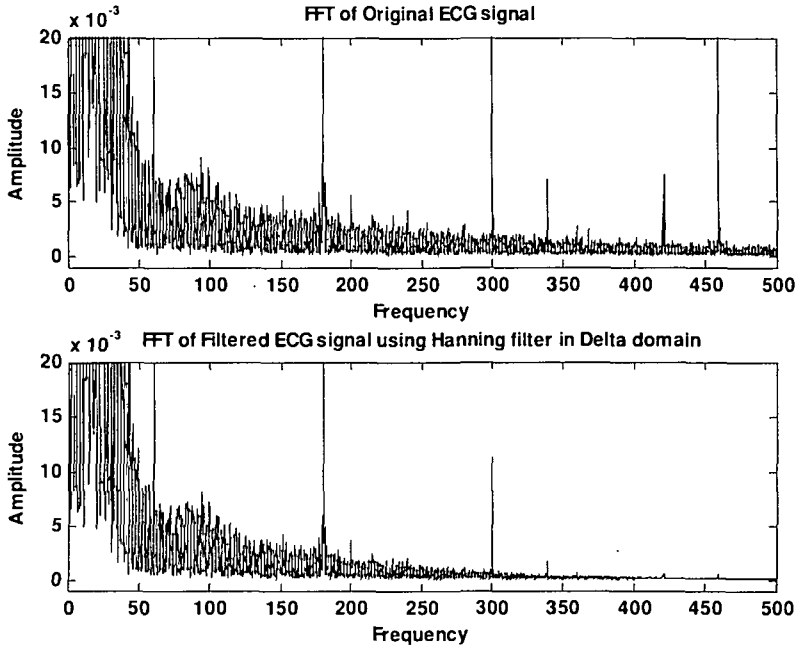

Figure 6.17: FFT of ECG and filtered signal with Hanning filter

It can be seen from the results of figure 6.16, the smoothness is less hence increased smoothing may be achieved by averaging signal samples over longer time windows, at the expense of increased filter delay [105]. If the signal samples over a window of eight samples are averaged, we get the output as:

$$y(n) = \frac{1}{8}\sum_{k=0}^{7} x(n-k) \tag{6.34}$$

The impulse response of the filter is

$$h(n) = \frac{1}{8}[\delta(n) + \delta(n-1) + \delta(n-2) + \delta(n-3) + \delta(n-4) + \delta(n-5) + \delta(n-6) + \delta(n-7)$$

The transfer function in delta domain is given as

$$H_\delta(\gamma) = \frac{1}{8}\sum_{k=0}^{7}(1 + \gamma\Delta)^{-k} \tag{6.35}$$

The frequency response by substituting $\gamma = \frac{e^{j\omega\Delta} - 1}{\Delta}$ in equation (6.35)

$$H_\delta(\omega) = \frac{1}{8}\sum_{k=0}^{7}(1 + \frac{e^{j\omega\Delta} - 1}{\Delta}\Delta)^{-k}$$
$$H_\delta(\omega) = \frac{1}{8}\sum_{k=0}^{7} e^{-jk\omega\Delta} \tag{6.36}$$

Setting $\Delta = 1$, $H_\delta(\omega) = \frac{1}{8}[1 + e^{-j4\omega}\{1 + 2\cos(\omega) + 2\cos(2\omega) + 2\cos(3)\}]$ (6.37)

The pole zero plot and frequency response of the 8-point MA filter is shown in Figure 6.18 and 6.19 respectively. It can be seen from pole zero plot that the filter has zeros at $\frac{f_s}{8} = 125\ Hz$, $\frac{f_s}{4} = 250\ Hz$, $\frac{3f_s}{8} = 375\ Hz$ *and* $\frac{f_s}{2} = 500\ Hz$. Comparing the frequency response of the 8-point MA filter with that of the Hanning filter in Figure 6.15, we see that the former provides increased attenuation in the range 90 – 400 Hz over the latter. Note that the attenuation provided by the filter after about 100 Hz is non uniform, which may not be desirable in certain applications. Furthermore, the phase response of the filter is not linear, although it is piece-wise linear.

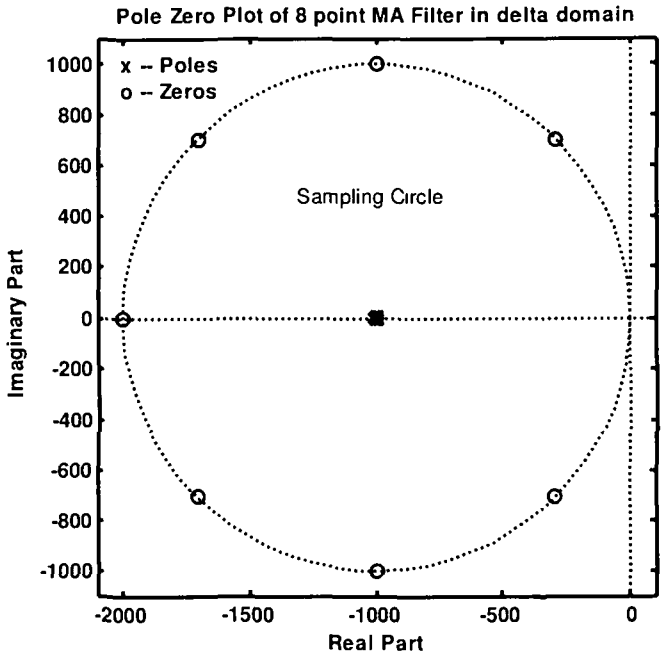

Figure 6.18: Pole zero plot of 8 point MA filter in delta domain with sampling frequency 1000 Hz

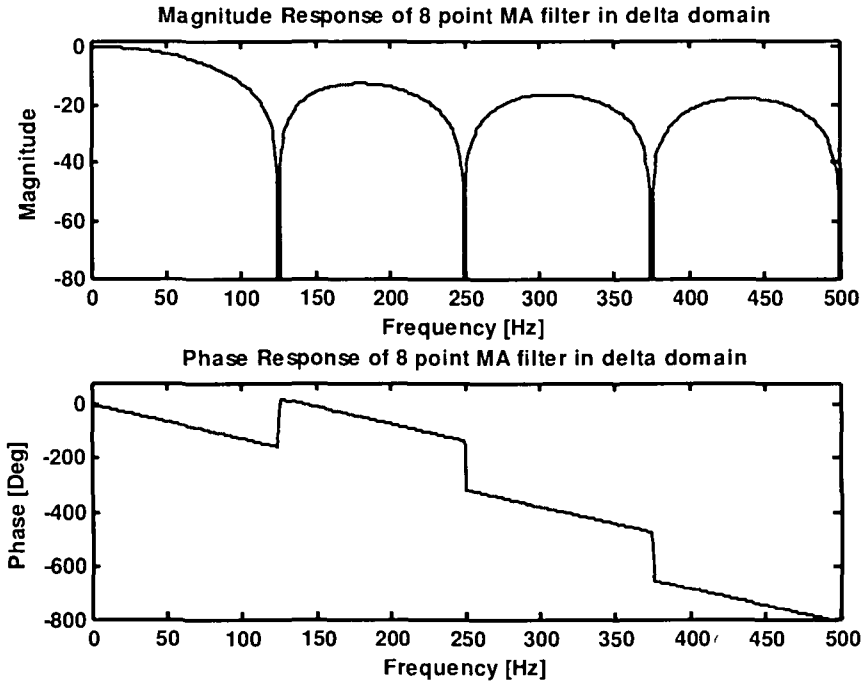

Figure 6.19: Magnitude and phase response of 8 point MA filter in delta domain

Figure 6.20 & 6.21 shows the filtering of ECG signal with high frequency noise and its FFT of filtered signal using 8 point MA filter.

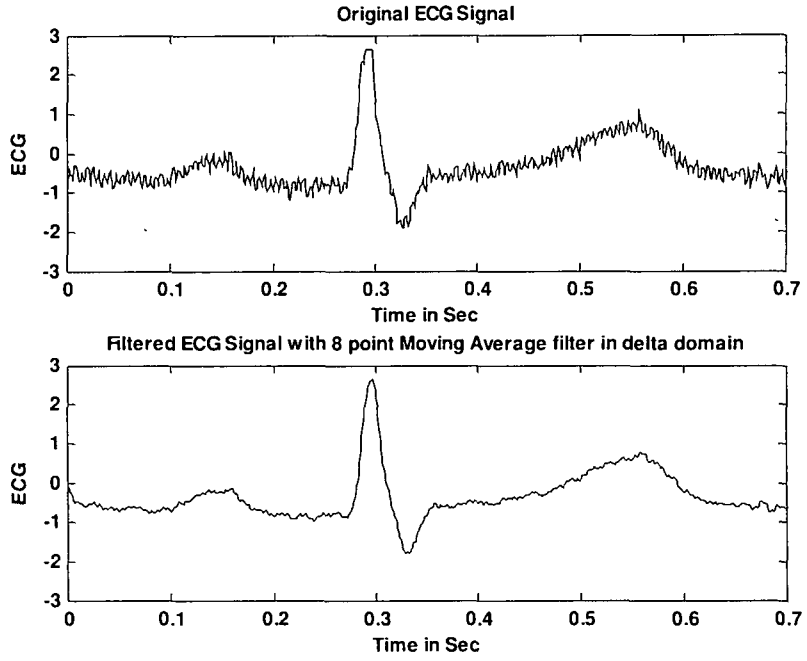

Figure 6.20: Filtering of ECG with high frequency noise using 8 point MA filter in delta domain

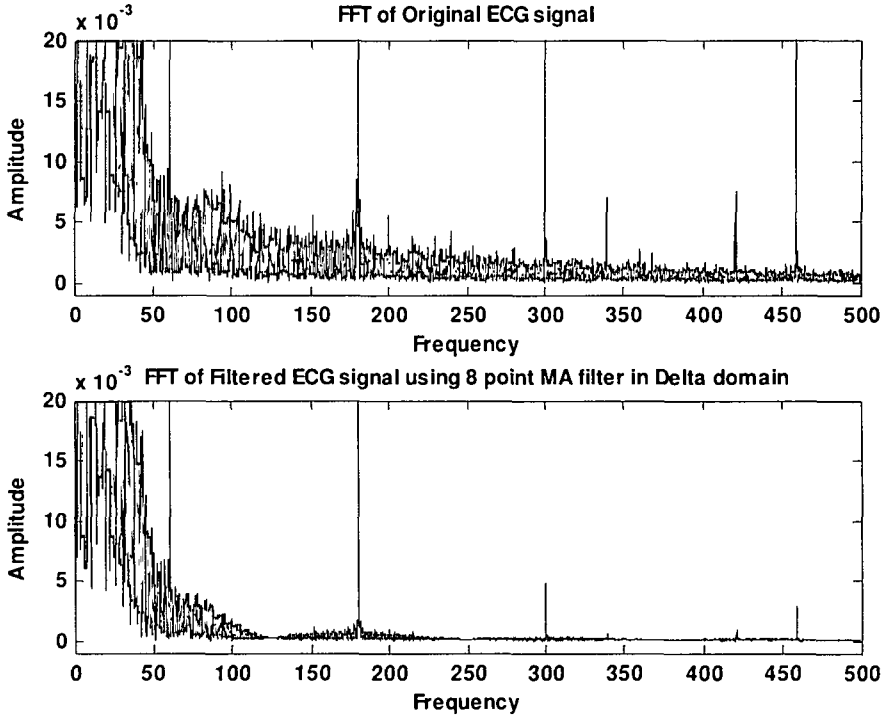

Figure 6.21: FFT of ECG and filtered signal with 8 point MA filter in delta domian

Comparing figures 6.16 with 6.20 and figure 6.17 with 6.21, it is seen that the output of 8 point MA average filter is smoother than that of Hanning filter in delta domain.

6.3.5 Derivative operator based filters:

The derivative operator in time domain removes the parts of the input that are constant. Large changes in the input lead to high magnitudes in the output of the derivative operator. Improved knowledge on the derivative operation may be obtained by studying its transform in the frequency domain. [105]

In digital signal processing, the basic derivative is obtained by first order difference operator [104] given as:

$$y(n) = \frac{1}{\Delta}[x(n) - x(n-1)] \tag{6.38}$$

The scale factor including the sampling interval Δ is required in order to obtain the rate of change of the signal with respect to the true time [105]. The transfer function in 'z' domain is

$$H(z) = \frac{1}{\Delta}(1 - z^{-1}) \tag{6.39}$$

Using equation (6.13), corresponding transfer function in delta domain is

$$H_\delta(\gamma) = \frac{\gamma}{1+\gamma\Delta}$$

or
$$H_\delta(\gamma) = \frac{1}{\Delta + \gamma^{-1}} \tag{6.40}$$

The frequency response of (6.40) can be obtained using $\gamma^{-1} = \dfrac{\Delta e^{-j\omega\Delta}}{1 - e^{-j\omega\Delta}}$

$$H_\delta(\omega) = \frac{1}{\Delta + \dfrac{\Delta e^{-j\omega\Delta}}{1-e^{-j\omega\Delta}}} = \frac{1}{\Delta}(1 - e^{-j\omega\Delta}) \tag{6.41}$$

or
$$H_\delta(\omega) = \frac{1}{\Delta} e^{-j\frac{\omega}{2}} \left[2j \sin\left(\frac{\omega}{2}\right)\right] \tag{6.42}$$

From equation (6.42)

$$|H_\delta(\omega)| = \frac{2}{\Delta}\left|\sin\left(\frac{\omega}{2}\right)\right| \tag{6.43}$$

$$\angle H_\delta(\omega) = \frac{\pi}{2} - \frac{\omega}{2} \tag{6.44}$$

The magnitude and phase response of the first order difference operator with sampling frequency of 1000 Hz are plotted in figure 6.22. Since delta transform itself is derivative type, hence the gain of the filter increases for higher frequencies up to folding frequency $f_s/2$ i.e half of the sampling frequency. Hence any high frequency noise present in the signal will be amplified significantly hence the result will be noisy.

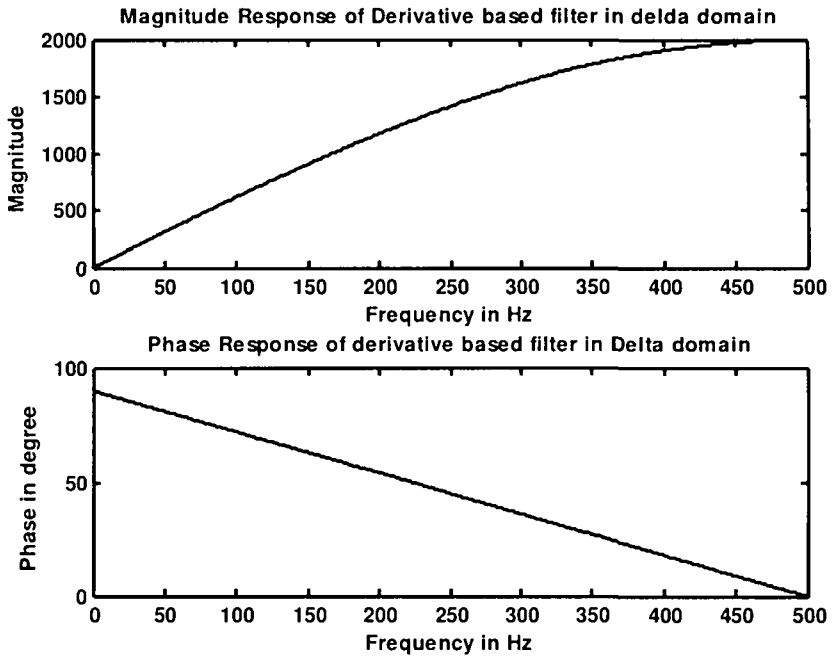

Figure 6.22: Magnitude and phase response of derivative based filter in delta domain

The noise amplification problem with the first order difference operator given in equation (6.38) may be controlled by taking the average of two successive output values [105]:

$$y_3(n) = \frac{1}{2}[y(n) + y(n-1)] \tag{6.45}$$

or $$y_3(n) = \frac{1}{2\Delta}[\{x(n) - x(n-1)\} + \{x(n-1) - x(n-2)\}] \quad (6.46)$$

$$y_3(n) = \frac{1}{2\Delta}[x(n) - x(n-2)] \quad (6.47)$$

The transfer function in delta domain given as

$$H_\delta(\gamma) = \frac{1}{2\Delta}\{1-(1+\gamma\Delta)^{-2}\} = \left[\frac{1}{\Delta}\{1-(1+\gamma\Delta)^{-1}\}\right]\left[\frac{1}{2}\{1+(1+\gamma\Delta)^{-1}\}\right] \quad (6.48)$$

$$H_\delta(\gamma) = \frac{\frac{1}{2}\left[1 + \frac{2}{\Delta}\gamma^{-1}\right]}{\left[1 + \frac{2}{\Delta}\gamma^{-1} + \frac{1}{\Delta^2}\gamma^{-2}\right]} \quad (6.49)$$

From equation (6.48) it is clear that the three point central difference operator is the product of the transfer functions of the simple first order difference operator and a two point Moving Average filter.

Magnitude and phase responses with sampling frequency 1000 Hz are plotted in figure 6.23. In this case also noise amplification is not improved hence in delta domain derivative type filters are not suitable.

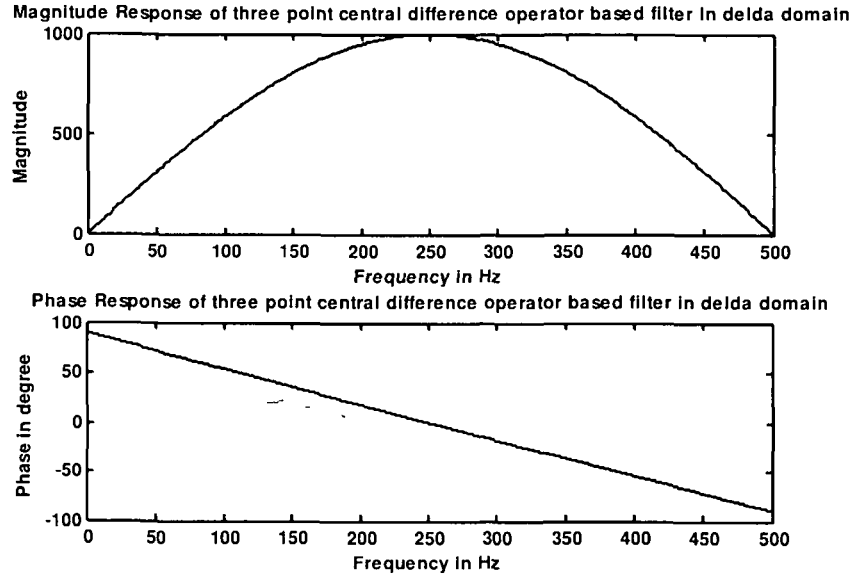

Figure 6.23: Magnitude and phase response of modified derivative based filter

The drawback of the first order difference and the three point central difference operator based filters lies in the fact that their magnitude responses remain low for the significant range of frequencies well beyond the band related to base-line wander. We would like to maintain the levels of the components present in the signal beyond about 0.5-1 Hz, that is, we would like the gain of the filter to be close to unity after about 0.5 Hz. [104]

The gain of a filter at specific frequencies may be improved by placing poles at related locations around the sampling circle in the gamma plane. For the sake of stability of the filter, the poles should be placed within the sampling circle. Since we are interested in maintaining a high gain at very low frequencies, we could place a pole on the real axis near the zero location. The transfer function in z-domain has been given in with zero located at 0.995 [104]. i.e

$$H(z) = \frac{1}{\Delta}\left[\frac{1 - z^{-1}}{1 - 0.995\, z^{-1}}\right] \tag{6.50}$$

or equivalently $$H(z) = \frac{1}{\Delta}\left[\frac{z - 1}{z - 0.995}\right] \tag{6.51}$$

Using equation (6.13), corresponding transfer function in delta domain is

$$H_\delta(\gamma) = \frac{1}{\Delta}\left[\frac{1 - (1 + \gamma\Delta)^{-1}}{1 - 0.995\,(1 + \gamma\Delta)^{-1}}\right] = \frac{1}{\Delta}\left[\frac{(1 + \gamma\Delta) - 1}{(1 + \gamma\Delta) - 0.995}\right] \tag{6.52}$$

or equivalently $$H_\delta(\gamma) = \frac{1}{\Delta}\left[\frac{\gamma}{\gamma - \frac{0.005}{\Delta}}\right] \tag{6.53}$$

The time domain input-output relationship is given as

$$y(n) = \frac{1}{\Delta}[x(n) - x(n-1) + 0.995\, y(n-1)] \tag{6.54}$$

The frequency response of a system is obtained by evaluating its transfer function at various points on the sampling circle in the complex gamma plane i.e by putting $\gamma = \frac{e^{j\omega\Delta} - 1}{\Delta}$ and evaluating $H_\delta(\gamma)$ for various values of the frequency variable ω of

interest. In general, the magnitude transfer function of a system for a particular value of γ is given by the product of the distances from the corresponding point in the complex gamma plane to all the zeros of the system's transfer function, divided by the product of the distances to its poles. The phase response is given by the sum of the angles of the vectors joining the point to all the zeros, minus the sum of the angles to the poles [126].

It is obvious that the magnitude response of the filter in Equations (6.52) and (6.53) is zero at $\gamma = 0$, due to the presence of a zero at that point. Furthermore, for values of γ away from $\gamma = 0$, the distances to the zero at $\gamma = 0$ and the pole at $\gamma = 0.0995 \times \Delta$ will be almost equal; therefore, the gain of the filter will be close to unity for frequencies greater than about 1 Hz. The magnitude and phase responses of the filter shown in Figure 6.24 confirm these observations; the filter is a highpass filter with nonlinear phase.

The result of application of the filter to the ECG signal with low frequency noise shown in Figure 6.25. It is evident that low frequency base line wandering has been removed without any significant distortion of the ECG. Close inspection, however, reveals that the S wave has been enhanced (made deeper) and that a negative undershoot has been introduced after the T wave. Removal of the low-frequency base-line artifact has been achieved at the cost of a slight distortion of ECG waves due to the use of a derivative based filter and its nonlinear phase response.

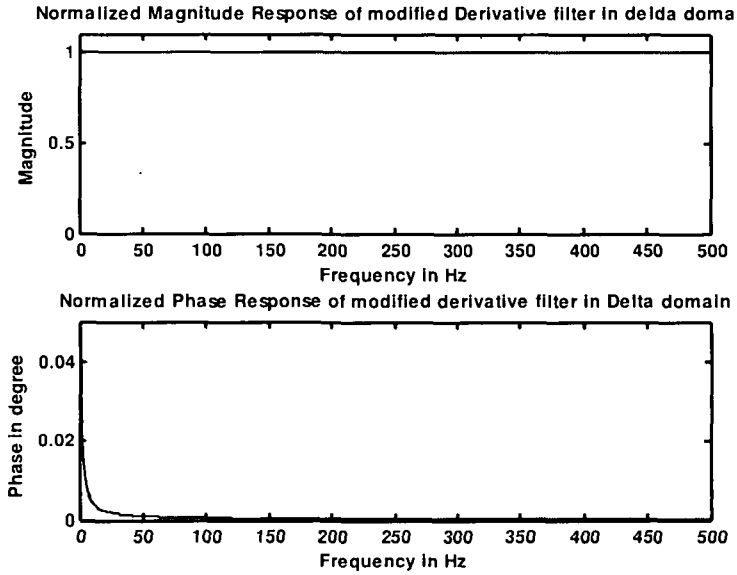

Figure 6.24: Normalized magnitude and phase responses of modified derivative filter in delta domain

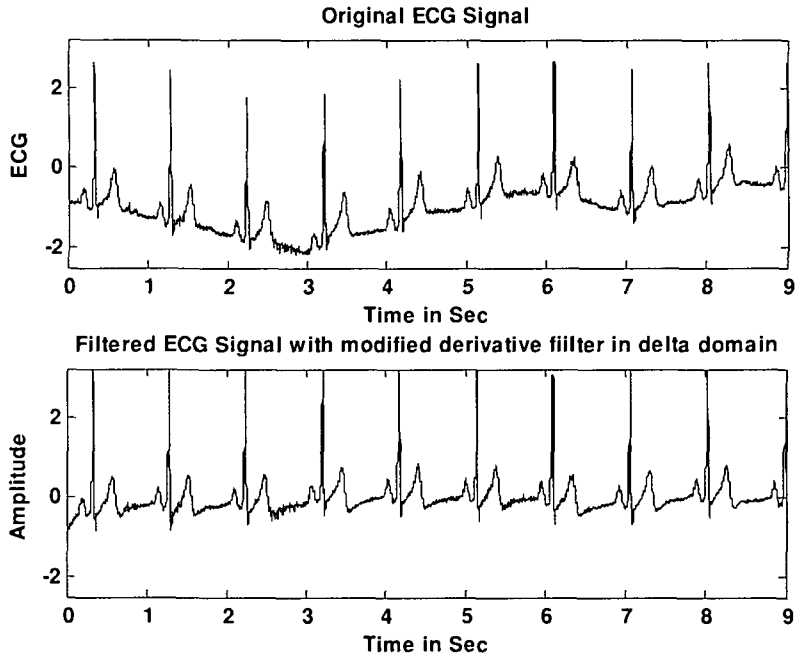

Figure 6.25: Results of modified derivative filter in delta domain to remove base line wander

6.3.6 Frequency Domain Filters :

The filters described in the previous section performed relatively simple operations in the time domain: although their frequency-domain characteristics were explored, the operators were not specifically designed to process any particular frequency response at the outset. The frequency response of the MA filter, in particular, was seen to be most attractive. The attenuation in the stop band was not uniform, with the gain falling below – 20 dB only around the zeros of the transfer function.

Filters may be designed in the frequency domain to provide specific lowpass, highpass, bandpass, or band-reject (notch) characteristics. Frequency domain filters may be implemented in software after obtaining the Fourier transform of the input signal, or converted into equivalent time–domain filters and applied directly upon the signal samples.

Many design procedures are available in the literature to design various types of filters: the most commonly used designs are the Butterworth, Chebyshev, elliptic and Bessel filters [132-136]. Since these filters have been well established in the analog–filter

domain, it is common to commence with an analog design and apply the delta transformation to obtain a digital filter in the delta domain. It is also common to design a lowpass filter with the desired pass-band, transition, and stop-band characteristics on a normalized-frequency axis, and then transformed it to the desired lowpass, highpass, bandpass, or band-reject characteristics [137]. Frequency-domain filters may also be specified directly in terms of the values of the desired frequency response at certain frequency samples only, and then transformed into the equivalent time-domain filters coefficients via the inverse Fourier transform. In the present work we will consider only the design of low pass butterworth and notch filter in delta domain. ECG signal will be processed with both the filters to remove low frequency noise and 50/60 Hz power line interference.

6.3.6.1 Butterworth lowpass filters :

The butterworth design is popular because of its simplicity, a monotonically decreasing magnitude response, and a maximally flat magnitude response in the pass-band. In order to design a Butterworth lowpass filter, we need to specify two parameters; ω_c and N where ω_c is the cutoff frequency in radian/sec and N is the order of the filter. The two parameters may be specified based on a knowledge of the characteristics of the filter as well as those of the signal and noise. [105]

Let us now design a Butterworth lowpass filter with f_c = 40 Hz, f_s = 200 Hz, and N = 4. We have $\omega_c = 2\pi \frac{f_c}{f_s} = 0.4\pi$ radians/sec . The prewarped s-domain cutoff frequency is Ω_c=1.453085 radians /sec. [105]

The poles of $H_a(s)H_a(-s)$ are placed around a circle of radius 1.453085 with an angular separation of $\frac{\pi}{N} = \frac{\pi}{4}$ radians. The poles of interest are located at angles $\frac{5}{8}\pi$ and $\frac{7}{8}\pi$ and the corresponding conjugate positions. The coordinates of the poles of interest are (-0.556072 ± j1.342475) and (-1.342475 ± j0.556072). The transfer function of the filter found as :

$$H_a(s) = \frac{4.458247}{(s^2 + 1.112143s + 2.111456)\,(s^2 + 2.684951s + 2.111456)} \qquad (6.55)$$

Applying the bilinear transformation, we get

$$H(z) = \frac{0.0465583(1+z^{-1})^4}{(1-0.447765\,z^{-1}+0.460815\,z^{-2})\,(1-0.328976\,z^{-1}+0.064588\,z^{-2})} \tag{6.56}$$

Using equation (6.13), the transfer function in delta domain obtained as

$$H_\delta(\gamma) = \frac{0.046583+74.53\gamma^{-1}+44719.59\gamma^{-2}+11925224.09\gamma^{-3}+1192522409.9\gamma^{-4}}{1+643.58\gamma^{-1}+173347.72\gamma^{-2}+22647966.09\gamma^{-3}+1192522409.9\gamma^{-4}} \tag{6.57}$$

The filter has four poles at (-1.546 e+02 ± j 1.288 e+02), (-1.671 e+02 ± j 0.387 e+02) and four zeros at (-400, -399.9, 399.9 ± j 0.115). Magnitude and phase response with sampling frequency 200 Hz is computed and shown in figure 6.26 and 6.27. Pole zero plot is shown in figure 6.28 and processing of ECG signal with lowpass butterworth filter and FFT of filtered signal are shown in figure 6.29 & 6.30 respectively. The pole-zero plot and the frequency response displays the excepted monotonic decrease in gain and –3 dB power point or 0.707 gain at 40 Hz.

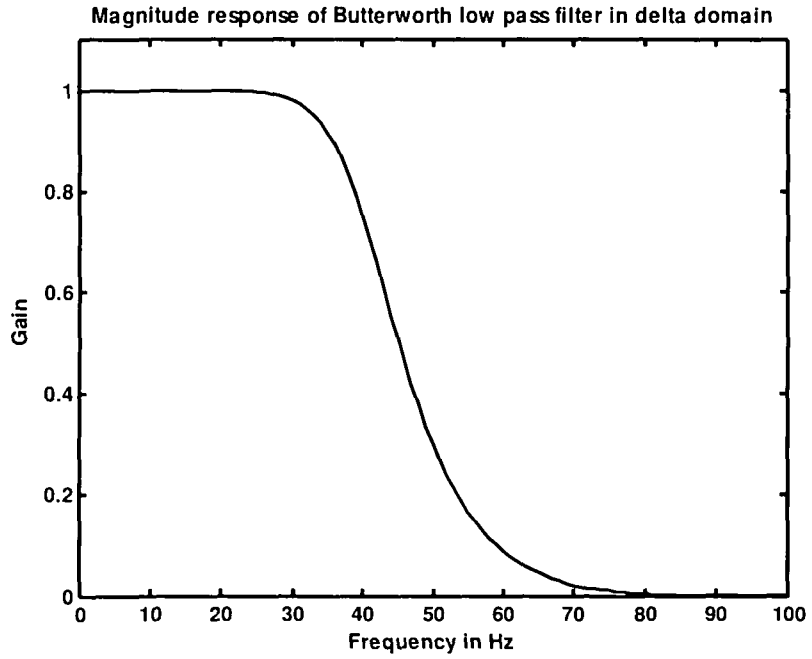

Figure 6.26: Magnitude response of butterworth low pass filter in delta domain with f_c =40 Hz, f_s=200 Hz and N=4

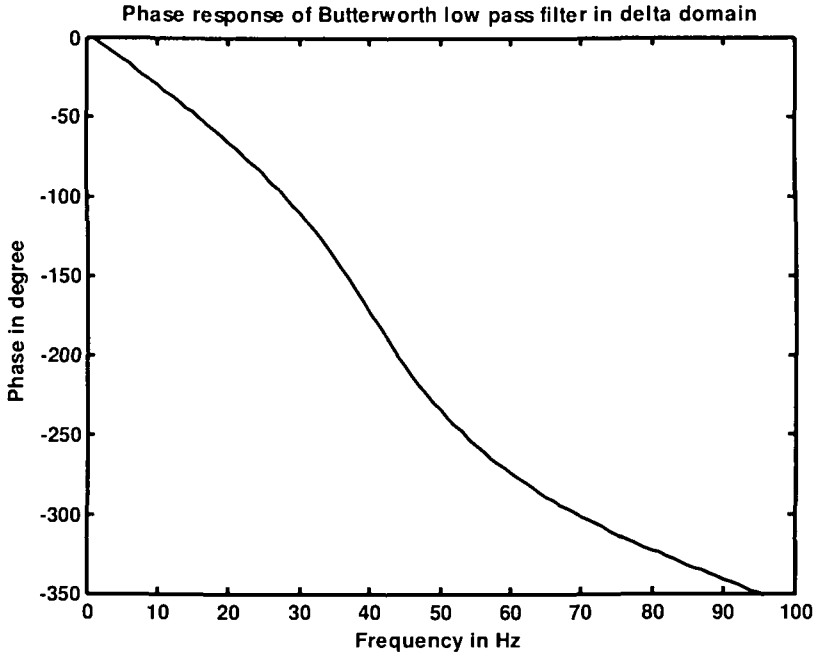

Figure 6.27: Phase response of butterworth low pass filter in delta domain with f_c =40 Hz, f_s=200 Hz and N=4

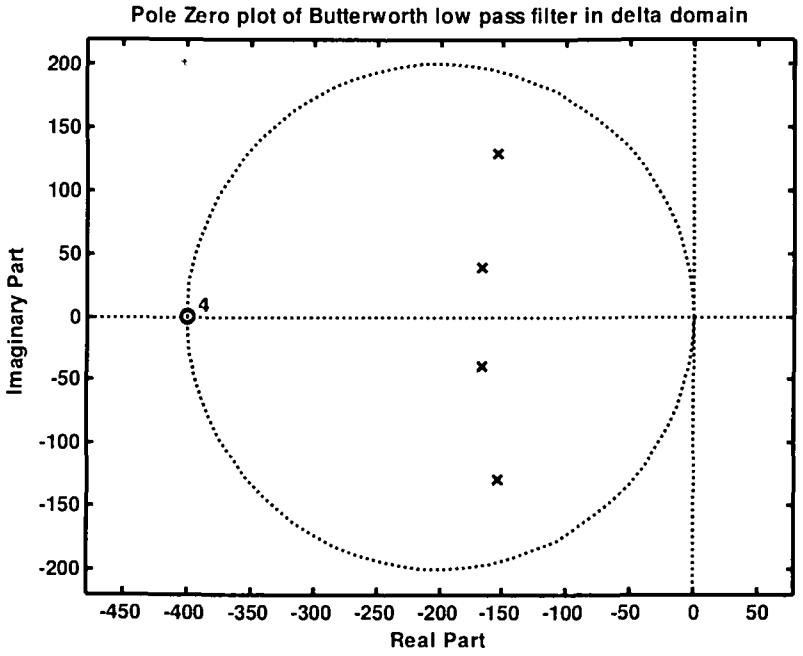

Figure 6.28: Pole zero plot of butterworth low pass filter in delta domain with f_c =40 Hz, f_s=200 Hz and N=4

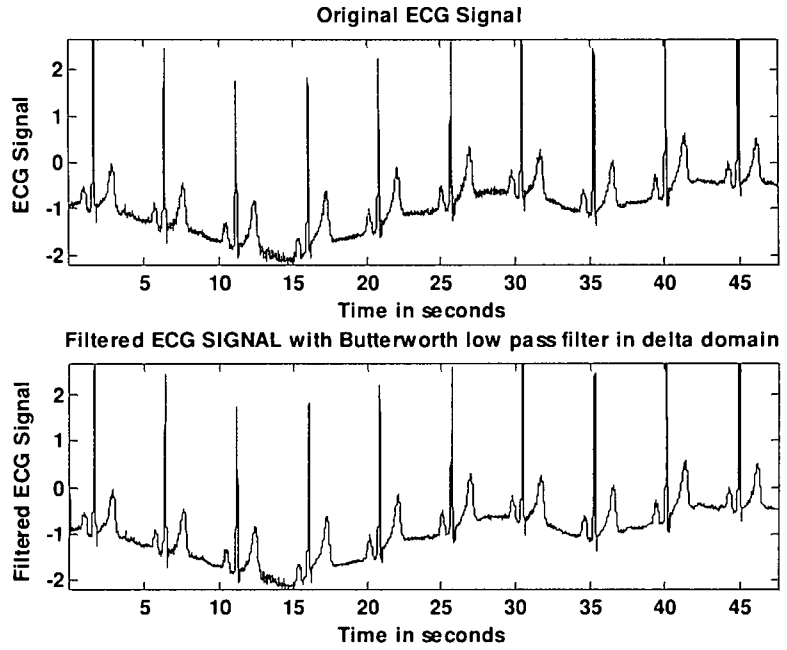

Figure 6.29: Processing of ECG signal with low frequency noise with butterworth low pass filter in delta domain with f_c =40 Hz, f_s=200 Hz and N=4

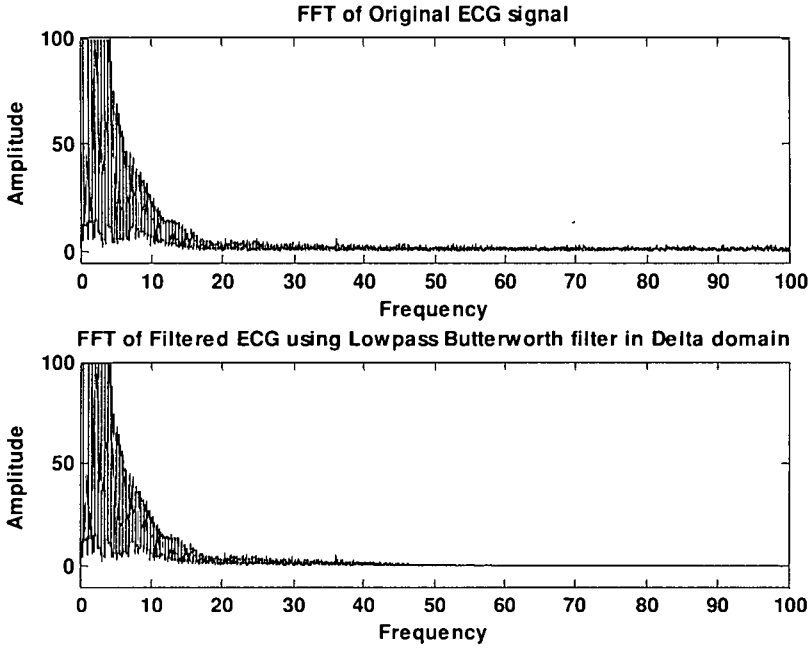

Figure 6.30: FFT of ECG and filtered signal with butterworth low pass filter in delta domain with f_c =40 Hz, f_s=200 Hz and N=4

Figure 6.31 compares the magnitude responses of three Butterworth lowpass filters in delta domain with f_c = 40 Hz, f_s = 200 Hz with order increasing from N=4, N=8, N=12. All three filters have their gain =0.707 a 40 Hz, but the transition band becomes sharper as the order N is increased.

The main disadvantages of Butterworth filter are a slow transition from the pass band to stop band and a nonlinear phase response. The nonlinear phase may be corrected for by passing the filter output again through the same filter but after a reversal in time [136].

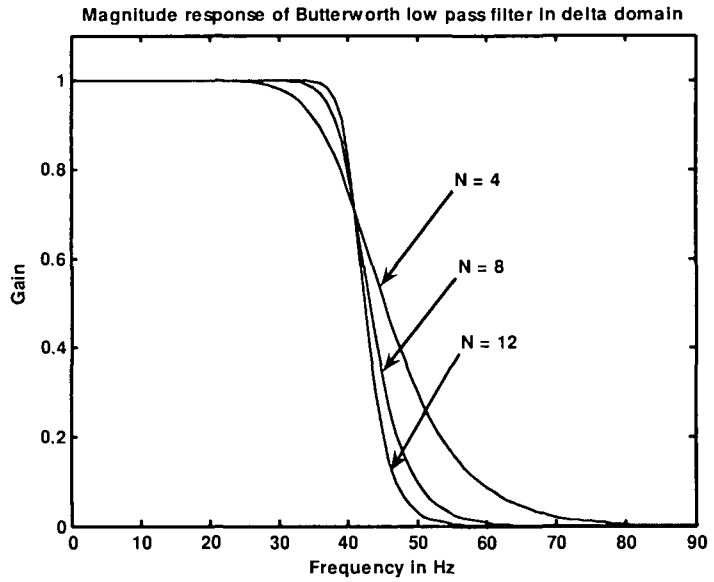

Figure 6.31: Magnitude responses of butterworth low pass filter in delta domain with f_c =40 Hz, f_s=200 Hz and N=4, 8, 12

6.3.6.2 Notch filters :

The nature of the influence of pole and zero locations on the frequency response is similar to that observed in continuous time systems with a minor difference. In place of the imaginary axis of the continuous time system, we have a sampling circle with the radius 1/Δ and cantered at -1/Δ in the complex delta domain. The nearer to the point $\gamma = \frac{e^{j\omega\Delta} - 1}{\Delta}$ representing some frequency ω and poles and zeros located at this point amplitude of magnitude response at that frequency.

Therefore to sacrifice the amplitude response at a frequency ω, we should place a pole as close as possible to the point $\gamma = \frac{e^{j\omega\Delta} - 1}{\Delta}$ representing frequency ω. Similarly to suppress the amplitude response at a frequency ω, we should place a zero as close as possible to the point $\gamma = \frac{e^{j\omega\Delta} - 1}{\Delta}$ on the sampling circle. Placing repeated poles or zeros will further enhance their influence.

Total suppression of signal transmission at any frequency can be achieved by placing a zero on the sampling circle at a point corresponding to that frequency. This is the principle of the notch filter.

Placing a pole or zero at the center (-1/Δ) does not influence the amplitude response because length of the vector connecting the (-1/Δ) to any point on the sampling circle is 1/Δ. However, a pole or zero at the center of sampling circle will generate an angle $\left(-\tan^{-1}\frac{\sin\omega\Delta}{\cos\omega\Delta - 1}\right)$ or $\left(\tan^{-1}\frac{\sin\omega\Delta}{\cos\omega\Delta - 1}\right)$ in $\angle H\left(\frac{(e^{j\omega\Delta} - 1)}{\Delta}\right)$.

Notch filter is also a frequency-domain filter and require to remove periodic artifacts such as power line interference from the ECG signals. If f_0 is the interference frequency, the angles of the (complex conjugate) zeros required will be $\pm\frac{f_0}{f_c}(2\pi)$; the radius of the zeros will be 1/Δ. If harmonics are also present, multiple zeros are required to be placed at $\pm\frac{n f_0}{f_c}(2\pi)$, where n representing the orders of all of the harmonics present.

Let us consider a signal with power line interference at f_0 = 60 Hz and sampling frequency is 1000 Hz. Since we need zero transmission at f_0, we must place zeros at $\omega = \pm\frac{f_0}{f_c}(2\pi)$ i.e ± 0.377 radians or 21.6° from the center of sampling circle as shown in figure 6.32. We also require a sharp recovery of gain on both sides of frequency i.e. 60 Hz which can be accomplished by placing two poles close to two zeros in order to cancel out the effect of the zeros as we move away from this point corresponding to frequency 60 Hz.

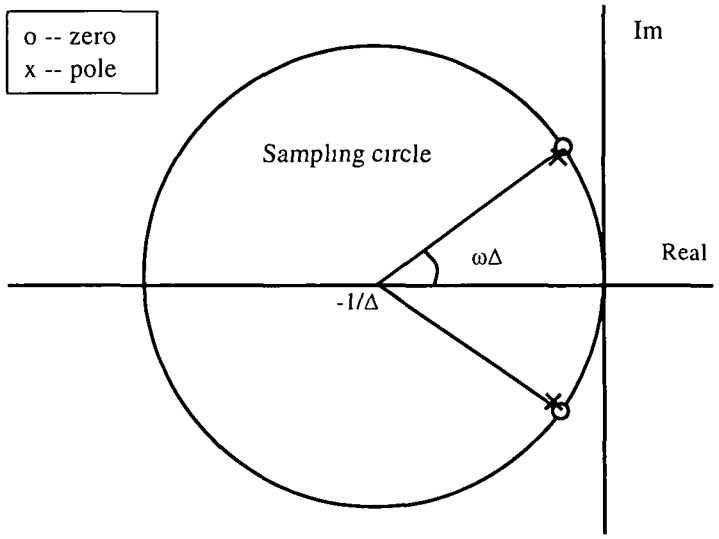

Figure 6.32: Location of zeros for notch filter to remove 60 Hz artifacts from ECG

Let γ_1 & γ_1^* are the zeros located at $\omega = \pm\frac{f_0}{f_c}(2\pi)$ then the location of poles must be $a\gamma_1$ & $a\gamma_1^*$ with a < 1/Δ for stability. Where γ_1^* is complex conjugate of γ_1. The resulting transfer function is

$$H(\gamma) = K\frac{(\gamma-\gamma_1)(\gamma-\gamma_1^*)}{(\gamma-a\gamma_1)(\gamma-a\gamma_1^*)} \tag{6.58}$$

Using equation (6.13) , $\gamma_1 = \frac{e^{j\omega\Delta}-1}{\Delta}$ & $\gamma_1^* = \frac{e^{-j\omega\Delta}-1}{\Delta}$ & selecting $K = a^2$ for unity dc gain, the filter transfer function is

$$H(\gamma) = \frac{a^2\left[1+\frac{2}{\Delta}(1-\cos\omega\Delta)\,\gamma^{-1}+\frac{2}{\Delta^2}(1-\cos\omega\Delta)\,\gamma^{-2}\right]}{\left[1+\frac{2a}{\Delta}(1-\cos\omega\Delta)\,\gamma^{-1}+\frac{2a^2}{\Delta^2}(1-\cos\omega\Delta)\,\gamma^{-2}\right]} \tag{6.59}$$

Where $(\gamma_1+\gamma_2) = \frac{2(\cos\omega\Delta-1)}{\Delta}$

$$\gamma_1\gamma_2 = \frac{2}{\Delta^2}(1-\cos\omega\Delta)$$

Where the bandwith of the notch is considered 4 Hz. Magnitude and phase responses for the filter given in equation (6.59) with sampling frequency 1000 Hz, Notch

frequency f_0 = 60 Hz and band width 4 Hz are shown in figure 6.33. Figure 3.34 and 3.35 shows filtering process of 60 Hz power line interference in ECG signal and FFT of the ECG signals. From FFT plot it is noticed that 60 Hz power line interference which is present in the original ECG is removed using notch filter in delta domain.

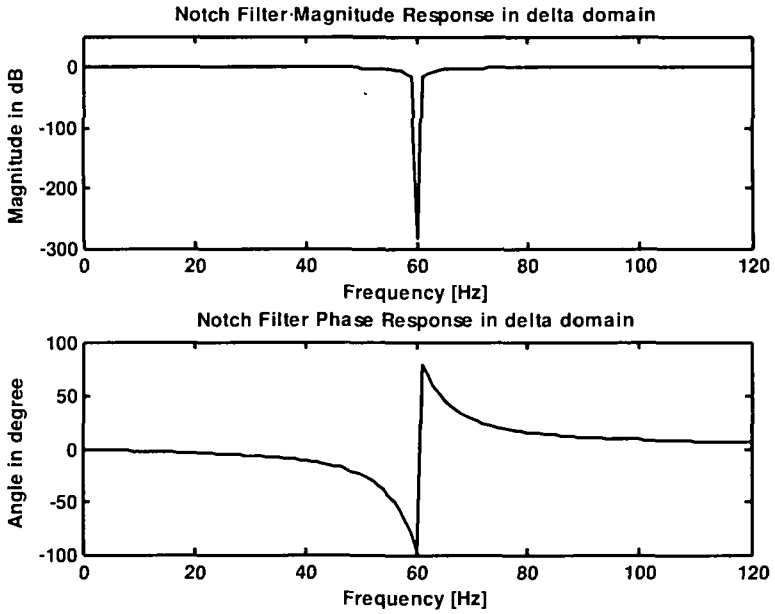

Figure 6.33 Magnitude and phase response of Notch filter with sampling frequency 1000 Hz, notch frequency 60 Hz and bandwidth 4 Hz

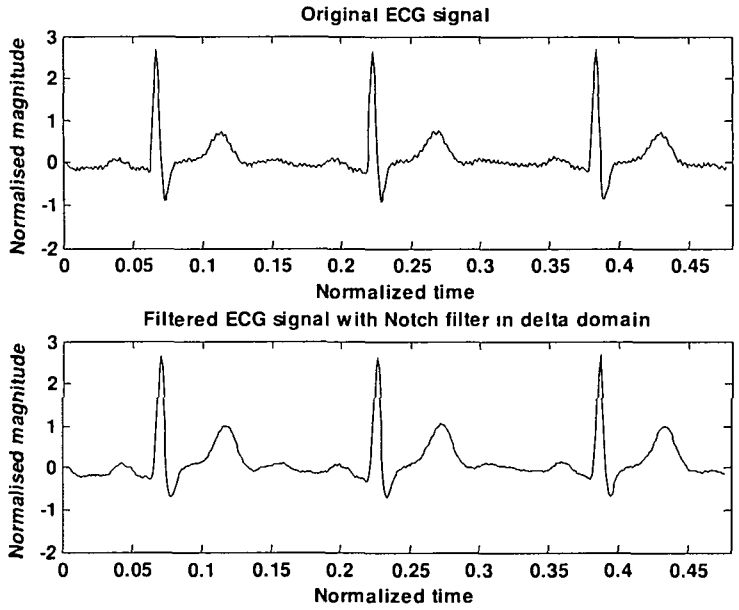

Figure 6.34: ECG signal filtered with Notch filter in delta domain with f_0 =60 Hz, f_s=1000 Hz and delF = 4 Hz

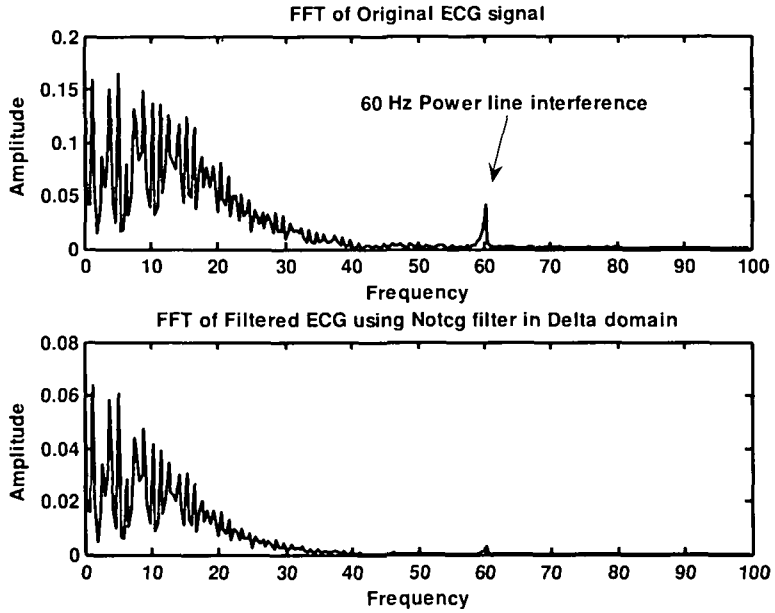

Figure 6.35: FFT of ECG signal filtered with Notch filter

6.4 Conclusion:

In this chapter we have investigated problems posed by artifacts, noise and interference of various forms in the acquisition and analysis of ECG signals. Different types of time and frequency domain digital filters in delta domain have been developed. Simulation results show that the filters designed in delta domain is as good as the filter designed in other domain. However number of adder and multiplier required for delay element in delta domain is more. Since sampling zeros are inducted, care must be taken while considering these sampling zeros otherwise the filter may be unstable and will show unsatisfactory performance.

Different filters may be suitable for different problems of biomedical signal analysis. It is unlikely that a single filter will address all of the problems hence the requirements are wide as per practical situations and applications. Attempts must be made at the outset to acquire artifact free signals to the extent possible.

Chapter 7

Conclusions and Future Recommendations:

7.1 Summary

The primary objective of this thesis is to present a unified framework for modelling of dynamical systems in discrete-time domain using the properties of delta operator and complex delta domain by using the properties of gamma transform. To develop systematic design procedure for a control system that retains the stability and performance characteristics of the classical designs, two methods of controller design have been discussed by capitalizing the computational capabilities of delta operator time moments and Genetic Algorithms. The result is a unified framework for control system that unify both discrete-time and continuous-time control together. The proposed design philosophy consists of constructing a reference model in the complex delta domain from the given time, frequency and complex domain specifications. First, the reference model parameters are determined from the initial specification of the control law. Secondly, a variant of time moments are developed in the complex delta domain called OGDTM and OFF in which Genetic algorithms, the artificial intelligence tools are used to search a set of either real or complex frequency points after minimising a scalar cost function. The cost function is developed between the step responses of the reference model and the controlled systems cascading controller with plant. Finally, OGDTM and OFF are used to obtain t he parameters of the controller using a sub class of Pade method. The computational framework developed is algebraic in nature and require solution of a set of linear equations only.

The design philosophy based on model matching control is a well-known procedure for applying in linear control theory that is widely applicable, especially in the aerospace and chemical processes industry. The model matching approach allows the formulation of the problem in such a way that the design specifications, both in time and frequency domains, are selected at the outset. This is in contrast to many design techniques in which the closed-loop model of the controlled system is not known until late in the design process. This unified approach for controller design for delta operator parameterized discrete-time systems has been shown to work well for SISO and MIMO systems and system

with time delays and as the sampling time (Δ) is decreased, the results approach the continuous-time results in the limit $\Delta \rightarrow 0$. Thus the proposed methods of the thesis are viable general in nature and may replace prevalent z-domain methods for model reduction and controller design. The thesis also deals with design of digital filter for biomedical signal processing utilising the properties of delta operator in which the technique developed is utilised to design digital filters which are fundamental to digital signal processing. Several time and frequency domain filters have been discussed and tested to reduce ECG artifacts.

7.2 Conclusions

The foundations have been laid for a novel approach to designing control systems that make the most of prior knowledge and experience, while capitalizing on the broader capabilities of model matching control theory and computational genetic algorithms. The principles introduced can be applied to SISO, MIMO and systems with time delays. Genetic algorithms are used for selection of a set of frequency points. These frequency points are GA parameters. These GA parameters are coded into binary strings called chromosome. A cost function is developed between the step response of the reference model and the overall controlled system. During evaluation of GA, this cost function is minimised to obtain the optimal frequency points based on which OGDTM and OFF are computed. GA is a global optimal search technique and therefore by intuitively selecting the search space, number of parameters, population size, crossover and mutation probability and selection methods like tournament or Roulette wheel it is possible to achieve global optimal solution.

7.3 Recommendations

The main recommendation for future work is to expand upon the findings of this thesis to investigate OGDTM and OFF for system identification and adaptive control system. Since the approach is iterative and relies heavily on computation, a rigorous analysis of the algorithms presented can be related to the first objective. In particular, it would be relevant to determine the worst-case computation times and error bounds with respect to the dimensions of the systems and control, as well as the number of stages. The algebraic techniques developed, together with existing theories on delta operator, time moment and GA show particular promise in this direction. Alternatively, other classical designs could be used in association with GA or other

artificial intelligence tools for minimisation of the performance index. The investigation using GA should remain a key ingredient in the process, as the GAs determine the class of control and cost functionals that can be approximated and, therefore, the optimal control problems that can be solved. One of the most desirable features of this approach is its flexibility. Not only is it unrestricted by the form of the governing dynamic equation, but it allows for extensions that can deal with system identification, stochastic processes and disturbances to name a few. The range of possibilities is at least as diverse as are the GA applications that already exist today in the literature. In particular, designs that can benefit both from *a-priori* and *a-posteriori* knowledge of the system would be ideal. Finally, there is considerable interest in the field for high-dimensional problems, where the system and control have many variables. Hence, the study of computation complexity should be a major focus of any solution method pursued hereon.

Biomedical signal processing is the area in which very less work is done in delta domain framework. There is ample scope in this field for modelling and problem specific digital filter design using the robust characteristics of delta operator.

Bibliography:

[1] Middleton R.H. and Goodwin G.C. "Improved finite word length characteristics in digital control using delta operator," *IEEE Trans. on Automatic Control*, vol. AC-31, no. 11, pp. 1015 - 1021, Nov. 1986.

[2] Ragazzaini J.R. and Franklin G.F., Sampled-Data Control Systems, *Mc-Graw Hill*, New York, 1958.

[3] Kuo B.C., Digital Control Systems, *Oxford University Press*, New York, 1992.

[4] Ogata K., Discrete-time Control Systems, *Prentice Hall, Englewood Cliffs*, New Jersey, 1987.

[5] Astorm K.J., Wittenmark B. and Workman M., "Computer Controlled Systems, Theory and Design", *Pearson Education Asia Pte. Ltd*, India, 2000.

[6] Franklin G.F. and Powell J.D., "Digital Control of Dynamic Systems", *Addison-Wesley*, Reading, India, 2000.

[7] Middleton R.H. and Goodwin G.C.,"High-speed digital signal processing and control," *Proc. IEEE*, vol. 80, no. 240, pp. 240 258, 1992.

[8] Gupta S.C., "Transform and State Variable Analysis in Linear Systems", *John Wiley,* New York, 1966.

[9] Neuman C.P., "Transformations between delta and forward shift operator transfer function models," *IEEE, Trans. on SMC*, vol. 23, no. 1, pp. 295 296, 1993.

[10] Middleton R.H. and Goodwin G.C., "Digital Control and Estimation: A Unifed Approach", *Prentice Hall*, New Jersey, 1990.

[11] Mukhopadhyay S., Patra A. and Rao G.P., "New class of discrete-time models for continuous-time systems," *International Journal of Control*, vol. 55, no. 5, pp. 1161-1187, 1992.

[12] Young P., Chotai A., McKenna P. and Tych W., "Proportional-integral plus (PIP) design for (δ) operator systems part 1. SISO, part 2. MIMO," *International Journal of Control,* vol. 70, pp. 123 167, 1998.

[13] P.Sarkar et. All, "A unified approach for controller reduction in delta domain", *IETE Journal of Research,* Vol-50, No-5, pp-373-375, 2004

[14] Sarkar.P et. All, "Controller Design in delta domain using generalized moment matching", *AMSE Journal,* Vol-61, No-1, PP-43-62, 2006.

[15] Lauritsen M.B. and Rostgaard M., "Delta-operator predictive control," *Proc. of the 36th IEEE Conference on Decision and Control*, vol. 1, pp. 884 889, 1997.

[16] Janecki D.,"Model reference adaptive control using the delta operator," *IEEE Trans. on Automatic Control,* vol. 33, no. 8, pp. 771 775, 1998.

[17] Masaru Sakamoto, Tadashi Matsushita, Yoshiki Mizukami and Kanya Tanaka, "Model Reference Adaptive Control Using Delta Operator with Neural Network for Pneumatic Servo System," pp-771-776, *SICE*, Aug 5-7, 2002, Osaka

[18] Erwin R.S. and Bernstein D.S., "Fixed-structure discrete-time H_2- optimal controller synthesis using the delta operator," *Proc. of the American Control Conference,* vol. 5, pp. 3185 -3189, 1997.

[19] Erwin R.S. and Bernstein D.S.,"Fixed-structure discrete-time mixed H_2/H_∞ controller synthesis using the delta-operator," *Proc of the 1997 American Control Conference*, vol. 5, pp. 3526-3530, 1997.

[20] Tadjine M., M'Saad M. and Dugard L.,"Discrete-time compensators with loop transfer recovery," *IEEE Trans. on Automatic Control*, vol. 39, no. 6, pp. 1259-1262, 1994.

[21] Lee, L.H., Goodwin G. and Kolodziej W., "Interconnections between continuous and discrete games with applications to H1," Proc. *of the 29th IEEE Conference on Decision and Control,* vol. 1.4, pp. 2425 -2430, 1990.

[22] Kyu-Hong Shim, Chariya Loescharataramdee,Edwin M. Sawan, King, "H-infinity Design for Two-Time-Scale Systems by Unified Approach using Delta Operators", *IEEE Trans* 0-7803-4547-9/98/$ 10.0/ 1998.

[23] P.Suchomski, "Robust PI and PID controller design in delta domain",. *IEE Proc.-Control Theory Appl.*, pp. 350.354, Sept. 2001.

[24] Hui-Guang Li, Xu-Dong Zhu, Ping Shun Wang, "Optimal Control Law of Robot Based On Delta Operator In Visual Servoing", *Procedings of the 3rd International Conference on Machine Learning and Cybernetics,* Shanghai, pp-533-537, 2004.

[25] Bengt Lennartson, Rick Middleton, Anna-Karin Christiansson and Tomas McKelvey, "Low Order Sampled Data H∞ Control using the Delta Operator and LMIs", *43rd IEEE Conference on Decision and Control* December 14-17, 2004.

[26] Kai-yu Wu, Yan-ming Fu and Shuang Li, "A Delta-operator Approach to Robust Stabilization for Uncertain Time-delay Systems with Jumping Parameter", *Proc, 6th World Congress on Intelligent Control and Automation,* China, pp 481- 485, 2006,

[27] Wang Qing,Ma Kemao, "Robust Stabilization and Robust H∞ Control of Uncertain Delta Operator Systems", *Proc. of the 26th Chinese Control Conference* July 26-31, 2007, Zhangjiajie, China.

[28] Qiu Jiqing, Yang Hongjiu, Xia Yuanqing, Zhang Jinhui, Gao Zhifeng, " Robust Stabilizatio for a class of discrete-time systems with delays via delta operators approach", *26th Chinese Control Conference*, pp 49-53, July 26-31, 2007.

[29] Linbo Xie, Weiyi Zhao and Zhicheng Ji, " LQG Control of Networked control system with long time delays using δ-operator", Proc. *6th International conference on Intelligent Systems Design an applications* (ISDA 06), IEEE.

[30] A. K. Ziarani and A. Konrad, "A nonlinear adaptive method of elimination of power line interference in ECG signals," *IEEE Trans. Biomed. Eng.*, vol. BME-49, no. 6, pp. 540–547, Jun. 2002.

[31] Markku Eraluoto and Iiro Harţimo, "Reducing Implemention Complexity of Fast Sampled Digital IIR Filters", pp *27* 1 - 274, *ICECS '96.*

[32] P.Tanelz Harp, Juha Kauraniema, and Seppo J. Ovaslca, *"Magnitude Response Optimization of Delta Opertaor Filters", Proceedings of ICSP* ' 96.

[33] Markku Eraluoto and Iiro Hartimo, "Design of Low-Power Narrowband Digital IIR Filters Using Delta Operator", 0-7803-3694-/19 7/$10.00 ©1997 *IEEE.*

[34] Fan H., "Delta-operator based efficient stability tests," *Proc. of the American Control Conference,* vol. 4, pp. 2508- 2512, 1997.

[35] Poor H.V.,"Delta-operator based signal processing: fast algorithms for rapidly sampled data," *Proc. of the 36th IEEE Conference on Decision and Control,* vol. 1, pp. 872- 877, 1997.

[36] R. Vijayan, H.V. Poor, "Lattice filters based on the delta operator", *IEE Proc.-Image Signal Process.,* Vol. 144, No. 3, June 1997.

[37] Juha Kauranietni', Titno I. Luakso2, Iiro Hartitmo', and Seppo J. Ovaska3, "Roundoff noise minimization in a direct form Delta operator structure", *proc. IEEE,* pp-1371-1374,. 1996

[38] Juha Kauraniemi, Timo I. Laakso, Iiro Hartimo, and Seppo J. Ovaska, "Delta Operator Realizations of Direct-Form IIR Filters", *IEEE Trans on Circuits and Systems-II: Analog and Digital Signal Processing,* Vol. 45m No. 1, pp 41 - 52, 1998

[39] Kyu-Hong Shim, M.Edwin Sawan, "Kalman Filter Design for Singularly Perturbed Systems by Unified ApproachnUsing Delta Operators", *Proceedings of the American Control Conference* San Diego, California 9 June 1999.

[40] M. B. Naumović and M. R. Stoji´c, "Comparative study of finite word length effects in digital filter design via the shift and delta transforms",. *Electrical Engineering,* vol. 82, pp. 213-216, Mar. 2000.

[41] Ngai Wong and Tung-Sang Ng, "Roundoff Noise Minimization in a Modified Direct-Form Delta Operator IIR Structure", *IEEE Trans on Circuit and Systems-II: Analog and Digital Signal Processing,* Vol. 47, No. 12, Dec 2000

[42] M.J.Newman and D.G.Holmes, "Delta Operator Digital Filters for High Performance Inverter Applications", pp 1407-1412, *0-7803-7262-*X/02/$10.00 © 2002 IEEE.

[43] Benson R.W., Bobrow J.E.and Jabbari F., "Experiments in system identification and pole-zero placement control using delta formulations," *Proc. of the 29th IEEE Conference on Decision and Control,* vol. 2, pp. 991 -993, 1990

[44] Wilkinson A.J., Roberts S., Taylor P.M. and Taylor G.E., "The application of recursive identification based on delta operators," *International Conference on Control,* vol. 1, pp. 627 -631, 1991.

[45] Soderstrom T., Fan H., Carlsson B. and Mossberg M., "Some approaches on how to use the delta operator when identifying continuous-time processes," *Proc. of the 36th IEEE Conference on Decision and Control,* vol. 1, pp. 890 -895, 1997.

[46] Soderstrom T., Fan H., Carlsson B., Mossberg M. and Yuanjie Zou, "Estimation of continuous-time AR process parameters from discrete time data," *IEEE Trans. on Signal Processing,* vol. 47, no. 5, pp. 1232-1244, 1999.

[47] Gessing R.,"Identification of shift and delta operator models for small sampling periods," *Proc. American Control Conference,* vol. 1, no. 1, pp. 346-350, 1999.

[48] Tinglun Song, Emmanuel G. Collins, Jr.and Robert H. Istepanian, "Improved Closed-Loop Stability for Fixed -point Controller Implementation Using the Delta Operator", *Proc. American Control Conference* San Diego, California June 1999.

[49] Zakian V., "Simplification of linear time invarient systems by moment approximants," *International Journal of Control*, vol. 18, no. 3, pp. 455-460, 1973.

[50] Bosley M. J., Kropholler H. W. and Lees F.P., "On the relation between the continued fraction expansion and moments matching methods of model reduction," *International Journal of Control*, vol. 18, no. 3, pp. 461-474, 1973.

[51] Shih Y.P. and Shieh C.S., "Model reduction of continuous and discrete multivariable systems by moment matching," *Computer and Chemical Engineering.*, vol. 2, pp. 127-132, 1978.

[52] Bultheel A. and Van Barel M., "Pade techniques for model reduction in linear system theory-a survey," *Journal of Computational and Applied Mathematics,* vol. 14, pp. 401-438, 1986.

[53] Rosenbrock H.H., "Design of multivariable control systems using inverse Nyquist array" *Proc. IEE*, vol. 116, no. 11, pp. 1929 -1936, 1969.

[54] MacFarlane A.G.J., "A survey of some recent results in linear multivariable feedback theory," *Automatica*, vol. 8, pp. 455-492, 1972.

[55] Mayne D.Q., "The design of linear multivariable system," *Automatica*, vol. 9, pp. 201 -208, 1973.

[56] Hung N.T. and Anderson B.D.O., "Triangularization technique for the design of multivariable control system," *IEEE Trans. on Automatic Control,* vol. AC-24, no. 3, pp. 455- 460, 1979.

[57] Stanley B., Quinn Jr. and Sanathana C.K., "A comparative study of controller design techniques," *Proc. 18th Annual Pittsburgh Conference on Modelling and Simulation,* 1987.

[58] D'Azzo J.G., "Automatic Feedback Control Systems Synthesis", *McGraw Hill*, New York, 1981.

[59] Tzasfestas S.G. (Ed.), *"Applied Digital Control", North Holland, Amsterdam*, 1985.

[60] Hanselmann H., "Implementation of digital controllers - a survey," *Automatica*, vol. 23, no. 1, pp. 1 -32, 1987.

[61] Rattan K.S., "Compensating for computational delay in digital equivalent of continuous control systems," *IEEE Trans on Automatic Control*, vol. 34, no. 8, pp. 895-899, 1989.

[62] Halawa J., "Comments on a new frequency domain technique for the simplification of linear dynamic systems and method for frequency domain simplification of tranfser functions," *International Journal of Control*, vol. 41, no. 1, pp. 297-301, 1985.

[63] Shi J. and Gibbard M.J., "Discrete system models based on simple performance specifications in the time, frequency or complex z-domains," *International Journal of Control,* vol. 42, no. 2, pp. 529 - 538, 1985.

[64] Janiszowski K., "A linear digital controller for single loop control systems," *International Journal of Control*, vol. 37, no. 1, pp. 159- 174, 1983.

[65] Zafiriou E. and Morari M., "Digital controllers for SISO systems : a review and a new algorithm," *International Journal of Control*, vol. 42, no. 4, pp. 855- 876, 1985.

[66] Houpis C.H. and Lamont G.B., "Digital Control Systems", *Prentice Hall, Englewood Cliffs,* New Jersey, 1985.

[67] Whitbeck R.F. and Hofmann L.G., "Digital control law synthesis in the w'-domain," *J. Guidance and Control*, vol. 1, no. 5, pp. 319-326, 1978.

[68] Knowles J.B., "Comprehensive, yet computationally simple, direct digital control systems design technique," *Proc. IEEE*, vol. 125, pp. 1383-1395, 1978.

[69] Inooka H., Obinata G. and Takeshima M., "Design of digital controller based on series expansions of pulse transfer functions," *Trans ASME, J. Dynamic Systems, Meas.and Control,* vol. 105, pp. 204-208, 1983.

[70] Inooka H., Watanabe T. and Imai Y., "Design of digital controllers for double loop systems based on series expansions," *International Journal of System Science*, vol. 19, no. 8, pp. 1539-1546, 1988.

[71] Porat B. and Friedlander B., "An output error method for reduced order controller design," *IEEE Trans. on Automatic Control*, vol. 29, no. 7, pp. 629-631, 1984.

[72] Obinata G., Nakamura T. and Inooka H., "An equation error method for the design of digital controllers," *IEEE Trans. on Automatic Con*trol, vol. 5, no. 3, pp. 123-135, 1988.

[73] Forsythe W., "Algorithms for digital control," *Trans. Inst. Meas. Control,* vol. 5, no. 3, pp. 123-135, 1983.

[74] Forsythe W., "A new method for the computation of digital fillter coefficients," *Simulation,* vol. 44, no. 1, pp. 23 31 and 75- 80, 1985.

[75] Kucera V., "Exact model matching, polynomial equation approach," *International Journal of System Science,* vol. 12, no. 12, pp. 1477-1484, 1981.

[76] J. Pal, " Control system design using approximate model matching", *System science (Poland)*, vol. 19, no. 3, pp. 5-23, 1993.

[77] Jr. Collins E.G. and Tinglun S., "A delta operator approach to discrete time H_∞ control," *International Journal of Control*, 1 vol. 72, no. 4, pp. 315-320, 1999.

[78] Katab A., Jury E.I. and Premaratne K., "Robust stability of delta operator discrete-time systems using frequency-domain graphical approach," *Proc. 34th IEEE Conference on Decision and Control, vol.* 1, pp. 774-779, 1995.

[79] Molchanov Alexander P. and Peter H. Bauer, "Robust stability of linear time-varying delta-operator formulated discrete-time systems," *IEEE Trans. on Automatic Control*, vol. 44, no. 2, pp. 325-327, 1999.

[80] J.H.Holland, "Adaptation in Natural and Artificial Systems", *Ann Arbor, MI Univ. Michigan Press,* 1975.

[81] D. E. Goldberg, 'Genetic Algorithms in Search, Optimisation, and Machine Learning', *Addison Wesley, Reading, 1989.*

[82] Alen Varsek, Tanja Urbancic and Bodgan Filipic, *"Genetic Algorithms in Controller Design and Tuning", IEEE Trans of Systems, Man and Cybernetics,* Vol. 23, No-5. 1993.

[83] B Porter and D L Hicks, "Genetic Robustification of Digital Model Following Flight Control Systems", *IEEE Trans* pp-556-570, 1994.

[84] B Porter and D L Hicks, "Genetic Design of Unconstrained Digital PID Controllers", *IEEE trans* pp-478-485, 1995.

[85] Jones A.H and De Moura Oliveira P B, "Genetic Auto Tuning of PID Controllers", *IEE Proc* No 414, pp-141-145, 1995.

[86] Bor-Sen Chen, Yu-Min Cheng and Ching Hsiang Lee, "A Genetic Approach to Mixed H_2/H_∞ Optimal PID Control", *IEEE trans* No-4, pp-51-59, 1995

[87] Jones A.H, Ajlouni N and Uzam M, "On line frequency domain identification and genetic tuning of PID controllers", *IEEE trans* No-5, pp-261-265, 1996.

[88] Sourav Kundu & Seiichi Kawata, " Genetic Algorithms for Optimal feedback Control Design", *Trans Engng Applic. Artif Intell* Vol. 9, No 4, pp 403-411 1996.

[89] Gary J Gray, Yun Li et all, "The Application of Genetic Algorithms to Gain Scheduling Controller Analysis and Design", *IEE Proc, Genetic algorithms in Engineering Systems: Innovation and applications,* No-446, pp-364-368, 1997.

[90] M. Reformat, E Kuffel, D Woodford and W Padrycz, "Application of genetic algorithms for control design in power systems", *IEE Proc* Vol. 145, 1998.

[91] S.M.Badran, H.N.Al-Duwaish, "Optimal output feedback controller based on genetic algorithms", *Elsevier Science SA, Electric Power Systems Research* 50, pp 7-15, 1999.

[92] Y.J.Cao and Q.H.Wu, " Optimization of control parameters in genetic algorithms: a stochastic approach", *International Journal of System Science*, Vol 30, No-2, pp-551-559, 1999.

[93] Mehdi Nasri, Hossein Nezamabadi pour and Malihe Maghfoori, "A PSO Based Optimum Design of PID Controller for a Linear Brushless DC Motor", *Proc. Of World Academy of Science Engg and Technology,* Vol. 20, pp-211-215, 2007.

[94] Arman Kiani B an Naser Pariz, "Fractional PID Controller Design Based on Evolutionary Algorithms for Robust two inertia Speed Control", *Proc First Joint congress on fuzzy an Intelligent Systems,* Iran, 2007.

[95] Donghal Li, Furong Gao, Yali Xue and Chongde Lu, " Optimization of Decentralized PI/PID Controllers Based on Genetic Algorithm", *Asian Journal of Control,* Vol. 9, No.3, pp 306-316, Sept. 2007.

[96] Mohsan Sayed Kazemi, " Designing Optimal PID Controller with genetic algorithms in view of controller location in the plant", *Proc. 7th WSEAS, International conference on Signal processing, Robotics an Automation,* pp-160-164, 2008.

[97] Peter H. Bauer , Roberto Castafieda & Kamal Premaratne, "Zero Input Behavior of Fixed-point Digital Filters in Delta-Operator Representation", *IEEE Proceedings of ASILOMAR-2 9*, pp-972-975, 1996

[98] Qiang Li, and H. Fan, " On Properties of Information Matrices of Delta-Operator based Adaptive Signal Processing Algorithms", IEEE *trans on signal processing,* vol. 45, no. 10, pp-2454-2467, 1997

[99] Kyu-Hong Shim, & M.Edwin Sawan, "Kalman Filter Design for Singularly Perturbed Systems by Unified Approach Using Delta Operators", *Proc. American Control Conference California*, pp-3873-3879 lune 1999.

[100] Ngai Wong and Tung-Sang Ng, "Roundoff Noise Minimization in a Modified Direct-Form Delta Operator IIR Structure", *IEEE trans. On circuits and systems—II: analog and digital signal processing*, vol. 47, NO. 12, pp-1533-1566, 2000

[101] C.Mehmet Hendekli and Ays¸in Ertüzün, "Design of a Multichannel Two-Dimensional Delta-Domain Lattice Filter for Noise Removal", *IEEE transactions on signal processing,*,vol. 49, NO. 7, pp -1581-1593, JULY 2001

[102] M.J. Newman and D.G. Holmes, "Delta Operator Digital Filters for High Performance Inverter Applications", *IEEE proc.* ,pp-1407-1412, *2002.*

[103] Hao Liu and Xiaohua Liu, "Guaranteed Cost Filtering for Polytypic Delta-Operator Uncertain Time Delay Systems", *Proc of 6th World Congress on Intelligent Control and Automation,* pp-2324-2326, 2006, China.

[104] Tompkins WJ, "Biomedical Digital Signal Processing", *Prentice-Hall,* Upper Saddle River, NJ, 1995

[105] Rangaraj M. Rangayyan, " Biomedical Signal Analysis a case study approach", *IEEE press*, 2001

[106] Patrick E. McSharry_, Gari D. Clifford, Lionel Tarassenko, and Leonard A. Smith, "A Dynamical Model for Generating Synthetic Electrocardiogram Signals", *Ieee Trans On Biomedical Engineering,* vol. 50, NO. 3, pp- 289-294, 2003.

[107] Alias Bin Ramli and Putri Aidawati Ahmad, " Correlation analysis for abnormal ECG signal Features extraction", *Proc. IEEE 4" National Conference on Telecommunication Technology Proceedings,* Malaysia , pp-232-237, 2003

[108] Ju-Won Lee and Gun-Ki Lee, "Design of an Adaptive Filter with a Dynamic structure for ECG Signal Processing,", *International Journal of Control, Automation, and Systems*, vol. 3, no. 1, pp. 137-142, March 2005.

[109] Reza Sameni, Mohammad B. Shamsollahi, Christian Jútten, and Gari D. "A Nonlinear Bayesian Filtering Framework for ECG Denoising", *IEEE Trans on Biomedical Engineering* , Vol. 54, No-12, pp-2172-2185, Dec.-2007.

[110] A Garcés Correa, E Laciar , H D Patiño & M E Valentinuzzi, "Artifact removal from EEG signals using adaptive filters in cascade", *proc. 16th Argentine Bioengineering Congress and the 5th Conference of Clinical Engineering,* Conference Series 90, pp 1-10, 2007.

[111] Astorm, K.J., Hagander P. and Sternby J., "Zeros of sampled systems," *Automatica*, vol. 20, pp. 31 38, 1984.

[112] Tesfaye A. and Tomizuka M., "Zeros of discretized continuous systems expressed in Euler operator an asymptotic analysis," *IEEE Trans. On Automatic Control*, vol. 40, no. 4, pp. 743 747, 1995.

[113] N.K.Sinha and G.P.Rao, "Identification of continuous Time systemes, Methodology and computer implementation", *Kluwer Academic Publishers*, 1991.

[114] Jury E.I., "Theory and Application of z-transform Method:, *John Wiley & Sons,* New York, 1964.

[115] Miline-Thomson L.M., "The Calculas of Finite Differences", *Macmillan,* London, 1960.

[116] Sanathanan C.K. and Quinn S.B, "Design of set point regulators for process involving time delay," *AIChE Jo*urnal, vol. 33, no. 11, pp. 1873-1881, 1987.

[117] H.N.Shankar, Ph.D Thesis titled "Adaptive control of general class of finite dimensional stable LTI systems", *IISC, Bangalore*, 2000.

[118] Chieh-Li Chen and Neil Murno, "Procedure to achive diagonal dominance using a PI/PID controller structure", *International Journal of control,* vol 50, no 5, pp 1771-1792, 1989.

[119] P. D. McMorran, S.M., "Design of gas-turbine controller using inverse Nyquist method", *Proc. IEE*, vol. 117, no. 10, pp. 2050-2056, 1970.

[120] Daniel L. Laughlin, Kenneth G. Jordan and Manfred Morari, " Internal model control and process uncertiainity: mapping uncertainity regions for SISO controller design", *International Jounal of Control*, vol. 44, no 6, pp 1675-1698, 1986.

[121] Wood R.K and Berry M.W., "Terminal composition of a binary distillation column", *Chemical Engineering Science*, vol. 28, pp 1707-1717, 1973

[122] A. Feuer and G. Goodwin, "Sampling in Digital Signal Processing and Control", *Boston: Birkh¨auser*, 1996.

[123] M. B. Naumovi´c, "Interrelationships between the one-sided discrete-time Fourier transform and one-sided delta transform",. *Electrical Engineering*, vol. 83, pp. 99. 101, May 2001.

[124] R. Middleton, "Delta toolbox for use with MATLAB", *Natick, MA: MathWorks, Inc.*, 1995.

[125] Hari c. Reddy et al, "Theory and test procedure for symmetries in the frequency response of complex Two-dimensional delta operator formulated discrete-time systems", *IEEE, international symposium on circuits and systems, H ong Kong pp-2373-2376, 1997*

[126] G. Li, .On the structure of digital controllers with finite word lenght consideration,.

IEEE Trans. Automat. Contr., pp. 689.693, May 1998.

[127] C. B. Rorabaugh, *"Digital Filter Designer's Handbook: With C++ Algorithms" 2nd ed. New York: McGraw Hill*, 1997.

[128] C.-T. Chen, "Digital Signal Processing: Spectral Computation and FilterDesign" *1st ed. New York: Oxford University Press,* 2001.

[129] Farooq Husain, "Digital Signal Processing and Applications", 2nd ed, *Umesh Publications*, India, 2004

[130] Rushmer R.F. Cardiovascular Dynamics, *W.B.Saunders, Philadelphia, PA, 4th edition,* 1976.

[131]Yue-Der Lin and Yu Hen Hu, "Power-Line Interference Detection and Suppression in ECG Signal Processing", Ieee Transactions On Biomedical Engineering, vol. 55, no. 1, pp- 353-357, 2008

[132] Oppenheim AV and Schafer RW, "Discrete time Signal Processing", *Prentice Hall, Englewood Cliffs,* NJ 1989.

[133] Platt RS, Hajduk E.A., Hullinger M and Easton PA, "A modified Bessel filter for amplitude demodulation of respiratory electrocardiogram", *Journal of Applied Physiology,* 84(1): 378-388, 1998.

[134] Williams C.S., "Designing Digital Filters", *Prentice Hall, Englewood Cliffs*, NJ, 1986

[135] Haykin S., "Modern Filters", *Macmillan,* NewYork, NY, 1989

[136] Sanjit K. Mitra "Digital Signal Processing", *TMH publication*, vol. 2 , Feb 2004.

[137]Hamming RW. "Digital Filters", Prentice Hall, Englewood Cliffs, NJ, 1983

[138] K. Kristinsson and G.A Dumont, "System identification and control using GAs", *IEEE trans*, SMC, pp 1033-1046, 1992.

[139] Michensen.M.L and Ostergaad K, "The use of residence time distribution data for estimation of parameters in the axial disperson model", *Chemical engineering Science,* vol. 25, pp 583-592, 1970.

Appendix-A

Discrete Data System Identification in Delta Domain:

A.1 Introduction:

Time moment matching methods are traditional tools widely used for parameter identification, particularly of chemical and flow processes. [138]. A major problem of parameter identification is that the higher moments are unreliable due to magnification of the signal tails. Michelsen [139] have applied weighted moment methods for parameter identification of axial dispersion model, in which moments of the signals were suitably modifiy by a damped exponential fitting. There are ample of literatures available on system identification in continuous and discrete z domain. Details of delta operator, delta time moment have already given in chapter-1 & chapter-3. Therefore we will discuss here the theory which is developed in delta operator framework for system identification using time moment matching method.

A.2 Ordinary delta time moments:

The i[th] ordinary moments of the distribution $f(k\Delta)$ is defined as

$$\begin{aligned} F(\gamma) &= \Delta\sum_{k=0}^{\infty} f(k\Delta)(1+\Delta\gamma)^{-k} \\ \frac{dF(\gamma)}{d\gamma} &= -\Delta\sum_{k=0}^{\infty} k\Delta f(k\Delta)(1+\Delta\gamma)^{-k-1} \\ &\vdots \quad \vdots \quad \vdots \\ \frac{d^{r}F(\gamma)}{d\gamma^{r}} &= (-1)^{r}\Delta\sum_{k=0}^{\infty} k\Delta(k\Delta+\Delta)\cdots(k\Delta+i\Delta-\Delta)(1+\Delta\gamma)^{-k-2} \end{aligned} \tag{A.1}$$

Ordinary Delta time moment about $\gamma = 0$ is defined as

$$\mu_{i} = \Delta\sum_{k=0}^{\infty}\frac{(k+i-1)!}{(k-1)!}\Delta^{i}f(k\Delta) \tag{A.2}$$

The Remann sum of equation (A.1) can be considered as the area of the distribution $f(k\Delta)$ by the weight

$$\frac{(k+i-1)!}{(k-1)!}\Delta^{i} \tag{A.3}$$

It can be noticed that as $t = k\Delta$ is large the weight also becomes large, and so increased emphasis is placed on the tails of the distribution. A better weight is one

which would approach zero for large value of $t = k\Delta$. A weight which could meet this requirement is

$$w_i(k\Delta) = \frac{(k+i-1)!}{(k-1)!}\Delta^i(1+\gamma\Delta)^{-(k+i)} \tag{A.4}$$

where γ is the real positive constant weighting factor.

A.3 Weighted time moments:

The weighting moments of the distribution $f(k\Delta)$ are defined as

$$M_i(\gamma) = \Delta\sum_{k=0}^{\infty}\frac{(k+i-1)!}{(k-1)!}\Delta^i f(k\Delta)(1+\Delta\gamma)^{-(k-i)} \tag{A.5}$$

Setting $\gamma = 0$ gives the ordinary moments, i.e.

$$M_i(0) = \mu_i \tag{A.6}$$

As γ increases, the weighting factor gives lesser emphasis to values of the signal when time is large. The zeroth weighted moments of $f(k\Delta)$ is is therefore the delta transform of the distribution i.e.

$$M_0(\gamma) = \Delta\sum_{k=0}^{\infty} f(k\Delta)(1+\Delta\gamma)^{-k} \tag{A.7}$$

if γ is taken as the delta transform variable, i.e

$$M_0(\gamma) = T[f(k\Delta)] = \bar{f}(\gamma) \tag{A.8}$$

Where T is the delta transform of the distribution $f(k\Delta)$. Since γ is chosen to be real, the delta transform strictly only applies along the real axis.

A.4 Properties of Delta Weighted Moments:

By using the properties of delta transform, simple derivation of the recurrence and linkage relations of the weighted moments is obtained as:

A.4.1 The Recurrence Relation:

From the properties of the delta transform [10]

$$T\left[\frac{(k+i-1)!}{(k-1)!}\Delta^i f(k\Delta)\right] = (-1)^i\frac{d^i}{d\gamma^i}(\bar{f}(\gamma)) \tag{A.9}$$

Therefore from equation (A.5) it is seen that

$$M_i(\gamma) = (-1)^i\frac{d^i}{d\gamma}(\bar{f}_i(\gamma)) \tag{A.10}$$

and corresponding recurrence relation can be written as as

$$M_{i+1}(\gamma) = -\frac{d}{d\gamma}(M_i(\gamma)) \tag{A.11}$$

These recurrence relations are utilized for determinations of the relationship between the weighted moments and model parameters.

A.4.2 The Linkage Relation:

The application of the conservation laws to a linear time invariant systems allows to establish relationships between input signal to the system $x(k\Delta)$, the output of the system $y(k\Delta)$ and $h(k\Delta)$, the impulse response of the system are linked by the convolution integral, i.e.

$$y(k\Delta) = \Delta\sum_{n=0}^{k\Delta} h(n\Delta)x(k\Delta - n\Delta) \tag{A.12}$$

Taking delta transforms

$$\bar{y}(\gamma) = \bar{x}(\gamma).\bar{h}(\gamma) \tag{A.13}$$

Hence from relation (14)

$$M_0(\gamma)_{output} = M_0(\gamma)_{system}.M_0(\gamma)_{input} \tag{A.14}$$

This gives a relation linking zeroth weighted moments of the input, output and system. Taking derivatives with respect to γ and dividing by relation (A.14))

$$\left(\frac{M_1(\gamma)}{M_0(\gamma)}\right)_{output} = \left(\frac{M_1(\gamma)}{M_0(\gamma)}\right)_{system} + \left(\frac{M_1(\gamma)}{M_0(\gamma)}\right)_{input} \tag{A.15}$$

Hence the general i^{th} derivatives of (A.15) is

$$\left(\frac{M_i(\gamma)}{M_0(\gamma)}\right)_{output} = \sum_{l=0}^{i}\binom{i}{l}\left(\frac{M_{i-l}(\gamma)}{M_0(\gamma)}\right)_{system}\left(\frac{M_l(\gamma)}{M_0(\gamma)}\right)_{input} \tag{A.16}$$

Equaion (A.16) is the general linkage relation, relating the i^{th} order weighted moments of the input, output and the system.

A.5 Parameter Identification algorithm:

Let us consider a linear n^{th} order discrete time SISO system in transfer matrix representation in delta domain.

$$G_\delta(\gamma) = \frac{N_\delta(\gamma)}{D_\delta(\gamma)} = \frac{b_1 + b_2\gamma + \cdots\cdots + b_n\gamma^{n-1}}{a_1 + a_2\gamma + \cdots + a_n\gamma^{n-1} + \gamma^n} \tag{A.17}$$

The objective of the system identification is to determine the coefficients, a_i and b_i of eqn. (A.17) from the input-output data. Here we discuss the procedure to obtain the weighted moments from the delta transfer model and thereafter from input-output data to obtain an ARMA model. The order of the system is to be known a priori.

A.5.1 Weighted Moments from the Delta Transfer Function

The weighted delta time moments can directly be obtained from the delta transfer function of the impulse response $h(k\Delta)$. From the definition of the delta transform we have

$$G_\delta(k\Delta) = \Delta\sum_{k=0}^{\infty} h(k\Delta)(1+\Delta\gamma)^{-k} \qquad \text{(A.18)}$$

using the recurrence relation in (A.11), from eqn.(A.17) the delta transfer function can be written as

$$D_\delta(\gamma)G_\delta(\gamma) = N_\delta(\gamma) \qquad \text{(A.19)}$$

differentiating both sides of eqn.(A.19) with respect to γ gives

$$\sum_{p=0}^{i}(-1)^p\binom{i}{p}M_p(\gamma)D_\chi^{(i-p)}(\gamma) = N_\delta^{(i)}(\gamma)\ , \quad i = 0,1,2,3\cdots \qquad \text{(A.20)}$$

where

$$\binom{i}{p} = \frac{i!}{p!(i-p)!}$$

$$D_\delta^{(i)}(\gamma) = \frac{d^i(D_\delta(\gamma))}{d\gamma^i}$$

$$N_\delta^{(i)}(\gamma) = \frac{d^i(N_\delta(\gamma))}{d\gamma^i}$$

Equation (A.20) in matrix for can be represented as:

$$\begin{bmatrix} D_\delta^{(0)}(\gamma) & 0 & 0 & 0 & \cdots & 0 \\ D_\delta^{(1)}(\gamma) & D_\delta^{(0)}(\gamma) & 0 & 0 & \cdots & 0 \\ D_\delta^{(2)}(\gamma) & 2D_\delta^{(1)}(\gamma) & D_\delta^{(0)}(\gamma) & 0 & \cdots & 0 \\ D_\delta^{(3)}(\gamma) & 3D_\delta^{(2)}(\gamma) & 3D_\delta^{(1)}(\gamma) & D_\delta^{(0)}(\gamma) & \cdots & 0 \\ \cdots & \cdots & \cdots & \cdots & \cdots & \cdots \end{bmatrix} \begin{bmatrix} M_0(\gamma) \\ -M_1(\gamma) \\ -M_2(\gamma) \\ M_3(\gamma) \\ \cdots \end{bmatrix} = \begin{bmatrix} N_\delta^{(0)}(\gamma) \\ N_\delta^{(1)}(\gamma) \\ N_\delta^{(2)}(\gamma) \\ N_\delta^{(3)}(\gamma) \\ \cdots \end{bmatrix} \qquad \text{(A.21)}$$

where

$$D_\delta^{(i)}(\gamma) = \sum_{k=1}^{n+1}\frac{(k-1)!}{(k-i-1)}a_k\gamma^{(k-i-1)} \quad \text{and } a_{n+1=1}\ , \quad i = 0,1,2\cdots\cdots n$$

$$N_{\delta}^{(i)}(\gamma)=\sum_{k=1}^{n}\frac{(k-1)!}{(k-i-1)!}b_k\gamma^{(k-i-1)}\ ,\quad i=0,1,2\cdots\cdots(n-1) \qquad \text{(A.22)}$$

The weighted time moments $M_i(\gamma)$ can be easily obtained from eqn.(A.21).

A.5.2 Weighted moments from input output data

We can directly obtain the weighted time moments from the time-domain input-output data using eqns.(A.5) and (A.21). Rearranging eqn.(A.21), we have another form

$$\begin{bmatrix} M_0(\gamma) & 0 & 0 & 0 & \cdots & 0 \\ -M_1(\gamma) & M_0(\gamma) & 0 & 0 & \cdots & 0 \\ M_2(\gamma) & -2M_1(\gamma) & M_0(\gamma) & 0 & \cdots & 0 \\ -M_3(\gamma) & 3M_2(\gamma) & -3M_1(\gamma) & M_0(\gamma) & \cdots & 0 \\ \cdots & \cdots & \cdots & \cdots & \cdots & \cdots \end{bmatrix}\begin{bmatrix} D_{\delta}^{(0)}(\gamma) \\ D_{\delta}^{(1)}(\gamma) \\ D_{\delta}^{(2)}(\gamma) \\ D_{\delta}^{(3)}(\gamma) \\ \cdots \end{bmatrix}=\begin{bmatrix} N_{\delta}^{(0)}(\gamma) \\ N_{\delta}^{(1)}(\gamma) \\ N_{\delta}^{(2)}(\gamma) \\ N_{\delta}^{(3)}(\gamma) \\ \cdots \end{bmatrix} \qquad \text{(A.23)}$$

From eqn. (A.22) the relations between $D_{\delta}^{(i)}(\gamma)$ and a_i, and $N_{\delta}^{(i)}(\gamma)$ and b_i are known. The matrix forms are written as

$$\begin{bmatrix} D_{\delta}^{(0)}(\gamma) \\ D_{\delta}^{(1)}(\gamma) \\ D_{\delta}^{(2)}(\gamma) \\ \vdots \\ D_{\delta}^{(i)}(\gamma) \\ D_{\delta}^{n}(\gamma) \end{bmatrix}=\begin{bmatrix} 1 & \gamma & \gamma^2 & \gamma^3 & \cdots & \gamma^n \\ 0 & 1 & 2\gamma & 3\gamma^2 & \cdots & n\gamma^{(n-1)} \\ 0 & 0 & 1 & 6\gamma & \cdots & n(n-1)\gamma^{(n-2)} \\ \vdots & \vdots & \vdots & \vdots & \vdots & \vdots \\ 0 & 0 & 0 & 0 & \cdots & \dfrac{n!}{(n-i-2)!}\gamma^{(n-i)} \\ 0 & 0 & 0 & 0 & 0 & n! \end{bmatrix}\begin{bmatrix} a_1 \\ a_2 \\ a_3 \\ \vdots \\ a_i \\ 1 \end{bmatrix}$$

and

$$\begin{bmatrix} N_{\delta}^{(0)}(\gamma) \\ N_{\delta}^{(1)}(\gamma) \\ N_{\delta}^{(2)}(\gamma) \\ \vdots \\ N_{\delta}^{(i)}(\gamma) \\ N_{\delta}^{(n-1)}(\gamma) \end{bmatrix}=\begin{bmatrix} 1 & \gamma & \gamma^2 & \gamma^3 & \cdots & \gamma^{(n-1)} \\ 0 & 1 & \gamma & r^2 & \cdots & \gamma^{(n-2)} \\ 0 & 0 & 1 & \gamma & \cdots & \gamma^{(n-3)} \\ \vdots & \vdots & \vdots & \vdots & \vdots & \vdots \\ 0 & 0 & 0 & 0 & \cdots & \dfrac{n!}{(n-i-2)!}\gamma^{(n-i)} \\ 0 & 0 & 0 & 0 & \cdots & (n-1)! \end{bmatrix}\begin{bmatrix} b_1 \\ b_2 \\ b_3 \\ \vdots \\ b_i \\ b_n \end{bmatrix} \qquad \text{(A.24)}$$

The equation (A.24) is now substituted in equation (A.23) and hence we can obtain a matrix equation which can be easily solved to obtain the system parameters a_i and b_i for optimal weighted parameter value γ.

A 5.3 Discussion:

The method of parameter identification of discrete-data system in delta domain is developed matching optimal weighted moments. The simulation results using genetic algorithm for the optimum value of weighted moment are amplified in the later part i.e. as time is increased. Hence this algorithm is included in this appendix to constitute the scope of further work.

Appendix-1.1

Table of delta transforms and its region of convergence

Function f[k] $(k \geq 0)$	**Description**	**Delta Transforms** T **[f(k)]**	**Region of Convergence**
$\frac{1}{\Delta}\delta_k[k]$	Impulse	1	$\lvert\gamma\rvert < \infty$
1	Unit Step	$\frac{1+\Delta\gamma}{\gamma}$	$\left\lvert\gamma+\frac{1}{\Delta}\right\rvert > \frac{1}{\Delta}$
$\mu[k]-\mu[k-1]$		$\frac{1}{\Delta}$	$\lvert\gamma\rvert < \infty$
k	Ramp	$\frac{1+\Delta\gamma}{\Delta\gamma^2}$	$\left\lvert\gamma+\frac{1}{\Delta}\right\rvert > \frac{1}{\Delta}$
k^2	Parabola	$\frac{(1+\Delta\gamma)(2+\Delta\gamma)}{\Delta^2\gamma^3}$	$\left\lvert\gamma+\frac{1}{\Delta}\right\rvert > \frac{1}{\Delta}$
$e^{\alpha k\Delta}\quad \alpha \in C$	Exponential	$\frac{1+\Delta\gamma}{\gamma-\frac{e^{\alpha\Delta}-1}{\Delta}}$	$\left\lvert\gamma+\frac{1}{\Delta}\right\rvert > \frac{e^{\alpha\Delta}}{\Delta}$
$ke^{\alpha k\Delta}\quad \alpha \in C$	- do -	$\frac{(1+\Delta\gamma)e^{\alpha\Delta}}{\Delta\left(\gamma-\frac{e^{\alpha\Delta}-1}{\Delta}\right)^2}$	$\left\lvert\gamma+\frac{1}{\Delta}\right\rvert > \frac{e^{\alpha\Delta}}{\Delta}$
$\sin(\omega k\Delta)$	Sin wave	$\frac{(1+\Delta\gamma)\omega\sin c(\omega\Delta)}{\gamma^2+\Delta\phi(\omega,\Delta)\gamma+\phi(\omega,\Delta)}$ Where $\sin c(\omega\Delta)=\frac{\sin(\omega\Delta)}{\omega\Delta}$ and $\phi(\omega,\Delta)=\frac{2(1-\cos(\omega\Delta))}{\Delta^2}$	$\left\lvert\gamma+\frac{1}{\Delta}\right\rvert > \frac{1}{\Delta}$
$\cos(\omega k\Delta)$	Cosine wave	$\frac{(1+\Delta\gamma)(\gamma+0.5\Delta\phi(\omega,\Delta))}{\gamma^2+\Delta\phi(\omega,\Delta)\gamma+\phi(\omega,\Delta)}$	$\left\lvert\gamma+\frac{1}{\Delta}\right\rvert > \frac{1}{\Delta}$

Appendix 1.2

Properties of delta transform

Function f[k] $(k \geq 0)]$	**Description**	**Delta Transforms** T **[f(k)]**
$\sum_{i=1}^{I} a_i f_i[k]$	Partial fractions	$\sum_{i=1}^{I} a_i F_i[\gamma]$
$f[k+1]$	Forward shift	$(1+\Delta\gamma)(F(\gamma)-f[0])$
$\frac{f[k+1]-f[k]}{\Delta}$	Scaled difference	$\gamma F(\gamma)-(1+\Delta\gamma)f[0]$
$\sum_{l=0}^{k-1} f[l]\,\Delta$	Reimann sum	$\frac{1}{\gamma}F(\gamma)$
$f[k-1]$	Backward shift	$(1+\Delta\gamma)^{-1}(F(\gamma)-f[-1])$
$f[k-l]\,\mu[k-l]$		$(1+\Delta\gamma)^{-1}(F(\gamma)$
$k\,f[k]$		$-\frac{(1+\Delta\gamma)}{\Delta}\frac{dF(\gamma)}{d\gamma}$
$\frac{1}{k}f[k]$		$\int_{\gamma}^{\infty}\frac{F(\varsigma)}{1+\Delta\varsigma}d\varsigma$
$\lim_{k\to\infty} f[k]$	Final value theorem	$\lim_{\gamma\to 0}\gamma F(\gamma)$
$\lim_{k\to 0} f[k]$	Initial value theorem	$\lim_{\gamma\to\infty}\frac{\gamma F(\gamma)}{1+\Delta\gamma}$
$\sum_{l=0}^{k-1} f_1[l]\,f_2[k-l]\Delta$	Convolution	$F_1(\gamma)\,F_2(\gamma)$
$f_1[k]f_2[k]$	Complex convolution	$\frac{1}{2\pi j}\oint F_1(\varsigma)\,F_2\left(\frac{\gamma-\varsigma}{1+\Delta\varsigma}\right)\frac{d\varsigma}{1+\Delta\varsigma}$
$(1+a\Delta)^k\,f[k]$		$F_1\left(\frac{\gamma-a}{1+a\Delta}\right)$

Note: Here $F_i(\gamma) = T[f_i(k)]$ and $\mu[k]$ denotes a unit step.

Appendix B

Matlab Programs

% The following Matlab programs and sub routines are used to generated different

% parameters, plot step/ impulse resoponses and locate poles – zeros in gamma plane.

% For delta domain parameterisation, Delta tool box[124] and for optimization, FlexGA tool

% box is used. The values of ω_n, ξ, Sampling time Δ and angle ρ can be changed to get

% different responses and other parameters.

%Authors: N.C.Sarcar, M. Bhuyan & P. Sarkar

%Date of revision: 01/02/2004 to 21/01/09

%==========

Chapter 2 (Reference Model) Programs:

```
%This program plots figure 2.2 to 2.7 and computes table 2.1, 2.2 & 2.3
%of reference model parameters

clear all;
clc;
format short;
wn=0.84;    % Given natural frequency for reference model
zita=0.7;   % Given damping ratio
wd=wn*sqrt(1-zita^2);
delta=0.5;
s=-zita*wn+wd*i;    % Calculation of poles in s domain
g=s2del(s,delta);   % Calculation of poles in delta domain
cong=conj(g);       % Calculation of conjugate pole in delta domain
p=[g;cong];
rden=conv([1,-g],[1,-cong]); % Denominator polynomial in delta domain
wdt=wd*delta;
roh1=-40;
roh=(pi/180)*roh1;
alpha=roh;
z=((tan(roh-(pi/2))*(abs(g))^2))/(abs(real(g))*tan(roh-(pi/2)).
-abs(imag(g)));
tp1=(1/(wn*sqrt(1-zita^2)))*(atan((-zita/sqrt(1-zita^2)))-alpha+pi);
tp=tp1/delta;
A=rden(3)/abs(real(z));
rnum=A*[1 z];
B=rnum(2);
C=rden(2);
num=[A  B];       % Numerator of Open Loop Transfer Function.
den=[1 (C-A) 0]; % Denominator of Open Loop Transfer Function.
printsys(rnum,rden,'y');
figure(1);
t=0:delta:15;
ts=t/delta;
y=delstep(rnum,rden,t,delta);
plot(ts,y);
xlabel('t/delta','Fontsize',12);
```

```
ylabel('Amplitude','Fontsize',12);
title('Step Response of Reference Model','Fontsize',12)
figure(2);
[mag,pha,w]=delbode(num,den,delta);
[Gm,Pm,Wcg,Wcp]=margin(mag,pha,w);
title('Magnitude and Phase plot of Reference Model','Fontsize',12);
figure(3);
[RE,IM,W] = DELNYQ(num,den,delta);
title('Nyquist Plot of Reference Model','Fontsize',12);
figure(4);
y=delimp(rnum,rden,t,delta);
plot(ts,y);
xlabel('t/delta','Fontsize',12);ylabel('Amplitude','Fontsize',12);
 title('Impulse Response of Reference Model','Fontsize',12);
 figure(5);
 [RE,IM,W] = delnic(num,den,delta);
 title('Nicholas Plot of Reference Model','Fontsize',12);
 figure(6);
 delplane(-z,p,delta);
 axis([-4.9,0.5,-2.3,2.3]);
 title('Pole Zero plot of of Reference Model','Fontsize',12);
      disp('Angle');disp(roh1);disp('wd*delta');disp(wdt);
      disp('Ploes');disp(g);disp('zeros');disp(-z);
      disp('tp/delta');disp(tp);disp('A');disp(A);
      disp('B');disp(B);disp('C');disp(C);
      disp('Gain Cross Over Frequency');disp(Wcp);
      disp('Gain Margin');disp(Gm);
      disp('Pnase Cross over Frequncy');disp(Wcg);
      disp('Phase Margin');disp(Pm);
%=========================================================================
% This program is for figure 2.8 to 2.9
%For Positive angles +80 to 0 and for negative angles -80 to 0 degree
clear all;
clc;
format short
wn=0.84;zta=0.7;delta=0.1;gain=1;
wd=wn*sqrt(1-zta*zta);
s=-zta*wn+(wn*sqrt(1-zta^2))*i ;    % pole in s-domain
g=s2del(s,delta);                   % pole in delta-domain
cong=conj(g);
rden=conv([1,-g],[1,-cong]);
p=[g;cong];
for ro =-80:10:80
    roh=(pi/180)*ro;
    alpa=roh;
    z= ((tan(roh-(pi/2))*(abs(g))^2))/(abs(real(g))*tan(roh-(pi/2))
       -abs(imag(g)));
tp=(1/(wn*sqrt(1-zta*zta)))*(atan((-zta/sqrt(1-zta*zta)))-alpa+pi);
tp=tp/delta;
wdT=wd*delta;
mp=abs(sec(alpa))*sqrt(1-zta*zta)*...
exp((-zta/sqrt(1-zta*zta))*(atan((-zta/sqrt(1-zta*zta)))-alpa+pi));
mp=mp*100;
ts=(-log(0.05*abs(cos(alpa)))*(sqrt(1-zta*zta)))/(wd*zta);
ts=ts/delta;
```

```
A=gain*(rden(3)/abs(real(z)));
rnum=A*[1 z];
       printsys(rnum,rden,'y');
       t=0:delta:15;
       y=delstep(rnum,rden,t,delta);
       plot(t,y);
       %axis([0,15,-1.25,1.75]);
       hold on;
       pause;
end
      title('Step Response of Reference Model','Fontsize',12);
      xlabel('Time in seconds','Fontsize',12);
      ylabel('Amplitude','Fontsize',12);
      hold off;
```

%==========

% This program plots figure 2.10

```
clear all;
clc;
format short
wn=0.84;zta=0.7;delta=0.1;gain=1;
wd=wn*sqrt(1-zta*zta);
s=-zta*wn+(wn*sqrt(1-zta^2))*i ;    % pole in s-domain
g=s2del(s,delta);                   % pole in delta-domain
cong=conj(g);
rden=conv([1,-g],[1,-cong]);
for ro=-80:10:80
    roh=(pi/180)*ro;
    alpa=roh;
    z=((tan(roh-(pi/2))*(abs(g))^2))/ (abs(real(g))* tan(roh-(pi/2))...
       - abs(imag(g)));
    tp=(1/(wn*sqrt(1-zta*zta)))*(atan((-zta/sqrt(1-zta*zta)))-alpa+pi);
    tp=tp/delta;
    wdT=wd*delta;
    mp=abs(sec(alpa))*sqrt(1-zta*zta)*...
    exp((-zta/sqrt(1-zta*zta))*(atan((-zta/sqrt(1-zta*zta)))-alpa+pi));
    mp=mp*100;
    %mp=[mp;mp1];
    ts=(-log(0.05*abs(cos(alpa)))*(sqrt(1-zta*zta)))/(wd*zta);
    ts=ts/delta;
       A=gain*(rden(3)/abs(real(z)));
       rnum=A*[1 z];
       disp('Angle');disp(roh);
       printsys(rnum,rden,'y');
       t=0:delta:10;
       tp=t/delta;
       y=delstep(rnum,rden,t,delta);
       plot(tp,y);
       hold on;
      pause;
end
      title('Step Response of Reference Model','Fontsize',12);
      xlabel('t/delta','Fontsize',12);ylabel('Amplitude','Fontsize',12);
      hold off;
```

%==========

```
% This program computes location of poles and zeros of reference model
% and plots figure 2.11 in delta domain.

clear all;
clc;
format short
wn=0.84;zta=0.7;delta=0.5;gain=1;
ro=[80,60,40,20,1,-10,-20,-30,-40,-45];
wd=wn*sqrt(1-zta*zta);
s=-zta*wn+(wn*sqrt(1-zta^2))*i ;    % pole in s-domain
g=s2del(s,delta);                   % pole in delta-domain
cong=conj(g);
rden=conv([1,-g],[1,-cong]);
p=[g;cong];
for k=1:10
    roh=(pi/180)*ro(k);
    alpa=roh;
    z=((tan(roh-(pi/2))*(abs(g))^2))/(-abs(real(g))*tan(roh-(pi/2))
      + abs(imag(g)));
    z1=num2str(z);
    z2=num2str(conj(z));
    tp1=(1/(wn*sqrt(1-zta*zta)))*(atan((-zta/sqrt(1-zta*zta)))-alpa+pi);
    tp=tp1/delta;
    wdT=wd*delta;
    mp1=abs(sec(alpa))*sqrt(1-zta*zta)*...
    exp((-zta/sqrt(1-zta*zta))*(atan((-zta/sqrt(1-zta*zta)))-alpa+pi));
    mp=mp1*100;
    ts1=(-log(0.05*abs(cos(alpa)))*(sqrt(1-zta*zta)))/(wd*zta);
    ts=ts1/delta;
       A=gain*(rden(3)/abs(real(z)));
       rnum=A*[1 z];
       disp('Angle');disp(ro(k));disp('Poles');disp(p);
       disp('zero');disp(z);
       delplane(z,p,delta);
       axis([-4.1,0.5,-2.3,2.3]);
       hold on;
        pause;
end
      hold off;
      title('Pole Zero Plot of Reference Model in Delta domain',
      'Fontsize',12);
%=========================================================================

% This program computes location of poles and zeros and parameters of
%reference model and plots figure 2.12 in delta domain for different
%values of ωdΔ and plot in delta plane

clear all;
clc;
format short
zta=0.7;delta=0.5;gain=1;ro=-45;
wdt=[0.1,0.2,0.3,0.6,0.7,0.9,1.1,1.3,1.5];
Roh=[];P=[];Z=[];Tp=[];Wdt=[];Wn=[];Mp=[];Ts=[];A=[];B=[];C=[];D=[];
for k=1:9
    Wdt=[Wdt;wdt(k)];
    wd=wdt(k)/delta;
    wn=wd/sqrt(1-zta*zta);
```

```
    Wn=[Wn;wn];
    s=-zta*wn+(wn*sqrt(1-zta^2))*i ;    % pole in s-domain
    g=s2del(s,delta);                   % pole in delta-domain
    cong=conj(g);
    rden=conv([1,-g],[1,-cong]);
    p=[g;cong];
    P=[P;g];
    Roh=[Roh;ro];
    roh=(pi/180)*ro;
    alpa=roh;
    z=((tan(roh-(pi/2))*(abs(g))^2))/(-abs(real(g))*tan(roh-(pi/2))
     + abs(imag(g)));
    Z=[Z;z];
    tp1=(1/(wn*sqrt(1-zta*zta)))*(atan((-zta/sqrt(1-zta*zta)))-alpa+pi);
    tp=tp1/delta;
    Tp=[Tp;tp];
    mp1=abs(sec(alpa))*sqrt(1-zta*zta)*...
    exp((-zta/sqrt(1-zta*zta))*(atan((-zta/sqrt(1-zta*zta)))-alpa+pi));
    mp=mp1*100;
    Mp=[Mp;mp];
    ts1=(-log(0.05*abs(cos(alpa)))*(sqrt(1-zta*zta)))/(wd*zta);
    ts=ts1/delta;
      Ts=[Ts;ts];
      A1=gain*(rden(3)/abs(real(z)));
      rnum=A1*[1 z];
      A=[A;A1];
      B1=rnum(2);
      B=[B;-B1];
      C1=rden(2);
      C=[C;C1];
      D=[D;-B1];
      delplane(z,p,delta);
      axis([-4.9,0.5,-2.3,2.3]);
      hold on;
      pause;
end
      hold off;
      title('Pole Zero Plot of Reference Model in Delta domain',
      'Fontsize',12);

%=========================================================================
% This program plots figure 2.14

clear all;
clc;
format short
wn=0.84;roh=20;zta=0.7;delta=0.1;gain=1;
wdt=[0.1,0.2,0.3,0.4,0.5,0.6,0.7,0.9];
for k=1:8
    wd=wdt(k)/delta;
    wn=wd/sqrt(1-zta*zta);
    s=-zta*wn+(wn*sqrt(1-zta^2))*i ;    % pole in s-domain
    g=s2del(s,delta);                   % pole in delta-domain
    cong=conj(g);
    rden=conv([1,-g],[1,-cong]);
    roh=(pi/180)*roh;
```

```
    alpa=roh;
    z= ((tan(roh-(pi/2))*(abs(g))^2))/ (abs(real(g))* tan(roh-(pi/2))...
       -abs(imag(g)));
    A=gain*(rden(3)/abs(real(z)));
    rnum=A*[1 z];
    t=0:0.1:5;
    ts=t/delta
    y=delstep(rnum,rden,t,delta);
    plot(ts,y);
    hold on;
    pause;
end
    title('Step Response of Reference
    Model','FontName','Times','Fontsize',12);
    xlabel('t/delta','FontName','Times','Fontsize',12);
    ylabel('Amplitude','FontName','Times','Fontsize',12);
    hold off;

%=========================================================================
% This program plots figure 2.15 and computes table 2.5 parameters

clear all;
clc;
format short
wn=0.84;delta=0.5;gain=1;ro=-20;
zt=[0.3,0.4,0.5,0.6,0.7,0.8,0.9];
Roh=[];P=[];Z=[];Tp=[];Zt=[];Wdt=[];Wn=[];Mp=[];Ts=[];A=[];B=[];C=[];D=[];
for k=1:7
    zta=zt(k);
    Zt=[Zt;zta];
    wd=wn*sqrt(1-zta*zta);
    wdt=wd*delta;
    Wdt=[Wdt;wdt];
    s=-zta*wn+(wn*sqrt(1-zta^2))*i ;    % pole in s-domain
    g=s2del(s,delta);                   % pole in delta-domain
    cong=conj(g);
    rden=conv([1,-g],[1,-cong]);
    p=[g;cong];
    P=[P;g];
    Roh=[Roh;ro];
    roh=(pi/180)*ro;
    alpa=roh;
    z=((tan(roh-(pi/2))*(abs(g))^2))/(-abs(real(g))*tan(roh-(pi/2))...
      + abs(imag(g)));
    Z=[Z;z];
    tp1=(1/(wn*sqrt(1-zta*zta)))*(atan((-zta/sqrt(1-zta*zta)))-alpa+pi);
    tp=tp1/delta;
    Tp=[Tp;tp];
    mp1=abs(sec(alpa))*sqrt(1-zta*zta)*...
    exp((-zta/sqrt(1-zta*zta))*(atan((-zta/sqrt(1-zta*zta)))-alpa+pi));
    mp=mp1*100;
    Mp=[Mp;mp];
    ts1=(-log(0.05*abs(cos(alpa)))*(sqrt(1-zta*zta)))/(wd*zta);
    ts=ts1/delta;
    Ts=[Ts;ts];
      A1=gain*(rden(3)/abs(real(z)));
      rnum=A1*[1 z];
```

```
      A=[A;A1];
      B1=rnum(2);
      B=[B;-B1];
      C1=rden(2);
      C=[C;C1];
      D=[D;-B1];
      delplane(z,p,delta);
      axis([-4.9,0.5,-2.3,2.3]);
      hold on;
      pause;
end
      hold off;
      title('Pole Zero Plot of Reference Model in Delta
      domain','Fontsize',12);
      disp('Angle');disp(ro);disp('Zita');disp(Zt);
      disp('Wd*Delta');disp(Wdt);disp('Wn');disp(Wn)
      disp('Poles');disp(P);disp('zero');disp(Z);
      disp('tp/Delta');disp(Tp);disp('Mp%');disp(Mp);
      disp('ts/Delta');disp(Ts);disp('A');disp(A);
      disp('B');disp(B);disp('C');disp(C);disp('D');disp(D);
%=================================================================
```

Chapter 3 (Controller design for SISO systems) Programs:

```
function del=comden(den,tol);
% This function computes the common denominator
% It eliminates the common roots, considering the tolerance specified.
% FILE NAME : comden.m

[n,x]=size(den);
del=den(1,:);
if n==1 return;end
% Default tol value
if ~exist('tol') tol=1e-4;end;
r=roots(del);
for i=2:n
    s=roots(den(i,:));
    lr=length(r);
    ls=length(s);
    for j=1:ls
        x=s(j);
        for k=1:lr
            if tol*round(x/tol)==tol*round(r(k)/tol) chk=0; break; end
            chk=1;
        end
              if chk  r=[r;x]; end;
        end
      end
        del=poly(r);
%=================================================================

function atm=agtm(ch,dl,n,anum,bdel,c)
% This function finds the Time moment matrix.
% FILE NAME: agtm.m
if ch ==2,
   atm=c*inv(dl*eye(size(anum))-anum)*bdel;
```

```
else
   valn=[];vald=[];
   for i=1:n*n
       valn=[valn;polyval(anum(i,:),dl)];
   end;
       vald=polyval(bdel,dl);
       atm=valn/vald;
       atm=reshape(atm,n,n);
       atm=atm';
   end;
%=============================================================

function [cg,cdel] = change(cnum,cden,n)
% This function forms a T.F.M. with common denominator.
% FILE NAME : change.m

cdel=mulrow(cden);
cg=conv(cnum(1,:),mulrow(cden(2:n*n,:)));
for i=2:n*n-1
     xx=[cden(1:i-1,:);cden(i+1:n*n,:)];
     xx=mulrow(xx);
     xx=conv(cnum(i,:),xx);
     cg=[cg;xx];
end
     xx=conv(cnum(n*n,:),mulrow(cden(1:n*n-1,:)));
     cg=[cg;xx];

%=============================================================

function [old]=cl2ol(cln,cld,n)
%This function computes the open-loop t.f.m. common denominator
%from the closed-loop t.f.m.(For diagonal t.f.m only).
%FILE NAME : cl2ol.m

old=[];
ln=length(cln(1,:));
ld=length(cld);
tempn=[];
for i=0:n-1
    temp=cln(1+i*(n+1),:);
    temp=cld-[zeros(1,ld-ln),temp];
   if abs(temp(ld))<1e-5 % to make last term zero
      temp(ld)=0;
   end
    tempn=[tempn;temp];
end
    old=comden(tempn,1e-5);

%=============================================================

function [tfmat,cdel]=mulnd(tfm,del,n);

% This function finds open-loop numerator and common denominator of
% reference model
% FILE NAME: mulnd.m

ln=length(tfm(1,:));
ld=length(del);
```

```
tempn=[];
for i=0:n-1
    temp=tfm(1+i*(n+1),:);
    temp=del-[zeros(1,ld-ln),temp];
    if abs(temp(ld))<1e-5 % to make last term zero
       temp(ld)=0;
    end
     tempn=[tempn;temp];
end
     x2=comden(tempn,1e-5);
     nn1=[];
for i=0:n-1
    [idn]=rmzero(conv(tfm(1+i*(n+1),:),x2));
    [idd]=rmzero(tempn(i+1,:));
     nn=deconv(idn,idd);
     nn1=[nn1;length(nn)];
 end
     nn2=max(nn1); % maximum order of the polynomial matrix
     nummo1=zeros(n*n,nn2);
     n2=[];n1=[];
for i=0:n-1
    [idn]=rmzero(conv(tfm(1+i*(n+1),:),x2)); % removing leading zeros
    [idd]=rmzero(tempn(i+1,:));
     n1=deconv(idn,idd);
     n1=[zeros(1,(nn2-length(n1))),n1];
     nummo1(1+i*(n+1),:)=n1;
 end
     cdel=x2;
     tfmat=nummo1;
```

```
%=============================================================
```

```
function product=mulrow(d);
% this function multiplies the rows of a t.f.m.
%FILE NAME: mulrow.m

[x,y]=size(d);
product=[1];
for i=1:x
      product=conv(product,d(i,:));
end;
```

```
%=============================================================
```

```
function [numm1,denm1]=refmodcalc(angle,delta)
% This routine computes numerator and denominator coefficients of
% reference model for different values of delta
% File name:  refmodelcal.m

format short;
n=1; % n==1 for SISO and 2 for MIMO systems
roh1=angle;
roh=(pi/180)*roh1;
alpa=roh;wn=0.84;zta=0.7;gain=1;
    wd=wn*sqrt(1-zta*zta);
    s=-zta*wn+(wn*sqrt(1-zta^2))*i ;   % pole in s-domain
    delta=[2 1 0.5 0.1 0.01 0.001];
    numm1=[];denm1=[];
```

```
for j=1:6
    g=s2del(s,delta(j));                    % pole in delta-domain
    cong=conj(g);
    denm=conv([1,-g],[1,-cong]);
    z= ((tan(roh-(pi/2))*(abs(g))^2))/ (abs(real(g))* tan(roh-(pi/2))
        - abs(imag(g)));
    A=gain*(denm(3)/abs(real(z)));
       numm=A*[1 z];
       numm1=[numm1;numm];
       denm1=[denm1;denm];
 end
```

```
%=============================================================
```

```
function [numm,denm]=refmodel28_40(delta)
% This routine computes numerator and denominator coefficients of
% refernce model for different values of angle roh
%File name:  refmodel28_40.m

angle=-40;
 [numm1,denm1]=refmodcalc(angle,delta);
if delta==2
      numm=numm1(1,:);denm=denm1(1,:);
elseif delta==1
      numm=numm1(2,:);denm=denm1(2,:);
elseif delta==0.5
      numm=numm1(3,:);denm=denm1(3,:);
elseif delta==0.1
      numm=numm1(4,:);denm=denm1(4,:);
elseif delta==0.01
      numm=numm1(5,:);denm=denm1(5,:);
else
      numm=numm1(6,:);denm=denm1(6,:);
end
```

```
%=============================================================
```

```
function [ng,dg]=tfsiso_con(ex_no)
% This function selects the plant transfer function coefficients
% for the examples of the thesis
% FILE NAME : tfsiso_con.m
% ex_no=input('Enter the Transfer function example No: ' );

if ex_no == 1
    % Ref. J Pal, "Control system design using approximate model
    % matching", System Science (Poland), vol.19,no.3,pp.5-23
    % Example 3.5.6.1

    ng=[0 0 3]; dg=[1 4 3];

elseif ex_no== 2
    % Sixth-order Tf, of a typical open-loop helicopter engine including
    % a fuel controller
    % Ref: Sanathanan, C.K. and  stanley B. Quinn Jr., " Controller
    % design via the synthesis equations" Journal of the Franklin
    % Institute, vol. 324, no.3, pp.431-451, 1987.
    % Example 3.5.6.2

    ng=[248.05 1483.339 91930.803 468732.64 634950.95];
```

```
    dg=[1 26.2401 1363.07 26802.8 326900 859173 528055];

elseif ex_no== 3
    % Ref. J Pal, "Control system design using approximate model
    % matching", System Science (Poland), vol.19,no.3,pp.5-23
    % Example 3.5.6.3

    ng=[0 0 200];dg=[2 10 100];

elseif ex_no== 4
     % Ref. H.N.Shankar, Ph.D thesis titled "Adaptive control of general
     % calss of finite dimensional stable LTI systems", IISC, Bangalore,
     % 2000.
     % Example 3.6.4

    ng=conv([1 2]);dg=conv([1 1],[1 3],[1 4]);
end
%=============================================================

% This program computes and plots the SISO controller by OGDTM method
% using genetic algorithms for different plants available in
% file tfsiso_con.m
% FILE NAME: msisoconogdtm.m

clear all;
clc;
f_name='sisoconogdtm';
siz=1;
p_max=1*ones(siz,1);
p_min=0.001*ones(siz,1);
p_res=0.01*ones(siz,1);
gap=fmga_def(5)
ptyp=2*ones(siz,1);
G_disp=1;
[maxp,minp,avp,bp,pi]=flexga(f_name,p_min,p_max,p_res,ptyp,gap,G_disp);
form_p=1;dl= bp;n=1;delta=0.1;
t=0:delta:20;
% ----- Call for plant transfer function ------
% Choose examples given in the file tfsiso_con.m
% Change the ex_no in the function sisoconogdtm.m also
 ex_no=1;
      [ng,dg]=tfsiso_con(ex_no);
      [nump denp]=c2del(ng,dg,delta);
      [numm,denm]=refmodel28_40(delta);
      opdenm=cl2ol(numm,denm,n);
      [npo]=zero(opdenm);% zero.m takes input as poly coef.and detects
                         % nos of zero at origin
      [npor]=zero(denp);
   cnr=2;          % Choose cnr=1 for PI and 2 for PID controller
   mr=cnr+1;
   u=[];q=[];
   for i=1:mr
       p=agtm(form_p,i*dl,n,nump,denp);
       m=agtm(form_p,i*dl,n,numm,denm );
       ql=inv(p)*(i*dl)^(npo-npor)*inv(eye(size(m))-m)*m;
       ql=reshape(ql',1,n*n);
```

```
        q=[q;q1];
        um=[1];
        for j=1:cnr
            um=[um,(i*dl)^j];
        end;
        u=[u;um];
    end;
       cnum=[];cden=[];
       x1=1;
    for i=1:n*n
        if npo==0
           u1=u(1:cnr+1,1:cnr+1);
           u2=[1:(x1+1) 0]'*dl.*q(:,i);
           z=inv(u1)*u2;
        else
           u1=u(1:cnr+1,1:cnr+1);
           u2=q(:,i);
           z=inv(u1)*u2;
        end
             zn=fliplr(z');
             zd=[1,0];
             cnum=[cnum;zn];
             cden=[cden;zd];
    end
       NUM=conv(cnum,nump);
       DEN=conv(cden,denp);
       sys=tf(NUM,DEN);
       SYS=feedback(sys,1,-1);
       [fnum,fden]=tfdata(SYS,'v');
       disp('Sampling Time');disp(delta);
%  Step response of reference model and system
       yf=delstep(numm,denm,t,delta);
       yc=delstep(fnum,fden,t,delta);

figure(2);
plot(t,yf,'k-',t,yc,'k--');xlabel('Time in sec');ylabel('Magnitude');
title('Step Response of SISO Reference Model and Designed System ');
legend('Reference Model','Closed Loop systen','location','Best');
legend BOXOFF;
% Impulse response of reference model and system
yf1=delimp(numm,denm,t,delta);
yc1=delimp(fnum,fden,t,delta);

figure(3);
plot(t,yf1,'k-',t,yc1,'k--');xlabel('Time in sec');ylabel('Magnitude');
title('Step Response of SISO Reference Model and Designed System ');
legend('Reference Model','Closed Loop systen','location','Best');
legend BOXOFF;
[z,p,k]=tf2zp(fnum,fden);
figure(4);
delplane(z,p,delta);
title('Pole Zero plot in delta domain');
legend('zeros','poles');
legend BOXOFF;
%----------------Numerator and Denominator coefficients-------------
disp('sampling time in seconds');disp(delta);disp('Angle');disp(-40);
disp('Optimum Ex. Point Value');disp(dl);
disp('Plant Transfer Function in s - Domain');printsys(ng,dg,'s');
```

```
disp('Plant Transfer Function in delta Domain');printsys(nump,denp,'y');
disp('Ref.Model Transfer Function in delta Domain');
printsys(numm,denm,'y');disp(numm);disp('coeff."A" of Reference Model');
if length(numm)==3
       disp(numm(2));
       else disp(numm(1));
end
       disp('coefficient "B" of Reference Model');
       if length(numm)==3
       disp(numm(3));
       else disp(numm(2));
end
       disp('coefficient "C" of Reference Model');
       disp(denm(2));
       disp('coefficient "D" of Reference Model');
       if length(numm)==3
       disp(numm(3));
       else disp(numm(2));
end

disp('Designed PI Controller Transfer Function in delta Domain');
      cden1=[0,cden];
printsys(cnum,cden1,'y');
disp('Designed system Transfer Function in delta Domain');
      printsys(fnum,fden,'y');

%------------time domain specifications------------
if n==1
      if length(cden)< length(cnum)
         cden=(conv([cden],[1,(0.1/delta)]));
      end
      [af,bf]=feedback(conv(cnum,nump),conv(cden,denp),1,1,-1);
      flag=ISSTABLE(roots(bf),delta);
      if flag==0
         disp('UNSTABLE SISO FEEDBACK SYSTEM in DELTA DOMAIN')
      elseif flag==1
         disp('STABLE SISO FEEDBACK SYSTEM in DELTA DAMAIN')
      end
      dyr=delstep(af,bf,t,delta);
      [mp tp tr ts]=tdspec(dyr);
      disp('Max percentage overshoot');disp(mp);
      disp('Peak time, Nos of sample');disp(tp);
      disp('Rise time, Nos of sample');disp(tr);
      disp('Settling time, Nos of sample');disp(ts);
      [mag,db,pha,wb]=deltabode(numm,(denm-[zeros(1,(length(denm)
                          -length(numm))),numm]),delta);
      [mag1,db1,pha1,wb1]=deltabode(conv(cnum,nump),conv(cden,denp),
      delta);
        [gmm,pmm,wcgm,wcpm]=margin(mag,pha,wb);
        disp('G M and Phase crossover frequency of reference model')
        disp(gmm);disp(wcpm);
        disp('P M and Gain crossover frequency of reference model')
        disp(pmm);disp(wcgm);
        [gm,pm,wcg,wcp]=margin(mag1,pha1,wb1);
        disp('G M and Phase crossover frequency of designed system')
        disp(gm);disp(wcp);
```

```
        disp('P M and Gain crossover frequency of designed system')
        disp(pm);disp(wcg);
end

%=============================================================
function [PI]=sisoconogdtm(x)
% This function computes basic SISO controller with OGDTMs and finds
% scalar fitness function.
% Finding the number of poles at origin for open-loop t.f.m.
% FILE NAME : sisoconogdtm.m

delta=0.1;
t=0:delta:20;
% ----- Call for plant transfer function ------
% Choose examples given in the file tfsiso_con.m
% Change the ex_no in the function msisoconogdtm.m also
 ex_no=1;
[ng,dg]=tfsiso_con(ex_no);
[nump denp]=c2del(ng,dg,delta);
[numm,denm]=refmodel28_40(delta);

% OGDTM program starts here
form_p=1;dl=x;n=1; % n=1 for SISO system
opdenm=cl2ol(numm,denm,n);
[npo]=zero(opdenm);% zero.m takes input as poly coef. and detects
                   % nos of zero at origin
[npor]=zero(denp);
   cnr=2;     % Choose cnr=1 for PI and 2 for PID controller
   mr=cnr+1;
   u=[];q=[];
   for i=1:mr
       p=agtm(form_p,i*dl,n,nump,denp);
       m=agtm(form_p,i*dl,n,numm,denm );
       q1=inv(p)*(i*dl)^(npo-npor)*inv(eye(size(m))-m)*m;
       q1=reshape(q1',1,n*n);
       q=[q;q1];
       um=[1];
       for j=1:cnr
           um=[um,(i*dl)^j];
       end;
       u=[u;um];
   end;
      cnum=[];cden=[];
      disp('Nos of open-loop ref model pole at origin');disp(npo)
      disp('Nos of plant pole at origin');disp(npor)
   x1=1;
   for i=1:n*n
       if npo==0
          u1=u(1:cnr+1,1:cnr+1);
          u2=[1:(x1+1) 0]'*dl.*q(:,i);
          z=inv(u1)*u2;
       else
          u1=u(1:cnr+1,1:cnr+1);
          u2=q(:,i);
          z=inv(u1)*u2;
      end
```

```
            zn=fliplr(z');
            zd=[1,0];
            cnum=[cnum;zn];cden=[cden;zd];
    end
% Computation of scalar fitness function
        NUM=conv(cnum,nump);
        DEN=conv(cden,denp);
        sys=tf(NUM,DEN);
        SYS=feedback(sys,1,-1);
        [fnum,fden]=tfdata(SYS,'v');
        yf=delstep(numm,denm,t,delta);
        yc=delstep(fnum,fden,t,delta);
        er1=yf-yc;
        er=er1'*er1;
        PI=er;
```

%==========

Chapter 4 (Controller design for MIMO systems) Programs:

%==========

```
function [Tfmat,Cdel]=comnd(tfm,del,p,m);
% This function finds common denominator of multivariable system
% in Transfer matrix form
% Common denominator is taken out using LCM of all denominators
% FILE NAME: comnd.m
% tfm = numerators are arranged as n11,n12,n21,n22
% p = Nos. of output, m = Nos. of input
% del = denominators d11,d12,d21,d22
% tfmat= numerators n11,n12,n21,n22
% cdel =common denominator

yn=[];yd=[];
for i=1:p*m
    yn=[yn;tfm(i,:)]; %n11;n21;n12;n22
    yd=[yd;del(i,:)]; % d11;d21;d12;d22
 end
 x2=comden(yd);
 nn1=[];
for i=1:p*m
    if any(yn(i,.))==1 & any(yd(i,:))==1
       [idn]=rmzero(conv(yn(i,:),x2));
       [idd]=rmzero(yd(i,:));
       nn=deconv(idn,idd);
       nn1=[nn1;length(nn)];
    end
 end
 nn2=max(nn1); % maximum order of the polynomial matrix
 n2=[];n1=[];
 for i=1:p*m
    if any(yn(i,:))==1 & any(yd(i,:))==1
       [idn]=rmzero(conv(yn(i,:),x2)); % removing leading zeros for
division
       [idd]=rmzero(yd(i,:));
       n1=deconv(idn,idd);
```

```
        n1=[zeros(1,(nn2-length(n1))),n1];
        n2=[n2;n1];
    else
        n2=[n2;zeros(1,nn2)];
    end
end
     cdel=x2;
     tfmat=n2;
%=================================================================
function [numm1,denm1]=refmodcalcmimo(angle,delta)
% This function computes the numerator and denominator of reference
% model for multi variable system
% n==1 for SISO and 2 for 2x2 MIMO systems
% angle=input('Enter any one value of angle roh == ');

format short;
n=1; roh1=angle;
roh=(pi/180)*roh1;
alpa=roh;
    wn=0.84;zta=0.7;gain=1;
    wd=wn*sqrt(1-zta*zta);
    s=-zta*wn+(wn*sqrt(1-zta^2))*i ;   % pole in s-domain
    delta=[2 1 0.5 0.1 0.01 0.001];
    numm1=[];
    denm1=[];
for j=1:6
    g=s2del(s,delta(j));                  % pole in delta-domain
    cong=conj(g);
    denm=conv([1,-g],[1,-cong]);
    z= ((tan(roh-(pi/2))*(abs(g))^2))/ (abs(real(g))* tan(roh-(pi/2))..
        - abs(imag(g)));
    A=gain*(denm(3)/abs(real(z)));
       numm=A*[1 z];
       numm=[0 numm];
       numm1=[numm1;numm];
       denm1=[denm1;denm];
end
%=================================================================
function [numm,denm]=refmodel5_40(delta)
% This function computes reference model for MIMO system for different
% values of samling time given in the function refmodcalcmimo.m

angle=+40;
numm1,denm1]=refmodcalcmimo(angle,delta);
if delta==2
      numm(1,:)=numm1(1,:);numm(2,:)=zeros(1,3);numm(3,:)=zeros(1,3);
      numm(4,:)=numm1(1,:);denm(1,:)=denm1(1,:);denm(2,:)=zeros(1,3);
      denm(3,:)=zeros(1,3);denm(4,:)=denm1(1,:);
elseif delta==1
      numm(1,:)=numm1(2,:);numm(2,:)=zeros(1,3);numm(3,:)=zeros(1,3);
      numm(4,:)=numm1(2,:);denm(1,:)=denm1(2,:);denm(2,:)=zeros(1,3);
      denm(3,:)=zeros(1,3);denm(4,:)=denm1(2,:);
elseif delta==0.5
      numm(1,:)=numm1(3,:);numm(2,:)=zeros(1,3);numm(3,:)=zeros(1,3);
```

```
      numm(4,:)=numm1(3,:);denm(1,:)=denm1(3,:);denm(2,:)=zeros(1,3);
      denm(3,:)=zeros(1,3);denm(4,:)=denm1(3,:);
elseif delta==0.1
      numm(1,:)=numm1(4,:);numm(2,:)=zeros(1,3);numm(3,:)=zeros(1,3);
      numm(4,:)=numm1(4,:);denm(1,:)=denm1(4,:);denm(2,:)=zeros(1,3);
      denm(3,:)=zeros(1,3);denm(4,:)=denm1(4,:);
elseif delta==0.01
      numm(1,:)=numm1(5,:);numm(2,:)=zeros(1,3);numm(3,:)=zeros(1,3);
      numm(4,:)=numm1(5,:);denm(1,:)=denm1(5,:);denm(2,:)=zeros(1,3);
      denm(3,:)=zeros(1,3);denm(4,:)=denm1(5,:);
else
      numm(1,:)=numm1(6,:);numm(2,:)=zeros(1,3);numm(3,:)=zeros(1,3);
      numm(4,:)=numm1(6,:);denm(1,:)=denm1(6,:);denm(2,:)=zeros(1,3);
      denm(3,:)=zeros(1,3);denm(4,:)=denm1(6,:);
end
%=============================================================

function [colmat]=row2col(rowmat,n)
% This function converts a rowwise arranged polynomial matrix
% to columnwise arrangment.
% FILE NAME: row2col.m
colmat=[];
for i=1:n
    for j=0:n-1
        colmat=[colmat;rowmat(i+j*n,:)];
    end
end

%=============================================================

function [i,idl]=zero(dl)
% This function finds the number of roots of a polynomial at origin,
% it also returns the polynomial after removing those roots.
% FILE NAME: zero.m

dl=roots(dl)';dl=fliplr(dl);l=length(dl);i=0;
for j=1:l
   if dl(l-(j-1))~=0
      idl=dl(1:l-i);
      idl=fliplr(poly(idl));
      return;
   end;
    i=i+1;
end;
%=============================================================

function [ng,dg]=tfmimo_con(ex_no)
% This function outputs the numerator and denominator coefficients
% of multivariable plants given in the examples.
% ex_no=input('Enter Example Number : ');
% FILE NAME: tfmimo_con.m

if ex_no == 1
      % Ref. Rosenbrock, H.H," design of the multivariable control
      % systems using the  inverse nyquist array" Proc. IEE , vol. 116,
```

```
      % no. 11, pp. 1929-1936, Nov. 1969.
      % Thesis example no 4.4.1

    ng=[-1 1; -1 2;-3 1; -1 1];
    dg=[1 2 1; 1 2 1;3 6 3; 1 2 1];

elseif ex_no == 2

    % The open-loop transfer function of a pressurized flow-box
    % Ref. Hung, N.T. and Anderson, B.D.O., " Triangularization
    % Technique for the design of Multivariable control systems",
    % IEEE Trans. Automat. control, vol. AC-24, no. 3,
    % pp. 455-460, 1979.
    % Thesis example no 4.4.2
    % Numerator order [n11;n12;n21;n22];

    ng=[0 0 .0336; 0 1.03 0;0 9.66e-4 0.117e-4;0 0 -0.01141];
    dg=[0 1 0.395;1 0.395 1.26e-4;1 0.395 1.26e-4;1 0.395 1.26e-4];

elseif ex_no == 3
    % Four input four output gas fired furnace problem
    % Ref: Chieh-Li Chen and Neil Munro, "Procedure to achieve diagonal
    % dominance using PI/PID controller structure", International
    % Journal of Control, vol.50, no. 5, pp. 1771-1792, 1989.
    % Thesis example no 4.4.3

    ng=[0 1;0 0.7;0 0.3;0 0.2;0 0.6;0 1.0;0 0.4;0 0.35;0 0.35;0 0.4;
        0 1.0;0 0.6;0 0.2;0 0.3;0 0.7;0 1.0];
    dg=[4 1;5 1;5 1;5 1;5 1;4 1;5 1;5 1;5 1;5 1;4 1;5 1;5 1;5 1;5 1;
        4 1];

elseif ex_no == 4

      % Four input four output gat turbine
      % Ref: P.D.McMorran, S.M.,"Design of gas-turbine controller using
      % inverse Nyquist method", Proc. IEE, vol. 117, no. 10,
      % pp. 2050-2056, 1970.
      % Thesis example number 4.6.2

    ng=[0 0 14.96 1521.432 2543.2;0 0 95150 1132094.7 1805947;
        0 0 85.2 8642.688 12268.8;0 0 124000 1492588 2525880];
    dg=[1 113.225 1357.275 3502.75 2525;1 113.225 1357.275 3502.75 2525;
        1 113.225 1357.275 3502.75 2525;1 113.225 1357.275 3502.75 2525];
end
%=================================================================

function [PI]=mimoogdtm(x)
% This function computes basic MIMO controller with OGDTMs and finds
% scalar fitness function.
% Finding the number of poles at origin for open-loop t.f.m.
% FILE NAME : mimoogdtm.m

delta=0.1;tim=0:delta:30;
% ----- Call for plant transfer function ------
% Choose examples given in the file tfmimo_con.m
```

```
% Change the ex_no in the function mmimoogdtm.m also
 ex_no=1;
[ng,dg]=tfmimo_con(ex_no);
[ng1,dg1]=c2del(ng(1,:),dg(1,:),delta);
[ng2,dg2]=c2del(ng(2,:),dg(2,:),delta);
[ng3,dg3]=c2del(ng(3,:),dg(3,:),delta);
[ng4,dg4]=c2del(ng(4,:),dg(4,:),delta);
%ng1=[0,ng1];dg1=[0,dg1];
nump=[ng1;ng2;ng3;ng4];
denp=[dg1;dg2;dg3;dg4];
[nump,denp]=comnd(nump,denp,2,2);

% reference model zeta =0.7 wn=0.84 Delta =0.0001,0.001,0.01,0.1,0.5,2
[numm,denm]=refmodel5_40(delta);
[numm,denm]=comnd(numm,denm,2,2);
form_p=1;n=2;
flag=isstable(roots(denp),delta);
if flag ==0
   disp('PLANT IS NOT STABLE')
end
      x1=1;cnr=1;
      mr=cnr+1;
      dl=x;
      opdenm=cl2ol(numm,denm,n);
      [npo]=zero(opdenm);      % zero.m takes input as poly coef.
                               % and detects nos of zero at origin
      [npor]=zero(denp);
      u=[];q=[];
   for i=1:mr
       if form_p==1 p=agtm(form_p,i*dl,n,nump,denp);
          m=agtm(form_p,i*dl,n,numm,denm );
       else
          p=agtm(form_p,i*dl,n,ap,bp,cp);
          m=agtm(form_p,i*dl,n,am,bm,cm);
       end
            q1=inv(p)*(i*dl)^(npo-npor)*inv(eye(size(m))-m)*m;
            q1=reshape(q1',1,n*n);
            q=[q;q1];
            um=[1];
       for j=1:cnr
           um=[um,(i*dl)^j];
       end;
            u=[u;um];
   end;
            cnum=[];cden=[];
   for i=1:n*n
       if npo==0
            u1=u(1:cnr+1,1:cnr+1);
            u2=[1: (x1+1)]'*dl.*q(:,i);
            z=inv(u1)*u2;
       else
            u1=u(1:cnr+1,1:cnr+1);
            u2=q(:,i);
            z=inv(u1)*u2;
       end
            zn=fliplr(z');
            zd=[1,0];
```

```
            cnum=[cnum;zn];
            cden=[cden;zd];
    end
            [cnum1,cdel]=change(cnum,cden,n);
            cnum11=row2col(cnum1,n);    % arranging as [n11 n21 n12 n22]
            [ac,bc,cc,dc]=tfm2ss(cnum11,cdel,n,n);
            nump1=row2col(nump,n);      % arranging as [n11 n21 n12 n22]
            [ap,bp,cp,dp] = tfm2ss(nump1,denp,n,n);
      ymm=[];ym=[];
    for i=1:n*n
        ymm=[ymm,delstep(numm(i,:),denm,tim,delta)];
                % this will give y11,y12,y21,y22
    end
    for j=1:n
        for l=j:n:min(size(ymm)) % this will give y11,y21,y12,y22
            ym=[ym,ymm(:,l)];
        end
    end
            [acp,bcp,ccp,dcp]=series(ac,bc,cc,dc,ap,bp,cp,dp);
            [af,bf,cf,df1]=feedbk(acp,bcp,ccp,dcp,2);
      flag=isstable(af,delta);
      yr=[];yrout=[];
      dyr=delstep(af,bf,cf,df1,1,tim,delta);
   for j=1:n
       yrout1=[];
       for i=j:n:length(dyr)
           yrout1=[yrout1;dyr(i,:)];
       end
       yrout=[yrout,yrout1];
   end
   for j=1:n
       for l=j:n:min(size(yrout))
           yr=[yr,yrout(:,l)];
       end
   end
      er=ym-yr;
PI=er(:,1)'*er(:,1)+er(:,2)'*er(:,2)+er(:,3)'*er(:,3)+er(:,4)'*er(:,4);
%=============================================================

% This program computes basic MIMO controller with OGDTMs using genetic
% algorithms and finds optimum frequency points.
% FILE NAME: mmimoogdtm.m

clear all;
clc;
angle=-40;wn=0.84;zita=0.7;
fname='mimoogdtm';
siz=1;
p_max=1*ones(siz,1);
p_min=0.001*ones(siz,1);
p_res=0.01*ones(siz,1);
gap=fmga_def(1);
ptyp=2*ones(siz,1);
G_disp=1;
gap(9)=2;
[maxp,minp,avp,bp1,pi]=flexga(fname,p_min,p_max,p_res,ptyp,gap,G_disp);
[PI]=mimopb5ga(bp1);
```

```
form_p=1;
dl= bp1;n=2;delta=0.1;
tim=0:delta:30;
t=tim/delta;
ex_no=1;
[ng,dg]=tfmimo_con(ex_no);
[ng1,dg1]=c2del(ng(1,:),dg(1,:),delta);
[ng2,dg2]=c2del(ng(2,:),dg(2,:),delta);
[ng3,dg3]=c2del(ng(3,:),dg(3,:),delta);
[ng4,dg4]=c2del(ng(4,:),dg(4,:),delta);
%ng1=[0,ng1];dg1=[0,dg1];
nump=[ng1;ng2;ng3;ng4];
denp=[dg1;dg2;dg3;dg4];
[nump,denp]=comnd(nump,denp,2,2);

numpf=[];denpf=[];
for i=1:n*n
      sys1=tf(nump1(i,:),denp1(i,:));
      SYS1=feedback(sys1,1,-1);
      [numpf1,denpf1]=tfdata(SYS1,'v');
if length(numpf1)<3
      numpf1=[0,numpf1];
end
      numpf=[numpf;numpf1];
if length(denpf1)<3
      denpf1=[0,denpf1];
end
      denpf=[denpf;denpf1];
end

% reference model zeta =0.7 wn=0.84 Delta =0.0001,0.001,0.01,0.1,0.5,2

[numm1,denm1]=refmodel5_40(delta);
[numm,denm]=comnd(numm1,denm1,2,2);

figure(1);
opdenm=cl2ol(numm,denm,n);
   [npo]=zero(opdenm); % detects nos of zero at origin
   [npor]=zero(denp);
   cnr=1;
   mr=cnr+1;
   u=[];q=[];
   for i=1:mr
       if form_p==1 p=agtm(form_p,i*dl,n,nump,denp);
          m=agtm(form_p,i*dl,n,numm,denm );
       else
          p=agtm(form_p,i*dl,n,ap,bp,cp);
          m=agtm(form_p,i*dl,n,am,bm,cm);
       end
            q1=inv(p)*(i*dl)^(npo-npor)*inv(eye(size(m))-m)*m;
            q1=reshape(q1',1,n*n);
            q=[q;q1];
            um=[1];
       for j=1:cnr
            um=[um,(i*dl)^j];
       end;
```

```
          u=[u;um];
  end;
  cnum=[];cden=[];
  x1=1;
  for i=1:n*n
      if npo==0
         u1=u(1:cnr+1,1:cnr+1);
         u2=[1: (x1+1)]'*dl.*q(:,i);
         z=inv(u1)*u2;
      else
         u1=u(1:cnr+1,1:cnr+1);
         u2=q(:,i);
         z=inv(u1)*u2;
      end
      zn=fliplr(z');
      zd=[1,0];
      cnum=[cnum;zn];
      cden=[cden;zd];
  end
     disp('PI');disp(PI);disp('Angle roh');disp(angle);
     disp('Undamped Natural frequency');disp(wn);
     disp('Damping factor');disp(zita);disp('Sampling time');disp(delta);
     disp('Ex Point value');disp(dl);
     disp('Numeretor Coeff.of plant [n11 n12 n21 n22]');disp(nump);
     disp('Common Den.coeff. of plant [d11 d12 d21 d22]'); disp(denp);
     disp('Numeretor Coeff.of CL-plant [n11 n12 n21 n22]');disp(numpf);
     disp('Denominator coeff.of CL-plant [d11 d12 d21 d22]');disp(denpf);
     disp('Numerator Coeff.of Reference Model ');disp(numm);
     disp('Common Denominator Coeff.of Reference Model');disp(denm);
     disp('Numerator Coefficients of Controller');disp(cnum);
     disp('Denominator Coefficients of Controller');disp(cden);
     com_del=mulrow(cden);
     disp('POLES OF CONTROLLER:  ');disp(roots(com_del));
     disp('Nos of open-loop ref model pole at origin');disp(npo)
     disp('Nos of plant pole at origin');disp(npor)
[ro,cl]=size(cden);
[cnum1,cdel]=change(cnum,cden,n);
     cnum11=row2col(cnum1,n);    % arranging as [n11 n21 n12 n22]
     [ac,bc,cc,dc]=tfm2ss(cnum11,cdel,n,n);
     nump1=row2col(nump,n);      % arranging as [n11 n21 n12 n22]
     [ap,bp,cp,dp] = tfm2ss(nump1,denp,n,n);
  if n~=1
     [acp,bcp,ccp,dcp]=series(ac,bc,cc,dc,ap,bp,cp,dp);
     [af,bf,cf,df1]=feedbk(acp,bcp,ccp,dcp,2);
  flag=isstable(af,delta);
  if flag ==0
     disp('Design feedback system is unstable');
  else
     disp('Design feedback system is stable');
  end
     ypp=[];yp=[];
  for i=1:n*n
       ypp=[ypp,delstep(nump1(i,:),denp1(i,:),tim,delta)];
           % Arrange in y11,y12,y21,y22
  end
  for j=1:n
       for l=j:n:min(size(ypp)) % this will give y11,y21,y12,y22
```

```
        yp=[yp,ypp(:,l)];
   end
end
   ypcc=[];
   ypc=[];
for i=1:n*n
     ypcc=[ypcc,delstep(numpf(i,:),denpf(i,:),tim,delta)];
         % this will give y11,y12,y21,y22
end
for j=1:n
     for l=j:n:min(size(ypcc)) % this will give y11,y21,y12,y22
         ypc=[ypc,ypcc(:,l)];
     end
 end
   ymm=[];ym=[];
 for i=1:n*n
     ymm=[ymm,delstep(numm(i,:),denm,tim,delta)];
         % this will give y11,y12,y21,y22
 end
 for j=1:n
     for l=j:n:min(size(ymm)) % this will give y11,y21,y12,y22
         ym=[ym,ymm(:,l)];
     end
 end
   yr=[];yrout=[];
   dyr=delstep(af,bf,cf,df1,1,tim,delta);
 for j=1:n
   yrout1=[];
    for i=j:n:length(dyr)
        yrout1=[yrout1;dyr(i,:)];
    end
   yrout=[yrout,yrout1];
end
   for j=1:n
         for l=j:n:min(size(yrout))
               yr=[yr,yrout(:,l)];
         end
end
for i=1:n*n
figure(i+1);
plot(t,yp(:,i),'k:',t,ypc(:,i),'k-.',t,ym(:,i),'k-',t,yr(:,i),'k--');
legend('Plant','Plant with Unity feed back','Reference Model',...
       'Designed Closed-Loop System');
legend BOXOFF;
title('Step Response of MIMO Systion with PI controller');
xlabel('t/delta');
ylabel('Magnitude');
pause;
end
    k=[1,n*n];
 for j=1:2
       i=k(j);
         [mp tp ts]=tdspec1(yp(:,i));
         [mp1 tp1 ts1]=tdspec1(ym(:,i));
         [mp2 tp2 ts2]=tdspec1(yr(:,i));
         disp('Mp%:  Plant  Model  CL-system');disp([mp,mp1,mp2]);
         disp('tp/delta: Plant  Model  CL-system');disp([tp,tp1,tp2]);
```

```
            disp('ts/delta: Plant  Model  CL-system');disp([ts,ts1,ts2]);
    end

    % PLotting of control efforts [u11 u21 u12 u22]

    [au,bu,cu,du]=feedback(ac,bc,cc,dc,ap,bp,cp,dp,-1);
       yr1=[];yrout=[];
       dyr=delstep(au,bu,cu,du,1,tim,delta);
    for j=1:n
        yrout1=[];
        for i=j:n:length(dyr)
            yrout1=[yrout1;dyr(i,:)];
        end
        yrout=[yrout,yrout1];
    end
    for j=1:n
        for l=j:n:min(size(yrout))
            yr1=[yr1,yrout(:,l)];
        end
    end
    for i=1:n*n
             figure(i+5);
             plot(t,yr1(:,i),'k-');
             title('Control Effort ');
             xlabel('t/delta');
              ylabel('Magnitude');
             pause;
       end
    end
%=============================================================
function[PI]=mimooff(x)
% This function computes scalar fitness function for multivariable
% controller design by optimum frequency fitting method.
% Takes plant transfer function for the function tfmimo_con(ex_no);
% FILE NAME: mimooff.m

delta=0.1;
tim=0:delta:50;
ex_no=1;
[ng,dg]=tfmimo_con(ex_no);

[ng1,dg1]=c2del(ng(1,:),dg(1,:),delta);
[ng2,dg2]=c2del(ng(2,:),dg(2,:),delta);
[ng3,dg3]=c2del(ng(3,:),dg(3,:),delta);
[ng4,dg4]=c2del(ng(4,:),dg(4,:),delta);
ng3=[0,ng3];dg3=[0,dg3];

nump=[ng1;ng2;ng3;ng4];
denp=[dg1;dg2;dg3;dg4];

[nump,denp]=comnd(nump,denp,2,2);

% reference model zeta =0.7,wn=0.84,Delta =0.0001,0.001,0.01,0.1,0.5,2
[numm,denm]=refmodel5_40(delta);
```

```
[numm,denm]=comnd(numm,denm,2,2);
form_p=1;
n=2;
x1=1;
   cnr=1;
   mr=cnr+1;
   dl=x;
   opdenm=cl2ol(numm,denm,n);
   [npo]=zero(opdenm);  % detects nos of zero at origin
   [npor]=zero(denp);
   [nummo,denmo]=mulnd(numm,denm,n);
   denmo=fliplr(rmzero(fliplr(opdenm)));

% Formation of Q-matrix and U-matrix using Optimal frequency Fitting

      abs_u=[];q=[];ang_u=[];
for i=1:mr
    p=[];m=[];
          for j=1:n*n
           p=[p;delfreq(nump(j,:),denp,i*dl,delta)];
           m=[m;delfreq(nummo(j,:),denmo,i*dl,delta)];
        end
       p=reshape(p,n,n);p=p';  % AFF matrix of the plant in TFM form
       m=reshape(m,n,n);m=m';  % AFF matrix of the ref.model in TFM form
       q1=inv(p)*m;
       q1=reshape(q1',1,n*n);
       q=[q;q1];
       ddl=dl*sqrt(-1);
       ddl=s2del(i*ddl,delta);
    um=[1];um1=0;
    for jj=1:cnr
        um=[um,(abs(ddl))^jj];
        um1=[um1,(angle(ddl)*jj)];
    end
    abs_u=[abs_u;um];  % absolute values of U-matrix elements
    ang_u=[ang_u;um1]; % Angles of the U-matrix elements
end;
      abs_q=abs(q);      % absolute values of the q-matrix elements
      ang_q=angle(q);    % angles of the q-matrix elements
      cos_u=cos(ang_u);
      sin_u=sin(ang_u);
      [ro,cl]=size(abs_u);
      ur=[];ui=[];
for i=1:cl
      ur=[ur,abs_u(:,i).*cos_u(:,i)];
      ui=[ui,abs_u(:,i).*sin_u(:,i)];
end
w1=[ur;ui];
% Computation of numerator and denominator of the controller
      cnum=[];cden=[];
for i=1:n*n
    ang_qu=[];w2=[];v=[];ang_q1=[];
    for j=1:cl
       ang_qu=[ang_qu,ang_q(:,i)+ ang_u(:,j)];
       ang_q1=[ang_q1,ang_q(:,i)];
    end
```

```
      cos_ang_qu=cos(ang_qu);
      sin_ang_qu=sin(ang_qu);
      cos_ang_ql=cos(ang_ql);
      sin_ang_ql=sin(ang_ql);
      url=[];uil=[];ur2=[];ui2=[];
    for j=1:cl
        url=[url,abs_q(:,i).*abs_u(:,j).*cos_ang_qu(:,j)];
        uil=[uil,abs_q(:,i).*abs_u(:,j).*sin_ang_qu(:,j)];
        % wnen npo~=0 |u|*e^jtheta not required
        ur2=[ur2,abs_q(:,i).*cos_ang_ql(:,j)];  % When there is pole at
origin
        ui2=[ui2,abs_q(:,i).*sin_ang_ql(:,j)];  % in open-loop reference
model
     end
        w2=[url;uil];  % To be used for PI or PID when no pole at origin
        w3=[ur2;ui2];  % To be used for PI or PID when pole at origin
        [row,col]=size(w2);
        v=w2(:,col);
        if npo==0
           z(1:mr,1)=pinv(wl)*w2(:,2);
        else
           z(1:mr,1)=pinv(wl)*w3(:,2);
        end
        zn=fliplr(z(1:cnr+1)');
        zd=[1 0];
        cnum=[cnum;zn];
        cden=[cden;zd];
     end
      [cnuml,cdel]=change(cnum,cden,n);
      cnumll=row2col(cnuml,n);     % arranging as [n11 n21 n12 n22]
      [ac,bc,cc,dc]=tfm2ss(cnumll,cdel,n,n);
      numpl=row2col(nump,n);       % arranging as [n11 n21 n12 n22]
      [ap,bp,cp,dp] = tfm2ss(numpl,denp,n,n);
      ymm=[];ym=[];
    for i=1:n*n
        ymm=[ymm,delstep(numm(i,:),denm,tim,delta)];
            % this will give y11,y12,y21,y22
    end
    for j=1:n
        for l=j:n:min(size(ymm)) % this will give y11,y21,y12,y22
            ym=[ym,ymm(:,l)];
        end
    end
      [acp,bcp,ccp,dcp]=series(ac,bc,cc,dc,ap,bp,cp,dp);
      [af,bf,cf,dfl]=feedbk(acp,bcp,ccp,dcp,2);
      flag=isstable(af,delta);
      yr=[];yrout=[];
      dyr=delstep(af,bf,cf,dfl,1,tim,delta);
   for j=1:n
       yroutl=[];
       for i=j:n:length(dyr)
           yroutl=[yroutl;dyr(i,:)];
       end
       yrout=[yrout,yroutl];
   end
   for j=1:n
       for l=j:n:min(size(yrout))
```

```
            yr=[yr,yrout(:,1)];
        end
    end
        er=ym-yr;
PI=er(:,1)'*er(:,1)+er(:,2)'*er(:,2)+er(:,3)'*er(:,3)+er(:,4)'*er(:,4);

%=========================================================
% This program computes optimum frequency points for multivariable
% controller design by optimum frequency fitting method using genetic
% algorithms. It takes the value of scalar fitness function from the
% file mimooff.m
% Takes plant transfer function for the function tfmimo_con(ex_no);
% FILE NAME: mmimooff.m

Angle=-40;wn=0.84;zita=0.7;
fname='mimoaff5ga';
siz=1;
p_max=1*ones(siz,1);
p_min=0.001*ones(siz,1);
p_res=0.01*ones(siz,1);
gap=fmga_def(1);
ptyp=2*ones(siz,1);
G_disp=1;
gap(9)=2;
[maxp,minp,avp,bp1,pi]=flexga(fname,p_min,p_max,p_res,ptyp,gap,G_disp);
[PI]=mimoaff5ga(bp1);

form_p=1;dl= bp1;n=2;delta=0.1;
tim=0:delta:50;
t=tim/delta;
ex_no=1;
figure(1);
      [ng,dg]=tfmimo_con(ex_no);
      [ng1,dg1]=c2del(ng(1,:),dg(1,:),delta);
      [ng2,dg2]=c2del(ng(2,:),dg(2,:),delta);
      [ng3,dg3]=c2del(ng(3,:),dg(3,:),delta);
      [ng4,dg4]=c2del(ng(4,:),dg(4,:),delta);
      ng3=[0,ng3];dg3=[0,dg3];
      nump1=[ng1;ng2;ng3;ng4];
      denp1=[dg1;dg2;dg3;dg4];
      [nump,denp]=comnd(nump1,denp1,2,2);
      numpff=[];denpff=[];
for i=1:n*n
      sys1=tf(nump1(i,:),denp1(i,:));
      SYS1=feedback(sys1,1,-1);
      [numpf1,denpf1]=tfdata(SYS1,'v');
if length(numpf1)<3
      numpf1=[0,numpf1];
end
      numpff=[numpff;numpf1];
if length(denpf1)<3
      denpf1=[0,denpf1];
end
      denpff=[denpff;denpf1];
end
[numpf,denpf]=comnd(numpff,denpff,2,2);
```

```
% reference model zeta =0.7 wn=0.84 Delta =0.0001,0.001,0.01,0.1,0.5,2

[numm,denm]=refmodel5_40(delta);
[numm,denm]=comnd(numm,denm,2,2);

form_p=1;n=2;x1=1;cnr=1;
   mr=cnr+1;
   opdenm=cl2ol(numm,denm,n);
   [npo]=zero(opdenm);
   % zero.m takes input as poly coef. and detects nos of zero at origin
   [npor]=zero(denp);
   [nummo,denmo]=mulnd(numm,denm,n);
   denmo=fliplr(rmzero(fliplr(opdenm)));

% Formation of Q-matrix and U-matrix using AFF

abs_u=[];q=[];ang_u=[];
for i=1:mr
    p=[];m=[];
          for j=1:n*n
           p=[p;delfreq(nump(j,:),denp,i*dl,delta)];
           m=[m;delfreq(nummo(j,:),denmo,i*dl,delta)];
       end
       p=reshape(p,n,n);p=p';  % AFF matrix of the plant in TFM form
       m=reshape(m,n,n);m=m';  % AFF matrix of the ref.model in TFM form
       q1=inv(p)*m;
       q1=reshape(q1',1,n*n);
    q=[q;q1];
    ddl=dl*sqrt(-1);
    ddl=s2del(i*ddl,delta);
    um=[1];um1=0;
    for jj=1:cnr
        um=[um,(abs(ddl))^jj];
        um1=[um1,(angle(ddl)*jj)];
    end
    abs_u=[abs_u;um];  % absolute values of U-matrix elements
    ang_u=[ang_u;um1]; % Angles of the U-matrix elements
end;
      abs_q=abs(q);      % absolute values of the q-matrix elements
      ang_q=angle(q);    % angles of the q-matrix elements
      cos_u=cos(ang_u);
      sin_u=sin(ang_u);
      [ro,cl]=size(abs_u);
      ur=[];ui=[];
for i=1:cl
    ur=[ur,abs_u(:,i).*cos_u(:,i)];
    ui=[ui,abs_u(:,i).*sin_u(:,i)];
end
      w1=[ur;ui];
% Computation of numerator and denominator of the controller
cnum=[];cden=[];
for i=1:n*n
    ang_qu=[];w2=[];v=[];ang_q1=[];
    for j=1:cl
       ang_qu=[ang_qu,ang_q(:,i)+ ang_u(:,j)];
```

```
       ang_q1=[ang_q1,ang_q(:,i)];
    end
    cos_ang_qu=cos(ang_qu);
    sin_ang_qu=sin(ang_qu);
    cos_ang_q1=cos(ang_q1);
    sin_ang_q1=sin(ang_q1);
    ur1=[];ui1=[];ur2=[];ui2=[];
    for j=1:cl
        ur1=[ur1,abs_q(:,i).*abs_u(:,j).*cos_ang_qu(:,j)];
        ui1=[ui1,abs_q(:,i).*abs_u(:,j).*sin_ang_qu(:,j)];
        % when npo~=0 |u|*e^jtheta not required
        ur2=[ur2,abs_q(:,i).*cos_ang_q1(:,j)];  % When there is pole at
origin
        ui2=[ui2,abs_q(:,i).*sin_ang_q1(:,j)];  % in open-loop reference
model
     end
        w2=[ur1;ui1];    % To be used for PI or PID when no pole at origin
        [row,col]=size(w2);
        w=[w1,-w2(:,1:col-1)]; % to be used for other controller
        v=w2(:,col);
        if npo==0
           z(1:mr,1)=pinv(w1)*w2(:,2);
        else
           z(1:mr,1)=pinv(w1)*w3(:,2);
        end
        zn=fliplr(z(1:cnr+1)');
        zd=[1 0];
        cnum=[cnum;zn];
        cden=[cden;zd]; '
end
      disp('Error');disp(PI);disp('Angle roh');disp(Angle);
      disp('Undamped Natural frequency');disp(wn);disp('Damping factor');
      disp(zita);disp('Sampling time');disp(delta);
      disp('Ex Point value in delta');disp(ddl);
      disp('Numeretor Coeff.of plant [n11 n12 n21 n22]');disp(nump);
      disp('Denominator coeff.of plant [d11 d12 d21 d22]');disp(denp);
      disp('Reference Model Numerator Coefficients');disp(numm);
      disp('Reference Model Denominator Coefficients');disp(denm);
      disp('Numerator Coefficients of Controller');disp(cnum);
      disp('Denominator Coefficients of Controller'); disp(cden);
      com_del=mulrow(cden);
      com_del=mulrow(cden);
      disp('POLES OF CONTROLLER:  ');disp(roots(com_del));
      disp('Nos of open-loop ref model pole at origin');disp(npo)
      disp('Nos of plant pole at origin');disp(npor)

      [cnum1,cdel]=change(cnum,cden,n);
      cnum11=row2col(cnum1,n);    % arranging as [n11 n21 n12 n22]
      [ac,bc,cc,dc]=tfm2ss(cnum11,cdel,n,n);
      nump1=row2col(nump,n);      % arranging as [n11 n21 n12 n22]
      [ap,bp,cp,dp] = tfm2ss(nump1,denp,n,n);
      if n~=1
   [acp,bcp,ccp,dcp]=series(ac,bc,cc,dc,ap,bp,cp,dp);
   [af,bf,cf,df1]=feedbk(acp,bcp,ccp,dcp,2);
   flag=isstable(af,delta);
   if flag ==0
      disp('Design feedback system is stable');
```

```
else
   disp('Design feedback system is stable');
end
   ypp=[];yp=[];
 for i=1:n*n
     ypp=[ypp,delstep(nump(i,:),denp,tim,delta)];
         % this will give y11,y12,y21,y22
 end
 for j=1:n
     for l=j:n:min(size(ypp)) % this will give y11,y21,y12,y22
         yp=[yp,ypp(:,l)];
     end
 end
 ypcc=[];
 ypc=[];
 for i=1:n*n
     ypcc=[ypcc,delstep(numpff(i,:),denpff(i,:),tim,delta)];
         % this will give y11,y12,y21,y22
 end
 for j=1:n
     for l=j:n:min(size(ypcc)) % this will give y11,y21,y12,y22
         ypc=[ypc,ypcc(:,l)];
     end
 end

 ymm=[];ym=[];yp=[];
 for i=1:n*n
     ymm=[ymm,delstep(numm(i,:),denm,tim,delta)];
         % this will give y11,y12,y21,y22
 end
  for i=1:n*n
     yp=[yp,delstep(nump(i,:),denp,tim,delta)];
         % this will give yp11,yp12,yp21,yp22
 end
 for j=1:n
     for l=j:n:min(size(ymm))
         % this will give y11,y21,y12,y22
         ym=[ym,ymm(:,l)];
     end
 end
yr=[];yrout=[];
dyr=delstep(af,bf,cf,df1,1,tim,delta);
for j=1:n
    yrout1=[];
    for i=j:n:length(dyr)
        yrout1=[yrout1;dyr(i,:)];
    end
    yrout=[yrout,yrout1];
end
for j=1:n
    for l=j:n:min(size(yrout))
        yr=[yr,yrout(:,l)];
    end
end

for i=1:n*n
```

```
        figure(i+1);
        plot(t,yp(:,i),'k-.');
        legend('Plant','Plant with Unity feed back');
        legend BOXOFF;
        title('Step Response of MIMO uncontrolled Plant');
        xlabel('t/delta ');
        ylabel('Magnitude');
        pause;
        end
    for i=1:n*n
        figure(i+5);
        plot(t,ym(:,i),'k-',t,yr(:,i),'k--');
        legend('Reference Model','Designed Closed loop System');
        legend BOXOFF;
        title('Step Response of MIMO Systion with PI controller');
        xlabel('t/delta ');
        ylabel('Magnitude');
        pause;
    end

    % PLotting of control efforts [u11 u21 u12 u22]
       [au,bu,cu,du]=feedback(ac,bc,cc,dc,ap,bp,cp,dp,-1);
       yr1=[];yrout=[];
       dyr=delstep(au,bu,cu,du,1,tim,delta);
    for j=1:n
        yrout1=[];
        for i=j:n:length(dyr)
            yrout1=[yrout1;dyr(i,:)];
        end
        yrout=[yrout,yrout1];
    end
    for j=1:n
        for l=j:n:min(size(yrout))
            yr1=[yr1,yrout(:,l)];
        end
    end
    for i=1:n*n
       figure(i+9);
       plot(t,yr1(:,i),'k-');title('Control Effort ');
       xlabel('t/delta');ylabel('Magnitude');
       pause;
    end
 end
%=========================================================
```

Chapter 5 (Time Delay Systems)

```
% This program computes optimum frequency points for multivariable
% controller design for the systems with time delay by optimum frequency
% fitting method using genetic algorithms. It takes the value of scalar
% fitness function from the file mimoofftd.m
% Takes plant transfer function for the function tfmimo_con(ex_no);
% FILE NAME: mmimoofftd.m

clear all;
clc;
fname='mimoofftd';
```

```
siz=1;
p_max=1*ones(siz,1);
p_min=0.001*ones(siz,1);
p_res=0.01*ones(siz,1);
gap=fmga_def(1);
ptyp=2*ones(siz,1);
G_disp=1;
gap(9)=2;
[maxp,minp,avp,bp1,pi]=flexga(fname,p_min,p_max,p_res,ptyp,gap,G_disp);
form_p=1;dl= bp1;n=2;delta=1;
tim=0:delta:10;
t=tim/delta;
ex_no=1;
figure(1);
tdP1=1;tdP2=3;tdP3=7;
 [ng,dg]=tfmimo_con(ex_no);
 [ng1,dg1]=c2deld(ng(1,:),dg(1,:),tdP1,delta);
 [ng2,dg2]=c2deld(ng(2,:),dg(2,:),tdP2,delta);
 [ng3,dg3]=c2deld(ng(3,:),dg(3,:),tdP3,delta);
 [ng4,dg4]=c2deld(ng(4,:),dg(4,:),tdP2,delta);
 [m1,n1]=size(ng1);[m2,n2]=size(dg1);[m3,n3]=size(ng2);
 [m4,n4]=size(dg2);[m5,n5]=size(ng3);[m6,n6]=size(dg3);
     ng11(1,:)=[zeros(1,n5-n1),ng1(1,:)];
     dg11(1,:)=[zeros(1,n6-n2),dg1(1,:)];
     ng21(1,:)=[zeros(1,n5-n3),ng2(1,:)];
     dg21(1,:)=[zeros(1,n6-n4),dg2(1,:)];
     ng31(1,:)=ng3(1,:);
     dg31(1,:)=dg3(1,:);
     ng41(1,:)=[zeros(1,n5-n3),ng4(1,:)];
     dg41(1,:)=[zeros(1,n6-n4),dg4(1,:)];
nump=[ng11;ng21;ng31;ng41];
denp=[dg11;dg21;dg31;dg41];

[nump,denp]=comnd(nump,denp,2,2);

% reference model zeta =0.7 wn=0.84 Delta =0.0001,0.001,0.01,0.1,0.5,2

[numm,denm]=refmodel5_40aff(delta);
[numm,denm]=comnd(numm,denm,2,2);

form_p=1;n=2;x1=1;cnr=1;
   mr=cnr+1;
   opdenm=cl2ol(numm,denm,n);
   [npo]=zero(opdenm);  % detects nos of zero at origin
   [npor]=zero(denp);
   [nummo,denmo]=mulnd(numm,denm,n);
   denmo=fliplr(rmzero(fliplr(opdenm)));

% Formation of Q-matrix and U-matrix using AFF
abs_u=[];q=[];ang_u=[];
for i=1:mr
    p=[];m=[];
          for j=1:n*n
           p=[p;delfreq(nump(j,:),denp,i*dl,delta)];
           %m=[m;delfreq(numm(j,:),denm,i*dl,delta)];
           m=[m;delfreq(nummo(j,:),denmo,i*dl,delta)];
```

```
        end
        p=reshape(p,n,n);p=p';  % AFF matrix of the plant in TFM form
        m=reshape(m,n,n);m=m';  % AFF matrix of the ref.model in TFM form
        q1=inv(p)*m;
        q1=reshape(q1',1,n*n);
    q=[q;q1];
    ddl=dl*sqrt(-1);
    ddl=s2del(i*ddl,delta);
    um=[1];um1=0;
    for jj=1:cnr
        um=[um,(abs(ddl))^jj];
        um1=[um1,(angle(ddl)*jj)];
    end
    abs_u=[abs_u;um];  % absolute values of U-matrix elements
    ang_u=[ang_u;um1]; % Angles of the U-matrix elements
end;
abs_q=abs(q);      % absolute values of the q-matrix elements
ang_q=angle(q);    % angles of the q-matrix elements
cos_u=cos(ang_u);
sin_u=sin(ang_u);
[ro,cl]=size(abs_u);
ur=[];ui=[];
for i=1:cl
    ur=[ur,abs_u(:,i).*cos_u(:,i)];
    ui=[ui,abs_u(:,i).*sin_u(:,i)];
end
w1=[ur;ui];
% Computation of numerator and denominator of the controller
cnum=[];cden=[];
for i=1:n*n
    ang_qu=[];w2=[];v=[];ang_q1=[];
    for j=1:cl
       ang_qu=[ang_qu,ang_q(:,i)+ ang_u(:,j)];
       ang_q1=[ang_q1,ang_q(:,i)];
    end
    cos_ang_qu=cos(ang_qu);
    sin_ang_qu=sin(ang_qu);
    cos_ang_q1=cos(ang_q1);
    sin_ang_q1=sin(ang_q1);
    ur1=[];ui1=[];ur2=[];ui2=[];
    for j=1:cl
      ur1=[ur1,abs_q(:,i).*abs_u(:,j).*cos_ang_qu(:,j)];
      ui1=[ui1,abs_q(:,i).*abs_u(:,j).*sin_ang_qu(:,j)];
            % wnen npo~=0 |u|*e^jtheta not required
      ur2=[ur2,abs_q(:,i).*cos_ang_q1(:,j)];% When there is pole at origin
      ui2=[ui2,abs_q(:,i).*sin_ang_q1(:,j)];% in open-loop reference model
    end
        w2=[ur1;ui1];     % To be used for PI or PID when no pole at origin
        w3=[ur2;ui2];     % To be used for PI or PID when pole at origin
        [row,col]=size(w2);
        v=w2(:,col);
        if npo==0
           z(1:mr,1)=pinv(w1)*w2(:,2);
        else
           z(1:mr,1)=pinv(w1)*w3(:,2);
        end
        zn=fliplr(z(1:cnr+1)');
```

```
      zd=[1 0];
      cnum=[cnum;zn];
      cden=[cden;zd];
    end
   disp('Sampling time');disp(delta);
   disp('Ex Point value in delta');disp(dd1);
   disp('Plant transfer function for common dinominator in delta
        domain [p11 p12 p21 p22]')
     for i=1:n*n
          printsys(nump(i,:),denp,'y')
     end
  disp('Reference Model transfer function with common Dinominator
       in delta domain [m11 m12 m21 m22]');
  for i=1:n*n
          printsys(numm(i,:),denm,'y')
     end
  disp('Controller transfer function in delta domain');
  for i=1:n*n
          printsys(cnum(i,:),cden(i,:),'y')
     end
  com_del=mulrow(cden);
  com_del=mulrow(cden);
  disp('POLES OF CONTROLLER:  ');disp(roots(com_del));
  disp('Nos of open-loop ref model pole at origin');disp(npo)
  disp('Nos of plant pole at origin');disp(npor)

[cnum1,cdel]=change(cnum,cden,n);
     cnum11=row2col(cnum1,n);    % arranging as [n11 n21 n12 n22]
     [ac,bc,cc,dc]=tfm2ss(cnum11,cdel,n,n);
     nump1=row2col(nump,n);      % arranging as [n11 n21 n12 n22]
     [ap,bp,cp,dp] = tfm2ss(nump1,denp,n,n);
     if n~=1
  [acp,bcp,ccp,dcp]=series(ac,bc,cc,dc,ap,bp,cp,dp);
  [af,bf,cf,df1]=feedbk(acp,bcp,ccp,dcp,2);
  flag=isstable(af,delta);
  if flag ==0
     disp('Design feedback system is unstable');
  else
     disp('Design feedback system is stable');
  end
   ymm=[];ym=[];
   for i=1:n*n
       ymm=[ymm,delstep(numm(i,:),denm,tim,delta)];
           % this will give y11,y12,y21,y22
   end
   for j=1:n
       for l=j:n:min(size(ymm))
           % this will give y11,y21,y12,y22
           ym=[ym,ymm(:,l)];
       end
   end
  yr=[];yrout=[];
  dyr=delstep(af,bf,cf,df1,1,tim,delta);
  for j=1:n
      yrout1=[];
      for i=j:n:length(dyr)
          yrout1=[yrout1;dyr(i,:)];
```

```
        end
        yrout=[yrout,yrout1];
    end
    for j=1:n
        for l=j:n:min(size(yrout))
            yr=[yr,yrout(:,l)];
        end
    end
    for i=1:n*n
        figure(i+1);
        plot(t,ym(:,i),'k-',t,yr(:,i),'k-.');
        legend('Reference Model','Designed Closed loop System');
        legend BOXOFF;
        title('Step Response of MIMO Systion with PI controller');
        xlabel('Time in seconds');ylabel('Magnitude');
        pause;
        close;
    end

    % PLotting of control efforts [u11 u21 u12 u22]
    [au,bu,cu,du]=feedback(ac,bc,cc,dc,ap,bp,cp,dp,-1);
    yr1=[];yrout=[];
    dyr=delstep(au,bu,cu,du,1,tim,delta);
    for j=1:n
        yrout1=[];
        for i=j:n:length(dyr)
            yrout1=[yrout1;dyr(i,:)];
        end
        yrout=[yrout,yrout1];
    end
    for j=1:n
        for l=j:n:min(size(yrout))
            yr1=[yr1,yrout(:,l)];
        end
    end
    for i=1:n*n
        figure(i+5);
        plot(t,yr(:,i),'k-');title('Control Efforts');
        xlabel('t/delta');ylabel('Magnitude');
        pause;
        close;
    end
end
%=========================================================
function [PI]=mimoofftd(x)
% This function designs multivariable controller for the systems with
% time delay  by optimum frequency fitting using genetic algorithm.
% FILE NAME: mimoofftd.m
%format short g

delta=1;Angle=-40;tdP=1;
tim=0:delta:10;
ex_no=1;
tdP1=1;tdP2=3;tdP3=7;
[ng,dg]=tfmimo_con(ex_no);
```

```
      [ng1,dg1]=c2deld(ng(1,:),dg(1,:),tdP1,delta);
      [ng2,dg2]=c2deld(ng(2,:),dg(2,:),tdP2,delta);
      [ng3,dg3]=c2deld(ng(3,:),dg(3,:),tdP3,delta);
      [ng4,dg4]=c2deld(ng(4,:),dg(4,:),tdP2,delta);
      [m1,n1]=size(ng1);[m2,n2]=size(dg1);[m3,n3]=size(ng2);
      [m4,n4]=size(dg2);[m5,n5]=size(ng3);[m6,n6]=size(dg3);
      ng11(1,:)=[zeros(1,n5-n1),ng1(1,:)];
      dg11(1,:)=[zeros(1,n6-n2),dg1(1,:)];
      ng21(1,:)=[zeros(1,n5-n3),ng2(1,:)];
      dg21(1,:)=[zeros(1,n6-n4),dg2(1,:)];
      ng31(1,:)=ng3(1,:);dg31(1,:)=dg3(1,:);
      ng41(1,:)=[zeros(1,n5-n3),ng4(1,:)];
      dg41(1,:)=[zeros(1,n6-n4),dg4(1,:)];
      nump=[ng11;ng21;ng31;ng41];
      denp=[dg11;dg21;dg31;dg41];
 [nump,denp]=comnd(nump,denp,2,2);

% reference model zeta =0.7 wn=0.84 Delta =0.0001,0.001,0.01,0.1,0.5,2
[numm,denm]=refmodel5_40aff(delta);
[numm,denm]=comnd(numm,denm,2,2);
form_p=1;n=2;x1=1;cnr=1;
   mr=cnr+1;
   x=0.34;
   dl=x;
   opdenm=cl2ol(numm,denm,n);
   [npo]=zero(opdenm);  % zero.m takes input as poly coef. and detects
                        % nos of zero at origin
   [npor]=zero(denp);
   [nummo,denmo]=mulnd(numm,denm,n);
   denmo=fliplr(rmzero(fliplr(opdenm)));

% Formation of Q-matrix and U-matrix using AFF
abs_u=[];q=[];ang_u=[];
for i=1:mr
    p=[];m=[];
          for j=1:n*n
           p=[p;delfreq(nump(j,:),denp,i*dl,delta)];
           %m=[m;delfreq(numm(j,:),denm,i*dl,delta)];
           m=[m;delfreq(nummo(j,:),denmo,i*dl,delta)];

       end
       p=reshape(p,n,n);p=p';  % AFF matrix of the plant in TFM form
       m=reshape(m,n,n);m=m';  % AFF matrix of the ref.model in TFM form
       q1=inv(p)*m;
       q1=reshape(q1',1,n*n);
    q=[q;q1];
    dd1=dl*sqrt(-1);
    dd1=s2del(i*dd1,delta);
    um=[1];um1=0;
    for jj=1:cnr
        um=[um,(abs(dd1))^jj];
        um1=[um1,(angle(dd1)*jj)];
    end
    abs_u=[abs_u;um];  % absolute values of U-matrix elements
    ang_u=[ang_u;um1]; % Angles of the U-matrix elements
end;
```

```
abs_q=abs(q);      % absolute values of the q-matrix elements
ang_q=angle(q);    % angles of the q-matrix elements
cos_u=cos(ang_u);
sin_u=sin(ang_u);
[ro,cl]=size(abs_u);
ur=[];ui=[];
for i=1:cl
    ur=[ur,abs_u(:,i).*cos_u(:,i)];
    ui=[ui,abs_u(:,i).*sin_u(:,i)];
end
%ui(:,1)=1;
w1=[ur;ui];
% Computation of numerator and denominator of the controller
cnum=[];cden=[];
for i=1:n*n
    ang_qu=[];w2=[];v=[];ang_q1=[];
    for j=1:cl
       ang_qu=[ang_qu,ang_q(:,i)+ ang_u(:,j)];
       ang_q1=[ang_q1,ang_q(:,i)];
    end
    cos_ang_qu=cos(ang_qu);
    sin_ang_qu=sin(ang_qu);
    cos_ang_q1=cos(ang_q1);
    sin_ang_q1=sin(ang_q1);
    ur1=[];ui1=[];ur2=[];ui2=[];
    for j=1:cl
      ur1=[ur1,abs_q(:,i).*abs_u(:,j).*cos_ang_qu(:,j)];
      ui1=[ui1,abs_q(:,i).*abs_u(:,j).*sin_ang_qu(:,j)];
            % wnen npo~=0 |u|*e^jtheta not required
      ur2=[ur2,abs_q(:,i).*cos_ang_q1(:,j)]; % When there is pole at origin
      ui2=[ui2,abs_q(:,i).*sin_ang_q1(:,j)];% in open-loop reference model
    end
        w2=[ur1;ui1];  % To be used for PI or PID when no pole at origin
        w3=[ur2;ui2];  % To be used for PI or PID when pole at origin
        [row,col]=size(w2);
        v=w2(:,col);
        if npo==0
           z(1:mr,1)=pinv(w1)*w2(:,2);
        else
           z(1:mr,1)=pinv(w1)*w3(:,2);
        end
        zn=fliplr(z(1:cnr+1)');
        zd=[1 0];
        cnum=[cnum;zn];
        cden=[cden;zd];
     end
     [cnum1,cdel]=change(cnum,cden,n);
      cnum11=row2col(cnum1,n);    % arranging as [n11 n21 n12 n22]
      [ac,bc,cc,dc]=tfm2ss(cnum11,cdel,n,n);
      nump1=row2col(nump,n);      % arranging as [n11 n21 n12 n22]
      [ap,bp,cp,dp] = tfm2ss(nump1,denp,n,n);
  ymm=[];ym=[];
    for i=1:n*n
        ymm=[ymm,delstep(numm(i,:),denm,tim,delta)];
            % this will give y11,y12,y21,y22
    end
```

```
    for j=1:n
        for l=j:n:min(size(ymm))
                % this will give y11,y21,y12,y22
            ym=[ym,ymm(:,l)];
        end
    end
   [acp,bcp,ccp,dcp]=series(ac,bc,cc,dc,ap,bp,cp,dp);
   [af,bf,cf,df1]=feedbk(acp,bcp,ccp,dcp,2);
   flag=isstable(af,delta);
   yr=[];yrout=[];
   dyr=delstep(af,bf,cf,df1,1,tim,delta);
   for j=1:n
       yrout1=[];
       for i=j:n:length(dyr)
           yrout1=[yrout1;dyr(i,:)];
       end
       yrout=[yrout,yrout1];
   end
   for j=1:n
       for l=j:n:min(size(yrout))
           yr=[yr,yrout(:,l)];
       end
   end

er=ym-yr;
PI=er(:,1)'*er(:,1)+er(:,2)'*er(:,2)+er(:,3)'*er(:,3)+er(:,4)'*er(:,4);
```

%==========

Chapter 6 (Biomedical digital filters)

```
% This program generates ecg signal with 60 Hz power frequency
% interference
% FILE NAME: ecg2x60.m

clear all               % clears all active variables
close all
% the ECG signal in the file is sampled at 200 Hz
ecg = load('ecg2x60.dat');
fs = 200; %sampling rate
slen = length(ecg);
t=[1:slen]/fs;
figure
plot(t, ecg)
xlabel('Time in seconds');
ylabel('ECG');
axis tight;
```

%==========

```
% This program generates ecg signal with high frequency noise
% FILE NAME: ecg_hfn.m

clear all               % clears all active variables
close all
ecg = load('ecg_hfn.dat');
fs = 1000; %sampling rate = 1000 Hz
slen = length(ecg);
```

```
t=[1:slen]/fs;
figure
plot(t, ecg)
axis tight;
xlabel('Time in seconds');
ylabel('ECG');
title('ECG signal with high Fequency Noise');
```

```
%=================================================
% This program generates ecg signal with low frequency noise
% FILE NAME: ecg_lfn.m

clear all               % clears all active variables
close all
ecg = load('ecg_lfn.dat');
fs = 1000; %sampling rate = 1000 Hz
slen = length(ecg);
t=[1:slen]/fs;
figure
plot(t, ecg)
axis tight;
xlabel('Time in seconds');
ylabel('ECG');
title('ECG signal with low Fequency Noise');
```

```
%=================================================
%This program is designed for butter worth low pass and high pass filter
% in delta domain

clear all;
close all;
clc;
ecg = load ('ecg_hfn.dat' );
fs = 1000;      % Sampling Frequency
delta=1/fs;
%-------------------------------------------------------
%       Design of low pass Butterworth filter
%-------------------------------------------------------
fc = 40;        % Cutoff Frequency for LPF
slen = length( ecg );
t = [1:slen]/fs;        %Time Scale
w1 = (fc/fs)*2;         %Normalised frequency
N = 4;                  %Order of the filter of LPF
[bl,al] = butter ( N,w1);%,'low');   %Getting coefficients of filter
[bs,as]=butter(N,w1,'s');
[bd1,ad1]=c2del(bl,al,delta);
[bz1,az1]=bilinear(bl,al,fs);
disp('Low pass filter T.F in S domain');
printsys(bl,al,'s');
disp('Low pass filter T.F in Z domain');
printsys(bz1,az1,'z');
disp('Low pass filter T.F in Delta domain');
printsys(bd1,ad1,'y');
%-------------------------------------------------------
%       Filtering of signals
%-------------------------------------------------------
```

```
Yl = filter(bl,al,ecg);      %Low Filtering ecg signal in s domain
yzl=filter(bzl,azl,ecg);     %Low Filtering ecg signal in z domain
ydl=filter(bdl,adl,ecg);     %Low Filtering ecg signal in delta domain
%-------------------------------------------------------
%       Disign of High pass butter worth filter
%-------------------------------------------------------
fcl=2;                    %cuttoff frequency for highpass filter
w2=(fcl/fs)*2;             %normalised frequency for HPF
Nl=4;                      %order of HPF
[bh,ah]=butter(Nl,w2,'high');   %Getting coefficients of filter
[bd2,ad2]=c2del(bh,ah,delta);
[bz2,az2]=bilinear(bh,ah,fs);
disp('Low pass filter T.F in S domain');printsys(bh,ah,'s');
disp('Low pass filter T.F in Z domain');printsys(bz2,az2,'z');
disp('Low pass filter T.F in Delta domain');printsys(bd2,ad2,'y');
%-------------------------------------------------------------------
%       High Filtering ecg signal
%-------------------------------------------------------------------
Yh=filter(bh,ah,Yl);yz2=filter(bz2,az2,yz1);yd2=filter(bd2,ad2,ydl);
%-------------------------------------------------------------------
%   plots  of filtered signal in S domain
%-------------------------------------------------------------------
figure(1);
subplot(3,1,1)
plot(t,ecg);
xlabel('Time in seconds');ylabel('Amplitude');axis tight;
title('ORIGINAL ECG SIGNAL');
subplot(3,1,2)
plot(t,Yl);
xlabel('Time in seconds');ylabel('Amplitude');axis tight;
title('Low filtered ecg SIGNAL in S');
subplot(3,1,3)
plot(t,Yh);
xlabel('Time in seconds');ylabel('Amplitude');axis tight;
title('High FILTERED SIGNAL IN S');
%-------------------------------------------------------
%   plots  of filtered signal in Z domain
%-------------------------------------------------------
figure(2);
subplot(3,1,1)
plot(t,ecg);
xlabel('Time in seconds');ylabel('Amplitude');axis tight;
title('ORIGINAL ECG SIGNAL');
subplot(3,1,2)
plot(t,yz1);
xlabel('Time in seconds');ylabel('Amplitude');axis tight;
title('Low filtered ecg SIGNAL in Z');
subplot(3,1,3)
plot(t,yz2);
xlabel('Time in seconds');ylabel('Amplitude');axis tight;
title('High FILTERED SIGNAL IN Z');
%-------------------------------------------------------
%   plots  of filtered signal in delta domain
%-------------------------------------------------------
figure(3);
subplot(3,1,1)
plot(t,ecg);
```

```
xlabel('Time in seconds');ylabel('Amplitude');axis tight;
title('ORIGINAL ECG SIGNAL');
subplot(3,1,2)
plot(t,yd1);
xlabel('Time in seconds');ylabel('Amplitude');axis tight;
title('Low filtered ecg SIGNAL in Delta');
subplot(3,1,3)
plot(t,yd2);
xlabel('Time in seconds');ylabel('Amplitude');axis tight;
title('High FILTERED SIGNAL IN Delta');
%=================================================

% This program is for design of band stop filter in delta domain

clear all;
format long;
input= load('ecg2x60.dat');
gamma=0.9999911;
fs=360; %input('Enter the value of sampling frequency  =  ');
delta=1/fs;
fo=60;
N = length(input);       % Number of samples
t_len = N/fs;            % Length of input signal in seconds
fignum = 1;
t  = ((1:N)/fs)';
f=0:fs/2;
w=2*pi*f;
ff=(w/(2*pi));
fn=ff/fs;
theta=2*pi*fo/fs;
alpha=2*pi*w*delta;
bita=abs((gamma-1)/delta);
k=bita^2;
z=[(exp(j*theta)-1)/delta;(exp(-j*theta)-1)/delta];
p=[bita*(exp(j*theta)-1)/delta,bita*(exp(-j*theta))/delta];
[numd,dend]=zp2tf(z,p,k);
Hd=delfreq(numd,dend,w,delta);
magd=abs(Hd);
phased=180/pi*unwrap(angle(Hd));

%-------------------------------------------------
% Magnitude plot in delta domain in dB
%-------------------------------------------------
figure(fignum);
fignum=fignum+1;
subplot(2,1,1);
plot(ff,20*log10(abs(Hd)));
axis([0 125 -400 10]);
title('Band Stop Filter Magnitude Response in delta');
xlabel('Frequency [Hz]');ylabel('Magnitude in dB');
subplot(2,1,2);
y1=180/pi*(unwrap(angle(Hd)'))';
plot(ff,y1);
axis([0 125 -100 400]);
title('Band Stop Filter Phase Response in delta');
xlabel('Frequency [Hz]');ylabel('Angle in degree');
```

```
%-----------------------------------------------------
%  In z-domain
%-----------------------------------------------------
k1=(1-2*gamma*cos(theta)+gamma^2)/(2-2*cos(theta));
numz=k1*[1 -2*cos(theta) 1];
denz=[1 -2*gamma*cos(theta) gamma^2];
%---------------------------------------
% Fitltering
%---------------------------------------

outputz=filter(numz,denz,input);
outputd=filter(numd,dend,input);
%-------------------------------------
% plot of outpute in z domain
%-------------------------------------
figure(fignum);
fignum=fignum+1;
subplot(2,1,1);
plot(t,input);
axis([0 1 -2 3]);
title('Original ECG signal');
xlabel('Normalized time');ylabel('Normalised magnitude');
subplot(2,1,2);
plot(t,outputz);
axis([0 1 -2 3]);
title('Filtered ECG signal in designed z domain');
xlabel('Normalized time');ylabel('Normalised magnitude');
%-------------------------------------
%plot of output in delta domain
%-------------------------------------
figure(fignum);
fignum=fignum+1;
subplot(2,1,1);
plot(t,input);
axis([0 1 -2 3]);
title('Original ECG signal');
xlabel('Normalized time');ylabel('Normalised magnitude');
subplot(2,1,2);
plot(t,outputd);
axis([0 1 -2 3]);
title('Filtered ECG signal in designed delta domain');
xlabel('Normalized time');ylabel('Normalised magnitude');

%=========================================================
```

List of publications:

Journals:

[1] N.C.Sarcar, P. Sarkar & M. Bhuyan, "Delta Operator Based Controller Design by Optimal Frequency Fitting Method Using Genetic Algorithm", Paper communicated to *International Journal ACTA Press Canada*, 2008 and reviewed paper already sent for publishing in 2009.

[2] N.C.Sarcar, Prashant Sarkar & Manabendra Bhuyan, "Classical Control Design in Delta Domain by Optimal Generalised Moment Matching Using Genetic Algorithm", Paper communicated to *International Journal AMSE France*, 2008. Some corrections have been suggested which is being incorporated and will be sent soon for publication .

Conferences:

[1] N.C.Sarcar, M.Bhuyan & P.Sarkar, "Reference model selection for controller design based on performance specifications in delta domain", *proc. International Conference on Recent Advancements and Applications of Computer in Electrical Engineering (RACE),* vol. 1, sl-56, pp 277-282, Engineeing College Bikaner, India, 2007.

[2] N.C.Sarcar, M.Bhuyan & P.Sarkar, "Discrete reference model selection and use of Generalised Moment Matching method for Controller Design in Delta Domain", *proc. International Conference, IICT 2007*, Vol. 1, pp 500-510, DIT, DehraDoon, India, 2007.

[3] N.C.Sarcar, M. Bhuyan & P.Sarcar, *"Frequency domain specifications of reference model in delta domain",* National Conference on Control and Instrumentation, NIT, Kurukshetra India, 2007.

[4] P.Sarkar & N.C.Sarcar. "Modeling and Parameter identification of discrete data systems by matching weighted moments using delta domain technique", *proc. National Conference on Electric Power Technology, Management and IT application, (EPTMITA-06), pp 4-9,* at MMMEC, Gorakhpur India, 2006.

[5] N.C.Sarcar, M.Bhuyan & P.Sarcar, "Parameterisation of biomedical digital filters using fast sampling delta transformation", *National Conference on notechnology (Nanotech-2004)* at ITM, Gorakhpur India, 2004.

[6] N.C.Sarcar, "Suppression of Power line interference in ECG signals using delta domain techniqaue", *IEEE Sponsored state level Conference* organized by student chapter, UP Section at ITM, Gorakhpur India, 2008.

[7] N.C.Sarcar, P. Sarkar & M. Bhuyan, "Controller design for time delay systems by optimal generalised delta time moment matching using genetic algorithm", Paper has been accepted for the *National Conference, TICE-09, to be held on 29-30 Oct-2009 at Dept of Electronics and Comm. Engg., Thapar University,Patiala, Punjab (India).*